
Biomolecular Feedback Systems

Domitilla Del Vecchio
MIT

Richard M. Murray
Caltech

REVIEW VERSION, June 5, 2012
© California Institute of Technology
All rights reserved.

This manuscript is for review purposes only and may not be reproduced, in whole or in part, without written consent from the authors.

Contents

Contents	i
Preface	iii
Notation	v
1 Introductory Concepts	1-1
1.1 Systems Biology: Modeling, Analysis and Role of Feedback	1-1
1.2 Dynamics and Control in the Cell	1-8
1.3 Control and Dynamical Systems Tools [AM08]	1-21
1.4 Input/Output Modeling [AM08]	1-30
1.5 From Systems to Synthetic Biology	1-36
1.6 Further Reading	1-41
2 Dynamic Modeling of Core Processes	2-1
2.1 Modeling Techniques	2-1
2.2 Transcription and Translation	2-14
2.3 Transcriptional Regulation	2-19
2.4 Post-Transcriptional Regulation	2-29
2.5 Cellular subsystems	2-38
Exercises	2-45
3 Analysis of Dynamic Behavior	3-1
3.1 Analysis Near Equilibria	3-1
3.2 Robustness	3-14
3.3 Analysis of Reaction Rate Equations	3-26
3.4 Oscillatory Behavior	3-32
3.5 Bifurcations	3-43
3.6 Model Reduction Techniques	3-48
Exercises	3-53
4 Stochastic Modeling and Analysis	4-1
4.1 Stochastic Modeling of Biochemical Systems	4-5
4.2 Simulation of stochastic systems	4-19

4.3	Input/Output Linear Stochastic Systems	4-22
	Exercises	4-27
5	Feedback Examples	5-1
5.1	The <i>lac</i> Operon	5.1-1
5.2	Bacterial Chemotaxis	5.2-1
6	Biological Circuit Components	6-1
6.1	Introduction to Biological Circuit Design	6-1
6.2	Negative Autoregulation	6-4
6.3	The Toggle Switch	6-9
6.4	The Repressilator	6-11
6.5	Activator-repressor clock	6-14
6.6	An Incoherent Feedforward Loop (IFFL)	6-20
	Exercises	6-21
7	Interconnecting Components	7-1
7.1	Input/Output Modeling and the Modularity Assumption	7-1
7.2	Introduction to Retroactivity	7-2
7.3	Retroactivity in Gene Circuits	7-5
7.4	Retroactivity in Signaling Systems	7-11
7.5	Insulation Devices: Retroactivity Attenuation	7-16
	Exercises	7-32
8	Design Tradeoffs	8-1
8.1	Metabolic Burden	8-1
8.2	Stochastic Effects: Design Tradeoffs between Retroactivity and Noise	8-13
A	Cell Biology Primer	A-1
A.1	What is a Cell	A-2
A.2	What is a Genome	A-29
A.3	Molecular Genetics: Piecing It Together	A-46
B	Probability and Random Processes	B-1
B.1	Random Variables	B-1
B.2	Continuous-State Random Processes	B-8
B.3	Discrete-State Random Processes	B-15
	Bibliography	B-1
	Index	I-1

Preface

This text serves as a supplement to *Feedback Systems* by Åström and Murray [2] (referred to throughout the text as AM08) and is intended for researchers interested in the application of feedback and control to biomolecular systems. The text has been designed so that it can be used in parallel with *Feedback Systems* as part of a course on biomolecular feedback and control systems, or as a standalone reference for readers who have had a basic course in feedback and control theory. The full text for AM08, along with additional supplemental material and a copy of these notes, is available on a companion web site:

<http://www.cds.caltech.edu/~murray/amwiki/BFS>

The material in this book is intended to be useful to three overlapping audiences: graduate students in biology and bioengineering interested in understanding the role of feedback in natural and engineered biomolecular systems; advanced undergraduates and graduate students in engineering disciplines who are interested the use of feedback in biological circuit design; and established researchers in the the biological sciences who want to explore the potential application of principles and tools from control theory to biomolecular systems. We have written the text assuming some familiarity with basic concepts in feedback and control, but have tried to provide insights and specific results as needed, so that the material can be learned in parallel. We also assume some familiarity with cell biology, at the level of a first course for non-majors. The individual chapters in the text indicate the pre-requisites in more detail, most of which are covered either in AM08 or in the supplemental information available from the companion web site.

Domitilla Del Vecchio
Cambridge, Massachusetts

Richard M. Murray
Pasadena, California

Notation

This is an internal chapter that is intended for use by the authors in fixing the notation that is used throughout the text. In the first pass of the book we are anticipating several conflicts in notation and the notes here may be useful to early users of the text. Review

Protein dynamics

For a gene ‘gent’, we write $genX$ for the gene, m_{genX} for the mRNA and $GenX$ for the protein when they appear in text or chemical formulas. Superscripts are used for covalent modifications, e.g., X^P for phosphorylation. We also use superscripts to differentiate between isomers, so m_{genX}^* might be used to refer to mature RNA or $GenX^f$ to refer to the folded versions of a protein, if required. Mathematical formulas use the italic version of the variable name, but roman font for the gene or isomeric state. The concentration of mRNA is written in text or formulas as m_{genX} (m_{genX}^* for mature) and the concentration of protein as p_{genX} (p_{genX}^f for folded). The same naming conventions are used for common gene/protein combinations: the mRNA concentration of $tetR$ is m_{tetR} , the concentration of the associated protein is p_{tetR} and parameters are α_{tetR} , δ_{tetR} , etc.

For generic genes and proteins, use X to refer to a protein, m_x to refer to the mRNA associated with that protein and x to refer to the gene that encodes X . The concentration of X can be written either as X , p_x or $[X]$, with that order of preference. The concentration of m_x can be written either as m_x (preferred) or $[m_x]$. Parameters that are specific to gene p are written with a subscripted p : α_p , δ_p , etc. Note that although the protein is capitalized, the subscripts are lower case (so indexed by the gene, not the protein) and also in roman font (since they are not a variable).

The dynamics of protein production are given by

$$\frac{dm_p}{dt} = \alpha_{p,0} - \underbrace{\mu m_p - \bar{\gamma}_p m_p}_{-\gamma_p m_p}, \quad \frac{dP}{dt} = \beta_p m_p - \underbrace{\mu P - \bar{\delta}_p P}_{-\delta_p P},$$

where $\alpha_{p,0}$ is the (basal) rate of production, γ_p parameterizes the rate of degradation of the mRNA m_p , β_p is the kinetic rate of protein production, μ is the growth rate that leads to dilution of concentrations and δ_p parameterizes the rate of degradation

of the protein P . Since dilution and degradation enter in a similar fashion, we use $\gamma = \bar{\gamma} + \mu$ and $\delta = \bar{\delta} + \mu$ to represent the aggregate degradation and dilution rate. If we are looking at a single gene/protein, the various subscripts can be dropped.

When we ignore the mRNA concentration, we write the simplified protein dynamics as

$$\frac{dP}{dt} = \beta_{p,0} - \bar{\delta}_p P.$$

Assuming that the mRNA dynamics are fast compared to protein production, then the constant $\beta_{p,0}$ is given by

$$\beta_{p,0} = \beta_p \frac{\bar{\gamma}_p}{\alpha_{p,0}}.$$

For regulated production of proteins using Hill functions, we modify the constitutive rate of production to be $f_p(Q)$ instead of $\alpha_{p,0}$ or $\beta_{p,0}$ as appropriate. The Hill function is written in the forms

$$F_{p,q}(Q) = \frac{\alpha_{p,q}}{1 + (Q/K_{p,q})^{n_{p,q}}}, \quad F_{p,q}(Q) = \frac{\alpha_{p,q}(Q/K_{p,q})^{n_{p,q}}}{1 + (Q/K_{p,q})^{n_{p,q}}}.$$

The notation for F mirrors that of transfer functions: $F_{p,q}$ represents the input/output relationship between input Q and output P (rate). If the target gene is not particularly relevant, the subscript can represent just the transcription factor: single letters:

$$F_{lac}(Q) = \frac{\alpha_{lac}}{1 + (Q/K_{laq})^{n_{lac}}}.$$

The subscripts can be dropped completely if there is only one Hill function in use.

Some common symbols:

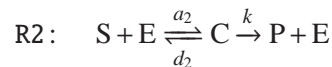
Symbol	LaTeX	Comment
X_{tot}	X_{tot}	Total concentration of a species
K_d	$\backslash Kd$	Dissociation constant
K_m	$\backslash Km$	Michaelis-Menten constant

Chemical reactions

We write the symbol for a chemical species A using roman type. The number of molecules of a species A is written as n_a . The concentration of the species is occasionally written as $[A]$, but we more often use the notation A , as in the case of proteins, or x_a . For a reaction $A + B \longleftrightarrow C$, we use the notation



This notation is primarily intended for situations where we have multiple reactions and need to distinguish between many different constants. Enzymatic reactions have the form



For a small number of reactions, the reaction number can be dropped.

It will often be the case that two species A and B will form a molecular bond, in which case we write the resulting species as AB. If we need to distinguish between covalent bonds and hydrogen bonds, we write the latter as A:B. Finally, in some situations we will have labeled section of DNA that are connected together, which we write as A–B, where here A represents the first portion of the DNA strand and B represents the second portion. When describing (single) strands of DNA, we write A' to represent the Watson-Crick complement of the strand A. Thus A–B:B'–A' would represent a double stranded length of DNA with domains A and B.

The choice of representing covalent molecules using the conventional chemical notation AB can lead to some confusion when writing the reaction dynamics using A and B to represent the concentrations of those species. Namely, the symbol AB could represent either the concentration of A times the concentration of B or the concentration of AB. To remove this ambiguity, when using this notation we write [A][B] as $A \cdot B$.

When working with a system of chemical reactions, we write S_i , $i = 1, \dots, n$ for the species and R_j , $j = 1, \dots, m$ for the reactions. We write n_i to refer to the molecular count for species i and $x_i = [S_i]$ to refer to the concentration of the species. The individual equations for a given species are written

$$\frac{dx_i}{dt} = \sum_{j=1}^m m_{k_{i,j}} x_j x_k.$$

The collection of reactions are written as

$$\frac{dx}{dt} = Nv(x, \theta), \quad \frac{dx_i}{dt} = N_{ij} v_j(x, \theta),$$

where x_i is the concentration of species S_i , $N \in \mathbb{R}^{n \times m}$ is the stoichiometry matrix, v_j is the reaction flux vector for reaction j , and θ is the collection of parameters that define the reaction rates. Occasionally it will be useful to write the fluxes as polynomials, in which case we use the notation

$$v_j(x, \theta) = \sum_k E_{jk} \prod_l x_l^{\epsilon_l^{jk}}$$

where E_{jk} is the rate constant for the k th term of the j th reaction and ϵ_l^{jk} is the stoichiometry coefficient for the species x_l .

Generally speaking, coefficients for propensity functions and reaction rate constants are written using lower case (c_ξ , k_i , etc). Two exceptions are the dissociation constant, which we write as K_d , and the Michaelis-Menten constant, which we write as K_m .

Figures

In the public version of the text, certain copyrighted figures are missing. The file-names for these figures are listed and many of the figures can be looked up in the following references:

- **Cou08** - *Mechanisms in Transcriptional Regulation* by A. J. Courey [16]
- **GNM93** - J. Greenblatt, J. R. Nodwell and S. W. Mason, “Transcriptional antitermination” [35]
- **Mad07** - *From a to alpha: Yeast as a Model for Cellular Differentiation* by H. Madhani [53]
- **MBoC** - *The Molecular Biology of the Cell* by Alberts et al. [3]
- **PKT08** - *Physical Biology of the Cell* by Phillips, Kondev and Theriot [68]

The remainder of the filename lists the chapter and figure number.

Review

Comments intended for reviewers are marked as in this paragraph. These comments generally explain missing material that will be included in the final text.

Chapter 1

Introductory Concepts

This chapter provides a brief introduction to concepts from systems biology, tools from differential equations and control theory, and approaches to modeling, analysis and design of biomolecular feedback systems. We begin with a discussion of the role of modeling, analysis and feedback in biological systems, followed by an overview of basic concepts from cell biology, focusing on the dynamics of protein production and control. This is followed by a short review of key concepts and tools from control and dynamical systems theory, intended to provide insight into the main methodology described in the text. Finally, we give a brief introduction to the field of synthetic biology, which is the primary topic of the latter portion of the text. Readers who are familiar with one or more of these areas can skip the corresponding sections without loss of continuity.

1.1 Systems Biology: Modeling, Analysis and Role of Feedback

At a variety of levels of organization—from molecular to cellular to organismal—biology is becoming more accessible to approaches that are commonly used in engineering: mathematical modeling, systems theory, computation and abstract approaches to synthesis. Conversely, the accelerating pace of discovery in biological science is suggesting new design principles that may have important practical applications in human-made systems. This synergy at the interface of biology and engineering offers many opportunities to meet challenges in both areas. The guiding principles of feedback and control are central to many of the key questions in biological science and engineering and can play an enabling role in understanding the complexity of biological systems.

In this section we summarize our view on the role that modeling and analysis should (eventually) play in the study and understanding of biological systems, and discuss some of the ways in which an understanding of feedback principles in biology can help us better understand and design complex biomolecular circuits.

There are a wide variety of biological phenomena that provide a rich source of examples for control, including gene regulation and signal transduction; hormonal, immunological, and cardiovascular feedback mechanisms; muscular control and locomotion; active sensing, vision, and proprioception; attention and consciousness; and population dynamics and epidemics. Each of these (and many more) provide opportunities to figure out what works, how it works and what can be done

to affect it. Our focus here is at the molecular scale, but the principles and approach that we describe can also be applied at larger time and length scales.

Modeling and analysis

Over the past several decades, there have been significant advances in modeling capabilities for biological systems that have provided new insights into the complex interactions of the molecular-scale processes that implement life. Reduced-order modeling has become commonplace as a mechanism for describing and documenting experimental results and high-dimensional stochastic models can now be simulated in reasonable periods of time to explore underlying stochastic effects. Coupled with our ability to collect large amounts of data from flow cytometry, micro-array analysis, single-cell microscopy and other modern experimental techniques, our understanding of biomolecular processes is advancing at a rapid pace.

Unfortunately, although models are becoming much more common in biological studies, they are still far from playing the central role in explaining complex biological phenomena. Although there are exceptions, the predominant use of models is to “document” experimental results: a hypothesis is proposed and tested using careful experiments, and then a model is developed to match the experimental results and help demonstrate that the proposed mechanisms can lead to the observed behavior. This necessarily limits our ability to explain complex phenomena to those for which controlled experimental evidence of the desired phenomena can be obtained.

This situation is much different than standard practice in the physical sciences and engineering, as illustrated in Figure 1.1 (in the context of modeling, analysis and control design for gas turbine aeroengines). In those disciplines, experiments are routinely used to help build models for individual components at a variety of levels of detail, and then these component-level models are interconnected to obtain a system-level model. This system-level model, carefully built to capture the appropriate level of detail for a given question or hypothesis, is used to explain, predict and systematically analyze the behaviors of a system. Because of the ways in which models are viewed, it becomes possible to prove (or invalidate) a hypothesis through analysis of the model, and the fidelity of the models is such that decisions can be made based on them. Indeed, in many areas of modern engineering—including electronics, aeronautics, robotics and chemical processing, to name a few—models play a primary role in the understanding of the underlying physics and/or chemistry, and these models are used in predictive ways to explore design tradeoffs and failure scenarios.

A key element in the successful application of modeling in engineering disciplines is the use of *reduced-order models* that capture the underlying dynamics of the system without necessarily modeling every detail of the underlying mechanisms. These reduced order models are often coupled with schematics diagrams,

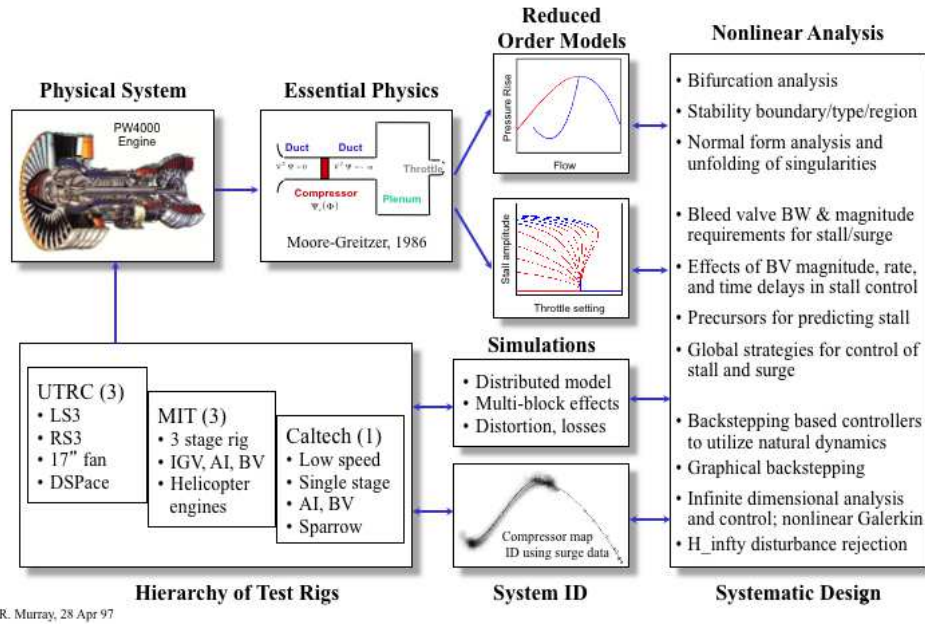


Figure 1.1: Sample modeling, analysis and design framework for an engineering system.

such as those shown in Figure 1.2, to provide a high level view of a complex system. The generation of these reduced-order models, either directly from data or through analytical or computational methods, is critical in the effective application of modeling since modeling of the detailed mechanisms produces high fidelity models that are too complicated to use with existing tools for analysis and design. One area in which the development of reduced order models is fairly advanced is in control theory, where input/output models such as input/output models, block diagrams and transfer functions are used to capture structured representations of dynamics at the appropriate level of fidelity for the task at hand [2].

While developing predictive models and corresponding analysis tools for biology is much more difficult, it is perhaps even more important that biology make use of models, particularly reduced-order models, as a central element of understanding. Biological systems are by their nature extremely complex and can behave in counterintuitive ways. Only by capturing the many interacting aspects of the system in a formal model can we ensure that we are reasoning properly about its behavior, especially in the presence of uncertainty. To do this will require substantial effort in building models that capture the relevant dynamics at the proper scales (depending on the question being asked) as well as building an analytical framework for answering questions of biological relevance.

The good news is that a variety of new techniques, ranging from experiments to computation to theory, are enabling us to explore new approaches to modeling

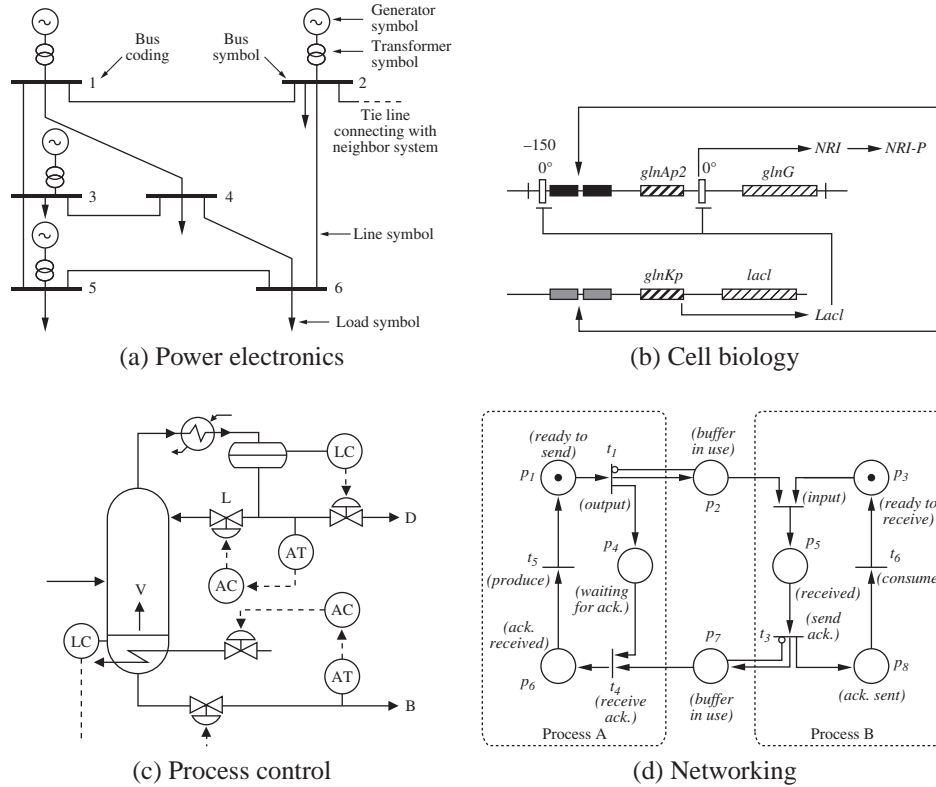


Figure 1.2: Schematic diagrams representing models in different disciplines. Each diagram is used to illustrate the dynamics of a feedback system: (a) electrical schematics for a power system [49], (b) a biological circuit diagram for a synthetic clock circuit [6], (c) a process diagram for a distillation column [78] and (d) a Petri net description of a communication protocol.

that attempt to address some of these challenges. In this text we focus on the use of a relevant classes of reduced-order models that can be used to capture many phenomena of biological relevance.

Dynamic behavior and phenotype

One of the key needs in developing a more systematic approach to the use of models in biology is to become more rigorous about the various behaviors that are important for biological systems. One of the key concepts that needs to be formalized is the notion of “phenotype”. This term is often associated with the existence of an equilibrium point in a reduced-order model for a system, but clearly more complex (non-equilibrium) behaviors can occur and the “phenotypic response” of a system to an input may not be well-modeled by a steady operating condition. Even more

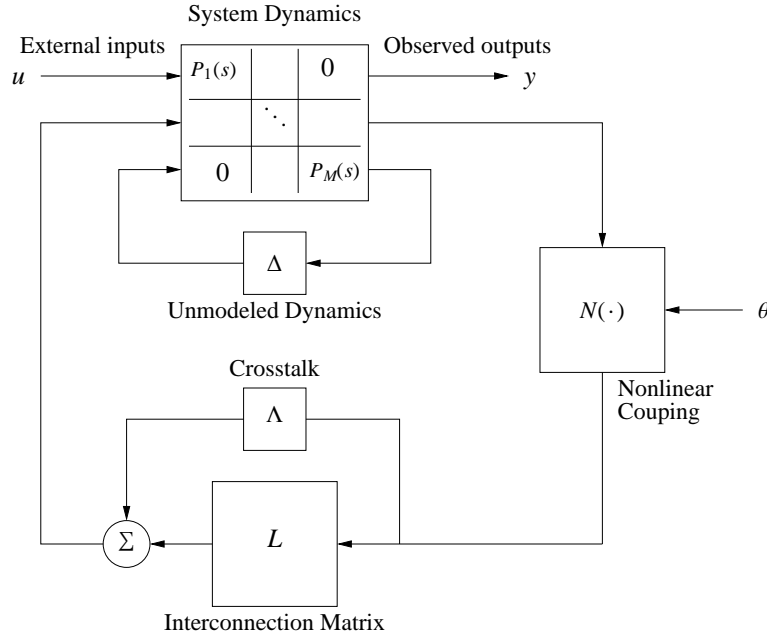


Figure 1.3: Conceptual modeling framework for biomolecular feedback systems. The dynamics consist of a set of linear dynamics, represented by the multi-input, multi-output transfer function $P(s)$, a static nonlinear map N and an interconnection matrix L . Uncertainty is represented as unmodeled dynamics Δ , crosstalk Λ and system context θ . The inputs and outputs to the system are denoted by u and y .

problematic is determining which regulatory structures are “active” in a given phenotype (versus those for which there is a regulatory pathway that is saturated and hence not active).

Figure 1.3 shows a graphical representation of a class of systems that captures many of the features we are interested in. The system is composed of M interconnected subsystems. The linear dynamics of the subsystems (possibly including delay) are captured via their frequency responses, represented in the diagram by the “transfer functions” $P_i(s)$. The outputs of the linear subsystems are transformed via a nonlinear map $N(\cdot)$ and then interconnected back to the inputs of the subsystems through the matrix L . The role of feedback is captured through the interconnection matrix L , which represents a weighted graph describing the interconnections between subsystems.

In addition to the internal dynamics and nonlinear coupling, we separately keep track of external inputs to the subsystems (u), measured outputs (y), stochastic disturbances (w , not shown), and measurement noise (v , not shown). Three other features are present in Fig. 1.3. The first is the uncertainty operator Δ , attached to the linear dynamics block. This operator represents both parametric uncertainty in the dynamics as well as unmodeled dynamics that have known (frequency-dependent)

bounds. Tools for understanding this class of uncertainty are available for both linear and nonlinear control systems [2] and allow stability and performance analyses in the presence of uncertainty. A similar term Λ is included in the interconnection matrix and represents (unmodeled) “crosstalk” between subsystems. Finally, θ represents the context- and environment-dependent parameters of the system.

This particular structure is useful because it captures a large number of modeling frameworks in a single formalism. Mass action kinetics and chemical reaction networks can be represented by equating the stoichiometry matrix with the interconnection matrix L and using the nonlinear terms to capture the fluxes, with θ representing the rate constants. We can also represent typical reduced-order models for transcriptional regulatory networks by letting the nonlinear functions $N()$ represent various types of Hill functions and including the effects of mRNA/protein production, degradation and dilution through the linear dynamics. These two classes of systems can also be combined, allowing a very expressive set of dynamics that is capable of capturing many relevant phenomena of interest in molecular biology.

In the context of the modeling framework described in Figure 1.3, it is possible to consider a working definition of phenotype in terms of the patterns of the dynamics that are present. In the simplest case, consisting of operation near a single equilibrium point, we can look at the effective gain of the different nonlinearities as a measure of which regulatory pathways are “active” in a given state. Consider, for example, labeling each nonlinearity in a system as being either *on*, *off* or *active*. A nonlinearity that is on or off represents one in which changes of the input produce very small deviations in the output, such as those that occur at very high or low concentrations in interactions modeled by a Hill function. An active nonlinearity is one in which there is a proportional response to changes in the input, with the slope of the nonlinearity giving the effective gain. In this setting, the phenotype of the system would consist of both a description of the nominal concentrations of the measurable species (y) as well as the state of each nonlinearity (on, off, active).

Another common situation is that a system may have multiple equilibrium points and the “phenotype” of the system is represented by the particular equilibrium point that the system converges to. In the simplest case, we can have *bistability*, in which there are two equilibrium points x_{1e} and x_{2e} for a fixed set of parameters. Depending on the initial conditions and external inputs, a given system may end up near one equilibrium point or the other, providing two distinct phenotypes. A model with bistability (or multi-stability) provides one method of modeling memory in a system: the cell or organism remembers its history by virtue of the equilibrium point to which it has converted.

For more complex phenotypes, where the subsystems are not at a steady operating point, one can consider temporal patterns such as limit cycles (periodic orbits) or non-equilibrium input/output responses. Analysis of these more complicated behaviors requires more sophisticated tools, but again model-based analysis of stability and input/output responses can be used to characterize the phenotypic

behavior of a biological system under different conditions or contexts.

Additional types of analysis that can be applied to systems of this form include sensitivity analysis (dependence of solution properties on selected parameters), uncertainty analysis (impact of disturbances, unknown parameters and unmodeled dynamics), bifurcation analysis (changes in phenotype as a function of input levels, context or parameters) and probabilistic analysis (distributions of states as a function of distributions of parameters, initial conditions or inputs). In each of these cases, there is a need to extend existing tools to exploit the particular structure of the problems we consider, as well as modify the techniques to provide relevance to biological questions.

Stochastic behavior

Another important feature of many biological systems is stochasticity: biological responses have an element of randomness so that even under carefully control conditions, the response of a system to a given input may vary from experiment to experiment. This randomness can have many possible sources, including external perturbations that are modeled as stochastic processes and internal processes such as molecular binding and unbinding, whose stochasticity stems from the underlying thermodynamics of molecular reactions.

While for many engineered systems it is common to try to eliminate stochastic behavior (yielding a “deterministic” response), for biological systems there appear to be many situations in which stochasticity is important for the way in which organisms survive. In biology, nothing is 100% and so there is always some chance that two identical organisms will respond differently. Thus viruses are never completely contagious and so some organisms will survive, and DNA replication is never error free, and so mutations and evolution can occur. In studying circuits where these types of effects are present, it thus becomes important to study the distribution of responses of a given biomolecular circuit, and to collect data in a manner that allows us to quantify these distributions.

One important indication of stochastic behavior is *bimodality*. We say that a circuit or system is bimodal if the response of the system to a given input or condition has two or more distinguishable classes of behaviors. An example of bimodality is shown in Figure 1.4, which shows the response of the galactose metabolic machinery in yeast. We see from the figure that even though genetically identical organisms are exposed to the same external environment (a fixed galactose concentration), the amount of activity in individual cells can have a large amount of variability. At some concentrations there are clearly two subpopulations of cells: those in which the galactose metabolic pathway is turned on (higher reporter fluorescence values on the y axis) and those for which it is off (lower reporter fluorescence).

Another characterization of stochasticity in cells is the separation of noisiness

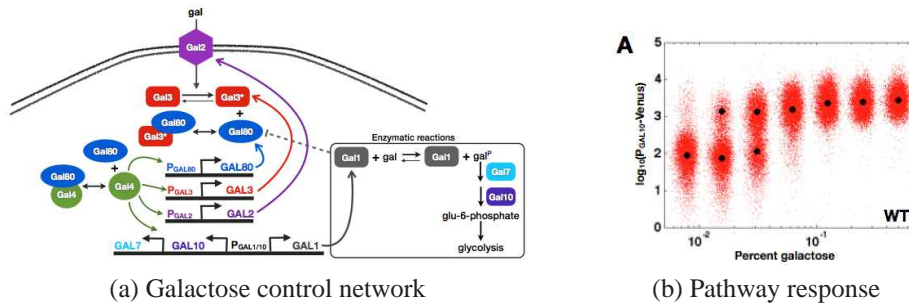


Figure 1.4: Galactose response in yeast [86]. (a) GAL signaling circuitry showing a number of different feedback pathways that are used to detect the presence of galactose and switch on the metabolic pathway. (b) Pathway activity as a function of galactose concentration. The points at each galactose concentration represent the activity level of the galactose metabolic pathway in an individual cell. Black dots indicate the mean of a Gaussian mixture model (GMM) classification [85]. Small random deviations were added to each galactose concentration (horizontal axis) to better visualize the distributions.

in protein expression into two categories: “intrinsic” noise and “extrinsic” noise. Roughly speaking, extrinsic noise represents variability in gene expression that effects all proteins in the cell in a correlated way. Extrinsic noise can be due to environmental changes that affect the entire cell (temperature, pH, oxygen level) or global changes in internal factors such as energy or metabolite levels (perhaps due to metabolic loading). Intrinsic noise, on the other hand, is the variability due to the inherent randomness of molecular events inside the cell and represents a collection of independent random processes. One way to attempt to measure the amount of intrinsic and extrinsic noise is to take two identical copies of a biomolecular circuit and compare their responses [27, 82]. Correlated variations in the output of the circuits corresponds (roughly) to extrinsic noise and uncorrelated variations to intrinsic noise [40, 82].

The types of models that are used to capture stochastic behavior are very different than those used for deterministic responses. Instead of writing differential equations that track average concentration levels, we must keep track of the individual events that can occur with some probability per unit time (or “propensity”). We will explore the methods for modeling and analysis of stochastic systems in Chapter 4.

1.2 Dynamics and Control in the Cell

The molecular processes inside a cell determine its behavior and are responsible for metabolizing nutrients, generating motion, enabling procreation and carrying out the other functions of the organism. In multi-cellular organisms, different types of cells work together to enable more complex functions. In this section we briefly

describe the role of dynamics and control within a cell and discuss the basic processes that govern its behavior and its interactions with its environment (including other cells). We assume knowledge of the basics of cell biology at the level provided in Appendix A; a much more detailed introduction to the biology of the cell and some of the processes described here can be found in standard textbooks on cell biology such as Alberts *et al.* [3] or Phillips *et al.* [68]. (Readers who are familiar with the material at the level described in these latter references can skip this section without any loss of continuity.)

The central dogma: production of proteins

The genetic material inside a cell, encoded in its DNA, governs the response of a cell to various conditions. DNA is organized into collections of genes, with each gene encoding a corresponding protein that performs a set of functions in the cell. The activation and repression of genes are determined through a series of complex interactions that give rise to a remarkable set of circuits that perform the functions required for life, ranging from basic metabolism to locomotion to procreation. Genetic circuits that occur in nature are robust to external disturbances and can function in a variety of conditions. To understand how these processes occur (and some of the dynamics that govern their behavior), it will be useful to present a relatively detailed description of the underlying biochemistry involved in the production of proteins.

DNA is a double stranded molecule with the “direction” of each strand specified by looking at the geometry of the sugars that make up its backbone (see Figure 1.5). The complementary strands of DNA are composed of a sequence of nucleotides that consist of a sugar molecule (deoxyribose) bound to one of 4 bases: adenine (A), cytosine (C), guanine (G) and thymine (T). The coding strand (by convention the top row of a DNA sequence when it is written in text form) is specified from the 5’ end of the DNA to the 3’ end of the DNA. (As described briefly in Appendix A, 5’ and 3’ refer to carbon locations on the deoxyribose backbone that are involved in linking together the nucleotides that make up DNA.) The DNA that encodes proteins consists of a promoter region, regulator regions (described in more detail below), a coding region and a termination region (see Figure 1.6). We informally refer to this entire sequence of DNA as a gene.

Expression of a gene begins with the *transcription* of DNA into mRNA by RNA polymerase, as illustrated in Figure 1.7. RNA polymerase enzymes are present in the nucleus (for eukaryotes) or cytoplasm (for prokaryotes) and must localize and bind to the promoter region of the DNA template. Once bound, the RNA polymerase “opens” the double stranded DNA to expose the nucleotides that make up the sequence. This reversible reaction, called *isomerization*, is said to transform the RNA polymerase and DNA from a *closed complex* to an *open complex*. After the open complex is formed, RNA polymerase begins to travel down the DNA

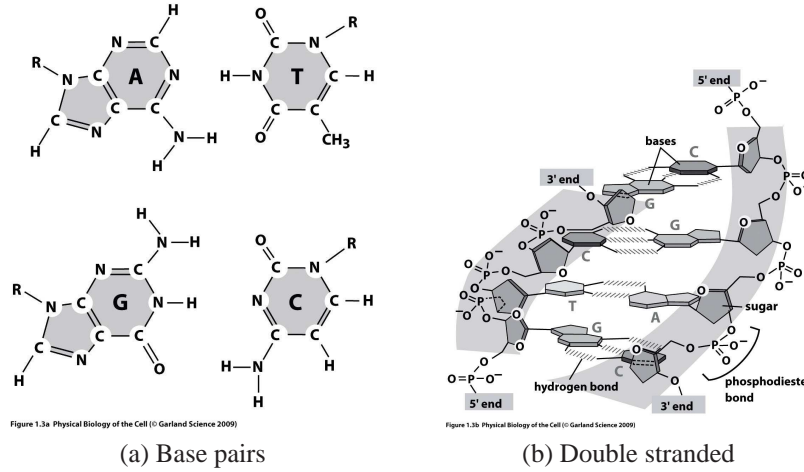


Figure 1.5: Molecular structure of DNA. (a) Individual bases (nucleotides) that make up DNA: adenine (A), cytosine (C), guanine (G) and thymine (T). (b) Double stranded DNA formed from individual nucleotides, with A binding to T and C binding to G. Each strand contains a 5' and 3' end, determined by the locations of the carbons where the next nucleotide binds. Figure from Phillips, Kondev and Theriot [68]; used with permission of Garland Science.

strand and constructs an mRNA sequence that matches the 5' to 3' sequence of the DNA to which it is bound. By convention, we number the first base pair that is transcribed as '+1' and the base pair prior to that (which is not transcribed) is labeled as '-1'. The promoter region is often shown with the -10 and -35 regions indicated, since these regions contain the nucleotide sequences to which the RNA polymerase enzyme binds (the locations vary in different cell types, but these two numbers are typically used).

The RNA strand that is produced by RNA polymerase is also a sequence of nucleotides with a sugar backbone. The sugar for RNA is ribose instead of deoxyribose and mRNA typically exists as a single stranded molecule. Another difference

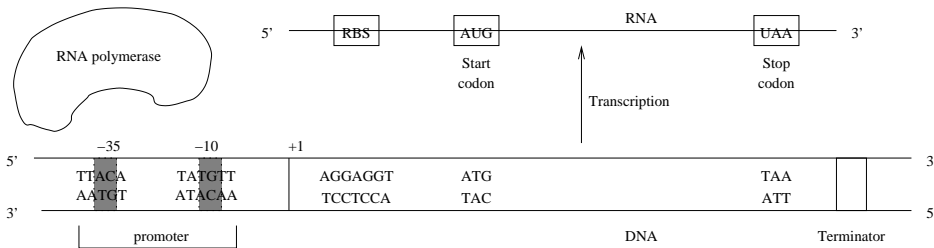


Figure 1.6: Geometric structure of DNA. The layout of the DNA is shown at the top. RNA polymerase binds to the promoter region of the DNA and transcribes the DNA starting at the +1 side and continuing to the termination site.

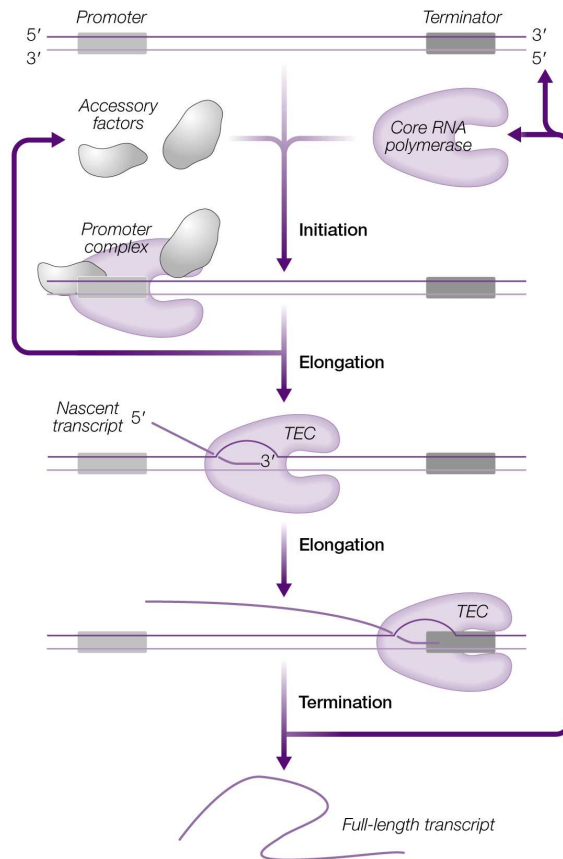


Figure 1.7: Production of messenger RNA from DNA. RNA polymerase, along with other accessory factors, binds to the promoter region of the DNA and then “opens” the DNA to begin transcription (initiation). As RNA polymerase moves down the DNA, producing an RNA transcript (elongation), which is later translated into a protein. The process ends when the RNA polymerase reaches the terminator (termination). Reproduced from Courey [16]; permission pending.

is that the base thymine (T) is replaced by uracil (U) in RNA sequences. RNA polymerase produces RNA one base pair at a time, as it moves from in the 5' to 3' direction along the DNA coding strand. RNA polymerase stops transcribing DNA when it reaches a *termination region* (or *terminator*) on the DNA. This termination region consists of a sequence that causes the RNA polymerase to unbind from the DNA. The sequence is not conserved across species and in many cells the termination sequence is sometimes “leaky”, so that transcription will occasionally occur across the terminator.

Once the mRNA is produced, it must be translated into a protein. This process is slightly different in prokaryotes and eukaryotes. In prokaryotes, there is a region of the mRNA in which the ribosome (a molecular complex consisting of of both

proteins and RNA) binds. This region, called the *ribosome binding site (RBS)*, has some variability between different cell species and between different genes in a given cell. The Shine-Delgarno sequence, AGGAGG, is the consensus sequence for the RBS. (A consensus sequence is a pattern of nucleotides that implements a given function across multiple organisms; it is not exactly conserved, so some variations in the sequence will be present from one organism to another.)

In eukaryotes, the RNA must undergo several additional steps before it is translated. The RNA sequence that has been created by RNA polymerase consists of *introns* that must be spliced out of the RNA (by a molecular complex called the spliceosome), leaving only the *exons*, which contain the coding sequence for the protein. The term *pre-mRNA* is often used to distinguish between the raw transcript and the spliced mRNA sequence, which is called *mature mRNA*. In addition to splicing, the mRNA is also modified to contain a *poly(A)* (polyadenine) *tail*, consisting of a long sequence of adenine (A) nucleotides on the 3' end of the mRNA. This processed sequence is then transported out of the nucleus into the cytoplasm, where the ribosomes can bind to it.

Unlike prokaryotes, eukaryotes do not have a well defined ribosome binding sequence and hence the process of the binding of the ribosome to the mRNA is more complicated. The *Kozak sequence* A/GCCACCAUGG is the rough equivalent of the ribosome binding site, where the underlined AUG is the start codon (described below). However, mRNA lacking the Kozak sequence can also be translated.

Once the ribosome is bound to the mRNA, it begins the process of *translation*. Proteins consist of a sequence of amino acids, with each amino acid specified by a codon that is used by the ribosome in the process of translation. Each codon consists of three base pairs and corresponds to one of the 20 amino acids or a “stop” codon. The genetic code mapping between codons and amino acids is shown in Table A.1. The ribosome translates each codon into the corresponding amino acid using transfer RNA (tRNA) to integrate the appropriate amino acid (which binds to the tRNA) into the polypeptide chain, as shown in Figure 1.8. The start codon (AUG) specifies the location at which translation begins, as well as coding for the amino acid methionine (a modified form is used in prokaryotes). All subsequent codons are translated by the ribosome into the corresponding amino acid until it reaches one of the stop codons (typically UAA, UAG and UGA).

The sequence of amino acids produced by the ribosome is a polypeptide chain that folds on itself to form a protein. The process of folding is complicated and involves a variety of chemical interactions that are not completely understood. Additional post-translational processing of the protein can also occur at this stage, until a folded and functional protein is produced. It is this molecule that is able to bind to other species in the cell and perform the chemical reactions that underly the behavior of the organism. The *maturation time* of a protein is the time required for the polypeptide chain to fold into a functional protein.

Each of the processes involved in transcription, translation and folding of the

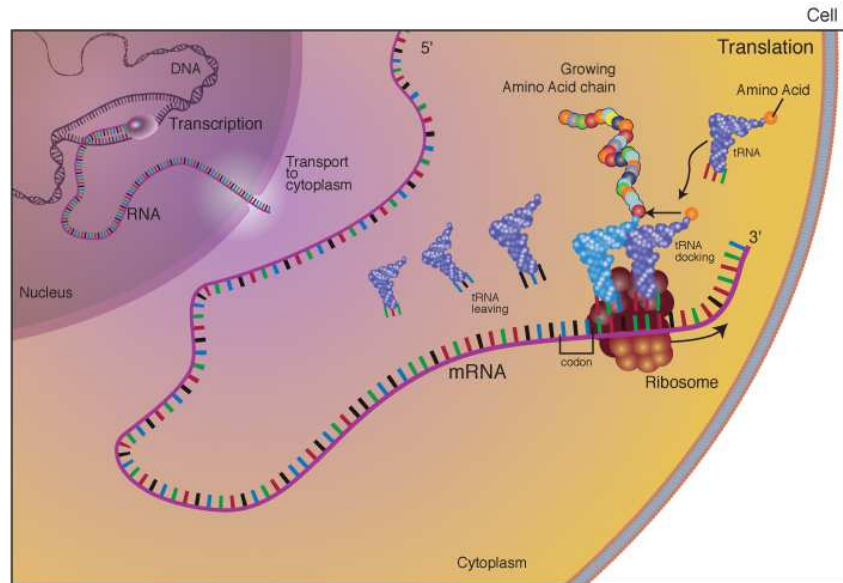


Figure 1.8: Translation is the process of translating the sequence of a messenger RNA (mRNA) molecule to a sequence of amino acids during protein synthesis. The genetic code describes the relationship between the sequence of base pairs in a gene and the corresponding amino acid sequence that it encodes. In the cell cytoplasm, the ribosome reads the sequence of the mRNA in groups of three bases to assemble the protein. Figure and caption courtesy the National Human Genome Research Institute.

protein takes time and affects the dynamics of the cell. Table 1.1 shows the rates of some of the key processes involved in the production of proteins. It is important to note that each of these steps is highly stochastic, with molecules binding together based on some propensity that depends on the binding energy but also the other molecules present in the cell. In addition, although we have described everything

Table 1.1: Rates of core processes involved in the creation of proteins from DNA in *E. coli*.

Process	Characteristic rate	Source
mRNA transcription rate	24-29 bp/sec	BioNumbers [1]
Protein translation rate	12-21 aa/sec	BioNumbers [1]
Maturation time (fluorescent proteins)	6-60 min	BioNumbers [1]
mRNA half life	~ 100 sec	YM03 [92]
<i>E. coli</i> cell division time	20-40 min	BioNumbers [1]
<i>Yeast</i> cell division time	70-140 min	BioNumbers [1]
Protein half life	~ 5×10^4 sec	YM03 [92]
Protein diffusion along DNA	up to 10^4 bp/sec	PKT [68]

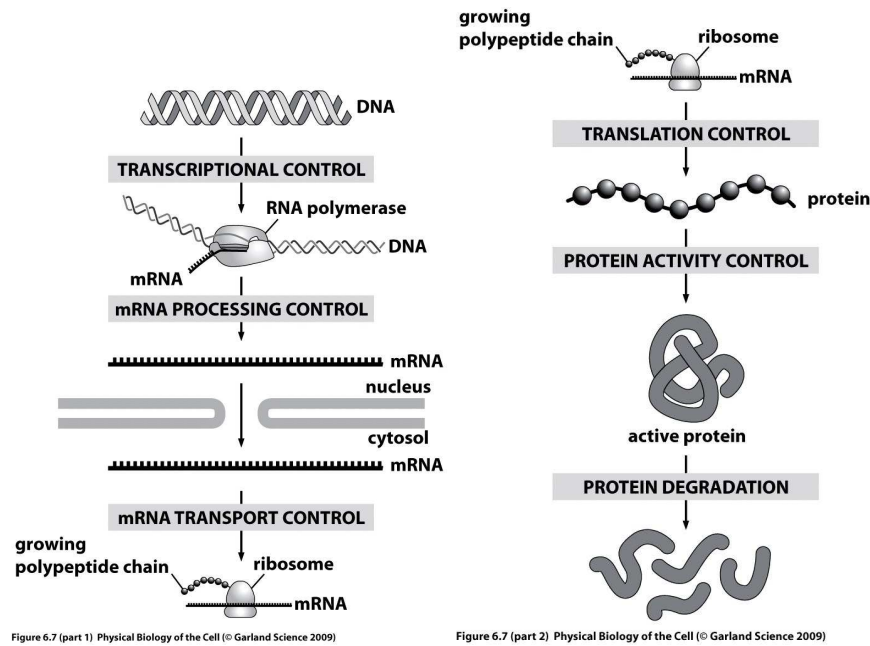


Figure 1.9: Regulation of proteins. Figure from Phillips, Kondev and Theriot [68]; used with permission of Garland Science.

as a sequential process, each of the steps of transcription, translation and folding are happening simultaneously. In fact, there can be multiple RNA polymerases that are bound to the DNA, each producing a transcript. In prokaryotes, as soon as the ribosome binding site has been transcribed, the ribosome can bind and begin translation. It is also possible to have multiple ribosomes bound to a single piece of mRNA. Hence the overall process can be extremely stochastic and asynchronous.

Transcriptional regulation of protein production

There are a variety of mechanisms in the cell to regulate the production of proteins. These regulatory mechanisms can occur at various points in the overall process that produces the protein. Figure 1.9 shows some of the common points of regulation in the protein production process. We focus first on *transcriptional regulation*, which refers to regulatory mechanisms that control whether or not a gene is transcribed.

The simplest forms of transcriptional regulation are repression and activation, which are controlled through *transcription factors*. In the case of *repression*, the presence of a transcription factor (often a protein that binds near the promoter) turns off the transcription of the gene and this type of regulation is often called negative regulation or “down regulation”. In the case of *activation* (or positive regulation), transcription is enhanced when an activator protein binds to the promoter site (facilitating binding of the RNA polymerase).

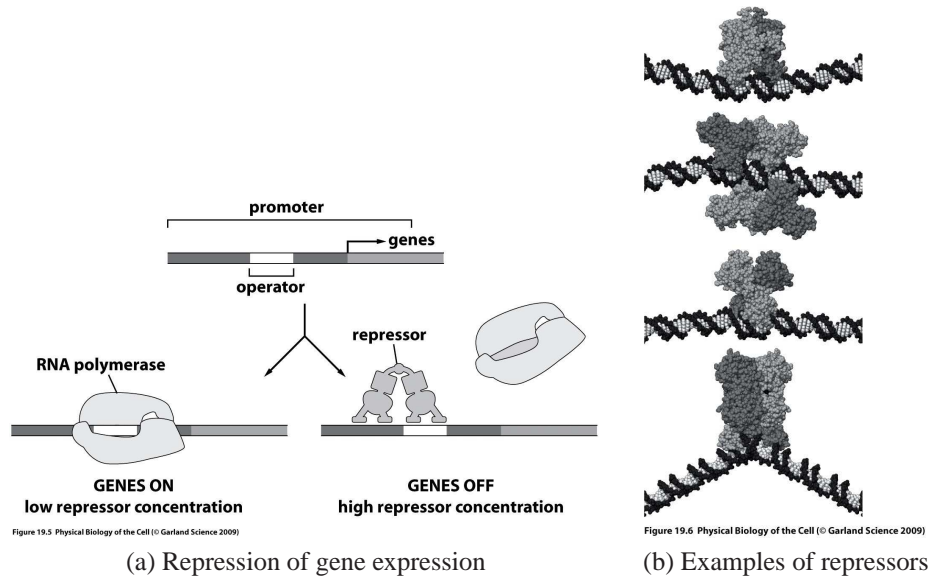


Figure 1.10: Repression of gene expression. Figure from Phillips, Kondev and Theriot [68]; used with permission of Garland Science.

Repression. A common mechanism for repression is that a protein binds to a region of DNA near the promoter and blocks RNA polymerase from binding. The region of DNA to which the repressor protein binds is called an *operator region* (see Figure 1.10a). If the operator region overlaps the promoter, then the presence of a protein at the promoter can “block” the DNA at that location and transcription cannot initiate, as illustrated in Figure 1.10a. Repressor proteins often bind to DNA as dimers or pairs of dimers (effectively tetramers). Figure 1.10b shows some examples of repressors bound to DNA.

A related mechanism for repression is *DNA looping*. In this setting, two repressor complexes (often dimers) bind in different locations on the DNA and then bind to each other. This can create a loop in the DNA and block the ability of RNA polymerase to bind to the promoter, thus inhibiting transcription. Figure 1.11 shows an example of this type of repression, in the *lac* operon. (An *operon* is a set of genes that is under control of a single promoter.)

Activation. The process of activation of a gene requires that an activator protein be present in order for transcription to occur. In this case, the protein must work to either recruit or enable RNA polymerase to begin transcription.

The simplest form of activation involves a protein binding to the DNA near the promoter in such a way that the combination of the activator and the promoter sequence bind RNA polymerase. Figure 1.12 illustrates the basic concept. Like repressors, many activators have inducers, which can act in either a positive or negative fashion (see Figure 1.14b). For example, cyclic AMP (cAMP) acts as a

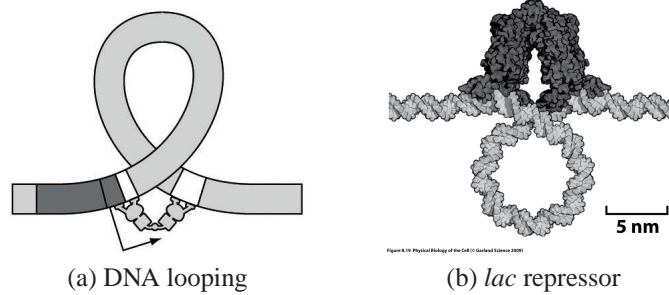


Figure 1.11: Repression via DNA looping. Figure from Phillips, Kondev and Theriot [68]; used with permission of Garland Science.

positive inducer for CAP.

Another mechanism for activation of transcription, specific to prokaryotes, is the use of *sigma factors*. Sigma factors are part of a modular set of proteins that bind to RNA polymerase and form the molecular complex that performs transcription. Different sigma factors enable RNA polymerase to bind to different promoters, so the sigma factor acts as a type of activating signal for transcription. Table 1.2 lists some of the common sigma factors in bacteria. One of the uses of sigma factors is to produce certain proteins only under special conditions, such as when the cell undergoes *heat shock*. Another use is to control the timing of the expression of certain genes, as illustrated in Figure 1.13.

Inducers. A feature that is present in some types of transcription factors is the existence of an *inducer molecule* that combines with the protein to either activate or inactivate its function. A *positive inducer* is a molecule that must be present in order for repression or activation to occur. A *negative inducer* is one in which the presence of the inducer molecule blocks repression or activation, either by changing the shape of the transcription factor protein or by blocking active sites on the protein that would normally bind to the DNA. Figure 1.14a summarizes the various possibilities. Common examples of repressor-inducer pairs include *lacI* and lactose (or IPTG), *tetR* and aTc, and tryptophan repressor and tryptophan. Lactose/IPTG and aTc are both negative inducers, so their presence causes the otherwise repressed

Table 1.2: Sigma factors in *E. coli* [3].

Sigma factor	Promoters recognized
σ^{70}	most genes
σ^{32}	genes associated with heat shock
σ^{28}	genes involved in stationary phase and stress response
σ^{28}	genes involved in motility and chemotaxis
σ^{24}	genes dealing with misfolded proteins in the periplasm

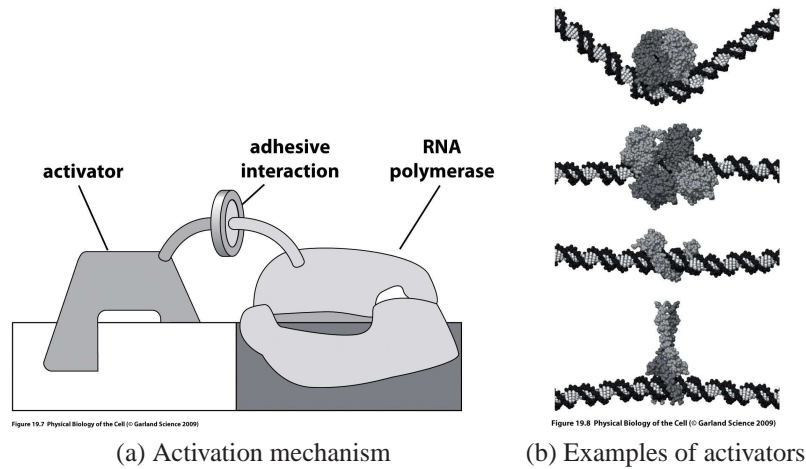


Figure 1.12: Activation of gene expression. (a) Conceptual operation of an activator. The activator binds to DNA upstream of the gene and attracts RNA polymerase to the DNA strand. (b) Examples of activators: catabolite activator protein (CAP), p53 tumor suppressor, zinc finger DNA binding domain and leucine zipper DNA binding domain. Figure from Phillips, Kondev and Theriot [68]; used with permission of Garland Science.

gene to be expressed, while tryptophan is a positive inducer.

Combinatorial promoters. In addition to repressors and activators, many genetic circuits also make use of *combinatorial promoters* that can act as either repressors or activators for genes. This allows genes to be switched on and off based on more complex conditions, represented by the concentrations of two or more activators or repressors.

Figure 1.15 shows one of the classic examples, a promoter for the *lac* system. In the *lac* system, the expression of genes for metabolizing lactose are under the control of a single (combinatorial) promoter. CAP, which is positively induced by cAMP, acts as an activator and LacI (also called “lac repressor”), which is neg-

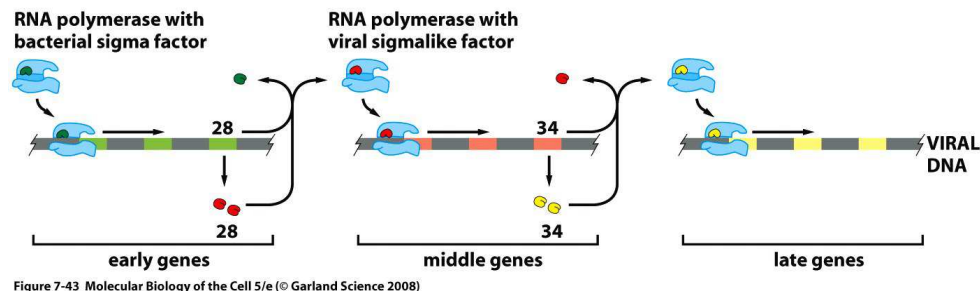


Figure 7-43 Molecular Biology of the Cell 5/e (© Garland Science 2008)

Figure 1.13: Use of sigma factors to controlling the timing of expression. Reproduced from Alberts et al. [3]; permission pending.

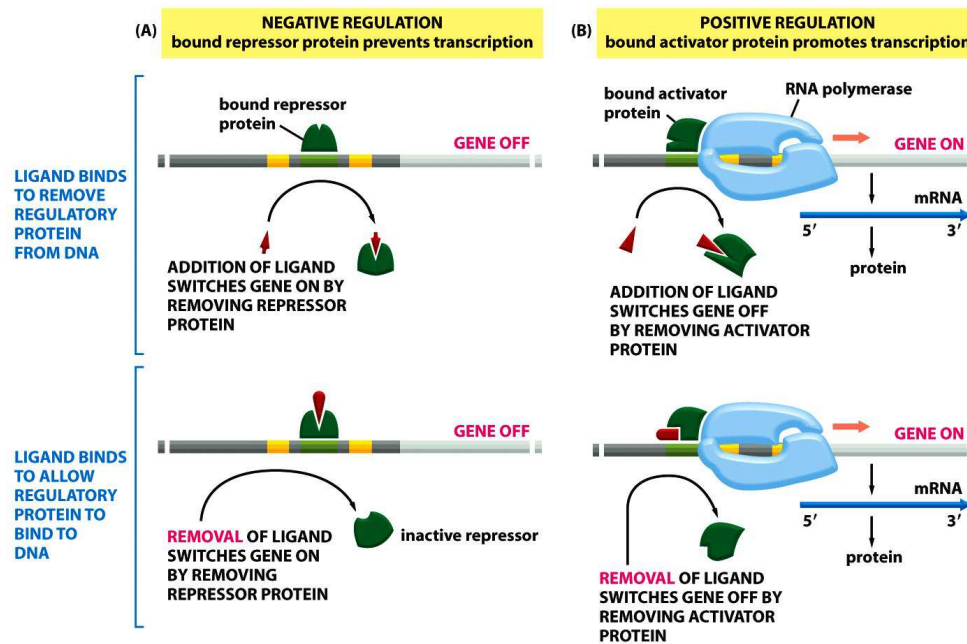


Figure 7-37 Molecular Biology of the Cell 5/e (© Garland Science 2008)

Figure 1.14: Effects of inducers. Reproduced from Alberts et al. [3]; permission pending.

actively induced by lactose, acts as a repressor. In addition, the inducer cAMP is expressed only when glucose levels are low. The resulting behavior is that the proteins for metabolizing lactose are expressed only in conditions where there is no glucose (so CAP is active) *and* lactose is present.

More complicated combinatorial promoters can also be used to control transcription in two different directions, an example that is found in some viruses.

Antitermination. A final method of activation in prokaryotes is the use of *antitermination*. The basic mechanism involves a protein that binds to DNA and deactivates a site that would normally serve as a termination site for RNA polymerase. Additional genes are located downstream from the termination site, but without a promoter region. Thus, in the presence of the anti-terminator protein, these genes are not expressed (or expressed with low probability). However, when the antitermination protein is present, the RNA polymerase maintains (or regains) its contact with the DNA and expression of the downstream genes is enhanced. In this way, antitermination allows downstream genes to be regulated by repressing “premature” termination. An example of an antitermination protein is the protein N in phage λ , which binds to a region of DNA labeled Nut (for N utilization), as shown in Figure 1.16 [36].

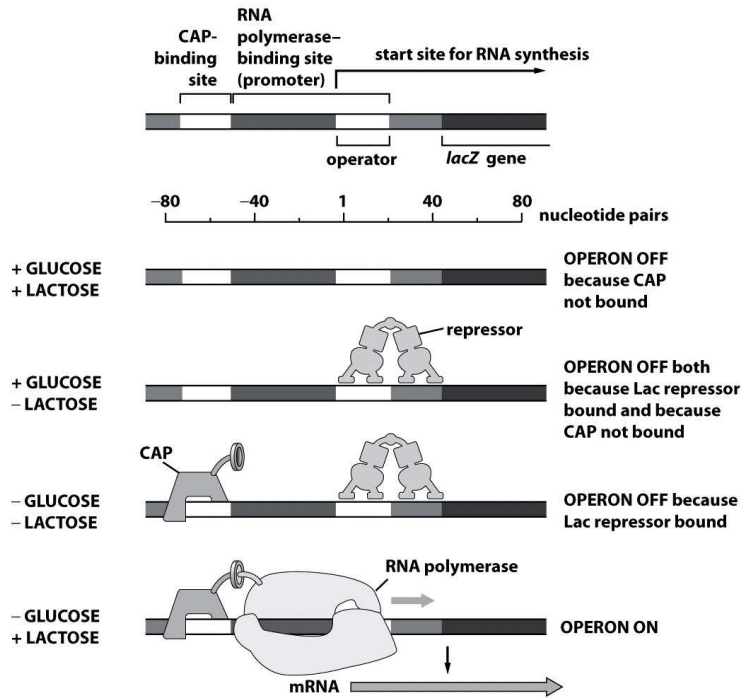


Figure 4.15 Physical Biology of the Cell (© Garland Science 2009)

Figure 1.15: Combinatorial logic for the *lac* operator. Figure from Phillips, Kondev and Theriot [68]; used with permission of Garland Science.

Post-transcriptional regulation of protein production

In addition to regulation that controls transcription of DNA into mRNA, a variety of mechanisms are available for controlling expression after mRNA is produced. These include control of splicing and transport from the nucleus (in eukaryotes), the use of various secondary structure patterns in mRNA that can interfere with ribosomal binding or cleave the mRNA into multiple pieces, and targeted degradation of mRNA. Once the polypeptide chain is formed, additional mechanisms are available that regulate the folding of the protein as well as its shape and activity

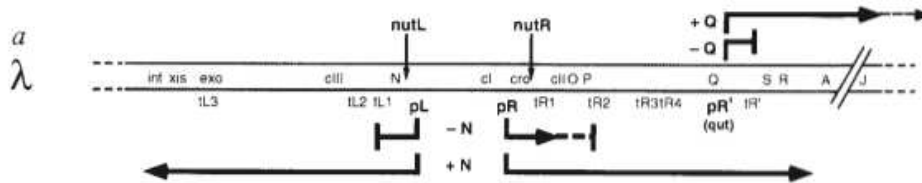


Figure 1.16: Antitermination. Reproduced from [36]; permission pending.

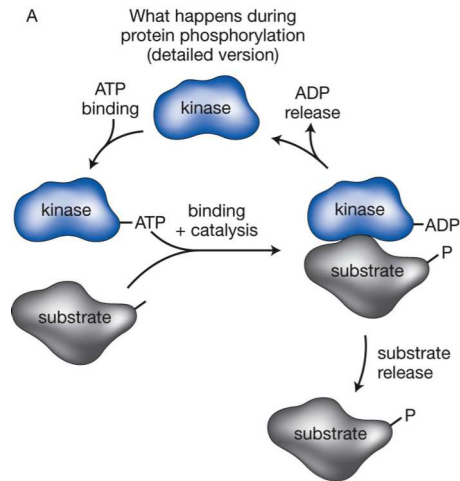


Figure 1.17: Phosphorylation of a protein via a kinase. Reproduced from Madhani [53]; permission pending.

level. We briefly describe some of the major mechanisms here.

Review

Material to be written: sRNA, riboswitches.

One of the most common types of post-transcriptional regulation is through the *phosphorylation* of proteins. Phosphorylation is an enzymatic process in which a phosphate group is added to a protein and the resulting conformation of the protein changes, usually from an inactive configuration to an active one. The enzyme that adds the phosphate group is called a *kinase* (or sometimes a *phosphotransferase*) and it operates by transferring a phosphate group from a bound ATP molecule to the protein, leaving behind ADP and the phosphorylated protein. *Dephosphorylation* is a complementary enzymatic process that can remove a phosphate group from a protein. The enzyme that performs dephosphorylation is called a *phosphatase*. Figure 1.17 shows the process of phosphorylation in more detail.

Phosphorylation is often used as a regulatory mechanism, with the phosphorylated version of the protein being the active conformation. Since phosphorylation and dephosphorylation can occur much more quickly than protein production and degradation, it is used in biological circuits in which a rapid response is required. One common pattern is that a signaling protein will bind to a ligand and the resulting allosteric change allows the signaling protein to serve as a kinase. The newly active kinase then phosphorylates a second protein, which modulates other functions in the cell. Phosphorylation cascades can also be used to amplify the effect of the original signal; we will describe this in more detail in Section 2.5.

Kinases in cells are usually very specific to a given protein, allowing detailed signaling networks to be constructed. Phosphatases, on the other hand, are much less specific, and a given phosphatase species may dephosphorylate many different

types of proteins. The combined action of kinases and phosphatases is important in signaling since the only way to deactivate a phosphorylated protein is by removing the phosphate group. Thus phosphatases are constantly “turning off” proteins, and the protein is activated only when sufficient kinase activity is present.

Phosphorylation of a protein occurs by the addition of a charged phosphate (PO_4) group to the serine (Ser), threonine (Thr) or tyrosine (Tyr) amino acids. Similar covalent modifications can occur by the attachment of other chemical groups to select amino acids. *Methylation* occurs when a methyl group (CH_3) is added to lysine (Lys) and is used for modulation of receptor activity and in modifying histones that are used in chromatin structures. *Acetylation* occurs when an acetyl group (COCH_3) is added to lysine and is also used to modify histones. *Ubiquitination* refers to the addition of a small protein, ubiquitin, to lysine; the addition of a polyubiquitin chain to a protein targets it for degradation.

1.3 Control and Dynamical Systems Tools [AM08]

To study the complex dynamics and feedback present in biological systems, we will make use of mathematical models combined with analytical and computational tools. In this section we present a brief introduction to some of the key concepts from control and dynamical systems that are relevant for the study of biomolecular systems considered in later chapters. More details on the application of specific concepts listed here to biomolecular systems is provided in the main body of the text. Readers who are familiar with introductory concepts in dynamical systems and control, at the level described in Åström and Murray [2] for example, can skip this section.

Dynamics, feedback and control

A *dynamical system* is a system whose behavior changes over time, often in response to external stimulation or forcing. The term *feedback* refers to a situation in which two (or more) dynamical systems are connected together such that each system influences the other and their dynamics are thus strongly coupled. Simple causal reasoning about a feedback system is difficult because the first system influences the second and the second system influences the first, leading to a circular argument. This makes reasoning based on cause and effect tricky, and it is necessary to analyze the system as a whole. A consequence of this is that the behavior of feedback systems is often counterintuitive, and it is therefore necessary to resort to formal methods to understand them.

Figure 1.18 illustrates in block diagram form the idea of feedback. We often use the terms *open loop* and *closed loop* when referring to such systems. A system is said to be a closed loop system if the systems are interconnected in a cycle, as

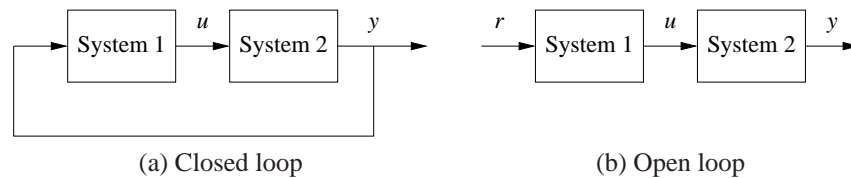


Figure 1.18: Open and closed loop systems. (a) The output of system 1 is used as the input of system 2, and the output of system 2 becomes the input of system 1, creating a closed loop system. (b) The interconnection between system 2 and system 1 is removed, and the system is said to be open loop.

shown in Figure 1.18a. If we break the interconnection, we refer to the configuration as an open loop system, as shown in Figure 1.18b.

Biological systems make use of feedback in an extraordinary number of ways, on scales ranging from molecules to cells to organisms to ecosystems. One example is the regulation of glucose in the bloodstream through the production of insulin and glucagon by the pancreas. The body attempts to maintain a constant concentration of glucose, which is used by the body's cells to produce energy. When glucose levels rise (after eating a meal, for example), the hormone insulin is released and causes the body to store excess glucose in the liver. When glucose levels are low, the pancreas secretes the hormone glucagon, which has the opposite effect. Referring to Figure 1.18, we can view the liver as system 1 and the pancreas as system 2. The output from the liver is the glucose concentration in the blood, and the output from the pancreas is the amount of insulin or glucagon produced. The interplay between insulin and glucagon secretions throughout the day helps to keep the blood-glucose concentration constant, at about 90 mg per 100 mL of blood.

Feedback has many interesting properties that can be exploited in designing systems. As in the case of glucose regulation, feedback can make a system resilient toward external influences. It can also be used to create linear behavior out of non-linear components, a common approach in electronics. More generally, feedback allows a system to be insensitive both to external disturbances and to variations in its individual elements.

Feedback has potential disadvantages as well. It can create dynamic instabilities in a system, causing oscillations or even runaway behavior. Another drawback, especially in engineering systems, is that feedback can introduce unwanted sensor noise into the system, requiring careful filtering of signals. It is for these reasons that a substantial portion of the study of feedback systems is devoted to developing an understanding of dynamics and a mastery of techniques in dynamical systems.

The mathematical study of the behavior of feedback systems is an area known as *control theory*. The term control has many meanings and often varies between communities. In engineering applications, we typically define control to be the use of algorithms and feedback in engineered systems. Thus, control includes such ex-

amples as feedback loops in electronic amplifiers, setpoint controllers in chemical and materials processing, “fly-by-wire” systems on aircraft and even router protocols that control traffic flow on the Internet. Emerging applications include high-confidence software systems, autonomous vehicles and robots, real-time resource management systems and biologically engineered systems. At its core, control is an *information* science and includes the use of information in both analog and digital representations.

Feedback properties

Feedback is a powerful idea that is used extensively in natural and technological systems. The principle of feedback is simple: implement correcting actions based on the difference between desired and actual performance. In engineering, feedback has been rediscovered and patented many times in many different contexts. The use of feedback has often resulted in vast improvements in system capability, and these improvements have sometimes been revolutionary, as discussed above. The reason for this is that feedback has some truly remarkable properties, which we discuss briefly here.

Robustness to Uncertainty. One of the key uses of feedback is to provide robustness to uncertainty. By measuring the difference between the sensed value of a regulated signal and its desired value, we can supply a corrective action. If the system undergoes some change that affects the regulated signal, then we sense this change and try to force the system back to the desired operating point. This is precisely the effect that Watt exploited in his use of the centrifugal governor on steam engines.

As an example of this principle, consider the simple feedback system shown in Figure 1.19. In this system, the speed of a vehicle is controlled by adjusting the amount of gas flowing to the engine. Simple *proportional-integral* (PI) feedback is used to make the amount of gas depend on both the error between the current and the desired speed and the integral of that error. The plot on the right shows the results of this feedback for a step change in the desired speed and a variety of different masses for the car, which might result from having a different number of passengers or towing a trailer. Notice that independent of the mass (which varies by a factor of 3!), the steady-state speed of the vehicle always approaches the desired speed and achieves that speed within approximately 5 s. Thus the performance of the system is robust with respect to this uncertainty.

Another early example of the use of feedback to provide robustness is the negative feedback amplifier. When telephone communications were developed, amplifiers were used to compensate for signal attenuation in long lines. A vacuum tube was a component that could be used to build amplifiers. Distortion caused by the nonlinear characteristics of the tube amplifier together with amplifier drift were obstacles that prevented the development of line amplifiers for a long time. A ma-

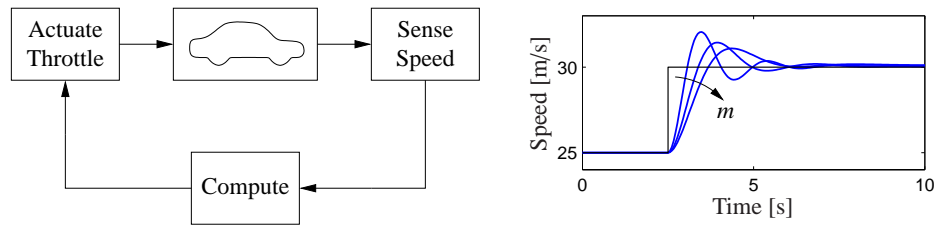


Figure 1.19: A feedback system for controlling the speed of a vehicle. In the block diagram on the left, the speed of the vehicle is measured and compared to the desired speed within the “Compute” block. Based on the difference in the actual and desired speeds, the throttle (or brake) is used to modify the force applied to the vehicle by the engine, drivetrain and wheels. The figure on the right shows the response of the control system to a commanded change in speed from 25 m/s to 30 m/s. The three different curves correspond to differing masses of the vehicle, between 1000 and 3000 kg, demonstrating the robustness of the closed loop system to a very large change in the vehicle characteristics.

major breakthrough was the invention of the feedback amplifier in 1927 by Harold S. Black, an electrical engineer at Bell Telephone Laboratories. Black used *negative feedback*, which reduces the gain but makes the amplifier insensitive to variations in tube characteristics. This invention made it possible to build stable amplifiers with linear characteristics despite the nonlinearities of the vacuum tube amplifier.

Feedback is also pervasive in biological systems, where transcriptional, translational and allosteric mechanisms are used to regulate internal concentrations of various species, and much more complex feedbacks are used to regulate properties at the organism level (such as body temperature, blood pressure and circadian rhythm). One difference in biological systems is that the separation of sensing, actuation and computation, a common approach in most engineering control systems, is less evident. Instead, the dynamics of the molecules that sense the environmental condition and make changes to the operation of internal components may be integrated together in ways that make it difficult to untangle the operation of the system. Similarly, the “reference value” to which we wish to regulate a system may not be an explicit signal, but rather a consequence of many different changes in the dynamics that are coupled back to the regulatory elements. Hence we do not see a clear “setpoint” for the desired ATP concentration, blood oxygen level or body temperature, for example. These difficulties complicate our analysis of biological systems, though many important insights can still be obtained.

Design of Dynamics. Another use of feedback is to change the dynamics of a system. Through feedback, we can alter the behavior of a system to meet the needs of an application: systems that are unstable can be stabilized, systems that are sluggish can be made responsive and systems that have drifting operating points can be held constant. Control theory provides a rich collection of techniques to analyze the stability and dynamic response of complex systems and to place bounds on the

behavior of such systems by analyzing the gains of linear and nonlinear operators that describe their components.

An example of the use of control in the design of dynamics comes from the area of flight control. The following quote, from a lecture presented by Wilbur Wright to the Western Society of Engineers in 1901 [58], illustrates the role of control in the development of the airplane:

Men already know how to construct wings or airplanes, which when driven through the air at sufficient speed, will not only sustain the weight of the wings themselves, but also that of the engine, and of the engineer as well. Men also know how to build engines and screws of sufficient lightness and power to drive these planes at sustaining speed ... Inability to balance and steer still confronts students of the flying problem ... When this one feature has been worked out, the age of flying will have arrived, for all other difficulties are of minor importance.

The Wright brothers thus realized that control was a key issue to enable flight. They resolved the compromise between stability and maneuverability by building an airplane, the Wright Flyer, that was unstable but maneuverable. The Flyer had a rudder in the front of the airplane, which made the plane very maneuverable. A disadvantage was the necessity for the pilot to keep adjusting the rudder to fly the plane: if the pilot let go of the stick, the plane would crash. Other early aviators tried to build stable airplanes. These would have been easier to fly, but because of their poor maneuverability they could not be brought up into the air. By using their insight and skillful experiments the Wright brothers made the first successful flight at Kitty Hawk in 1903.

Since it was quite tiresome to fly an unstable aircraft, there was strong motivation to find a mechanism that would stabilize an aircraft. Such a device, invented by Sperry, was based on the concept of feedback. Sperry used a gyro-stabilized pendulum to provide an indication of the vertical. He then arranged a feedback mechanism that would pull the stick to make the plane go up if it was pointing down, and vice versa. The Sperry autopilot was the first use of feedback in aeronautical engineering, and Sperry won a prize in a competition for the safest airplane in Paris in 1914. Figure 1.20 shows the Curtiss seaplane and the Sperry autopilot. The autopilot is a good example of how feedback can be used to stabilize an unstable system and hence “design the dynamics” of the aircraft.

One of the other advantages of designing the dynamics of a device is that it allows for increased modularity in the overall system design. By using feedback to create a system whose response matches a desired profile, we can hide the complexity and variability that may be present inside a subsystem. This allows us to create more complex systems by not having to simultaneously tune the responses of a large number of interacting components. This was one of the advantages of

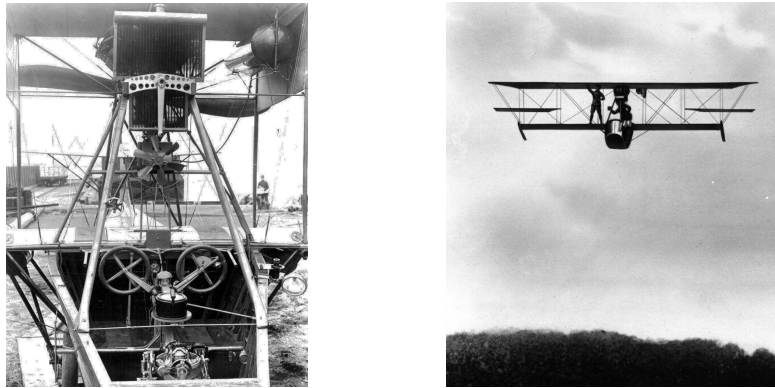


Figure 1.20: Aircraft autopilot system. The Sperry autopilot (left) contained a set of four gyros coupled to a set of air valves that controlled the wing surfaces. The 1912 Curtiss used an autopilot to stabilize the roll, pitch and yaw of the aircraft and was able to maintain level flight as a mechanic walked on the wing (right) [42].

Black's use of negative feedback in vacuum tube amplifiers: the resulting device had a well-defined linear input/output response that did not depend on the individual characteristics of the vacuum tubes being used.

Drawbacks of Feedback. While feedback has many advantages, it also has some drawbacks. Chief among these is the possibility of instability if the system is not designed properly. We are all familiar with the undesirable effects of feedback when the amplification on a microphone is turned up too high in a room. This is an example of feedback instability, something that we obviously want to avoid. This is tricky because we must design the system not only to be stable under nominal conditions but also to remain stable under all possible perturbations of the dynamics.

In addition to the potential for instability, feedback inherently couples different parts of a system. One common problem is that feedback often injects measurement noise into the system. Measurements must be carefully filtered so that the actuation and process dynamics do not respond to them, while at the same time ensuring that the measurement signal from the sensor is properly coupled into the closed loop dynamics (so that the proper levels of performance are achieved).

Another potential drawback of control is the complexity of embedding a control system in a product. While the cost of sensing, computation and actuation has decreased dramatically in the past few decades, the fact remains that control systems are often complicated, and hence one must carefully balance the costs and benefits. An early engineering example of this is the use of microprocessor-based feedback systems in automobiles. The use of microprocessors in automotive applications began in the early 1970s and was driven by increasingly strict emissions standards, which could be met only through electronic controls. Early systems were expensive

and failed more often than desired, leading to frequent customer dissatisfaction. It was only through aggressive improvements in technology that the performance, reliability and cost of these systems allowed them to be used in a transparent fashion. Even today, the complexity of these systems is such that it is difficult for an individual car owner to fix problems.

Feedforward. Feedback is reactive: there must be an error before corrective actions are taken. However, in some circumstances it is possible to measure a disturbance before it enters the system, and this information can then be used to take corrective action before the disturbance has influenced the system. The effect of the disturbance is thus reduced by measuring it and generating a control signal that counteracts it. This way of controlling a system is called *feedforward*. Feedforward is particularly useful in shaping the response to command signals because command signals are always available. Since feedforward attempts to match two signals, it requires good process models; otherwise the corrections may have the wrong size or may be badly timed.

The ideas of feedback and feedforward are very general and appear in many different fields. In economics, feedback and feedforward are analogous to a market-based economy versus a planned economy. In business, a feedforward strategy corresponds to running a company based on extensive strategic planning, while a feedback strategy corresponds to a reactive approach. In biology, feedforward has been suggested as an essential element for motion control in humans that is tuned during training. Experience indicates that it is often advantageous to combine feedback and feedforward, and the correct balance requires insight and understanding of their respective properties.

Positive Feedback. In most of control theory, the emphasis is on the role of *negative feedback*, in which we attempt to regulate the system by reacting to disturbances in a way that decreases the effect of those disturbances. In some systems, particularly biological systems, *positive feedback* can play an important role. In a system with positive feedback, the increase in some variable or signal leads to a situation in which that quantity is further increased through its dynamics. This has a destabilizing effect and is usually accompanied by a saturation that limits the growth of the quantity. Although often considered undesirable, this behavior is used in biological (and engineering) systems to obtain a very fast response to a condition or signal.

One example of the use of positive feedback is to create switching behavior, in which a system maintains a given state until some input crosses a threshold. Hysteresis is often present so that noisy inputs near the threshold do not cause the system to jitter. This type of behavior is called *bistability* and is often associated with memory devices.

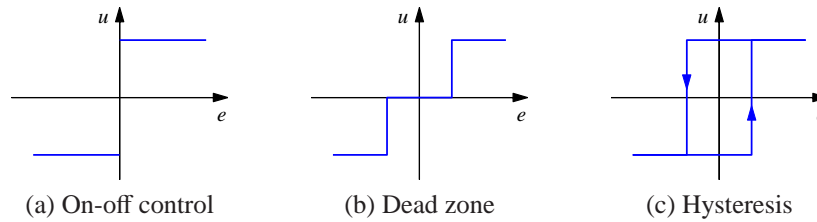


Figure 1.21: Input/output characteristics of on-off controllers. Each plot shows the input on the horizontal axis and the corresponding output on the vertical axis. Ideal on-off control is shown in (a), with modifications for a dead zone (b) or hysteresis (c). Note that for on-off control with hysteresis, the output depends on the value of past inputs.

Simple forms of feedback

The idea of feedback to make corrective actions based on the difference between the desired and the actual values of a quantity can be implemented in many different ways. The benefits of feedback can be obtained by very simple feedback laws such as on-off control, proportional control and proportional-integral-derivative control. In this section we provide a brief preview of some of these topics to provide a basis of understanding for their use in the chapters that follows.

On-Off Control. A simple feedback mechanism can be described as follows:

$$u = \begin{cases} u_{\max} & \text{if } e > 0 \\ u_{\min} & \text{if } e < 0, \end{cases} \quad (1.1)$$

where the *control error* $e = r - y$ is the difference between the reference signal (or command signal) r and the output of the system y and u is the actuation command. Figure 1.21a shows the relation between error and control. This control law implies that maximum corrective action is always used.

The feedback in equation (1.1) is called *on-off control*. One of its chief advantages is that it is simple and there are no parameters to choose. On-off control often succeeds in keeping the process variable close to the reference, such as the use of a simple thermostat to maintain the temperature of a room. It typically results in a system where the controlled variables oscillate, which is often acceptable if the oscillation is sufficiently small.

Notice that in equation (1.1) the control variable is not defined when the error is zero. It is common to make modifications by introducing either a dead zone or hysteresis (see Figure 1.21b and 1.21c).

PID Control. The reason why on-off control often gives rise to oscillations is that the system overreacts since a small change in the error makes the actuated variable change over the full range. This effect is avoided in *proportional control*, where the characteristic of the controller is proportional to the control error for small errors.

This can be achieved with the control law

$$u = \begin{cases} u_{\max} & \text{if } e \geq e_{\max} \\ k_p e & \text{if } e_{\min} < e < e_{\max} \\ u_{\min} & \text{if } e \leq e_{\min}, \end{cases} \quad (1.2)$$

where k_p is the controller gain, $e_{\min} = u_{\min}/k_p$ and $e_{\max} = u_{\max}/k_p$. The interval (e_{\min}, e_{\max}) is called the *proportional band* because the behavior of the controller is linear when the error is in this interval:

$$u = k_p(r - y) = k_p e \quad \text{if } e_{\min} \leq e \leq e_{\max}. \quad (1.3)$$

While a vast improvement over on-off control, proportional control has the drawback that the process variable often deviates from its reference value. In particular, if some level of control signal is required for the system to maintain a desired value, then we must have $e \neq 0$ in order to generate the requisite input.

This can be avoided by making the control action proportional to the integral of the error:

$$u(t) = k_i \int_0^t e(\tau) d\tau. \quad (1.4)$$

This control form is called *integral control*, and k_i is the integral gain. It can be shown through simple arguments that a controller with integral action has zero steady-state error. The catch is that there may not always be a steady state because the system may be oscillating.

An additional refinement is to provide the controller with an anticipative ability by using a prediction of the error. A simple prediction is given by the linear extrapolation

$$e(t + T_d) \approx e(t) + T_d \frac{de(t)}{dt},$$

which predicts the error T_d time units ahead. Combining proportional, integral and derivative control, we obtain a controller that can be expressed mathematically as

$$u(t) = k_p e(t) + k_i \int_0^t e(\tau) d\tau + k_d \frac{de(t)}{dt}. \quad (1.5)$$

The control action is thus a sum of three terms: the past as represented by the integral of the error, the present as represented by the proportional term and the future as represented by a linear extrapolation of the error (the derivative term). This form of feedback is called a *proportional-integral-derivative (PID) controller* and its action is illustrated in Figure 1.22.

A PID controller is very useful and is capable of solving a wide range of control problems. More than 95% of all industrial control problems are solved by PID control, although many of these controllers are actually *proportional-integral (PI) controllers* because derivative action is often not included [22]. There are also more advanced controllers, which differ from PID controllers by using more sophisticated methods for prediction.

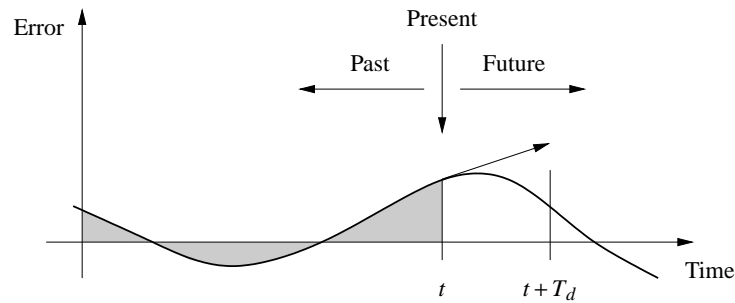


Figure 1.22: Action of a PID controller. At time t , the proportional term depends on the instantaneous value of the error. The integral portion of the feedback is based on the integral of the error up to time t (shaded portion). The derivative term provides an estimate of the growth or decay of the error over time by looking at the rate of change of the error. T_d represents the approximate amount of time in which the error is projected forward (see text).

1.4 Input/Output Modeling [AM08]

A model is a mathematical representation of a physical, biological or information system. Models allow us to reason about a system and make predictions about how a system will behave. In this text, we will mainly be interested in models of dynamical systems describing the input/output behavior of systems, and we will often work in “state space” form. In the remainder of this section we provide an overview of some of the key concepts in input/output modeling. The mathematical details introduced here are explored more fully in Chapter 3.

The heritage of electrical engineering

The approach to modeling that we take builds on the view of models that emerged from electrical engineering, where the design of electronic amplifiers led to a focus on input/output behavior. A system was considered a device that transforms inputs to outputs, as illustrated in Figure 1.23. Conceptually an input/output model can be viewed as a giant table of inputs and outputs. Given an input signal $u(t)$ over some interval of time, the model should produce the resulting output $y(t)$.

The input/output framework is used in many engineering disciplines since it allows us to decompose a system into individual components connected through their inputs and outputs. Thus, we can take a complicated system such as a radio or a television and break it down into manageable pieces such as the receiver, demodulator, amplifier and speakers. Each of these pieces has a set of inputs and outputs and, through proper design, these components can be interconnected to form the entire system.

The input/output view is particularly useful for the special class of *linear time-invariant systems*. This term will be defined more carefully below, but roughly

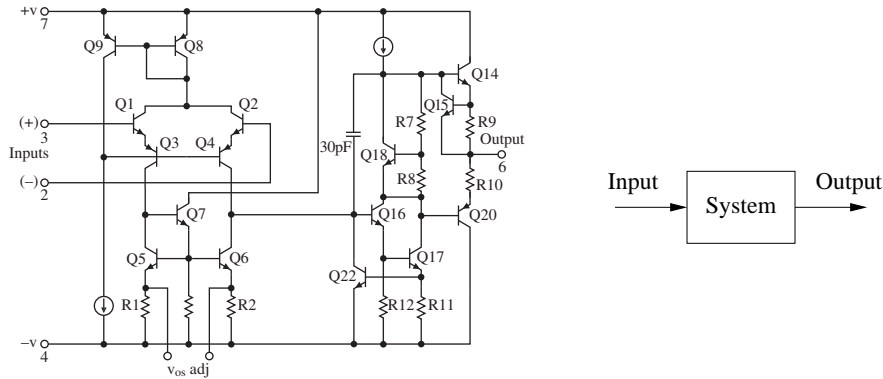


Figure 1.23: Illustration of the input/output view of a dynamical system. The figure on the left shows a detailed circuit diagram for an electronic amplifier; the one on the right is its representation as a block diagram.

speaking a system is linear if the superposition (addition) of two inputs yields an output that is the sum of the outputs that would correspond to individual inputs being applied separately. A system is time-invariant if the output response for a given input does not depend on when that input is applied. While most biomolecular systems are neither linear nor time-invariant, they can often be approximated by such models, often by looking at perturbations of the system from its nominal behavior, in a fixed context.

One of the reasons that linear time-invariant systems are so prevalent in modeling of input/output systems is that a large number of tools have been developed to analyze them. One such tool is the *step response*, which describes the relationship between an input that changes from zero to a constant value abruptly (a step input) and the corresponding output. The step response is very useful in characterizing the performance of a dynamical system, and it is often used to specify the desired dynamics. A sample step response is shown in Figure 1.24a.

Another way to describe a linear time-invariant system is to represent it by its response to sinusoidal input signals. This is called the *frequency response*, and a rich, powerful theory with many concepts and strong, useful results has emerged for systems that can be described by their frequency response. The results are based on the theory of complex variables and Laplace transforms. The basic idea behind frequency response is that we can completely characterize the behavior of a system by its steady-state response to sinusoidal inputs. Roughly speaking, this is done by decomposing any arbitrary signal into a linear combination of sinusoids (e.g., by using the Fourier transform) and then using linearity to compute the output by combining the response to the individual frequencies. A sample frequency response is shown in Figure 1.24b.

The input/output view lends itself naturally to experimental determination of system dynamics, where a system is characterized by recording its response to

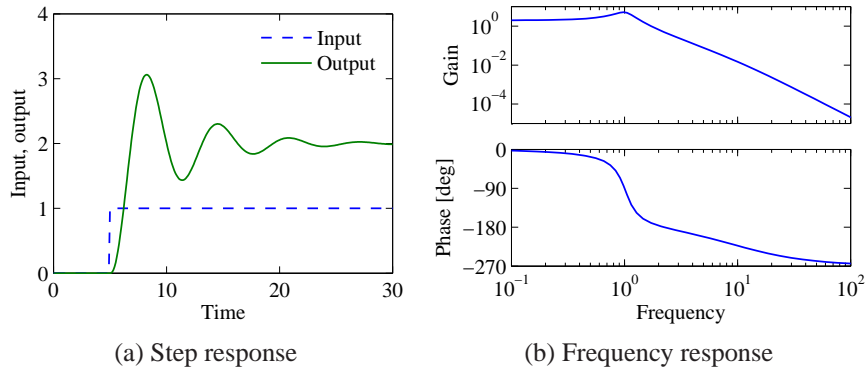


Figure 1.24: Input/output response of a linear system. The step response (a) shows the output of the system due to an input that changes from 0 to 1 at time $t = 5$ s. The frequency response (b) shows the amplitude gain and phase change due to a sinusoidal input at different frequencies.

particular inputs, e.g., a step or a set of sinusoids over a range of frequencies.

The control view

When control theory emerged as a discipline in the 1940s, the approach to dynamics was strongly influenced by the electrical engineering (input/output) view. A second wave of developments in control, starting in the late 1950s, was inspired by mechanics, where the state space perspective was used. The emergence of space flight is a typical example, where precise control of the orbit of a spacecraft is essential. These two points of view gradually merged into what is today the state space representation of input/output systems.

The development of state space models involved modifying the models from mechanics to include external actuators and sensors and utilizing more general forms of equations. In control, models often take the form

$$\frac{dx}{dt} = f(x, u), \quad y = h(x, u), \quad (1.6)$$

where x is a vector of state variables, u is a vector of control signals and y is a vector of measurements. The term dx/dt (sometimes also written as \dot{x}) represents the derivative of x with respect to time, now considered a vector, and f and h are (possibly nonlinear) mappings of their arguments to vectors of the appropriate dimension.

Adding inputs and outputs has increased the richness of the classical problems and led to many new concepts. For example, it is natural to ask if possible states x can be reached with the proper choice of u (reachability) and if the measurement y contains enough information to reconstruct the state (observability). These topics are addressed in greater detail in AM08.

A final development in building the control point of view was the emergence of disturbances and model uncertainty as critical elements in the theory. The simple way of modeling disturbances as deterministic signals like steps and sinusoids has the drawback that such signals cannot be predicted precisely. A more realistic approach is to model disturbances as random signals. This viewpoint gives a natural connection between prediction and control. The dual views of input/output representations and state space representations are particularly useful when modeling uncertainty since state models are convenient to describe a nominal model but uncertainties are easier to describe using input/output models (often via a frequency response description).

An interesting observation in the design of control systems is that feedback systems can often be analyzed and designed based on comparatively simple models. The reason for this is the inherent robustness of feedback systems. However, other uses of models may require more complexity and more accuracy. One example is feedforward control strategies, where one uses a model to precompute the inputs that cause the system to respond in a certain way. Another area is system validation, where one wishes to verify that the detailed response of the system performs as it was designed. Because of these different uses of models, it is common to use a hierarchy of models having different complexity and fidelity.

State space systems

The state of a system is a collection of variables that summarize the past of a system for the purpose of predicting the future. For a biochemical system the state is composed of the variables required to account for the current context of the cell, including the concentrations of the various species and complexes that are present. It may also include the spatial locations of the various molecules. A key issue in modeling is to decide how accurately this information has to be represented. The state variables are gathered in a vector $x \in \mathbb{R}^n$ called the *state vector*. The control variables are represented by another vector $u \in \mathbb{R}^p$, and the measured signal by the vector $y \in \mathbb{R}^q$. A system can then be represented by the differential equation

$$\frac{dx}{dt} = f(x, u), \quad y = h(x, u), \quad (1.7)$$

where $f : \mathbb{R}^n \times \mathbb{R}^p \rightarrow \mathbb{R}^n$ and $h : \mathbb{R}^n \times \mathbb{R}^p \rightarrow \mathbb{R}^q$ are smooth mappings. We call a model of this form a *state space model*.

The dimension of the state vector is called the *order* of the system. The system (1.7) is called *time-invariant* because the functions f and h do not depend explicitly on time t ; there are more general time-varying systems where the functions do depend on time. The model consists of two functions: the function f gives the rate of change of the state vector as a function of state x and control u , and the function h gives the measured values as functions of state x and control u .

A system is called a *linear* state space system if the functions f and h are linear in x and u . A linear state space system can thus be represented by

$$\frac{dx}{dt} = Ax + Bu, \quad y = Cx + Du, \quad (1.8)$$

where A , B , C and D are constant matrices. Such a system is said to be *linear and time-invariant*, or LTI for short. The matrix A is called the *dynamics matrix*, the matrix B is called the *control matrix*, the matrix C is called the *sensor matrix* and the matrix D is called the *direct term*. Frequently systems will not have a direct term, indicating that the control signal does not influence the output directly.

Input/output formalisms for biomolecular modeling

A key challenge in developing models for any class of problems is the selection of an appropriate mathematical framework for the models. Among the features that we believe are important for a wide variety of biological systems are capturing the temporal response of a biomolecular system to various inputs and understanding how the underlying dynamic behavior leads to a given phenotypes. The models should reflect the subsystem structure of the underlying dynamical system to allow prediction of results, but need not necessarily be mechanistically accurate at a detailed biochemical level. We are particularly interested in those problems that include a number of molecular “subsystems” that interact with each other, and so our models should support a level of modularity (with the additional advantage of allowing multiple groups to develop detailed models for each module that can be combined to form more complex models of the interacting components). Since we are likely to be building models based on high-throughput experiments, it is also key that the models capture the measurable outputs of the systems.

For many of the systems that we are interested in, a good starting point is to use reduced-order models consisting of nonlinear differential equations, possible with some time delay. Using the basic structure shown in Figure 1.3, a model for a multi-component system might be described using a set of input/output differential equations of the form

$$\begin{aligned} \frac{dx_i}{dt} &= Ax_i + N(x_i, Ly^*, \theta) + Bu_i + Fw_i, \\ y_i &= Cx_i + Hv_i \quad y_i^*(t) = y_i(t - \tau_i). \end{aligned} \quad (1.9)$$

The internal state of the i th component (subsystem) is captured by the state $x_i \in \mathbb{R}^{n_i}$, which might represent the concentrations of various species and complexes as well as other internal variables required to describe the dynamics. The “outputs” of the system, which describe those species (or other quantities) that interact with other subsystems in the cell is captured by the variable $y_i \in \mathbb{R}^{p_i}$. The internal dynamics consist of a set of linear dynamics (Ax) as well as nonlinear terms that depend

both on the internal state and the outputs of other subsystems ($N(\cdot)$), where Ly^* represents interconnections with other subsystems and θ is a set of parameters that represent the context of the system (described in more detail below). We also allow for the possibility of time delays (due to folding, transport or other processes) and write y_i^* for the “functional” output seen by other subsystems.

The coupling between subsystems is captured using a weighted graph, whose elements are represented by the coefficients interconnection matrix L . In the simplest version of the model, we simply combine different outputs from other modules in some linear combination to obtain the “input” Ly^* . More general interconnections are possible, including allowing multiple outputs from different subsystems to interact in nonlinear ways (such as one often sees on combinatorial promoters in gene regulatory networks).

Finally, in addition to the internal dynamics and nonlinear coupling, we separately keep track of external inputs to the subsystem (Bu), stochastic disturbances (Fw) and measurement noise (Hv). We treat the external inputs u as deterministic variables (representing inducer concentrations, nutrient levels, temperature, etc) and the disturbances and noise w and v as (vector) random processes. If desired, the mappings from the various inputs to the states and outputs, represented by the matrices B , F and H can also depend on the system state x (resulting in additional nonlinearities).

This particular structure is useful because it captures a large number of modeling frameworks in a single formalism. In particular, mass action kinetics and chemical reaction networks can be represented by equating the stoichiometry matrix with the interconnection matrix L and using the nonlinear terms to capture the fluxes, with θ representing the rate constants. We can also represent typical reduced-order models for transcriptional regulatory networks by letting the nonlinear functions N represent various types of Hill functions and including the effects of mRNA/protein production, degradation and dilution through the linear dynamics. These two classes of systems can also be combined, allowing a very expressive set of dynamics that is capable of capturing many relevant phenomena of interest in molecular biology.

Despite being a well-studied class of systems, there are still many open questions with this framework, especially in the context of biomolecular systems. For example, a rigorous theory of the effects of crosstalk, the role of context on the nonlinear elements, and combining the effects of interconnection, uncertainty and nonlinearity is just emerging. Adding stochastic effects, either through the disturbance and noise terms, initial conditions or in a more fundamental way, is also largely unexplored. And the critical need for methods for performing model reduction in a way that respects of the structure of the subsystems has only recently begun to be explored. Nonetheless, many of these research directions are being pursued and we attempt to provide some insights in this text into the underlying techniques that are available.

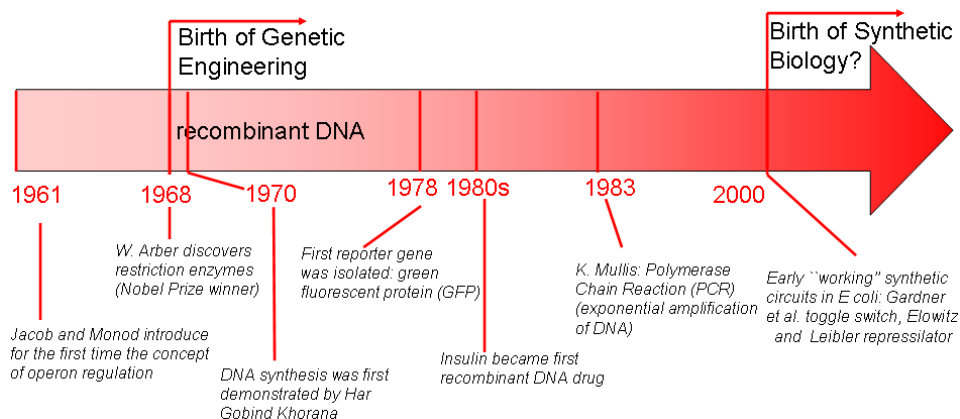


Figure 1.25: Milestones in the history of synthetic biology.

1.5 From Systems to Synthetic Biology

The rapidly growing field of synthetic biology seeks to use biological principles and processes to build useful engineering devices and systems. Applications of synthetic biology range from materials production (drugs, biofuels) to biological sensing and diagnostics (chemical detection, medical diagnostics) to biological machines (bioremediation, nanoscale robotics). Like many other fields at the time of their infancy (electronics, software, networks), it is not yet clear where synthetic biology will have its greatest impact. However, recent advances such as the ability to “boot up” a chemically synthesized genome [30] demonstrate the ability to synthesize systems that offer the possibility of creating devices with substantial functionality. At the same time, the tools and processes available to design systems of this complexity are much more primitive, and *de novo* synthetic circuits typically use a tiny fraction of the number of genetic elements of even the smallest microorganisms [70].

Several scientific and technological developments over the past four decades have set the stage for the design and fabrication of early synthetic biomolecular circuits (see Figure 1.25). An early milestone in the history of synthetic biology can be traced back to the discovery of mathematical logic in gene regulation. In their 1961 paper, Jacob and Monod introduced for the first time the idea of gene expression regulation through transcriptional feedback [44]. Only a few years later (1969), *restriction enzymes* that cut double-stranded DNA at specific recognition sites were discovered by Arber and co-workers [5]. These enzymes were a major enabler of recombinant DNA technology, in which genes from one organism are extracted and spliced into the chromosome of another. One of the most celebrated products of this technology was the large scale production of insulin by employing *E. coli* bacteria as a cell factory [87].

Another key innovation was the development of the polymerase chain reaction (PCR), devised in the 1980s, which allows exponential amplification of small amounts of DNA and can be used to obtain sufficient quantities for use in a variety of molecular biology laboratory protocols where higher concentrations of DNA are required. Using PCR, it is possible to “copy” genes and other DNA sequences out of their host organisms.

The developments of recombinant DNA technology, PCR and artificial synthesis of DNA provided the ability to “cut and paste” natural or synthetic promoters and genes in almost any fashion. This cut and paste procedure is called *cloning* and consists of four primary steps: *fragmentation*, *ligation*, *transfection* and *screening*. The DNA of interest is first isolated using restriction enzymes and/or PCR amplification. Then, a ligation procedure is employed in which the amplified fragment is inserted into a vector. The vector is often a piece of circular DNA, called a plasmid, that has been linearized by means of restriction enzymes that cleave it at appropriate restriction sites. The vector is then incubated with the fragment of interest with an enzyme called *DNA ligase*, producing a single piece of DNA with the target DNA inserted. The next step is to transfect (or transform) the DNA into living cells, where the natural replication mechanisms of the cell will duplicate the DNA when the cell divides. This process does not transfect all cells, and so a selection procedure is required to isolate those cells that have the desired DNA inserted in them. This is typically done by using a plasmid that gives the cell resistance to a specific antibiotic; cells grown in the presence of that antibiotic will only live if they contain the plasmid. Further selection can be done to insure that the inserted DNA is also present.

Once a circuit has been constructed, its performance must be verified and, if necessary, debugged. This is often done with the help of *fluorescent reporters*. The most famous of these is GFP, which was isolated from the jellyfish *Aequorea victoria* in 1978 by Shimomura [80]. Further work by Chalfie and others in the 1990s enabled the use of GFP in *E. coli* as a fluorescent reporter by inserting it into an appropriate point in an artificial circuit [15]. By using spectrofluorometry, fluorescent microscopy or flow cytometry, it is possible to measure the amount of fluorescence in individual cells or collections of cells and characterize the performance of a circuit in the presence of inducers or other factors.

Two early examples of the application of these technologies were the *repressilator* [26] and a synthetic genetic switch [29].

The repressilator is a synthetic circuit in which three proteins each repress another in a cycle. This is shown schematically in Figure 1.26a, where the three proteins are TetR, λ cI and LacI. The basic idea of the repressilator is that if TetR is present, then it represses the production of λ cI. If λ cI is absent, then LacI is produced (at the unregulated transcription rate), which in turn represses TetR. Once TetR is repressed, then λ cI is no longer repressed, and so on. If the dynamics of the circuit are designed properly, the resulting protein concentrations will oscillate,

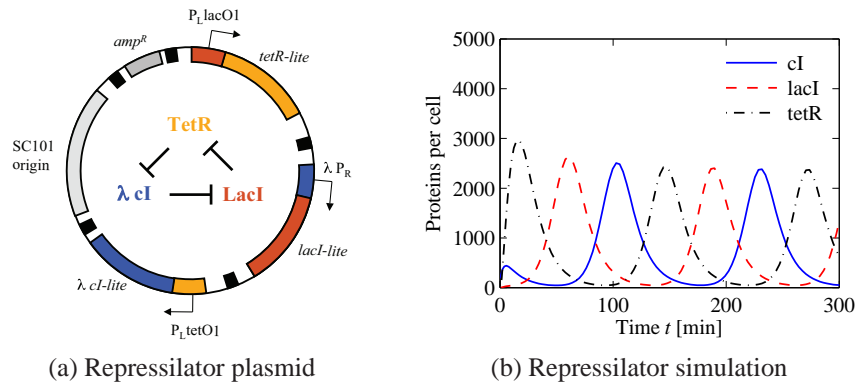


Figure 1.26: The repressilator genetic regulatory network. (a) A schematic diagram of the repressilator, showing the layout of the genes in the plasmid that holds the circuit as well as the circuit diagram (center). The flat headed arrow between the protein names represents repression. (b) A simulation of a simple model for the repressilator, showing the oscillation of the individual protein concentrations. (Figure courtesy M. Elowitz.)

as shown in Figure 1.26b.

The repressilator can be constructed using the techniques described above. First, we can make copies of the individual promoters and genes that form our circuit by using PCR to amplify the selected sequences out of the original organisms in which they were found. TetR is the tetracycline resistance repressor protein that is found in gram-negative bacteria (such as *E. coli*) and is part of the circuitry that provides resistance to tetracycline. LacI is the gene that produces *lac* repressor, responsible for turning off the *lac* operon in the lactose metabolic pathway in *E. coli* (see Section 5.1). And λcI comes from λ phage, where it is part of the regulatory circuitry that regulates lysis and lysogeny.

By using restriction enzymes and related techniques, we can separate the natural promoters from their associated genes, and then ligate (reassemble) them in a new order and insert them into a “backbone” vector (the rest of the plasmid, including the origin of replication and appropriate antibiotic resistance). These DNA is then transformed into cells that are grown in the presence of an antibiotic, so that only those cells that contain the repressilator can replicate. Finally, we can take individual cells containing our circuit and let them grow under a microscope to image fluorescent reporters coupled to the oscillator.

Another early circuit in the synthetic biology toolkit is a genetic switch built by Gardner *et al.* [29]. The genetic switch consists of two repressors connected together in a cycle, as shown in Figure 1.27a. The intuition behind this circuit is that if the gene A is being expressed, it will repress production of B and maintain its expression level (since the protein corresponding to B will not be present to repress A). Similarly, if B is being expressed, it will repress the production of A and maintain its expression level. This circuit thus implements a type of *bistability* that

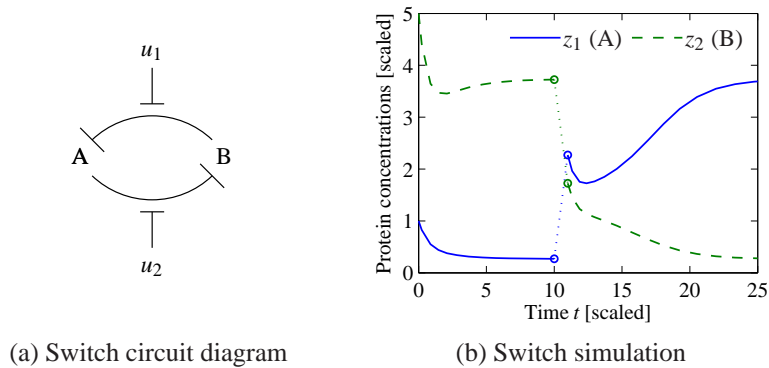


Figure 1.27: Stability of a genetic switch. The circuit diagram in (a) represents two proteins that are each repressing the production of the other. The inputs u_1 and u_2 interfere with this repression, allowing the circuit dynamics to be modified. The simulation in (b) shows the time response of the system starting from two different initial conditions. The initial portion of the curve corresponds to protein B having higher concentration than A, and converges to an equilibrium where A is off and B is on. At time $t = 10$, the concentrations are perturbed, moving the concentrations into a region of the state space where solutions converge to the equilibrium point with the A on and B off.

can be used as a simple form of memory. Figure 1.27b shows the time traces for a system, illustrating the bistable nature of the circuit. When the initial condition starts with a concentration of protein B greater than that of A, the solution converges to the equilibrium point where B is on and A is off. If A is greater than B, then the opposite situation results.

These seemingly simple circuits took years to get to work, but showed that it was possible to synthesize a biological circuit that performed a desired function that was not originally present in a natural system. Today, commercial synthesis of DNA sequences and genes has become cheaper and faster, with a price often below \$0.30 per base pair.¹ The combination of inexpensive synthesis technologies, new advances in cloning techniques, and improved devices for imaging and measurement has vastly simplified the process of producing a sequence of DNA that encodes a given set of genes, operator sites, promoters and other functions, and these techniques are a routine part of undergraduate courses in molecular and synthetic biology.

As illustrated by the examples above, current techniques in synthetic biology have demonstrated the ability to program biological function by designing DNA sequences that implement simple circuits. Most current devices make use of transcriptional or post-transcriptional processing, resulting in very slow timescales (response times typically measured in tens of minutes to hours). This restricts their use in systems where faster response to environmental signals is needed, such as

¹As of this writing; divide by a factor of two for every two years after the publication date.

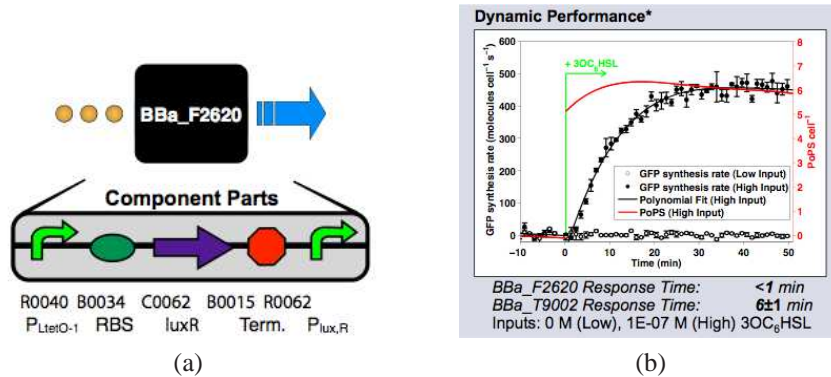


Figure 1.28: Expression of a protein using an inducible promoter [14]. (a) The circuit diagram indicates the DNA sequences that are used to construct the part (chosen from the BioBrick library). (b) The measured response of the system to a step change in the inducer level (HSL).

rapid detection of a chemical signal or fast response to changes in the internal environment of the cell. In addition, existing methods for biological circuit design have limited modularity (reuse of circuit elements requires substantial redesign or tuning) and typically operate in very narrow operating regimes (e.g., a single species grown in a single type of media under carefully controlled conditions). Furthermore, engineered circuits inserted into cells can interact with the host organism and have other unintended interactions.

As an illustration of the dynamics of synthetic devices in use today, Figure 1.28 shows a typical response of a genetic element to an inducer molecule [14]. In this circuit, an external signal of homoserine lactone (HSL) is applied at time zero and the system reaches 10% of the steady state value in approximately 15 minutes. This response is limited in part by the time required to synthesize the output protein (GFP), including delays due to transcription, translation and folding. Since this is the response time for the underlying “actuator”, circuits that are composed of feedback interconnections of such genetic elements will typically operate at 5–10 times slower speeds. While these speeds are appropriate in many applications (e.g., regulation of steady state enzyme levels for materials production), in the context of biochemical sensors or systems that must maintain a steady operating point in more rapidly changing thermal or chemical environments, this response time is too slow to be used as an effective engineering approach.

By comparison, the input/output response for the signaling component in *E. coli* chemotaxis is shown in Figure 1.29 [79]. Here the response of the kinase CheA is plotted in response to an exponential ramp in the ligand concentration. The response is extremely rapid, with the timescale measured in seconds. This rapid response is implemented by conformational changes in the proteins involved in the circuit, rather than regulation of transcription or other slower processes.

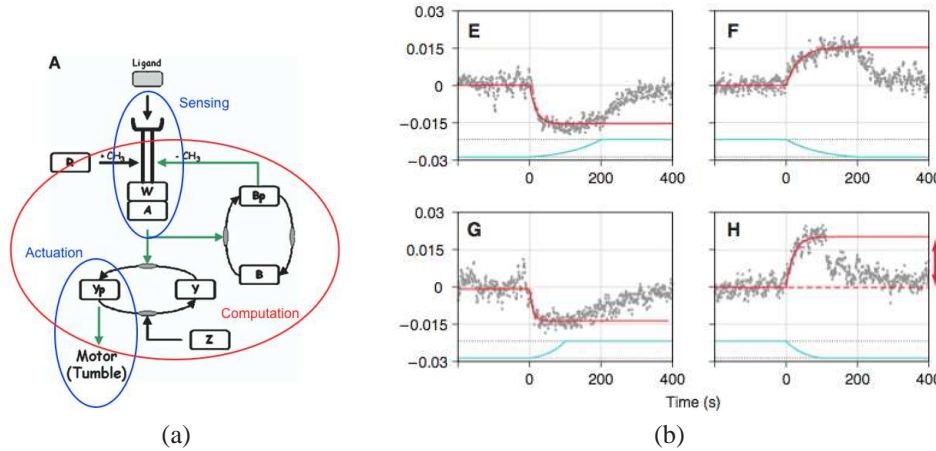


Figure 1.29: Responses of *E. coli* signaling network to exponential ramps in ligand concentration. (a) A simplified circuit diagram for chemotaxis, showing the biomolecular processes involved in regulating flagellar motion. (b) Time responses of the “sensing” subsystem (from Shimizu, Tu and Berg; *Molecular Systems Biology*, 2010), showing the response to exponential inputs.

The field of synthetic biology has the opportunity to provide new approaches to solving engineering and scientific problems. Sample engineering applications include the development of synthetic circuits for producing biofuels, ultrasensitive chemical sensors, or production of materials with specific properties that are tuned to commercial needs. In addition to the potential impact on new biologically engineered devices, there is also the potential for impact in improved understanding of biological processes. For example, many diseases such as cancer and Parkinson’s disease are closely tied to kinase dysfunction. Our analysis of robust systems of kinases and the ability to synthesize systems that support or invalidate biological hypotheses may lead to a better systems understanding of failure modes that lead to such diseases.

1.6 Further Reading

There are numerous survey articles and textbooks that provide more detailed introductions to the topics introduced in this chapter. In the area of systems biology, the textbook by Alon [4] provides a broad view of some of the key elements of modern systems biology. A more comprehensive set of topics is covered in the recent textbook by Klipp [48], while a more engineering-oriented treatment of modeling of biological circuits can be found in the text by Myers [63]. Two other books that are particularly noteworthy are Ptashne’s book on the phage λ [69] and Madhani’s book on yeast [53], both of which use well-studied model systems to describe a

general set of mechanisms and principles that are present in many different types of organisms.

Several textbooks and research monographs provide excellent resources for modeling and analysis of biomolecular dynamics and regulation. J. D. Murray's two-volume text [61] on biological modeling is an excellent reference with many examples of biomolecular dynamics. The textbook by Phillips, Kondev and Theriot [68] provides a quantitative approach to understanding biological systems, including many of the concepts discussed in this chapter. Courey [16] gives a detailed description of mechanisms transcriptional regulation.

The topics in dynamical systems and control theory that are briefly introduced here are covered in more detail in AM08 [2], to which this text is a supplement. Other books that introduce tools for modeling and analysis of dynamical systems with applications in biology include J. D. Murray's text [61] and the recent text by Ellner and Guckenheimer [25].

Synthetic biology is a rapidly evolving field that includes many different sub-areas of research, but few textbooks are currently available. In the specific area of biological circuit design that we focus on here, there are a number of good survey and review articles. The article by Baker *et al.* [8] provides a high level description of the basic approach and opportunities. Recent survey and review papers include Voigt [88] and Khalil and Collins [47].

Chapter 2

Dynamic Modeling of Core Processes

The goal of this chapter is to describe basic biological mechanisms in a way that can be represented by simple dynamical models. We begin the chapter with a discussion of the basic modeling formalisms that we will utilize to model biomolecular feedback systems. We then proceed to study a number of core processes within the cell, providing different model-based descriptions of the dynamics that will be used in later chapters to analyze and design biomolecular systems. The focus in this chapter and the next is on deterministic models using ordinary differential equations; Chapter 4 describes how to model the stochastic nature of biomolecular systems.

Prerequisites. Readers should have some basic familiarity with cell biology, at the level of the description in Section 1.2 (see also Appendix A), and a basic understanding of ordinary differential equations, at the level of Chapter 2 of AM08.

2.1 Modeling Techniques

In order to develop models for some of the core processes of the cell, we will need to build up a basic description of the biochemical reactions that take place, including production and degradation of proteins, regulation of transcription and translation, intracellular sensing, action and computation, and intercellular signaling. As in other disciplines, biomolecular systems can be modeled in a variety of different ways, at many different levels of resolution, as illustrated in Figure 2.1. The choice of which model to use depends on the questions that we want to answer, and good modeling takes practice, experience, and iteration. We must properly capture the aspects of the system that are important, reason about the appropriate temporal and spatial scales to be included, and take into account the types of simulation and analysis tools to be applied. Models that are to be used for analyzing existing systems should make testable predictions and provide insight into the underlying dynamics. Design models must additionally capture enough of the important behavior to allow decisions to be made regarding how to interconnect subsystems, choose parameters and design regulatory elements.

In this section we describe some of the basic modeling frameworks that we will build on throughout the rest of the text. We begin with brief descriptions of the relevant physics and chemistry of the system, and then quickly move to models that focus on capturing the behavior using reaction rate equations. In this chapter

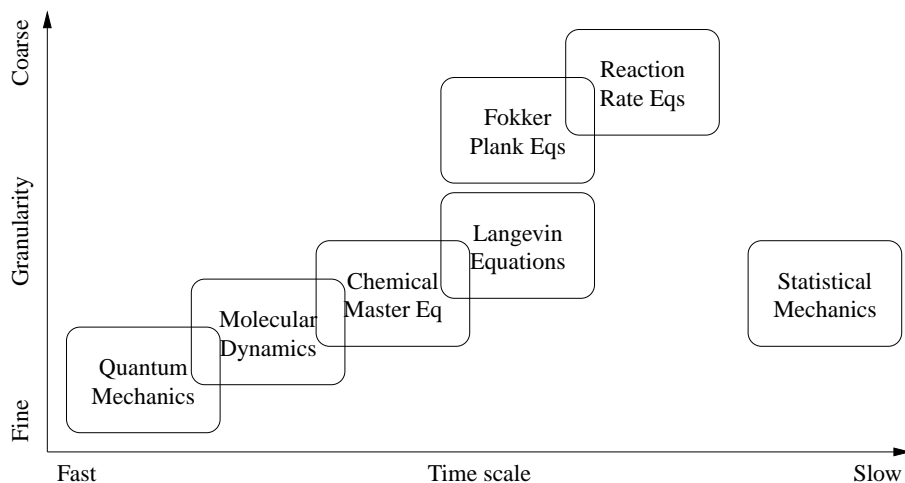


Figure 2.1: Different methods of modeling biomolecular systems.

our emphasis will be on dynamics with time scales measured in seconds to hours and mean behavior averaged across a large number of molecules. We touch only briefly on modeling in the case where stochastic behavior dominates and defer a more detailed treatment until Chapter 4.

Statistical mechanics and chemical kinetics

At the fine end of the modeling scale depicted in Figure 2.1, we can attempt to model the *molecular dynamics* of the cell, in which we attempt to model the individual proteins and other species and their interactions via molecular-scale forces and motions. At this scale, the individual interactions between protein domains, DNA and RNA are resolved, resulting in a highly detailed model of the dynamics of the cell.

For our purposes in this text, we will not require the use of such a detailed scale. Instead, we will start with the abstraction of molecules that interact with each other through stochastic events that are guided by the laws of thermodynamics. We begin with an equilibrium point of view, commonly referred to as *statistical mechanics*, and then briefly describe how to model the (statistical) dynamics of the system using chemical kinetics. We cover both of these points of view very briefly here, primarily as a stepping stone to more deterministic models, and present a more detailed description in Chapter 4.

The underlying representation for both statistical mechanics and chemical kinetics is to identify the appropriate *microstates* of the system. A microstate corresponds to a given configuration of the components (species) in the system relative to each other and we must enumerate all possible configurations between the molecules that are being modeled. As an example, consider the distribution of RNA

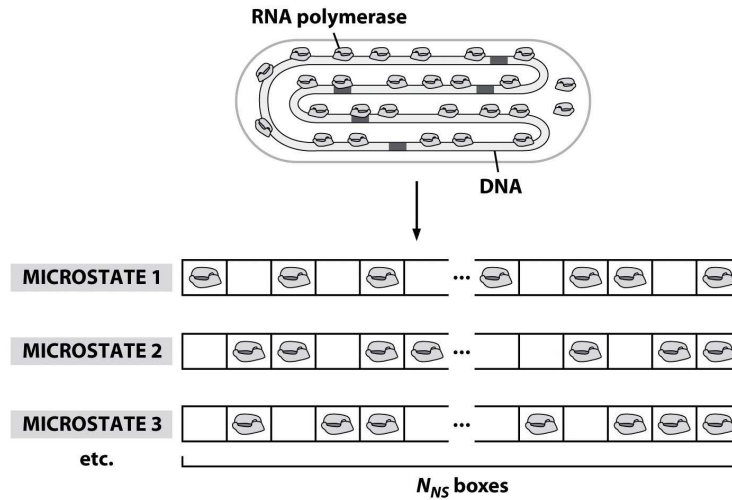


Figure 6.9 Physical Biology of the Cell (© Garland Science 2009)

Figure 2.2: Microstates for RNA polymerase. Each microstate of the system corresponds to the RNA polymerase being located at some position in the cell. If we discretize the possible locations on the DNA and in the cell, the microstates corresponds to all possible non-overlapping locations of the RNA polymerases. Figure from Phillips, Kondev and Theriot [68]; used with permission of Garland Science.

polymerase in the cell. It is known that most RNA polymerases are bound to the DNA in a cell, either as they produce RNA or as they diffuse along the DNA in search of a promoter site. Hence we can model the microstates of the RNA polymerase system as all possible locations of the RNA polymerase in the cell, with the vast majority of these corresponding to the RNA polymerase at some location on the DNA. This is illustrated in Figure 2.2.

In statistical mechanics, we model the configuration of the cell by the probability that system is in a given microstate. This probability can be calculated based on the energy levels of the different microstates. The laws of statistical mechanics state that if we have a set of microstates Q , then the steady state probability that the system is in a particular microstate q is given by

$$\mathbb{P}(q) = \frac{1}{Z} e^{-E_q/(k_B T)}, \quad (2.1)$$

where E_q is the energy associated with the microstate $q \in Q$, k_B is the Boltzmann constant, T is the temperature in degrees Kelvin, and Z is a normalizing factor, known as the *partition function*,

$$Z = \sum_{q \in Q} e^{-E_q/(k_B T)}.$$

(These formulas are described in more detail in Chapter 4.)

By keeping track of those microstates that correspond to a given system state (also called a *macrostate*), we can compute the overall probability that a given macrostate is reached. Thus, if we have a set of states $S \subset Q$ that correspond to a given macrostate, then the probability of being in the set S is given by

$$P(S) = \frac{1}{Z} \sum_{q \in S} e^{-E_q/(k_B T)} = \frac{\sum_{q \in S} e^{-E_q/(k_B T)}}{\sum_{q \in Q} e^{-E_q/(k_B T)}}. \quad (2.2)$$

This can be used, for example, to compute the probability that some RNA polymerase is bound to a given promoter, averaged over many independent samples, and from this we can reason about the rate of expression of the corresponding gene. More details and several examples will be illustrated in Chapter 4.

Statistical mechanics describes the steady state distribution of microstates, but does not tell us how the microstates evolve in time. To include the dynamics, we must consider the *chemical kinetics* of the system and model the probability that we transition from one microstate to another in a given period of time. Let q represent the microstate of the system, which we shall take as a vector of integers that represents the number of molecules of a specific types in given configurations or locations. Assume we have a set of M reactions R_j , $j = 1, \dots, M$, with ξ_j representing the change in state q associated with reaction R_j . We describe the kinetics of the system by making use of the *propensity function* $a_j(q, t)$ associated with reaction R_j , which captures the instantaneous probability that at time t a system will transition between state q and state $q + \xi_j$.

More specifically, the propensity function is defined such that

$$a_j(q, t) dt = \text{Probability that reaction } R_j \text{ will occur between time } t \text{ and time } t + dt \text{ given that the microstate is } q.$$

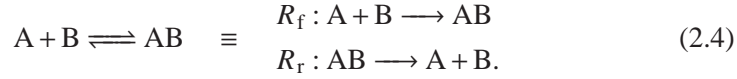
We will give more detail in Chapter 4 regarding the validity of this functional form, but for now we simply assume that such a function can be defined for our system.

Using the propensity function, we can keep track of the probability distribution for the state by looking at all possible transitions into and out of the current state. Specifically, given $P(q, t)$, the probability of being in state q at time t , we can compute the time derivative $dP(q, t)/dt$ as

$$\frac{dP}{dt}(q, t) = \sum_{j=1}^M (a_j(q - \xi_j) P(q - \xi_j, t) - a_j(q) P(q, t)) \quad (2.3)$$

This equation (and its many variants) is called the *chemical master equation* (CME). The first sum on the right hand side represents the transitions into the state q from some other state $q - \xi_j$ and the second sum represents that transitions out of the state q . The variable ξ_j in the sum ranges over all possible reactions.

Clearly the dynamics of the distribution $P(q, t)$ depend on the form of the propensity functions $a_j(q)$. Consider a simple reaction of the form



We assume that the reaction takes place in a well-stirred volume Ω and let the configurations q be represented by the number of each species that is present. The forward reaction R_f is a bimolecular reaction and we will see in Chapter 4 that it has a propensity function

$$a_f(q) = \frac{k_f}{\Omega} n_A n_B,$$

where k_f is a parameter that depends on the forward reaction, and n_A and n_B are the number of molecules of each species. The reverse reaction R_r is a unimolecular reaction and we will see that it has a propensity function

$$a_r(q) = k_r n_{AB},$$

where k_r is a parameter that depends on the reverse reaction and n_{AB} is the number of molecules of AB that are present.

If we now let $q = (n_A, n_B, n_{AB})$ represent the microstate of the system, then we can write the chemical master equation as

$$\frac{dP}{dt}(n_A, n_B, n_{AB}) = k_r n_{AB} P(n_A - 1, n_B - 1, n_{AB} + 1) - k_f n_A n_B P(n_A, n_B, n_{AB}).$$

The first term on the right hand side represents the transitions into the microstate $q = (n_A, n_B, n_{AB})$ and the second term represents the transitions out of that state.

The number of differential equations depends on the number of molecules of A, B and AB that are present. For example, if we start with 1 molecules of A, 1 molecule of B, and 3 molecules of AB, then the possible states and dynamics are

$$\begin{array}{ll} q_0 = (1, 0, 4) & dP_0/dt = 3k_r P_1 \\ q_1 = (2, 1, 3) & dP_1/dt = 4k_r P_0 - 2(k_f/\Omega)P_1 \\ q_2 = (3, 2, 2) & dP_2/dt = 3k_r P_1 - 6(k_f/\Omega)P_2 \\ q_3 = (4, 3, 1) & dP_3/dt = 2k_r P_2 - 12(k_f/\Omega)P_3 \\ q_4 = (5, 4, 0) & dP_4/dt = 1k_r P_3 - 20(k_f/\Omega)P_4, \end{array}$$

where $P_i = P(q_i, t)$. Note that the states of the chemical master equation are the probabilities that we are in a specific microstate, and the chemical master equation is a *linear* differential equation (we see from equation (2.3) that this is true in general).

The primary difference between the statistical mechanics description given by equation (2.1) and the chemical kinetics description in equation (2.3) is that the master

equation formulation describes how the probability of being in a given microstate evolves over time. Of course, if the propensity functions and energy levels are modeled properly, the steady state, average probabilities of being in a given microstate should be the same for both formulations.

Reaction rate equations

Although very general in form, the chemical master equation suffers from being a very high dimensional representation of the dynamics of the system. We shall see in Chapter 4 how to implement simulations that obey the master equation, but in many instances we will not need this level of detail in our modeling. In particular, there are many situations in which the number of molecules of a given species is such that we can reason about the behavior of a chemically reacting system by keeping track of the *concentration* of each species as a real number. This is of course an approximation, but if the number of molecules is sufficiently large, then the approximation will generally be valid and our models can be dramatically simplified.

To go from the chemical master equation to a simplified form of the dynamics, we begin by making a number of assumptions. First, we assume that we can represent the state of a given species by its concentration n_A/Ω , where n_A is the number of molecules of A in a given volume Ω . We also treat this concentration as a real number, ignoring the fact that the real concentration is quantized. Finally, we assume that our reactions take place in a well-stirred volume, so that the rate of interactions between two species is solely determined by the concentrations of the species.

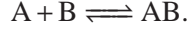
Before proceeding, we should recall that in many (and perhaps most) situations inside of cells, these assumptions are *not* particularly good ones. Biomolecular systems often have very small molecular counts and are anything but well mixed. Hence, we should not expect that models based on these assumptions should perform well at all. However, experience indicates that in many cases the basic form of the equations provides a good model for the underlying dynamics and hence we often find it convenient to proceed in this manner.

Putting aside our potential concerns, we can now proceed to write the dynamics of a system consisting of a set of species S_i , $i = 1, \dots, n$ undergoing a set of reactions R_j , $j = 1, \dots, m$. We write $x_i = [S_i] = n_{S_i}/\Omega$ for the concentration of species i (viewed as a real number). Because we are interested in the case where the number of molecules is large, we no longer attempt to keep track of every possible configuration, but rather simply assume that the state of the system at any given time is given by the concentrations x_i . Hence the state space for our system is given by $x \in \mathbb{R}^n$ and we seek to write our dynamics in the form of a differential equation

$$\frac{dx}{dt} = f(x, \theta),$$

where $f : \mathbb{R}^n \rightarrow \mathbb{R}^n$ describes the rate of change of the concentrations as a function of the instantaneous concentrations and θ represents the parameters that govern the dynamic behavior.

To illustrate the general form of the dynamics, we consider again the case of a basic bimolecular reaction



Each time the forward reaction occurs, we decrease the number of molecules of A and B by 1 and increase the number of molecules of AB (a separate species) by 1. Similarly, each time the reverse reaction occurs, we decrease the number of molecules of AB by one and increase the number of molecules of A and B.

Using our discussion of the chemical master equation, we know that the likelihood that the forward reaction occurs in a given interval dt is given by $a_f(q)dt = (k_f/\Omega)n_A n_B dt$ and the reverse reaction has likelihood $a_r(q) = k_r n_{AB}$. It follows that the concentration of the complex AB satisfies

$$\begin{aligned} [AB](t+dt) - [AB](t) &= \mathbb{E}(n_{AB}(t+dt)/\Omega - n_{AB}(t)/\Omega) \\ &= (a_f(q - \xi_f, t) - a_r(q))/\Omega \cdot dt \\ &= (k_f n_A n_B / \Omega^2 - k_r n_{AB} / \Omega) dt \\ &= (k_f [A][B] - k_r [AB]) dt. \end{aligned}$$

Taking the limit as dt approaches zero (but remains large enough that we can still average across multiple reactions, as described in more detail in Chapter 4), we obtain

$$\frac{d}{dt}[AB] = k_f [A][B] - k_r [AB].$$

In a similar fashion we can write equations to describe the dynamics of A and B and the entire system of equations is given by

$$\begin{aligned} \frac{d}{dt}[A] &= k_r [AB] - k_f [A][B] & \frac{dA}{dt} &= k_r C - k_f A \cdot B \\ \frac{d}{dt}[B] &= k_r [AB] - k_f [A][B] & \text{or } \frac{dB}{dt} &= k_r C - k_f A \cdot B \\ \frac{d}{dt}[AB] &= k_f [A][B] - k_r [AB] & \frac{dC}{dt} &= k_f A \cdot B - k_r C, \end{aligned}$$

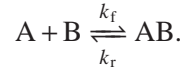
where $C = [AB]$, $A = [A]$, and $B = [B]$. These equations are known as the *mass action kinetics* or the *reaction rate equations* for the system. The parameters k_f and k_r are called the *rate constants* and they match the parameters that were used in the underlying propensity functions.

Note that the same rate constants appear in each term, since the rate of production of AB must match the rate of depletion of A and B and vice versa. We

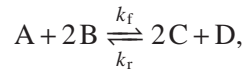
adopt the standard notation for chemical reactions with specified rates and write the individual reactions as



where k_f and k_r are the reaction rates. For bidirectional reactions we can also write



It is easy to generalize these dynamics to more complex reactions. For example, if we have a reversible reaction of the form



where A, B, C and D are appropriate species and complexes, then the dynamics for the species concentrations can be written as

$$\begin{aligned} \frac{d}{dt}A &= k_r C^2 \cdot D - k_f A \cdot B^2, & \frac{d}{dt}C &= 2k_f A \cdot B^2 - 2k_r C^2 \cdot D, \\ \frac{d}{dt}B &= 2k_r C^2 \cdot D - 2k_f A \cdot B^2, & \frac{d}{dt}D &= k_f A \cdot B^2 - k_r C^2 \cdot D. \end{aligned} \quad (2.5)$$

Rearranging this equation, we can write the dynamics as

$$\frac{d}{dt} \begin{pmatrix} A \\ B \\ C \\ D \end{pmatrix} = \begin{pmatrix} -1 & 1 \\ -2 & 2 \\ 2 & -2 \\ 1 & -1 \end{pmatrix} \begin{pmatrix} k_f A \cdot B^2 \\ k_r C^2 \cdot D \end{pmatrix}. \quad (2.6)$$

We see that in this decomposition, the first term on the right hand side is a matrix of integers reflecting the stoichiometry of the reactions and the second term is a vector of rates of the individual reactions.

Often, the following notation will be employed to denote birth and death of species



We attach to the first reaction the differential equation

$$\frac{dA}{dt} = k_f,$$

and to the second reaction we attach the differential equation

$$\frac{dA}{dt} = -k_r A.$$

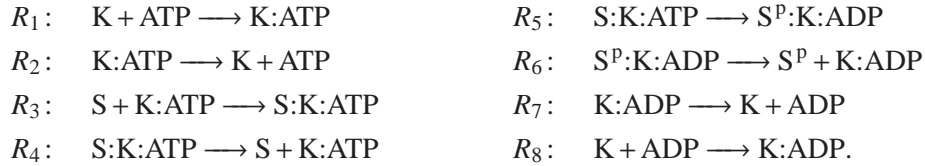
From a physical point of view, these reactions simply the representation of more complex processes, such as transcription of mRNA or degradation of proteins due to proteases.

More generally, given a chemical reaction consisting of a set of species S_i , $i = 1, \dots, n$ and a set of reactions R_j , $j = 1, \dots, m$, we can write the mass action kinetics in the form

$$\frac{dx}{dt} = Nv(x),$$

where $N \in \mathbb{R}^{n \times m}$ is the *stoichiometry matrix* for the system and $v(x) \in \mathbb{R}^m$ is the *reaction flux vector*. Each row of $v(x)$ corresponds to the rate at which a given reaction occurs and the corresponding column of the stoichiometry matrix corresponds to the changes in concentration of the relevant species. As we shall see in the next chapter, the structured form of this equation will allow us to explore some of the properties of the dynamics of chemically reacting systems.

Example 2.1 (Covalent modification of a protein). Consider the set of reactions involved in the phosphorylation of a protein by a kinase, as shown in Figure 1.17. Let S represent the substrate, K represent the kinase and S^P represent the phosphorylated (activated) substrate. The sets of reactions illustrated in Figure 1.17 are



We now write the kinetics for each reaction:

$$\begin{array}{ll} v_1 = k_1 [K][\text{ATP}], & v_5 = k_5 [S:K:\text{ATP}], \\ v_2 = k_2 [K:\text{ATP}], & v_6 = k_6 [S^P:K:\text{ADP}], \\ v_3 = k_3 [S][K:\text{ATP}], & v_7 = k_7 [K:\text{ADP}], \\ v_4 = k_4 [S:K:\text{ATP}], & v_8 = k_8 [K][\text{ADP}]. \end{array}$$

We treat $[\text{ATP}]$ as a constant (regulated by the cell) and hence do not directly track its concentration. (If desired, we could similarly ignore the concentration of ADP since we have chosen not to include the many additional reactions in which it participates.)

The kinetics for each species are thus given by

$$\begin{array}{ll} \frac{d}{dt}[K] = -v_1 + v_2 + v_7 - v_8 & \frac{d}{dt}[K:\text{ATP}] = v_1 - v_2 - v_3 + v_4 \\ \frac{d}{dt}[S] = -v_3 + v_4 & \frac{d}{dt}[S:K:\text{ATP}] = v_3 - v_4 - v_5 \\ \frac{d}{dt}[S^P] = v_6 & \frac{d}{dt}[S^P:K:\text{ADP}] = v_5 - v_6 \\ \frac{d}{dt}[\text{ADP}] = v_7 - v_8 & \frac{d}{dt}[K:\text{ADP}] = v_6 - v_7 + v_8. \end{array}$$

Collecting these equations together and writing the state as a vector, we obtain

$$\frac{d}{dt} \underbrace{\begin{pmatrix} [\text{K}] \\ [\text{K:ATP}] \\ [\text{S}] \\ [\text{S:K:ATP}] \\ [\text{S}^{\text{P}}] \\ [\text{S}^{\text{P}}:\text{K:ADP}] \\ [\text{ADP}] \\ [\text{K:ADP}] \end{pmatrix}}_x = \underbrace{\begin{pmatrix} -1 & 1 & 0 & 0 & 0 & 0 & 1 & -1 \\ 1 & -1 & 1 & -1 & 0 & 0 & 0 & 0 \\ 0 & 0 & -1 & 1 & 0 & 0 & 0 & 0 \\ 0 & 0 & 1 & -1 & -1 & 0 & 0 & 0 \\ 0 & 0 & 0 & 0 & 0 & 1 & 0 & 0 \\ 0 & 0 & 0 & 0 & 1 & -1 & 0 & 0 \\ 0 & 0 & 0 & 0 & 0 & 0 & 1 & -1 \\ 0 & 0 & 0 & 0 & 0 & 1 & -1 & 1 \end{pmatrix}}_N \underbrace{\begin{pmatrix} v_1 \\ v_2 \\ v_3 \\ v_4 \\ v_5 \\ v_6 \\ v_7 \\ v_8 \end{pmatrix}}_{v(x)},$$

which is in standard stoichiometric form. ∇

Reduced order mechanisms

In this section, we look at dynamics of some common reactions that occur in biomolecular systems. Under some assumptions on the relative rates of reactions and concentrations of species, it is possible to derive reduced order expressions for the dynamics of the system. We focus here on an informal derivation of the relevant results, but return to these examples in the next chapter to illustrate that the same results can be derived using a more formal and rigorous approach.

Simple binding reaction. Consider the reaction in which two species A and B bind reversibly to form a complex $C=AB$:



where a is the association rate and b is the dissociation rate. Assume that B is a species that is controlled by other reactions in the cell and that the total concentration of A is conserved, so that $A + C = [A] + [AB] = A_{\text{tot}}$. If the dynamics of this reaction are fast compared to other reactions in the cell, then the amount of A and C present can be computed as a (steady state) function of B.

To compute how A and C depend on the concentration of B at the steady state, we must solve for the equilibrium concentrations of A and C. The rate equation for C is given by

$$\frac{dC}{dt} = aB \cdot (A_{\text{tot}} - C) - dC.$$

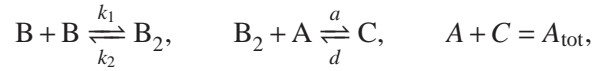
By setting $dC/dt = 0$ and letting $K_d := d/a$, we obtain the expressions

$$C = \frac{(B/K_d)A_{\text{tot}}}{(B/K_d) + 1}, \quad A = \frac{A_{\text{tot}}}{(B/K_d) + 1}.$$

The constant K_d is the inverse of the affinity of A to B and is called the *dissociation constant* for the reaction. The steady state value of C increases with B while the steady state value of A decreases with B as more of A is found in the complex C.

Note that when $B \approx K_d$, A and C have roughly equal concentration. Thus the higher the value of K_d , the more B is required for A to form the complex C. K_d has the units of concentration and it can be interpreted as the concentration of B at which half of the total number of molecules of A are associated with B. Therefore a high K_d represents a weak affinity between A and B, while a low K_d represents a strong affinity.

Cooperative binding reaction. Assume now that B binds to A only after dimerization, that is, only after binding another molecule of B. Then, we have that reactions (2.7) become



in which B_2 denotes the dimer of B. The corresponding ODE model is given by

$$\frac{dB_2}{dt} = 2k_1B^2 - 2k_2B_2 - aB_2 \cdot (A_{\text{tot}} - C) + dC, \quad \frac{dC}{dt} = aB_2 \cdot (A_{\text{tot}} - C) - dC.$$

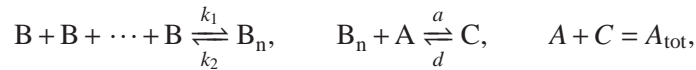
By setting $dB_2/dt = 0$, $dC/dt = 0$, and by defining $K_m := k_2/k_1$, we obtain that

$$B_2 = B^2/K_m, \quad C = \frac{(B_2/K_d)A_{\text{tot}}}{(B_2/K_d) + 1}, \quad A = \frac{A_{\text{tot}}}{(B_2/K_d) + 1},$$

so that

$$C = \frac{A_{\text{tot}} \frac{B^2}{K_m K_d}}{\frac{B^2}{K_m K_d} + 1}, \quad A = \frac{A_{\text{tot}}}{\frac{B^2}{K_m K_d} + 1}.$$

As an exercise, the reader can verify that if B binds to A only as a complex of n copies of B, that is,

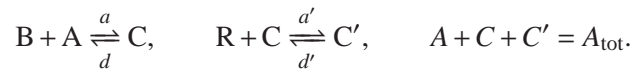


then we have that

$$C = \frac{A_{\text{tot}} \frac{B^n}{K_m K_d}}{\frac{B^n}{K_m K_d} + 1}, \quad A = \frac{A_{\text{tot}}}{\frac{B^n}{K_m K_d} + 1}.$$

In this case, one says that the binding of B to A is *cooperative* with cooperativity n . Figure 2.3 shows the above functions, which are often referred to as *Hill functions*.

Another type of cooperative binding is when a species R can bind A only after another species B is bound. In this case, the reactions are given by



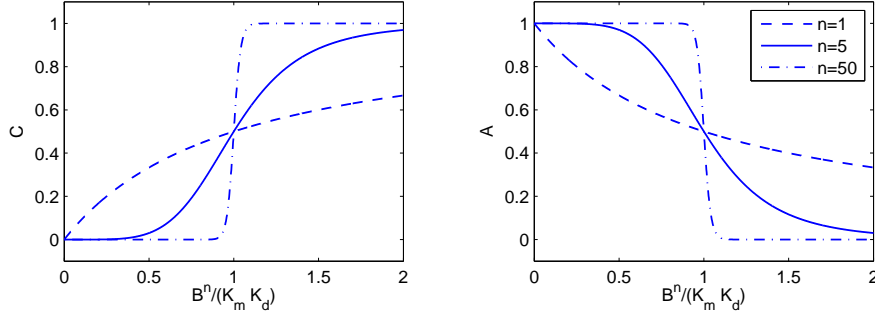


Figure 2.3: Steady state concentrations of the complex C and of A as functions of the concentration of B .

Proceeding as above by writing the ODE model and equating the time derivatives to zero to obtain the equilibrium, one obtains

$$C = \frac{1}{K_d} B(A_{\text{tot}} - C - C'), \quad C' = \frac{1}{K'_d K_d} R(A_{\text{tot}} - C - C').$$

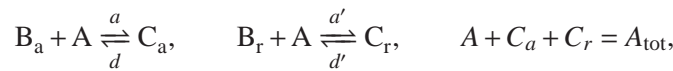
By solving this system of two equations for the unknowns C' and C , one obtains

$$C' = \frac{(RB)/(K_d K'_d) A_{\text{tot}}}{(B/K_d)(R/K'_d + 1) + 1}, \quad C = \frac{(B/K_d) A_{\text{tot}}}{(B/K_d)(R/K'_d + 1) + 1}.$$

In the case in which B would first bind cooperatively with other copies of B with cooperativity n , the above expressions would modify to

$$C' = \frac{(RB^n)/(K_d K'_d k_m) A_{\text{tot}}}{(B^n/K_d k_m)(R/K'_d + 1) + 1}, \quad C = \frac{(B^n/K_d k_m) A_{\text{tot}}}{(B^n/K_d k_m)(R/K'_d + 1) + 1}.$$

Competitive binding reaction. Finally, consider the case in which two species B_a and B_r both bind to A competitively, that is, they cannot be bound to A at the same time. Let C_a be the complex formed between B_a and A and let C_r be the complex formed between B_r and A . Then, we have the following reactions



for which we can write the dynamics as

$$\frac{dC_a}{dt} = aB_a \cdot (A_{\text{tot}} - C_a - C_r) - dC_a, \quad \frac{dC_r}{dt} = a'B_r \cdot (A_{\text{tot}} - C_a - C_r) - d'C_r.$$

By setting the derivatives to zero, we obtain that

$$C_a(aB_a + d) = aB_a(A_{\text{tot}} - C_r), \quad C_r(a'B_r + d') = a'B_r(A_{\text{tot}} - C_a),$$

and defining $K_{d,a} := d/a$, $K_{d,r} := d'/a'$ leads to

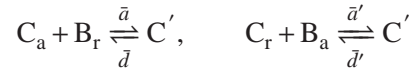
$$C_r = \frac{B_r(A_{\text{tot}} - C_a)}{B_r + K_{d,r}}, \quad C_a \left(B_a + K_{d,a} - \frac{B_a B_r}{B_r + K_{d,r}} \right) = B_a \left(\frac{K_{d,r}}{B_r + K_{d,r}} \right) A_{\text{tot}},$$

from which we finally obtain that

$$C_a = \frac{(B_a/K_{d,a})A_{\text{tot}}}{(B_a/K_{d,a}) + (B_r/K_{d,r}) + 1}, \quad C_r = \frac{(B_r/K_{d,r})A_{\text{tot}}}{(B_r/K_{d,r}) + (B_a/K_{d,a}) + 1}.$$

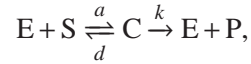
In this derivation, we have assumed that both B_a and B_r bind A as monomers. If they were binding as dimers, the reader should verify as an exercise (see Exercises) that they would appear in the final expressions with a power of two.

Note also that in this derivation we have assumed that the binding is competitive, that is, B_a and B_r cannot simultaneously bind to A. If they were binding simultaneously to A, we would have included another complex comprising B_a and B_r and A. Denoting this new complex by C' , we would have added also the two additional reactions



and we would have modified the conservation law for A to $A_{\text{tot}} = A + C_a + C_r + C'$. The reader can verify as an exercise (see Exercises) that in this case a mixed term $B_r B_a$ would appear in the equilibrium expressions.

Enzymatic reaction. A general enzymatic reaction can be written as



in which E is an enzyme, S is the substrate to which the enzyme binds to form the complex C, and P is the product resulting from the modification of the substrate S due to the binding with the enzyme E. The parameter a is referred to as association rate, d as dissociation rate, and k as the catalytic rate. Enzymatic reactions are very common and we will see specific instances of them in the sequel, e.g., phosphorylation and dephosphorylation reactions. The corresponding ODE system is given by

$$\begin{aligned} \frac{dS}{dt} &= -aE \cdot S + dC, & \frac{dC}{dt} &= aE \cdot S - (d+k)C, \\ \frac{dE}{dt} &= -aE \cdot S + dC + kC, & \frac{dP}{dt} &= kC. \end{aligned}$$

The total enzyme concentration is usually constant and denoted by E_{tot} , so that $E + C = E_{\text{tot}}$. Substituting in the above equations $E = E_{\text{tot}} - C$, we obtain

$$\begin{aligned} \frac{dE}{dt} &= -a(E_{\text{tot}} - C) \cdot S + dC + kC, & \frac{dC}{dt} &= a(E_{\text{tot}} - C) \cdot S - (d+k)C, \\ \frac{dS}{dt} &= -a(E_{\text{tot}} - C) \cdot S + dC, & \frac{dP}{dt} &= kC. \end{aligned}$$

This system cannot be solved analytically, therefore assumptions have been used in order to reduce it to a simpler form. Michaelis and Menten assumed that the conversion of E and S to C and *vice versa* is much faster than the decomposition of C into E and P. This approximation is called the *quasi-steady state approximation* between the enzyme and the complex. This assumption can be translated into the condition

$$a, d \gg k$$

on the rate constants. Under this assumption and assuming that $S \gg E$ (at least at time 0; see Example ??), C immediately reaches its steady state value (while P is still changing). The steady state value of C is given by solving $a(E_{\text{tot}} - C)S - (d + k)C = 0$ for C , which gives

$$C = \frac{E_{\text{tot}}S}{S + K_m}, \quad \text{with} \quad K_m = \frac{d + k}{a},$$

in which the constant K_m is called the *Michaelis-Menten constant*. Letting $V_{\text{max}} = kE_{\text{tot}}$, the resulting kinetics

$$\frac{dP}{dt} = k \frac{E_{\text{tot}}S}{S + K_m} = V_{\text{max}} \frac{S}{S + K_m}$$

is called *Michaelis-Menten kinetics*. The constant V_{max} is called the maximal velocity (or maximal flux) of modification and it represents the maximal rate that can be obtained when the enzyme is completely saturated by the substrate. The value of K_m corresponds to the value of S that leads to a half-maximal value of the P production rate. When the enzyme complex can be neglected with respect to the total substrate amount S_{tot} , we have that $S_{\text{tot}} \approx S + P$, so that the above equation can be also re-written as

$$\frac{dP}{dt} = \frac{V_{\text{max}}(S_{\text{tot}} - P)}{(S_{\text{tot}} - P) + K_m}.$$

When $K_m \ll S_{\text{tot}}$ and the substrate has not yet been all converted to product, that is, $S_{\text{tot}} - P \ll K_m$, we have that the rate of product formation becomes approximately $dP/dt \approx V_{\text{max}}$, which is the maximal speed of reaction. Since this rate is constant and does not depend on the reactant concentrations, it is usually referred to zero-order kinetics. When $S_{\text{tot}} - P \ll K_m$, the system is said to operate in the zero-order regime (see Figure 2.4).

2.2 Transcription and Translation

In this section we consider the processes of transcription and translation, using the modeling techniques described in the previous section to capture the fundamental dynamic behavior. Models of transcription and translation can be done at a variety of levels of detail and which model to use depends on the questions that one wants

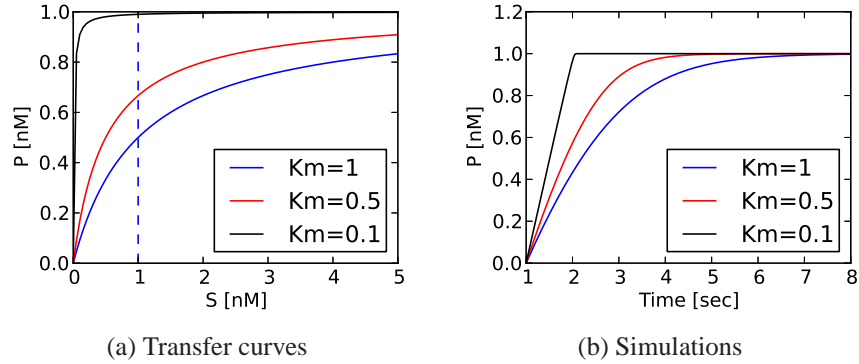


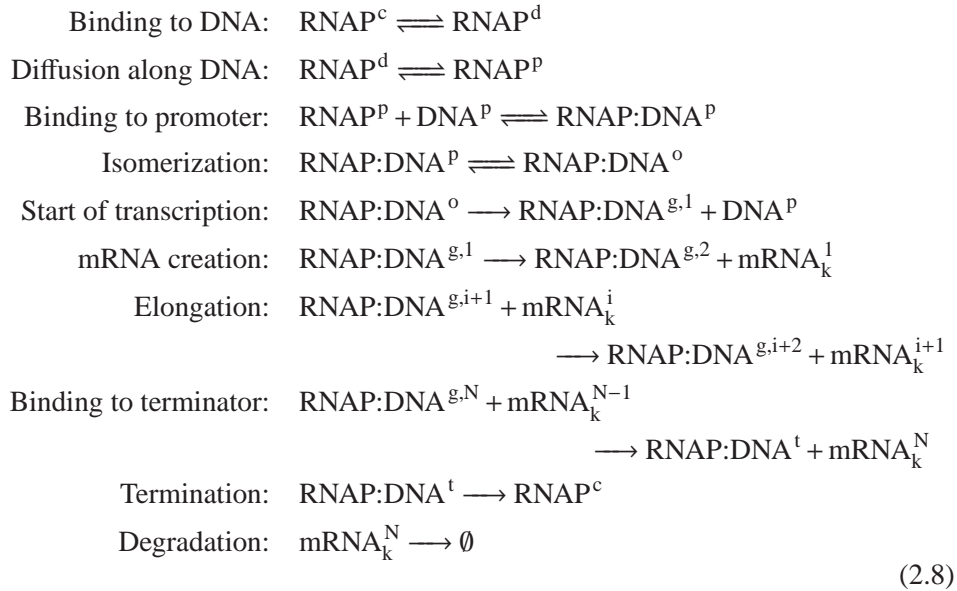
Figure 2.4: Enzymatic reactions. (a) Transfer curve showing the production rate for P as a function of substrate concentration. (b) Time plots of product $P(t)$ for different values of the K_m . In the plots $S_{\text{tot}} = 1$ and $V_{\text{max}} = 1$. The black plot shows the behavior for a value of K_m much smaller than the total substrate amount S_{tot} . This corresponds to a constant product formation rate (at least before the substrate is almost all converted to product, that is, $S_{\text{tot}} - P \approx K_m$), which is referred to *zero-order kinetics*.

to consider. We present several levels of modeling here, starting with a fairly detailed set of reactions and ending with highly simplified models that can be used when we are only interested in average production rate of proteins at relatively long time scales.

The basic reactions that underly transcription include the diffusion of RNA polymerase from one part of the cell to the promoter region, binding of an RNA polymerase to the promoter, isomerization from the closed complex to the open complex, and finally the production of mRNA, one base pair at a time. To capture this set of reactions, we keep track of the various forms of RNA polymerase according to its location and state: RNAP^c represents RNA polymerase in the cytoplasm and RNAP^d is non-specific binding of RNA polymerase to the DNA. We must similarly keep track of the state of the DNA, to insure that multiple RNA polymerases do not bind to the same section of DNA. Thus we can write DNA^p for the promoter region, $\text{DNA}^{g,i}$ for the i th section of a gene g (whose length can depend on the desired resolution) and DNA^t for the termination sequence. We write $\text{RNAP}:\text{DNA}$ to represent RNA polymerase bound to DNA (assumed closed) and $\text{RNAP}:\text{DNA}^o$ to indicate the open complex. Finally, we must keep track of the mRNA that is produced by transcription: we write mRNA^i to represent an mRNA strand of length i and assume that the length of the gene of interest is N .

Using these various states of the RNA polymerase and locations on the DNA,

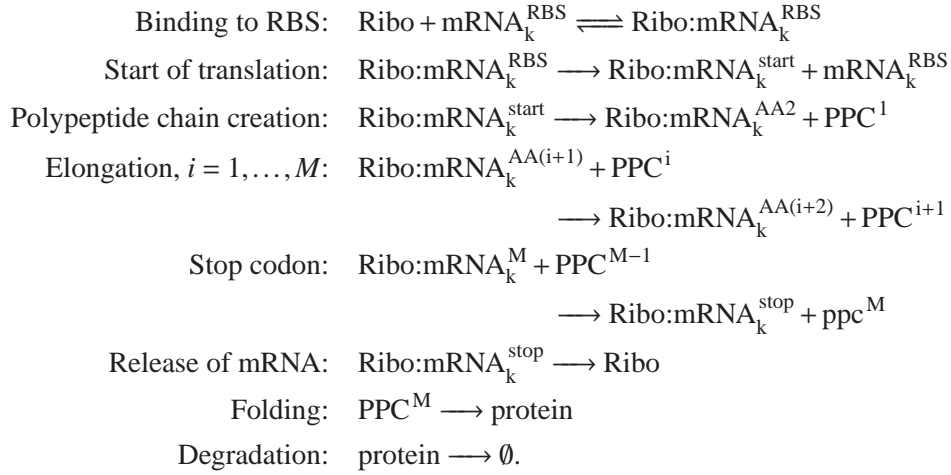
we can write a set of reactions modeling the basic elements of transcription as



This reaction has been written for prokaryotes, but a similar set of reactions could be written for eukaryotes: the main differences would be that the RNA polymerase remains in the nucleus and the mRNA must be spliced and transported to the cytosol. Note that at the start of transcription we “release” the promoter region of the DNA, thus allowing a second RNA polymerase to bind to the promoter while the first RNA polymerase is still transcribing the gene.

A similar set of reactions can be written to model the process of translation. Here we must keep track of the binding of the ribosome to the mRNA, translation of the mRNA sequence into a polypeptide chain, and folding of the polypeptide chain into a functional protein. Let $\text{Ribo:mRNA}^{\text{RBS}}$ indicate the ribosome bound to the ribosome binding site, $\text{Ribo:mRNA}^{\text{AA}i}$ the ribosome bound to the i th codon, $\text{Ribo:mRNA}^{\text{start}}$ and $\text{Ribo:mRNA}^{\text{stop}}$ for the start and stop codons, and PPC^i for a polypeptide chain consisting of i amino acids. The reactions describing translation

can then be written as



As in the case of transcription, we see that these reactions allow multiple ribosomes to translate the same piece of mRNA by freeing up the ribosome binding site (RBS) when translation begins.

As complex as these reactions are, they are still missing many important effects. For example, we have not accounted for the existence and effects of the 5' and 3' untranslated regions (UTRs) of a gene and we have also left out various error correction mechanisms in which ribosomes can step back and release an incorrect amino acid that has been incorporated into the polypeptide chain. We have also left out the many chemical species that must be present in order for a variety of the reactions to happen (NTPs for mRNA production, amino acids for protein production, etc). Incorporation of these effects requires additional reactions that track the many possible states of the molecular machinery that underlies transcription and translation.

Given a set of reactions, the various stochastic processes that underly detailed models of transcription and translation can be specified using the stochastic modeling framework described briefly in the previous section. In particular, using either models of binding energy or measured rates, we can construct propensity functions for each of the many reactions that lead to production of proteins, including the motion of RNA polymerase and the ribosome along DNA and RNA. For many problems in which the detailed stochastic nature of the molecular dynamics of the cell are important, these models are the most relevant and they are covered in some detail in Chapter 4.

Alternatively, we can move to the reaction rate formalism and model the reactions using differential equations. To do so, we must compute the various reaction rates, which can be obtained from the propensity functions or measured experimentally. In moving to this formalism, we approximate the concentrations of various species as real numbers, which may not be accurate since some species exist at

low molecular counts in the cell. Despite all of these approximations, in many situations the reaction rate equations are perfectly sufficient, particularly if we are interested in the average behavior of a large number of cells.

In some situations, an even simpler model of the transcription, translation and folding processes can be utilized. Let the “active” mRNA be the mRNA that is available for translation by the ribosome. We model its concentration through a simple time delay of length τ^m that accounts for the transcription of the ribosome binding site in prokaryotes or splicing and transport from the nucleus in eukaryotes. If we assume that RNA polymerase binds to DNA at some average rate (which includes both the binding and isomerization reactions) and that transcription takes some fixed time (depending on the length of the gene), then the process of transcription can be described using the delay differential equation

$$\frac{dm}{dt} = \alpha_{p,0} - \mu m - \bar{\gamma} m, \quad m^*(t) = e^{-\mu\tau^m} m(t - \tau^m), \quad (2.9)$$

where m is the concentration of mRNA for protein P, m^* is the concentration of active mRNA, $\alpha_{p,0}$ is the rate of production of the mRNA for protein P, μ is the growth rate of the cell (which results in dilution of the concentration) and $\bar{\gamma}$ is the rate of degradation of the mRNA. Since the dilution and degradation terms are of the same form, we will often combine these terms in the mRNA dynamics and use a single coefficient γ . The exponential factor accounts for dilution due to the change in volume of the cell, where μ is the cell growth rate. The constants $\alpha_{p,0}$ and γ capture the average rates of production and degradation, which in turn depend on the more detailed biochemical reactions that underlie transcription.

Once the active mRNA is produced, the process of translation can be described via a similar ordinary differential equation that describes the production of a functional protein:

$$\frac{dP}{dt} = \beta_{p,0} m^* - \delta P, \quad P^f(t) = e^{-\mu\tau^f} P(t - \tau^f). \quad (2.10)$$

Here P represents the concentration of the polypeptide chain for the protein, P^f represents the concentration of functional protein (after folding). The parameters that govern the dynamics are $\beta_{p,0}$, the rate of translation of mRNA; δ the rate of degradation and dilution of P; and τ^f , the time delay associated with folding and other processes required to make the protein functional. The exponential term again accounts for dilution due to cell growth. The degradation and dilution term, parameterized by δ , captures both rate at which the polypeptide chain is degraded and the rate at which the concentration is diluted due to cell growth.

It will often be convenient to write the dynamics for transcription and translation in terms of the functional mRNA and functional protein. Differentiating the

expression for m^* , we see that

$$\begin{aligned}\frac{dm^*(t)}{dt} &= e^{-\mu\tau^m} \dot{m}(t - \tau^m) \\ &= e^{-\mu\tau^m} (\alpha_{p,0} - \gamma m(t - \tau^m)) = \bar{\alpha}_{p,0} - \gamma m^*(t),\end{aligned}\quad (2.11)$$

where $\bar{\alpha}_{p,0} = e^{-\mu\tau^m} \alpha_{p,0}$. A similar expansion for the active protein dynamics yields

$$\frac{dP^f(t)}{dt} = \bar{\beta}_{p,0} m^*(t - \tau^f) - \delta P^f(t), \quad (2.12)$$

where $\bar{\beta}_{p,0} = e^{-\mu\tau^f} \beta_{p,0}$. We shall typically use equations (2.11) and (2.12) as our (reduced) description of protein folding, dropping the superscript f and overbars when there is no risk of confusion.

In many situations the time delays described in the dynamics of protein production are small compared with the time scales at which the protein concentration changes (depending on the values of the other parameters in the system). In such cases, we can simplify our model of the dynamics of protein production even further and write

$$\frac{dm}{dt} = \alpha_{p,0} - \gamma m, \quad \frac{dP}{dt} = \beta_{p,0} m - \delta P. \quad (2.13)$$

Note that we here have dropped the superscripts $*$ and f since we are assuming that all mRNA is active and proteins are functional and dropped the overbar on α and β since we are assuming the time delays are negligible.

Finally, the simplest model for protein production is one in which we only keep track of the basal rate of production of the protein, without including the mRNA dynamics. This essentially amounts to assuming the mRNA dynamics reach steady state quickly and replacing the first differential equation in equation (2.13) with its equilibrium value. This is often a good assumption as mRNA degradation is usually about 100–1000 times faster than protein degradation (see Table 1.1). Thus we obtain

$$\frac{dP}{dt} = \beta - \delta P, \quad \beta := \beta_{p,0} \frac{\alpha_{p,0}}{\gamma}.$$

This model represents a simple first order, linear differential equation for the rate of production of a protein. In many cases this will be a sufficiently good approximate model, although we will see that in many cases it is too simple to capture the observed behavior of a biological circuit.

2.3 Transcriptional Regulation

The operation of a cell is governed in part by the selective expression of genes in the DNA of the organism, which control the various functions the cell is able to perform at any given time. Regulation of protein activity is a major component of

activator. The relative reaction rates determine how strong the activator is and the “leakiness” of transcription in the absence of the activator.

A simplified version of the dynamics can be obtained by assuming that transcription factors bind to the DNA rapidly, so that they are in steady state configurations. In this case, we can make use of the reduced order models described in Section 2.1. We can consider the competitive binding case to model that a strong repressor prevents RNAP to bind to the DNA. In the sequel, we remove the superscripts “p” from the DNA and RNAP for simplifying notation. The steady state amount of the complex of DNA bound to the repressor will have the expression

$$[\text{DNA:Rep}] = \frac{([\text{Rep}]/K_d)[\text{DNA}]}{1 + [\text{Rep}]/K_d + [\text{RNAP}]/K'_d}$$

and the steady state amount of free DNA (not bound to the repressor) will be given by

$$C = [\text{DNA}] - [\text{DNA:Rep}] = \frac{([\text{RNAP}]/K'_d)[\text{DNA}]}{1 + [\text{RNAP}]/K'_d + [\text{Rep}]/K_d},$$

in which K'_d is the dissociation constant of RNAP from the promoter while K_d is the dissociation constant of Rep from the promoter. The complex C, having RNAP bound, will allow transcription, while the complex [DNA:Rep] will not allow transcription as it is not bound to RNAP. The transcription rate will be proportional to C, so that the rate of change of mRNA is described by

$$\frac{d[\text{mRNA}]}{dt} = \alpha_0 \frac{([\text{RNAP}]/K'_d)[\text{DNA}]}{1 + [\text{RNAP}]/K'_d + [\text{Rep}]/K_d} - \gamma[\text{mRNA}],$$

in which the production rate is given by

$$f([\text{Rep}]) = \alpha_0 \frac{([\text{RNAP}]/K'_d)[\text{DNA}]}{1 + [\text{RNAP}]/K'_d + [\text{Rep}]/K_d}.$$

If the repressor binds to the promoter with cooperativity n , the above expression becomes (see Section 2.1)

$$f([\text{Rep}]) = \alpha_0 \frac{([\text{RNAP}]/K'_d)[\text{DNA}]}{1 + [\text{RNAP}]/K'_d + [\text{Rep}]^n/(K_d k_m)},$$

in which k_m is the dissociation constant of the reaction of n molecules of Rep binding together. The function f is usually denoted by the standard Hill function form

$$f([\text{Rep}]) = \frac{\alpha}{1 + ([\text{Rep}]/K)^n},$$

in which α and K are implicitly defined. In practice we have that $[\text{RNAP}]/K_{d,a} \gg 1$ since there is plenty of RNAP in the cell. As a consequence we obtain the expressions $\alpha = \alpha_0[\text{DNA}]$ and $K = K_d K'_d k_m / [\text{RNAP}]$.

Finally, if the repressor is not strong and allows RNAP to still bind to the promoter at a small rate, the above expression modifies to the new form (see Section 2.1)

$$f([\text{Rep}]) = \frac{\alpha}{1 + ([\text{Rep}]/K)^n} + \bar{\alpha},$$

in which $\bar{\alpha}$ is the basal expression level when the promoter is fully repressed, usually referred to as “leakiness”.

To model the production rate of mRNA in the case in which an activator Act binds to the promoter with cooperativity n , we can consider first the case in which RNAP binds only when the activator is already bound to the promoter. This can be well modeled by a cooperative binding scenario as illustrated in Section 2.1. According to this scenario, the concentration of the complex $[\text{RNAP:DNA}^\circ]$ is given by

$$[\text{RNAP:DNA}^\circ] = C' = \frac{([\text{RNAP}][\text{Act}]^n)/(K_d K'_d k_m)[\text{DNA}]}{1 + ([\text{Act}]^n/K_d k_m)(1 + [\text{RNAP}]/K'_d)},$$

in which K'_d is the dissociation constant of RNAP with the complex of DNA bound to Act and K_d is the dissociation constant of Act with DNA. Since the production rate of mRNA is proportional to $[\text{RNAP:DNA}^\circ]$, we have that

$$\frac{d[\text{mRNA}]}{dt} = f([\text{Act}]) - \gamma[\text{mRNA}]$$

with

$$f([\text{Act}]) = \alpha_0 \frac{([\text{RNAP}][\text{Act}]^n)/(K_d K'_d k_m)[\text{DNA}]}{1 + ([\text{Act}]^n/K_d k_m)(1 + [\text{RNAP}]/K'_d)} =: \frac{\alpha([\text{Act}]/K)^n}{1 + ([\text{Act}]/K)^n},$$

in which α and K are implicitly defined. Since in practice $[\text{RNAP}]/K_{d,a} \gg 1$, we have that $\alpha = \alpha_0[\text{DNA}]$ and $K = K_d K'_d k_m / [\text{RNAP}]$.

The right-hand side expression is in the standard Hill function form. Figure 2.5 shows the shape of these Hill functions both for an activator and a repressor. If we assume that RNAP can still bind to DNA even when the activator is not bound, we have an additional basal expression rate $\bar{\alpha}$ so that the new form of the production rate is given by

$$f([\text{Act}]) = \frac{\alpha([\text{Act}]/K)^n}{1 + ([\text{Act}]/K)^n} + \bar{\alpha}.$$

Example 2.2 (Repressilator). As an example of how these models can be used, we consider the model of a “repressilator,” originally due to Elowitz and Leibler [26] and briefly described in Section 1.5. The repressilator is a synthetic circuit in which three proteins each repress another in a cycle. This is shown schematically in Figure 2.6a, where the three proteins are TetR, λ cI and LacI.

We can model this system using three copies of equation (4.2), with A and B replaced by the appropriate combination of TetR, cI and LacI. The state of the

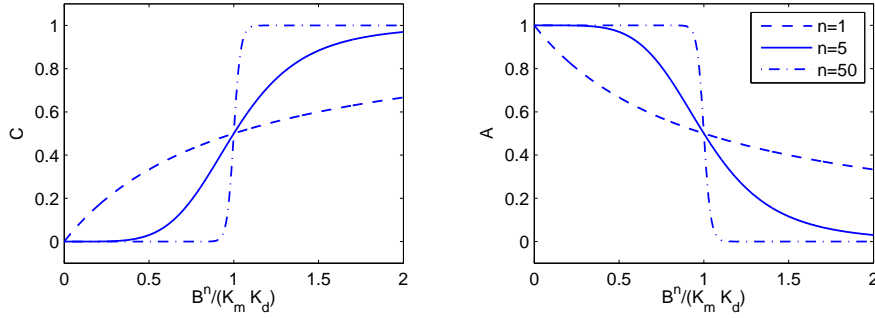


Figure 2.5: Hill function for an activator (left) and a repressor (right).

system is then given by $x = (m_{\text{TetR}}, p_{\text{TetR}}, m_{\text{cI}}, p_{\text{cI}}, m_{\text{LacI}}, p_{\text{LacI}})$. The full dynamics become

$$\frac{d}{dt} \begin{pmatrix} m_{\text{TetR}} \\ p_{\text{TetR}} \\ m_{\text{cI}} \\ p_{\text{cI}} \\ m_{\text{LacI}} \\ p_{\text{LacI}} \end{pmatrix} = \begin{pmatrix} \frac{\alpha_{\text{LacI}}}{1 + (p_{\text{LacI}}/K_{\text{LacI}})^n} + \bar{\alpha}_{\text{TetR}} - \gamma m_{\text{TetR}} \\ \beta_{\text{TetR}} m_{\text{TetR}} - \delta p_{\text{TetR}} \\ \frac{\alpha_{\text{TetR}}}{1 + (p_{\text{TetR}}/K_{\text{TetR}})^n} + \bar{\alpha}_{\text{cI}} - \gamma m_{\text{cI}} \\ \beta_{\text{cI}} m_{\text{cI}} - \delta p_{\text{cI}} \\ \frac{\alpha_{\text{cI}}}{1 + (p_{\text{cI}}/K_{\text{cI}})^n} + \bar{\alpha}_{\text{LacI}} - \gamma m_{\text{LacI}} \\ \beta_{\text{LacI}} m_{\text{LacI}} - \delta p_{\text{LacI}} \end{pmatrix} \quad (2.14)$$

Figure 2.6b shows the traces of the three protein concentrations for (symmetric) parameters $n = 2$, $\alpha = 0.5$, $K = 6.25 \times 10^{-4}$, $\alpha_0 = 5 \times 10^{-4}$, $\gamma = 5.8 \times 10^{-3}$, $\beta = 0.12$ and $\delta = 1.2 \times 10^{-3}$ with initial conditions $x(0) = (1, 200, 0, 0, 0, 0)$ (following [26]).

▽

As indicated earlier, many activators and repressors operate in the presence of inducers. To incorporate these dynamics in our description, we simply have to add the reactions that correspond to the interaction of the inducer with the relevant protein. For a negative inducer, we can simply add a reaction in which the inducer binds the regulator protein and effectively sequesters it so that it cannot interact with the DNA. For example, a negative inducer operating on a repressor could be modeled by adding the reaction



Since the above reactions are very fast compared to transcription, they can be assumed at the quasi-steady state. Hence, the free amount of repressor that can still bind to the promoter can be calculated by writing the ODE model corresponding

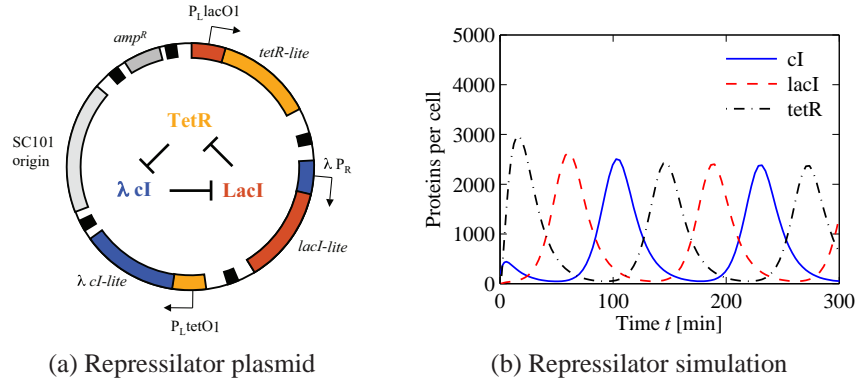


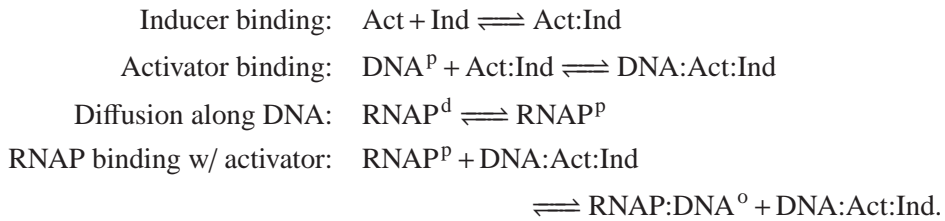
Figure 2.6: The repressilator genetic regulatory network. (a) A schematic diagram of the repressilator, showing the layout of the genes in the plasmid that holds the circuit as well as the circuit diagram (center). (b) A simulation of a simple model for the repressilator, showing the oscillation of the individual protein concentrations. (Figure courtesy M. Elowitz.)

to the above reactions and by setting the time derivatives to zero. This yields to

$$[\text{Rep}] = \frac{[\text{Rep}]_{\text{tot}}}{1 + [\text{Ind}]/\bar{K}_d},$$

in which $[\text{Rep}]_{\text{tot}} = [\text{Rep}] + [\text{Rep}:\text{Ind}]$ is the total amount of repressor (bound and not bound to the inducer) and \bar{K}_d is the dissociation constant of Ind binding to Rep. This expression of the repressor concentration needs to be substituted in the expression of the production rate $f([\text{Rep}])$.

Positive inducers can be handled similarly, except now we have to modify the binding reactions to only work in the presence of a regulatory protein bound to an inducer. For example, a positive inducer on an activator would have the modified reactions



Hence, in the expression of the production rate $f([\text{Act}])$, we should substitute in place of $[\text{Act}]$ the concentration $[\text{Act:Ind}]$. This concentration, in turn, can be simply computed at the quasi-steady state by writing the ODE model for the inducer binding reaction and equating the time derivatives to zero. This yields

$$[\text{Act:Ind}] = \frac{[\text{Act}]_{\text{tot}}[\text{Ind}]/\bar{K}_d}{1 + [\text{Ind}]/\bar{K}_d},$$

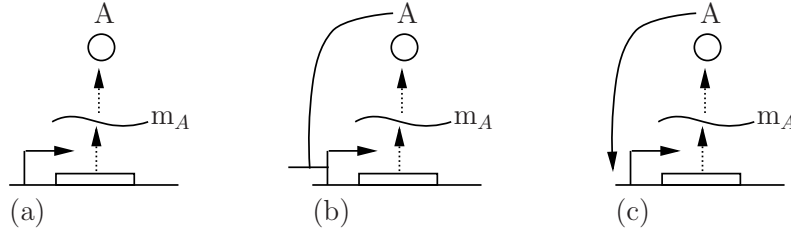


Figure 2.7: Autoregulation of gene expression. The three circuits control the expression of gene regulation using (a) unregulated, (b) negative autoregulation and (c) positive autoregulation.

in which $[\text{Act}]_{\text{tot}} = [\text{Act}] + [\text{Act:Ind}]$ and \bar{K}_d is the dissociation constant of the binding of Ind with Act.

Example 2.3 (Autoregulation of gene expression). Consider the three circuits shown in Figure 2.7, representing a unregulated gene, a negatively autoregulated gene and a positively autoregulated gene. We want to model the dynamics of the protein A starting from zero initial conditions for the three different cases to understand how the three different circuit topologies affect dynamics.

The dynamics of the three circuits can be written in a common form,

$$\frac{dm_A}{dt} = f(A) - \gamma m_A, \quad \frac{dA}{dt} = \beta m_A - \delta A, \quad (2.15)$$

where $f(A)$ has the form

$$f_{\text{unreg}}(A) = \alpha_B, \quad f_{\text{repress}}(A) = \frac{\alpha_B K}{K + A^n} + \alpha_0, \quad f_{\text{activate}}(A) = \frac{\alpha_A A^n}{K + A^n} + \alpha_B$$

We choose the parameters to be

$$\begin{aligned} \alpha_A &= 1/3, & \alpha_B &= 1/2, & \alpha_0 &= 5 \times 10^{-4}, \\ \beta &= 20 \log(2)/120, & \gamma &= \log(2)/120, & \delta &= \log(2)/600, \\ K &= 10^8, & n &= 2, \end{aligned}$$

corresponding to biologically plausible values. Note that the parameters are chosen so that $f(0) \approx \alpha_B$ for each circuit.

Figure 2.8a shows the results of the simulation. We see that initial increase in protein concentration is identical for each circuit, consistent with our choice of Hill functions and parameters. As the expression level increases, the effects of positive and negative are seen, leading to different steady state expression levels. In particular, the negative feedback circuit reaches a lower steady state expression level while the positive feedback circuit settles to a higher value.

In some situations, it makes sense to ask whether different circuit topologies have different properties that might lead us to choose one over another. In the case

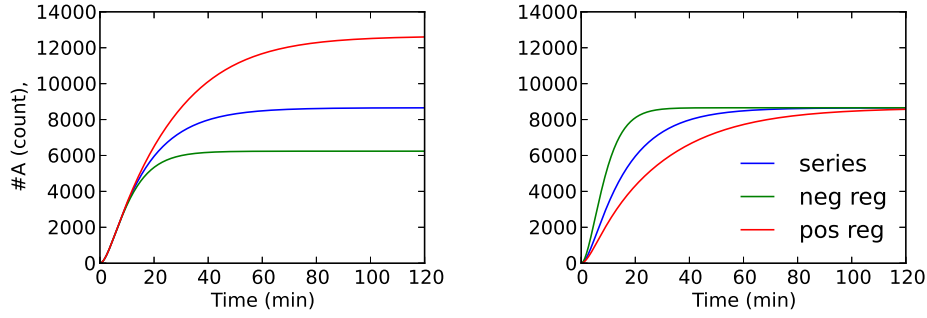


Figure 2.8: Simulations for autoregulated gene expression. (a) Non-normalized expression levels. (b) Normalized expression.

where the circuit is going to be used as part of a more complex pathway, it may make the most sense to compare circuits that produce the same steady state concentration of the protein A. To do this, we must modify the parameters of the individual circuits, which can be done in a number of different ways: we can modify the promoter strengths, degradation rates, or other molecular mechanisms reflected in the parameters.

The steady state expression level for the negative autoregulation case can be adjusted by using a stronger promoter (modeled by α_B) or ribosome binding site (modeled by β). The equilibrium point for the negative autoregulation case is given by the solution of the equations

$$m_{A,e} = \frac{\alpha K}{\gamma(K + A_e^n)}, \quad A_e = \frac{\beta}{\delta} m_{A,e}.$$

These coupled equations can be solved for $m_{A,e}$ and A_e , but in this case we simply need to find values α'_B and β' that give the same values as the unregulated case. For example, if we equate the mRNA levels of the unregulated system with that of the negatively autoregulated system, we have

$$\frac{\alpha_B}{\gamma} = \frac{1}{\gamma} \left(\frac{\alpha'_B K}{K + A_e^n} + \alpha_0 \right) \implies \alpha'_B = (\alpha_B - \alpha_0) \frac{K + A_e^n}{K}, \quad A_e = \frac{\alpha_B \beta}{\gamma \delta},$$

where A_e is the desired equilibrium value (which we choose using the unregulated case as a guide).

A similar calculation can be done for the case of positive autoregulation, in this case decreasing the promoter parameters α_A and α_B so that the steady state values match. A simple way to do this is to leave α_A unchanged and decrease α_B to account for the positive feedback. Solving for α'_B to give the same mRNA levels as the unregulated case yields

$$\alpha'_B = \alpha_B - \alpha_A \frac{A_e^n}{K + A_e^n}.$$

Figure 2.8b shows simulations of the expression levels over time for the modified circuits. We see now that the expression levels all reach the same steady state value. The negative autoregulated circuit has the property that it reaches the steady state more quickly, due to the increased rate of protein expression when A is small ($\alpha'_B > \alpha_B$). Conversely, the positive autoregulated circuit has a slower rate of expression than the constitutive case, since we have lowered the rate of protein expression when A is small. The initial higher and lower expression rates are compensated for via the autoregulation, resulting in the same expression level in steady state. ∇

We have described how the Hill function can model the regulation of a gene by a single transcription factor. However, genes can also be regulated by multiple transcription factors, some of which may be activators and some may be repressors. In this case, the promoter controlling the expression of the gene is called a combinatorial promoter. The mRNA production rate can thus take several forms depending on the roles (activators versus repressors) of the various transcription factors [4]. In general, the production rate resulting from a promoter that takes as input transcription factors p_i for $i \in \{1, \dots, N\}$ will be denoted $f(p_1, \dots, p_n)$.

Thus, the dynamics of a transcriptional module is often well captured by the ordinary differential equations

$$\frac{dm_y}{dt} = f(p_1, \dots, p_n) - \gamma_y m_y, \quad \frac{dp_y}{dt} = \beta_y m_y - \delta_y p_y, \quad (2.16)$$

where m_y denotes the concentration of mRNA translated by gene y , the constants γ_y and δ_y incorporate the dilution and degradation processes, and β_y is a constant that establishes the rate at which the mRNA is translated.

For a combinatorial promoter with two input proteins, an activator p_a and a repressor p_r , in which the activator cannot bind if the repressor is bound to the promoter, the function $f(p_a, p_r)$ can be obtained by employing the competitive binding in the reduced order models of Section 2.1. In this case, assuming the activator has cooperativity n and the repressor has cooperativity m , we obtain the expression

$$f(p_a, p_r) = \alpha \frac{(p_a^n)/(K_{m,a}K_{d,a})}{1 + p_a^n/(K_{m,a}K_{d,a}) + p_r^m/(K_{m,r}K_{d,r})}.$$

Here, $K_{d,a}$ and $K_{d,r}$ are the dissociation constant of the activator and repressor, respectively, from the DNA promoter site, while $K_{m,a}$ and $K_{m,r}$ are the dissociation constants for the cooperative binding reactions for the activator and repressor. In the case in which the activator is “leaky”, that is, some transcription still occurs even when there is no activator, the above expression will be modified to

$$f(p_a, p_r) = \alpha \frac{(p_a^n)/(K_{m,a}K_{d,a}) + \bar{\alpha}}{1 + p_a^n/(K_{m,a}K_{d,a}) + p_r^m/(K_{m,r}K_{d,r})},$$

in which $\bar{\alpha}$ is the basal transcription rate when no activator and no repressor are present.

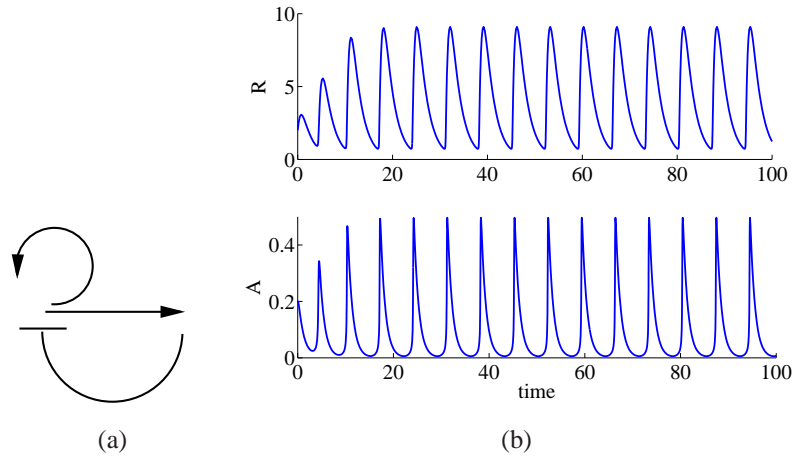


Figure 2.9: The activator-repressor clock network. (a) A schematic diagram of the circuit. (b) A simulation of a simple model for the clock, showing the oscillation of the individual protein concentrations. In the simulation, we have chosen $K_a = K_r = 1$, $\alpha_A = \alpha_R = 100$, $\bar{\alpha}_A = 0.4$, $\bar{\alpha}_R = 0.004$, $\delta_A = 1$, $\delta_R = 0.5$, $n = 2$, and $m = 4$.

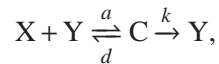
Example 2.4 (Activator-repressor clock). As an example of where combinatorial promoters are used, we illustrate in this example an activator-repressor clock that was fabricated in *E. coli* and is shown in Figure 2.9(a) [?].

The activator A is self activated and is also repressed by the repressor R. Hence, the promoter controlling the expression of A is a combinatorial promoter. The model describing this system, assuming the mRNA dynamics have reached its quasi-steady state, is given by

$$\frac{dA}{dt} = \frac{\alpha_A A^n / K_a + \bar{\alpha}_A}{A^n / K_a + R^m / K_r + 1} - \delta_A A, \quad \frac{dR}{dt} = \frac{\alpha_R A^n / K_a + \bar{\alpha}_R}{A^n / K_a + 1} - \delta_R R$$

Figure 2.9 (b) shows the behavior of the activator and the repressor concentrations. We will come back to this design in Chapter 6, in which we will use the tools introduced in Chapter 3 to establish parameter conditions under which the system admits a periodic solution. ∇

Finally, a simple regulation mechanism is based on altering the half life of a protein. Specifically, the degradation rate of a protein is determined by the amounts of proteases present, which bind to recognition sites (degradation tags) and then degrade the protein. Degradation of a protein X by a protease Y can then be modeled by the following two-step reaction



in which C is the complex of the protease bound to the protein. By the end of the reaction, protein X has been degraded to nothing.

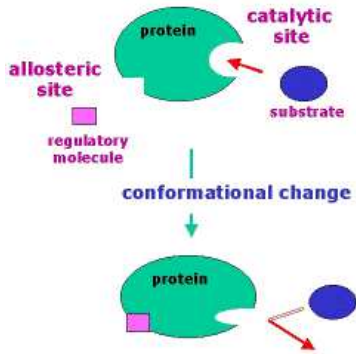


Figure 2.10: In allosteric regulation, a regulatory molecule binds to a site separate from the catalytic site (active site) of an enzyme. This binding causes a change in the three dimension conformation of the protein, turning off (or turning on) the catalytic site. Permission pending.

2.4 Post-Transcriptional Regulation

In addition to regulation of expression through modifications of the process of transcription, cells can also regulate the production and activity of proteins via a collection of other post-transcriptional modifications. These include methods of modulating the translation of proteins, as well as affecting the activity of a protein via changes in its conformation, as shown in Figure 1.9.

Allosteric modifications to proteins

In allosteric regulation, a regulatory molecule binds to a site separate from the catalytic site (active site) of an enzyme. This binding causes a change in the three dimension conformation of the protein, turning off (or turning on) the catalytic site (Figure 2.10).

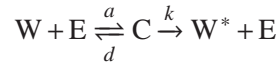
Enzyme activity can often be altered by small signaling molecules called allosteric effectors, which can either be activators or inhibitors, just like inducers work for activation or inhibition of transcription factors. Inhibition can either be competitive or not competitive. In the case of competitive inhibition, the inhibitor competes with the substrate for binding the enzyme; that is, the substrate can bind to the enzyme only if the inhibitor is not bound. In the case of non-competitive inhibition, the substrate can be bound to the enzyme even if the latter is bound to the inhibitor. In this case, however, the product may not be able to form or may form at a lower rate, in which case, we have partial inhibition.

Activation can be absolute or not. Specifically, an activator is absolute when the enzyme can bind to the substrate only when bound to the activator. Otherwise, the

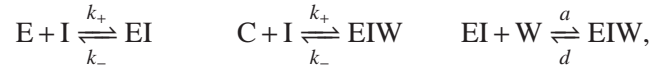
activator is not absolute. In this section, we derive the expressions for the production rate of the active protein in an enzymatic reaction in the two most common cases: when we have a (non-competitive) inhibitor I or an (absolute) activator A of the enzyme.

Allosteric inhibition

Consider the standard enzymatic reaction



in which enzyme E activates protein W and transforms it to the active form W^{*} . Let I be a (non-competitive) inhibitor of enzyme E so that when E is bound to I, the complex EI can still bind to inactive protein W, however, the complex EIW is non-productive, that is, it does not produce the active protein W^{*} . Then, we have the following additional reactions:



with the conservation laws (assuming W_{tot} is in much greater amounts than E_{tot})

$$E_{\text{tot}} = E + C + EI + EIW, \quad W_{\text{tot}} = W + W^{*} + C + EIW \approx W + W^{*}.$$

Hence, the production rate of W^{*} is given by $dW^{*}/dt = kC$. Since we have that $k_{+}, k_{-}, a, b \gg k$, we can assume all the complexes to be at the quasi steady state. This gives

$$EIW = \frac{a}{d} EI \cdot W, \quad EI = \frac{k_{+}}{k_{-}} E \cdot I, \quad C = \frac{1}{K_m} W \cdot E,$$

in which $K_m = (d+k)/a$ is the Michaelis-Menten constant. Using these expressions, the conservation law for the enzyme, and the fact that $a/d \approx 1/K_m$, we obtain

$$E = \frac{E_{\text{tot}}}{(I/K_d + 1)(1 + W/K_m)}, \quad \text{with } K_d = k_{-}/k_{+},$$

so that

$$C = \frac{W}{W + K_m} \frac{E_{\text{tot}}}{1 + I/K_d}$$

and, as a consequence,

$$\frac{dW^{*}}{dt} = k_1 E_{\text{tot}} \left(\frac{1}{1 + I/K_d} \right) \left(\frac{W}{W + K_m} \right).$$

Using the conservation law for W , this is also equivalent to

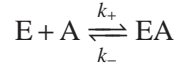
$$\frac{dW^*}{dt} = k_1 E_{\text{tot}} \left(\frac{1}{1 + I/K_d} \right) \left(\frac{(W_{\text{tot}} - W^*)}{(W_{\text{tot}} - W^*) + K_m} \right).$$

In our earlier derivations of the Michaelis-Menten kinetics $V_{\text{max}} = k_1 E_{\text{tot}}$ was called the maximal speed of modification, which occurs when the enzyme is completely saturated by the substrate (Section 2.1). Hence, the effect of a non-competitive inhibitor is to decrease the maximal speed of modification by a factor $1/(1 + I/K_d)$.

Another type of inhibition occurs when the inhibitor is competitive, that is, when I is bound to E , the complex EI cannot bind to protein W . Since E can either bind to I or W (not both), I competes against W for binding to E . See Exercise 2.11.

Allosteric activation

In this case, the enzyme E can transform W to its active form only when it is bound to A . Also, we assume that E cannot bind W unless E is bound to A (from here, the name absolute activator). The reactions are therefore modified to be



and



with conservation laws

$$E_{\text{tot}} = E + EA + EAW, \quad W_{\text{tot}} \approx W + W^*.$$

The production rate of W^* is given by $dW^*/dt = kEAW$. Assuming as above that the complexes are at the quasi-steady state, we have that

$$EA = \frac{E \cdot A}{K_d}, \quad EAW = \frac{W \cdot EA}{K_m},$$

which, using the conservation law for E , leads to

$$E = \frac{E_{\text{tot}}}{(1 + W/K_m)(1 + A/K_d)} \quad \text{and} \quad EAW = \left(\frac{A}{A + K_d} \right) \left(\frac{W}{W + K_m} \right) E_{\text{tot}}.$$

Hence, we have that

$$\frac{dW^*}{dt} = kE_{\text{tot}} \left(\frac{A}{A + K_d} \right) \left(\frac{W}{W + K_m} \right).$$

Using the conservation law for W , this is also equivalent to

$$\frac{dW^*}{dt} = kE_{\text{tot}} \left(\frac{A}{A + K_d} \right) \left(\frac{(W_{\text{tot}} - W^*)}{(W_{\text{tot}} - W^*) + K_m} \right).$$

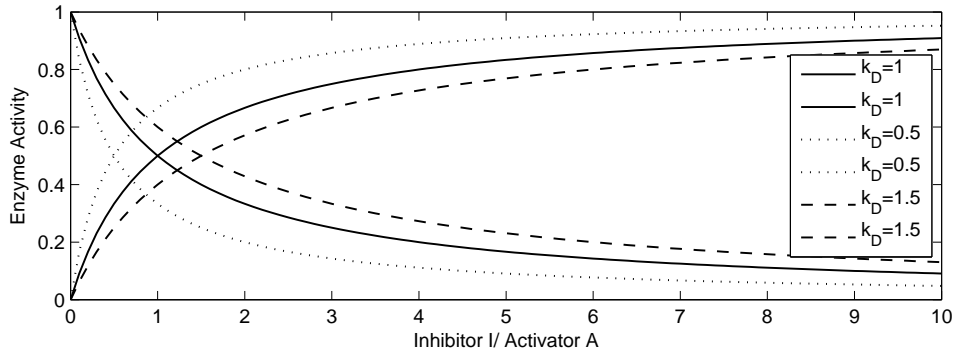


Figure 2.11: Enzyme activity in the presence of allosteric effectors (activators or inhibitors). The red plots show the enzyme activity in the presence of an inhibitor as a function of the inhibitor concentration. The green plots show the enzyme activity in the presence of an activator as a function of the activator concentration. The different plots show the effect of the dissociation constant.

The effect of an absolute activator is to modulate the maximal speed of modification by a factor $A/(A + K_d)$.

Figure 2.11 shows the behavior of the enzyme activity as a function of the allosteric effector. As the dissociation constant decreases, that is, the affinity of the effector increases, a very small amount of effector will cause the enzyme activity to be completely “on” in the case of the activator and completely “off” in the case of the inhibitor.

Another type of activation occurs when the activator is not absolute, that is, when E can bind to W directly, but cannot activate W unless the complex EW first binds A (see Exercise 2.12).

Covalent modifications to proteins

Covalent modification is a post-translational protein modification that affects the activity of the protein. It plays an important role both in the control of metabolism and in signal transduction. Here, we focus on *reversible* cycles of modification, in which a protein is interconverted between two forms that differ in activity either because of effects on the kinetics relative to substrates or for altered sensitivity to effectors.

At a high level, a covalent modification cycle involves a target protein X, an enzyme Z for modifying it, and a second enzyme Y for reversing the modification (see Figure 2.12). We call X^* the activated protein. There are often allosteric effectors or further covalent modification systems that regulate the activity of the modifying enzymes, but we do not consider this added level of complexity here. There are several types of covalent modification, depending on the type of acti-

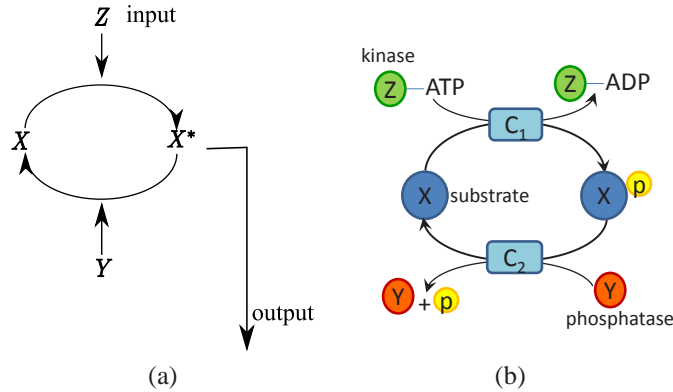


Figure 2.12: (Left) General diagram representing a covalent modification cycle. (Right) Detailed view of a phosphorylation cycle including ATP, ADP, and the exchange of the phosphate group “p”.

vation of the protein. *Phosphorylation* is a covalent modification that takes place mainly in eukaryotes and involves activation of the inactive protein X by addition of a phosphate group, PO_4 . In this case, the enzyme Z is called a *kinase* while the enzyme Y is called *phosphatase*. Another type of covalent modification, which is very common in both prokaryotes and eukaryotes, is *methylation*. Here, the inactive protein is activated by the addition of a methyl group, CH_3 .

The reactions describing this system are given by the following two enzymatic reactions, also called a two step reaction model,



The corresponding ODE model is given by

$$\begin{aligned} \frac{dZ}{dt} &= -a_1 Z \cdot X + (k_1 + d_1) C_1, & \frac{dX^*}{dt} &= k_1 C_1 - a_2 Y \cdot X^* + d_2 C_2, \\ \frac{dX}{dt} &= -a_1 Z \cdot X + d_1 C_1 + k_2 C_2, & \frac{dC_2}{dt} &= a_2 Y \cdot X^* - (d_2 + k_2) C_2, \\ \frac{dC_1}{dt} &= a_1 Z \cdot X - (d_1 + k_1) C_1, & \frac{dY}{dt} &= -a_2 Y \cdot X^* + (d_2 + k_2) C_2. \end{aligned}$$

Furthermore, we have that the total amounts of enzymes Z and Y are conserved. Denote the total concentrations of Z and Y by Z_{tot} , Y_{tot} , respectively. Then, we have also the conservation laws $Z + C_1 = Z_{\text{tot}}$ and $Y + C_2 = Y_{\text{tot}}$. We can thus reduce the above system of ODE to the following one, in which we have substituted $Z =$

$Z_{\text{tot}} - C_1$ and $Y = Y_{\text{tot}} - C_2$:

$$\begin{aligned}\frac{dC_1}{dt} &= a_1(Z_{\text{tot}} - C_1) \cdot X - (d_1 + k_1)C_1, \\ \frac{dX^*}{dt} &= k_1C_1 - a_2(Y_{\text{tot}} - C_2) \cdot X^* + d_2C_2, \\ \frac{dC_2}{dt} &= a_2(Y_{\text{tot}} - C_2) \cdot X^* - (d_2 + k_2)C_2.\end{aligned}$$

As for the case of the enzymatic reaction, this system cannot be analytically integrated. To simplify it, we can perform a similar approximation as done for the enzymatic reaction. In particular, the complexes C_1 and C_2 are often assumed to reach their steady state values very quickly because $a_1, d_1, a_2, d_2 \gg k_1, k_2$. Therefore, we can approximate the above system by substituting for C_1 and C_2 their steady state values, given by the solutions to

$$a_1(Z_{\text{tot}} - C_1) \cdot X - (d_1 + k_1)C_1 = 0$$

and

$$a_2(Y_{\text{tot}} - C_2) \cdot X^* - (d_2 + k_2)C_2 = 0.$$

By solving these equations, we obtain that

$$C_2 = \frac{Y_{\text{tot}}X^*}{X^* + K_{m,2}}, \quad \text{with} \quad K_{m,2} = \frac{d_2 + k_2}{a_2}$$

and

$$C_1 = \frac{Z_{\text{tot}}X}{X + K_{m,1}}, \quad \text{with} \quad K_{m,1} = \frac{d_1 + k_1}{a_1}.$$

As a consequence, the ODE model of the phosphorylation system can be well approximated by

$$\frac{dX^*}{dt} = k_1 \frac{Z_{\text{tot}}X}{X + K_{m,1}} - a_2 \frac{Y_{\text{tot}}K_{m,2}}{X^* + K_{m,2}} \cdot X^* + d_2 \frac{Y_{\text{tot}}X^*}{X^* + K_{m,2}},$$

which, considering that $a_2K_{m,2} - d_2 = k_2$, leads finally to

$$\frac{dX^*}{dt} = k_1 \frac{Z_{\text{tot}}X}{X + K_{m,1}} - k_2 \frac{Y_{\text{tot}}X^*}{X^* + K_{m,2}}. \quad (2.17)$$

We will come back to the modeling of this system after we have introduced singular perturbation theory, through which we will be able to perform a formal analysis and mathematically characterize the assumptions needed for approximating the original system by the first order ODE model (2.17). In the model of equation (2.17), we have that $X = X_{\text{tot}} - X^* - C_1 - C_2$ by the conservation laws. A standard assumption is that the amounts of enzymes are small compared to the amount of substrate, so that $X \approx X_{\text{tot}} - X^*$ [34].

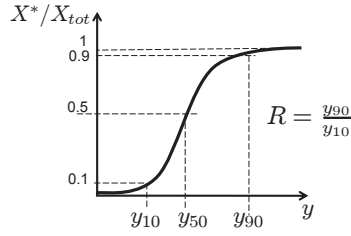


Figure 2.13: Steady state characteristic curve showing the relevance of the response coefficient for ultrasensitivity. As $R \rightarrow 1$, the points y_{10} and y_{90} tend to each other.

Ultrasensitivity

One relevant aspect of the response of the covalent modification cycle to its input is the sensitivity of the steady state characteristic curve. Specifically, what parameters affect the shape of the steady state response is a crucial question. To determine the steady state characteristics, which shows how the steady state of X^* changes when the input stimulus Z_{tot} is changed, we set $dX^*/dt = 0$ in equation (2.17). Using the approximation $X \approx X_{\text{tot}} - X^*$, denoting $V_1 := k_1 Z_{\text{tot}}$, $V_2 := k_2 Y_{\text{tot}}$, $\bar{K}_1 := K_{m,1}/X_{\text{tot}}$, and $\bar{K}_2 := K_{m,2}/X_{\text{tot}}$, we obtain

$$y := \frac{V_1}{V_2} = \frac{X^*/X_{\text{tot}} (\bar{K}_1 + (1 - X^*/X_{\text{tot}}))}{(\bar{K}_2 + X^*/X_{\text{tot}})(1 - X^*/X_{\text{tot}})}. \quad (2.18)$$

We are interested in the shape of the steady state curve of X^* as function of y . This shape is usually characterized by two key parameters: the response coefficient, denoted R , and the point of half maximal induction, denoted y_{50} . Let y_α denote the value of y corresponding to having X^* equal $\alpha\%$ of the maximum value of X^* obtained for $y = \infty$, which is equal to X_{tot} . Then, the response coefficient is defined as

$$R := \frac{y_{90}}{y_{10}},$$

and measures how switch-like the response is (Figure 2.13). When $R \rightarrow 1$ the response becomes switch-like. In the case in which the steady state characteristic is a Hill function, we have that $X^* = y^n / (K + y^n)$, so that $y_\alpha = (\alpha / (100 - \alpha))^{1/n}$ and as a consequence

$$R = (81)^{(1/n)}, \text{ or equivalently } n = \frac{\log(81)}{\log(R)}.$$

Hence, when $n = 1$, that is, the characteristic is of the Michaelis-Menten type, we have that $R = 81$, while when n increases, R decreases. Usually, when $n > 1$ the response is referred to as *ultrasensitive*. The formula $n = \log(81)/\log(R)$ is often

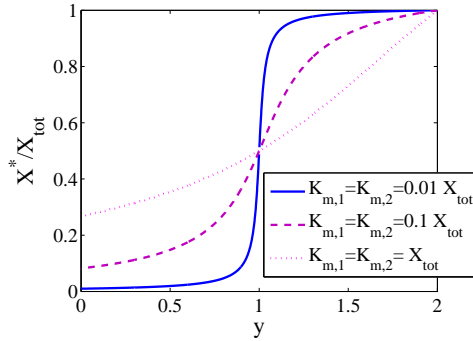


Figure 2.14: Steady state characteristics of a covalent modification cycle as a function of the Michaelis-Menten constants K_1 and K_2 .

employed to estimate the *apparent Hill coefficient* of a dose response curve (the input/output steady state characteristic curve obtained from experimental data) since R can be calculated for any response curve directly from the data points.

In the case of the current system, from equation (2.18), we have that

$$y_{90} = \frac{(\bar{K}_1 + 0.1) 0.9}{(\bar{K}_2 + 0.9) 0.1} \quad \text{and} \quad y_{10} = \frac{(\bar{K}_1 + 0.9) 0.1}{(\bar{K}_2 + 0.1) 0.9},$$

so that

$$R = 81 \frac{(\bar{K}_1 + 0.1)(\bar{K}_2 + 0.1)}{(\bar{K}_2 + 0.9)(\bar{K}_1 + 0.9)}.$$

As a consequence, when $\bar{K}_1, \bar{K}_2 \gg 1$, we have that $R \rightarrow 81$, which gives a Michaelis-Menten type of response. If instead $\bar{K}_1, \bar{K}_2 \ll 0.1$, we have that $R \rightarrow 1$, which corresponds to a theoretic Hill coefficient $n \gg 1$, that is, a switch-like response (Figure 2.14). In particular, if we have, for example, $\bar{K}_1 = \bar{K}_2 = 10^{-2}$, we obtain an apparent Hill coefficient greater than 13. This type of ultrasensitivity is usually referred to as *zero-order ultrasensitivity* because it is zero-order in the protein substrate, which saturates the enzyme surface. That is, referring to equation (2.17), when $K_{m,1}$ is much smaller than the amount of protein substrate X , we have that (at the steady state) $Z_{tot}X/(K_{m,1} + X) \approx Z_{tot}$. This rate is “zero order” in the substrate concentration since the enzyme is completely saturated by the substrate (no free enzyme is left, all is bound to the substrate).

One can study the behavior also of the point of half maximal induction

$$y_{50} = \frac{\bar{K}_1 + 0.5}{\bar{K}_2 + 0.5},$$

to find that as \bar{K}_2 increases, it decreases and that as \bar{K}_1 increases, it increases.

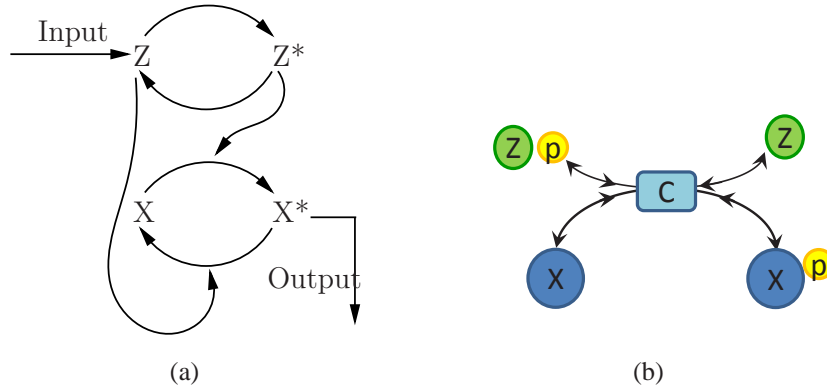
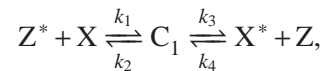


Figure 2.15: (a) Diagram of a phosphotransfer system. (b) Proteins X and Z are transferring the phosphate group p to each other.

Phosphotransfer systems

Phosphotransfer systems are also a common motif in cellular signal transduction. These structures are composed of proteins that can phosphorylate each other. In contrast to kinase-mediated phosphorylation, where the phosphate donor is usually ATP, in phosphotransfer the phosphate group comes from the donor protein itself (Figure 2.15). Each protein carrying a phosphate group can donate it to the next protein in the system through a reversible reaction. In this section, we describe a module extracted from the phosphotransferase system [?]. The complete cascade is discussed in next Section 2.5.

Let X be a transcription factor in its inactive form and let X* be the same transcription factor once it has been activated by the addition of a phosphate group. Let Z* be a phosphate donor, that is, a protein that can transfer its phosphate group to the acceptor X. The standard phosphotransfer reactions [74] can be modeled according to the two-step reaction model



in which C_1 is the complex of Z bound to X bound to the phosphate group. Additionally, protein Z can be phosphorylated and protein X* dephosphorylated by other phosphotransfer interactions. These reactions are modeled as one step reactions depending only on the concentrations of Z and X*, that is,



Protein X is assumed to be conserved in the system, that is, $X_{\text{tot}} = X + C_1 + X^*$. We assume that protein Z is produced with time-varying production rate $k(t)$ and

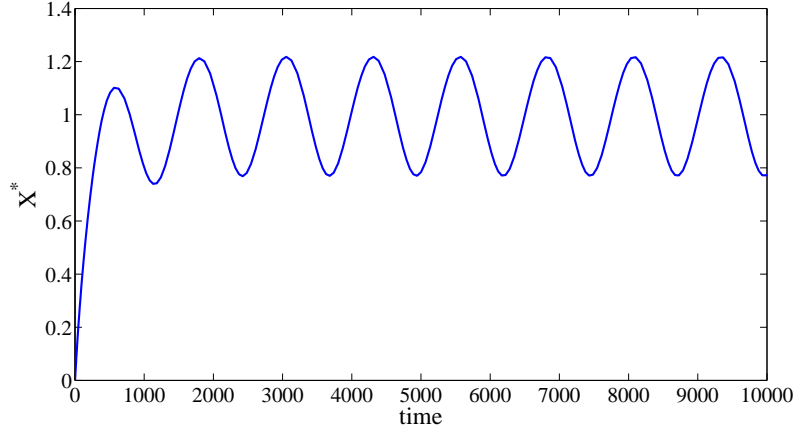


Figure 2.16: Output response of the phosphotransfer system with a step signal $k(t) = 1 + 0.5 \sin(\omega t)$. The parameters are given by $\delta = 0.01$, $X_{\text{tot}} = 5000$, $k_1 = k_2 = k_3 = k_4 = \pi_1 = \pi_2 = 0.01$.

decays with rate δ . The ODE model corresponding to this system is thus given by the equations

$$\begin{aligned}
 \frac{dZ}{dt} &= k(t) - \delta Z + k_3 C_1 - k_4 X^* Z - \pi_1 Z \\
 \frac{dC_1}{dt} &= k_1 X_{\text{tot}} \left(1 - \frac{X^*}{X_{\text{tot}}} - \frac{C_1}{X_{\text{tot}}} \right) Z^* - k_3 C_1 - k_2 C_1 + k_4 X^* Z \\
 \frac{dZ^*}{dt} &= \pi_1 Z + k_2 C_1 - k_1 X_{\text{tot}} \left(1 - \frac{X^*}{X_{\text{tot}}} - \frac{C_1}{X_{\text{tot}}} \right) Z^* \\
 \frac{dX^*}{dt} &= k_3 C_1 - k_4 X^* Z - \pi_2 X^*
 \end{aligned} \tag{2.19}$$

Sample simulation results when the input is a time-varying (periodic) stimulus are shown in Figure 2.16. The output X^* well tracks the input stimulus by virtue of the fast phosphotransfer reactions.

This model will be considered again in Chapter 7 when the phosphotransfer system is proposed as a possible realization of an insulation device to buffer systems from retroactivity effects.

2.5 Cellular subsystems

In the previous section we have studied how to model a variety of core processes that occur in cells. In this section we consider a few common “subsystems” in which these processes are combined for specific purposes.

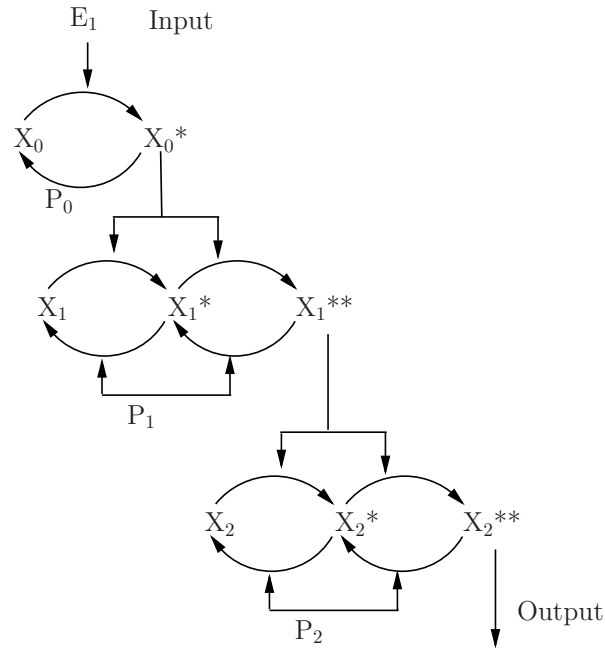


Figure 2.17: Schematic representing the MAPK cascade. It has three levels: the first one has a single phosphorylation, while the second and the third ones have a double phosphorylation.

Intercellular signaling: MAPK cascades

The Mitogen Activated Protein Kinase (MAPK) cascade is a recurrent structural motif in several signal transduction pathways (Figure 2.17). The cascade consists of a MAPK kinase kinase (MAPKKK), a MAPK kinase (MAPKK), and a MAPK. MAPKKKs activate MAPKKs by phosphorylation at two conserved sites and MAPKKs activate MAPKs by also phosphorylation at conserved sites. The cascade relays signals from the plasma membrane to targets in the cytoplasm and nucleus. It has been extensively studied and modeled. Here, we provide two different models. First, we build a modular model by viewing the system as the composition of single phosphorylation cycle modules (whose ODE model was derived earlier) and double phosphorylation cycle modules, whose ODE model we derive here. Then, we provide the full list of reactions describing the cascade and construct a mechanistic ODE model from scratch. We will then highlight the difference between the two derived models.

Double phosphorylation model. Consider the double phosphorylation motif in Figure 2.18. The reactions describing the system are given by

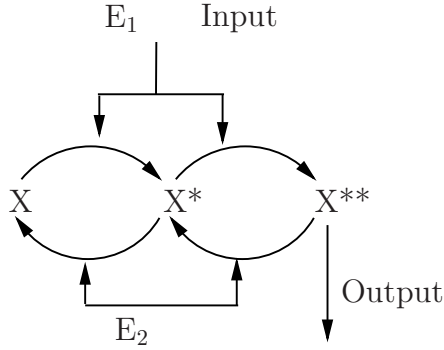
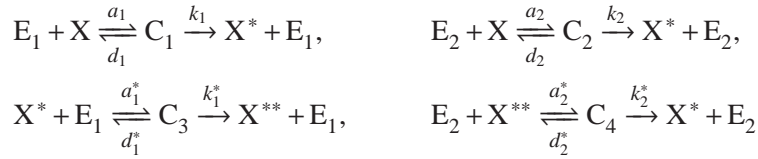


Figure 2.18: Schematic representing a double phosphorylation cycle. E_1 is the input and X^{**} is the output.



With conservation laws

$$\begin{aligned}
 E_1 + C_1 + C_3 &= E_{1,\text{tot}}, & E_2 + C_2 + C_4 &= E_{2,\text{tot}}, \\
 X_{\text{tot}} &= X + X^* + X^{**} + C_1 + C_2 + C_3 + C_4 \approx X + X^* + X^{**},
 \end{aligned}$$

in which we have assumed the the total amounts of enzymes are small compared to the total amount of substrate as we have explained earlier. Since $a_i, d_i \gg k_i$ and $a_i^*, d_i^* \gg k_i^*$, we can assume that the complexes are at the quasi-steady state (i.e., $\dot{C}_i \approx 0$), which gives the Michaelis-Menten form for the amount of formed complexes:

$$\begin{aligned}
 C_1 &= E_{1,\text{tot}} \frac{K_1^* X}{K_1^* X + K_1 X^* + K_1 K_1^*}, & C_3 &= E_{1,\text{tot}} \frac{K_1 X^*}{K_1^* X + K_1 X^* + K_1 K_1^*}, \\
 C_2 &= E_{2,\text{tot}} \frac{K_2^* X^*}{K_2^* X^* + K_2 X^{**} + K_2 K_2^*}, & C_4 &= E_{2,\text{tot}} \frac{K_2 X^{**}}{K_2^* X^* + K_2 X^{**} + K_2 K_2^*},
 \end{aligned}$$

in which $K_i = (d_i + k_i)/a_i$ and $K_i^* = (d_i^* + k_i^*)/a_i^*$ are the Michaelis-Menten constants for the enzymatic reactions. Since the complexes are at the quasi steady state, it follows that

$$\begin{aligned}
 \frac{d}{dt} X^* &= k_1 C_1 - k_2 C_2 - k_1^* C_3 + k_2^* C_4, \\
 \frac{d}{dt} X^{**} &= k_1^* C_3 - k_2^* C_4,
 \end{aligned}$$

from which, substituting the expressions of the complexes, we obtain that

$$\begin{aligned}\frac{d}{dt} X^* &= E_{1,\text{tot}} \frac{k_1 X K_1^* - k_1^* X^* K_1}{K_1^* X + K_1 X^* + K_1 K_1^*} + E_{2,\text{tot}} \frac{k_2^* X^{**} K_2 - k_2 X^* K_2^*}{K_2^* X^* + K_2 X^{**} + K_2 K_2^*} \\ \frac{d}{dt} X^{**} &= k_1^* E_{1,\text{tot}} \frac{K_1 X^*}{K_1^* X + K_1 X^* + K_1 K_1^*} - k_2^* E_{2,\text{tot}} \frac{K_2 X^{**}}{K_2^* X^* + K_2 X^{**} + K_2 K_2^*},\end{aligned}$$

in which $X = X_{\text{tot}} - X^* - X^{**}$.

Modular model of MAPK cascades

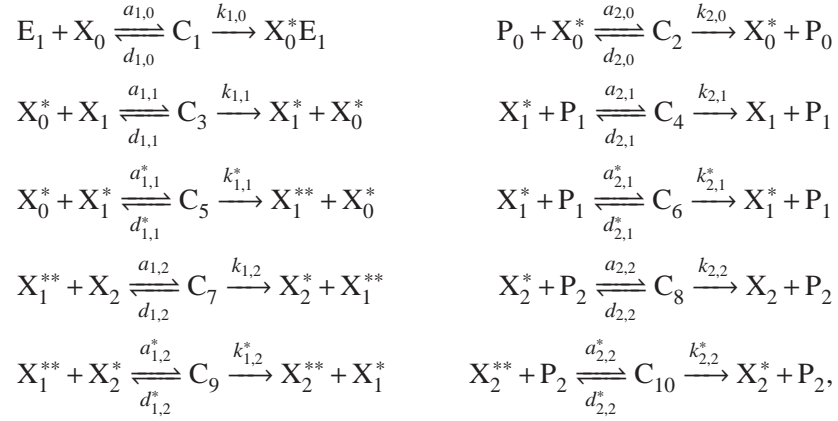
In this section, to simplify notation, we denote ‘‘MAPK’’ by X_2 . In a modular composition framework, the output of one stage becomes an input to the next stage downstream of it. Hence, X_0^* becomes the input enzyme that activates the phosphorylation of X_1 , and X_1^{**} becomes the input enzyme that activates the phosphorylation of X_2 . Let $(a_{1,i}, d_{1,i}, k_{1,i})$ and $(a_{2,i}, d_{2,i}, k_{2,i})$ be the association, dissociation, and catalytic rates for the forward and backward enzymatic reactions, respectively, for the first cycle at stage $i \in \{0, 1, 2\}$. Similarly, let $(a_{1,i}^*, d_{1,i}^*, k_{1,i}^*)$ and $(a_{2,i}^*, d_{2,i}^*, k_{2,i}^*)$ be the association, dissociation, and catalytic rates for the forward and backward enzymatic reactions, respectively, for the second cycle at stage $i \in \{1, 2\}$. Also, denote by $K_{1,i}$ and $K_{2,i}$ for $i \in \{0, 1, 2\}$ the Michaelis-Menten constants of the forward and backward enzymatic reactions, respectively, of the first cycle at stage i . Similarly, denote $K_{1,i}^*$ and $K_{2,i}^*$ for $i \in \{1, 2\}$ be the Michaelis-Menten constants of the forward and backward enzymatic reactions, respectively, of the second cycle at stage i . Let $P_{1,\text{tot}}$ and $P_{2,\text{tot}}$ be the total amounts of the X_1 and X_2 phosphatases, respectively. Then, the modular ODE model of the MAPK cascade is given by

$$\begin{aligned}\frac{d}{dt} X_0^* &= k_{1,0} E_{1,\text{tot}} \frac{X_0}{X_0 + K_{1,0}} - k_{2,0} P_{0,\text{tot}} \frac{X_0^*}{X_0^* + K_{2,0}} \\ \frac{d}{dt} X_1^* &= X_0^* \frac{k_{1,1} X_0 K_{1,1}^* - k_{1,1}^* X_1^* K_{1,1}}{K_{1,1}^* X_1 + K_{1,1} X_1^* + K_{1,1} K_{1,1}^*} + P_{1,\text{tot}} \frac{k_{2,1}^* K_{2,1} X_1^{**} - k_{2,1} X_1^* K_{2,1}^*}{K_{2,1}^* X_1^* + K_{2,1} X_1^{**} + K_{2,1} K_{2,1}^*} \\ \frac{d}{dt} X_1^{**} &= k_{1,1}^* X_0^* \frac{X_1^* K_{1,1}}{K_{1,1}^* X_1 + K_{1,1} X_1^* + K_{1,1} K_{1,1}^*} - k_{2,1}^* P_{1,\text{tot}} \frac{X_1^{**} K_{2,1}}{K_{2,1}^* X_1^* + K_{2,1} X_1^{**} + K_{2,1} K_{2,1}^*} \\ \frac{d}{dt} X_2^* &= X_1^{**} \frac{k_{1,2} X_2 K_{1,2}^* - k_{1,2}^* X_2^* K_{1,2}}{K_{1,2}^* X_2 + K_{1,2} X_2^* + K_{1,2} K_{1,2}^*} + P_{2,\text{tot}} \frac{k_{2,2}^* K_{2,2} X_2^{**} - k_{2,2} X_2^* K_{2,2}^*}{K_{2,2}^* X_2^* + K_{2,2} X_2^{**} + K_{2,2} K_{2,2}^*} \\ \frac{d}{dt} X_2^{**} &= k_{1,2}^* X_1^{**} \frac{X_2^* K_{1,2}}{K_{1,2}^* X_2 + K_{1,2} X_2^* + K_{1,2} K_{1,2}^*} - k_{2,2}^* P_{2,\text{tot}} \frac{X_2^{**} K_{2,2}}{K_{2,2}^* X_2^* + K_{2,2} X_2^{**} + K_{2,2} K_{2,2}^*}\end{aligned} \quad (2.20)$$

in which, letting $X_{0,\text{tot}}, X_{1,\text{tot}}$ and $X_{2,\text{tot}}$ represent the total amounts of each stage protein, we have $X_0 = X_{0,\text{tot}} - X_0^*$, $X_1 = X_{1,\text{tot}} - X_1^* - X_1^{**}$ and $X_2 = X_{2,\text{tot}} - X_2^* - X_2^{**}$.

Mechanistic model of the MAPK cascade

We now give the entire set of reactions for the MAPK cascade of Figure 2.17 as they are found in standard references (Huang-Ferrell model [41]):



with conservation laws

$$\begin{aligned}
 X_{0,\text{tot}} &= X_0 + X_0^* + C_1 + C_2 + C_3 + C_5 \\
 X_{1,\text{tot}} &= X_1 + X_1^* + C_3 + X_1^{**} + C_4 + C_5 + C_6 + C_7 + C_9 \\
 X_{2,\text{tot}} &= X_2 + X_2^* + X_2^{**} + C_7 + C_8 + C_9 + C_{10} \\
 E_{1,\text{tot}} &= E_1 + C_1, \quad P_{0,\text{tot}} = P_0 + C_2 \\
 P_{1,\text{tot}} &= P_1 + C_4 + C_6 \\
 P_{2,\text{tot}} &= P_2 + C_8 + C_{10}.
 \end{aligned}$$

The corresponding ODE model is given by

$$\begin{aligned}
\frac{d}{dt} C_1 &= a_{1,0} E_1 X_0 - (d_{1,0} + k_{1,0}) C_1 \\
\frac{d}{dt} X_0^* &= k_{1,0} C_1 + d_{2,0} C_2 - a_{2,0} P_0 X_0^* + (d_{1,1} + k_{1,1}) C_3 - a_{1,1} X_1 X_0^* \\
&\quad + (d_{1,1}^* + k_{1,1}^*) C_5 - a_{1,1}^* X_0^* X_1^* \\
\frac{d}{dt} C_2 &= a_{2,0} P_0 X_0^* - (d_{2,0} + k_{2,0}) C_2 \\
\frac{d}{dt} C_3 &= a_{1,1} X_1 X_0^* - (d_{1,1} + k_{1,1}) C_3 \\
\frac{d}{dt} X_1^* &= k_{1,1} C_3 + d_{2,1} C_4 - a_{2,1} X_1^* P_1 + d_{1,1}^* C_5 - a_{1,1}^* X_1^* X_0^* + k_{2,1}^* C_6 \\
\frac{d}{dt} C_4 &= a_{2,1} X_1^* P_1 - (d_{2,1} + k_{2,1}) C_4 \\
\frac{d}{dt} C_5 &= a_{1,1}^* X_0^* X_1^* - (d_{1,1}^* + k_{1,1}^*) C_5 \\
\frac{d}{dt} X_1^{**} &= k_{1,1}^* C_5 - a_{2,1}^* X_1^* P_1 + d_{2,1}^* C_6 - a_{1,2} X_1^{**} X_2 \\
&\quad + (d_{1,2} + k_{1,2}) C_7 - a_{1,2}^* X_1^{**} X_2^* + (d_{1,2}^* + k_{1,2}^*) C_9 \\
\frac{d}{dt} C_6 &= a_{2,1}^* X_1^* P_1 - (d_{2,1}^* + k_{2,1}^*) C_6 \\
\frac{d}{dt} C_7 &= a_{1,2}^* X_1^* X_2 - (d_{1,2}^* + k_{1,2}^*) C_7 \\
\frac{d}{dt} X_2^* &= -a_{2,2} X_2^* P_2 + d_{2,2} C_8 - a_{1,2}^* X_2^* X_2^{**} + d_{1,2}^* C_9 + C_{10} K_{10} \\
\frac{d}{dt} C_8 &= a_{2,2}^* X_2^* P_2 - (d_{2,2} + k_{2,2}) C_8 \\
\frac{d}{dt} X_2^{**} &= k_{1,2}^* C_9 - a_{2,2}^* X_2^* P_2 + d_{2,2}^* C_{10} \\
\frac{d}{dt} C_9 &= a_{1,2}^* X_1^* X_2^* - (d_{1,2}^* + k_{1,2}^*) C_9 \\
\frac{d}{dt} C_{10} &= a_{2,2}^* X_2^* P_2 - (d_{2,2}^* + k_{2,2}^*) C_{10}.
\end{aligned}$$

Assuming as before that the total amounts of enzymes are much smaller than the total amounts of substrates ($E_{1,\text{tot}}, P_{0,\text{tot}}, P_{1,\text{tot}}, P_{2,\text{tot}} \ll X_{0,\text{tot}}, X_{1,\text{tot}}, X_{2,\text{tot}}$), we can approximate the conservation laws as

$$\begin{aligned}
X_{0,\text{tot}} &\approx X_0 + X_0^* + C_3 + C_5, \\
X_{1,\text{tot}} &\approx X_1 + X_1^* + C_3 + X_1^{**} + C_5 + C_7 + C_9, \\
X_{2,\text{tot}} &\approx X_2 + X_2^* + X_2^{**} + C_7 + C_9.
\end{aligned}$$

Using these and assuming that the complexes are at the quasi-steady state, we obtain the following functional dependencies:

$$\begin{aligned} C_1 &= f_1(X_0^*, X_1^*, X_1^{**}, X_2^*, X_2^{**}), & C_2 &= f_2(X_0^*), \\ C_3 &= f_3(X_0^*, X_1^*, X_1^{**}, X_2^*, X_2^{**}), & C_5 &= f_5(X_0^*, X_1^*), \\ C_7 &= f_7(X_1^*, X_1^{**}, X_2^*, X_2^{**}), & C_9 &= f_9(X_1^{**}, X_2^*). \end{aligned}$$

The fact that C_7 depends on X_2^* and X_2^{**} illustrates that the dynamics of the second stage are influenced by those of the third stage. Similarly, the fact that C_3 depends on X_1^* , X_1^{**} , X_2^* , X_2^{**} indicates that the dynamics of the first stage are influenced by those of the second stage and by that of the third stage. The phenomenon by which the behavior of a “module” is influenced by that of its downstream clients is called *retroactivity*, which is a phenomenon similar to impedance in electrical systems and to back-effect in mechanical systems. It will be studied at length in Chapter 7.

This fact is in clear contrast with the ODE model obtained by modular composition, in which each stage dynamics depended upon the variables of the upstream stages and not upon those of the downstream stages. That is, from equations (2.20), it is apparent that the dynamics of X_0^* (first stage) do not depend on the variables of the second stage (X_1, X_1^*, X_1^{**}). In turn, the dynamics of X_1^* and X_1^{**} (second stage) do not depend on the variables of the third stage (X_2^* and X_2^{**}). Indeed modular composition does not consider the fact that the proteins of each stage are “used-up” in the process of transmitting information to the downstream stages. This backward effect has been theoretically shown to lead to sustained oscillations in the MAPK cascade [72]. By contrast, the modular ODE model of MAPK cascades does not give rise to sustained oscillations.

Properties of the MAPK Cascade

The stimulus-response curve obtained with the mechanistic model predicts that the response of the MAPKKK to the stimulus $E_{1,\text{tot}}$ is of the Michaelis-Menten type. By contrast, the stimulus-response curve obtained for the MAPKK and MAPK are sigmoidal and show high Hill coefficients, which increases from the MAPKK response to the MAPK response. That is, an increase ultrasensitivity is observed moving down in the cascade (Figure 2.19). These model observations persist when key parameters, such as the Michaelis-Menten constants are changed [41]. Furthermore, zero-order ultrasensitivity effects can be observed. Specifically, if the amounts of MAPKK were increased, one would observe a higher apparent Hill coefficient for the response of MAPK. Similarly, if the values of the K_m for the reactions in which the MAPKK takes place were decreased, one would also observe a higher apparent Hill coefficient for the response of MAPK. Double phosphorylation is also key to obtain a high apparent Hill coefficient. In fact, a cascade in which the double phosphorylation was assumed to occur through a one-step model

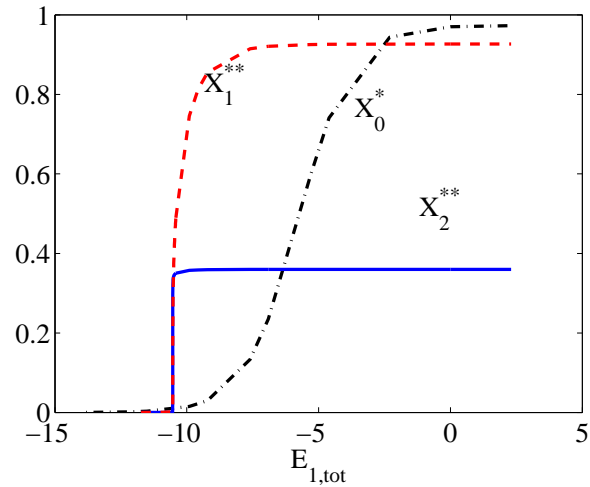


Figure 2.19: Dose response of the MAPK cascade for every stage. Simulations from the model of [72].

(similar to single phosphorylation) predicted substantially lower apparent Hill coefficients.

Additional topics to be added later:

Review

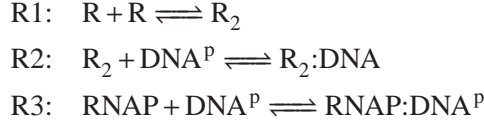
1. Transport across the membrane
2. Membrane receptors, ligand binding, G-proteins

Exercises

2.1 (BE 150, Winter 2011) Consider a cascade of three activators $X \rightarrow Y \rightarrow Z$. Protein X is initially present in the cell in its inactive form. The input signal of X , S_x , appears at time $t=0$. As a result, X rapidly becomes active and binds the promoter of gene Y , so that protein Y starts to be produced at rate β . When Y levels exceed a threshold K , gene Z begins to be transcribed and translated at rate γ . All proteins have the same degradation/dilution rate α .

- (a) What are the concentrations of proteins Y and Z as a function of time?
- (b) What is the minimum duration of the pulse S_x such that Z will be produced?
- (c) What is response time of protein Z with respect to the time of addition of S_x ?

2.2 (Hill function for a cooperative repressor) Consider a repressor that binds to an operator site as a dimer:

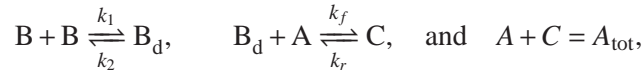


Assume that the reactions are at equilibrium and that the RNA polymerase concentration is large (so that [RNAP] is roughly constant). Show that the ratio of the concentration of RNA:DNA^P to the total amount of DNA, D_{tot} , can be written as a Hill function

$$f(R) = \frac{[\text{RNAP}:\text{DNA}]}{D_{\text{tot}}} = \frac{\alpha}{K + R^2}$$

and give expressions for α and K .

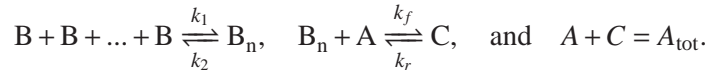
2.3 (Switch-like behavior in cooperative binding) For a cooperative binding reaction



the steady state values of C and A are

$$C = \frac{k_M A_{\text{tot}} B^2}{k_M B^2 + K_d}, \quad \text{and} \quad A = \frac{A_{\text{tot}} K_d}{k_M B^2 + K_d}.$$

Derive the expressions of C and A at the steady state when you modify these reactions to

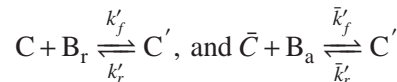


Make MATLAB plots of the expressions that you obtain and verify that as n increases the functions become more switch-like.

2.4 Consider the following modification of the competitive binding reactions:

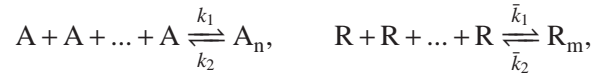


and



with $A_{\text{tot}} = A + C + \bar{C} + C'$. What are the steady state expressions for A and C ? What information do you deduce from these expressions if A is a promoter, B_a is an activator protein, and C is the activator/DNA complex that makes the gene transcriptionally active?

2.5 Consider the case of a competitive binding of an activator A and a repressor R with D and assume that before they can bind D they have to cooperatively bind according to the following reactions:



in which the complex A_n contains n molecules of A and the complex R_m contains m molecules of R. The competitive binding reactions with A are given by



and $D_{\text{tot}} = D + C + C'$. What are the steady state expressions for C and D?

2.6 Assume that we have an activator B_a and a repressor protein B_r . We want to obtain an input function such that when a lot of B_a is present, the gene is transcriptionally active only if there is no B_r , when low amounts of B_a are present, the gene is transcriptionally inactive (with or without B_r). Write down the reactions among B_a , B_r , and complexes with the DNA (A) that lead to such an input function. Demonstrate that indeed the set of reactions you picked leads to the desired input function.

2.7 (BE 150, Winter 2011) Consider a positive transcriptional feedback loop composed of two negative interactions $X \dashv Y$ and $Y \dashv X$.

(a) Write the ODEs for the system above. Assume that the two transcription/repression mechanisms have the same dynamics and both genes are degraded at the same rate 0.2. Let the basal transcription rate be 1, $K = 2$, $n = 2$.

(b) To solve for the steady states, plot the *nullclines* by solving $\frac{dX}{dt} = 0$ and $\frac{dY}{dt} = 0$ (i.e. solve for $Y = g_1(X)$ where $\frac{dX}{dt} = 0$ and $Y = g_2(X)$ where $\frac{dY}{dt} = 0$ and plot both solutions). The steady states are given by the intersections of the two nullclines.

(c) Plot the time response of X and Y using the following two initial conditions:

$$(X(0), Y(0)) = (1, 4) \quad \text{and} \quad (4, 1).$$

Next, plot the phase plane of the system using *pplane* in MATLAB. How do the responses change with initial conditions? Describe a situation where this type of interaction would be useful.

2.8 Consider the phosphorylation reactions described in Section 2.4, but suppose that the kinase concentration Z is not constant, but is produced and decays according to the reaction $Z \xrightleftharpoons[k(t)]{\delta} \emptyset$. How should the system in equation (2.17) be modified?

Use a MATLAB simulation to apply a periodic input stimulus $k(t)$ using parameter values: $k_{\text{cat}} = k'_{\text{cat}} = 1$, $k_f = k'_f = k_r = k'_r = 10$, $\delta = 0.01$. Is the cycle capable of “tracking” the input stimulus? If yes, to what extent? What are the tracking properties depending on?

2.9 Another model for the phosphorylation reactions, referred to as one step reaction model, is given by $Z + X \rightleftharpoons X^* + Z$ and $Y + X^* \rightleftharpoons X + Y$, in which the complex formations are neglected. Write down the ODE model and comparing the differential equation of X^* to that of equation (2.17), list the assumptions under which the one step reaction model is a good approximation of the two step reaction model.

2.10 (Transcriptional regulation with delay) Consider a repressor or activator B^* modeled by a Hill function $F(B)$. Show that in the presence of transcriptional delay τ^m , the dynamics of the active mRNA can be written as

$$\frac{dm^*(t)}{dt} = e^{-\tau^m} F(B(t - \tau^m)) - \bar{\gamma}m^*.$$

2.11 (Competitive Inhibition) Derive the expression of the production rate of W^* in the presence of a competitive inhibitor I.

2.12 (Non-absolute activator) Derive the expression of the production rate of W^* in the presence of a non-absolute activator A.

2.13 (BE 150, Winter 2011) Consider the following network $X \rightarrow Y$ and $X \rightarrow X$.

(a) Write the ODEs for the system above. Use basal expression $\beta_X = \beta_Y = 2$ and activation coefficients $K_X = 1$, $K_Y = 2$, $n_1 = n_2 = 2$. The degradation coefficients for X and Y are both 0.5.

(b) Plot the vector field using pplane. How many steady states do you observe?

(c) Solve for the steady states of the system using the derived ODEs, linearize the system and do a stability analysis.

Chapter 3

Analysis of Dynamic Behavior

In this chapter, we describe some of the tools from dynamical systems and feedback control theory that will be used in the rest of the text to analyze and design biological circuits, building on tools already described in AM08. We focus here on deterministic models and the associated analyses; stochastic methods are given in Chapter 4.

Prerequisites. Readers should have a understanding of the tools for analyzing stability of solutions to ordinary differential equations, at the level of Chapter 4 of AM08. We will also make use of linearized input/output models in state space, based on the techniques described in Chapter 5 of AM08 and the frequency domain techniques described in Chapters 8–10.

3.1 Analysis Near Equilibria

As in the case of many other classes of dynamical systems, a great deal of insight into the behavior of a biological system can be obtained by analyzing the dynamics of the system subject to small perturbations around a known solution. We begin by considering the dynamics of the system near an equilibrium point, which is one of the simplest cases and provides a rich set of methods and tools.

In this section we will model the dynamics of our system using the input/output modeling formalism described in Chapter 1:

$$\dot{x} = f(x, \theta, u), \quad y = h(x, \theta) \quad (3.1)$$

where $x \in \mathbb{R}^n$ is the system state, $\theta \in \mathbb{R}^p$ are the system parameters and $u \in \mathbb{R}^q$ is a set of external inputs (including disturbances and noise). The system state x is a vector whose components will represent concentration of species, such as proteins, kinases, DNA promoter sites, inducers, allosteric effectors, etc. The system parameters θ is also a vector, whose components will represent biochemical parameters such as association and dissociation rates, production rates, decay rates, dissociation constants, etc. The input u is a vector whose components will represent a number of possible physical entities, including the concentration of transcription factors, DNA concentration, kinases concentration, etc. The output $y \in \mathbb{R}^m$ of the system represents quantities that can be measured or that are used to interconnect subsystem models to form larger models.

Example 3.1 (Transcriptional component). Consider a promoter controlling a gene g that can be regulated by a transcription factor Z . Let m_G and G represent the mRNA and protein expressed by gene g . This system can be viewed as a system, in which $u = Z$ is the concentration of transcription factor regulating the promoter, the state $x = (x_1, x_2)$ is such that $x_1 = m_G$ is the concentration of mRNA and $x_2 = G$ is the concentration of protein, and $y = G = x_2$ is the concentration of protein G . Assuming that the transcription factor regulating the promoter is a repressor, the system dynamics can be described by the following system

$$\frac{dx_1}{dt} = \frac{\alpha}{1 + (u/K)^n} - \gamma x_1, \quad \frac{dx_2}{dt} = \beta x_1 - \delta x_2, \quad y = x_2$$

in which $\theta = (\alpha, K, \gamma, \beta, \delta, n)$ is the vector of system parameters. In this case, we have that

$$f(x, \theta, u) = \begin{pmatrix} \frac{\alpha}{1 + (u/K)^n} - \gamma x_1 \\ \beta x_1 - \delta x_2 \end{pmatrix}, \quad h(x, \theta) = x_2.$$

▽

Note that we have chosen to explicitly model the system parameters θ , which can be thought of as an additional set of (mainly constant) inputs to the system.

Equilibrium points and stability [AM08]

We begin by considering the case where the input u and parameters θ in equation (3.1) are fixed and hence we can write the dynamics of the system as

$$\frac{dx}{dt} = F(x). \quad (3.2)$$

An *equilibrium point* of a dynamical system represents a stationary condition for the dynamics. We say that a state x_e is an equilibrium point for a dynamical system if $F(x_e) = 0$. If a dynamical system has an initial condition $x(0) = x_e$, then it will stay at the equilibrium point: $x(t) = x_e$ for all $t \geq 0$.

Equilibrium points are one of the most important features of a dynamical system since they define the states corresponding to constant operating conditions. A dynamical system can have zero, one or more equilibrium points.

The *stability* of an equilibrium point determines whether or not solutions nearby the equilibrium point remain close, get closer or move further away. An equilibrium point x_e is *stable* if solutions that start near x_e stay close to x_e . Formally, we say that the equilibrium point x_e is stable if for all $\epsilon > 0$, there exists a $\delta > 0$ such that

$$\|x(0) - x_e\| < \delta \implies \|x(t) - x_e\| < \epsilon \quad \text{for all } t > 0,$$

where $x(t)$ represents the solution to the differential equation (3.2) with initial condition $x(0)$. Note that this definition does not imply that $x(t)$ approaches x_e as

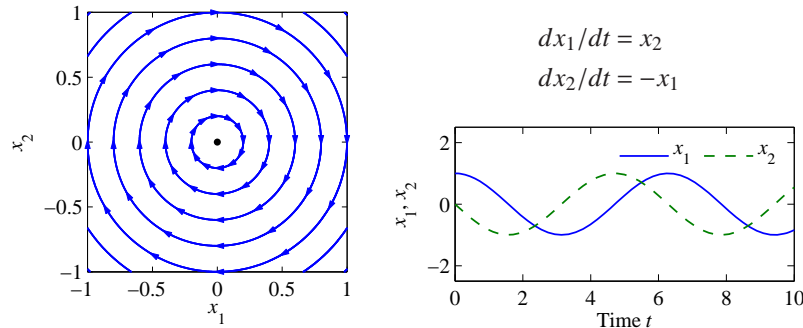


Figure 3.1: Phase portrait (trajectories in the state space) on the left and time domain simulation on the right for a system with a single stable equilibrium point. The equilibrium point x_e at the origin is stable since all trajectories that start near x_e stay near x_e .

time increases but just that it stays nearby. Furthermore, the value of δ may depend on ϵ , so that if we wish to stay very close to the solution, we may have to start very, very close ($\delta \ll \epsilon$). This type of stability, which is illustrated in Figure 3.1, is also called *stability in the sense of Lyapunov*. If an equilibrium point is stable in this sense and the trajectories do not converge, we say that the equilibrium point is *neutrally stable*.

An example of a neutrally stable equilibrium point is shown in Figure 3.1. From the phase portrait, we see that if we start near the equilibrium point, then we stay near the equilibrium point. Indeed, for this example, given any ϵ that defines the range of possible initial conditions, we can simply choose $\delta = \epsilon$ to satisfy the definition of stability since the trajectories are perfect circles.

An equilibrium point x_e is *asymptotically stable* if it is stable in the sense of Lyapunov and also $x(t) \rightarrow x_e$ as $t \rightarrow \infty$ for $x(0)$ sufficiently close to x_e . This corresponds to the case where all nearby trajectories converge to the stable solution for large time. Figure 3.2 shows an example of an asymptotically stable equilibrium point.

Note from the phase portraits that not only do all trajectories stay near the equilibrium point at the origin, but that they also all approach the origin as t gets large (the directions of the arrows on the phase portrait show the direction in which the trajectories move).

An equilibrium point x_e is *unstable* if it is not stable. More specifically, we say that an equilibrium point x_e is unstable if given some $\epsilon > 0$, there does *not* exist a $\delta > 0$ such that if $\|x(0) - x_e\| < \delta$, then $\|x(t) - x_e\| < \epsilon$ for all t . An example of an unstable equilibrium point is shown in Figure 3.3.

The definitions above are given without careful description of their domain of applicability. More formally, we define an equilibrium point to be *locally stable* (or *locally asymptotically stable*) if it is stable for all initial conditions $x \in B_r(a)$,

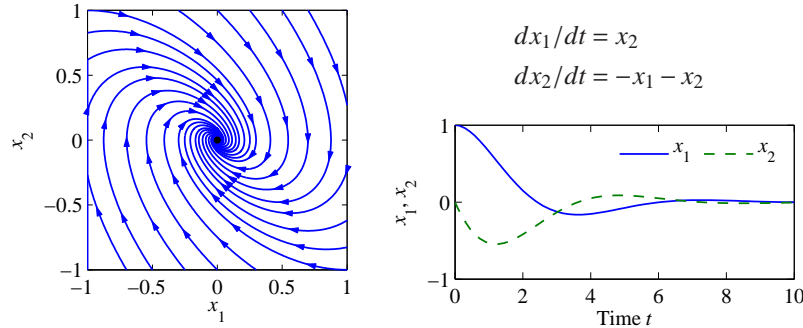


Figure 3.2: Phase portrait and time domain simulation for a system with a single asymptotically stable equilibrium point. The equilibrium point x_e at the origin is asymptotically stable since the trajectories converge to this point as $t \rightarrow \infty$.

where

$$B_r(a) = \{x : \|x - a\| < r\}$$

is a ball of radius r around a and $r > 0$. A system is *globally stable* if it is stable for all $r > 0$. Systems whose equilibrium points are only locally stable can have interesting behavior away from equilibrium points, as we explore in the next section.

To better understand the dynamics of the system, we can examine the set of all initial conditions that converge to a given asymptotically stable equilibrium point. This set is called the *region of attraction* for the equilibrium point. In general, computing regions of attraction is difficult. However, even if we cannot determine the region of attraction, we can often obtain patches around the stable equilibria that are attracting. This gives partial information about the behavior of the system.

For planar dynamical systems, equilibrium points have been assigned names based on their stability type. An asymptotically stable equilibrium point is called a *sink* or sometimes an *attractor*. An unstable equilibrium point can be either a *source*, if all trajectories lead away from the equilibrium point, or a *saddle*, if some trajectories lead to the equilibrium point and others move away (this is the situation pictured in Figure 3.3). Finally, an equilibrium point that is stable but not asymptotically stable (i.e., neutrally stable, such as the one in Figure 3.1) is called a *center*.

Example 3.2 (Bistable gene circuit). Consider a system composed of two genes that express transcription factors that repress each other as shown in Figure 3.4. Denoting the concentration of protein A by x_1 and that of protein B by x_2 and neglecting the mRNA dynamics, the system can be modeled by the following differential equations:

$$\frac{dx_1}{dt} = \frac{\alpha_1}{(x_2^n/K_2) + 1} - \delta x_1, \quad \frac{dx_2}{dt} = \frac{\alpha_2}{(x_1^n/K_1) + 1} - \delta x_2.$$

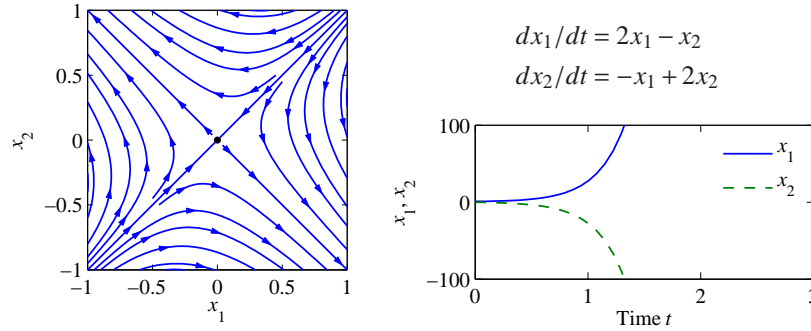


Figure 3.3: Phase portrait and time domain simulation for a system with a single unstable equilibrium point. The equilibrium point x_e at the origin is unstable since not all trajectories that start near x_e stay near x_e . The sample trajectory on the right shows that the trajectories very quickly depart from zero.

Figure 3.4(b) shows the phase portrait of the system. This system is bi-stable because there are two (asymptotically) stable equilibria. Specifically, the trajectories converge to either of two possible equilibria: one where x_1 is high and x_2 is low and the other where x_1 is low and x_2 is high. A trajectory will approach the first one if the initial condition is below the dashed line, called the separatrix, while it will approach the second one if the initial condition is above the separatrix. Hence, the region of attraction of the first equilibrium is the region of the plane below the separatrix and the region of attraction of the second one is the portion of plane above the separatrix. ∇

Nullcline Analysis

Nullcline analysis is a simple and intuitive way to determine the stability of an equilibrium point for systems in \mathbb{R}^2 . Consider the system with $x = (x_1, x_2) \in \mathbb{R}^2$ described by the differential equations

$$\frac{dx_1}{dt} = F_1(x_1, x_2), \quad \frac{dx_2}{dt} = F_2(x_1, x_2).$$

The nullclines of this system are given by the two curves in the x_1, x_2 plane in which $F_1(x_1, x_2) = 0$ and $F_2(x_1, x_2) = 0$. The nullclines intersect at the equilibria of the system x_e . Figure 3.5 shows an example in which there is a unique equilibrium.

The stability of the equilibrium is deduced by inspecting the direction of the trajectory of the system starting at initial conditions x close to the equilibrium x_e . The direction of the trajectory can be obtained by determining the signs of F_1 and F_2 in each of the regions in which the nullclines partition the plane around the equilibrium x_e . If $F_1 < 0$ ($F_1 > 0$), we have that x_1 is going to decrease (increase) and similarly if $F_2 < 0$ ($F_2 > 0$), we have that x_2 is going to decrease (increase). In

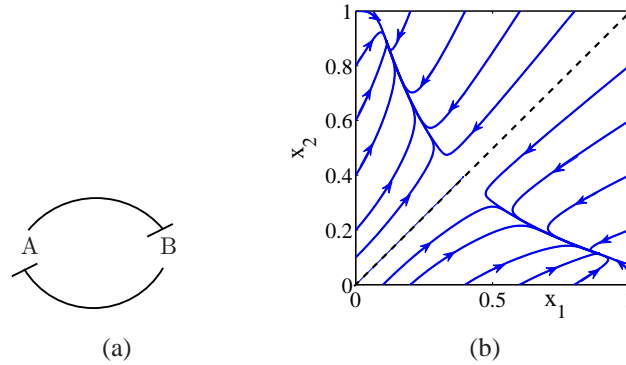


Figure 3.4: (a) Diagram of a bistable gene circuit composed of two genes. (b) Phase plot showing the trajectories converging to either one of the two possible stable equilibria depending on the initial condition. The parameters are $\alpha_1 = \alpha_2 = 1$, $K_1 = K_2 = 0.1$, and $\delta = 1$.

Figure 3.5, we show a case in which $F_1 < 0$ on the right-hand side of the nullcline $F_1 = 0$ and $F_1 > 0$ on the left-hand side of the same nullcline. Similarly, we have chosen a case in which $F_2 < 0$ above the nullcline $F_2 = 0$ and $F_2 > 0$ below the same nullcline. Given these signs, it is clear (see the figure) that starting from any point x close to x_e the vector field will always point toward the equilibrium x_e and hence the trajectory will tend toward such equilibrium. In this case, it then follows that the equilibrium x_e is asymptotically stable.

Example 3.3 (Negative autoregulation). As an example, consider expression of a gene with negative feedback. Let x_1 represent the mRNA concentration and x_2 represent the protein concentration. Then, a simple model (in which for simplicity we have assumed all parameters to be 1) is given by

$$\frac{dx_1}{dt} = \frac{1}{1+x_2} - x_1, \quad \frac{dx_2}{dt} = x_1 - x_2,$$

so that $F_1(x_1, x_2) = 1/(1+x_2) - x_1$ and $F_2(x_1, x_2) = x_1 - x_2$. Figure 3.5(a) exactly represents the situation for this example. In fact, we have that

$$F_1(x_1, x_2) < 0 \iff x_1 > \frac{1}{1+x_2}, \quad F_2(x_1, x_2) < 0 \iff x_2 > x_1,$$

which provides the direction of the vector field as shown in Figure 3.5. As a consequence, the equilibrium point is stable. The phase plot of Figure 3.5(b) confirms this fact since the trajectories all converge to the unique equilibrium point. ∇

Stability analysis via linearization

For systems with more than two states, the graphical technique of nullcline analysis cannot be used. Hence, we must resort to other techniques to determine stability.

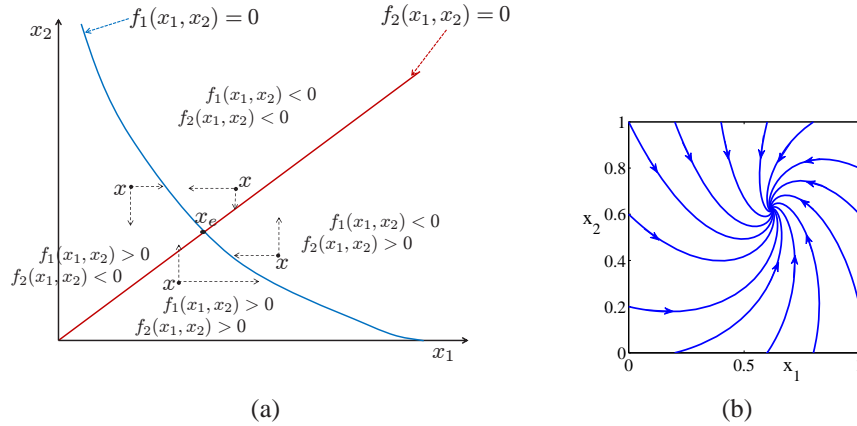


Figure 3.5: (a) Example of nullclines for a system with a single equilibrium point x_e . To understand the stability of the equilibrium point x_e , one traces the direction of the vector field (f_1, f_2) in each of the four regions in which the nullcline partition the plane. If in each region the vector field points toward the equilibrium point, then such a point is asymptotically stable. (b) Phase plot diagram for the negative autoregulation example.

Consider a linear dynamical system of the form

$$\frac{dx}{dt} = Ax, \quad x(0) = x_0, \quad (3.3)$$

where $A \in \mathbb{R}^{n \times n}$. For a linear system, the stability of the equilibrium at the origin can be determined from the eigenvalues of the matrix A :

$$\lambda(A) = \{s \in \mathbb{C} : \det(sI - A) = 0\}.$$

The polynomial $\det(sI - A)$ is the *characteristic polynomial* and the eigenvalues are its roots. We use the notation λ_j for the j th eigenvalue of A and $\lambda(A)$ for the set of all eigenvalues of A , so that $\lambda_j \in \lambda(A)$. For each eigenvalue λ_j there is a corresponding eigenvector $v_j \in \mathbb{R}^n$, which satisfies the equation $Av_j = \lambda_j v_j$.

In general λ can be complex-valued, although if A is real-valued, then for any eigenvalue λ , its complex conjugate λ^* will also be an eigenvalue. The origin is always an equilibrium point for a linear system. Since the stability of a linear system depends only on the matrix A , we find that stability is a property of the system. For a linear system we can therefore talk about the stability of the system rather than the stability of a particular solution or equilibrium point.

The easiest class of linear systems to analyze are those whose system matrices are in diagonal form. In this case, the dynamics have the form

$$\frac{dx}{dt} = \begin{pmatrix} \lambda_1 & & 0 \\ & \lambda_2 & \\ 0 & & \ddots \\ & & & \lambda_n \end{pmatrix} x. \quad (3.4)$$

It is easy to see that the state trajectories for this system are independent of each other, so that we can write the solution in terms of n individual systems $\dot{x}_j = \lambda_j x_j$. Each of these scalar solutions is of the form

$$x_j(t) = e^{\lambda_j t} x_j(0).$$

We see that the equilibrium point $x_e = 0$ is stable if $\lambda_j \leq 0$ and asymptotically stable if $\lambda_j < 0$.

Another simple case is when the dynamics are in the block diagonal form

$$\frac{dx}{dt} = \begin{pmatrix} \sigma_1 & \omega_1 & & 0 & 0 \\ -\omega_1 & \sigma_1 & & 0 & 0 \\ 0 & 0 & \ddots & \vdots & \vdots \\ 0 & 0 & & \sigma_m & \omega_m \\ 0 & 0 & & -\omega_m & \sigma_m \end{pmatrix} x.$$

In this case, the eigenvalues can be shown to be $\lambda_j = \sigma_j \pm i\omega_j$. We once again can separate the state trajectories into independent solutions for each pair of states, and the solutions are of the form

$$\begin{aligned} x_{2j-1}(t) &= e^{\sigma_j t} (x_{2j-1}(0) \cos \omega_j t + x_{2j}(0) \sin \omega_j t), \\ x_{2j}(t) &= e^{\sigma_j t} (-x_{2j-1}(0) \sin \omega_j t + x_{2j}(0) \cos \omega_j t), \end{aligned}$$

where $j = 1, 2, \dots, m$. We see that this system is asymptotically stable if and only if $\sigma_j = \operatorname{Re} \lambda_j < 0$. It is also possible to combine real and complex eigenvalues in (block) diagonal form, resulting in a mixture of solutions of the two types.

Very few systems are in one of the diagonal forms above, but some systems can be transformed into these forms via coordinate transformations. One such class of systems is those for which the dynamics matrix has distinct (non-repeating) eigenvalues. In this case there is a matrix $T \in \mathbb{R}^{n \times n}$ such that the matrix TAT^{-1} is in (block) diagonal form, with the block diagonal elements corresponding to the eigenvalues of the original matrix A . If we choose new coordinates $z = Tx$, then

$$\frac{dz}{dt} = T\dot{x} = TAx = TAT^{-1}z$$

and the linear system has a (block) diagonal dynamics matrix. Furthermore, the eigenvalues of the transformed system are the same as the original system since if v is an eigenvector of A , then $w = Tv$ can be shown to be an eigenvector of TAT^{-1} . We can reason about the stability of the original system by noting that $x(t) = T^{-1}z(t)$, and so if the transformed system is stable (or asymptotically stable), then the original system has the same type of stability.

This analysis shows that for linear systems with distinct eigenvalues, the stability of the system can be completely determined by examining the real part of the eigenvalues of the dynamics matrix. For more general systems, we make use of the following theorem, proved in the next chapter:

Theorem 3.1 (Stability of a linear system). *The system*

$$\frac{dx}{dt} = Ax$$

is asymptotically stable if and only if all eigenvalues of A all have a strictly negative real part and is unstable if any eigenvalue of A has a strictly positive real part.

In the case in which the system state is two-dimensional, that is, $x \in \mathbb{R}^2$, we have a simple way of determining the eigenvalues of a matrix A . Specifically, denote by $\text{tr}(A)$ the trace of A , that is, the sum of the diagonal terms, and let $\det(A)$ be the determinant of A . Then, we have that the two eigenvalues are given by

$$\lambda_{1,2} = \frac{1}{2} \left(\text{tr}(A) \pm \sqrt{\text{tr}(A)^2 - 4 \det(A)} \right).$$

Both eigenvalues have negative real parts when (1) $\text{tr}(A) < 0$ and (2) $\det(A) > 0$. By contrast, if condition (2) is satisfied but $\text{tr}(A) > 0$, the eigenvalues have positive real parts.

An important feature of differential equations is that it is often possible to determine the local stability of an equilibrium point by approximating the system by a linear system. Suppose that we have a nonlinear system

$$\frac{dx}{dt} = F(x)$$

that has an equilibrium point at x_e . Computing the Taylor series expansion of the vector field, we can write

$$\frac{dx}{dt} = F(x_e) + \left. \frac{\partial F}{\partial x} \right|_{x_e} (x - x_e) + \text{higher-order terms in } (x - x_e).$$

Since $F(x_e) = 0$, we can approximate the system by choosing a new state variable $z = x - x_e$ and writing

$$\frac{dz}{dt} = Az, \quad \text{where } A = \left. \frac{\partial F}{\partial x} \right|_{x_e}. \quad (3.5)$$

We call the system (3.5) the *linear approximation* of the original nonlinear system or the *linearization* at x_e . We also refer to matrix A as the *Jacobian matrix* of the original nonlinear system.

The fact that a linear model can be used to study the behavior of a nonlinear system near an equilibrium point is a powerful one. Indeed, we can take this even further and use a local linear approximation of a nonlinear system to design a feedback law that keeps the system near its equilibrium point (design of dynamics). Thus, feedback can be used to make sure that solutions remain close to the equilibrium point, which in turn ensures that the linear approximation used to stabilize it is valid.

Example 3.4 (Negative autoregulation). Consider again the self repressed gene modeled by the equations

$$\frac{dx_1}{dt} = \frac{1}{1+x_2} - x_1, \quad \frac{dx_2}{dt} = x_1 - x_2.$$

In this case,

$$F(x) = \begin{pmatrix} \frac{1}{1+x_2} - x_1 \\ x_1 - x_2 \end{pmatrix},$$

so that, letting $x_e = (x_{1,e}, x_{2,e})$, the Jacobian matrix is given by

$$A = \left. \frac{\partial F}{\partial x} \right|_{x_e} = \begin{pmatrix} -1 & -\frac{1}{(1+x_{2,e})^2} \\ 1 & -1 \end{pmatrix}.$$

In this case, we have that $\text{tr}(A) = -2 < 0$ and that $\det(A) = 1 + \frac{1}{(1+x_{2,e})^2} > 0$. Hence, independently of the value of the equilibrium point, the eigenvalues have both negative real parts, which implies that the equilibrium point x_e is asymptotically stable. ∇

Frequency domain analysis

Frequency domain analysis is a way to understand how well a system can respond to rapidly changing input stimuli. As a general rule, most physical systems display an increased difficulty in responding to input stimuli as the frequency of variation increases: when the input stimulus changes faster than the natural time scales of the system, the system becomes incapable of responding. If instead the input stimulus is changing much slower than the natural time scales of the system, the system will respond very accurately. That is, the system behaves like a “low-pass filter”. The cut-off frequency at which the system does not display a significant response is called the *bandwidth* and quantifies the dominant time scale. To identify this dominant time scale, we can perform input/output experiments in which the system is excited with periodic input at various frequencies.

Example 3.5 (Phosphorylation cycle). To illustrate the basic ideas, consider the frequency response of a phosphorylation cycle, in which enzymatic reactions are modeled by a first order reaction. Referring to Figure 3.6a, we have that the one step reactions involved are given by



with conservation law $X + X^* = X_{\text{tot}}$. Let Y_{tot} be the total amount of phosphatase. We assume that the kinase Z has a time-varying concentration, which we view as the *input* to the system, while X^* is the *output* of the system.

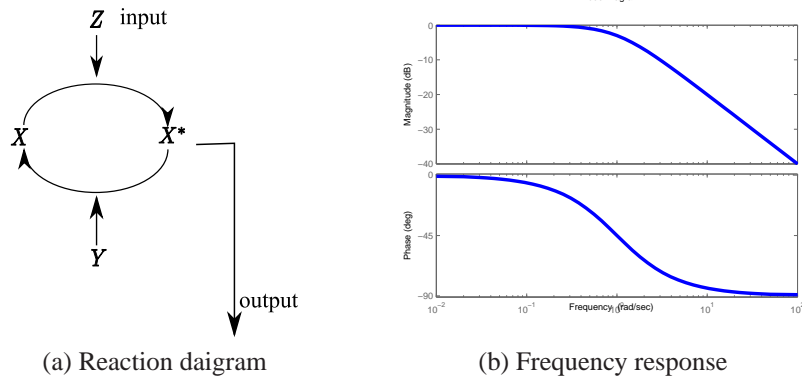


Figure 3.6: (a) Diagram of a phosphorylation cycle, in which Z is the kinase, X is the substrate, and Y is the phosphatase. (b) Bode plot showing the magnitude and phase lag for the frequency response of a one step reaction model of the phosphorylation system on the left. The magnitude is plotted in decibels (dB), in which $M_{dB} = 20\log_{10}(M)$. The parameters are $\beta = \delta = 1$.

The differential equation model is given by

$$\frac{dX^*}{dt} = k_1 Z(t)(X_{\text{tot}} - X^*) - k_2 Y_{\text{tot}} X^*,$$

If we assume that the cycle is weakly activated ($X^* \ll X_{\text{tot}}$), the above equation is well approximated by

$$\frac{dX^*}{dt} = \beta Z(t) - \delta X^*, \quad (3.6)$$

where $\beta = k_1 X_{\text{tot}}$ and $\delta = k_2 Y_{\text{tot}}$. To determine the frequency response, we set the input $Z(t)$ to a periodic function. It is customary to take sinusoidal functions as the input signal as they lead to an easy way to calculate the frequency response. Let then $Z(t) = A_0 \sin(\omega t)$.

Since equation (3.6) is linear in the state X^* and input Z , it can be directly integrated to lead to

$$X^*(t) = \frac{A_0 \beta}{\sqrt{\omega^2 + \delta^2}} \sin(\omega t - \tan^{-1}(\omega/\delta)) - \frac{A_0 \beta \omega}{(\omega^2 + \delta^2)} e^{-\delta t}.$$

The second term dies out for t large enough. Hence, the steady state response is given by the first term. The amplitude of response is thus given by $A_0 \beta / \sqrt{\omega^2 + \delta^2}$, in which the gain $\beta / \sqrt{\omega^2 + \delta^2}$ depends on the system parameters and on the frequency of the input stimulation.

As this frequency increases, the amplitude decreases and approaches zero for infinite frequencies. Also, the argument of the sine function shows a negative phase shift of $\tan^{-1}(\omega/\delta)$, which indicates that there is an increased delay in responding

to the input as the frequency increases. Hence, the key quantities in the frequency response are the magnitude gain $M(\omega)$ and phase lag $\phi(\omega)$ given by

$$M(\omega) = \frac{\beta}{\sqrt{\omega^2 + \delta^2}}, \quad \phi(\omega) = \tan^{-1}\left(\frac{\omega}{\delta}\right).$$

These are plotted in Figure 3.6b, a type of figure known as a *Bode plot*.

The bandwidth of the system, denoted ω_B is the frequency at which the magnitude gain drops below $M(0)/\sqrt{2}$. In this case, the bandwidth is given by $\omega_B = \delta = k_2 Y_{\text{tot}}$, which implies that the bandwidth of the system can be made larger by increasing the amount of phosphatase. However, note that since $M(0) = \beta/\delta = k_1 X_{\text{tot}}/(k_2 Y_{\text{tot}})$, increased phosphatase will also result in decreased amplitude of response. Hence, if one wants to increase the bandwidth of the system while keeping the value of $M(0)$ (also called the *zero frequency gain*) unchanged, one should increase the total amounts of substrate and phosphatase in comparable proportions. Fixing the value of the zero frequency gain, the bandwidth of the system increases with increased amounts of phosphatase and kinase. ∇

More generally, the *frequency response* of a linear system with one input and one output

$$\dot{x} = Ax + Bu, \quad y = Cx + Du$$

is the response of the system to a sinusoidal input $u = a \sin \omega t$ with input amplitude a and frequency ω . The *transfer function* for a linear system is given by

$$G_{yu}(s) = C(sI - A)^{-1}B + D$$

and represents the response of a system to an exponential signal of the form $u(t) = e^{st}$ where $s \in \mathbb{C}$. In particular, the response to a sinusoid $u = a \sin \omega t$ is given by $y = Ma \sin(\omega t + \phi)$ where the gain M and phase shift ϕ can be determined from the transfer function evaluated at $s = i\omega$:

$$G_{yu}(i\omega) = Me^{i\phi}, \quad M = |G_{yu}(i\omega)| = \sqrt{\text{Im}(G_{yu}(i\omega))^2 + \text{Re}(G_{yu}(i\omega))^2}$$

$$\phi = \tan^{-1}\left(\frac{\text{Im}(G_{yu}(i\omega))}{\text{Re}(G_{yu}(i\omega))}\right).$$

where $\text{Re}(\cdot)$ and $\text{Im}(\cdot)$ represent the real and imaginary parts of a complex number.

For finite dimensional linear (or linearized) systems, the transfer function be written as a ratio of polynomials in s :

$$G(s) = \frac{b(s)}{a(s)}.$$

The values of s at which the numerator vanishes are called the *zeros* of the transfer function and the values of s at which the denominator vanishes are called the *poles*.

The transfer function representation of an input/output linear system is essentially equivalent to the state space description, but we reason about the dynamics by looking at the transfer function instead of the state space matrices. For example, it can be shown that the poles of a transfer function correspond to the eigenvalues of the matrix A , and hence the poles determine the stability of the system. In addition, interconnections between subsystems often have simple representations in terms of transfer functions. For example, two systems G_1 and G_2 in series (with the output of the first connected to the input of the second) have a combined transfer function $G_{\text{series}}(s) = G_1(s)G_2(s)$ and two systems in parallel (a single input goes to both systems and the outputs are summed) has the transfer function $G_{\text{parallel}}(s) = G_1(s) + G_2(s)$.

Transfer functions are useful representations of linear systems because the properties of the transfer function can be related to the properties of the dynamics. In particular, the shape of the frequency response describes how the system response to inputs and disturbances, as well as allows us to reason about the stability of interconnected systems. The Bode plot of a transfer function gives the magnitude and phase of the frequency response as a function of frequency and the *Nyquist plot* can be used to reason about stability of a closed loop system from the open loop frequency response (AM08, Section 9.2).

Returning to our analysis of biomolecular systems, suppose we have a systems whose dynamics can be written as

$$\dot{x} = f(x, \theta, u)$$

and we wish to understand how the solutions of the system depend on the parameters θ and input disturbances u . We focus on the case of an equilibrium solution $x(t; x_0, \theta_0) = x_e$. Let $z = x - x_e$, $\tilde{u} = u - u_0$ and $\tilde{\theta} = \theta - \theta_0$ represent the deviation of the state, input and parameters from their nominal values. Linearization can be performed in a way similar to the way it was performed for a system with no inputs. Specifically, we can write the dynamics of the perturbed system using its linearization as

$$\frac{dz}{dt} = \left(\frac{\partial f}{\partial x} \right)_{(x_e, \theta_0, u_0)} \cdot z + \left(\frac{\partial f}{\partial \theta} \right)_{(x_e, \theta_0, u_0)} \cdot \tilde{\theta} + \left(\frac{\partial f}{\partial w} \right)_{(x_e, \theta_0, u_0)} \cdot \tilde{u}.$$

This linear system describes small deviations from $x_e(\theta_0, w_0)$ but allows $\tilde{\theta}$ and \tilde{w} to be time-varying instead of the constant case considered earlier.

To analyze the resulting deviations, it is convenient to look at the system in the frequency domain. Let $y = Cx$ be a set of values of interest. The transfer functions between $\tilde{\theta}$, \tilde{w} and y are given by

$$H_{y\tilde{\theta}}(s) = C(sI - A)^{-1}B_{\theta}, \quad H_{y\tilde{w}}(s) = C(sI - A)^{-1}B_w,$$

where

$$A = \left. \frac{\partial f}{\partial x} \right|_{(x_e, \theta_0, w_0)}, \quad B_{\theta} = \left. \frac{\partial f}{\partial \theta} \right|_{(x_e, \theta_0, w_0)}, \quad B_w = \left. \frac{\partial f}{\partial w} \right|_{(x_e, \theta_0, w_0)}.$$

Note that if we let $s = 0$, we get the response to small, constant changes in parameters. For example, the change in the outputs y as a function of constant changes in the parameters is given by

$$H_{y\tilde{\theta}}(0) = CA^{-1}B_{\theta} = CS_{x,\theta}.$$

Example 3.6 (Transcriptional regulation). Consider a genetic circuit consisting of a single gene. The dynamics of the system are given by

$$\frac{dm}{dt} = F(P) - \gamma m, \quad \frac{dP}{dt} = \beta m - \delta P,$$

where m is the mRNA concentration and P is the protein concentration. Suppose that the mRNA degradation rate γ can change as a function of time and that we wish to understand the sensitivity with respect to this (time-varying) parameter. Linearizing the dynamics around an equilibrium point

$$A = \begin{pmatrix} -\gamma & F'(p_e) \\ \beta & -\delta \end{pmatrix}, \quad B_{\gamma} = \begin{pmatrix} -m_e \\ 0 \end{pmatrix}.$$

For the case of no feedback we have $F(P) = \alpha_0$, and the system has an equilibrium point at $m_e = \alpha_0/\gamma$, $P_e = \beta\alpha_0/(\delta\gamma)$. The transfer function from γ to p , after linearization about the steady state, is given by

$$G_{P\gamma}^{\text{ol}}(s) = \frac{-\beta m_e}{(s + \gamma)(s + \delta)},$$

where γ_0 represents the nominal value of γ around which we are linearizing. For the case of negative regulation, we have

$$F(P) = \frac{\alpha}{1 + P^n/K} + \alpha_0,$$

and the resulting transfer function is given by

$$G_{P\gamma}^{\text{cl}}(s) = \frac{\beta m_e}{(s + \gamma_0)(s + \delta) + \beta\sigma}, \quad \sigma = F'(P_e) = \frac{n\alpha P_e^{n-1}/K}{(1 + P_e^n/K)^2}.$$

Figure 3.7 shows the frequency response for the two circuits. We see that the feedback circuit attenuates the response of the system to disturbances with low-frequency content but slightly amplifies disturbances at high frequency (compared to the open loop system). ∇

3.2 Robustness

The term ‘‘robustness’’ refers to the general ability of a system to continue to function in the presence of uncertainty. In the context of this text, we will want to be

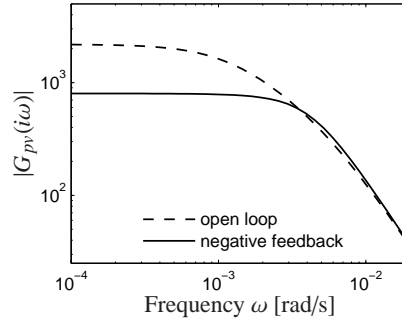


Figure 3.7: Noise attenuation in a genetic circuit.

more precise. We say that a given function (of the circuit) is robust with respect to a set of specified perturbations if the sensitivity of that function to perturbations is small. Thus, to study robustness, we must specify both the function we are interested in and the set of perturbations that we wish to consider.

In this section we study the robustness of the system

$$\dot{x} = f(x, \theta, u), \quad y = h(x, \theta)$$

to various perturbations in the parameters θ and disturbance inputs u . The function we are interested in is modeled by the outputs y and hence we seek to understand how y changes if the parameters θ are changed by a small amount or if external disturbances u are present. We say that a system is robust with respect to these perturbations if y undergoes little changes as these perturbations are introduced.

Parametric uncertainty

In addition to studying the input/output transfer curve and the stability of a given equilibrium point, we can also study how these features change with respect to changes in the system parameters θ . Let $y_e(\theta_0, u_0)$ represent the output corresponding to an equilibrium point x_e with fixed parameters θ_0 and external input u_0 , so that $f(x_e, \theta_0, u_0) = 0$. We assume that the equilibrium point is stable and focus here on understanding how the value of the output, the location of the equilibrium point and the dynamics near the equilibrium point vary as a function of changes in the parameters θ and external inputs w .

We start by assuming that $u = 0$ and investigating how x_e and y_e depend on θ . The simplest approach is to analytically solve the equation $f(x_e, \theta_0) = 0$ for x_e and then set $y_e = h(x_e, \theta_0)$. However, this is often difficult to do in closed form and so as an alternative we instead look at the linearized response given by

$$S_{x,\theta} := \left. \frac{dx_e}{d\theta} \right|_{\theta_0}, \quad S_{y,\theta} := \left. \frac{dy_e}{d\theta} \right|_{\theta_0},$$

which is the (infinitesimal) change in the equilibrium state and the output due to a change in the parameter. To determine $S_{x,\theta}$ we begin by differentiating the relationship $f(x_e(\theta), \theta) = 0$ with respect to θ :

$$\frac{df}{d\theta} = \frac{\partial f}{\partial x} \frac{dx_e}{d\theta} + \frac{\partial f}{\partial \theta} = 0 \quad \implies \quad S_{x,\theta} = \frac{dx_e}{d\theta} = - \left(\frac{\partial f}{\partial x} \right)^{-1} \frac{\partial f}{\partial \theta} \Big|_{(x_e, \theta_0)}. \quad (3.7)$$

Similarly, we can compute the change in the output sensitivity as

$$S_{y,\theta} = \frac{dy_e}{d\theta} = \frac{\partial h}{\partial x} \frac{dx_e}{d\theta} + \frac{\partial h}{\partial \theta} = - \left(\frac{\partial h}{\partial x} \left(\frac{\partial f}{\partial x} \right)^{-1} \frac{\partial f}{\partial \theta} + \frac{\partial h}{\partial \theta} \right) \Big|_{(x_e, \theta_0)}.$$

These quantities can be computed numerically and hence we can evaluate the effect of small (but constant) changes in the parameters θ on the equilibrium state x_e and corresponding output value y_e .

A similar analysis can be performed to determine the effects of small (but constant) changes in the external input u . Suppose that x_e depends on both θ and u , with $f(x_e, \theta_0, u_0) = 0$ and θ_0 and u_0 representing the nominal values. Then

$$\frac{dx_e}{d\theta} = - \left(\frac{\partial f}{\partial x} \right)^{-1} \frac{\partial f}{\partial \theta} \Big|_{(x_e, \theta_0, u_0)}, \quad \frac{dx_e}{du} = - \left(\frac{\partial f}{\partial x} \right)^{-1} \frac{\partial f}{\partial u} \Big|_{(x_e, \theta_0, u_0)}.$$

The sensitivity matrix can be normalized by dividing the parameters by their nominal values and rescaling the outputs (or states) by their equilibrium values. If we define the scaling matrices

$$D^{x_e} = \text{diag}\{x_e\}, \quad D^{y_e} = \text{diag}\{y_e\}, \quad D^\theta = \text{diag}\{\theta\},$$

Then the scaled sensitivity matrices can be written as

$$\bar{S}_{x,\theta} = (D^{x_e})^{-1} S_{x\theta} D^\theta, \quad \bar{S}_{y,\theta} = (D^{y_e})^{-1} S_{y\theta} D^\theta.$$

The entries in this matrix describe how a fractional change in a parameter gives a fractional change in the output, relative to the nominal values of the parameters and outputs.

Example 3.7 (Transcriptional regulation). Consider again the case of transcriptional regulation described in Example 3.6. We wish to study the response of the protein concentration to fluctuations in its parameters in two cases: a *constitutive promoter* (no regulation) and self-repression (negative feedback), illustrated in Figure 3.8.

For the case of no feedback we have $F(p) = \alpha_0$, and the system has an equilibrium point at $m_e = \alpha_0/\gamma$, $P_e = \beta\alpha_0/(\delta\gamma)$. The parameter vector can be taken as

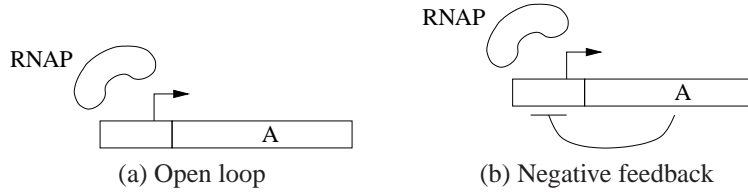


Figure 3.8: Parameter sensitivity in a genetic circuit. The open loop system (a) consists of a constitutive promoter, while the closed loop circuit (b) is self-regulated with negative feedback (repressor).

$\theta = (\alpha_0, \gamma, \beta, \delta)$. Since we have a simple expression for the equilibrium concentrations, we can compute the sensitivity to the parameters directly:

$$\frac{\partial x_e}{\partial \theta} = \begin{pmatrix} \frac{1}{\gamma} & -\frac{\alpha_0}{\gamma^2} & 0 & 0 \\ \frac{\beta}{\delta\gamma} & -\frac{\beta\alpha_0}{\delta\gamma^2} & \frac{\alpha_0}{\delta\gamma} & -\frac{\beta\alpha_0}{\gamma\delta^2} \end{pmatrix},$$

where the parameters are evaluated at their nominal values, but we leave off the subscript 0 on the individual parameters for simplicity. If we choose the parameters as $\theta_0 = (0.00138, 0.00578, 0.115, 0.00116)$, then the resulting sensitivity matrix evaluates to

$$S_{x_e, \theta}^{\text{open}} \approx \begin{pmatrix} 170 & -41 & 0 & 0 \\ 17000 & -4100 & 210 & -21000 \end{pmatrix}. \quad (3.8)$$

If we look instead at the scaled sensitivity matrix, then the open loop nature of the system yields a particularly simple form:

$$\bar{S}_{x_e, \theta}^{\text{open}} = \begin{pmatrix} 1 & -1 & 0 & 0 \\ 1 & -1 & 1 & -1 \end{pmatrix}. \quad (3.9)$$

In other words, a 10% change in any of the parameters will lead to a comparable positive or negative change in the equilibrium values.

For the case of negative regulation, we have

$$F(P) = \frac{\alpha}{1 + P^n/K} + \alpha_0,$$

and the equilibrium points satisfy

$$m_e = \frac{\delta}{\beta} P_e, \quad \frac{\alpha}{1 + P_e^n/K} + \alpha_0 = \gamma m_e = \frac{\gamma\delta}{\beta} P_e. \quad (3.10)$$

In order to make a proper comparison with the previous case, we need to be careful to choose the parameters so that the equilibrium concentration P_e matches that of the open loop system. We can do this by modifying the promoter strength α or the RBS strength β so that the second formula in equation (3.10) is satisfied or,

equivalently, choose the parameters for the open loop case so that they match the closed loop steady state protein concentration (see Example 2.3).

Rather than attempt to solve for the equilibrium point in closed form, we instead investigate the sensitivity using the computations in equation (3.10). The state, dynamics and parameters are given by

$$x = \begin{pmatrix} m & P \end{pmatrix}, \quad f(x, \theta) = \begin{pmatrix} F(P) - \gamma m \\ \beta m - \delta P \end{pmatrix}, \quad \theta = (\alpha_0 \quad \gamma \quad \beta \quad \delta \quad \alpha \quad n \quad K).$$

Note that the parameters are ordered such that the first four parameters match the open loop system. The linearizations are given by

$$\frac{\partial f}{\partial x} = \begin{pmatrix} -\gamma & F'(P_e) \\ \beta & -\delta \end{pmatrix}, \quad \frac{\partial f}{\partial \theta} = \begin{pmatrix} 1 & -m & 0 & 0 & \frac{1}{1+P^n/K} & \frac{K\alpha P^n \log(P)}{(K+P^n)^2} & \frac{\alpha}{(1+P^n/K)^2} \\ 0 & 0 & m & -P & 0 & 0 & 0 \end{pmatrix},$$

where again the parameters are taken to be their nominal values. From this we can compute the sensitivity matrix as

$$S_{x,\theta} = \begin{pmatrix} -\frac{\delta}{\delta\gamma - \beta F'} & \frac{\delta m}{\delta\gamma - \beta F'} & -\frac{mF'}{\delta\gamma - \beta F'} & \frac{PF'}{\delta\gamma - \beta F'} & -\frac{\delta \frac{\partial F}{\partial \alpha_1}}{\delta\gamma - \beta F'} & -\frac{\delta \frac{\partial F}{\partial n}}{\delta\gamma - \beta F'} & -\frac{\delta \frac{\partial F}{\partial K}}{\delta\gamma - \beta F'} \\ -\frac{\beta}{\delta\gamma - \beta F'} & \frac{\beta m}{\delta\gamma - \beta F'} & -\frac{\gamma m}{\delta\gamma - \beta F'} & \frac{\gamma P}{\delta\gamma - \beta F'} & -\frac{\beta \frac{\partial F}{\partial \alpha_1}}{\delta\gamma - \beta F'} & -\frac{\beta \frac{\partial F}{\partial n}}{\delta\gamma - \beta F'} & -\frac{\beta \frac{\partial F}{\partial K}}{\delta\gamma - \beta F'} \end{pmatrix},$$

where $F' = \partial F / \partial P$ and all other derivatives of F are evaluated at the nominal parameter values.

We can now evaluate the sensitivity at the same protein concentration as we use in the open loop case. The equilibrium point is given by

$$x_e = \begin{pmatrix} m_e \\ P_e \end{pmatrix} = \begin{pmatrix} \frac{\alpha_0}{\gamma} \\ \frac{\alpha_0 \beta}{\delta \gamma} \end{pmatrix} = \begin{pmatrix} 0.239 \\ 23.9 \end{pmatrix}$$

and the sensitivity matrix is

$$S_{x_e, \theta}^{\text{closed}} \approx \begin{pmatrix} 76.1 & -18.2 & -1.16 & 116. & 0.134 & -0.212 & -0.000117 \\ 7610. & -1820. & 90.8 & -9080. & 13.4 & -21.2 & -0.0117 \end{pmatrix}.$$

The scaled sensitivity matrix becomes

$$\bar{S}_{x_e, \theta}^{\text{closed}} \approx \begin{pmatrix} 0.16 & -0.44 & -0.56 & 0.56 & 0.28 & -1.78 & -3.08 \times 10^{-7} \\ 0.16 & -0.44 & 0.44 & -0.44 & 0.28 & -1.78 & -3.08 \times 10^{-7} \end{pmatrix}. \quad (3.11)$$

Comparing this equation with equation (3.9), we see that there is reduction in the sensitivity with respect to most parameters. In particular, we become less sensitive to those parameters that are not part of the feedback (columns 2–4), but there is higher sensitivity with respect to some of the parameters that are part of the feedback mechanisms (particularly n). ∇

More generally, we may wish to evaluate the sensitivity of a (non-constant) solution to parameter changes. This can be done by computing the function $dx(t)/d\theta$, which describes how the state changes at each instant in time as a function of (small) changes in the parameters θ . We assume $u = 0$ for simplicity of exposition.

Let $x(t; x_0, \theta_0)$ be a solution of the dynamics with initial condition x_0 and parameters θ_0 . To compute $dx/d\theta$, we write down a differential equation for how it evolves in time:

$$\begin{aligned} \frac{d}{dt} \left(\frac{dx}{d\theta} \right) &= \frac{d}{d\theta} \left(\frac{dx}{dt} \right) = \frac{d}{d\theta} (f(x, \theta, u)) \\ &= \frac{\partial f}{\partial x} \frac{dx}{d\theta} + \frac{\partial f}{\partial \theta}. \end{aligned}$$

This is a differential equation with $n \times m$ states $S_{ij} = dx_i/d\theta_j$ and with initial condition $S_{ij}(0) = 0$ (since changes to the parameters do not affect the initial conditions).

To solve these equations, we must simultaneously solve for the state x and the sensitivity S (whose dynamics depend on x). Thus, we must solve the set of $n + nm$ coupled differential equations

$$\frac{dx}{dt} = f(x, \theta, u), \quad \frac{dS_{x\theta}}{dt} = \frac{\partial f}{\partial x}(x, \theta, u) S_{x\theta} + \frac{\partial f}{\partial \theta}(x, \theta, u). \quad (3.12)$$

This differential equation generalizes our previous results by allowing us to evaluate the sensitivity around a (non-constant) trajectory. Note that in the special case that we are at an equilibrium point and the dynamics for $S_{x,\theta}$ are stable, the steady state solution of equation (3.12) is identical to that obtained in equation (3.7). However, equation (3.12) is much more general, allowing us to determine the change in the state of the system at a fixed time T , for example. This equation also does not require that our solution stay near an equilibrium point, it only requires that our perturbations in the parameters are sufficiently small.

Example 3.8 (Repressilator). Consider the example of the repressilator, which was described in Example 2.2. The dynamics of this system can be written as

$$\begin{aligned} \frac{dm_1}{dt} &= F_{\text{rep}}(P_3) - \gamma m_1 & \frac{dP_1}{dt} &= \beta m_1 - \delta P_1 \\ \frac{dm_2}{dt} &= F_{\text{rep}}(P_1) - \gamma m_2 & \frac{dP_2}{dt} &= \beta m_2 - \delta P_2 \\ \frac{dm_3}{dt} &= F_{\text{rep}}(P_2) - \gamma m_3 & \frac{dP_3}{dt} &= \beta m_3 - \delta P_3, \end{aligned}$$

where the repressor is modeled using a Hill function

$$F_{\text{rep}}(P) = \frac{\alpha}{1 + (P/K)^n} + \alpha_0.$$

The dynamics of this system lead to a limit cycle in the protein concentrations, as shown in Figure 3.9a.

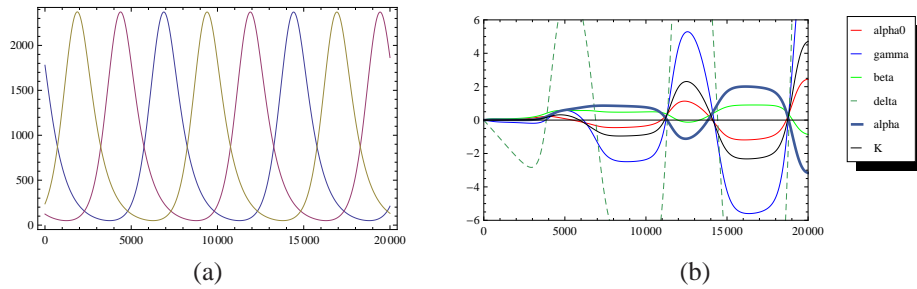


Figure 3.9: Repressilator sensitivity plots

We can analyze the sensitivity of the protein concentrations to changes in the parameters using the sensitivity differential equation. Since our solution is periodic, the sensitivity dynamics will satisfy an equation of the form

$$\frac{dS_{x,\theta}}{dt} = A(t)S_{x,\theta} + B(t),$$

where $A(t)$ and $B(t)$ are both periodic in time. Letting $x = (m_1, P_1, m_2, P_2, m_3, P_3)$ and $\theta = (\alpha_0, \gamma, \beta, \delta, \alpha, K)$, we can compute $S_{x,\theta}$ along the limit cycle. If the dynamics for $S_{x,\theta}$ are stable then the resulting solutions will be periodic, showing how the dynamics around the limit cycle depend on the parameter values. The results are shown in Figure 3.9b, where we plot the steady state sensitivity of P_1 as a function of time. We see, for example, that the limit cycle depends strongly on the protein degradation and dilution rate γ , indicating that changes in this value can lead to (relatively) large variations in the magnitude of the limit cycle.

▽

Several simulation tools include the ability to do sensitivity analysis of this sort, including COPASI.

Adaptation and disturbance rejection

A system is said to adapt to the input u when the steady state value of its output y is independent of the actual (constant) value of the input (Figure 3.10). Basically, after the input changes to a constant value, the output returns to its original value after a transient perturbation. Adaptation corresponds to the concept of *disturbance rejection* in control theory. The full notion of disturbance rejection is more general and depends on the specific disturbance input and it is studied using the internal model principle [81].

For example, for adaptation to constant signals, the internal model principle requires integral feedback. The internal model principle is a powerful way to uncover biochemical structures in natural networks that are known to have the adaptation

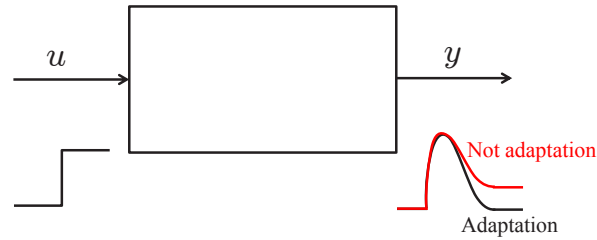


Figure 3.10: Adaptation property. The system is said to have the adaptation property if the steady state value of the output does not depend on the steady state value of the input. Hence, after a constant input perturbation, the output returns to its original value.

property. An example of this is the bacterial chemotaxis described in more detail in Chapter 5.

We illustrate two main mechanisms to attain adaptation: integral feedback and incoherent feedforward loops (IFFLs). We next study these two mechanisms from a mathematical standpoint to illustrate how they achieve adaptation. Possible biomolecular implementations are presented in later chapters.

Integral feedback

In integral feedback systems, a “memory” variable z keeps track of the accumulated difference between $y(t)$ and its nominal steady state value y_0 . A comparison is performed between this memory variable and the current input u , providing an error term that is used to drive the feedback mechanism that brings the system output back to the desired value y_0 (Figure 3.11).

In this system, the output $y(t)$, after any constant input perturbation u , tends to y_0 for $t \rightarrow \infty$ independently of the (constant) value of u . The equations representing the system are given by:

$$\frac{dz}{dt} = y_1, \quad y_1 = y - y_0, \quad y = k(u - z),$$

so that the equilibrium is obtained by setting $\dot{z} = 0$, from which we obtain $y = y_0$. That is, the steady state of y does not depend on u . The additional question to answer is whether, after a perturbation u occurs, $y_1(t)$ tends to zero for $t \rightarrow \infty$. This is the case if and only if $\dot{z} \rightarrow 0$ as $t \rightarrow \infty$, which is satisfied if the equilibrium of the system $\dot{z} = -kz + ku - y_0$ is asymptotically stable. This, in turn, is satisfied whenever $k > 0$ and u is a constant. Hence, after a constant perturbation u is applied, the system output y approaches back its original steady state value y_0 , that is, y is robust to constant perturbations.

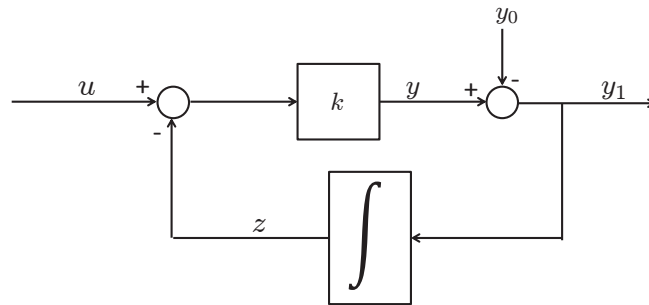


Figure 3.11: Basic block diagram representing a system with integral action.

More generally, a system with integral action can take the form

$$\frac{dx}{dt} = f(x, u, k), \quad y = h(x), \quad \frac{dz}{dt} = y - y_0, \quad k = k(x, z)$$

in which the steady state value of y , being the solution to $y - y_0 = 0$, does not depend on u . In turn, y tends to this steady state value for $t \rightarrow \infty$ if and only if $\dot{z} \rightarrow 0$ as $t \rightarrow \infty$. This, in turn, is the case if z tends to a constant value for $t \rightarrow \infty$, which is satisfied if u is a constant and the steady state of the above system is asymptotically stable.

Integral feedback is recognized as a key mechanism of perfectly adapting biological systems, both at the physiological level and at the cellular level, such as in blood calcium homeostasis [24], in the regulation of tryptophan in *E. coli* [84], in neuronal control of the prefrontal cortex [59], and in *E. coli* chemotaxis [91].

Incoherent feedforward loops

Feedforward motifs (Figure 3.12) are common in transcriptional networks and it has been shown they are over-represented in *E. coli* gene transcription networks, compared to other motifs composed of three nodes [4]. These are systems in which

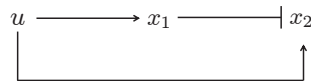


Figure 3.12: Incoherent feedforward loop. The input u affects the output through two channels. It indirectly represses it through an intermediate variable x_1 and it activates it directly.

the input u directly helps promote the production of the output x_2 and also acts as a delayed inhibitor of the output through an intermediate variable x_1 . This incoherent counterbalance between positive and negative effects gives rise, under appropriate conditions, to adaptation. A large number of incoherent feedforward loops participate in important biological processes such as the EGF to ERK activation [64], the glucose to insulin release [67], ATP to intracellular calcium release [56], micro-RNA regulation [83], and many others.

Several variants of incoherent feedforward loops exist for perfect adaptation. The “sniffer”, for example, is one in which the intermediate variable promotes degradation:

$$\frac{dx_1}{dt} = \alpha u - \delta x_1, \quad \frac{dx_2}{dt} = \beta u - \gamma x_1 x_2. \quad (3.13)$$

In this system, the steady state value of the output x_2 is obtained by setting the time derivatives to zero. Specifically, we have that $\dot{x}_1 = 0$ given $x_1 = \alpha u / \delta$ and $\dot{x}_2 = 0$ gives $x_2 = \beta u / (\gamma x_1)$, which combined together result in $x_2 = (\beta \delta) / (\gamma \alpha)$, which is a constant independent of the input u . The linearization of the system at the equilibrium is given by

$$A = \begin{pmatrix} -\delta & 0 \\ -\gamma(\beta\delta)/(\gamma\alpha) & -\gamma(\alpha u/\delta) \end{pmatrix}$$

which has eigenvalues $-\delta$ and $-\gamma(\alpha u/\delta)$. Since these are both negative, the equilibrium point is asymptotically stable. The sniffer appears in models of neutrophil motion and *Dictyostelium* chemotaxis [90].

Another form for a feedforward loop is one in which the intermediate variable x_1 inhibits production of the output x_2 , such as in the system:

$$\frac{dx_1}{dt} = \alpha u - \delta x_1, \quad \frac{dx_2}{dt} = \beta \frac{u}{x_1} - \gamma x_2. \quad (3.14)$$

The equilibrium point of this system is given by setting the time derivatives to zero. From $\dot{x}_1 = 0$, one obtains $x_1 = \alpha u / \delta$ and from $\dot{x}_2 = 0$ one still obtains that $x_2 = \beta u / (\gamma x_1)$, which combined together result in $x_2 = (\beta \delta) / (\gamma \alpha)$, which is a constant independent of the input u .

By calculating the linearization at the equilibrium, one obtains

$$A = \begin{pmatrix} -\delta & 0 \\ -\frac{u}{x_1^2} & -\gamma \end{pmatrix},$$

whose eigenvalues are given by $-\delta$ and $-\gamma$. Hence, the equilibrium point is asymptotically stable. Further, one can show that the equilibrium point is globally asymptotically stable because the x_1 subsystem is linear, stable, and x_1 approaches a constant value (for constant u) and the x_2 subsystem, in which $\beta u / x_1$ is viewed as an external input is also linear and exponentially stable.

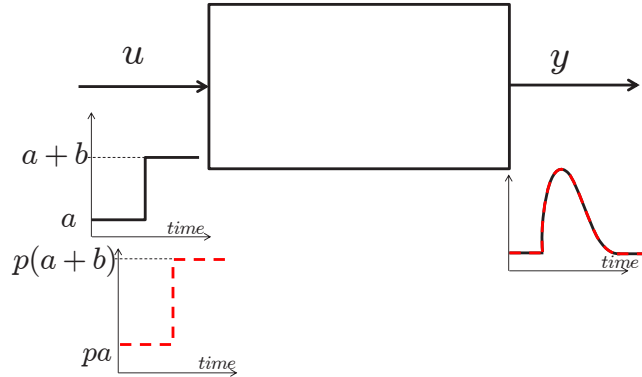


Figure 3.13: Fold-change detection. The output response does not depend on the absolute magnitude of the input but only on the fold change of the input.

Scale Invariance and fold-change detection

Scale invariance is the property by which the output $x_2(t)$ of the system does not depend on the amplitude of the input $u(t)$ (Figure 3.13). Specifically, consider an adapting system and assume that it pre-adapted to a constant background value a , then apply input $a + b$ and let $x_2(t)$ be the resulting output. Now consider a new background value pa for the input and let the system pre-adapt to it. Then apply the input $p(a + b)$ and let $\bar{x}_2(t)$ be the resulting output. The system has the scale invariance property if $x_2(t) = \bar{x}_2(t)$. This also means that the output responds in the same way to inputs changing by the same multiplicative factor (fold), hence this property is also called fold-change detection. Looking at Figure 3.13, the output would present different pulses for different fold changes b/a .

Incoherent feedforward loops can implement the fold-change detection property [33]. As an example, consider the feedforward motif represented by the sniffer and consider two inputs: $u_1(t) = a + b_1(t - t_0)$ and $u_2(t) = pa + pb_1(t - t_0)$. Assume also, as said above, that at time t_0 the system is at the steady state, that is, it pre-adapted. Hence, we have that the two steady states from which the system starts at $t = t_0$ are given by $x_{1,1} = a\alpha/\delta$ and $x_{1,2} = pa\alpha/\delta$ for the x_1 variable and by $x_{2,1} = x_{2,2} = (\beta\delta)/(\gamma\alpha)$ for the x_2 variable. Integrating system (3.14) starting from these initial conditions, we obtain for $t \geq t_0$

$$x_{1,1}(t) = a \frac{\alpha}{\delta} e^{-\delta(t-t_0)} + (a+b)(1 - e^{-\delta(t-t_0)}) \quad \text{and}$$

$$x_{1,2}(t) = pa \frac{\alpha}{\delta} e^{-\delta(t-t_0)} + p(a+b)(1 - e^{-\delta(t-t_0)}).$$

Using these in the expression of \dot{x}_2 in equation (3.14) gives the differential

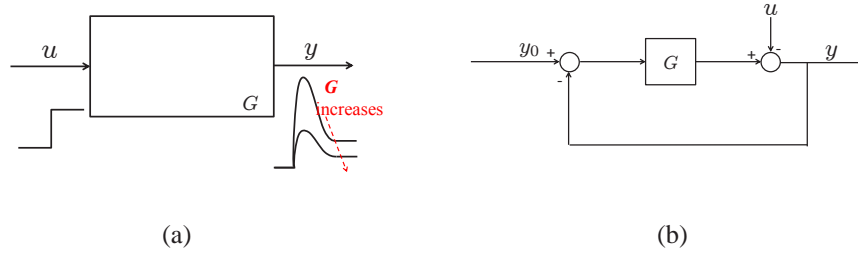


Figure 3.14: (a) Disturbance attenuation. A system is said to have the disturbance attenuation property if there is an internal system parameter G such that the system output response becomes arbitrarily close to a nominal output (independent of the input u) by increasing the value of G . (b) High gain feedback. A possible mechanism to attain disturbance attenuation is to feedback the error between the nominal output y_0 and the actual output y through a large gain G .

equations to which $x_{2,1}(t)$ and $x_{2,2}(t)$ obey for $t \geq t_0$ as

$$\frac{dx_{2,1}}{dt} = \frac{\beta(a+b)}{a\frac{\alpha}{\delta}e^{-\delta(t-t_0)} + (a+b)(1-e^{-\delta(t-t_0)})} - \gamma x_{2,1}, \quad x_{2,1}(t_0) = (\beta\delta)/(\gamma\alpha)$$

and

$$\frac{dx_{2,2}}{dt} = \frac{p\beta(a+b)}{pa\frac{\alpha}{\delta}e^{-\delta(t-t_0)} + p(a+b)(1-e^{-\delta(t-t_0)})} - \gamma x_{2,2}, \quad x_{2,2}(t_0) = (\beta\delta)/(\gamma\alpha),$$

which give $x_{2,1}(t) = x_{2,2}(t)$ for all $t \geq t_0$. Hence, the system responds exactly the same way after changes in the input of the same fold. The output response is not dependent on the scale of the input but only on its shape.

Disturbance attenuation

A system has the property of disturbance attenuation if there is a system parameter G such that the output response $y(t)$ to the input $u(t)$ can be made arbitrarily small as G is increased (Figure 3.14a). A possible mechanism for disturbance attenuation is high gain feedback (Figure 3.14b). In a high gain feedback configuration, the error between the output y , perturbed by some exogenous disturbance u , and a desired nominal output y_0 is fed back with a negative sign to produce the output y itself. If $y_0 > y$, this will result in an increase of y , otherwise it will result in a decrease of y . Mathematically, one obtains from the block diagram that

$$y = \frac{u}{1+G} + y_0 \frac{G}{1+G},$$

so that as G increases the (relative) contribution of u on the output of the system can be arbitrarily reduced.

High gain feedback can take a much more general form. Consider a system with $x \in \mathbb{R}^n$ in the form $\dot{x} = F(x, t)$. We say that this system is *contracting* if any two trajectories starting from different initial conditions tend to each other as time increase to infinity. A sufficient condition for the system to be contracting is that in some set of coordinates, with matrix transformation denoted Θ , the symmetric part of the linearization matrix (Jacobian) is negative definite. That is, that the largest eigenvalue of

$$\frac{1}{2} \left(\frac{\partial F}{\partial x} + \frac{\partial F^T}{\partial x} \right),$$

is negative. We denote this eigenvalue by $-\lambda$ for $\lambda > 0$ and call it the contraction rate of the system.

Now, consider the nominal system $\dot{x} = Gf(x, t)$ for $G > 0$ and its perturbed version $\dot{x}_p = Gf(x_p, t) + u(t)$. Assume that the input $u(t)$ is bounded everywhere in norm by a constant $C > 0$. If the system is contracting, we have the following robustness result:

$$\|x(t) - x_p(t)\| \leq \chi \|x(0) - x_p(0)\| e^{-G\lambda t} + \frac{\chi C}{\lambda G},$$

in which χ is an upper bound on the condition number (ratio between the largest and the smallest eigenvalue of $\Theta^T \Theta$) of the transformation matrix Θ [52]. Hence, if the perturbed and the nominal systems start from the same initial conditions, the difference between their states can be made arbitrarily small by increasing the gain G . Hence, the system has the disturbance attenuation property.

3.3 Analysis of Reaction Rate Equations

The previous section considered analysis techniques for general dynamical systems with small perturbations. In this section, we specialize to the case where the dynamics have the form of a reaction rate equation:

$$\frac{ds}{dt} = Nv(x, \theta), \quad (3.15)$$

where x is the vector of species concentrations, θ is the vector of reaction parameters, N is the stoichiometry matrix and $v(x, \theta)$ is the reaction rate (or flux) vector.

Reduced reaction dynamics

When analyzing reaction rate equations, it is often the case that there are conserved quantities in the dynamics. For example, conservation of mass will imply that if all compounds containing a given species are captured by the model, the total mass of that species will be constant. This type of constraint will then give a conserved quantity of the form $c_i = H_i x$ where H_i represents that combinations of species in

which the given element appears. Since c_i is constant, it follows that $dc_i/dt = 0$ and, aggregating the set of all conserved species, we have

$$0 = \frac{dc}{dt} = H \frac{ds}{dt} = HNv(x, \theta) \quad \text{for all } x.$$

If we assume that the vector of fluxes spans \mathbb{R}^m (the range of $v : \mathbb{R}^n \times \mathbb{R}^p \rightarrow \mathbb{R}^m$), then this implies that the conserved quantities correspond to the left null space of the stoichiometry matrix N .

It is often useful to remove the conserved quantities from the description of the dynamics and write the dynamics for a set of independent species. To do this, we transform the state of the system into two sets of variables:

$$\begin{pmatrix} x_i \\ x_d \end{pmatrix} = \begin{pmatrix} P \\ H \end{pmatrix} x. \quad (3.16)$$

The vector $x_i = Px$ is the set of independent species and is typically chosen as a subset of the original species of the model (so that the rows P consists of all zeros and a single 1 in the column corresponding to the selected species). The matrix H should span the left null space of N , so that x_d represents the set of dependent concentrations. These dependent species do not necessarily correspond to individual species, but instead are often combinations of species (for example, the total concentration of a given element that appears in a number of molecules that participate in the reaction).

Given the decomposition (3.16), we can rewrite the dynamics of the system in terms of the independent variables x_i . We start by noting that given x_i and x_d , we can reconstruct the full set of species x :

$$x = \begin{pmatrix} P \\ H \end{pmatrix}^{-1} \begin{pmatrix} x_i \\ x_d \end{pmatrix} = Lx_i + c_0, \quad L = \begin{pmatrix} P \\ H \end{pmatrix}^{-1} \begin{pmatrix} I \\ 0 \end{pmatrix}, \quad c_0 = \begin{pmatrix} P \\ H \end{pmatrix}^{-1} \begin{pmatrix} 0 \\ c \end{pmatrix}$$

where c_0 represents the conserved quantities. We now write the dynamics for x_i as

$$\frac{dx_i}{dt} = P \frac{dx}{dt} = PNv(Lx_i + c_0, \theta) = N_r v_r(x_i, c_0, \theta), \quad (3.17)$$

where N_r is the *reduced stoichiometry matrix* and v_r is the rate vector with the conserved quantities separated out as constant parameters.

The reduced order dynamics in equation (3.17) represent the evolution of the independent species in the reaction. Given x_i , we can reconstruct the full set of species from the dynamics of the independent species by writing $x = Lx_i + c_0$. The vector c_0 represents the values of the conserved quantities, which must be specified in order to compute the values of the full set of species. In addition, since $x = Lx_i + c_0$, we have that

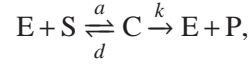
$$\frac{dx}{dt} = L \frac{dx_i}{dt} = LN_r v_r(x_i, c_0, p) = LN_r v(x, \theta),$$

which implies that

$$N = LN_r.$$

Thus, L also reconstruct the reduced stoichiometry matrix from the reduced space to the full space.

Example 3.9 (Enzyme kinetics). Consider an enzymatic reaction



whose full dynamics can be written as

$$\frac{d}{dt} \begin{pmatrix} S \\ E \\ C \\ P \end{pmatrix} = \begin{pmatrix} -1 & 1 & 0 \\ -1 & 1 & 1 \\ 1 & -1 & -1 \\ 0 & 0 & 1 \end{pmatrix} \begin{pmatrix} aE \cdot S \\ dC \\ kC \end{pmatrix}.$$

The conserved quantities are given by

$$H = \begin{pmatrix} 0 & 1 & 1 & 0 \\ 1 & -1 & 0 & 1 \end{pmatrix}.$$

The first of these is the total enzyme concentration $E_{\text{tot}} = E + C$, while the second asserts that the concentration of product P is equal to the free enzyme concentration E minus the substrate concentration S . If we assume that we start with substrate concentration S_0 , enzyme concentration E_{tot} and no product or bound enzyme, then the conserved quantities are given by

$$c = \begin{pmatrix} E + C \\ S - E + P \end{pmatrix} = \begin{pmatrix} E_{\text{tot}} \\ S_0 - E_{\text{tot}} \end{pmatrix}.$$

There are many possible choices for the set of independent species $x_i = Px$, but since we are interested in the substrate and the product, we choose P as

$$P = \begin{pmatrix} 1 & 0 & 0 & 0 \\ 0 & 0 & 0 & 1 \end{pmatrix}.$$

Once P is chosen then we can compute

$$L = \begin{pmatrix} P \\ H \end{pmatrix}^{-1} \begin{pmatrix} I \\ 0 \end{pmatrix} = \begin{pmatrix} 1 & 0 \\ 1 & 1 \\ -1 & -1 \\ 0 & 1 \end{pmatrix}, \quad c_0 = \begin{pmatrix} P \\ H \end{pmatrix}^{-1} \begin{pmatrix} 0 \\ c \end{pmatrix} = \begin{pmatrix} 0 \\ E_{\text{tot}} - S_0 \\ S_0 \\ 0 \end{pmatrix},$$

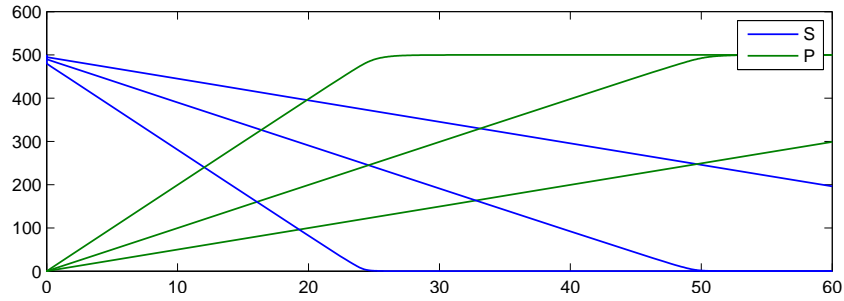


Figure 3.15: Enzyme dynamics. The simulations were carried out $a = d = 10$, $k = 1$, $S_0 = 500$ and $E_{\text{tot}} = 5, 10, 20$. The top plot shows the concentration of substrate S and product P , with the fastest case corresponding to $E_{\text{tot}} = 20$. The figures on the lower left zoom in on the substrate and product concentrations at the initial time and the figures on the lower right at one of the transition times.

The resulting reduced order dynamics can be computed to be

$$\begin{aligned} \frac{d}{dt} \begin{pmatrix} S \\ P \end{pmatrix} &= \begin{pmatrix} -1 & 1 & 0 \\ 0 & 0 & 1 \end{pmatrix} \begin{pmatrix} a(P + S + E_{\text{tot}} - S_0)S \\ d(-P - S + S_0) \\ k(-P - S + S_0) \end{pmatrix} \\ &= \begin{pmatrix} -a(P + S + E_{\text{tot}} - S_0)S - d(P + S - S_0) \\ k(S_0 - S - P) \end{pmatrix}. \end{aligned}$$

A simulation of the dynamics is shown in Figure 3.15. We see that the dynamics are very well approximated as being a constant rate of production until we exhaust the substrate (consistent with the Michaelis-Menten approximation).

▽

Metabolic control analysis

Metabolic control analysis (MCA) focuses on the study of the sensitivity of steady state concentrations and fluxes to changes in various system parameters. The basic concepts are equivalent to the sensitivity analysis tools described in Section 3.1, specialized to the case of reaction rate equations. In this section we provide a brief introduction to the key ideas, emphasizing the mapping between the general concepts and MCA terminology (as originally done by Ingalls [43]).

Consider the reduced set of chemical reactions

$$\frac{dx_i}{dt} = N_r v_r(x_i, \theta) = N_r v(Lx_i + c_0, \theta).$$

We wish to compute the sensitivity of the equilibrium concentrations x_e and equilibrium fluxes v_e to the parameters θ . We start by linearizing the dynamics around

an equilibrium point x_e . Defining $z = x - x_e$, $u = \theta - \theta_0$ and $f(z, u) = N_r v(x_e + z, \theta_0 + u)$, we can write the linearized dynamics as

$$\frac{dx}{dt} = Ax + Bu, \quad A = \left(N_r \frac{\partial v}{\partial s} L \right), \quad B = \left(N_r \frac{\partial v}{\partial p} \right), \quad (3.18)$$

which has the form of a linear differential equation with state z and input u .

In metabolic control analysis, the following terms are defined:

$$\begin{aligned} \bar{\epsilon}_\theta &= \left. \frac{dv}{d\theta} \right|_{x_e, \theta_0} & \bar{\epsilon}_\theta &= \text{flux control coefficients} \\ \bar{R}_\theta^x &= \frac{\partial x_e}{\partial \theta} = \bar{C}^x \bar{\epsilon}_\theta & \bar{R}_\theta^x &= \\ & & \bar{C}^x &= \text{concentration control coefficients} \\ \bar{R}_\theta^v &= \frac{\partial v_e}{\partial \theta} = \bar{C}^v \bar{\epsilon}_\theta & \bar{R}_\theta^v &= \\ & & \bar{C}^v &= \text{rate control coefficients} \end{aligned}$$

These relationships describe how the equilibrium concentration and equilibrium rates change as a function of the perturbations in the parameters. The two control matrices provide a mapping between the variation in the flux vector evaluated at equilibrium,

$$\left(\frac{\partial v}{\partial \theta} \right)_{x_e, \theta_0},$$

and the corresponding differential changes in the equilibrium point, $\partial x_e / \partial \theta$ and $\partial v_e / \partial \theta$. Note that

$$\frac{\partial v_e}{\partial \theta} \neq \left(\frac{\partial v}{\partial \theta} \right)_{x_e, \theta_0}.$$

The left side is the relative change in the equilibrium rates, while the right side is the change in the rate function $v(x, \theta)$ evaluated at an equilibrium point.

To derive the coefficient matrices \bar{C}^x and \bar{C}^v , we simply take the linear equation (3.18) and choose outputs corresponding to s and v :

$$y_x = Ix, \quad y_v = \frac{\partial v}{\partial x} Lx + \frac{\partial v}{\partial \theta} u.$$

Using these relationships, we can compute the transfer functions

$$\begin{aligned} H_x(s) &= (sI - A)^{-1} B = \left[(sI - N_r \frac{\partial v}{\partial x} L)^{-1} N_r \right] \frac{\partial v}{\partial \theta}, \\ H_v(s) &= \frac{\partial v}{\partial s} L (sI - A)^{-1} B + \frac{\partial v}{\partial \theta} = \left[\frac{\partial v}{\partial x} L (sI - N_r \frac{\partial v}{\partial x} L)^{-1} N_r + I \right] \frac{\partial v}{\partial \theta}. \end{aligned}$$

Classical metabolic control analysis considers only the equilibrium concentrations, and so these transfer functions would be evaluated at $x = 0$ to obtain the equilibrium equations.

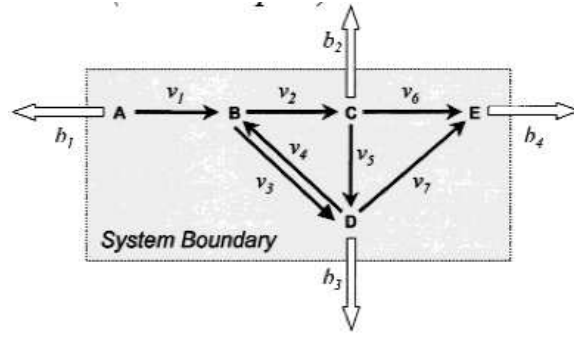


Figure 3.16: Flux balance analysis.

These equations are often normalized by the equilibrium concentrations and parameter values, so that all quantities are expressed as fractional quantities. If we define

$$D^x = \text{diag}\{x_e\}, \quad D^v = \text{diag}\{v(x_e, \theta_0)\}, \quad D^\theta = \text{diag}\{\theta_0\},$$

then the normalized coefficient matrices (without the overbar) are given by

$$\begin{aligned} C^x &= (D^x)^{-1} \bar{C}^x D^v, & C^v &= (D^v)^{-1} \bar{C}^v D^v, \\ R_\theta^x &= (D^x)^{-1} \bar{R}_\theta^x D^\theta, & R_\theta^v &= (D^v)^{-1} \bar{R}_\theta^v D^\theta. \end{aligned}$$

Flux balance analysis

Flux balance analysis is a technique for studying the relative rate of different reactions in a complex reaction system. We are most interested in the case where there may be multiple pathways in a system, so that the number of reactions m is greater than the number of species n . The dynamics

$$\frac{dx}{dt} = Nv(x, \theta)$$

thus have the property that the matrix N has more columns than rows and hence there are multiple reactions that can produce a given set of species. Flux balance is often applied to pathway analysis in metabolic systems to understand the limiting pathways for a given species and the effects of changes in the network (e.g., through gene deletions) to the production capacity.

To perform a flux balance analysis, we begin by separating the reactions of the pathway into internal fluxes v_i versus exchanges flux v_e , as illustrated in Figure 3.16. The dynamics of the resulting system now be written as

$$\frac{dx}{dt} = Nv(x, \theta) = N \begin{pmatrix} v_i \\ v_e \end{pmatrix} = Nv_i(x, \theta) - b_e,$$

where $b_e = -Nv_e$ represents the effects of external fluxes on the species dynamics. Since the matrix N has more columns than rows, it has a *right* null space and hence there are many different internal fluxes that can produce a given change in species.

In particular, we are interested studying the steady state properties of the system. In this case, we have that $dx/dt = 0$ and we are left with an algebraic system

$$Nv_i = b_e.$$

Review

Material to be completed.

3.4 Oscillatory Behavior

In addition to equilibrium behavior, a variety of cellular processes involve oscillatory behavior in which the system state is constantly changing, but in a repeating pattern. Two examples of biological oscillations are the cell cycle and circadian rhythm. Both of these dynamic behaviors involve repeating changes in the concentrations of various proteins, complexes and other molecular species in the cell, though they are very different in their operation. In this section we discuss some of the underlying ideas for how to model this type of oscillatory behavior, focusing on those types of oscillations that are most common in biomolecular systems.

Biomolecular oscillators

Biological systems have a number of natural oscillatory processes that govern the behavior of subsystems and whole organisms. These range from internal oscillations within cells to the oscillatory nature of the beating heart to various tremors and other undesirable oscillations in the neuro-muscular system. At the biomolecular level, two of the most studied classes of oscillations are the cell cycle and circadian rhythm.

The cell cycle consists of a set “phases” that govern the duplication and division of cells into two new cells:

- G1 phase - gap phase, terminated by “G1 checkpoint”
- S phase - synthesis phase (DNA replication)
- G2 phase - gap phase, terminated by “G2 checkpoint”
- M - mitosis (cell division)

The cell goes through these stages in a cyclical fashion, with the different enzymes and pathways active in different phases. The cell cycle is regulated by many different proteins, often divided into two major classes. *Cyclins* are a class of proteins that sense environmental conditions internal and external to the cell and are also used to implement various logical operations that control transition out of

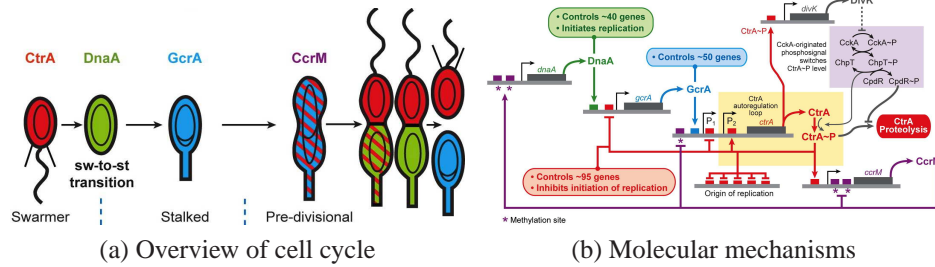


Figure 3.17: The *Caulobacter crescentus* cell cycle. (a) *Caulobacter* cells divide asymmetrically into a stalked cell, which is attached to a surface, and a swarmer cell, that is motile. The swarmer cells can become stalked cells in a new location and begin the cell cycle anew. The transcriptional regulators CtrA, DnaA and GcrA are the primary factors that control the various phases of the cell cycle. (b) The genetic circuitry controlling the cell cycle consists of a large variety of regulatory mechanisms, described in more detail in the text. Figure obtained from [50] (permission TBD).

the G1 and G2 phases. *Cyclin dependent kinases* (CDKs) are proteins that serve as “actuators” by turning on various pathways during different cell cycles.

An example of the control circuitry of the cell cycle for the bacterium *Caulobacter crescentus* (henceforth *Caulobacter*) is shown in Figure 3.17 [50]. This organism uses a variety of different biomolecular mechanisms, including transcriptional activation and repression, positive autoregulation (CtrA), phosphotransfer and methylation of DNA.

The cell cycle is an example of an oscillator that does not have a fixed period. Instead, the length of the individual phases and the transitioning of the different phases are determined by the environmental conditions. As one example, the cell division time for *E. coli* can vary between 20 minutes and 90 minutes due to changes in nutrient concentrations, temperature or other external factors.

A different type of oscillation is the highly regular pattern encoding in circadian rhythm, which repeats with a period of roughly 24 hours. The observation of circadian rhythms dates as far back as 400 BCE, when Androsthenes described observations of daily leaf movements of the tamarind tree [57]. There are three defining characteristics associated with circadian rhythm: (1) the time to complete one cycle is approximately 24 hours, (2) the rhythm is endogenously generated and self-sustaining and (3) the period remains relatively constant under changes in ambient temperature. Oscillations that have these properties appear in many different organisms, including micro-organisms, plants, insects and mammals. Some common features of the circuitry implementing circadian rhythms in these organisms is the combination of positive and negative feedback loops, often with the positive elements activating the expression of clock genes and the negative elements repressing the positive elements [12]. Figure 3.18 shows some of the different organisms in which circadian oscillations can be found and the primary genes responsible for

different positive and negative factors.

Clocks, oscillators and limit cycles

To begin our study of oscillators, we consider a nonlinear model of the system described by the differential equation

$$\frac{dx}{dt} = f(x, u, \theta), \quad y = h(x, \theta)$$

where $x \in \mathbb{R}^n$ represents the state of the system (typically concentrations of various proteins and other species and complexes), $u \in \mathbb{R}^q$ represents the external inputs, $y \in \mathbb{R}^p$ represents the (measured) outputs and $\theta \in \mathbb{R}^K$ represents the model parameters. We say that a solution $(x(t), u(t))$ is *oscillatory with period T* if $y(t+T) = y(t)$. For simplicity, we will often assume that $p = q = 1$, so that we have a single input and single output, but most of the results can be generalized to the multi-input, multi-output case.

There are multiple ways in which a solution can be oscillatory. One of the simplest is that the input $u(t)$ is oscillatory, in which case we say that we have a *forced oscillation*. In the case of a linear system, an input of the form $u(t) = A \sin \omega t$ then we now already the output will be of the form $y(t) = M \cdot A \sin(\omega t + \phi)$ where M and ϕ represent the gain and phase of the system (at frequency ω). In the case of a nonlinear system, if the output is periodic then we can write it in terms of a set of harmonics,

$$y(t) = B_0 + B_1 \sin(\omega t + \phi_1) + B_2 \sin(2\omega t + \phi_2) + \dots$$

The term B_0 represents the average value of the output (also called the bias), the terms B_i are the magnitudes of the i th harmonic and ϕ_i are the phases of the harmonics (relative to the input). The *oscillation frequency* ω is given by $\omega = 2\pi/T$ where T is the oscillation period.

A different situation occurs when we have no input (or a constant input) and still obtain an oscillatory output. In this case we say that the system has a *self-sustained oscillation*. This type of behavior is what is required for oscillations such as the cell cycle and circadian rhythm, where there is either no obvious forcing function or the forcing function is removed by the oscillation persists. If we assume that the input is constant, $u(t) = A_0$, then we are particularly interested in how the period T (or equivalently frequency ω), amplitudes B_i and phases ϕ_i depend on the input A_0 and system parameters θ .

To simplify our notation slightly, we consider a system of the form

$$\frac{dx}{dt} = F(x, \theta), \quad y = h(x, \theta) \tag{3.19}$$

where $F(x, \theta) = f(x, u, \theta)$ reflects the fact that the input is ignored (or taken to be one of the constant parameters) in the analysis that follows. We have focused on

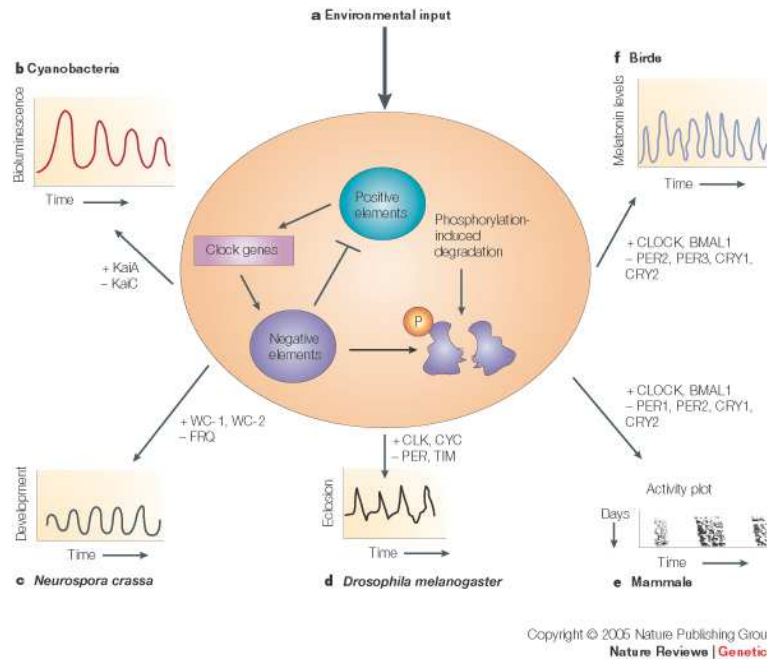


Figure 3.18: (a) Most circadian systems use a clock mechanism involving oscillators that are composed of positive and negative elements, which form feedback loops. In these loops, the positive elements activate the expression of the clock genes. The clock genes, as well as driving rhythmic biological outputs, encode negative elements that inhibit the activities of the positive elements. Phosphorylation of the negative elements leads to their eventual degradation, allowing the positive elements to restart the cycle. Clock genes can sometimes also function positively to increase the expression of the positive elements (not shown). (b–f) Although the same basic mechanism is present, the components vary in different organisms. The core oscillator components are indicated for the model organisms discussed in this review (positive elements (indicated by '+' symbols): KaiA, WHITE COLLAR-1 (WC-1), WHITE COLLAR-2 (WC-2), CLOCK (CLK in *Drosophila melanogaster*), CYCLE (CYC), and brain and muscle Arnt-like protein 1 (BMAL1, also known as MOP3 and ARNT1); negative elements (indicated by '-' symbols): KaiC, FREQUENCY (FRQ), period (PER), timeless (TIM), cryptochrome (CRY)). Examples of circadian activities that are commonly experimentally assayed in these organisms are also shown. These oscillators receive environmental input and, either alone or coupled to other oscillators, send signals through an unknown mechanism to the rest of the organism to control rhythmic behaviours. In cyanobacteria (b), rhythmic output is measured by fusing the promoters of rhythmic genes to a luciferase reporter gene to monitor the resulting bioluminescence. In *Neurospora crassa* (c), rhythmicity in the development of asexual conidiospores is monitored. In flies (d), mammals (e) and birds (f), rhythms in locomotor activity can be monitored using automated equipment. Another rhythmic event in flies is eclosion (d), which is the emergence of adult flies from their pupal case. For mammals (e), activity (dark lines) is shown as a vertical stack (in chronological order, with each horizontal row representing activity for one day) and double plotted for clarity. In addition, rhythms in gene expression and biochemical activities, such as those shown for melatonin levels in birds (f), provide further measures of rhythmicity. Figure and caption from [12].

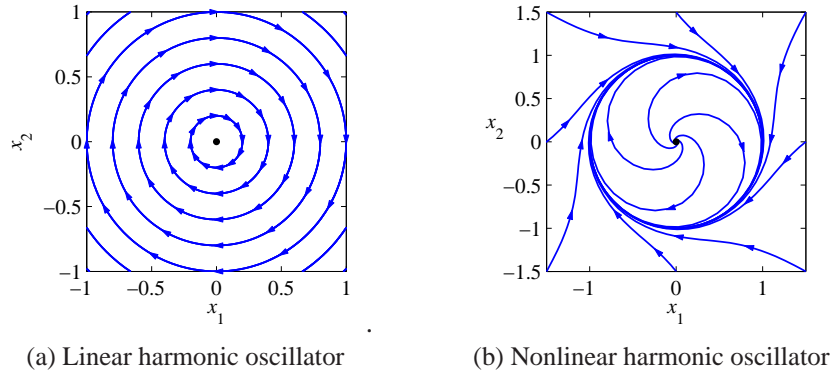


Figure 3.19: Examples of harmonic oscillators.

the oscillatory nature of the output $y(t)$ thus far, but we note that if the states $x(t)$ are periodic then the output is as well, as this is the most common case. Hence we will often talk about the *system* being oscillatory, by which we mean that there is a solution for the dynamics in which the state satisfies $x(t+T) = x(t)$.

More formally, we say that a closed curve $\Gamma \in \mathbb{R}^n$ is an *orbit* if trajectories that start on Γ remain on Γ for all time and if Γ is not an equilibrium point of the system. As in the case of equilibrium points, we say that the orbit is *stable* if trajectories that start near Γ stay near Γ , *asymptotically stable* if in addition nearby trajectories approach Γ as $t \rightarrow \infty$ and *unstable* if it is not stable. The orbit Γ is periodic with period T if for any $x(t) \in \Gamma$, $x(t+T) = x(t)$.

There are many different types of periodic orbits that can occur in a system whose dynamics are modeled as in equation (3.19). A *harmonic oscillator* refers to a system that oscillates around an equilibrium point, but does not (usually) get near the equilibrium point. The classical harmonic oscillator is a linear system of the form

$$\frac{d}{dt} \begin{pmatrix} 0 & \omega \\ -\omega & 0 \end{pmatrix} \begin{pmatrix} x_1 \\ x_2 \end{pmatrix},$$

whose solutions are given by

$$\begin{pmatrix} x_1(t) \\ x_2(t) \end{pmatrix} = \begin{pmatrix} \cos \omega t & \sin \omega t \\ -\sin \omega t & \cos \omega t \end{pmatrix} \begin{pmatrix} x_1(0) \\ x_2(0) \end{pmatrix}.$$

The frequency of this oscillation is fixed, but the amplitude depends on the values of the initial conditions, as shown in Figure 3.19. Note that this system has a single equilibrium point at $x = (0,0)$ and the eigenvalues of the equilibrium point have zero real part, so trajectories neither expand nor contract, but simply oscillate.

An example of a nonlinear harmonic oscillator is given by the equation

$$\frac{dx_1}{dt} = x_2 + x_1(1 - x_1^2 - x_2^2), \quad \frac{dx_2}{dt} = -x_1 + x_2(1 - x_1^2 - x_2^2). \quad (3.20)$$

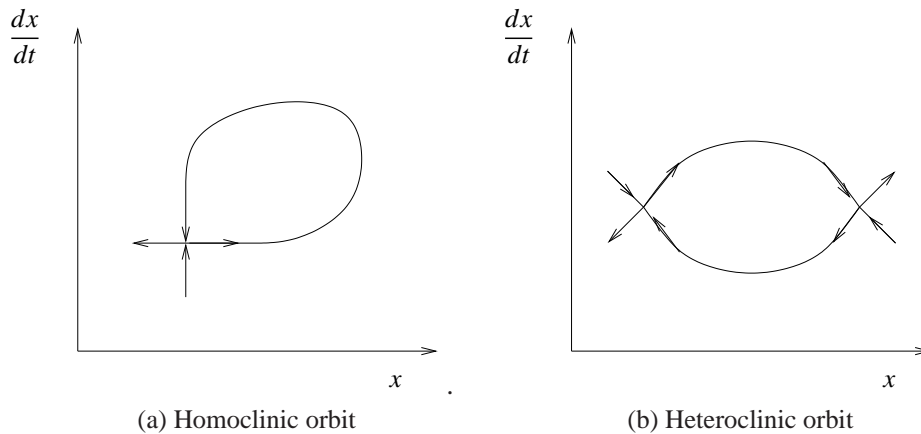


Figure 3.20: Homoclinic and heteroclinic orbits

This system has an equilibrium point at $x = (0, 0)$, but the linearization of this equilibrium point is unstable. The phase portrait in Figure 3.19b shows that the solutions in the phase plane converge to a circular trajectory. In the time domain this corresponds to an oscillatory solution. Mathematically the circle is called a *limit cycle*. Note that in this case, the solution for any initial condition approaches the limit cycle and the amplitude and frequency of oscillation “in steady state” (once we have reached the limit cycle) are independent of the initial condition.

A different type of oscillation can occur in nonlinear systems in which the equilibrium points are saddle points, having both stable and unstable eigenvalues. Of particular interest is the case where the stable and unstable orbits of one or more equilibrium points join together. Two such situations are shown in Figure 3.20. The figure on the left is an example of a *homoclinic orbit*. In this system, trajectories that start near the equilibrium point quickly diverge away (in the directions corresponding to the unstable eigenvalues) and then slowly return to the equilibrium point along the stable directions. If the initial conditions are chosen to be precisely on the homoclinic orbit Γ then the system slowly converges to the equilibrium point, but in practice there are often disturbances present that will perturb the system off of the orbit and trigger a “burst” in which the system rapidly escapes from the equilibrium point and then slowly converges again.

A somewhat similar type of orbit is a *heteroclinic orbit*, in which the orbit connects two different equilibrium points, as shown in Figure 3.20b.

An example of a system with a homoclinic orbit is given by the system

$$\frac{dx_1}{dt} = x_2, \quad \frac{dx_2}{dt} = x_1 - x_1^3 \quad (3.21)$$

The phase portrait and time domain solutions are shown in Figure 3.21. In this system, there are periodic orbits both inside and outside the two homoclinic cy-

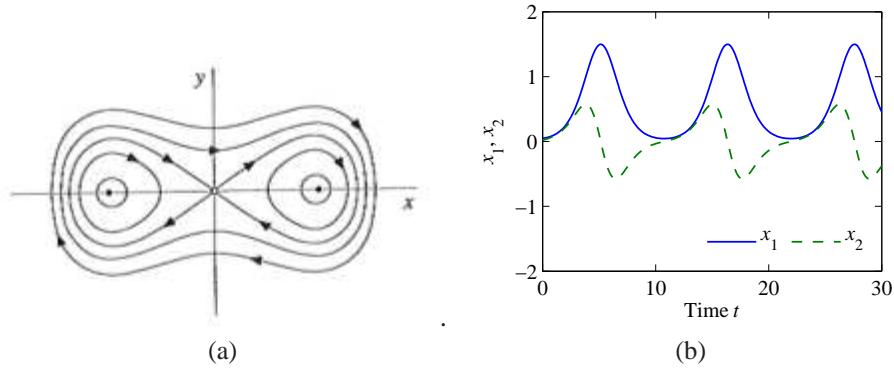


Figure 3.21: Example of a homoclinic orbit.

cles (left and right). Note that the trajectory we have chosen to plot in the time domain has the property that it rapidly moves away from the equilibrium point and then slowly re-converges to the equilibrium point, before begin carried away again. This type of oscillation, in which one slowly returns to an equilibrium point before rapidly diverging is often called a *relaxation oscillation*. Note that for this system, there are also oscillations that look more like the harmonic oscillator case described above, in which we oscillate around the unstable equilibrium points at $x = (\pm 1, 0)$.

Example 3.10 (Glycolytic oscillations). Glycolysis is one of the principal metabolic networks involved in energy production. It is a sequence of enzyme-catalyzed reactions that converts sugar into pyruvate, which is then further degraded to alcohol (in yeast fermentation) and lactic acid (in muscles) in anaerobic conditions, and ATP (the cell's major energy supply) is produced as a result. Both damped and sustained oscillations have been observed. Damped oscillations were first reported by [23] while sustained oscillations in yeast cell free extracts were observed when glucose-6-phosphate (G6P), fructose-6-phosphate (F6P) [39] or trehalose [71] were used as substrates.

Here, we introduce the fundamental motif which is known to be at the core of these oscillatory phenomenon. This is depicted in Figure 3.22 (a). A simple model for the system is given by the two differential equations

$$\frac{dS}{dt} = v_0 - v_1, \quad \frac{dP}{dt} = v_1 - v_2,$$

in which

$$v_1 = S f(P), \quad f(P) = \frac{\alpha P^2}{K + P^2}, \quad v_2 = k_2 P,$$

where $f(P)$ is the Hill function. Under the assumption that $K \gg P^2$, we have $f(P) \approx k_1 P^2$, in which we have defined $k_1 := \alpha/K$. This second order system admits a stable limit cycle under suitable parameter conditions (Figure 3.22(b)). ∇

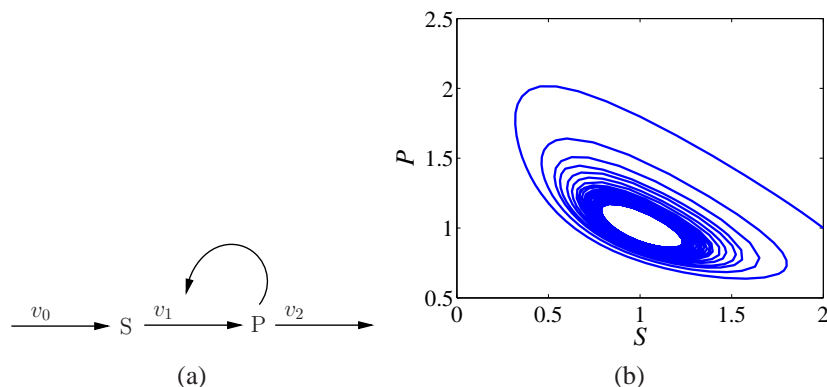


Figure 3.22: (a) The Glycolysis pathway. “S” is a substrate, which is converted into product “P”. This, in turn, is activating its own production by enhancing the rate v_2 . (b) Oscillations in the glycolysis pathway. Parameters are $v_0 = 1$, $k_1 = 1$, and $k_2 = 1.00001$.

The example above illustrates some of the types of questions we would like to answer for oscillatory systems. For example, Under what parameter conditions do oscillations occur in the glycolytic system? How much can the parameter change before the limit cycle disappears? To analyze these sorts of questions, we need to introduce tools that allow to infer the existence and robustness of limit cycle behavior from a differential equation model. The objective of this section is to address these questions.

Consider the system $\dot{x} = F(x)$ and let $x(t, x_0)$ denote its solution starting at x_0 at time $t = 0$, that is, $\dot{x}(t, x_0) = F(x(t, x_0))$ and $x(0, x_0) = x_0$. We say that $x(t, x_0)$ is a *periodic solution* if there is $T > 0$ such that $x(t, x_0) = x(t + T, x_0)$ for all $t \in \mathbb{R}$. Here, we seek to answer two questions: (a) when does a system $\dot{x} = F(x)$ admit periodic solutions? (b) When are these periodic solutions stable or asymptotically stable?

In order to provide the main result to state the existence of a stable periodic solution, we need the concept of omega-limit set of a point p , denoted $\omega(p)$. Basically, the omega-limit set $\omega(p)$ denotes the set of all points to which the trajectory of the system starting from p tends as time approaches infinity. This is formally defined in the following definition.

Definition 3.1. A point $\bar{x} \in \mathbb{R}^n$ is called an *omega-limit point* of $p \in \mathbb{R}^n$ if there is a sequence of times $\{t_i\}$ with $t_i \rightarrow \infty$ for $i \rightarrow \infty$ such that $x(t_i, p) \rightarrow \bar{x}$ as $i \rightarrow \infty$. The *omega limit set* of p , denoted $\omega(p)$, is the set of all omega-limit points of p .

The omega-limit set of a system has several relevant properties, among which the fact that it cannot be empty and that it must be a connected set.

Limit cycles in the plane

Before studying periodic behavior of systems in \mathbb{R}^n , we study the behavior of systems in \mathbb{R}^2 as several high dimensional systems can be often well approximated by systems in two dimensions by, for example, employing quasi-steady state approximations. For systems in \mathbb{R}^2 , we will see that there are easy-to-check conditions that guarantee the existence of a limit cycle.

The first result that we next give provides a simple check to rule out periodic solutions for system in \mathbb{R}^2 . Specifically, let $x \in \mathbb{R}^2$ and consider

$$\dot{x}_1 = F_1(x_1, x_2) \quad \dot{x}_2 = F_2(x_1, x_2), \quad (3.22)$$

in which the functions $F : \mathbb{R}^2 \rightarrow \mathbb{R}^2$ is smooth. Then, we have the following result:

Theorem 3.2 (Bendixson's criterion). *If on a simply connected region $D \subset \mathbb{R}^2$ (i.e., there are no holes in it) the expression*

$$\frac{\partial F_1}{\partial x_1} + \frac{\partial F_2}{\partial x_2}$$

is not identically zero and does not change sign, then system (3.22) has no closed orbits that lie entirely in D .

Example 3.11. Consider the system

$$\dot{x}_1 = -x_2^3 + \delta x_1^3, \quad \dot{x}_2 = x_1^3,$$

with $\delta \geq 0$. We can compute $\frac{\partial F_1}{\partial x_1} + \frac{\partial F_2}{\partial x_2} = 3\delta x_1^2$, which is positive in all \mathbb{R}^2 if $\delta \neq 0$. If $\delta \neq 0$, we can thus conclude from Bendixson's criterion that there are no periodic solutions. Investigate as an exercise what happens when $\delta = 0$. ∇

The following theorem, completely characterizes the omega limit set of any point for a system in \mathbb{R}^2 .

Theorem 3.3 (Poincaré-Bendixson). *Let M be a bounded and closed positively invariant region for the system $\dot{x} = F(x)$ with $x \in M$ (i.e., any trajectory that starts in M stays in M for all $t \geq 0$). Let $p \in M$, then one of the following possibilities holds for $\omega(p)$:*

- (i) $\omega(p)$ is a steady state;
- (ii) $\omega(p)$ is a closed orbit;
- (iii) $\omega(p)$ consists of a finite number of steady states and orbits, each starting (for $t = 0$) and ending (for $t \rightarrow \infty$) at one of the fixed points.

This theorem has two important consequences:

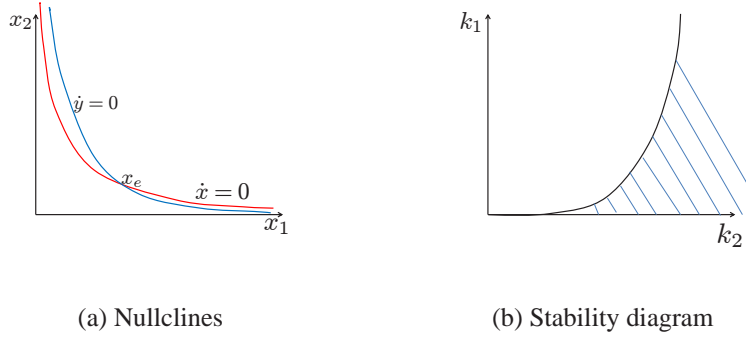


Figure 3.23: (a) The nullclines and the equilibrium of the system. (b) Parameter space leading to oscillatory behavior.

1. If the system does not have steady states in M , since $\omega(p)$ is not empty, it must be a periodic solution;
2. If there is only one steady state in M and it is unstable and not a saddle (i.e., the eigenvalues of the linearization at the steady state are both positive), then $\omega(p)$ is a periodic solution.

Example 3.12 (Glycolytic oscillations). Consider again the glycolysis example. Let $x_1 = S$ and $x_2 = P$ and rewrite the system (3.10) as

$$\frac{dx_1}{dt} = v_0 - k_1 x_1 x_2^2 =: F_1(x_1, x_2), \quad \frac{dx_2}{dt} = k_1 x_1 x_2^2 - k_2 x_2 =: F_2(x_1, x_2).$$

As a first step, we need to determine the number of steady states. From $\dot{x} = 0$, we obtain

$$x = \frac{v_0}{k_1 y^2},$$

while from $\dot{y} = 0$, we obtain

$$x = \frac{k_2}{k_1 y}.$$

The intersection between these two curves (the nullclines) in the (x_1, x_2) plane gives rise to one steady state only (Figure 3.23a). The reader can determine a positively invariant region that is compact. Then, it is enough to verify that the steady state $(x_{1,e}, x_{2,e})$ is unstable and not a saddle to guarantee the existence of a stable limit cycle. Thus,

$$J = \begin{pmatrix} \frac{\partial F_1}{\partial x_1} & \frac{\partial F_1}{\partial x_2} \\ \frac{\partial F_2}{\partial x_1} & \frac{\partial F_2}{\partial x_2} \end{pmatrix} \Bigg|_{(x_{1,e}, x_{2,e})} = \begin{pmatrix} -k_1 x_{2,e}^2 & -2k_1 x_{1,e} x_{2,e} \\ k_1 x_{2,e}^2 & -k_2 + 2k_1 x_{1,e} x_{2,e} \end{pmatrix},$$

in which $x_{1,e} = k_2^2/(k_1 v_0)$ and $x_{2,e} = v_0/k_2$. The eigenvalues are such that

$$\lambda_{1,2} = \frac{\text{tr}(J) \pm \sqrt{\text{tr}(J)^2 - 4 \det(J)}}{2},$$

in which

$$\text{tr}(J) = k_2 - k_1 \left(\frac{v_0}{k_2} \right)^2 \quad \text{and} \quad \det(J) = k_1 \left(\frac{v_0}{k_2} \right)^2.$$

Since $\det(J) > 0$, in order to have an unstable equilibrium that is not a saddle, it is necessary and sufficient to have $\text{tr}(J) > 0$, which leads to

$$k_1 < k_2^3/v_0^2.$$

This region is depicted in Figure 3.23b. Hence, if k_2 is large enough (i.e., the outflux is large enough compared to the strength of the self activation) a stable limit cycle arises. ∇

Limit cycles in \mathbb{R}^n

The results above holds only for systems in two dimensions. However, there have been recent extensions of this theorem to systems with special structure in \mathbb{R}^n . In particular, we have the following result due to Hastings et al. (1977).

Theorem 3.4 (Hastings et al. 1977). *Consider a system $\dot{x} = F(x)$, which is of the form*

$$\begin{aligned} \dot{x}_1 &= F_1(x_n, x_1) \\ \dot{x}_j &= F_j(x_{j-1}, x_j), \quad 2 \leq j \leq n \end{aligned}$$

on the set M defined by $x_i \geq 0$ for all i with the following inequalities holding in M :

- (i) $\frac{\partial F_i}{\partial x_i} < 0$ and $\frac{\partial F_i}{\partial x_{i-1}} > 0$, for $2 \leq i \leq n$, and $\frac{\partial F_1}{\partial x_n} < 0$;
- (ii) $F_i(0,0) \geq 0$ and $F_1(x_n, 0) > 0$ for all $x_n \geq 0$;
- (iii) The system has a unique steady state $x^* = (x_1^*, \dots, x_n^*)$ in M such that $F_1(x_n, x_1) < 0$ if $x_n > x_n^*$ and $x_1 > x_1^*$, while $F_1(x_n, x_1) > 0$ if $x_n < x_n^*$ and $x_1 < x_1^*$;
- (iv) $\frac{\partial F_1}{\partial x_1}$ is bounded above in M .

Then, if the Jacobian of f at x^* has no repeated eigenvalues and has any eigenvalue with positive real part, then the system has a non-constant periodic solution in M .

This theorem states that for a system with cyclic structure in which the cycle “has negative gain”, the instability of the steady state (under some technical assumption) is equivalent to the existence of a periodic solution. This theorem,

however, does not provide information about whether the orbit is attractive or not, that is, of whether it is an omega-limit set of any point in M . This stability result is implied by a more recent theorem due to Mallet-Paret and Smith (1990), for which we provide a simplified statement as follows.

Theorem 3.5 (Mallet-Paret and Smith, 1990). *Consider the system $\dot{x} = F(x)$ with the following cyclic feedback structure*

$$\begin{aligned}\dot{x}_1 &= F_1(x_n, x_1) \\ \dot{x}_j &= F_j(x_{j-1}, x_j), \quad 2 \leq j \leq n\end{aligned}$$

on a set M defined by $x_i \geq 0$ for all i with all trajectories starting in M bounded for $t \geq 0$. Then, the ω -limit set $\omega(p)$ of any point $p \in M$ can be one of the following:

- (a) A steady state;
- (b) A non-constant periodic orbit;
- (c) A set of steady states connected by homoclinic or heteroclinic orbits.

As a consequence of the theorem, we have that for a system with cyclic feedback structure that admits one steady state only and at which the linearization has all eigenvalues with positive real part, the omega limit set must be a periodic orbit.

Let for some $\delta_i \in \{1, -1\}$ be $\delta_i \frac{\partial F_i(x, x_{i-1})}{\partial x_{i-1}} > 0$ for all $0 \leq i \leq n$ and define $\Delta := \delta_1 \cdot \dots \cdot \delta_n$. One can show that the sign of Δ is related to whether the system has one or multiple steady states.

In Chapter 6, we will apply these results to determine the parameter space that makes the repressilator (see Example 2.2) oscillate.

3.5 Bifurcations

Another important property of nonlinear systems is how their behavior changes as the parameters governing the dynamics change. We can study this in the context of models by exploring how the location of equilibrium points, their stability, their regions of attraction and other dynamic phenomena, such as limit cycles, vary based on the values of the parameters in the model.

Parametric stability

Consider a differential equation of the form

$$\frac{dx}{dt} = F(x, \theta), \quad x \in \mathbb{R}^n, \theta \in \mathbb{R}^k, \quad (3.23)$$

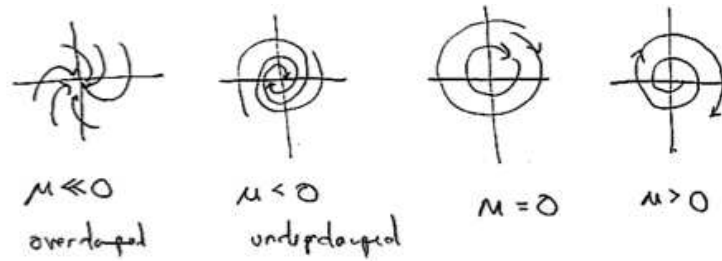


Figure 3.24: Phase portraits for a simple bifurcation.

where x is the state and θ is a set of parameters that describe the family of equations. The equilibrium solutions satisfy

$$F(x, \theta) = 0,$$

and as θ is varied, the corresponding solutions $x_e(\theta)$ can also vary. We say that the system (3.23) has a *bifurcation* at $\theta = \theta^*$ if the behavior of the system changes qualitatively at θ^* . This can occur either because of a change in stability type or a change in the number of solutions at a given value of θ .

As an example of a bifurcation, consider the linear system

$$\frac{dx_1}{dt} = x_2, \quad \frac{dx_2}{dt} = -kx_1 - \mu x_2,$$

where $k > 0$ is fixed and θ is our bifurcation parameter. Figure 3.24 shows the phase portraits for different values of θ . We see that at $\theta = 0$ the system transitions from a single stable equilibrium point at the origin to having an unstable equilibrium. Hence, as θ goes from negative to positive values, the behavior of the system changes in a significant way, indicating a bifurcation.

A common way to visualize a bifurcation is through the use of a *bifurcation diagram*. To create a bifurcation diagram, we choose a function $y = h(x)$ such that the value of y at an equilibrium point has some useful meaning for the question we are studying. We then plot the value of $y_e = h(x_e(\theta))$ as a function of θ for all equilibria that exist for a given parameter value θ . By convention, we use dashed lines if the corresponding equilibrium point is unstable and solid lines otherwise. Figure 3.25 shows examples of some common bifurcation diagrams. Note that for some types of bifurcations, such as the pitchfork bifurcation, there exist values of θ where there is more than one equilibrium point. A system that exhibits this type of behavior is said to be *multistable*. A common case is that there are two stable equilibria, in which case the system is said to be *bistable*.

Another type of diagram that is useful in understanding parametric dependence is a *parametric stability diagram*, an example of which was shown in Figure ???. In this type of diagram, we pick one or two (or sometimes three) parameters in the

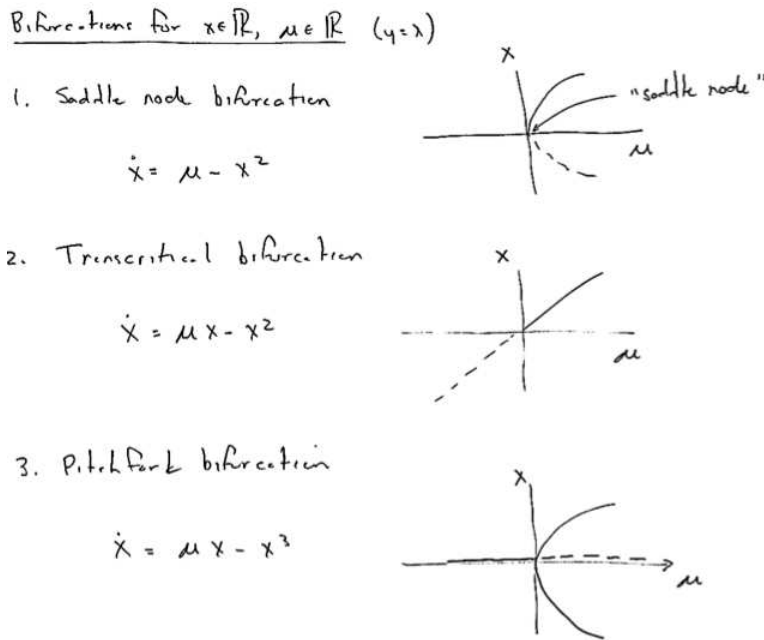


Figure 3.25: Bifurcation diagrams for some common bifurcations

system and then analyze the stability type for the system over all possible combinations of those parameters. The resulting diagram shows those regions in parameter space where the system exhibits qualitatively different behaviors; an example is shown in Figure 3.26a.

A particular form of bifurcation that is very common when controlling linear systems is that the equilibrium remains fixed but the stability of the equilibrium changes as the parameters are varied. In such a case it is revealing to plot the eigenvalues of the system as a function of the parameters. Such plots are called *root locus diagrams* because they give the locus of the eigenvalues when parameters change. An example is shown in Figure 3.26b. Bifurcations occur when parameter values are such that there are eigenvalues with zero real part. Computing environments such LabVIEW, MATLAB and Mathematica have tools for plotting root loci.

Parametric stability diagrams and bifurcation diagrams can provide valuable insights into the dynamics of a nonlinear system. It is usually necessary to carefully choose the parameters that one plots, including combining the natural parameters of the system to eliminate extra parameters when possible. Computer programs such as AUTO, LOCBIF and XPPAUT provide numerical algorithms for producing stability and bifurcation diagrams.

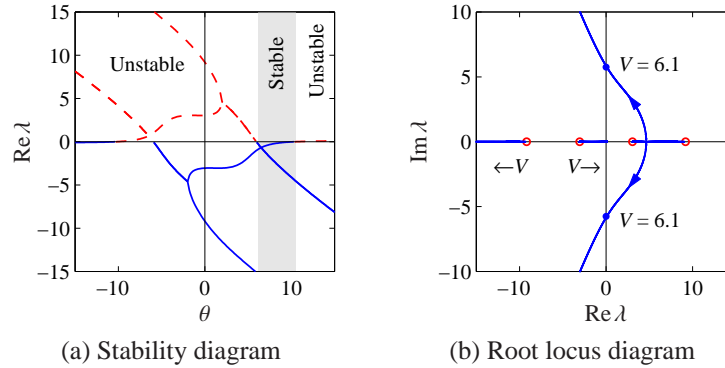


Figure 3.26: Stability plots a nonlinear system. The plot in (a) shows the real part of the system eigenvalues as a function of the parameter θ . The system is stable when all eigenvalues have negative real part (shaded region). The plot in (b) shows the locus of eigenvalues on the complex plane as the parameter θ is varied and gives a different view of the stability of the system. This type of plot is called a *root locus diagram*.

Hopf bifurcation

The bifurcations discussed above involved bifurcation of equilibrium points. Another type of bifurcation that can occur is that a system with an equilibrium point admits a limit cycle as a parameter is changed through a critical value. The Hopf bifurcation theorem provides a technique that is often used to understand whether a system admits a periodic orbit when some parameter is varied. Usually, such an orbit is a small amplitude periodic orbit that is present in the close vicinity of an unstable steady state.

Consider the system dependent on a parameter α :

$$\frac{dx}{dt} = g(x, \alpha), x \in \mathbb{R}^n, \alpha \in \mathbb{R},$$

and assume that at the steady state \bar{x} corresponding to $\alpha = \bar{\alpha}$ (i.e., $g(\bar{x}, \bar{\alpha}) = 0$), the linearization $\partial g / \partial x(\bar{x}, \bar{\alpha})$ has a pair of (non zero) imaginary eigenvalues with the remaining eigenvalues having negative real parts. Define the new parameter $\theta := \alpha - \bar{\alpha}$ and re-define the system as

$$\frac{dx}{dt} = f(x, \theta) =: g(x, \theta + \bar{\alpha}),$$

so that the linearization $\partial f / \partial x(\bar{x}, 0)$ has a pair of (non zero) imaginary eigenvalues with the remaining eigenvalues having negative real parts. Denote by $\lambda(\theta) = \beta(\theta) + i\omega(\theta)$ the eigenvalue such that $\beta(0) = 0$. Then, if $\frac{\partial \beta}{\partial \theta} \theta(0) \neq 0$ the system admits a small amplitude almost sinusoidal periodic orbit for θ small enough and the system is said to go through a Hopf bifurcation at $\theta = 0$. If the small amplitude periodic

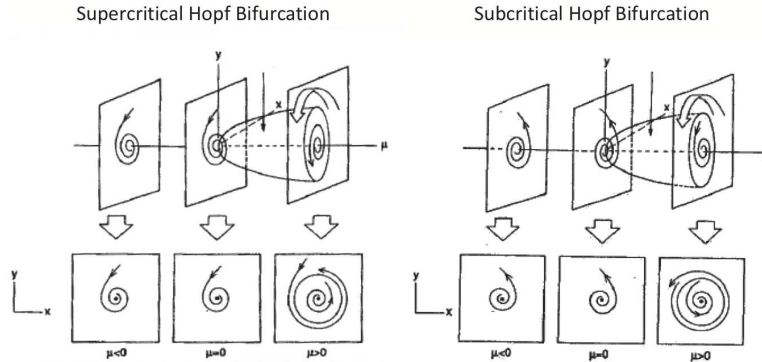


Figure 3.27: Hopf Bifurcation. On the left hand, as θ increases a stable limit cycle appears. On the right hand side, as θ increases a limit cycle appears but it is unstable.

orbit is stable, the Hopf bifurcation is said *supercritical*, while if it is unstable it is said *subcritical*. Figure 3.27 shows diagrams corresponding to these bifurcations.

In order to determine whether a Hopf bifurcation is supercritical or subcritical, it is necessary to calculate a “curvature” coefficient, for which there are formulas (Marsden and McCracken, 1976) and available bifurcation software, such as AUTO. In practice, it is often enough to calculate the value $\bar{\alpha}$ of the parameter at which Hopf bifurcation occurs and simulate the system for values of the parameter α close to $\bar{\alpha}$. If a small amplitude limit cycle appears, then the bifurcation must be supercritical.

Example 3.13 (Glycolytic oscillations). Recalling the model (3.10) for the glycolytic oscillator, we ask whether such an oscillator goes through a Hopf bifurcation. In order to answer this question, we consider again the expression of the eigenvalues

$$\lambda_{1,2} = \frac{\operatorname{tr}(J) \pm \sqrt{\operatorname{tr}(J)^2 - 4\det(J)}}{2},$$

in which

$$\operatorname{tr}(J) = k_2 - k_1 \left(\frac{v_0}{k_2}\right)^2 \quad \text{and} \quad \det(J) = k_1 \left(\frac{v_0}{k_2}\right)^2.$$

The eigenvalues are imaginary if $\operatorname{tr}(J) = 0$, that is, if $k_1 = k_2^3/v_0^2$. Furthermore, the frequency of oscillations is given by $\omega = \sqrt{4\det(J)} = 4k_1(v_0/k_2)^2$. When $k_1 \approx k_2^3/v_0^2$, an approximately sinusoidal oscillation appears. When k_1 is large, the Hopf bifurcation theorem does not imply the existence of a periodic solution. This is because the Hopf theorem provides only local results. For obtaining global results, one has to apply other tools, such as the Poincaré-Bendixson theorem. ∇

The Hopf bifurcation theorem is based on center manifold theory for nonlinear dynamical systems. For a rigorous treatment of Hopf bifurcation is thus necessary

to study center manifold theory first, which is outside the scope of this text. For details, the reader is referred to standard text in dynamical systems [89, 37].

3.6 Model Reduction Techniques

The techniques that we have developed in this chapter can be applied to a wide variety of dynamical systems. However, many of the methods require significant computation and hence we would like to reduce the complexity of the models as much as possible before applying them. In this section, we review methods for doing such a reduction in the complexity of the models. Most of the techniques are based on the common idea that if we are interested in the slower time scale dynamics of a system, the fast time scale dynamics can be approximated by their equilibrium solutions. This idea was introduced in Chapter 2 in the context of reduced order mechanisms; we present a more mathematical analysis of such systems here.

Singular perturbation analysis

Singular perturbation techniques apply to systems that have processes that evolve on both fast and slow time scales and that can be written in a standard form, which we now introduce. Let $(x, y) \in D := D_x \times D_y \subset \mathbb{R}^n \times \mathbb{R}^m$ and consider the vector field

$$\begin{aligned} \frac{dx}{dt} &= f(x, y, \epsilon), & x(0) &= x_0 \\ \epsilon \frac{dy}{dt} &= g(x, y, \epsilon), & y(0) &= y_0 \end{aligned}$$

in which $0 < \epsilon \ll 1$ is a small parameter and both $f(x, y, 0)$ and $g(x, y, 0)$ are well defined. Since $\epsilon \ll 1$, the absolute value of the time derivative of y can be much larger than the time derivative of x , resulting in y dynamics that are much faster than the x dynamics. That is, this system has a slow time scale evolution (in x) and a fast time-scale evolution (in y).

If we are interested only in the slower time scale, then the above system can be approximated (under suitable conditions) by the *reduced system*

$$\begin{aligned} \frac{d\bar{x}}{dt} &= f(\bar{x}, \bar{y}, 0), & \bar{x}(0) &= x_0, \\ 0 &= g(\bar{x}, \bar{y}, 0). \end{aligned}$$

Let $y = \gamma(x)$ denote *slow manifold* given by the locally unique solution of $g(x, y, 0) = 0$. The *implicit function theorem* [55] shows that this solution exists whenever $\partial g / \partial y$ is non singular. Furthermore, the theorem also shows that

$$\frac{d\gamma}{dx} = -\frac{\partial g^{-1}}{\partial y} \frac{\partial g}{\partial x}.$$

We can now approximate the dynamics in x (i.e., on the slow manifold) as

$$\frac{d\bar{x}}{dt} = f(\bar{x}, \gamma(\bar{x}), 0), \quad x(0) = x_0.$$

We seek to determine under what conditions the solution $x(t)$ is “close” to the solution $\bar{x}(t)$ of the reduced system. This problem can be addressed by analyzing the fast dynamics. Letting $\tau = t/\epsilon$ be the fast time scale, we have that

$$\frac{dx}{d\tau} = \epsilon f(x, y, \epsilon), \quad \frac{dy}{d\tau} = g(x, y, \epsilon), \quad (x(0), y(0)) = (x_0, y_0),$$

so that when $\epsilon \ll 1$, $x(\tau)$ does not appreciably change. Therefore, the above system in the τ time scale can be approximated by

$$\frac{dy}{d\tau} = g(x_0, y, 0), \quad y(0) = y_0,$$

in which x is “frozen” at the initial condition. This system is usually referred to as the *boundary layer* system. If for all x_0 , we have that $y(\tau)$ converges to $\gamma(x_0)$, then for $t > 0$ we will have that the solution $x(t)$ is well approximated by the solution $\bar{x}(t)$ to the reduced system. This qualitative explanation is more precisely captured by the following theorem [?].

Theorem 3.6. *Assume that*

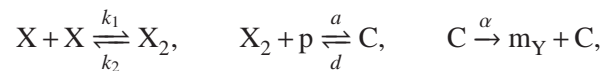
$$\text{Real} \left(\lambda \left(\frac{\partial}{\partial y} g(x, y) \Big|_{y=\gamma(x)} \right) \right) < 0$$

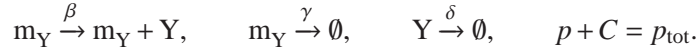
uniformly for $x \in D_x$. Let the solution of the reduced system be uniquely defined for $t \in [0, t_f]$. Then, for all $t_b \in (0, t_f]$ there is a constant $\epsilon^ > 0$ and set $\Omega \subseteq D$ such that*

$$\begin{aligned} x(t) - \bar{x}(t) &= O(\epsilon) \text{ uniformly for } t \in [0, t_f], \\ y(t) - \gamma(\bar{x}(t)) &= O(\epsilon) \text{ uniformly for } t \in [t_b, t_f], \end{aligned}$$

provided $\epsilon < \epsilon^$ and $(x_0, y_0) \in \Omega$.*

Example 3.14 (Hill function). In Section 2.1, we obtained the expression of the Hill function by making a quasi-steady state approximation on the dynamics of binding. Here, we illustrate how Hill function expressions can be derived by a formal application of singular perturbation. Specifically, consider the simple binding scenario of a transcription factor X with DNA promoter sites p. Assume that such a transcription factor is acting as an activator of the promoter and let Y be the protein expressed under promoter p. Assume further that X dimerizes before binding to promoter p. The reaction equations describing this system are given by





The corresponding differential equation model is given by

$$\begin{aligned} \frac{dX_2}{dt} &= k_1 X^2 - k_2 X_2 - a X_2 (p_{\text{tot}} - C) + dC \\ \frac{dC}{dt} &= a X_2 (p_{\text{tot}} - C) - dC \\ \frac{dm_Y}{dt} &= \alpha C - \gamma m_Y \\ \frac{dY}{dt} &= \beta m_Y - \delta Y. \end{aligned}$$

Since all the binding reactions are much faster than mRNA and protein production and decay, we have that $k_1, k_2, a, d \gg \alpha, \beta, \gamma, \delta$. Let $k_m := k_2/k_1$, $K_d := d/a$, $c := k_2/d$, and $\epsilon := \delta/d$. Then, we can re-write the above system by using the substitutions

$$d = \frac{\delta}{\epsilon}, \quad a = \frac{\delta}{K_d \epsilon}, \quad k_2 = c \frac{\delta}{\epsilon}, \quad k_1 = c \frac{\delta}{k_m \epsilon},$$

so that we obtain

$$\begin{aligned} \epsilon \frac{dX_2}{dt} &= c \frac{\delta}{k_m} X^2 - c \delta X_2 - \frac{\delta}{K_d} X_2 (p_{\text{tot}} - C) + \delta C \\ \epsilon \frac{dC}{dt} &= \frac{\delta}{K_d} X_2 (p_{\text{tot}} - C) - \delta C \\ \frac{dm_Y}{dt} &= \alpha C - \gamma m_Y \\ \frac{dY}{dt} &= \beta m_Y - \delta Y. \end{aligned}$$

This system is in the standard singular perturbation form 3.6. As an exercise, the reader can verify that the slow manifold is locally asymptotically stable (see Exercises). The slow manifold is obtained by setting $\epsilon = 0$ and determines X_2 and C as functions of X . These functions are given by

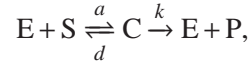
$$X_2 = \frac{X^2}{k_m}, \quad C = \frac{p_{\text{tot}} X^2 / (k_m K_d)}{1 + X^2 / (k_m K_d)}.$$

As a consequence, the reduced system becomes

$$\begin{aligned} \frac{dm_Y}{dt} &= \alpha \frac{p_{\text{tot}} X^2 / (k_m K_d)}{1 + X^2 / (k_m K_d)} - \gamma m_Y \\ \frac{dY}{dt} &= \beta m_Y - \delta Y, \end{aligned}$$

which is the familiar expression for the dynamics of gene expression with an activator as derived in Chapter 2. ∇

Example 3.15 (Enzymatic reaction). Let's go back to the enzymatic reaction



in which E is an enzyme, S is the substrate to which the enzyme binds to form the complex C , and P is the product resulting from the modification of the substrate S due to the binding with the enzyme E . The corresponding system of differential equations is given by

$$\begin{aligned} \frac{dE}{dt} &= -aE \cdot S + dC + kC, & \frac{dC}{dt} &= aE \cdot S - (d+k)C, \\ \frac{dS}{dt} &= -aE \cdot S + dC, & \frac{dP}{dt} &= kC. \end{aligned}$$

By assuming that $a, d \gg k$, we obtained before that approximately $dC/dt = 0$ and thus that $C = E_{\text{tot}}S/(S + K_m)$, with $k_m = (d+k)/a$ and $dP/dt = V_{\text{max}}S/(S + k_m)$ with $V_{\text{max}} = kE_{\text{tot}}$. From this, it also follows that

$$\frac{dE}{dt} \approx 0 \text{ and } \frac{dS}{dt} \approx -\frac{dP}{dt}. \quad (3.24)$$

How good is this approximation? By applying the singular perturbation method, we will obtain a clear answer to this question. Specifically, define $K_d := d/a$ and take the system to standard singular perturbation form by defining the small parameter $\epsilon := k/d$, so that $d = k/\epsilon$, $a = k/(K_d\epsilon)$, and the system becomes

$$\begin{aligned} \epsilon \frac{dE}{dt} &= -\frac{k}{K_d} E \cdot S + kC + \epsilon kC, & \epsilon \frac{dC}{dt} &= \frac{k}{K_d} E \cdot S - kC - \epsilon kC, \\ \epsilon \frac{dS}{dt} &= -\frac{k}{K_d} E \cdot S + kC, & \frac{dP}{dt} &= kC. \end{aligned}$$

One cannot directly apply singular perturbation theory on this system because one can verify from the linearization of the first three equations that the boundary layer dynamics are not locally exponentially stable since there are two zero eigenvalues. This is because the three variables E, S, C are not independent. Specifically, $E = E_{\text{tot}} - C$ and $S + C + P = S(0) = S_{\text{tot}}$, assuming that initially we have S in amount $S(0)$ and no amount of P and C in the system. Given these conservation laws, the system can be re-written as

$$\epsilon \frac{dC}{dt} = \frac{k}{K_d} (E_{\text{tot}} - C) \cdot (S_{\text{tot}} - C - P) - kC - \epsilon kC, \quad \frac{dP}{dt} = kC.$$

Under the assumption made in the analysis of the enzymatic reaction that $S_{\text{tot}} \gg E_{\text{tot}}$, we have that $C \ll S_{\text{tot}}$ so that the equations finally become

$$\epsilon \frac{dC}{dt} = \frac{k}{K_d} (E_{\text{tot}} - C) \cdot (S_{\text{tot}} - P) - kC - \epsilon kC, \quad \frac{dP}{dt} = kC.$$

One can verify (see Exercises) that in this system, the boundary layer dynamics is locally exponentially stable, so that setting $\epsilon = 0$ one obtains

$$\bar{C} = \frac{E_{\text{tot}}(S_{\text{tot}} - \bar{P})}{(S_{\text{tot}} - \bar{P}) + k_m} =: \gamma(\bar{P})$$

and thus that the reduced system is given by

$$\frac{d\bar{P}}{dt} = V_{\text{max}} \frac{(S_{\text{tot}} - \bar{P})}{(S_{\text{tot}} - \bar{P}) + k_m}.$$

This system is the same as that obtained in Chapter 2. However, $dC(t)/dt$ and $dE(t)/dt$ are not close to zero as obtained earlier. In fact, from the conservation law $\bar{S} + \bar{C} + \bar{P} = S(0) = S_{\text{tot}}$, we obtain that $\frac{d\bar{S}}{dt} = -\frac{d\bar{P}}{dt} - \frac{d\bar{C}}{dt}$, in which now $\frac{d\bar{C}}{dt} = \frac{\partial\gamma}{\partial P}(\bar{P}) \cdot \frac{d\bar{P}}{dt}$. Therefore

$$\frac{d\bar{S}}{dt} = -\frac{d\bar{P}}{dt} \left(1 + \frac{\partial\gamma}{\partial P}(\bar{P})\right), \quad \bar{S}(0) = S_{\text{tot}} - \gamma(\bar{P}(0)) - \bar{P}(0) \quad (3.25)$$

and

$$\frac{d\bar{E}}{dt} = -\frac{d\bar{C}}{dt} = -\frac{\partial\gamma}{\partial P}(\bar{P}) \frac{d\bar{P}}{dt}, \quad E(0) = E_{\text{tot}} - \gamma(\bar{P}(0)), \quad (3.26)$$

which are different from expressions (3.24).

These expressions are close to those in equation (3.24) only when $\partial\gamma/\partial P(\bar{P})$ is small enough. In the plots of Figure 3.28, we show the time trajectories of the original system, of the Michaelis-Menten quasi-steady state approximation (QSSA), and of the singular perturbation approximation. In the full model (solid line in Figure 3.28), $E(t)$ starts from a unit concentration and immediately collapses to zero as the enzyme is all consumed to form the complex C by the substrate, which is in excess. Similarly, $C(t)$ starts from zero and immediately reaches the maximum possible value of one.

In the QSSA, both $E(t)$ and $C(t)$ are assumed to stabilize immediately to their (quasi) steady state and then stay constant. This is depicted by the dotted plots in Figure 3.28, in which $E(t)$ stays at zero for the whole time and $C(t)$ stays at one for the whole time. This approximation is fairly good as long as there is an excess of substrate. When the substrate concentration goes to zero as it is all converted to product, also the complex concentration C goes to zero (see solid line of Figure 3.28). At this time, the concentrations of complex and enzyme substantially change with time and the QSSA is unsatisfactory. By contrast, the reduced dynamics obtained from the singular perturbation approach well represent the dynamics of the full system even during this transient behavior. Hence, while the QSSA is a good approximation only as long as there is excess of substrate in the system, the reduced dynamics obtained by singular perturbation is a good approximation even when the substrate concentration goes to zero.

In Figure 3.29, we show the curve $C = \gamma(P)$ (in red) and the trajectories of the full system in black. All of the trajectories of the system immediately collapse into

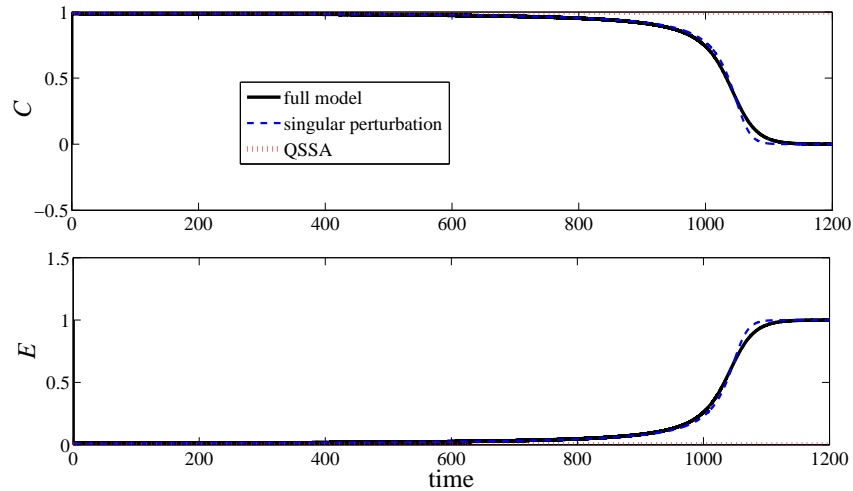


Figure 3.28: Simulation results for the enzymatic reaction comparing the approximations from singular perturbation and from the quasi-steady state approximation (QSSA). Here, we have $S_{\text{tot}} = 100$, $E_{\text{tot}} = 1$, $a = d = 10$, and $k = 0.1$. The full model is the one in equations (??).

an ϵ -neighbor of the curve $C = \gamma(P)$. From this plot, it is clear that $\partial\gamma/\partial P$ is small as long as the product concentration P is small enough, which corresponds to a substrate concentration S large enough. This confirms that the QSSA is good only as long as there is excess of substrate S . ∇

Exercises

3.1 (Frequency response of a phosphorylation cycle) Consider the model of a covalent modification cycle as illustrated in Chapter 2 in which the kinase Z is not constant, but it is produced and decays according to the reaction $Z \xrightleftharpoons[u(t)]{\delta}$. Let $u(t)$ be the input stimulus of the cycle and let X^* be the output. Determine the frequency response of X^* to u , determine its bandwidth, and make plots of it. What parameters can be used to tune the bandwidth?

3.2 (Design for robustness) Consider a one-step reaction model for a phosphorylation cycle as seen in Homework 1, in which the input stimulus is the time-varying concentration of kinase $Z(t)$. When found in the cellular environment, this cycle is subject to possible interactions with other cellular components, such as the non-specific or specific binding of X^* to target sites, to noise due to stochasticity of the cellular environment, and to other cross-talk phenomena. We will come back to these “disturbances” later during the course. For now, we can think of these distur-

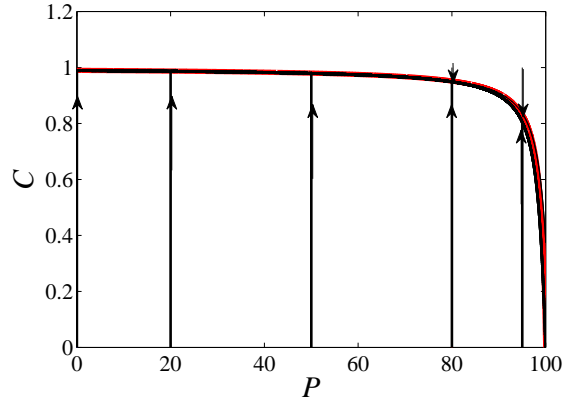


Figure 3.29: The slow manifold of the system $C = \gamma(P)$ is shown in red. In black, we show the trajectories of the full system. These trajectories collapse into an ϵ -neighbor of the slow manifold. Here, we have $S_{\text{tot}} = 100$, $E_{\text{tot}} = 1$, $a = d = 10$, and $k = 0.1$.

bances as acting like an aggregate rate of change on the output protein X^* , which we call $d(t)$. Hence, we can model the “perturbed” cycle by

$$\dot{X}^* = Z(t)k_1X_{\text{tot}}\left(1 - \frac{X^*}{X_{\text{tot}}}\right) - k_2Y_{\text{tot}}X^* + d(t),$$

which is the same as you found in Homework 1, except for the presence of the disturbance $d(t)$. Assume that you can tune all the parameters in this system (we will see later that this is actually possible to large extent by suitably fabricating genetic circuits). Can you tune these parameters so that the response of $X^*(t)$ to $d(t)$ is arbitrarily attenuated while the response of $X^*(t)$ to $Z(t)$ remains arbitrarily large? If yes, explain how these parameters should be tuned to reach this design objective and justify your answer through a careful mathematical reasoning using the tools introduced in class.

3.3 (Adaptation) Show that the equation of the sniffer 3.13 can be taken into the standard integral feedback form through a suitable change of coordinates.

3.4 (Design limitations) This problem is meant to have you think about possible trade-offs and limitations that are involved in any realistic design question (we will come back to this when we start design). Here, we examine this through the open loop and negative feedback transcriptional component seen in class (see Figure 3-8 in the Lecture Notes). Specifically, we want to compare the robustness of these two topologies to cellular noise, crosstalk, and other cellular interactions. As performed in Problem 1, we model these phenomena as a time-varying disturbance affecting the production rate of mRNA m and protein P . To slightly simplify the problem, we focus only on disturbances affecting the production of protein. The open loop

model becomes

$$\dot{m} = \alpha_0 - \gamma m \quad \dot{P} = \beta m - \delta P + d(t)$$

and the negative feedback system becomes

$$\dot{m} = \alpha_0 + \frac{\alpha}{K + P^n} - \gamma m \quad \dot{P} = \beta m - \delta P + d(t).$$

Answer the following questions:

- After performing linearization about the equilibrium point, determine analytically the frequency response of P to d for both systems.
- Sketch the magnitude plot of this response by hand for both systems, compare them, and determine what happens as β and α increase (note: if your calculations are correct, you should find that what really matters for the negative feedback system is the product $\alpha\beta$, which we can view as the *feedback gain*). So, is increasing the feedback gain to arbitrarily large values the best strategy to decrease the sensitivity of the system to the disturbance? Comment.
- Pick parameter values and use Matlab to draw Bode plots as the feedback gain increases and validate your predictions of (b). (Suggested parameters: $\gamma = 1$, $\delta = 1$, $K = 1$, $n = 1$, $\alpha\beta = \{1, 10, 100, 1000, \dots\}$). Note: in Matlab, once you have determined the matrices A , B , C , and D for the linearization, you can just do: `SYS=ss(A,B,C,D)`; `bode(SYS)` and the Bode plot will pop up.
- Investigate the answer to (c) when you have $\gamma = 20$, that is, the timescale of the mRNA dynamics becomes faster than that of the protein dynamics. What does change with respect to what you found in (c)? Note: when γ increases you are reducing the (phase) lag within the negative feedback loop...
- When γ is at least 10 times larger than δ , you can approximate the m dynamics to the quasi-steady state. So, the two above systems can be reduced to one differential equation each for the protein concentration P . For these two reduced systems, determine analytically the frequency response to d and use it to find out whether arbitrarily increasing the feedback gain is a good strategy to decrease the sensitivity of response to the disturbance.

3.5 (Bendixson criterion) Consider the possible circuit topologies of Figure 3.30, in which A and B are transcriptional components. Model each transcriptional component by a first order system, in which you have approximated the mRNA dynamics at the quasi-steady state. Hence, each topology will be represented by a dynamical system in the plane \mathbb{R}^2 . Use Bendixson criterion to rule out topologies that cannot give rise to closed orbits.

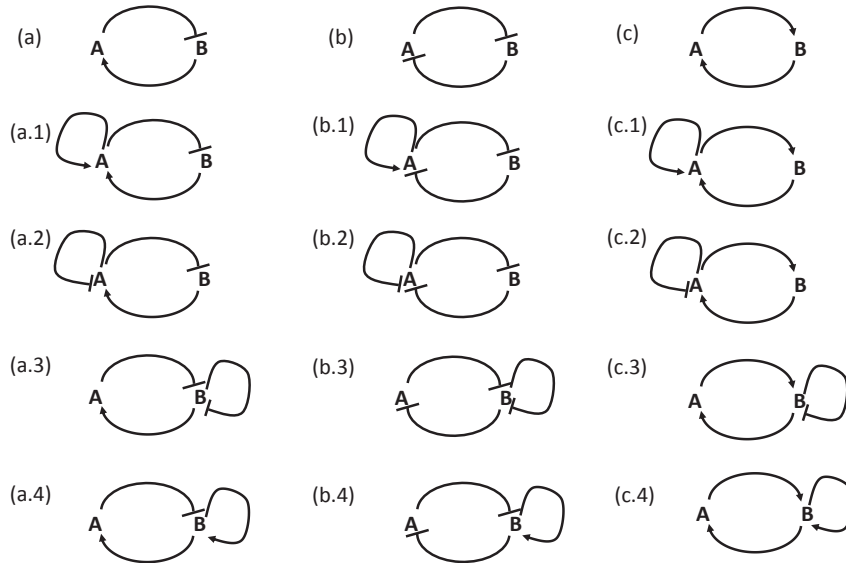


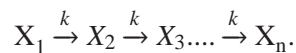
Figure 3.30: Circuit topologies with two components (proteins): A and B.

3.6 (Two gene oscillator) Consider the feedback system composed of two genes expressing proteins A (activator) and R (repressor), in which we denote by A , R , m_A , and m_R , the concentrations of the activator protein, the repressor protein, the mRNA for the activator protein, and the mRNA for the repressor protein, respectively. The ODE model corresponding to this system is given by

$$\begin{aligned} \frac{dm_A}{dt} &= \frac{\alpha_0}{K_1 + R^n} - \gamma m_A & \frac{dm_R}{dt} &= \frac{\alpha A^m}{K_2 + A^m} - \gamma m_R \\ \frac{dA}{dt} &= \beta m_A - \delta A & \frac{dR}{dt} &= \beta m_R - \delta R. \end{aligned}$$

Determine parameter conditions under which this system admits a stable limit cycle. Validate your finding through simulation.

3.7 (Goodwin oscillator) Consider the simple set of reactions



Assume further that X_n is a transcription factor that represses the production of protein X_1 through transcriptional regulation (assume simple binding of X_n to DNA). Neglecting the mRNA dynamics of X_1 , write down the ODE model of this system and determine conditions on the length n of the cascade for which the system admits a stable limit cycle. Validate your finding through simulation.

3.8 (Activator-repressor clock) A well known oscillating motif is given by the activator-repressor clock by Atkinson et al. [?] in which an activator protein A activates its own production and the one of a repressor protein R, which in turn acts as a repressor for A. The ODE model corresponding to this clock is given by

$$\begin{aligned}\frac{dm_A}{dt} &= \frac{\alpha A^m + \alpha_0}{K_1 + R^n + A^m} - \gamma m_A & \frac{dm_R}{dt} &= \frac{\alpha A^m}{K_2 + A^m} - \gamma m_R \\ \frac{dA}{dt} &= \mu(\beta m_A - \delta A) & \frac{dR}{dt} &= \beta m_R - \delta R,\end{aligned}$$

in which $\mu > 0$ models the difference of speeds between the dynamics of the activator and that of the repressor. Indeed a key requirement for this system to oscillate is that the dynamics of the activator are sufficiently faster than that of the repressor. Demonstrate that this system goes through a Hopf Bifurcation with bifurcation parameter μ . Validate your findings with simulation by showing the small amplitude periodic orbit.

3.9 (Phosphorylation via singular perturbation) Consider again the model of a covalent modification cycle as illustrated in Chapter 2 in which the kinase Z is not constant, but it is produced and decays according to the reaction $Z \xrightleftharpoons[u(t)]{\delta} \emptyset$.

(a) Consider that $k_f, k_r \gg k_{\text{cat}}, \delta, u(t)$ and employ singular perturbation with small parameter, for example, $\epsilon = \delta/k_r$ to obtain the approximated dynamics of $Z(t)$ and $X^*(t)$. How is this different from the result obtained in Exercise 2.9? Explain.

(b) Simulate these approximated dynamics when $u(t)$ is a periodic signal with frequency ω and compare the responses of Z of this approximated dynamics to those obtained in Exercise 2.9 as you change ω . What do you observe? Explain.

3.10 (Hill function via singular perturbation) Show that the slow manifold of the following system is asymptotically stable:

$$\begin{aligned}\epsilon \frac{dX_2}{dt} &= c \frac{\delta}{k_m} X^2 - c \delta X_2 - \frac{\delta}{K_d} X_2 (p_{\text{tot}} - C) + \delta C, & \frac{dm_Y}{dt} &= \alpha C - \gamma m_Y, \\ \epsilon \frac{dC}{dt} &= \frac{\delta}{K_d} X_2 (p_{\text{tot}} - C) - \delta C, & \frac{dY}{dt} &= \beta m_Y - \delta Y.\end{aligned}$$

3.11 (Enzyme dynamics via singular perturbation) Show that the slow manifold of the following system is asymptotically stable:

$$\epsilon \frac{dC}{dt} = \frac{k}{K_d} (E_{\text{tot}} - C) \cdot (S_{\text{tot}} - P) - kC - \epsilon kC, \quad \frac{dP}{dt} = kC.$$

3.12 (BE 150, Winter 2011; Based on Alon 4.6—Shaping the pulse) Consider a situation where X in an I1-FFL begins to be produced at time $t=0$, so that the level of protein X gradually increases. The input signal S_x and S_y are present throughout.

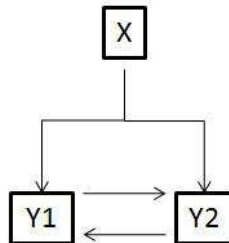
(a) How does the pulse shape generated by the I1-FFL depend on the thresholds K_{xz} , K_{xy} , and K_{yz} , and on β , the production rate of protein X ? (i.e. How does increasing or decreasing these parameters change the height or position of the pulse peak, the slope of the rise of the pulse, etc?)

(b) Analyze a set of genes Z_1, Z_2, \dots, Z_n , all regulated by the same X and Y in I1-FFLs. Design thresholds such that the genes are turned ON in the rising phase of the pulse in a certain temporal order and turned OFF in the declining phase of the pulse with the same order.

(c) Design thresholds such that the turn-OFF order is opposite the turn-ON order. Plot the resulting dynamics.

3.13 (BE 150, Winter 2011; Based on Alon 5.6—Bi-fan dynamics) Consider a bi-fan in which activators X_1 and X_2 regulate genes Z_1 and Z_2 . The input signal of X_1, S_{X1} , appears at time $t=0$ and vanishes at time $t=D$. The input signal of X_2, S_{X2} , appears at time $t=D/2$ and vanishes at $t=2D$. Plot the dynamics of the promoter activity of Z_1 and Z_2 given that the input functions of Z_1 and Z_2 are AND and OR logic, respectively.

3.14 (BE 150, Winter 2011; Based on Alon 6.1—Memory in the regulated-feedback network motif) Transcription factor X activates transcription factor Y_1 and Y_2 . Y_1 and Y_2 mutually activate each other. The input function at the Y_1 and Y_2 promoters is an OR gate (Y_2 is activated when either X or Y_1 binds the promoter). At time $t=0$, X begins to be produced from an initial concentration of $X=0$. Initially $Y_1 = Y_2 = 0$. All production rates are $\beta = 1$ and degradation rates are $\alpha = 1$. All of the activation thresholds are $K=0.5$. At time $t=3$, production of X stops.



(a) Plot the dynamics of X, Y_1, Y_2 . What happens to Y_1 and Y_2 after X decays away?

(b) Consider the same problem, but now Y_1 and Y_2 repress each other and X activates Y_1 and represses Y_2 . At time $t=0$, X begins to be produced and the initial

levels are $X = 0, Y_1 = 0, Y_2 = 1$. At time $t=3$, X production stops. Plot the dynamics of the system. What happens after X decays away?

3.15 (BE 150, Winter 2011; Repressilator) Simulate the following simplified version of the repressilator:

$$\begin{aligned} \frac{dm_1}{dt} &= \frac{k_p}{1 + \left(\frac{p_3}{K_M}\right)^n} - k_{mdeg}m_1 & \frac{dp_1}{dt} &= k_{trans}m_1 - k_{pdeg}p_1 \\ \frac{dm_2}{dt} &= \frac{k_p}{1 + \left(\frac{p_1}{K_M}\right)^n} - k_{mdeg}m_2 & \frac{dp_2}{dt} &= k_{trans}m_2 - k_{pdeg}p_2 \\ \frac{dm_3}{dt} &= \frac{k_p}{1 + \left(\frac{p_2}{K_M}\right)^n} - k_{mdeg}m_3 & \frac{dp_3}{dt} &= k_{trans}m_3 - k_{pdeg}p_3 \end{aligned}$$

(a) Simulate the system using the following parameters: $k_p = 0.5, n = 2, K_M = 40, k_{mdeg} = 0.0058, k_{pdeg} = 0.0012, k_{trans} = 0.116$.

(b) Suppose the protein half-life suddenly decreases by half. Which parameter(s) will change and how? Simulate what happens. What if the protein half-life is doubled? How do these two changes affect the oscillatory behavior?

(c) Now assume that there is leakiness in the transcription process. How does the system's ODE change? Simulate the system with a small leakiness (say, $5e-3$) and comment on how it affects the oscillatory behavior.

3.16 (BE 150, Winter 2011; Glycolytic oscillations) In almost all living cells, glucose is broken down into the cell's energy currency, ATP, via the glycolysis pathway. Glycolysis is autocatalytic in the sense that ATP must first be consumed in the early steps before being produced later and oscillations in glycolytic metabolites have been observed experimentally. We will look at a minimal model of glycolysis:

$$\frac{dX}{dt} = \frac{2Vy^a}{1+y^h} - kx \quad \frac{dY}{dt} = (q+1)kx - q\frac{2Vy^a}{1+y^h} - 1$$

Note that this system has been normalized such that $Y_{ss} = 1$.

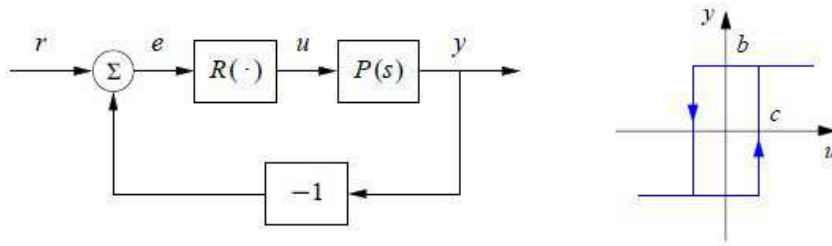
(a) While a system may have the potential to oscillate, the behavior still depends on the parameter values. The glycolysis system undergoes multiple *bifurcations* as the parameters are varied. Using linear stability analysis, find the parameter conditions where the system is stable vs. unstable. Next, find the conditions where the system has eigenvalues with nonzero imaginary parts.

(b) Let $q=k=V=1$. Find the relationship between h and a where the system is stable or not. Draw the stability diagram and mark the regions where the system is stable vs. unstable. In the same plot, mark the regions where the system has eigenvalues with nonzero imaginary parts.

(c) Let $q=k=V=1$. Choose h and a such that the eigenvalues are unstable and have nonzero imaginary parts. Use these parameter values and simulate the nonlinear system in MATLAB. Sketch the time response of the system starting with initial condition $X(0)=1.2$, $Y(0)=0.5$ (you may use MATLAB or sketch by hand). Comment on what you see compared to what linear stability analysis told you about the system.

3.17 (BE 150, Winter 2011) Finding limit cycles for nonlinear systems and understanding how changes in parameters affect the amplitude and period of the oscillation is difficult to do in analytical form. A graphical technique that gives some insight into this problem is the use of *describing functions*, which is described in *Feedback Systems*, Section 9.5. In this problem we will use describing functions for a simple feedback system to approximate the amplitude and frequency of a limit cycle in analytical form.

Consider the system with the block diagram shown below. The block R is a relay



with hysteresis whose input/output response is shown on the right and the process transfer function is $P(s) = e^{-s\tau}/s$. Use describing function analysis to determine frequency and amplitude of possible limit cycles. Simulate the system and compare with the results of the describing function analysis.

3.18 (BE 150, Winter 2011) In this problem we will compare the model with single methylation site vs. double methylation sites. The model with a single methylation site is given by:

$$\frac{d(X + X^*)}{dt} = V_R R - \frac{V_B B X^*}{K + X^*}$$

where the *activity* is given by $A = X^*$. The model with two methylation sites is given by

$$\begin{aligned} \frac{d(X_2 + X_2^*)}{dt} &= \frac{R V_R X_1}{X_1 + X_0} - B V_B X_2^* \\ \frac{d(X_1 + X_1^*)}{dt} &= B V_B X_2^* + \frac{R V_R X_0}{X_1 + X_0} - \frac{R V_R X_1}{X_1 + X_0} - B V_B X_1^* \\ \frac{dX_0}{dt} &= -\frac{R V_R X_0}{X_0 + X_1} + B V_B X_1^* \end{aligned}$$

and the activity is given by $A = X_1 + X_2$. Let $K = 10, V_R R = 1, V_B B = 2$. Derive the parameter sensitivities of the activities ($\frac{dA}{dp_i}$) for both the single and double methylation models. Comment on which parameter each model is most robust and most sensitive to.

3.19 (BE 150, Winter 2011) Consider a toy model of protein production:

$$\frac{dm}{dt} = f(p) - \gamma m \qquad \frac{dp}{dt} = g(p) - \delta p$$

(a) Assume that there is transcriptional self-regulation ($f(p) = \frac{\alpha}{K+p^n}$). We now know that the mRNA transcription process and thus we want to understand the sensitivity with respect to the mRNA transcription rate α_0 . Compute the transfer function from α to p . Plot this transfer function for $\alpha = 0.002, \beta_0 = 0.1, \gamma = 0.005, \delta = 0.001, K = 0.002$. Compare it with the transfer function from α_0 to p without regulation ($f(p) = \alpha_0 = 0.001$). (Note: As a reminder on how to compute these transfer functions, see BFS chapter 3 page 3-11).

(b) Now assume that there is no transcriptional regulation ($f(p) = \alpha_0$) but there is translational self-regulation such that $g(p) = \frac{\beta m}{K+p^n}$. Compute the transfer function from α_0 to p when $\beta = 0.2$. Compare again with the case with no regulation.

3.20 (BE 150, Winter 2011) Consider a simple model of chemotaxis:

$$\frac{dX_m}{dt} = k_R R + k^f(L)X_m^* - k^r X_m$$

$$\frac{dX_m^*}{dt} = -k_B B^P \frac{X_m^*}{K X_m^* + X_m^*} - k^f(L)X_m^* + k^r X_m$$

where X_m is the concentration of methylated receptor complex, and X_m^* is the concentration of activated, methylated receptor complex. Ligand concentration enters into the equation through the rate $k^f(L)$. In this model, $CheR$ (R) and $CheB^P$ (B^P) concentrations are constant. (BFS, Section 5)

(a) Pick parameter values such that $k_B B^P > k_R R$ and plot the dynamics, doubling the ligand concentration at time $t=20$. Compare to figure 5.12 in BFS.

(b) Now assume that CheR no longer acts in saturation. Rederive the dynamics and plot. Comment on how this assumption affects adaptation.

Chapter 4

Stochastic Modeling and Analysis

In this chapter we explore stochastic behavior in biomolecular systems, building on our preliminary discussion of stochastic modeling in Section 2.1. We begin by reviewing the various methods for modeling stochastic processes, including the chemical master equation (CME), the chemical Langevin equation (CLE) and the Fokker-Planck equation (FPE). Given a stochastic description, we can then analyze the behavior of the system using a variety of stochastic simulation and analysis tools. In many cases, we must simplify the dynamics of the system in order to obtain a tractable model, and we describe several methods for doing so, including finite state projection, linearization and Markov chain representations. We also investigate how to use data to identify some the structure and parameters of stochastic models.

Prerequisites. This chapter makes use of a variety of topics in stochastic processes that are not covered in AM08. Readers should have a good working knowledge of basic probability and some exposure to simple stochastic processes (e.g., Brownian motion), at the level of the material presented in Appendix B (drawn from [62]).

TAKEN FROM CHAPTER 2:

Example 4.1 (Combinatorial promoter). A combinatorial promoter is a region of DNA in which multiple transcription factors can bind and influence the subsequent binding of RNA polymerase. Combinatorial promoters appear in a number of natural and engineered circuits and represent a mechanism for creating switch-like behavior, for example by having a gene that controls expression of its own transcription factors.

One method to model a combinatorial promoter is to use the binding energies of the different combinations of proteins to the operator region, and then compute the probability of being in a given promoter state given the concentration of each of the transcription factors. Table 4.1 shows the possible states of a notional promoter that has two operator regions—one that binds a repressor protein R and another that binds an activator protein A. As indicated in the table, the promoter has three (possibly overlapping) regions of DNA: OR1 and OR2 are binding sites for the repressor and activator proteins, and Prom is the location where RNA polymerase binds. (The individual labels are primarily for bookkeeping purposes and may not correspond to physically separate regions of DNA.)

To determine the probabilities of being in a given macrostate, we must compute the individual microstates that occur at a given concentrations of repressor, ac-

Table 4.1: Configurations for a combinatorial promoter with an activator and a repressor. Each row corresponds to a specific macrostate of the promoter in which the listed molecules are bound to the target region. The relative energy of state compared with the ground state provides a measure of the likelihood of that state occurring, with more negative numbers corresponding to more energetically favorable configurations.

State	OR1	OR2	Prom	$E_q (\Delta G)$	Comment
S_1	–	–	–	0	No binding (ground state)
S_2	–	–	RNAP	–5	RNA polymerase bound
S_3	R	–	–	–10	Repressor bound
S_4	–	A	–	–12	Activator bound
S_5	–	A	RNAP	–15	Activator and RNA polymerase

tivator and RNA polymerase. Each microstate corresponds to an individual set of molecules binding in a specific configuration. So if we have n_R repressor molecules, then there is one microstate corresponding to *each* different repressor molecule that is bound, resulting in n_R individual microstates. In the case of configuration S_5 , where two different molecules are bound, the number of combinations is given by the product of the numbers of individual molecules, $n_A \cdot n_{\text{RNAP}}$, reflecting the possible combinations of molecules that can occupy the promoter sites. The overall partition function is given by summing up the contributions from each microstate:

$$Z = e^{-E_0/(k_B T)} + n_{\text{RNAP}} e^{-E_{\text{RNAP}}/(k_B T)} + n_R e^{-E_R/(k_B T)} + n_A e^{-E_A/(k_B T)} + n_A n_{\text{RNAP}} e^{-E_{A:\text{RNAP}}/(k_B T)}. \quad (4.1)$$

The probability of a given macrostate is determined using equation (2.2). For example, if we define the promoter to be “active” if RNA polymerase is bound to the DNA, then the probability of being in this macrostate as a function of the various molecular counts is given by

$$P_{\text{active}}(n_R, n_A, n_{\text{RNAP}}) = \frac{1}{Z} \left(n_{\text{RNAP}} e^{-E_{\text{RNAP}}/(k_B T)} + n_A n_{\text{RNAP}} e^{-E_{A:\text{RNAP}}/(k_B T)} \right) = \frac{k_{A:\text{RNAP}} n_A + k_{\text{RNAP}}}{1 + k_{\text{RNAP}} + k_R n_R + (k_A + k_{A:\text{RNAP}}) n_A},$$

where

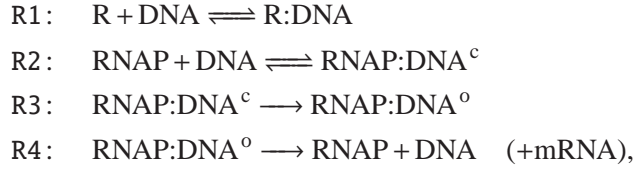
$$k_X = e^{-(E_X - E_0)/(k_B T)}.$$

From this expression we see that if $n_R \gg n_A$ then P_{active} tends to 0 while if $n_A \gg n_R$ then P_{active} tends to 1, as expected. ∇

Example 4.2 (Repression of gene expression). We consider a simple model of repression in which we have a promoter that contains binding sites for RNA polymerase and a repressor protein R. RNA polymerase only binds when the repressor

is absent, after which it can undergo an isomerization reaction to form an open complex and initiate transcription. Once the RNA polymerase begins to create mRNA, we assume the promoter region is uncovered, allowing another repressor or RNA polymerase to bind.

The following reactions describe this process:

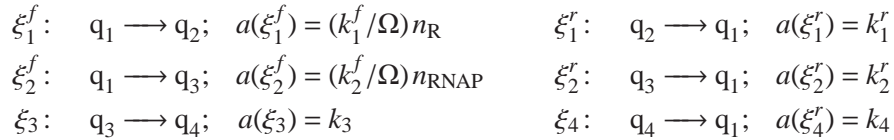


where RNAP:DNA^c represents the closed complex and RNAP:DNA^o represents the open complex. The states for the system depend on the number of molecules of each species and complex that are present. If we assume that we start with n_R repressors and n_{RNAP} RNA polymerases, then the possible states for our system are given by

State	DNA	R	RNAP	R:DNA	RNAP:DNA ^c	RNAP:DNA ^o
q_1	1	n_R	n_{RNAP}	0	0	0
q_2	0	$n_R - 1$	n_{RNAP}	1	0	0
q_3	0	n_R	$n_{\text{RNAP}} - 1$	0	1	0
q_4	0	n_R	$n_{\text{RNAP}} - 1$	0	0	1

Note that we do not keep track of each individual repressor or RNA polymerase molecule that binds to the DNA, but simply keep track of whether they are bound or not.

We can now rewrite the chemical reactions as a set of transitions between the possible microstates of the system. Assuming that all reactions take place in a volume Ω , we use the propensity functions for unimolecular and bimolecular reactions to obtain:



The chemical master equation can now be written down using the propensity functions for each reaction:

$$\frac{d}{dt} \begin{pmatrix} P(q_1, t) \\ P(q_2, t) \\ P(q_3, t) \\ P(q_4, t) \end{pmatrix} = \begin{pmatrix} -(k_1^f/\Omega)n_R - (k_2^f/\Omega)n_{\text{RNAP}} & k_1^r & k_2^r & k_4 \\ (k_1^f/\Omega)n_R & -k_1^r & 0 & 0 \\ (k_2^f/\Omega)n_{\text{RNAP}} & 0 & -k_2^r - k_3 & 0 \\ 0 & 0 & k_3 & -k_4 \end{pmatrix} \begin{pmatrix} P(q_1, t) \\ P(q_2, t) \\ P(q_3, t) \\ P(q_4, t) \end{pmatrix}.$$

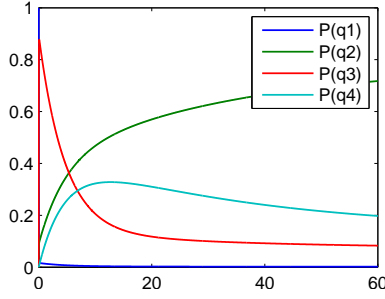


Figure 4.1: Numerical solution of chemical master equation for simple repression model.

The initial condition for the system can be taken as $P(q, 0) = (1, 0, 0, 0)$, corresponding to the state q_1 . A simulation showing the evolution of the probabilities is shown in Figure 4.1.

The equilibrium solution for the probabilities can be solved by setting $\dot{P} = 0$, which yields:

$$P_e(q_1) = \frac{k_1^r k_4 \Omega (k_2^r + k_3)}{k_1^f k_4 n_R (k_2^r + k_3) + k_1^r k_2^f n_{\text{RNAP}} (k_3 + k_4) + k_1^r k_4 \Omega (k_2^r + k_3)}$$

$$P_e(q_2) = \frac{k_1^f k_4 n_R (k_2^r + k_3)}{k_1^f k_4 n_R (k_2^r + k_3) + k_1^r k_2^f n_{\text{RNAP}} (k_3 + k_4) + k_1^r k_4 \Omega (k_2^r + k_3)}$$

$$P_e(q_3) = \frac{k_1^r k_2^f k_4 n_{\text{RNAP}}}{k_1^f k_4 n_R (k_2^r + k_3) + k_1^r k_2^f n_{\text{RNAP}} (k_3 + k_4) + k_1^r k_4 \Omega (k_2^r + k_3)}$$

$$P_e(q_4) = \frac{k_1^r k_2^f k_3 n_{\text{RNAP}}}{k_1^f k_4 n_R (k_2^r + k_3) + k_1^r k_2^f n_{\text{RNAP}} (k_3 + k_4) + k_1^r k_4 \Omega (k_2^r + k_3)}$$

We see that the functional dependencies are similar to the case of the combinatorial promoter of Example 4.1, but with the binding energies replaced by kinetic rate constants. ∇

A simplified version of the dynamics can be obtained by assuming that transcription factors bind to the DNA rapidly, so that they are in steady state configurations. In this case, we can make use of the steady state statistical mechanics techniques described in Section 2.1 and relate the expression of the gene to the probability that the activator or repressor is bound to the DNA (P_{bound}). This can be done at the level of the reaction rate equation by replacing the differential equations for activator or repressor binding with their steady state values. Here instead we demonstrate how to account for this rapid binding in the simplified differential equation models presented at the end of Section 2.2.

Recall that given the relative energies of the different microstates of the system, we can compute the probability of a given configuration using equation (2.1):

$$\mathbb{P}(q) = \frac{1}{Z} e^{-E_q/(k_B T)}.$$

Consider the regulation of a gene a with a protein concentration given by p_a and a corresponding mRNA concentration m_a . Let b be a second gene with protein concentration p_b that represses the production of protein A through transcriptional regulation. If we let q_{bound} represent the microstate corresponding to the appropriate activator or repressor bound to the DNA, then we can compute $\mathbb{P}(q_{\text{bound}})$ as a function of the concentration p_b , which we write as $P_{\text{bound}}(p_b)$. For a repressor, the resulting mRNA dynamics can be written as

$$\frac{dm_a}{dt} = (1 - P_{\text{bound}}(p_b))\alpha_{a0} - \gamma_a m_a. \quad (4.2)$$

We see that the effect of the repression is modeled by a modification of the rate of transcription depending on the probability that the repressor is bound to the DNA.

In the case of an activator, we proceed similarly. The modified mRNA dynamics are given by

$$\frac{dm_a}{dt} = P_{\text{bound}}(p_b)\alpha_{a0} - \gamma_a m_a, \quad (4.3)$$

where now we see that B must be bound to the DNA in order for transcription to occur.

As we shall see in Chapter 4 (see also Exercise 2.2), the functional form of P_{bound} can be nicely approximated by a monotonic rational function in the form of a Hill function [18, 61]. For a repressor, the Hill function is given by

$$f_a^r(p_b) = 1 - P_{\text{bound}}(p_b) = \frac{\alpha_{ab}}{k_{ab} + p_b^{n_{ab}}} + \alpha_{a0},$$

where the subscripts correspond to a protein B repressing production of a protein A, and the parameters α_{ab} , k_{ab} and n_{ab} describe how B represses A. The maximum transcription rate occurs when $p_b = 0$ and is given by $\alpha_{ab}/k_{ab} + \alpha_{a0}$. The minimum rate of transcription occurs when $p_b \rightarrow \infty$, giving α_{a0} , which describes the “leakiness” of the promoter. The parameter n_{ab} is called the *Hill coefficient* and determines how close the Hill function is to a step function. The Hill coefficient is often called the *degree of cooperativity* of the reaction, as it often arises from molecular reactions that involve multiple (“cooperating”) copies of the protein X, as seen in Section 2.1.

4.1 Stochastic Modeling of Biochemical Systems

Chemical reactions in the cell can be modeled as a collection of stochastic events corresponding to chemical reactions between species, including binding and unbinding of molecules (such as RNA polymerase and DNA), conversion of one set

of species into another, and enzymatically controlled covalent modifications such as phosphorylation. In this section we will briefly survey some of the different representations that can be used for stochastic models of biochemical systems, following the material in the textbooks by Phillips *et al.* [68], Gillespie [31] and Van Kampen [46].

Statistical physics

At the core of many of the reactions and multi-molecular interactions that take place inside of cells is the chemical physics associated with binding between two molecules. One way to capture some of the properties of these interactions is through the use of statistical mechanics and thermodynamics.

As described briefly already in Chapter 2, the underlying representation for both statistical mechanics and chemical kinetics is to identify the appropriate microstates of the system. A microstate corresponds to a given configuration of the components (species) in the system relative to each other and we must enumerate all possible configurations between the molecules that are being modeled.

In statistical mechanics, we model the configuration of the cell by the probability that system is in a given microstate. This probability can be calculated based on the energy levels of the different microstates. Consider a setting in which our system is contained within a reservoir. The total (conserved) energy is given by E_{tot} and we let E_r represent the energy in the reservoir. Let $E_s^{(1)}$ and $E_s^{(2)}$ represent two different energy levels for the system of interest and let $W_r(E_r)$ be the number of possible microstates of the reservoir with energy E_r . The laws of statistical mechanics state that the ratio of probabilities of being at the energy levels $E_s^{(1)}$ and $E_s^{(2)}$ is given by the ratio of number of possible states of the reservoir:

$$\frac{P(E_s^{(1)})}{P(E_s^{(2)})} = \frac{W_r(E_{\text{tot}} - E_s^{(1)})}{W_r(E_{\text{tot}} - E_s^{(2)})}. \quad (4.4)$$

Defining the entropy of the system as $S = k_B \ln W$, we can rewrite equation (4.4) as

$$\frac{W_r(E_{\text{tot}} - E_s^{(1)})}{W_r(E_{\text{tot}} - E_s^{(2)})} = \frac{e^{S_r(E_{\text{tot}} - E_s^{(1)})/k_B}}{e^{S_r(E_{\text{tot}} - E_s^{(2)})/k_B}}.$$

We now approximate $S_r(E_{\text{tot}} - E_s)$ in a Taylor series expansion around E_{tot} , under the assumption that $E_r \gg E_s$:

$$S_r(E_{\text{tot}} - E_s) \approx S_r(E_{\text{tot}}) - \frac{\partial S_r}{\partial E} E_s.$$

From the properties of thermodynamics, if we hold the volume and number of molecules constant, then we can define the temperature as

$$\left. \frac{\partial S}{\partial E} \right|_{V,N} = \frac{1}{T}$$

and we obtain

$$\frac{P(E_s^{(1)})}{P(E_s^{(2)})} = \frac{e^{-E_s^{(1)}/k_B T}}{e^{-E_s^{(2)}/k_B T}}.$$

This implies that

$$\mathbb{P}(E_s^{(q)}) \propto e^{-E_s^{(q)}/(k_B T)}$$

and hence the probability of being in a microstate q is given by

$$\mathbb{P}(q) = \frac{1}{Z} e^{-E_q/(k_B T)}, \quad (4.5)$$

where we have written E_q for the energy of the microstate and Z is a normalizing factor, known as the *partition function*, defined by

$$Z = \sum_{q \in Q} e^{-E_q/(k_B T)}.$$

By keeping track of those microstates that correspond to a given system state (also called a macrostate), we can compute the overall probability that a given macrostate is reached.

In order to determine the energy levels associated with different microstates, we will often make use of the *free energy* of the system. Consider an elementary reaction $A + B \rightleftharpoons AB$. Let E be the energy of the system, taken to be operating at pressure P in a volume V . The *enthalpy* of the system is defined as $H = E + PV$ and the *Gibbs free energy* is defined as $G = H - TS$ where T is the temperature of the system and S is its entropy (defined above). The change in bond energy due to the reaction is given by

$$\Delta H = \Delta G + T \Delta S,$$

where the Δ represents the change in the respective quantity. $-\Delta H$ represents the amount of heat that is absorbed from the reservoir, which then affects the entropy of the reservoir.

The resulting formula for the probability of being in a microstate q is given by

$$P(q) = \frac{1}{Z} e^{-\Delta G/k_B T}.$$

Example 4.3 (Ligand-receptor binding). To illustrate how these ideas can be applied in a cellular setting, consider the problem of determining the probability that a ligand binds to a receptor protein, as illustrated in Figure 4.2. We model the system by breaking up the cell into Ω different locations, each of the size of a ligand molecule, and keeping track of the locations of the L ligand molecules. The microstates of the system consist of all possible locations of the ligand molecules, including those in which one of the ligand molecules is bound to the receptor molecule.

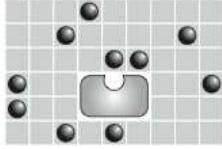
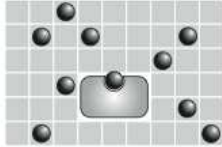
STATE	ENERGY	MULTIPLICITY	WEIGHT
	$L\varepsilon_{\text{sol}}$	$\frac{\Omega!}{L!(\Omega-L)!} \approx \frac{\Omega^L}{L!}$	$\frac{\Omega^L}{L!} e^{-\beta L\varepsilon_{\text{sol}}}$
	$(L-1)\varepsilon_{\text{sol}} + \varepsilon_{\text{b}}$	$\frac{\Omega!}{(L-1)!(\Omega-L+1)!} \approx \frac{\Omega^{L-1}}{(L-1)!}$	$\frac{\Omega^{L-1}}{(L-1)!} e^{-\beta[(L-1)\varepsilon_{\text{sol}} + \varepsilon_{\text{b}}]}$

Figure 4.2: Statistical physics description of ligand-receptor binding. The cell is modeled as a compartment with Ω sites, one of which contains a receptor protein. Ligand molecules can occupy any of the sites (first column) and we can compute the Gibbs free energy associated with each configuration (second column). The first row represents all possible microstates in which the receptor protein is not bound, while the second represents all configurations in which one of the ligands binds to the receptor. By accounting for the multiplicity of each microstate (third column), we can compute the weight of the given collection of microstates (fourth column). Figure from Phillips, Kondev and Theriot [68].

To compute the probability that the ligand is bound to the receptor, we must compute the energy associated with each possible microstate and then compute the weighted sum of the microstates corresponding to the ligand being bound, normalized by the partition function. We let E_{sol} represent the free energy associated with a ligand in free solution and E_{bound} represent the free energy associated with the ligand being bound to the receptor. Thus, the energy associated with microstates in which the ligand is not bound to the receptor is given by

$$\Delta G_{\text{sol}} = LE_{\text{sol}}$$

and the energy associated with microstates in which one ligand is bound to the receptor is given by

$$\Delta G_{\text{bound}} = (L-1)E_{\text{sol}} + E_{\text{bound}}.$$

Next, we compute the number of possible ways in which each of these two situations can occur. For the unbound ligand, we have L molecules that can be in any one of Ω locations, and hence the total number of combinations is given by

$$N_{\text{sol}} = \binom{\Omega}{L} = \frac{\Omega!}{L!(\Omega-L)!} \approx \frac{\Omega^L}{L!},$$

where the final approximation is valid in the case when $L \ll \Omega$. Similarly, the number of microstates in which the ligand is bound to the receptor is

$$N_{\text{sol}} = \binom{\Omega}{L-1} = \frac{\Omega!}{(L-1)!(\Omega-L+1)!} \approx \frac{\Omega^{L-1}}{(L-1)!}.$$

Using these two counts, the partition function for the system is given by

$$Z \approx \frac{\Omega^L}{L!} e^{-\frac{LE_{\text{sol}}}{k_B T}} + \frac{\Omega^{L-1}}{(L-1)!} e^{-\frac{(L-1)E_{\text{sol}} + E_{\text{bound}}}{k_B T}}.$$

Finally, we can compute the steady state probability that the ligand is bound by computing the ratio of the weights for the desired states divided by the partition function

$$P_{\text{bound}} = \frac{1}{Z} \cdot \frac{\Omega^{L-1}}{(L-1)!} e^{-\frac{(L-1)E_{\text{sol}} + E_{\text{bound}}}{k_B T}}.$$

▽

While the previous example was carried out for the special case of a ligand molecule binding to a receptor protein, in fact this same type of computation can be used to compute the probability that a transcription factor is attached to a piece of DNA or that two freely moving molecules bind to each other. Each of these cases simply comes down to enumerating all possible microstates, computing the energy associated with each, and then computing the ratio of the sum of the weights for the desired states to the complete partition function.

Example 4.4 (Transcription factor binding). Suppose that we have a transcription factor R that binds to a specific target region on a DNA strand (such as the promoter region upstream of a gene). We wish to find the probability P_{bound} that the transcription factor will be bound to this location as a function of the number of transcription factor molecules n_R in the system. If the transcription factor is a repressor, for example, knowing $P_{\text{bound}}(n_R)$ will allow us to calculate the likelihood of transcription occurring.

To compute the probability of binding, we assume that the transcription factor can bind non-specifically to other sections of the DNA (or other locations in the cell) and we let N_{ns} represent the number of such sites. We let E_{bound} represent the free energy associated with R bound to its specified target region and E_{ns} represent the free energy for R in any other non-specific location, where we assume that $E_{\text{extbound}} < E_{\text{ns}}$. The microstates of the system consist of all possible assignments of the n_R transcription factors to either a non-specific location or the target region of the DNA. Since there is only one target site, there can be at most one transcription factor attached there and hence we must count all of the ways in which either zero or one molecule of R are attached to the target site.

If none of the n_R copies of R are bound to the target region then these must be distributed between the n_{NS} non-specific locations. Each bound protein has energy E_{ns} , so the total energy for any such configuration is $n_R E_{\text{ns}}$. The number of such combinations is $\binom{N_{\text{ns}}}{n_R}$ and so the contribution to the partition function from these microstates is

$$Z_{\text{ns}} = \binom{N_{\text{ns}}}{n_R} e^{-n_R E_{\text{ns}}/(k_B T)} = \frac{N_{\text{ns}}!}{n_R!(N_{\text{ns}} - n_R)!} e^{-n_R E_{\text{ns}}/(k_B T)}$$

For the microstates in which one molecule of R is bound at a target site and the other $n_R - 1$ molecules are at the non-specific locations, we have a total energy of $E_{\text{bound}} + (n_R - 1)E_{\text{ns}}$ and $\binom{N_{\text{ns}}}{(n_R - 1)}$ possible such states. The resulting contribution to the partition function is

$$Z_{\text{bound}} = \frac{N_{\text{ns}}!}{(n_R - 1)!(N_{\text{ns}} - n_R + 1)!} e^{-(E_{\text{bound}} - (n_R - 1)E_{\text{ns}})/(k_B T)}.$$

The probability that the target site is occupied is now computed by looking at the ratio of the Z_{bound} to $Z = Z_{\text{ns}} + Z_{\text{bound}}$. After some basic algebraic manipulations, it can be shown that

$$P_{\text{bound}}(n_R) = \frac{\binom{n_R}{N_{\text{ns}} - n_R + 1} \exp[-(E_{\text{bound}} + E_{\text{ns}})/(k_B T)]}{1 + \binom{n_R}{N_{\text{ns}} - n_R + 1} \exp[-(E_{\text{bound}} + E_{\text{ns}})/(k_B T)]}.$$

If we assume that $N_{\text{ns}} \gg n_R$, then we can write

$$P_{\text{bound}}(n_R) \approx \frac{kn_R}{1 + kn_R}, \quad \text{where} \quad k = \frac{1}{N_{\text{ns}}} \exp[-(E_{\text{bound}} - E_{\text{ns}})/(k_B T)].$$

As we would expect, this says that for very small numbers of repressors, P_{bound} is close to zero, while for large numbers of repressors, $P_{\text{bound}} \rightarrow 1$. The point at which we get a binding probability of 0.5 is when $n_R = 1/k$, which depends on the relative binding energies and the number of non-specific binding sites. ∇

Chemical master equation (CME)

The statistical physics model we have just considered gives a description of the *steady state* properties of the system. In many cases, it is clear that the system reaches this steady state quickly and hence we can reason about the behavior of the system just by modeling the free energy of the system. In other situations, however, we care about the transient behavior of a system or the dynamics of a system that does not have an equilibrium configuration. In these instances, we must extend our formulation to keep track of how quickly the system transitions from one microstate to another, known as the *chemical kinetics* of the system.

To model these dynamics, we return to our enumeration of all possible microstates of the system. Let $P(q, t)$ represent the probability that the system is in microstate q at a given time t . Here q can be any of the very large number of possible microstates for the system. We wish to write an explicit expression for how $P(q, t)$ varies as a function of time, from which we can study the stochastic dynamics of the system.

We begin by assuming we have a set of M reactions R_j , $j = 1, \dots, M$, with ξ_j representing the change in state associated with reaction R_j . Specifically, ξ_j is given by the j th column of the stoichiometry matrix N . The *propensity function* defines the probability that a given reaction occurs in a sufficiently small time step dt :

$a_j(q, t)dt$ = Probability that reaction R_j will occur between time t and time $t + dt$ given that $X(t) = q$.

The linear dependence on dt relies on the fact that dt is chosen sufficiently small. We will typically assume that a_j does not depend on the time t and write $a_j(q)dt$ for the probability that reaction j occurs in state q .

Using the propensity function, we can compute the distribution of states at time $t + dt$ given the distribution at time t :

$$\begin{aligned} P(q, t + dt | q_0, t_0) &= P(q, t | q_0, t_0) \left(1 - \sum_{j=1}^M a_j(q)dt \right) + \sum_{j=1}^M P(q - \xi_j | q_0, t_0) a_j(q - \xi_j)dt \\ &= P(q, t | q_0, t_0) + \sum_{j=1}^M \left(a_j(q - \xi_j)P(q - \xi_j, t | q_0, t_0) - a_j(q)P(q, t | q_0, t_0) \right) dt. \end{aligned} \quad (4.6)$$

Since dt is small, we can take the limit as $dt \rightarrow 0$ and we obtain the *chemical master equation* (CME):

$$\frac{\partial P}{\partial t}(q, t | q_0, t_0) = \sum_{j=1}^M \left(a_j(q - \xi_j)P(q - \xi_j, t | q_0, t_0) - a_j(q)P(q, t | q_0, t_0) \right) \quad (4.7)$$

This equation is also referred to as the *forward Kolmogorov equation* for a discrete state, continuous time random process.

We will sometimes find it convenient to use a slightly different notation in which we let ξ represent any transition in the system state (without enumerating the reactions). In this case, we write the propensity function as $a(\xi; q, t)$, which represents the incremental probability that we will transition from state q to state $q + \xi$ at time t . When the propensities are not explicitly dependent on time, we simply write $a(\xi; q)$. In this notation, the chemical master equation becomes

$$\frac{\partial P}{\partial t}(q, t | q_0, t_0) = \sum_{\xi} \left(a(\xi; q - \xi)P(q - \xi, t | q_0, t_0) - a(\xi; q)P(q, t | q_0, t_0) \right), \quad (4.8)$$

where the sum is understood to be over all allowable transitions.

Under some additional assumptions, we can rewrite the master equation in differential form as

$$\frac{d}{dt}P(q, t) = \sum_{\xi} a(\xi; q - \xi)P(q - \xi, t) - \sum_{\xi} a(\xi; q)P(q, t), \quad (4.9)$$

where we have dropped the dependence on the initial condition for notational convenience. We see that the master equation is a *linear* differential equation with state $P(q, t)$. However, it is important to note that the size of the state vector can be very

large: we must keep track of the probability of every possible microstate of the system. For example, in the case of the ligand-receptor problem discussed earlier, this has a factorial number of states based on the number of possible sites in the model. Hence, even for very simple systems, the master equation cannot typically be solved either analytically or in a numerically efficient fashion.

Despite its complexity, the master equation does capture many of the important details of the chemical physics of the system and we shall use it as our basic representation of the underlying dynamics. As we shall see, starting from this equation we can then derive a variety of alternative approximations that allow us to answer specific equations of interest.

The key element of the master equation is the propensity function $a(\xi; q, t)$, which governs the rate of transition between microstates. Although the detailed value of the propensity function can be quite complex, its functional form is often relatively simple. In particular, for a unimolecular reaction ξ of the form $A \rightarrow B$, the propensity function is proportional to the number of molecules of A that are present:

$$a(\xi; q, t) = c_\xi n_A. \quad (4.10)$$

This follows from the fact that each reaction is independent and hence the likelihood of a reaction happening depends directly on the number of copies of A that are present.

Similarly, for a bimolecular reaction, we have that the likelihood of a reaction occurring is proportional to the product of the number of molecules of each type that are present (since this is the number of independent reactions that can occur) and inversely proportional to the volume Ω . Hence, for a reaction ξ of the form $A + B \rightarrow C$ we have

$$a(\xi; q, t) = \frac{c_\xi}{\Omega} n_A n_B. \quad (4.11)$$

The rigorous verification of this functional form is beyond the scope of this text, but roughly we keep track of the likelihood of a single reaction occurring between A and B and then multiply by the total number of combinations of the two molecules that can react ($n_A \cdot n_B$).

A special case of a bimolecular reaction occurs when $A = B$, so that our reaction is given by $2A \rightarrow B$. In this case we must take into account that a molecule cannot react with itself, and so the propensity function is of the form

$$a(\xi; q, t) = \frac{c_\xi}{\Omega} n_A (n_A - 1). \quad (4.12)$$

Although it is tempting to extend this formula to the case of more than two species being involved in a reaction, usually such reactions actually involve combinations of bimolecular reactions, e.g.:

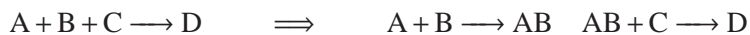


Table 4.2: Examples of propensity functions for some common cases [32]. Here we take r_a and r_b to be the effective radii of the molecules, $m^* = m_a m_b / (m_a + m_b)$ is the reduced mass of the two molecules, Ω is the volume over which the reaction occurs, T is temperature, k_B is Boltzmann's constant and n_a, n_b are the numbers of molecules of A and B present.

Reaction type	Propensity function coefficient, c_ξ
Reaction occurs if molecules "touch"	$\left(\frac{8k_B T}{\pi m^*}\right)^{1/2} \pi(r_a + r_b)^2$
Reaction occurs if molecules collide with energy ϵ	$\left(\frac{8k_B T}{\pi m^*}\right)^{1/2} \pi(r_a + r_b)^2 \cdot e^{-\epsilon/k_B T}$
Steady state transcription factor	$P_{\text{bound}} k_{\text{oc}} n_{\text{RNAP}}$

This more detailed description reflects that fact that it is extremely unlikely that three molecules will all come together at precisely the same instant, versus the much more likely possibility that two molecules will initially react, followed by a second reaction involving the third molecule.

The propensity functions for these cases and some others are given in Table 4.2.

Example 4.5 (Transcription of mRNA). Consider the production of mRNA from a single copy of DNA. We have two basic reactions that can occur: mRNA can be produced by RNA polymerase transcribing the DNA and producing an mRNA strand, or mRNA can be degraded. We represent the microstate q of the system in terms of the number of mRNA's that are present, which we write as n for ease of notation. The reactions can now be represented as $\xi = +1$, corresponding to transcription and $\xi = -1$, corresponding to degradation. We choose as our propensity functions

$$a(+1; n, t) = \alpha, \quad a(-1; n, t) = \gamma n,$$

by which we mean that the probability of that a gene is transcribed in time dt is αdt and the probability that a transcript in time dt is $\gamma n dt$ (proportional to the number of mRNA's).

We can now write down the master equation as described above. Equation (4.6) becomes

$$\begin{aligned} P(n, t + dt) &= P(n, t) \left(1 - \sum_{\xi=+1, -1} a(\xi; n, t) dt\right) + \sum_{\xi=+1, -1} P(n - \xi, t) a(\xi; n - \xi) dt \\ &= P(n, t) - a(+1; n, t) P(n, t) - a(-1; n, t) P(n, t) \\ &\quad + a(+1; n - 1, t) P(n - 1, t) + a(-1; n + 1, t) P(n + 1) \\ &= P(n, t) + \alpha P(n - 1, t) dt - (\alpha - \gamma n) P(n, t) dt + \gamma(n + 1) P(n + 1, t) dt. \end{aligned}$$

This formula holds for $n > 0$, with the $n = 0$ case satisfying

$$P(0, t + dt) = P(0, t) - \alpha P(0, t) dt + \gamma P(1, t) dt.$$

Notice that we have an infinite number of equations, since n can be any positive integer.

We can write the differential equation version of the master equation by subtracting the first term on the right hand side and dividing by dt :

$$\begin{aligned}\frac{d}{dt}P(n,t) &= \alpha P(n-1,t) - (\alpha + \gamma n)P(n,t) + \gamma(n+1)P(n+1,t), & n > 0 \\ \frac{d}{dt}P(0,t) &= -\alpha P(0,t) + \gamma P(1,t).\end{aligned}$$

Again, this is an infinite number of differential equations, although we could take some limit N and simply declare that $P(N,t) = 0$ to yield a finite number.

One simple type of analysis that can be done on this equation without truncating it to a finite number is to look for a steady state solution to the equation. In this case, we set $\dot{P}(n,t) = 0$ and look for a constant solution $P(n,t) = p_e(n)$. This yields an algebraic set of relations

$$\begin{aligned}0 &= -\alpha p_e(0) + \gamma p_e(1) & \implies & \alpha p_e(0) = \gamma p_e(1) \\ 0 &= \alpha p_e(0) - (\alpha + \gamma)p_e(1) + 2\gamma p_e(2) & & \alpha p_e(1) = 2\gamma p_e(2) \\ 0 &= \alpha p_e(1) - (\alpha + 2\gamma)p_e(2) + 3\gamma p_e(3) & & \alpha p_e(2) = 3\gamma p_e(3) \\ &\vdots & & \vdots \\ & & & \alpha p(n-1) = n\gamma p(n).\end{aligned}$$

It follows that the distribution of steady state probabilities is given by the Poisson distribution

$$p(n) = e^{-\alpha/\gamma} \frac{(\alpha/\gamma)^n}{n!},$$

and the mean, variance and coefficient of variation are thus

$$\mu = \frac{\alpha}{\gamma}, \quad \sigma^2 = \frac{\alpha}{\gamma}, \quad CV = \frac{\mu}{\sigma} = \frac{1}{\sqrt{\mu}} = \sqrt{\frac{\gamma}{\alpha}}.$$

▽

Chemical Langevin equation (CLE)

The chemical master equation gives a complete description of the evolution of the distribution of a system, but it can often be quite cumbersome to work with directly. A number of approximations to the master equation are thus used to provide more tractable formulations of the dynamics. The first of these that we shall consider is known as the *chemical Langevin equation* (CLE).

To derive the chemical Langevin equation, we start by assuming that the number of molecules in the system is large and that we can therefore represent the system using a vector of real numbers X , with X_i representing the (real-valued) number of molecules in S_i . (Often X_i will be divided by the volume to give a real-valued concentration of species S_i .) In addition, we assume that we are interested in the

dynamics on time scales in which individual reactions are not important and so we can look at how the system state changes over time intervals in which many reactions occur and hence the system state evolves in a smooth fashion.

Let $X(t)$ be the state vector for the system, where we assume now that the elements of X are real-valued rather than integer valued. We make the further approximation that we can lump together multiple reactions so that instead of keeping track of the individual reactions, we can average across a number of reactions over a time τ to allow the continuous state to evolve in continuous time. The resulting dynamics can be described by a stochastic process of the form

$$X_i(t + \tau) = X_i(t) + \sum_{j=1}^M \xi_{ij} a_j(X(t)) \tau + \sum_{j=1}^M \xi_{ij} a_j^{1/2}(X(t)) \mathcal{N}_j(0, \sqrt{\tau}),$$

where a_j are the propensity functions for the individual reactions, ξ_{ij} are the corresponding changes in the system states X_i and \mathcal{N}_j are a set of independent Gaussian random variables with zero mean and variance τ .

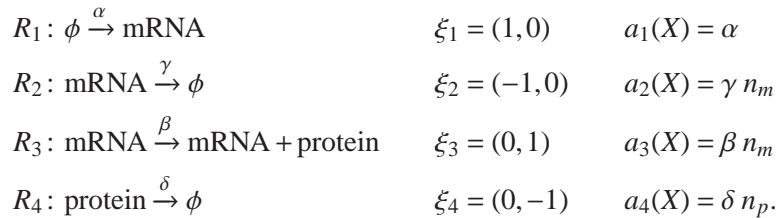
If we assume that τ is small enough that we can use the derivative to approximate the previous equation (but still large enough that we can average over multiple reactions), then we can write

$$\frac{dX_i(t)}{dt} = \sum_{j=1}^M \xi_{ji} a_j(X(t)) + \sum_{j=1}^M \xi_{ji} a_j^{1/2}(X(t)) \Gamma_j(t) =: A_i(X(t)) + \sum_{j=1}^M B_{ij}(X(t)) \Gamma_j(t), \quad (4.13)$$

where Γ_j are white noise processes (see Appendix B.2). This equation is called the *chemical Langevin equation* (CLE).

Example 4.6 (Protein production). Consider a simplified model of protein production in which mRNAs are produced by transcription and proteins by translation. We also include degradation of both mRNAs and proteins, but we do not model the detailed processes of elongation of the mRNA and polypeptide chains.

We can capture the state of the system by keeping track of the number of copies of mRNA and proteins. We further approximate this by assuming that the number of each of these is sufficiently large that we can keep track of its concentration, and hence $X = (n_m, n_p)$ where $n_m \in \mathbb{R}$ is the amount of mRNA and $n_p \in \mathbb{R}$ is the concentration of protein. Letting Ω represent the volume, the reactions that govern the dynamics of the system are given by:



Substituting these expressions into equation (4.13), we obtain a stochastic differential equation of the form

$$\frac{d}{dt} \begin{pmatrix} n_m \\ n_p \end{pmatrix} = \begin{pmatrix} -\gamma & 0 \\ \beta & -\delta \end{pmatrix} \begin{pmatrix} n_m \\ n_p \end{pmatrix} + \begin{pmatrix} \alpha \\ 0 \end{pmatrix} + \sqrt{\Omega} \begin{pmatrix} (\sqrt{\alpha + \gamma n_m}) \Gamma_m \\ (\sqrt{\beta n_m + \delta n_p}) \Gamma_p \end{pmatrix},$$

where Γ_m and Γ_p are independent white noise processes with unit variance. (Note that in deriving this equation we have used the fact that the sum of two independent Gaussian processes is a Gaussian process.) ∇

Fokker-Planck equations (FPE)

The chemical Langevin equation provides a stochastic ordinary differential equation that describes the evolution of the system state. A slightly different (but completely equivalent) representation of the dynamics is to model how the probability distribution $P(q, t)$ evolves in time. As in the case of the chemical Langevin equation, we will assume that the system state is continuous and write down a formula for the evolution of the density function $p(x, t)$. This formula is known as the *Fokker-Planck equations* (FPE) and is essentially an approximation on the chemical master equation.

Consider first the case of a random process in one dimension. We assume that the random process is in the same form as the previous section:

$$\frac{dX(t)}{dt} = A(X(t)) + B(X(t))\Gamma(t). \quad (4.14)$$

The function $A(X)$ is called the *drift term* and $B(X)$ is the *diffusion term*. It can be shown that the probability density function for X , $p(x, t | x_0, t_0)$, satisfies the partial differential equation

$$\frac{\partial p}{\partial t}(x, t | x_0, t_0) = -\frac{\partial}{\partial x}(A(x, t)p(x, t | x_0, t_0)) + \frac{1}{2} \frac{\partial^2}{\partial x^2}(B^2(x, t)p(x, t | x_0, t_0)) \quad (4.15)$$

Note that here we have shifted to the probability density function since we are considering X to be a continuous state random process.

In the multivariate case, a bit more care is required. Using the chemical Langevin equation (4.13), we define

$$D_i(x, t) = \sum_{j=1}^M B_{ij}^2(x, t), \quad C_{ij}(x, t) = \sum_{k=1}^M B_{ik}(x, t)B_{jk}(x, t), \quad i < j = 1, \dots, M.$$

The Fokker-Planck equation now becomes

$$\begin{aligned}
\frac{\partial p}{\partial t}(x, t | x_0, t_0) = & - \sum_{i=1}^M \frac{\partial}{\partial x_i} (A_i(x, t) p(x, t | x_0, t_0)) \\
& + \frac{1}{2} \sum_{i=1}^M \frac{\partial}{\partial x_i} \frac{\partial^2}{\partial x_i^2} (D_i(x, t) p(x, t | x_0, t_0)) \\
& + \sum_{\substack{i, j=1 \\ i < j}}^M \frac{\partial^2}{\partial x_i \partial x_j} (C_{ij}(x, t) p(x, t | x_0, t_0)).
\end{aligned} \tag{4.16}$$

Linear noise approximation (LNA)

The chemical Langevin equation and the Fokker-Planck equation provide approximations to the chemical master equation. A slightly different approximation can be obtained by expanding the density function in terms of a size parameter Ω . This approximation is known as the *linear noise approximation* (LNA) or the Ω *expansion* [46].

We begin with a master equation for a continuous random variable X , which we take to be of the form

$$\frac{\partial p}{\partial t}(x, t) = \int (a_\Omega(\xi; x - \xi) p(x - \xi, t) - a_\Omega(\xi; x) p(x, t)) d\xi,$$

where we have dropped the dependence on the initial condition for notational simplicity. As before, the propensity function $a_\Omega(\xi; x)$ represents the transition probability between a state x and a state $x + \xi$ and we assume that it is a function of a parameter Ω that represents the size of the system (typically the volume). Since we are working with continuous variables, we now have an integral in place of our previous sum.

We now assume that the mean of X can be written as $\Omega\phi(t)$ where $\phi(t)$ is a continuous function of time that represents the evolution of the mean of X/Ω . To understand the fluctuations of the system about this mean, we write

$$X = \Omega\phi + \Omega^{\frac{1}{2}}Z,$$

where Z is a new variable representing the perturbations of the system about its mean. We can write the distribution for Z as

$$p_Z(z, t) = p_X(\Omega\phi(t) + \Omega^{\frac{1}{2}}z, t)$$

and it follows that the derivatives of p_Z can be written as

$$\begin{aligned}
\frac{\partial^v p_Z}{z^v} &= \Omega^{\frac{1}{2}v} \frac{\partial^v p_X}{x^v} \\
\frac{\partial p_Z}{\partial t} &= \frac{\partial p_X}{\partial t} + \Omega \frac{d\phi}{dt} \frac{\partial p_X}{\partial x} = \frac{\partial p_X}{\partial t} + \Omega^{\frac{1}{2}} \frac{d\phi}{dt} \frac{\partial p_Z}{\partial z}.
\end{aligned}$$

We further assume that the Ω dependence of the propensity function is such that

$$a_{\Omega}(\xi, \Omega\phi) = f(\Omega)\tilde{a}(\xi; \phi),$$

where \tilde{a} is not dependent on Ω . From these relations, we can now derive the master equation for p_Z in terms of powers of Ω (derivation omitted).

The $\Omega^{1/2}$ term in the expansion turns out to yield

$$\frac{d\phi}{dt} = \int \xi a(\xi, \Omega\phi) d\xi, \quad \phi(0) = \frac{X(0)}{\Omega},$$

which is precisely the equation for the mean of the concentration. It can further be shown that the terms in Ω^0 are given by

$$\frac{\partial p_Z(z, \tau)}{\partial \tau} = -\alpha'_1(\phi) \frac{\partial}{\partial z} (z p_Z(z, t)) + \frac{1}{2} \alpha_2(\phi) \frac{\partial^2 p_Z(z, t)}{\partial z^2}, \quad (4.17)$$

where

$$\alpha_v(x) = \int \xi^v \tilde{a}(\xi; x) d\xi, \quad \tau = \Omega^{-1} f(\Omega) t.$$

Notice that in the case that $\phi(t) = \phi_0$ (a constant), this equation becomes the Fokker-Planck equation derived previously.

Higher order approximations to this equation can also be carried out by keeping track of the expansion terms in higher order powers of Ω . In the case where Ω represents the volume of the system, the next term in the expansion is Ω^{-1} and this represents fluctuations that are on the order of a single molecule, which can usually be ignored.

Rate reaction equations (RRE)

As we already saw in Chapter 2, the reaction rate equations can be used to describe the dynamics of a chemical system in the case where there are a large number of molecules whose state can be approximated using just the concentrations of the molecules. We re-derive the results from Section 2.1 here, being more careful to point out what approximations are being made.

We start with the chemical Langevin equations (4.13), from which we can write the dynamics for the average quantity of the each species at each point in time:

$$\frac{d\langle X_i(t) \rangle}{dt} = \sum_{j=1}^M \xi_{ji} \langle a_j(X(t)) \rangle,$$

where the second order term drops out under the assumption that the Γ_j 's are independent processes. We see that the reaction rate equations follow by defining $x_i = \langle X_i \rangle / \Omega$ and *assuming* that $\langle a_j(X(t)) \rangle = a_j(\langle X(t) \rangle)$. This relationship is true when a_j is linear (e.g., in the case of a unimolecular reaction), but is an approximation otherwise.

4.2 Simulation of stochastic systems

Suppose that we want to generate a collection of sample trajectories for a stochastic system whose evolution is described by the chemical master equation (4.7):

$$\frac{d}{dt}P(q, t) = \sum_{\xi} a(\xi; q - \xi)P(q - \xi, t) - \sum_{\xi} a(\xi; q)P(q, t),$$

where $P(q, t)$ is the probability of being in a microstate q at time t (starting from q_0 at time t_0) and $a(\xi; q)$ is the propensity function for a reaction ξ starting at a microstate q and ending at microstate $q + \xi$. Instead of simulating the distribution function $P(q, t)$, we wish to simulate a specific instance $q(t)$ starting from some initial condition $q_0(t_0)$. If we simulate many such instances of $q(t)$, their distribution at time t should match $P(q, t)$.

To illustrate the basic ideas that we will use, consider first a simple birth process in which the microstate is given by an integer $q \in \{0, 1, 2, \dots\}$ and we assume that the propensity function is given by

$$a(\xi; q) dt = \lambda dt, \quad \xi = +1.$$

Thus the probability of transition increases linearly with the time increment dt (so birth events occur at rate λ , on average). If we assume that the birth events are independent of each other, then it can be shown (see Appendix B) that this process has Poisson distribution with parameter $\lambda\tau$:

$$P(q(t + \tau) - q(t) = \ell) = \frac{(\lambda\tau)^\ell}{\ell!} e^{-\lambda\tau},$$

where τ is the difference in time and ℓ is the difference in count q . In fact, this distribution is a joint distribution in time τ and count ℓ , and by setting $\ell = 1$ it can be seen that the time to the next reaction T follows an exponential distribution and has density function

$$p_T(\tau) = \lambda e^{-\lambda\tau}.$$

The exponential distribution has expectation $1/\lambda$ and so we see that the average time between events is inversely proportional to the reaction rate λ .

Consider next a more general case in which we have a countable number of microstates $q \in \{0, 1, 2, \dots\}$ and we let k_{ji} represent the transition probability between a microstate i and microstate j . The birth process is a special case given by $k_{i+1,i} = \lambda$ and all other $k_{ji} = 0$. The chemical master equation describes the joint probability that we are in state $q = i$ at a particular time t . We would like to know the probability that we transition to a new state $q = j$ at time $t + dt$. Given this probability, we can attempt to generate an instance of the variable $q(t)$ by first determining which reaction occurs and then when the reaction occurs.

Let $P(j, \tau) := P(j, t + \tau + d\tau \mid i, t + \tau)$ represent the probability that we transition from the state i to the state j in the time interval $[t + \tau, t + \tau + d\tau]$. For simplicity and ease of notation, we will take $t = 0$. Let $T := T_{j,i}$ be the time at which the reaction first occurs. We can write the probability that we transition to state j in the interval $[\tau, \tau + d\tau]$ as

$$P(j, \tau) = P(T > \tau) k_{ji} d\tau, \quad (4.18)$$

where $P(T > \tau)$ is the probability that no reaction occurs in the time interval $[0, \tau]$ and $k_{ji}d\tau$ is the probability that the reaction taking state i to state j occurs in the next $d\tau$ seconds (assumed to be independent events, giving the product of these probabilities).

To compute $P(T > \tau)$, define

$$\bar{k}_i = \sum_j k_{ji}$$

so that $(1 - \bar{k}_i)d\tau$ is the probability that no transition occurs from state i in the next $d\tau$ seconds. Then, the probability that no reaction occurs in the interval $[\tau, \tau + d\tau]$ can be written as

$$P(T > \tau + d\tau) = P(T > \tau)(1 - \bar{k}_i) d\tau. \quad (4.19)$$

It follows that

$$\frac{d}{d\tau} P(T > \tau) = \lim_{d\tau \rightarrow 0} \frac{P(T > \tau + d\tau) - P(T > \tau)}{d\tau} = -P(T > \tau) \bar{k}_i.$$

Solving this differential equation, we obtain

$$P(T > \tau) = e^{-\bar{k}_i \tau}, \quad (4.20)$$

so that the probability that no reaction occurs in time τ decreases exponentially with the amount of time that we wait, with rate given by the sum of all the reactions that can occur from state i .

We can now combine equation (4.20) with equation (4.18) to obtain

$$P(j, \tau) = P(j, \tau + d\tau \mid i, 0) = k_{ji} e^{-\bar{k}_i \tau} d\tau.$$

We see that this has the form of a density function in time and hence the probability that the next reaction is reaction j , independent of the time in which it occurs, is

$$P_{ji} = \int_0^\infty k_{ji} e^{-\bar{k}_i \tau} d\tau = \frac{k_{ji}}{\bar{k}_i}. \quad (4.21)$$

Thus, to choose the next reaction to occur from a state i , we choose between N possible reactions, with the probability of each reaction weighted by k_{ji}/\bar{k}_i .

To determine the time that the next reaction occurs, we sum over all possible reactions j to get the density function for the reaction time:

$$p_T(\tau) = \sum_j k_{ji} e^{-\bar{k}_i \tau} = \bar{k}_i e^{-\bar{k}_i \tau}.$$

This is the density function associated with a Poisson distribution. To compute a time of reaction Δt that draws from this distribution, we note that the cumulative distribution function for T is given by

$$\int_0^{\Delta t} f_T(\tau) d\tau = \int_0^{\Delta t} \bar{k}_i e^{-\bar{k}_i \tau} d\tau = 1 - e^{-\bar{k}_i \Delta t}.$$

The cumulative distribution function is always in the range $[0, 1]$ and hence we can compute Δt by choosing a (uniformly distributed) random number r in $[0, 1]$ and then computing

$$\Delta t = \frac{1}{\bar{k}_i} \ln \frac{1}{1-r}. \quad (4.22)$$

(This equation can be simplified somewhat by replacing $1 - r$ with r' and noting that r' can also be drawn from a uniform distribution on $[0, 1]$.)

Note that in the case of a birth process, this computation agrees with our earlier analysis. Namely, $\bar{k}_i = \lambda$ and hence the (only) reaction occurs according to an exponential distribution with parameter λ .

This set of calculations gives the following algorithm for computing an instance of the chemical master equation:

1. Choose an initial condition q at time $t = 0$.
2. Calculate the propensity functions $a_\xi(q)$ for each possible reaction q .
3. Choose the time for the reaction according to equation (4.22), where $r \in [0, 1]$ is chosen from a uniform distribution.
4. Use a weighted random number generator to identify which reaction will take place next, using the weights in equation (4.21).
5. Update q by implementing the reaction ξ and update the time t by δt .
6. If $T < T_{\text{stop}}$, goto step 2.

This method is sometimes called ‘‘Gillespie’s direct method’’ [31, ?], but we shall refer to it here as the ‘‘stochastic simulation algorithm’’ (SSA). We note that the reaction number in step 4 can be computed by calculating a uniform random number on $[0, 1]$, scaling this by the total propensity $\sum_i a(\xi_i, q)$, and then finding the first reaction i such that $\sum_0^i a(\xi_i, q)$ is larger than this scaled random number.

Example 4.7.

∇

4.3 Input/Output Linear Stochastic Systems

In many situations, we wish to know how noise propagates through a biomolecular system. For example, we may wish to understand how stochastic variations in RNA polymerase concentration affect gene expression. In order to analyze these cases, we specialize to the case of a biomolecular system operating around a fixed operating point.

We now consider the problem of how to compute the response of a linear system to a random process. We assume we have a linear system described in state space as

$$\dot{X} = AX + FW, \quad Y = CX \quad (4.23)$$

Given an “input” W , which is itself a random process with mean $\mu(t)$, variance $\sigma^2(t)$ and correlation $r(t, t + \tau)$, what is the description of the random process Y ?

Let W be a white noise process, with zero mean and noise intensity Q :

$$r(\tau) = Q\delta(\tau).$$

We can write the output of the system in terms of the convolution integral

$$Y(t) = \int_0^t h(t-\tau)W(\tau) d\tau,$$

where $h(t-\tau)$ is the impulse response for the system

$$h(t-\tau) = Ce^{A(t-\tau)}B + D\delta(t-\tau).$$

We now compute the statistics of the output, starting with the mean:

$$\begin{aligned} \mathbb{E}(Y(t)) &= \mathbb{E}\left(\int_0^t h(t-\eta)W(\eta) d\eta\right) \\ &= \int_0^t h(t-\eta)\mathbb{E}(W(\eta)) d\eta = 0. \end{aligned}$$

Note here that we have relied on the linearity of the convolution integral to pull the expectation inside the integral.

We can compute the covariance of the output by computing the correlation $r(\tau)$ and setting $\sigma^2 = r(0)$. The correlation function for y is

$$\begin{aligned} r_Y(t, s) &= \mathbb{E}(Y(t)Y(s)) = \mathbb{E}\left(\int_0^t h(t-\eta)W(\eta) d\eta \cdot \int_0^s h(s-\xi)W(\xi) d\xi\right) \\ &= \mathbb{E}\left(\int_0^t \int_0^s h(t-\eta)W(\eta)W(\xi)h(s-\xi) d\eta d\xi\right) \end{aligned}$$

Once again linearity allows us to exchange expectation and integration

$$\begin{aligned}
 r_Y(t, s) &= \int_0^t \int_0^s h(t-\eta) \mathbb{E}(W(\eta)W(\xi)) h(s-\xi) d\eta d\xi \\
 &= \int_0^t \int_0^s h(t-\eta) Q \delta(\eta-\xi) h(s-\xi) d\eta d\xi \\
 &= \int_0^t h(t-\eta) Q h(s-\eta) d\eta
 \end{aligned}$$

Now let $\tau = s - t$ and write

$$\begin{aligned}
 r_Y(\tau) &= r_Y(t, t + \tau) = \int_0^t h(t-\eta) Q h(t + \tau - \eta) d\eta \\
 &= \int_0^t h(\xi) Q h(\xi + \tau) d\xi \quad (\text{setting } \xi = t - \eta)
 \end{aligned}$$

Finally, we let $t \rightarrow \infty$ (steady state)

$$\lim_{t \rightarrow \infty} r_Y(t, t + \tau) = \bar{r}_Y(\tau) = \int_0^\infty h(\xi) Q h(\xi + \tau) d\xi \quad (4.24)$$

If this integral exists, then we can compute the second order statistics for the output Y .

We can provide a more explicit formula for the correlation function r in terms of the matrices A , F and C by expanding equation (4.24). We will consider the general case where $W \in \mathbb{R}^p$ and $Y \in \mathbb{R}^q$ and use the correlation matrix $R(t, s)$ instead of the correlation function $r(t, s)$. Define the *state transition matrix* $\Phi(t, t_0) = e^{A(t-t_0)}$ so that the solution of system (4.23) is given by

$$x(t) = \Phi(t, t_0)x(t_0) + \int_{t_0}^t \Phi(t, \lambda) F w(\lambda) d\lambda$$

Proposition 4.1 (Stochastic response to white noise). *Let $\mathbb{E}(X(t_0)X^T(t_0)) = P(t_0)$ and W be white noise with $\mathbb{E}(W(\lambda)W^T(\xi)) = R_W \delta(\lambda - \xi)$. Then the correlation matrix for X is given by*

$$R_X(t, s) = P(t)\Phi^T(s, t)$$

where $P(t)$ satisfies the linear matrix differential equation

$$\dot{P}(t) = AP + PA^T + FR_W F, \quad P(0) = P_0.$$

Proof. Using the definition of the correlation matrix, we have

$$\begin{aligned}
\mathbb{E}(X(t)X^T(s)) &= \mathbb{E}\left(\Phi(t,0)X(0)X^T(0)\Phi^T(t,0) + \text{cross terms}\right. \\
&\quad \left. + \int_0^t \Phi(t,\xi)FW(\xi)d\xi \int_0^s W^T(\lambda)F^T\Phi(s,\lambda)d\lambda\right) \\
&= \Phi(t,0)\mathbb{E}(X(0)X^T(0))\Phi(s,0) \\
&\quad + \int_0^t \int_0^s \Phi(t,\xi)F\mathbb{E}(W(\xi)W^T(\lambda))F^T\Phi(s,\lambda)d\xi d\lambda \\
&= \Phi(t,0)P(0)\Phi^T(s,0) + \int_0^t \Phi(t,\lambda)FR_W(\lambda)F^T\Phi(s,\lambda)d\lambda.
\end{aligned}$$

Now use the fact that $\Phi(s,0) = \Phi(s,t)\Phi(t,0)$ (and similar relations) to obtain

$$R_X(t,s) = P(t)\Phi^T(s,t)$$

where

$$P(t) = \Phi(t,0)P(0)\Phi^T(t,0) + \int_0^t \Phi(t,\lambda)FR_WF^T(\lambda)\Phi^T(t,\lambda)d\lambda$$

Finally, differentiate to obtain

$$\dot{P}(t) = AP + PA^T + FR_WF, \quad P(0) = P_0$$

(see Friedland for details). □

The correlation matrix for the output Y can be computed using the fact that $Y = CX$ and hence $R_Y = C^T R_X C$. We will often be interested in the steady state properties of the output, which are given by the following proposition.

Proposition 4.2 (Steady state response to white noise). *For a time-invariant linear system driven by white noise, the correlation matrices for the state and output converge in steady state to*

$$R_X(\tau) = R_X(t, t + \tau) = Pe^{A^T\tau}, \quad R_Y(\tau) = CR_X(\tau)C^T$$

where P satisfies the algebraic equation

$$AP + PA^T + FR_WF^T = 0 \quad P > 0. \quad (4.25)$$

Equation (4.25) is called the *Lyapunov equation* and can be solved in MATLAB using the function `lyap`.

Example 4.8 (First-order system). Consider a scalar linear process

$$\dot{X} = -aX + W, \quad Y = cX,$$

where W is a white, Gaussian random process with noise intensity σ^2 . Using the results of Proposition 4.1, the correlation function for X is given by

$$R_X(t, t + \tau) = p(t)e^{-a\tau}$$

where $p(t) > 0$ satisfies

$$p(t) = -2ap + \sigma^2.$$

We can solve explicitly for $p(t)$ since it is a (non-homogeneous) linear differential equation:

$$p(t) = e^{-2at} p(0) + (1 - e^{-2at}) \frac{\sigma^2}{2a}.$$

Finally, making use of the fact that $Y = cX$ we have

$$r(t, t + \tau) = c^2(e^{-2at} p(0) + (1 - e^{-2at}) \frac{\sigma^2}{2a}) e^{-a\tau}.$$

In steady state, the correlation function for the output becomes

$$r(\tau) = \frac{c^2 \sigma^2}{2a} e^{-a\tau}.$$

Note correlation function has the same form as the Ornstein-Uhlenbeck process in Example B.7 (with $Q = c^2 \sigma^2$). ∇

As in the case of deterministic linear systems, we can analyze a stochastic linear system either in the state space or the frequency domain. The frequency domain approach provides a very rich set of tools for modeling and analysis of interconnected systems, relying on the frequency response and transfer functions to represent the flow of signals around the system.

Given a random process $X(t)$, we can look at the frequency content of the properties of the response. In particular, if we let $\rho(\tau)$ be the correlation function for a (scalar) random process, then we define the *power spectral density function* as the Fourier transform of ρ :

$$S(\omega) = \int_{-\infty}^{\infty} \rho(\tau) e^{-j\omega\tau} d\tau, \quad \rho(\tau) = \frac{1}{2\pi} \int_{-\infty}^{\infty} S(\omega) e^{j\omega\tau} d\omega.$$

The power spectral density provides an indication of how quickly the values of a random process can change through the frequency content: if there is high frequency content in the power spectral density, the values of the random variable can change quickly in time.

Example 4.9 (First-order Markov process). To illustrate the use of these measures, consider a first-order Markov process as defined in Example B.7. The correlation function is

$$\rho(\tau) = \frac{Q}{2\omega_0} e^{-\omega_0|\tau|}.$$

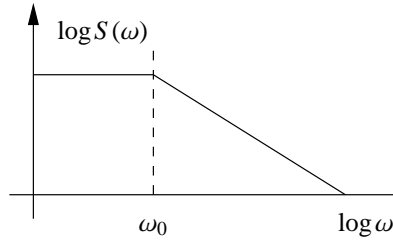


Figure 4.3: Spectral power density for a first-order Markov process.

The power spectral density becomes

$$\begin{aligned} S(\omega) &= \int_{-\infty}^{\infty} \frac{Q}{2\omega_0} e^{-\omega|\tau|} e^{-j\omega\tau} d\tau \\ &= \int_{-\infty}^0 \frac{Q}{2\omega_0} e^{(\omega-j\omega)\tau} d\tau + \int_0^{\infty} \frac{Q}{2\omega_0} e^{(-\omega-j\omega)\tau} d\tau = \frac{Q}{\omega^2 + \omega_0^2}. \end{aligned}$$

We see that the power spectral density is similar to a transfer function and we can plot $S(\omega)$ as a function of ω in a manner similar to a Bode plot, as shown in Figure 4.3. Note that although $S(\omega)$ has a form similar to a transfer function, it is a real-valued function and is not defined for complex s . ∇

Using the power spectral density, we can more formally define “white noise”: a *white noise process* is a zero-mean, random process with power spectral density $S(\omega) = W = \text{constant}$ for all ω . If $X(t) \in \mathbb{R}^n$ (a random vector), then $W \in \mathbb{R}^{n \times n}$. We see that a random process is white if all frequencies are equally represented in its power spectral density; this spectral property is the reason for the terminology “white”. The following proposition verifies that this formal definition agrees with our previous (time domain) definition.

Proposition 4.3. *For a white noise process,*

$$\rho(\tau) = \frac{1}{2\pi} \int_{-\infty}^{\infty} S(\omega) e^{j\omega\tau} d\omega = W\delta(\tau),$$

where $\delta(\tau)$ is the unit impulse function.

Proof. If $\tau \neq 0$ then

$$\rho(\tau) = \frac{1}{2\pi} \int_{-\infty}^{\infty} W(\cos(\omega\tau) + j\sin(\omega\tau)) d\omega = 0$$

If $\tau = 0$ then $\rho(\tau) = \infty$. Can show that

$$\rho(0) = \lim_{\epsilon \rightarrow 0} \int_{-\epsilon}^{\epsilon} \int_{-\infty}^{\infty} (\dots) d\omega d\tau = W\delta(0)$$

□

Given a linear system

$$\dot{X} = AX + FW, \quad Y = CX,$$

with W given by white noise, we can compute the spectral density function corresponding to the output Y . We start by computing the Fourier transform of the steady state correlation function (4.24):

$$\begin{aligned} S_Y(\omega) &= \int_{-\infty}^{\infty} \left[\int_0^{\infty} h(\xi) Q h(\xi + \tau) d\xi \right] e^{-j\omega\tau} d\tau \\ &= \int_0^{\infty} h(\xi) Q \left[\int_{-\infty}^{\infty} h(\xi + \tau) e^{-j\omega\tau} d\tau \right] d\xi \\ &= \int_0^{\infty} h(\xi) Q \left[\int_0^{\infty} h(\lambda) e^{-j\omega(\lambda - \xi)} d\lambda \right] d\xi \\ &= \int_0^{\infty} h(\xi) e^{j\omega\xi} d\xi \cdot QH(j\omega) = H(-j\omega)QH(j\omega) \end{aligned}$$

This is then the (steady state) response of a linear system to white noise.

As with transfer functions, one of the advantages of computations in the frequency domain is that the composition of two linear systems can be represented by multiplication. In the case of the power spectral density, if we pass white noise through a system with transfer function $H_1(s)$ followed by transfer function $H_2(s)$, the resulting power spectral density of the output is given by

$$S_Y(\omega) = H_1(-j\omega)H_2(-j\omega)Q_uH_2(j\omega)H_1(j\omega).$$

As stated earlier, white noise is an idealized signal that is not seen in practice. One of the ways to produce more realistic models of noise and disturbances is to apply a filter to white noise that matches a measured power spectral density function. Thus, we wish to find a covariance W and filter $H(s)$ such that we match the statistics $S(\omega)$ of a measured noise or disturbance signal. In other words, given $S(\omega)$, find $W > 0$ and $H(s)$ such that $S(\omega) = H(-j\omega)WH(j\omega)$. This problem is known as the *spectral factorization problem*.

Figure 4.4 summarizes the relationship between the time and frequency domains.

Exercises

4.1 (BE 150, Winter 2011) For this problem, we return to our standard model of transcription and transcription process with probabilistic creation and degradation of discrete mRNA and protein molecules. The *propensity functions* for each reaction are as follows:

Probability of transcribing 1 mRNA molecule: $0.2dt$

$$\begin{array}{ccc}
 p(v) = \frac{1}{\sqrt{2\pi R_V}} e^{-\frac{v^2}{2R_V}} & V \longrightarrow \boxed{H} \longrightarrow Y & p(y) = \frac{1}{\sqrt{2\pi R_Y}} e^{-\frac{y^2}{2R_Y}} \\
 S_V(\omega) = R_V & & S_Y(\omega) = H(-j\omega)R_V H(j\omega) \\
 \rho_V(\tau) = R_V \delta(\tau) & \begin{array}{l} \dot{X} = AX + FV \\ Y = CX \end{array} & \begin{array}{l} \rho_Y(\tau) = R_Y(\tau) = C P e^{-A|\tau|} C^T \\ AP + PA^T + FR_V F^T = 0 \end{array}
 \end{array}$$

Figure 4.4: Summary of steady state stochastic response.

Probability of degrading 1 mRNA molecule: $0.5dt$ and is proportional to the number of mRNA molecules.

Probability of translating 1 protein: $5dt$ and is proportional to the number of mRNA molecules.

Probability of degrading 1 protein molecule: $0.5dt$ and is proportional to the number of protein molecules.

dt is the time step chosen for your simulation. Here we choose $dt = 0.05$.

(a) Simulate the stochastic system above until time $T = 100$. Plot the resulting number of mRNA and protein over time.

(b) Now assume that the proteins are degraded much more slowly than mRNA and the propensity function of protein degradation is now $0.05dt$. To maintain similar protein levels, the translation probability is now $0.5dt$ (and still proportional to the number of mRNA molecules). Simulate this system as above. What difference do you see in protein level? Comment on the effect of protein degradation rates on noise.

4.2 (BE 150, Winter 2011) Compare a simple model of negative autoregulation with one without autoregulation:

$$\frac{dX}{dt} = \beta_0 - \gamma X$$

and

$$\frac{dX}{dt} = \frac{\beta}{1 + \frac{X}{K}} - \gamma X$$

(a) Assume that the basal transcription rates β and β_0 vary between cells, following a Gaussian distribution with $\frac{\sigma^2}{\langle X \rangle} = 0.1$. Simulate time courses of both models for 100 different "cells" using the following parameters: $\beta = 2, \beta_0 = 1, \gamma = 1, K = 1$. Plot the nonregulated and autoregulated systems in two separate plots. Comment on the variation you see in the time courses.

(b) Calculate the deterministic steady state for both models above. How does variation in the basal transcription rate β or β_0 enter into the steady state and relate it to what you see in part (a).

4.3 Consider gene expression: $\phi \xrightarrow{k} m$, $m \xrightarrow{\beta} m + P$, $m \xrightarrow{\gamma} \phi$, and $P \xrightarrow{\delta} \phi$. Answer the following questions:

(a) Use the stochastic simulation algorithm (SSA) to obtain realizations of the stochastic process of gene expression and numerically compare with the deterministic ODE solution. Explore how the realizations become close to or apart from the ODE solution when the volume is changed. Determine the stationary probability distribution for the protein (you can do this numerically, but note that this process is linear, so you can compute the probability distribution analytically in closed form).

(b) Now consider the additional binding reaction of protein P with downstream DNA binding sites D : $P + D \xrightleftharpoons[k_{off}]{k_{on}} C$. Note that the system no longer linear due to the presence of a bi-molecular reaction. Use the SSA algorithm to obtain sample realizations and numerically compute the probability distribution of the protein and compare it to what you obtained in part (a). Explore how this probability distribution and the one of C change as the rates k_{on} and k_{off} become larger and larger with respect to δ, k, β, γ . Do you think we can use a QSS approximation similar to what we have done for ODE models?

(c) Determine the Langevin equation for the system in part (b) and obtain sample realizations. Explore numerically how good this approximation is when the volume decreases/increases.

4.4 Consider the bi-molecular reaction $A + B \xrightleftharpoons[k_2]{k_1} C$, in which A and B are in total amounts A_T and B_T , respectively. Compare the steady state value of C obtained from the deterministic model to the mean value of C obtained from the stochastic model as the volume is changed in the stochastic model. What do you observe? You can perform this investigation through numerical simulation.

4.5 Consider the simple birth and death process: $Z \xrightleftharpoons[k_1 G]{k_2 G} \emptyset$, in which G is a “gain”. Assume that the reactions are catalyzed by enzymes and that the gain G can be tuned by changing the amounts of these enzymes. A deterministic ODE model for this system incorporating noise and disturbances due to the stochasticity of the cellular environment is given by

$$\dot{Z} = k_1 G - k_2 G Z + d(t),$$

in which $d(t)$ incorporates noise, as seen in the previous homework. Determine the Langevin equation for this birth and death process and compare its form to the deterministic one. Also, determine the frequency response of Z to noise for both the deterministic model and for the Langevin model. Does increasing the gain G has the same effect in both models? Explain.

4.6 Consider a second order system with dynamics

$$\begin{pmatrix} \dot{X}_1 \\ \dot{X}_2 \end{pmatrix} = \begin{pmatrix} -a & 0 \\ 0 & -b \end{pmatrix} \begin{pmatrix} X_1 \\ X_2 \end{pmatrix} + \begin{pmatrix} 1 \\ 1 \end{pmatrix} v, \quad Y = \begin{pmatrix} 1 & 1 \end{pmatrix} \begin{pmatrix} X_1 \\ X_2 \end{pmatrix}$$

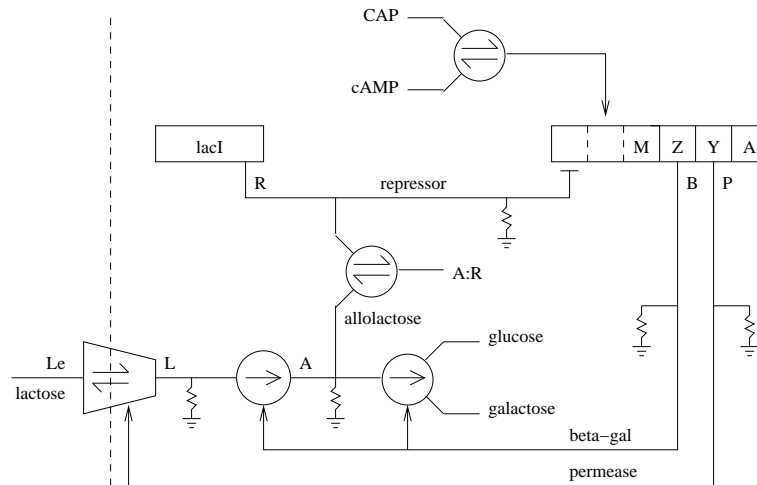
that is forced by Gaussian white noise with zero mean and variance σ^2 . Assume $a, b > 0$.

- (a) Compute the correlation function $\rho(\tau)$ for the output of the system. Your answer should be an explicit formula in terms of a , b and σ .
- (b) Assuming that the input transients have died out, compute the mean and variance of the output.

Chapter 5

Feedback Examples

Pagination in this chapter is broken down by section to facilitate author editing. Review
Some extraneous blank pages may be included due to LaTeX processing.

Figure 5.1: Schematic diagram for the *lac* system.

5.1 The *lac* Operon

Modeling

The *lac* operon is one of the most studied regulatory networks in molecular biology. Its function is to determine when the cell should produce the proteins and enzymes necessary to import and metabolize lactose from its external environment. Since glucose is a more efficient source of carbon, the lactose machinery is not produced unless lactose is present and glucose is not present. The *lac* control system implements this computation.

In constructing a model for the *lac* system, we need to decide what questions we wish to answer. Here we will attempt to develop a model that allows us to understand what levels of lactose are required for the *lac* system to become active in the absence of glucose. We will focus on the so-called “bi-stability” of the *lac* operon: there are two steady operating conditions—at low lactose levels the machinery is off and at high lactose levels the machinery is on. The system has hysteresis, so once the operon is activated, it remains active even if the lactose concentration decreases. We will construct a differential equation model of the system, with various simplifying assumptions along the way.

A schematic diagram of the *lac* control system is shown in Figure 5.1. Starting at the bottom of the figure, lactose permease is an integral membrane protein that helps transport lactose into the cell. Once in the cell, lactose is converted to allolactose, and allolactose is then broken down into glucose and galactose, both with the assistance of the enzyme β -galactosidase (β -gal for short). From here, the glucose is processed using the usual glucose metabolic pathway and the galactose.

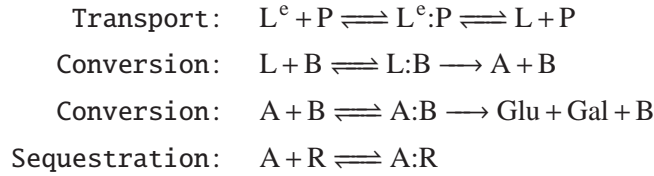
The control circuitry is implemented via the reactions and transcriptional reg-

ulation shown in the top portion of the diagram. The *lac* operon, consisting of the genes *lacZ* (coding for β -gal), *lacY* (coding for lactose permease) and *lacA* (coding for a transacetylase), has a combinatorial promoter. Normally, lac repressor (*lacI*) is present and the operon is off. The activator for the operon is CAP, which has a positive inducer cAMP. The concentration of cAMP is controlled by glucose: when glucose is present, there is very little cAMP available in the cell (and hence CAP is not active).

The bistable switching behavior in the *lac* control system is implemented with a feedback circuit involving the *lac* repressor. Allolactose binds *lac* repressor and so when lactose is being metabolized, then the repressor is sequestered by allolactose and the *lac* operon is no longer repressed.

To model this circuit, we need to write down the dynamics of all of the reactions and protein production for the circuitry shown in Figure 5.1. We will denote the concentration of the β -gal mRNA and protein as m_b and B . We assume that the internal concentration of lactose is given by L , ignoring the dynamics of lactose permease and transport of lactose into the cell. Similarly, we assume that the concentration of repressor protein, denoted R , is constant.

We start by keeping track of the concentration of free allolactose A . The relevant reactions are given by the transport of lactose into the cell, the conversion of lactose into allolactose and then into glucose and lactose and finally the sequestration of repressor R by allolactose:



We see that the dynamics involve a number of enzymatic reactions and hence we can use Michaelis-Menten kinetics to model the response at a slightly reduced level of detail. The differential equation for the internal lactose concentration L becomes

$$\frac{dL}{dt} = \alpha_{LL^e} P \frac{L^e}{K_{L^e} + L^e} - \alpha_{PL} B \frac{L}{K_{PL} + L} - \alpha_{AL} B \frac{L}{K_{AL} + L} - \delta_L L, \quad (5.1)$$

where the first two terms arise from the transport of lactose into and out of the cell, the third term is the conversion of lactose to allolactose and the final term is due to degradation and dilution. Similarly, the dynamics for the allolactose concentration can be modeled as

$$\frac{dA}{dt} = \alpha_{AL} B \frac{L}{K_{AL} + L} - \alpha_{AB} B \frac{A}{K_A + A} + k_{AR}^r [A:R] - k_{AR}^f [A][R] - \delta_A A.$$

The dynamics of the production of β -gal and lactose permease are given by the transcription and translational dynamics of protein production. These genes

are both part of the same operon (along with *lacA*) and hence they use a single mRNA strand for translation. To determine the production rate of mRNA, we need to determine the amount of repression that is present as a function of the amount of repressor, which in turn depends on the amount of allolactose that is present. We make the simplifying assumption that the sequestration reaction is fast, so that it is in equilibrium and hence

$$[A:R] = k_{AR}[A][R], \quad k_{AR} = k_{AR}^f/k_{AR}^r.$$

We also assume that the total repressor concentration is constant (production matches degradation and dilution). Letting $R_{\text{tot}} = [R] + [A:R]$ represent the total repressor concentration, we can write

$$[R] = R_{\text{tot}} - k_{AR}[A][R] \quad \implies \quad [R] = \frac{R_{\text{tot}}}{1 + k_{AR}[A]}. \quad (5.2)$$

The simplification that the sequestration reaction is in equilibrium also simplifies the reaction dynamics for allolactose, which becomes

$$\frac{dA}{dt} = \alpha_{AL}B \frac{L}{K_{AL} + L} - \alpha_A B \frac{A}{K_A + A} - \delta_A A. \quad (5.3)$$

We next need to compute the effect of the repressor on the production of β -gal and lactose permease. It will be useful to express the promoter state in terms of the allolactose concentration A rather than R , using equation (5.2). We model this using a Hill function of the form

$$F_{BA}(A) = \frac{\alpha_R}{K_R + R^n} = \frac{\alpha_R(1 + K_{AR}A)^n}{K_R(1 + K_{AR}A)^n + R_{\text{tot}}}$$

Letting M represent the concentration of the (common) mRNA, the resulting form of the protein production dynamics becomes

$$\begin{aligned} \frac{dM}{dt} &= e^{-\mu\tau_M} F_{BA}(A(t - \tau_m)) - \bar{\gamma}_M M, \\ \frac{dB}{dt} &= \beta_B e^{-\mu\tau_B} M(t - \tau_B) - \bar{\delta}_B B, \\ \frac{dP}{dt} &= \beta_P e^{-\mu(\tau_M + \tau_P)} M(t - \tau_M - \tau_P) - \bar{\delta}_P P. \end{aligned} \quad (5.4)$$

This model includes the degradation and dilution of mRNA ($\bar{\gamma}_M$), the transcriptional delays β -gal mRNA (τ_M), the degradation and dilution of the proteins ($\bar{\delta}_B$, $\bar{\delta}_P$) and the delays in the translation and folding of the final proteins (τ_B , τ_P).

To study the dynamics of the circuit, we consider a slightly simplified situation in which we study the response to the internal lactose concentration L . In this case, we can take $L(t)$ as a constant and ignore the dynamics of the permease P .

Table 5.1: Parameter values for *lac* dynamics (from [?]).

Parameter	Value	Description
$\bar{\mu}$	$3.03 \times 10^{-2} \text{ min}^{-1}$	dilution rate
α_M	997 nMmin^{-1}	production rate of β -gal mRNA
β_B	$1.66 \times 10^{-2} \text{ min}^{-1}$	production rate of β -galactosidase
β_P	$???\text{ min}^{-1}$	production rate of lactose permease
α_A	$1.76 \times 10^4 \text{ min}^{-1}$	production rate of allolactose
$\bar{\gamma}_M$	0.411 min^{-1}	degradation and dilution of β -gal mRNA
$\bar{\delta}_B$	$8.33 \times 10^{-4} \text{ min}^{-1}$	degradation and dilution of β -gal
$\bar{\delta}_P$	$?? \text{ min}^{-1}$	degradation and dilution of lactose permease
$\bar{\delta}_A$	$1.35 \times 10^{-2} \text{ min}^{-1}$	degradation and dilution of allolactose
n	2	Hill coefficient for repressor
K	7200	
k_1	$2.52 \times 10^{-2} (\mu\text{M})^{-2}$	
K_L	$0.97 \mu\text{M}$	
K_A	$1.95 \mu\text{M}$	
β_A	$2.15 \times 10^4 \text{ min}^{-1}$	
τ_M	0.10 min	
τ_B	2.00 min	
τ_P	$???\text{ min}$	

Figure 5.2a shows the time response of the system for an internal lactose concentration of $100 \mu\text{M}$. As a test of the effect of time delays, we consider in Figure 5.2b the case when we set the delays τ_M and τ_B to both be zero. We see that the response has very little difference, consistent with our intuition that the delays are short compared to the dynamics of the underlying processes.

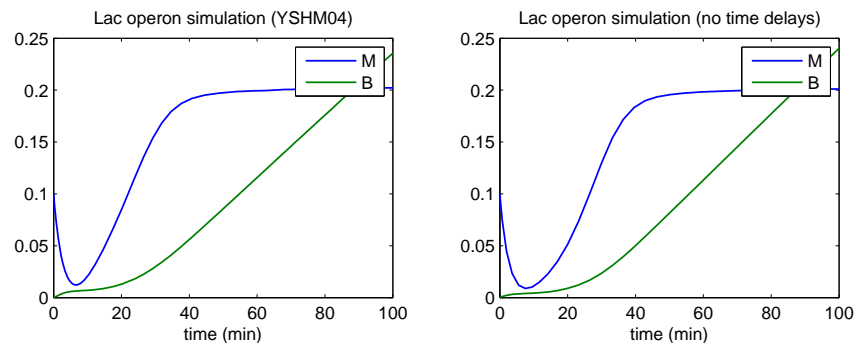


Figure 5.2: Time response of the Lac system.

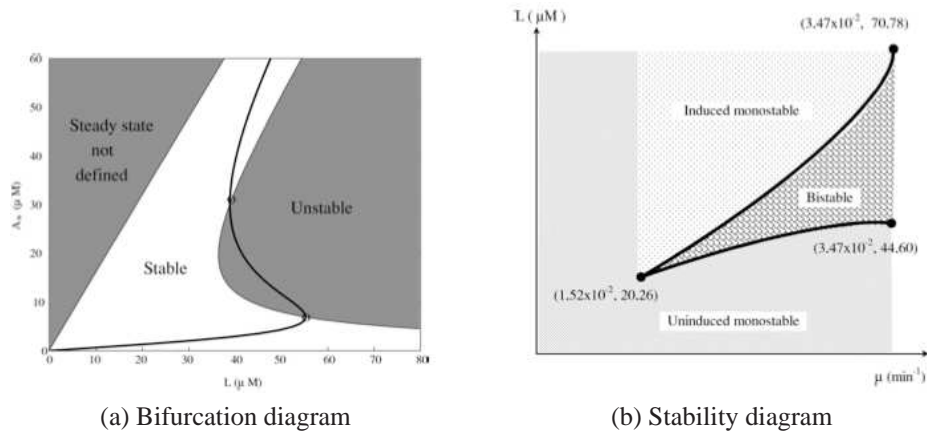


Figure 5.3: Bifurcation and stability diagram for the *lac* system. Figures from [?].

Bifurcation analysis

To further explore the different types of dynamics that can be exhibited by the *Lac* system, we make use of bifurcation analysis. If we vary the amount of lactose present in the environment, we expect that the *lac* circuitry will turn on at some point. Figure 5.3a shows the concentration of allolactose A as a function of the internal lactose concentration L . We see that the behavior of the *lac* system depends on the amount of lactose that is present in the cell. At low concentrations of lactose, the *lac* operon is turned off and the proteins required to metabolize lactose are not expressed. At high concentrations of lactose, the *lac* operon is turned on and the metabolic machinery is activated. In our model, these two operating conditions are measured by the concentration of β -galactosidase B and allolactose A . At intermediate concentrations of lactose, the system has multiple equilibrium points, with two stable equilibrium points corresponding to high and low concentrations of A (and B , as can be verified separately).

The parametric stability plot in Figure 5.3b shows the different types of behavior that can result based on the dilution rate μ and the lactose concentration L . We see that we get bistability only in a certain range of these parameters. Otherwise, we get that the circuitry is either uninduced or induced.

Sensitivity analysis

We now explore how the equilibrium conditions vary if the parameters in our model are changed.

For the gene *lacZ* (which encodes the protein β -galactosidase), we let B represent the protein concentration and M represent the mRNA concentration. We also consider the concentration of the lactose L inside the cell, which we will treat as an external input, and the concentration of allolactose, A . Assuming that the time de-

lays considered previously can be ignored, the dynamics in terms of these variables are

$$\begin{aligned} \frac{dM}{dt} &= F_{BA}(A, \theta) - \gamma_b M, & F_{BA}(A, \theta) &= \alpha_{AB} \frac{1 + k_1 A^n}{K + k_1 A^n}, \\ \frac{dB}{dt} &= \beta_B M - \delta_B B, & F_{AL}(L, \theta) &= \alpha_A \frac{L}{k_L + L}, \\ \frac{dA}{dt} &= BF_{AL}(L, \theta) - BF_{AA}(A, \theta) - \gamma_A A, & F_{AA}(A, \theta) &= \beta_A \frac{A}{k_A + A}. \end{aligned} \quad (5.5)$$

Here the state is $x = (M, B, A) \in \mathbb{R}^3$, the input is $w = L \in \mathbb{R}$ and the parameters are $\theta = (\alpha_B, \beta_B, \alpha_A, \gamma_B, \delta_B, \gamma_A, n, k, k_1, k_L, k_A, \beta_A) \in \mathbb{R}^{12}$. The values for the parameters are listed in Table 5.1.

We investigate the dynamics around one of the equilibrium points, corresponding to an intermediate input of $L = 40 \mu\text{M}$. There are three equilibrium points at this value of the input:

$$x_{1,e} = (0.000393, 0.000210, 3.17), \quad x_{2,e} = (0.00328, 0.00174, 19.4), \quad x_{3,e} = (0.0142, 0.00758, 42.1).$$

We choose the third equilibrium point, corresponding to the lactose metabolic machinery being activated and study the sensitivity of the steady state concentrations of allolactose (A) and β -galactosidase (B) to changes in the parameter values.

The dynamics of the system can be represented in the form $\dot{x} = f(x, \theta, L)$ with

$$f(x, \theta, L) = \begin{pmatrix} F_{BA}(A) - \gamma_B M - \mu M \\ \beta_B M - \delta_B B - \mu B \\ F_{AL}(L)B - F_{AA}(A)B - \delta_A A - \mu A \end{pmatrix}.$$

To compute the sensitivity with respect to the parameters, we compute the derivatives of f with respect to the state x ,

$$\frac{\partial f}{\partial x} = \begin{pmatrix} -\gamma_B - \mu & 0 & \frac{\partial F_{BA}}{\partial A} \\ \beta_B & -\delta_B - \mu & 0 \\ 0 & F_{AL} - F_{AA} & -B \frac{\partial F_{AA}}{\partial A} \end{pmatrix}$$

and the parameters θ ,

$$\frac{\partial f}{\partial \theta} = \begin{pmatrix} F_{BA} & 0 & 0 & -M & 0 & 0 & \frac{\partial F_{BA}}{\partial n} & \frac{\partial F_{BA}}{\partial k} & \frac{\partial F_{BA}}{\partial k_1} & 0 & 0 & 0 \end{pmatrix}.$$

Carrying out the relevant computations and evaluating the resulting expression numerically, we obtain

$$\frac{\partial}{\partial \theta} \begin{pmatrix} B_e \\ A_e \end{pmatrix} = \begin{pmatrix} -1.21 & 0.0243 & -3.35 \times 10^{-6} & 0.935 & 1.46 & \dots & 0.00115 \\ -2720. & 47.7 & -0.00656 & 1830. & 2860. & \dots & 3.27 \end{pmatrix}.$$

We can also normalize the sensitivity computation

$$\bar{S}_{x_e\theta} = \frac{\partial x_e/x_e}{\partial \theta/\theta_0} = (D^x)^{-1} S_{x_e\theta} D^\theta,$$

where $D^x = \text{diag}\{x_e\}$ and $D^\theta = \text{diag}\{\theta_0\}$, which yields

$$\bar{S}_{y_e\theta} = \begin{pmatrix} -4.85 & 3.2 & -3.18 & 3.11 & 3.2 & 6.3 & -6.05 & -4.1 & 4.02 & 6.05 \\ -1.96 & 1.13 & -1.12 & 1.1 & 1.13 & 3.24 & -3.11 & -2.11 & 2.07 & 3.11 \end{pmatrix}$$

where

$$\theta = (\mu \quad \alpha_M \quad K \quad K_1 \quad \beta_B \quad \alpha_A \quad K_L \quad \beta_A \quad K_A \quad L).$$

We see from this computation that increasing the growth rate decreases the equilibrium concentration of *B* and *A*, while increasing the lactose concentration by 2-fold increases the equilibrium β -gal concentration 12-fold (6X) and the allolactose concentration by 6-fold (3X).

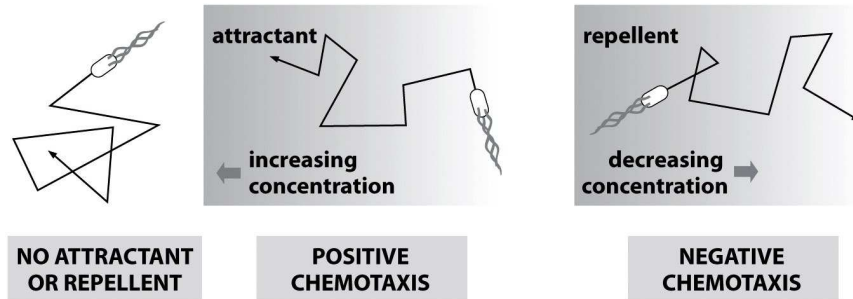


Figure 4.16d Physical Biology of the Cell (© Garland Science 2009)

Figure 5.4: Examples of chemotaxis. Figure from Phillips, Kondev and Theriot [68]; used with permission of Garland Science.

5.2 Bacterial Chemotaxis

Chemotaxis refers to the process by which micro-organisms move in response to chemical stimuli. Examples of chemotaxis include the ability of organisms to move in the direction of nutrients or move away from toxins in the environment. Chemotaxis is called *positive chemotaxis* if the motion is in the direction of the stimulus and *negative chemotaxis* if the motion is away from the stimulant, as shown in Figure 5.4. Many chemotaxis mechanisms are stochastic in nature, with biased random motions causing the average behavior to be either positive, negative or neutral (in the absence of stimuli).

In this section we look in some detail at bacterial chemotaxis, which *E. coli* use to move in the direction of increasing nutrients. The material in this section is based primarily on the work of Barkai and Leibler [9] and Rao, Kirby and Arkin [73].

Control system overview

The chemotaxis system in *E. coli* consists of a sensing system that detects the presence of nutrients, and actuation system that propels the organism in its environment, and control circuitry that determines how the cell should move in the presence of chemicals that stimulate the sensing system.

The actuation system in the *E. coli* consists of a set of flagella that can be spun using a flagellar motor embedded in the outer membrane of the cell, as shown in Figure 5.5a. When the flagella all spin in the counter clockwise direction, the individual flagella form a bundle and cause the organism to move roughly in a straight line. This behavior is called a “run” motion. Alternatively, if the flagella spin in the clockwise direction, the individual flagella do not form a bundle and the organism “tumbles”, causing it to rotate (Figure 5.5b). The selection of the motor direction is controlled by the protein CheY: if phosphorylated CheY binds to the motor complex, the motor spins clockwise (tumble), otherwise it spins counter-

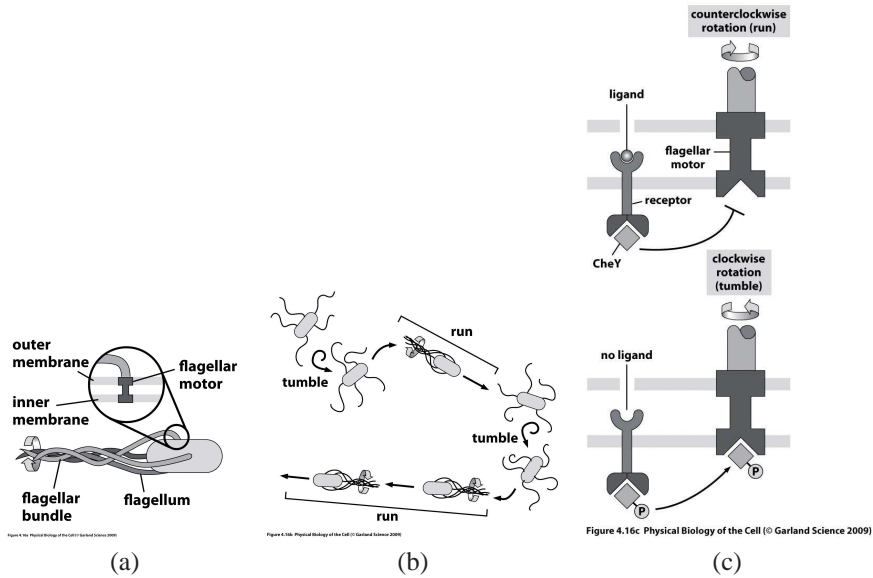


Figure 5.5: Bacterial chemotaxis. Figures from Phillips, Kondev and Theriot [68]; used with permission of Garland Science.

clockwise (run).

Because of the size of the organism, it is not possible for a bacterium to sense gradients across its length. Hence, a more sophisticated strategy is used, in which the organism undergoes a combination of run and tumble motions. The basic idea is illustrated in Figure 5.5c: when high concentration of ligand (nutrient) is present, the CheY protein is left unphosphorylated and does not bind to the actuation complex, resulting in a counter-clockwise rotation of the flagellar motor (run). Conversely, if the ligand is not present then the molecular machinery of the cell causes CheY to be phosphorylated and this modifies the flagellar motor dynamics so that a clockwise rotation occurs (tumble). The net effect of this combination of behaviors is that when the organism is traveling through regions of higher nutrient concentration, it continues to move in a straight line for a longer period before tumbling, causing it to move in directions of increasing nutrient concentration.

A simple model for the molecular control system that regulates chemotaxis is shown in Figure 5.6. We start with the basic sensing and actuation mechanisms. A membrane bound protein MCP (methyl-accepting chemotaxis protein) that is capable of binding to the external ligand serves as a signal transducing element from the cell exterior to the cytoplasm. Two other proteins, CheW and CheA, form a complex with MCP. This complex can either be in an active or inactive state. In the active state, CheA is autophosphorylated and serves as a phosphotransferase for two additional proteins, CheB and CheY. The phosphorylated form of CheY then binds to the motor complex, causing clockwise rotation of the motor.

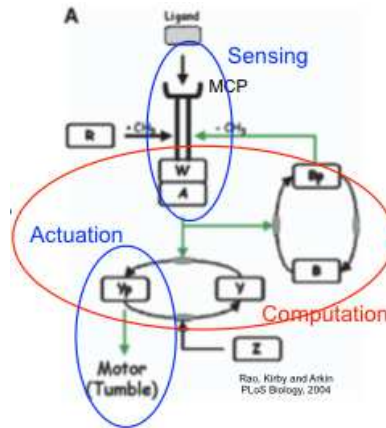


Figure 5.6: Control system for chemotaxis. Figure from Rao *et al.* [73] (Figure 1A).

The activity of the receptor complex is governed by two primary factors: the binding of a ligand molecule to the MCP protein and the presence or absence of up to 4 methyl groups on the MCP protein. The specific dependence on each of these factors is somewhat complicated. Roughly speaking, when the ligand L is bound to the receptor then the complex is less likely to be active. Furthermore, as more methyl groups are present, the ligand binding probability increases, allowing the gain of the sensor to be adjusted through methylation. Finally, even in the absence of ligand the receptor complex can be active, with the probability of it being active increasing with increased methylation. Figure 5.7 summarizes the possible states, their free energies and the probability of activity.

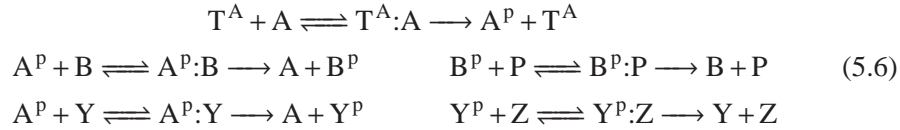
Several other elements are contained in the chemotaxis control circuit. The most important of these are implemented by the proteins CheR and CheB, both of which affect the receptor complex. CheR, which is constitutively produced in the cell, methylates the receptor complex at one of the four different methylation sites. Conversely, the phosphorylated form of CheB demethylates the receptor complex. As described above, the methylation patterns of the receptor complex affect its activity, which affects the phosphorylation of CheA and, in turn, phosphorylation of CheY and CheB. The combination of CheA, CheB and the methylation of the receptor complex forms a negative feedback loop: if the receptor is active, then CheA phosphorylates CheB, which in turn demethylates the receptor complex, making it less active. As we shall see when we investigate the detailed dynamics below, this feedback loop corresponds to a type of integral feedback law. This integral action allows the cell to adjust to different levels of ligand concentration, so that the behavior of the system is invariant to the absolute nutrient levels.

Non-ligand bound			Ligand bound		
Species	p	ΔG (kcal/mol)	Species	p	ΔG (kcal/mol)
	0.017	2.37		0.003	3.55
	0.125	1.18		0.017	2.37
	0.500	0.00		0.125	1.18
	0.874	-1.18		0.500	0.00
	0.997	-3.55		0.980	-2.37

Figure 5.7: Receptor complex states. The probability of a given state being in an active configuration is given by p . Figure obtained from [60].

Modeling

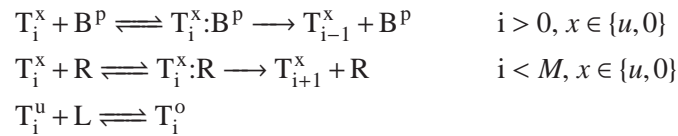
The detailed reactions that implement chemotaxis are illustrated in Figure 5.8. Letting T represent the receptor complex and T^A represent an active form, the basic reactions can be written as



where CheA, CheB, CheY and CheZ are written simply as A , B , Y and Z for simplicity and P is a non-specific phosphatase. We see that these are basically three linked sets of phosphorylation and dephosphorylation reactions, with CheA serving as a phosphotransferase and P and CheZ serving as phosphatases.

The description of the methylation of the receptor complex is a bit more complicated. Each receptor complex can have multiple methyl groups attached and the activity of the receptor complex depends on both the amount of methylation and whether a ligand is attached to the receptor site. Furthermore, the binding probabilities for the receptor also depend on the methylation pattern. To capture this, we use the set of reactions that are illustrated in Figures 5.6 and 5.8. In this diagram, T_i^s represents a receptor that has i methylation sites filled and ligand state s (which can be either u if unoccupied or o if occupied). We let M represent the maximum number of methylation sites ($M = 4$ for *E. coli*).

Using this notation, the transitions between the states correspond to the reactions shown in Figure 5.9:



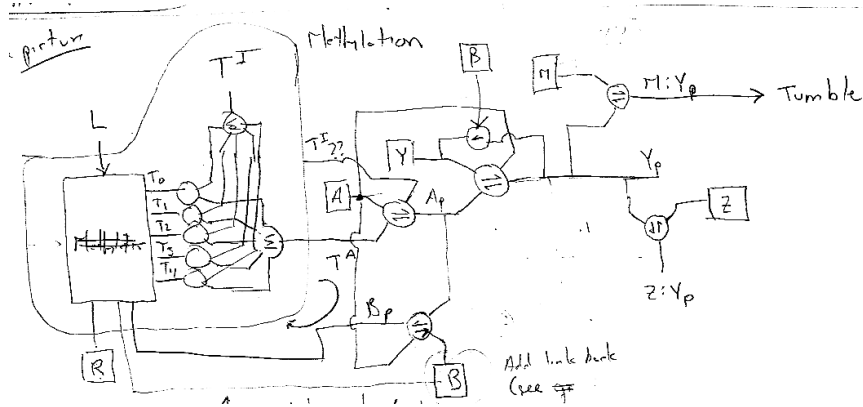
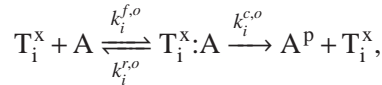


Figure 5.8: Circuit diagram for chemotaxis.

We now must write reactions for each of the receptor complexes with CheA. Each form of the receptor complex has a different activity level and so the most complete description is to write a separate reaction for each T_i^o and T_i^u species:



where $x \in \{o, u\}$ and $i = 0, \dots, M$. This set of reactions replaces the placeholder reaction $T^A + A \rightleftharpoons T^A:A \rightarrow A^p + T^A$ used earlier.

Approximate model

The detailed model described above is sufficiently complicated that it can be difficult to analyze. In this section we develop a slightly simpler model that can be used to explore the adaptation properties of the circuit, which happen on a slower time-scale.

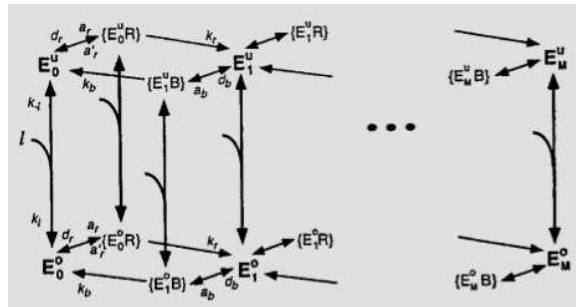


Figure 5.9: Methylation model for chemotaxis. Figure from Barkai and Leibler [9] (Box 1). Note: the figure uses the notation E_i^s for the receptor complex instead of T_i^s .

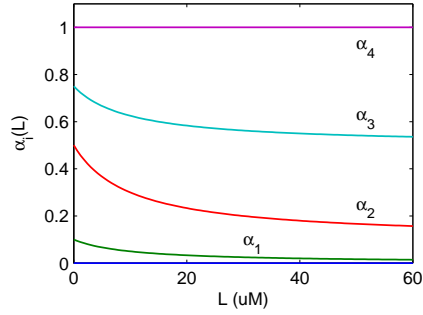


Figure 5.10: Probability of activity.

We begin by simplifying the representation of the receptor complex and its methylation pattern. Let $L(t)$ represent the ligand concentration and T_i represent the concentration of the receptor complex with i sides methylated. If we assume that the binding reaction of the ligand L to the complex is fast, we can write the probability that a receptor complex with i sites methylated is in its active state as a static function $\alpha_i(L)$, which we take to be of the form

$$\alpha_i(L) = \frac{\alpha_i^o L}{K_L + L} + \frac{\alpha_i K_L}{K_L + L}.$$

The coefficients α_i^o and α_i capture the effect of presence or absence of the ligand on the activity level of the complex. Note that α_i has the form of a Michaelis-Menten function, reflecting our assumption that ligand binding is fast compared to the rest of the dynamics in the model. Following [73], we take the coefficients to be

$$\begin{aligned} a_0 = 0, & \quad a_1 = 0.1, & \quad a_2 = 0.5, & \quad a_3 = 0.75, & \quad a_4 = 1, \\ a_0^o = 0, & \quad a_1^o = 0, & \quad a_2^o = 0.1, & \quad a_3^o = 0.5, & \quad a_4^o = 1. \end{aligned}$$

and choose $K_L = 10 \mu\text{M}$. Figure 5.10 shows how each α_i varies with L .

The total concentration of active receptors can now be written in terms of the receptor complex concentrations T_i and the activity probabilities $\alpha_i(L)$. We write the concentration of activated complex T^A and inactivated complex T^I as

$$T^A = \sum_{i=0}^4 \alpha_i(L) T_i, \quad T^I = \sum_{i=0}^4 (1 - \alpha_i(L)) T_i.$$

These formulas can now be used in our dynamics as an effective concentration of active or inactive receptors, justifying the notation that we used in equation (5.6).

We next model the transition between the methylation patterns on the receptor. We assume that the rate of methylation depends on the activity of the receptor complex, with active receptors less likely to be demethylated and inactive receptors

less likely to be methylated [73, 60]. Let

$$r_B = k_B \frac{B^p}{K_B + T^A}, \quad r_R = k_R \frac{R}{K_R + T^I},$$

represent rates of the methylation and demethylation reactions. We choose the coefficients as

$$k_B = 0.5, \quad K_B = 5.5, \quad k_R = 0.255, \quad K_R = 0.251,$$

We can now write the methylation dynamics as

$$\frac{d}{dt}T_i = r_R(1 - \alpha_{i+1}(L))T_{i-1} + r_B\alpha_{i+1}(L)T_{i+1} - r_R(1 - \alpha_i(L))T_i - r_B\alpha_i(L)T_i,$$

where the first and second terms represent transitions into this state via methylation or demethylation of neighboring states (see Figure 5.9) and the last two terms represent transitions out of the current state by methylation and demethylation, respectively. Note that the equations for T_0 and T_4 are slightly different since the demethylation and methylation reactions are not present, respectively.

Finally, we write the dynamics of the phosphorylation and dephosphorylation reactions, and the binding of CheY^P to the motor complex. Under the assumption that the concentrations of the phosphorylated proteins are small relative to the total protein concentrations, we can approximate the reaction dynamics as

$$\begin{aligned} \frac{d}{dt}A^p &= 50T^A A - 100A^p Y - 30A^p B, \\ \frac{d}{dt}Y^p &= 100A^p Y - 0.1Y^p - 5[M]Y^p + 19[M:Y^p] - 30Y^p, \\ \frac{d}{dt}B^p &= 30A^p B - B^p, \\ \frac{d}{dt}[M:Y^p] &= 5[M]Y^p - 19[M:Y^p]. \end{aligned}$$

The total concentrations of the species are given by

$$\begin{aligned} A + A^p &= 5 \text{ nM}, & B + B^p &= 2 \text{ nM}, & Y + Y^p + [M:Y^p] &= 17.9 \text{ nM}, \\ [M] + [M:Y^p] &= 5.8 \text{ nM}, & R &= 0.2 \text{ nM}, & \sum_{i=0}^4 T_i &= 5 \text{ nM}. \end{aligned}$$

The reaction coefficients and concentrations are taken from Rao *et al.* [73].

Figure 5.11a shows a the concentration of the phosphorylated proteins based on a simulation of the model. Initially, all species are started in their unphosphorylated and demethylated states. At time $T = 500$ s the ligand concentration is increased to $L = 10 \mu\text{M}$ and at time $T = 1000$ it is returned to zero. We see that immediately after the ligand is added, the CheY^P concentration drops, allowing longer runs between tumble motions. After a short period, however, the CheY^P concentration adapts to

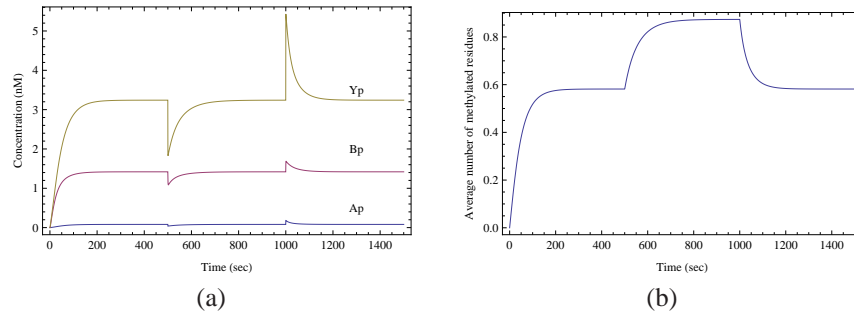


Figure 5.11: Simulation and analysis of reduced-order chemotaxis model.

the higher concentration and the nominal run versus tumble behavior is restored. Similarly, after the ligand concentration is decreased the concentration of CheY^P increases, causing a larger fraction of tumbles (and subsequent changes in direction). Again, adaptation over a longer time scale returns that CheY concentration to its nominal value.

Figure 5.11b helps explain the adaptation response. We see that the average amount of methylation of the receptor proteins increases when the ligand concentration is high, which decreases the activity of CheA (and hence decreases the phosphorylation of CheY).

Integral action

The perfect adaptation mechanism in the chemotaxis control circuitry has the same function as the use of integral action in control system design: by including a feedback on the integral of the error, it is possible to provide exact cancellation to constant disturbances. In this section we demonstrate that a simplified version of the dynamics can indeed be regarded as integral action of an appropriate signal. This interpretation was first pointed out by Yi *et al* [91].

We begin by formulating an even simpler model for the system dynamics that captures the basic features required to understand the integral action. Let X represent the receptor complex and assume that it is either methylated or not. We let X_m represent the methylated state and we further assume that this methylated state can be activated, which we write as X_m^* . This simplified description replaces the multiple states T_i and probabilities $\alpha_i(L)$. We also ignore the additional phosphorylation dynamics of CheY and simply take the activated receptor concentration X_m^* as our measure of overall activity.

Figure 5.12 shows the transitions between the various forms X . As before, CheR methylates the receptor and CheB^P demethylates it. We simplify the picture by only allowing CheB^P to act on the active state X_m^* and CheR to act on the inactive state. We take the ligand into account by assuming that the transition between the active form X_m^* and the inactive form X_m depends on the ligand concentration: higher

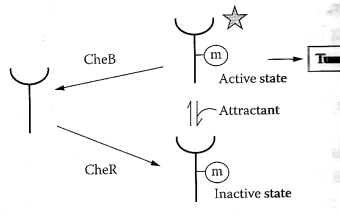
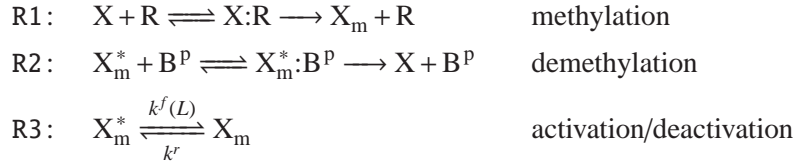


Figure 5.12: Reduced order model of receptor activity. Obtained from [4], Figure 7.9.

ligand concentration will increase the rate of transition to the inactive state.

This model is a considerable simplification from the ligand binding model that is illustrated in Figures 5.7 and 5.9. In the previous models, there is some probability of activity with or without methylation and with or without ligand. In this simplified model, we assume that only three states are of interest: demethylated, methylated/inactive and methylated/active. We also modify the way that ligand binding is captured and instead of keeping track of all of the possibilities in Figure 5.7, we assume that the ligand transitions us from an active state X_m^* to an inactive X_m . These states and transitions are roughly consistent with the different energy levels and probabilities in Figure 5.7, but it is clearly a much coarser model.

Accepting these approximations, the model illustrated in Figure 5.12 results in a set of chemical reactions of the form



For simplicity we take both R and B^P to have constant concentration.

We can approximate the first and second reactions by their Michaelis-Menten forms, which yield net methylation and demethylation rates (for those reactions)

$$v_+ = k_R R \frac{X}{K_X + X}, \quad v_- = k_B B^P \frac{X_m^*}{K_{X_m^*} + X_m^*}.$$

If we further assume that $X \gg K_X > 1$, then the methylation rate can be further simplified:

$$v_+ = k_R R \frac{X}{K_X + X} \approx K_R R.$$

Using these approximations, we can write the resulting dynamics for the overall system as

$$\begin{aligned}
 \frac{d}{dt} X_m &= k_R R + k^f(L) X_m^* - k^r X_m \\
 \frac{d}{dt} X_m^* &= -k_B B^P \frac{X_m^*}{K_{X_m^*} + X_m^*} - k^f(L) X_m^* + k^r X_m.
 \end{aligned}$$

We wish to use this model to understand how the steady state activity level X_m^* depends on the ligand concentration L (which enters through the deactivation rate $k^f(L)$).

It will be useful to rewrite the dynamics in terms of the activated complex concentration X_m^* and the *total* methylated complex concentration $X_m^t = X_m + X_m^*$. A simple set of algebraic manipulations yields

$$\begin{aligned}\frac{dX_m^*}{dt} &= k^r(X_m^t - X_m^*) - k_B B^p \frac{X_m^*}{K_{X_m^*} + X_m^*} - k^f(L)X_m^*, \\ \frac{dX_m^t}{dt} &= k_R R - k_B B^p \frac{X_m^*}{K_{X_m^*} + X_m^*}.\end{aligned}$$

From the second equation, we see that the the concentration of methylated complex X_m^t is a balance between the action of the methylation reaction (R1, characterized by v_+) and the demethylation reaction (R2, at rate v_-). Since the action of a ligand binding to the receptor complex increases the rate of deactivation of the complex (R3), in the presence of a ligand we will increase the amount of methylated complex (and, via reaction R1) eventually restore the amount of the activated complex. This represents the adaptation mechanism in this simplified model.

To further explore the effect of adaptation, we compute the equilibrium points for the system. Setting the time derivatives to zero, we obtain

$$\begin{aligned}X_{m,e}^* &= \frac{K_{X_m^*} k_R R}{k_B B^p - k_R R} \\ X_{m,e}^t &= \frac{1}{k^r} \left(k^r X_m^* + k_B B^p \frac{X_m^*}{K_{X_m^*} + X_m^*} + k^f(L)X_m^* \right).\end{aligned}$$

Note that the solution for the active complex $X_{m,e}^*$ in the first equation does not depend on $k^f(L)$ (or k^r) and hence the steady state solution is independent of the ligand concentration. Thus, in steady state, the concentration of activated complex adapts to the steady state value of the ligand that is present, making it insensitive to the steady state value of this input.

The dynamics for X_m^t can be viewed as an integral action: when the concentration of X_m^* matches its reference value (with no ligand present), the quantity of methylated complex X_m^t remains constant. But if X_m^t does not match this reference value, then X_m^t increases at a rate proportional to the methylation “error” (measured here by difference in the nominal reaction rates v_+ and v_-). It can be shown that this type of integral action is necessary to achieve perfect adaptation in a robust manner [91].

Chapter 6

Biological Circuit Components

In this chapter, we describe some simple circuits components that have been constructed in *E. coli* cells using the technology of synthetic biology. We will analyze their behavior employing mainly the tools from Chapter 3 and some of the tools from Chapter 4. The basic knowledge of Chapter 2 will be assumed.

6.1 Introduction to Biological Circuit Design

In Chapter 2 we have introduced a number of core processes and their modeling. These include gene expression, transcriptional regulation, post-translational regulation such as covalent modification of proteins, allosteric regulation of enzymes, activity regulation of transcription factors through inducers, etc. These core processes provide a rich set of functional building blocks, which can be combined together to create circuits with prescribed functionalities.

For example, if we want to create an inverter, a device that returns high output when the input is low and vice versa, we can use a gene regulated by a transcription repressor. If we want to create a signal amplifier, we can employ a cascade of covalent modification cycles. Specifically, if we want the amplifier to be linear, we should tune the Michaelis-Menten constants to be small enough compared to the amounts of protein substrates. If instead we are looking for an almost digital response, we could employ a covalent modification cycle with high amounts of substrates compared to the Michaelis-Menten constants. Furthermore, if we are looking for a fast input/output response, phosphorylation cycles are better candidates than transcriptional systems.

In this chapter and in the next one, we illustrate how one can build circuits with prescribed functionality using some of the building blocks of Chapter 2 and the design techniques illustrated in Chapter 3. We will focus on two types of circuits: gene circuits and signal transduction circuits. In some cases, we will illustrate designs that incorporate both.

A gene circuit is usually depicted by a set of nodes, each representing a gene, connected by unidirectional edges, representing a transcriptional activation or a repression. Inducers will often appear as additional nodes, which activate or inhibit a specific edge. Early examples of such circuits include an activator-repressor system that can display toggle switch or clock behavior [6], a loop oscillator called the repressilator obtained by connecting three inverters in a ring topology [26], a

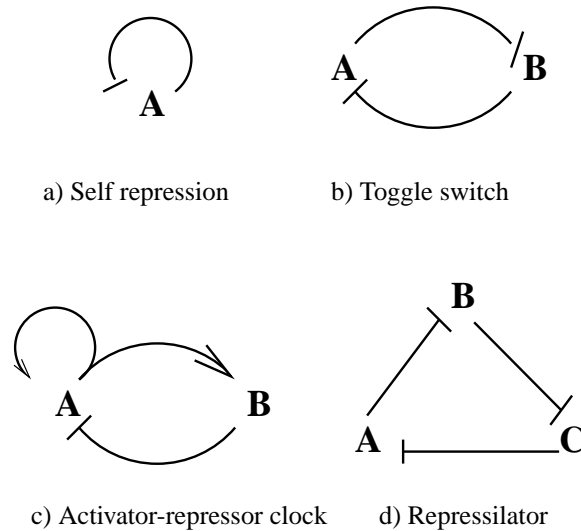


Figure 6.1: Early transcriptional circuits that have been fabricated in bacteria *E. coli*: the negatively autoregulated gene [11], the toggle switch [29], the activator-repressor clock [6], and the repressilator [26].

toggle switch obtained connecting two inverters in a ring fashion [29], and an autorepressed circuit [11] (Figure 6.1). Each node represents a gene and each arrow from node Z to node X indicates that the transcription factor encoded in gene z , denoted Z , regulates gene x [4]. If z represses the expression of x , the interaction is represented by $Z \dashv X$. If z activates the expression of x , the interaction is represented by $Z \rightarrow X$ [4].

Basic synthetic biology technology

Simple synthetic gene circuits can be constituted by a set of (connected) transcriptional components, which are made up by the DNA base-pair sequences that compose the desired promoters, ribosome binding sites, gene coding region, and terminators. We can choose these components from a library of basic interchangeable parts, which are classified based on biochemical properties such as affinity (of promoter, operator, or ribosome binding sites), strength (of a promoter), and efficiency (of a terminator). The desired sequence of parts is usually assembled on plasmids, which are circular pieces of DNA, separate from the host cell chromosome, with their own origin of replication. These plasmids are then inserted, through a process called transformation in bacteria and transfection in yeast, in the host cell. Once in the host cell, they express the proteins they code for by using the transcription and translation machinery of the cell. There are three main types of plasmids: low copy number (5-10 copies), medium copy number (15-20 copies), and high copy number (up to hundreds). The copy number reflects the average number of copies of

the plasmid inside the host cell. The higher the copy number, the more efficient the plasmid is at replicating itself. The exact number of plasmids in each cell fluctuates stochastically and cannot be exactly controlled.

In order to measure the amounts of proteins of interest, we make use of *reporter genes*. A reporter gene codes for a protein that fluoresces in a specific color (red, blue, green, yellow, etc.) when it is exposed to light of the correct wave-length. For instance, green fluorescent protein (GFP) is a protein with the property that it fluoresces in green when exposed to UV light. It is produced by the jellyfish *Aequoria victoria*, and its gene has been isolated so that it can be used as a reporter. Other fluorescent proteins, such as yellow fluorescent protein (YFP) and red fluorescent protein (RFP) are genetic variations of GFP.

A reporter gene is usually inserted downstream of the gene expressing the protein whose concentration we want to measure. In this case, both genes are under the control of the same promoter and are transcribed into a single mRNA molecule. The mRNA is then translated to protein and the two proteins will be fused together. This technique sometimes affects the functionality of the protein of interest because some of the regulatory sites may be occluded by the fluorescent protein. To prevent this, another viable technique is to clone after the protein of interest the reporter gene under the control of a copy of the same promoter that also controls the expression of the protein. This way the protein is not fused to the reporter protein, which guarantees that the protein function is not affected. Also, the expression levels of both proteins should be close to each other since they are controlled by (different copies of) the same promoter.

Just as fluorescent proteins can be used as a read out of a circuit, inducers function as external inputs that can be used to probe the system. Inducers function by either disabling repressor proteins (negative inducers) or by enabling activator proteins (positive inducers). Two commonly used negative inducers are IPTG and aTc. Isopropyl- β -D-1-thiogalactopyranoside (IPTG) induces activity of beta-galactosidase, which is an enzyme that promotes lactose utilization, through binding and inhibiting the *lac* repressor LacI. The anhydrotetracycline (aTc) binds the wild-type repressor (TetR) and prevents it from binding the Tet operator. Two common positive inducers are arabinose and AHL. Arabinose activates the transcriptional activator AraC, which activates the pBAD promoter. Similarly, AHL is a signaling molecule that activates the LuxR transcription factor, which activates the pLux promoter.

Protein dynamics can be usually altered by the addition of a degradation tag at the end of the coding region. A degradation tag is a sequence of base pairs that adds an amino acid sequence to the functional protein that is recognized by proteases. Proteases then bind to the protein, degrading it into a non-functional molecule. As a consequence, the half life of the protein decreases, resulting into an increased decay rate. Degradation tags are often employed to obtain a faster response of the protein concentration to input stimulation and to prevent protein accumulation.

6.2 Negative Autoregulation

In this section, we analyze the negatively autoregulated gene of Figure 6.1 and focus on analyzing how the presence of the negative feedback affects the dynamics of the system [75] and how the negative feedback affects the noise properties of the system [11, 7]. This system was introduced in Example 3.6.

Let X denote the concentration of protein X and let X be a transcriptional repressor for its own production. Assuming that the mRNA dynamics are at the quasi-steady state, the ODE model describing the self repressed system is given by

$$\frac{dX}{dt} = \frac{\beta}{1 + (X/K)^n} - \delta X.$$

We seek to compare the behavior of this autoregulated system to the behavior of the unregulated one:

$$\frac{dX}{dt} = \beta_0 - \delta X,$$

in which β_0 is the unrepressed production rate.

Dynamic effects of negative autoregulation

As we showed via simulation in Example 2.3, negative autoregulation speeds up the response to perturbations. Hence, the time the system takes to reach its steady state decreases with negative feedback. In this section, we show this result analytically by employing linearization about the steady state and by explicitly calculating the time the system takes to reach it.

Let $X_e = \beta_0/\delta$ be the steady state of the unregulated system and denote $z = X - X_e$ the perturbation with respect to such a steady state. The dynamics of z are given by

$$\frac{dz}{dt} = -\delta z.$$

Given a small initial perturbation z_0 , the time response of z is given by the exponential

$$z(t) = z_0 e^{-\delta t}.$$

The “half-life” of the signal $z(t)$ is the time it takes to reach half of z_0 . This is a common measure for the speed of response of a system to an initial perturbation. Simple mathematical calculation shows that $t_{\text{half}} = \ln(2)/\delta$.

Let now X_e be the steady state of the autoregulated system. Assuming that the perturbation z with respect to such a steady state is small enough, we can employ linearization to describe the dynamics of z . These dynamics are given by

$$\frac{dz}{dt} = -\bar{\delta} z,$$

in which

$$\bar{\delta} = \delta + \frac{nX_e^{n-1}/K^n}{(1 + (X_e/K)^n)^2}.$$

In this case, we have that $t_{\text{half}} = \ln(2)/\bar{\delta}$.

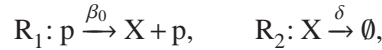
Since $\bar{\delta} > \delta$ (independently of the steady state X_e), we have that the dynamic response to a perturbation is faster in the system with negative autoregulation. This confirms the simulation findings of Example 2.3.

Noise filtering

In this section, we investigate the effect of the negative feedback on the noise spectrum of the system. In order to do this, we employ the Langevin modeling framework and determine the frequency response to the noise on the various reaction channels. We perform two different studies. In the first one, we assume that the decay rate of the protein is much smaller than that of the mRNA. As a consequence, the mRNA is at its quasi-steady state and we focus on the dynamics of the protein only. In the second study, we investigate the consequence of having the mRNA and protein decay rates in the same range so that the quasi-steady state assumption cannot be made. In either case, we study both the open loop system and the closed loop system (the system with negative autoregulation) and compare the corresponding frequency responses.

Assuming mRNA at the quasi-steady state

In this case, the reactions for the open loop system are given by



in which β_0 is the constitutive production rate, p is the DNA promoter, and δ is the decay rate of the protein. Since the concentration of DNA promoter p is not changed by these reactions, it is a constant, which we call p_{tot} .

Employing the Langevin equation (4.13) of Section 4.1 and denoting by n_X the real-valued number of molecules of X and by n_p the real-valued number of molecules of p , we obtain

$$\frac{dn_X}{dt} = \beta_0 n_p - \delta n_X + \sqrt{\beta_0 n_p} N_1 - \sqrt{\delta n_X} N_2.$$

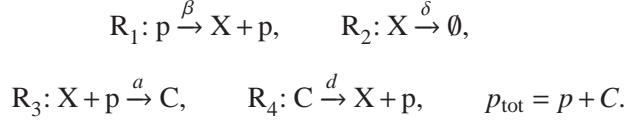
By denoting $X = n_X/\Omega$ the concentration of X and $p = n_p/\Omega = p_{\text{tot}}$ the concentration of p , we have that

$$\frac{dX}{dt} = \beta_0 p_{\text{tot}} - \delta X + \frac{1}{\sqrt{\Omega}} (\sqrt{\beta_0 p_{\text{tot}}} N_1 - \sqrt{\delta X} N_2).$$

This is a linear system and therefore we can calculate the frequency response to any of the two inputs N_1 and N_2 . The frequency response to input N_1 is given by

$$G_{XN_1}(\omega) = \frac{\sqrt{\beta_0 p_{\text{tot}}/\Omega}}{\sqrt{\omega^2 + \delta^2}}.$$

We now consider the autoregulated system. The reactions are given by



Employing the Langevin equation (4.13) of Section 4.1 and dividing both sides of the equation to obtain concentrations, we obtain

$$\begin{aligned} \frac{dp}{dt} &= -aXp + d(p_{\text{tot}} - p) + \frac{1}{\sqrt{\Omega}}(-\sqrt{aXp}N_3 + \sqrt{d(p_{\text{tot}} - p)}N_4) \\ \frac{dX}{dt} &= \beta p - \delta X - aXp + d(p_{\text{tot}} - p) + \frac{1}{\sqrt{\Omega}}(\sqrt{\beta p}N_1 - \sqrt{\delta X}N_2 - \sqrt{aXp}N_3 + \sqrt{d(p_{\text{tot}} - p)}N_4). \end{aligned}$$

Denoting $K_d = d/a$, $\Gamma_1(t) = \frac{1}{\sqrt{\Omega}}(-\sqrt{aXp/K_d}N_3 + \sqrt{d(p_{\text{tot}} - p)}N_4)$, and $\Gamma_2(t) = \frac{1}{\sqrt{\Omega}}(\sqrt{\beta p}N_1 - \sqrt{\delta X}N_2)$, we can rewrite the above system in the following form:

$$\begin{aligned} \frac{dp}{dt} &= -aXp + d(p_{\text{tot}} - p) + \sqrt{d}\Gamma_1(t) \\ \frac{dX}{dt} &= \beta p - \delta X - aXp + d(p_{\text{tot}} - p) + \Gamma_2(t) + \sqrt{d}\Gamma_1(t). \end{aligned}$$

Since $a, d \gg \delta, \beta p$, this system displays two time scales. Denoting $\epsilon := \delta/d$ and defining $y := X - p$, the system can be further rewritten in standard singular perturbation form (3.6):

$$\begin{aligned} \epsilon \frac{dp}{dt} &= -\delta Xp/K_d + \delta(p_{\text{tot}} - p) + \sqrt{\epsilon} \sqrt{d}\Gamma_1(t) \\ \frac{dy}{dt} &= \beta p - \delta(y + p) + \Gamma_2(t). \end{aligned}$$

By setting $\epsilon = 0$ and assuming that p_{tot}/K_d is sufficiently small, we obtain the reduced system describing the dynamics of X as

$$\frac{dX}{dt} = \beta \frac{p_{\text{tot}}}{X/K_d + 1} - \delta X + \frac{1}{\sqrt{\Omega}}(\sqrt{\beta p}N_1 - \sqrt{\delta X}N_2) =: f(X, N_1, N_2).$$

The equilibrium point for this system corresponding to the mean values $N_1 = 0$ and $N_2 = 0$ of the inputs is given by

$$X_e = \frac{1}{2}(\sqrt{K_d^2 + 4\beta p_{\text{tot}}K_d/\delta} - K_d).$$

The linearization of the system about this equilibrium point is given by

$$A = \left. \frac{\partial f}{\partial X} \right|_{X_e, N_1=0, N_2=0} = -\beta \frac{p_{\text{tot}}/K_d}{(X_e/K_d + 1)^2 + 1} - \delta,$$

$$b_1 = \left. \frac{\partial f}{\partial N_1} \right|_{X_e, N_1=0, N_2=0} = \frac{1}{\sqrt{\Omega}} \sqrt{\frac{\beta p_{\text{tot}}}{X_e/K_d + 1}}, \quad b_2 = \left. \frac{\partial f}{\partial N_2} \right|_{X_e, N_1=0, N_2=0} = -\sqrt{\delta X_e}.$$

Hence, the frequency response to N_1 is given by

$$G_{XN_1}^c(\omega) = \frac{b_1}{\sqrt{\omega^2 + A^2}}.$$

In order to make a fair comparison between this response and that of the open loop system, we need to make sure that the steady states of both systems are the same. In order to do so, we set

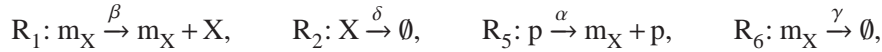
$$\beta_0 = \frac{\beta}{X_e/K_d + 1}.$$

This can be attained by adjusting the strength of the promoter and of the ribosome binding site.

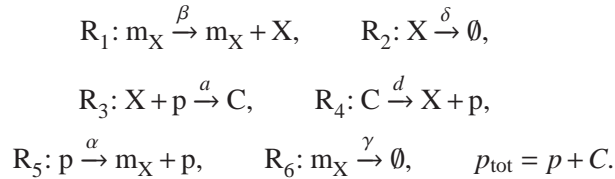
As a consequence, $b_1 = \sqrt{\beta_0 p_{\text{tot}}/\Omega}$. Since also $A > \delta$, it is clear that $G_{XN_1}^c(\omega) < G_{XN_1}(\omega)$ for all ω . This result implies that the negative feedback attenuates the noise at all frequencies. The two frequency responses are plotted in Figure 6.2(a).

mRNA decay close to protein decay

In this case, we need to model the processes of transcription and translation separately. Denoting m_X the mRNA of X, the reactions describing the open loop system modify to



while those describing the closed loop system modify to



Employing the Langevin equation in terms of concentrations, and applying singular perturbation as performed before, we obtain the dynamics of the system as

$$\frac{dm_X}{dt} = f(X) - \gamma m_X + \frac{1}{\sqrt{\Omega}} (\sqrt{f(X)} N_5 - \sqrt{\gamma m_X} N_6)$$

$$\frac{dX}{dt} = \beta m_X - \delta X + \frac{1}{\sqrt{\Omega}} (\sqrt{\beta m_X} N_1 - \sqrt{\delta X} N_2),$$

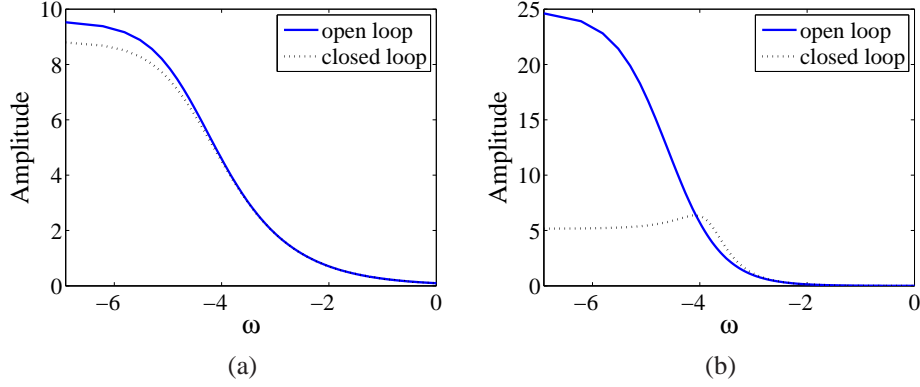


Figure 6.2: (a) Frequency response to noise $N_1(t)$ for both open loop and closed loop for the model in which mRNA is assumed at its quasi-steady state. The parameters are $p_{\text{tot}} = 10$, $K_d = 10$, $\beta = 0.001$, $\delta = 0.01$, $\Omega = 1$, and $\beta_0 = 0.00092$. (b) Frequency response to noise $N_6(t)$ for both open loop and closed loop for the model in which mRNA decay is close to protein decay. The parameters are $p_{\text{tot}} = 10$, $K_d = 10$, $\alpha = 0.001$, $\beta = 0.01$, $\gamma = 0.01$, $\delta = 0.01$, and $\alpha_0 = 0.0618$.

in which for the open loop system $f(X) = \alpha_0 p_{\text{tot}}$, while for the closed loop system

$$f(X) = \frac{\alpha p_{\text{tot}}}{X/K_d + 1}.$$

The steady state for the open loop system is given by

$$m_e^o = \frac{\alpha_0}{\gamma}, \quad X_e^o = \frac{\alpha_0 \beta}{\gamma \delta}.$$

Considering N_6 to be the input of interest, the linearization of the system at this equilibrium is given by

$$A^o = \begin{pmatrix} -\gamma & 0 \\ \beta & -\delta \end{pmatrix}, \quad B^o = \begin{pmatrix} \sqrt{\gamma m_e^o / \Omega} \\ 0 \end{pmatrix}.$$

Letting $K = \beta / (\delta K_d)$, the steady state for the closed loop system is given by

$$X_e^c = \frac{\beta m_e}{\delta}, \quad m_e^c = (-1/K + \sqrt{(1/K)^2 + 4\alpha p_{\text{tot}} / (K\gamma)}) / 2.$$

The linearization of the closed loop system at this equilibrium point is given by

$$A^c = \begin{pmatrix} -\gamma & -G \\ \beta & -\delta \end{pmatrix}, \quad B^c = \begin{pmatrix} \sqrt{\gamma m_e^c / \Omega} \\ 0 \end{pmatrix},$$

in which $G = \alpha p_{\text{tot}} / (X_e^c / K_d + 1)^2$ represents the contribution of the negative feedback. The larger the value of G the stronger the negative feedback.

In order to make a fair comparison between the two systems, we need to make the steady states be the same. In order to do this, we can set $\alpha_0 = \alpha/(X_e^c/K_d + 1)$, which can be done by suitable changing the promoter and ribosome binding site strengths.

The open loop and closed loop transfer functions are given by

$$G_{XN_6}^o(s) = \frac{\beta \sqrt{\gamma m_e / \Omega}}{(s + \gamma)(s + \delta)},$$

and by

$$G_{XN_6}^c(s) = \frac{\beta \sqrt{\gamma m_e / \Omega}}{s^2 + s(\gamma + \delta) + \gamma\delta + G},$$

respectively. By looking at these expressions, it is clear that the open loop transfer function has two real poles, while the closed loop transfer function can have complex conjugate poles when G is sufficiently large. As a consequence, noise N_6 can be amplified at sufficiently high frequencies. Figure 6.2(b) shows the corresponding frequency responses for both the open loop and the closed loop system.

It is clear that the presence of the negative feedback attenuates noise with respect to the open loop system at low frequency, but it amplifies it at higher frequency. This is a very well known effect known as the “water bed effect”, according to which negative feedback decreases the effect of disturbances at low frequency, but it can amplify it at higher frequency. This effect is not found in first order models, as demonstrated by the derivations when mRNA is at the quasi-steady state. This illustrates the spectral shift of the intrinsic noise toward the high frequency, as also experimentally demonstrated [7].

6.3 The Toggle Switch

The toggle switch is composed of two genes that mutually repress each other, as shown in the diagram of Figure 6.3 [29]. We start by describing a simple model with no inducers. By assuming that the mRNA dynamics are at the quasi-steady state, we obtain a two dimensional differential equation model given by

$$\frac{dA}{dt} = \frac{\beta}{1 + (B/K)^n} - \delta A, \quad \frac{dB}{dt} = \frac{\beta}{1 + (A/K)^n} - \delta B,$$

in which we have assumed for simplicity that the parameters of the repression functions are the same for A and B.

The number and stability of equilibria can be analyzed by performing nullcline analysis since the system is two-dimensional. Specifically, by setting $\dot{A} = 0$ and $\dot{B} = 0$, we obtain the nullclines shown in Figure 6.3. In the case in which the parameters are the same for both A and B, the nullclines intersect at three points, which determine the steady states of this system.

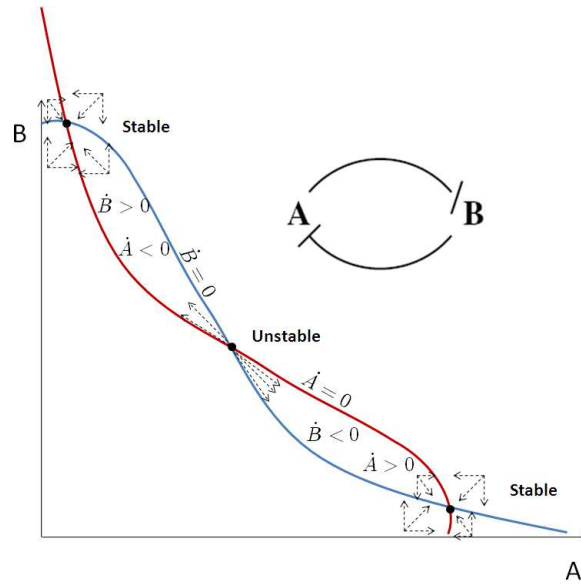


Figure 6.3: Nullclines for the toggle switch. By analyzing the direction of the vector field in the proximity of the equilibria, one can deduce their stability as described in Chapter 3.

The nullclines partition the plane into six regions. By determining the sign of \dot{A} and \dot{B} in each of these six regions, one determines the direction in which the vector field is pointing in each of these regions. From these directions, one immediately deduces that the steady state for which $A = B$ is unstable while the other two are stable. This is thus a bistable system.

The system converges to one steady state or the other depending on the initial condition. If the initial condition is in the region of attraction of one steady state, it converges to that steady state. The 45 degree line divides the plane into the two regions of attraction of the stable steady states. Once the system has converged to one of the two steady states, it cannot switch to the other unless an external stimulation is applied that moves the initial condition to the region of attraction of the other steady state [29].

In the toggle switch by [29], external stimulations were added in form of negative inducers for A and B. Let u_1 be the negative inducer for A and u_2 be the negative inducer for B. Then, as we have seen in Section 2.3, the expressions of the Hill functions need to be modified to replace A by $A/(1+(u_1/K_{d,1}))$ and B by $B/(1+(u_2/K_{d,2}))$, in which $K_{d,1}$ and $K_{d,2}$ are the dissociation constants of u_1 with A and of u_2 with B, respectively. We show in Figure 6.4 time traces for $A(t)$ and $B(t)$ when the inducer concentrations are changed. Specifically, initially u_1 is high until time 100 while u_2 is low until this time. As a consequence, A does not repress B while B represses A. Accordingly, the concentration of A stays low until time 100 and the concentration of B stays high. After time 100, u_2 is high and u_1 is low.

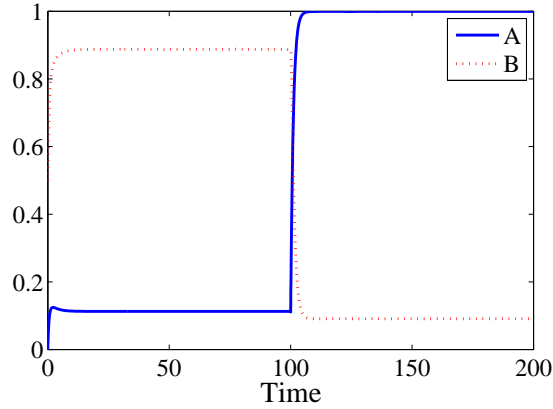


Figure 6.4: time traces for $A(t)$ and $B(t)$ when inducer concentrations u_1 and u_2 are changed. In the simulation, we have $n = 2$, $K_{d,1} = K_{d,2} = 1$, $K^2 = 0.1$, $\beta = 1$, and $\delta = 1$. The inducers are such that $u_1 = 10$ for $t < 100$ and $u_1 = 0$ for $t \geq 100$, while $u_2 = 0$ for $t < 100$ and $u_2 = 10$ for $t \geq 100$.

As a consequence B does not repress A while A represses B. In this situation, A switches to its high value and B switches to its low value.

6.4 The Repressilator

Elowitz and Leibler [26] constructed the first operational oscillatory genetic circuit consisting of three repressors arranged in ring fashion, and coined it the “repressilator” (Figure 6.1d). The repressilator exhibits sinusoidal, limit cycle oscillations in periods of hours, slower than the cell-division life cycle. Therefore, the state of the oscillator is transmitted between generations from mother to daughter cells.

The dynamical model of the repressilator can be obtained by composing three transcriptional modules in a loop fashion. The dynamics can be written as

$$\begin{aligned} \frac{dm_A}{dt} &= -\delta m_A + f_1(C) & \frac{dm_B}{dt} &= -\delta m_B + f_2(A) & \frac{dm_C}{dt} &= -\delta m_C + f_3(B) \\ \frac{dA}{dt} &= m_A - \delta A & \frac{dB}{dt} &= m_B - \delta B & \frac{dC}{dt} &= m_C - \delta C, \end{aligned}$$

where we take

$$f_1(p) = f_2(p) = f_3(p) = \frac{\alpha^2}{1 + p^n}.$$

This structure belongs to the class of cyclic feedback systems that we have studied in earlier chapters. In particular, the Mallet-Paret and Smith theorem and Hastings

theorem (see Section 3.4 for the details) can be applied to infer that if the system has a unique equilibrium point and this is unstable, then it admits a periodic solution. Therefore, we first determine the number of equilibria and their stability.

The equilibria of the system can be found by setting the time derivatives to zero. We thus obtain that

$$A = \frac{f_1(C)}{\delta^2}, \quad B = \frac{f_2(A)}{\delta^2}, \quad C = \frac{f_3(B)}{\delta^2},$$

which combined together yield to

$$A = \frac{1}{\delta^2} f_1 \left(\frac{1}{\delta^2} f_3 \left(\frac{1}{\delta^2} f_2(A) \right) \right) =: g(A).$$

The solution to this equation determines the set of steady states of the system. The number of steady states is given by the number of crossings of the two functions $h_1(A) = g(A)$ and $h_2(A) = A$. Since h_2 is strictly monotonically increasing, we obtain a unique steady state if h_1 is monotonically decreasing. This is the case when $g'(A) = \frac{dg(A)}{dA} < 0$. Otherwise, there could be multiple steady states. Since we have that

$$\text{sign}(g'(A)) = \prod_{i=1}^3 \text{sign}(f'_i(P)),$$

then if $\prod_{i=1}^3 \text{sign}(f'_i(P)) < 0$ the system has a unique steady state. We call the product $\prod_{i=1}^3 \text{sign}(f'_i(P))$ the *loop gain*.

Thus, any cyclic feedback system with negative loop gain will have a unique steady state. It can be shown that a cyclic feedback system with positive loop gain belongs to the class of monotone systems and hence cannot have periodic orbits [54]. In the present case, system (6.4) is such that $f'_i < 0$, so that the loop gain is negative and there is a unique steady state. We next study the stability of this steady state by studying the linearization of the system.

Letting P denote the steady state value of the protein concentrations for A, B, and C, the linearization of the system is given by

$$J = \begin{pmatrix} -\delta & 0 & 0 & 0 & 0 & f'_1(P) \\ 1 & -\delta & 0 & 0 & 0 & 0 \\ 0 & f'_2(P) & -\delta & 0 & 0 & 0 \\ 0 & 0 & 1 & -\delta & 0 & 0 \\ 0 & 0 & 0 & f'_3(P) & -\delta & 0 \\ 0 & 0 & 0 & 0 & 1 & -\delta \end{pmatrix},$$

whose characteristic polynomial is given by

$$\det(\lambda I - J) = (\lambda + \delta)^6 - \prod_{i=1}^3 f'_i(P). \quad (6.1)$$

In the case in which $f_i(P) = \alpha^2 / (1 + p^n)$ for $i \in \{1, 2, 3\}$, this characteristic polynomial has a root with positive real part if the ratio α/δ satisfies the relation

$$\alpha^2 / \delta^2 > \sqrt[n]{\frac{4/3}{n-4/3}} \left(1 + \frac{4/3}{n-4/3} \right).$$

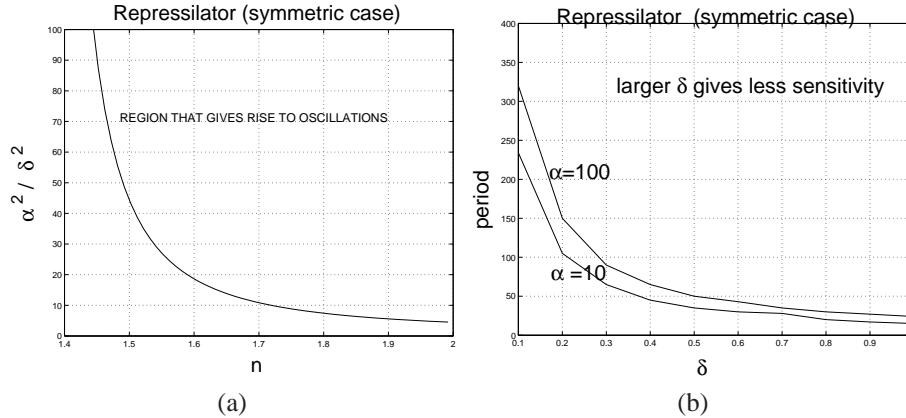


Figure 6.5: (a) Space of parameters that give rise to oscillations for the repressilator in equation (6.4). (b) Period as a function of δ and α .

For the proof of this statement, the reader is referred to [20]. This relationship is plotted in the left plot of Figure 6.5.

When n increases, the existence of an unstable equilibrium point is guaranteed for larger ranges of the other parameter values. Of course, this “behavioral” robustness does not guarantee that other important features of the oscillator, such as the period are not changed when parameters vary. Numerical studies indicate that the period T approximately follows $T \propto 1/\delta$, and varies little with respect to α (Figure 6.5b). From the figure, we see that as the value of δ increases, the sensitivity of the period to the variation of δ itself decreases. However, increasing δ would necessitate the increase of the cooperativity n , therefore indicating a possible tradeoff that should be taken into account in the design process in order to balance the system complexity and robustness of the oscillations. From a practical point of view, n can be changed by selecting repressors that bind cooperatively to the promoter. In practice, it is usually hard to obtain values of n greater than two.

A similar result for the existence of a periodic solution can be obtained for the non-symmetric case in which the input functions of the three transcriptional modules are modified to

$$f_1(p) = \frac{\alpha_3^2}{1+p^n}, \quad f_2(p) = \frac{\alpha^2 p^n}{1+p^n}, \quad f_3(p) = \frac{\alpha^2 p^n}{1+p^n}.$$

That is, two interactions are activations and one only is a repression. Since the loop gain is still negative, there is only one equilibrium point only. We can thus obtain the condition for oscillations again by establishing conditions on the parameters that guarantee that at least one root of the characteristic polynomial (6.1) has

positive real part, that is,

$$(0.86)^2 n^3 \sqrt[3]{\frac{p_3^n}{(1+p_3^n)(1+p_2^n)(1+p_1^n)}} > 1. \quad (6.2)$$

We rewrite p_1 and p_3 as functions of p_2 by using two of the equilibrium relations:

$$p_1 = \sqrt[n]{\frac{p_2}{\alpha^2/\delta^2 - p_2}}, \quad p_3 = \frac{\alpha^2/\delta^2 p_2^n}{1 + p_2^n}.$$

Using these expressions in (6.2), we can find all possible values of p_2 that satisfy (6.2) for a fixed pair $(\alpha^2/\delta^2, n)$. These values of p_2 correspond to the possible values of α_3^2/δ^2 by means of the third equilibrium condition

$$\alpha_3^2/\delta^2 = p_1(1 + p_3^n).$$

For each pair $(\alpha^2/\delta^2, n)$, we finally obtain all possible values of α_3^2/δ^2 that satisfy the equilibrium conditions and inequality (6.2). These conditions are reported in Figure 6.6 (see [20] for the detailed derivations).

One can conclude that it is possible to “over design” the circuit to be in the region of parameter space that gives rise to oscillations. In practice, values of n between one and two can be obtained by employing repressors that have cooperativity higher than or equal to two. There are plenty of such repressors, including those originally used in the repressilator design [26]. However, values of n greater than two may be hard to reach in practice. It is also possible to show that increasing the number of elements in the oscillatory loop, the value of n sufficient for oscillatory behavior decreases.

6.5 Activator-repressor clock

Consider the activator-repressor clock diagram shown in Figure 6.1(c). The transcriptional module A has an input function that takes two inputs: an activator A and a repressor B. The transcriptional module B has an input function that takes only an activator A as its input. Let m_A and m_B represent the concentration of mRNA of the activator and of the repressor, respectively. Let A and B denote the protein concentration of the activator and of the repressor, respectively. Then, we consider the following four-dimensional model describing the rate of change of the species concentrations:

$$\begin{aligned} \frac{dm_A}{dt} &= -\delta_1 m_A + F_1(A, B), & \frac{dm_B}{dt} &= -\delta_2 m_B + F_2(A), \\ \frac{dA}{dt} &= -\delta_A A + \beta_1 m_A, & \frac{dB}{dt} &= -\delta_B B + \beta_2 m_B, \end{aligned}$$

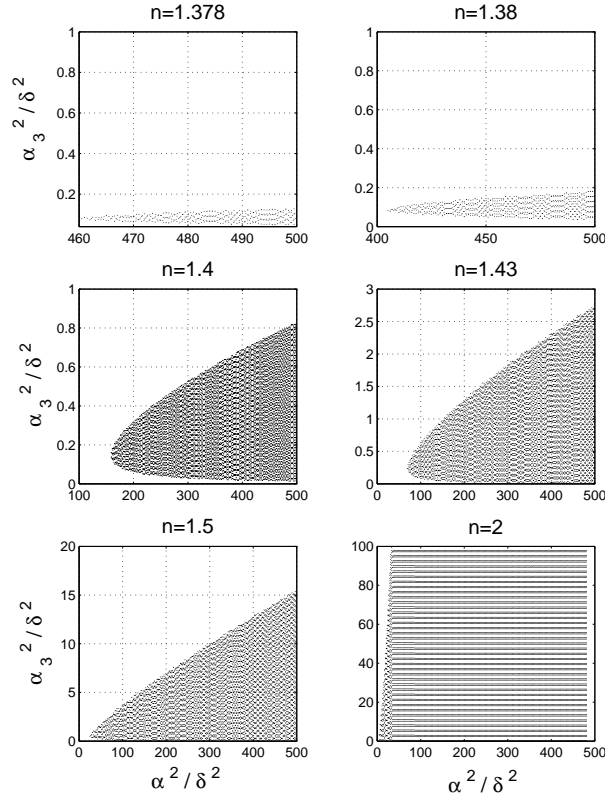


Figure 6.6: Space of parameters that give rise to oscillations for the repressilator (non-symmetric case). As the value of n is increased, the ranges of the other parameters for which sustained oscillations exist become larger.

in which the functions F_1 and F_2 are the Hill functions and are given by

$$F_1(A, B) = \frac{K_1 A^n + K_{A0}}{1 + (A/k_1)^n + (B/k_2)^m}, \quad F_2(A) = \frac{K_2 A^n + K_{B0}}{1 + (A/k_1)^n}.$$

The Hill function F_1 can be obtained through a combinatorial promoter, where there are sites both for an activator and for a repressor (see Section 2.3).

Two-dimensional analysis

We first assume the mRNA dynamics to be at the quasi-steady state so that we can perform two dimensional analysis and invoke the Poincarè-Bendixson theorem. Then, we analyze the four dimensional system and perform a bifurcation study.

We denote $f_1(A, B) := (\beta_1/\delta_1)F_1(A, B)$ and $f_2(A) := (\beta_2/\delta_2)F_2(A)$. For simplicity, we also denote $f(A, B) := -\delta_A A + f_1(A, B)$ and $g(A, B) := -\delta_B B + f_2(A)$ so

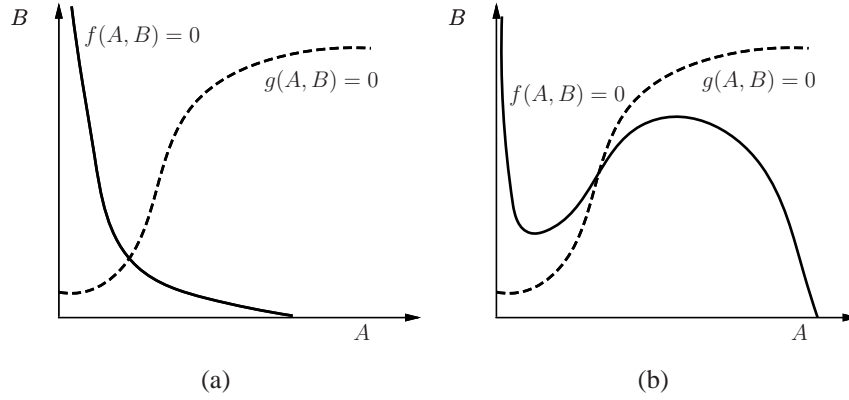


Figure 6.7: Nullclines for the two-dimensional system of equation (6.5). (a) shows the only possible configuration of the nullclines when $n = 1$. (b) shows a possible configuration of the nullclines when $n = 2$. In this configuration, there is a unique equilibrium, which can be unstable.

that the two-dimensional system is given by

$$\frac{dA}{dt} = f(A, B), \quad \frac{dB}{dt} = g(A, B).$$

For simplicity, we assume $m = 1$ and $k_i = 1$ for all i .

We first study whether the system admits a periodic solution for $n = 1$. To do so, we analyze the nullclines to determine the number and location of steady states. Denote $\bar{K}_1 = K_1(\beta_1/\delta_1)$, $\bar{K}_2 = K_2(\beta_2/\delta_2)$, $\bar{K}_{A0} = K_{A0}(\beta_1/\delta_1)$, and $\bar{K}_{B0} = K_{B0}(\beta_1/\delta_1)$. Then, $g(A, B) = 0$ leads to

$$B = \frac{\bar{K}_2 A + \bar{K}_{B0}}{(1 + A)\delta_A},$$

which is an increasing function of A . Setting $f(A, B) = 0$, we obtain that

$$B = \frac{\bar{K}_1 A + \bar{K}_{A0} - \delta_A A(1 + A)}{\delta_A A},$$

which is a monotonically decreasing function of A . These nullclines are displayed in Figure 6.7(a).

We see that we have one equilibrium only. To determine the stability of such an equilibrium, we calculate the linearization of the system at such an equilibrium. This is given by

$$J = \begin{pmatrix} \frac{\partial f}{\partial A} & \frac{\partial f}{\partial B} \\ \frac{\partial g}{\partial A} & \frac{\partial g}{\partial B} \end{pmatrix}$$

In order for the equilibrium to be unstable and not a saddle, it is necessary and sufficient that

$$\text{tr}(J) > 0 \text{ and } \det(J) > 0.$$

Graphical inspection of the nullclines at the equilibrium (see 6.7(a)), shows that

$$\left. \frac{dB}{dA} \right|_{f(A,B)=0} < 0$$

By the implicit function theorem ([55]), we further have that

$$\left. \frac{dB}{dA} \right|_{f(A,B)=0} = -\frac{\partial f/\partial A}{\partial f/\partial B},$$

so that $\partial f/\partial A < 0$ because $\partial f/\partial B < 0$. As a consequence, we have that $\text{tr}(J) < 0$ and hence the equilibrium point is either stable or a saddle.

To determine which one of these two, we further inspect the nullclines and find that

$$\left. \frac{dB}{dA} \right|_{g(A,B)=0} > \left. \frac{dB}{dA} \right|_{f(A,B)=0}.$$

Again using the implicit function theorem we have that

$$\left. \frac{dB}{dA} \right|_{g(A,B)=0} = -\frac{\partial g/\partial A}{\partial g/\partial B},$$

so that $\det(J) > 0$. Hence, the ω -limit set (Section 3.4) of any point in the plane is not necessarily a periodic orbit. Hence, to guarantee that any initial condition converges to a periodic orbit, we need to require that $n > 1$.

We now study the case $n = 2$. In this case, the nullcline $f(A, B) = 0$ changes and can have the shape shown in Figure 6.7 (b). In the case in which, as in the figure, there is an equilibrium point only and the nullclines intersect both with positive slope (equivalent to $\det(J) > 0$), the equilibrium is unstable and not a saddle if $\text{tr}(J) > 0$, which is satisfied if

$$\frac{\delta_B}{\partial f_1/\partial A - \delta_A} < 1.$$

This condition reveals the crucial design requirement for the functioning of the clock. Specifically the repressor B time scale must be sufficiently slower than the activator A time scale. This point is illustrated in the simulations of Figure 6.8, in which we see that if δ_B is too large, the trace becomes negative and oscillations disappear.

Four-dimensional analysis

In order to specifically study time scale separation between activator and repressor as a crucial design requirement for the clock, we perform a time scale analysis employing bifurcation tools . To this end, we consider the following four-dimensional

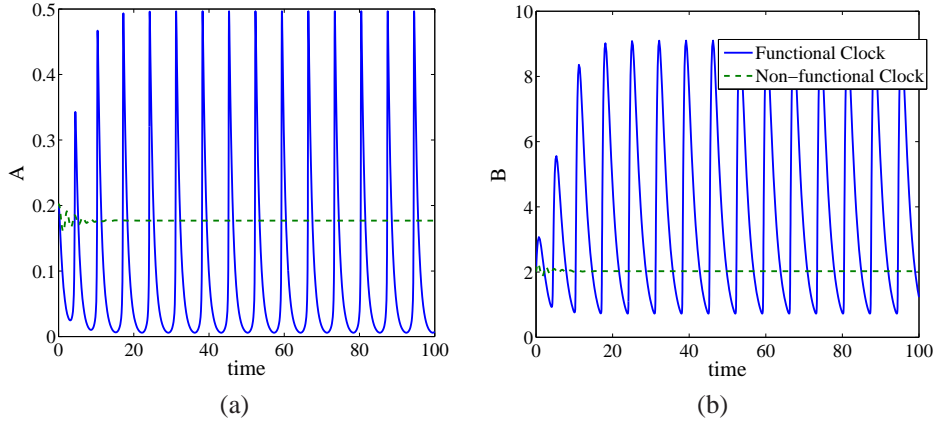


Figure 6.8: *Effect of the trace of the Jacobian on the stability of the equilibrium.* The above plots illustrate the trajectories of system (6.5) for both Functional ($\text{tr}(J) > 0$) and a Non-Functional ($\text{tr}(J) < 0$) Clocks. The parameters in the simulation are $\delta_1 = \delta_2 = 1$, $K_1 = K_2 = 100$, $K_{A0} = .04$, $K_{B0} = .004$, $\delta_A = 1$, $\beta_1 = \beta_2 = 1$, and $k_1 = k_2 = 1$. In the Functional Clock, $\delta_B = 0.5$ whereas in the Non-Functional Clock, $\delta_B = 1.5$. Parameters K_1 and K_2 were chosen to give about 500-2000 copies of protein per cell for activated promoters. Parameters K_{A0} and K_{B0} were chosen to give about 1-10 copies per cell for non-activated promoters.

model describing the rate of change of the species concentrations:

$$\begin{aligned} \frac{dm_A}{dt} &= -\delta_1/\epsilon m_A + F_1(A, B) & \frac{dm_B}{dt} &= -\delta_2/\epsilon m_B + F_2(A) \\ \frac{dA}{dt} &= \nu(-\delta_A A + \beta_1/\epsilon m_A) & \frac{dB}{dt} &= -\delta_B B + \beta_2/\epsilon m_B. \end{aligned}$$

This system is the same as system (6.5) where we have explicitly introduced two parameters, ν and ϵ , which model time scale differences as follows. The parameter ν regulates the difference of time scale between the repressor and the activator dynamics while ϵ regulates the difference of time scale between the mRNA and the protein dynamics. The parameter ϵ determines how close model (6.5) is to the two-dimensional model (6.5), in which the mRNA dynamics are considered at the quasi-steady state. Thus, ϵ is a singular perturbation parameter (equations (6.5) can be taken to standard singular perturbation form by considering the change of variables $\bar{m}_A = m_A/\epsilon$ and $\bar{m}_B = m_B/\epsilon$). The details on singular perturbation can be found in Section 3.6.

The values of ϵ and of ν do not affect the number of equilibria of the system.

We then perform bifurcation analysis with ϵ and ν the two bifurcation parameters. The bifurcation analysis results are summarized by Figure 6.9. The reader is referred to [19] for the details of the numerical analysis. In terms of the ϵ and

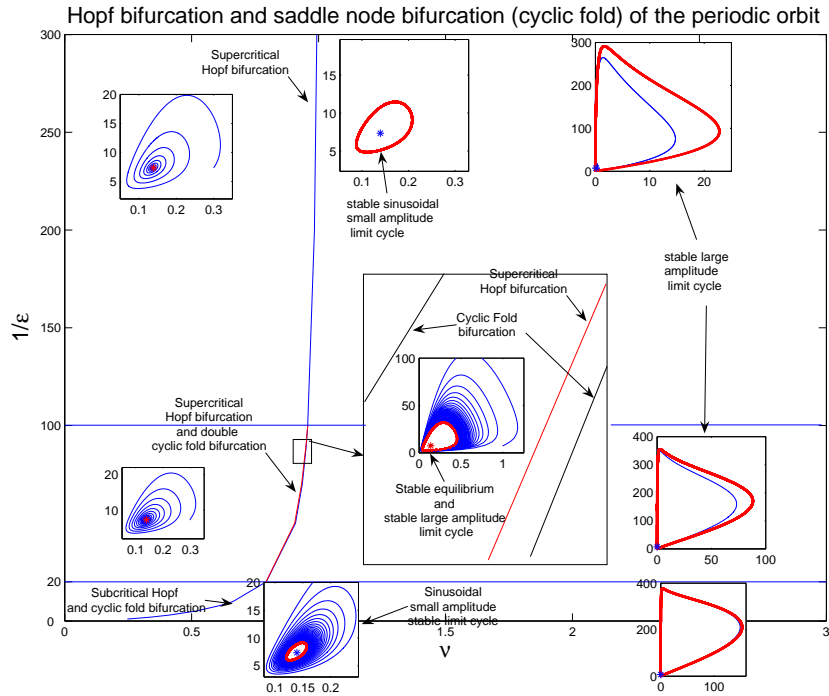


Figure 6.9: Design chart for the relaxation oscillator. We obtain sustained oscillations past the Hopf bifurcation, for values of ν sufficiently large independently of the difference of time scales between the protein and the mRNA dynamics. We also notice that there are values of ν for which a stable equilibrium point and a stable orbit coexist and values of ν for which two stable orbits coexist. The interval of ν values for which two stable orbits coexist is too small to be able to numerically set ν in such an interval. Thus, this interval is not practically relevant. The values of ν for which a stable equilibrium and a stable periodic orbit coexist is instead relevant. This situation corresponds to the *hard excitation* condition [51] and occurs for realistic values of the separation of time-scales between protein and m-RNA dynamics. Therefore, this simple oscillator motif described by a four-dimensional model can capture the features that lead to the long term suppression of the rhythm by external inputs.

ν parameters, it is thus possible to “over design” the system: if the activator dynamics are sufficiently sped up with respect to the repressor dynamics, the system undergoes a Hopf bifurcation (Hopf bifurcation was introduced in Section 3.4) and stable oscillations will arise. From a fabrication point of view, the activator dynamics can be sped up by adding suitable degradation tags to the activator protein. Similarly, the repressor dynamics can be slowed down by adding repressor DNA binding sites (see Chapter 7 and the effects of retroactivity on dynamic behavior).

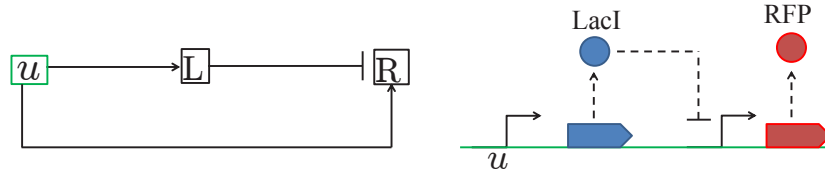


Figure 6.10: (Left) The incoherent feedforward motif. (Right) A possible implementation of the incoherent feedforward motif. Here, LacI (L) is under the control of a constitutive promoter in amounts u , while RFP (R) is under the control of the lac promoter, also in amounts u . Hence RFP is also activated by u as the RFP gene is found in amounts u just like the LacI gene.

6.6 An Incoherent Feedforward Loop (IFFL)

Several genetic implementations of incoherent feedforward loops are possible [4]. Here, we describe an implementation proposed for making the steady state levels of protein expression adapt to DNA plasmid copy number [13]. In this implementation, the input u is the amount of DNA plasmid coding for both the intermediate regulator LacI (L) with concentration L and the output RFP (R) with concentration R . The intermediate regulator LacI represses through transcriptional repression the expression of the output protein RFP (Figure 6.10). The expectation is that the steady state value of the RFP expression is independent of the concentration u of the plasmid. That is, the concentration of RFP should adapt to the copy number of its own plasmid.

In order to analyze whether the adaptation property holds, we write the differential equation model describing the system, assuming the mRNA dynamics are at the quasi-steady state. This model is given by

$$\frac{dL}{dt} = k_0 u - \delta L, \quad \frac{dR}{dt} = \frac{k_1 u}{1 + (L/K_d)} - \delta R, \quad (6.3)$$

in which k_0 is the constitutive rate at which LacI is expressed and K_d is the dissociation constant of LacI from the operator sites on the lac promoter. This implementation has been called the sniffer in Section 3.2. The steady state of the system is obtained by setting the time derivatives to zero and gives

$$L = \frac{k_0}{\delta} u, \quad R = \frac{k_1 u}{\delta + k_0 u / K_d}.$$

From this expression, one can easily note that as K_d decreases, the denominator of the right-side expression tends to $k_0 u / K_d$ resulting into the steady state value $R = k_1 K_d / k_0$, which does not depend on the input u . Hence, in this case, adaptation

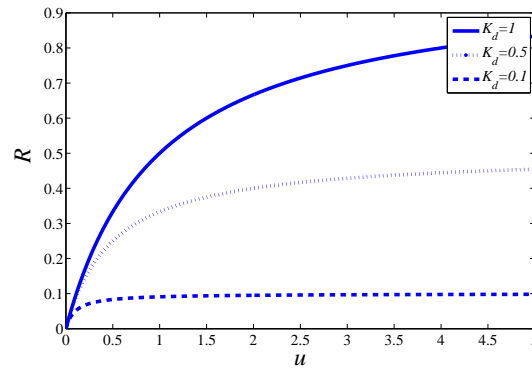


Figure 6.11: Behavior of the steady state value of y as a function of the input u .

would be reached. This is the case if the affinity of LacI to its operator sites is extremely high, resulting also in a strong repression and hence a lower value of R . In practice, however, the value of K_d is non-zero, hence the adaptation is not perfect. We show in Figure 6.11 the behavior of the steady state of R as a function of the input u for different values of K_d . Ideally, for perfect adaptation, this should be a horizontal line.

In this study, we have modeled protein L as binding with its promoter with no cooperativity. If L is LacI, the cooperativity of binding is $n = 4$. We leave as an exercise to show that the adaptation behavior persist in this case.

For engineering a system with prescribed behavior, one has to be able to change the physical features so as to change the values of the parameters of the model. This is often possible. For example, the binding affinity ($1/K_d$ in the Hill function model) of a transcription factor to its site on the promoter can be affected by single or multiple base pairs substitutions. The protein decay rate can be increased by adding degradation tags at the end of the gene expressing protein Y. Promoters that can accept multiple input transcription factors (combinatorial promoters) to implement regulation functions that take multiple inputs can be realized by combining the operator sites of several simple promoters [17].

Exercises

6.1 Consider the Toggle Switch that we have seen in class:

$$\dot{A} = \frac{\beta}{1 + (B/K_1)^n} - \alpha_1 A, \quad \dot{B} = \frac{\gamma}{1 + (A/K_2)^m} - \alpha_2 B.$$

Here, we are going to explore the parameter space that makes the system work as a toggle. To do so, answer the following questions:

- (a) Consider $m = n = 1$. Determine the number and stability of the equilibria.
- (b) Consider $m = 1$ and $n > 1$ and determine the number and stability of the equilibria (as other parameters change).
- (c) Consider $m = n = 2$. Determine parameter conditions on $\beta, \gamma, \alpha_1, \alpha_2$ for which the system is bistable, i.e., there are two stable steady states.

6.2 Consider the oscillator design of Stricker et al. [?]. Build a four dimensional model including mRNA concentration and protein concentration. Then reduce this fourth order model to a second order model using the QSS approximation for the mRNA dynamics. Then, investigate the following points:

- (a) Use the Poincaré-Bendixson theorem to determine under what conditions the system in 2D admits a periodic orbit.
- (b) Simulate the four dimensional system and the two dimensional system for parameter values that give oscillations and study how close the trajectories of the 2D approximation are to those of the 4D system.
- (c) Determine whether the four dimensional system has a Hopf bifurcation (either analytically or numerically).

6.3 Consider the feedforward circuit shown in Figure 6.11. Assume now to model the fact that the cooperativity of binding of LacI to its promoter is 4. The model then modifies to

$$\frac{dL}{dt} = k_0 u - \delta L, \quad \frac{dR}{dt} = \frac{k_1 u}{1 + (L/K_d)^4} - \delta R. \quad (6.4)$$

Show that the adaptation property still holds under suitable parameter conditions.

Chapter 7

Interconnecting Components

In Chapter 6 and Chapter 2, we studied the behavior of simple biomolecular modules, such as oscillators, toggles, self repressing circuits, signal transduction and amplification systems, based on reduced order models. One natural step forward is to create larger and more complex systems by composing these modules together. In this chapter, we illustrate problems that need to be overcome when interconnecting components and propose a number of engineering solutions based on the feedback principles introduced in Chapter 3. Specifically, we explain how impedance-like effects arise at the interconnection between modules, which change the expected circuit behavior. These impedance problems appear in several other engineering domains, including electrical, mechanical, and hydraulic systems, and have been largely addressed by the respective engineering communities. In this chapter, we explain how similar engineering solutions can be employed in biomolecular systems to defeat impedance effects and guarantee “modular” interconnection of circuits. In Chapter 8, we further study loading of the cellular environment by synthetic circuits employing the same framework developed in this chapter.

7.1 Input/Output Modeling and the Modularity Assumption

The input/output modeling introduced in Chapter 1 and further developed in Chapter 3 has been employed so far to describe the behavior of various modules and subsystems. Such an input/output description of a system allows to connect systems together by setting the input u_2 of a downstream system equal to the output of the upstream system.

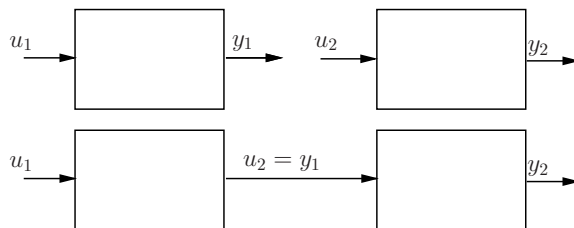


Figure 7.1: In the input/output modeling framework, systems are interconnected by statically assigning to the input of the downstream system the value of the output of the upstream system.

y_1 of the upstream system (Figure 7.1). This interconnection framework has been used extensively in the previous chapters.

Specifically, each node of a gene circuit has been modeled as an input/output module taking as input the concentrations of transcription factors that regulate a gene y and giving as output the concentration of protein Y expressed by gene y . This is of course not the only possible choice for delimiting a module. We could in fact let the mRNA or the RNA polymerase flowing along the DNA, called PoPS (Polymerase Per Second) [28], play the role of input and output signals. Similarly, each node of a signal transduction network is usually a protein covalent modification module, which takes as input a modifying enzyme (a kinase in the case of phosphorylation) and gives as an output the modified protein.

For example, one of the models of the MAPK cascade considered in Section 2.5 was obtained by setting the value of the kinase concentration of a downstream cycle equal to the value of the concentration of the modified protein of the upstream cycle. A similar technique was employed for designing all the circuits of Chapter 6. For example, the repressilator model was obtained by setting the concentration of the input transcription factor of each gene equal to the concentration of the output transcription factor of the upstream gene.

This input/output modeling framework is extremely useful because it allows us to predict the behavior of an interconnected system based on the behavior of the isolated modules. For example, the location and number of steady states in the toggle switch of Section 6.3 was predicted by intersecting the steady state input/output characteristics of the isolated modules A and B. Similarly, the number of steady states in the repressilator was predicted by modularly composing the input/output steady state characteristics of the three modules composing the circuit.

For this input/output interconnection framework to reliably predict the behavior of connected modules, however, one must have that the input/output (dynamic) behavior of a system does not change upon interconnection to another system. We refer to the property by which a system input/output behavior does not change upon interconnection as *modularity*. Of course, all the designs and modeling described in the previous chapter assume that the modularity property holds. In this chapter, we question this assumption and investigate when modularity holds in gene and in signal transduction circuits.

7.2 Introduction to Retroactivity

The modularity assumption implies that when two modules are connected together, their behavior does not change because of the interconnection. However, a fundamental systems-engineering issue that arises when interconnecting subsystems is how the process of transmitting a signal to a “downstream” component affects the dynamic state of the sending component. This issue, the effect of “loads” on the output of a system, is well-understood in many engineering fields such as electrical

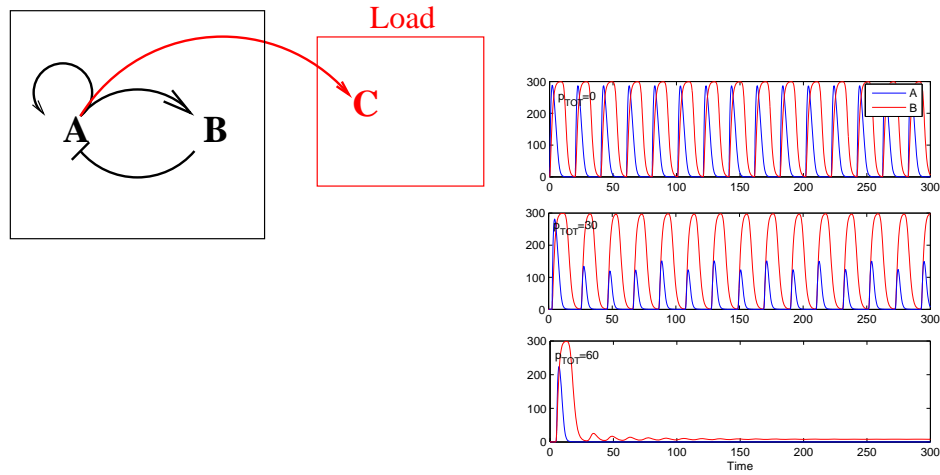


Figure 7.2: The clock behavior can be destroyed by a load. As the number of downstream binding sites for A, p_{tot} , is increased in the load, the activator and repressor dynamics lose their synchronization and ultimately the oscillations disappear.

engineering. It has often been pointed out that similar issues may arise for biological systems. These questions are especially delicate in design problems, such as those described in Chapter 6.

For example, consider a biomolecular clock, such as the activator-repressor clock introduced in Section 6.5. Assume that the activator protein concentration $A(t)$ is now used as a means to synchronize or time some downstream systems. From a systems/signals point of view, $A(t)$ becomes an *input* to the second system (Figure 7.2). The terms “upstream” and “downstream” reflect the direction in which we think of signals as traveling, *from* the clock *to* the systems being synchronized. However, this is only an idealization, because, as seen in Figure 7.2, the binding and unbinding of A to promoter sites in a downstream system competes with the biochemical interactions that constitute the upstream clock and may therefore disrupt the operation of the clock itself. We call this “back-effect” *retroactivity* to extend the notion of impedance or loading to non-electrical systems and in particular to biomolecular systems. This phenomenon, while in principle may be used in an advantageous way from natural systems, can be deleterious when designing synthetic systems.

One possible approach to avoid disrupting the behavior of the clock is to introduce a gene coding for a new protein X, placed under the control of the same promoter as the gene for A, and using the concentration of X, which presumably mirrors that of A, to drive the downstream system. This approach, however, still has the problem that the behavior of the X concentration in time may be altered and even disrupted by the addition of downstream systems that drain X, as we shall see in the next section. The net result is that the downstream systems are not prop-

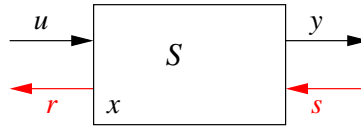


Figure 7.3: A system S input and output signals. The r and s signals denote signals originating by retroactivity upon interconnection [21].

erly timed as X does not transmit the desired signal. Methods to model and prevent retroactivity is the subject of this chapter.

To model a system with retroactivity, we add to the input/output modeling framework used so far, an additional input, called s , to model any change that may occur upon interconnection with a downstream system. That is, s models the fact that whenever y is taken as an input to a downstream system the value of y may change, because of the physics of the interconnection. This phenomenon is also called in the physics literature “the observer effect”, implying that no physical quantity can be measured without being altered by the measurement device. Similarly, we add a signal r as an additional output to model the fact that when a system is connected downstream of another one, it will send a signal upstream that will alter the dynamics of that system. More generally, we define a system S to have internal state x , two types of inputs, and two types of outputs: an input “ u ”, an output “ y ” (as before), a *retroactivity to the input* “ r ”, and a *retroactivity to the output* “ s ” (Figure 7.3). We will thus represent a system S by the equations

$$\frac{dx}{dt} = f(x, u, s), \quad y = h(x, u, s), \quad r = R(x, u, s), \quad (7.1)$$

where f , g , and R are arbitrary functions and the signals x , u , s , r , and y may be scalars or vectors. In such a formalism, we define the input/output model of the isolated system as the one in equation (7.1) without r in which we have also set $s = 0$.

Let S_i be a system with inputs u_i and s_i and with outputs y_i and r_i . Let S_1 and S_2 be two systems with disjoint sets of internal states. We define the interconnection of an upstream system S_1 with a downstream system S_2 by simply setting $y_1 = u_2$ and $s_1 = r_2$. For interconnecting two systems, we require that the two systems do not have internal states in common.

Inset. As a simple example, which may be more familiar to an engineering audience, consider the one-tank system shown on the left of Figure 7.4. We consider a constant input flow f_0 as input to the tank system and the pressure p at the output pipe is considered the output of the tank system. The corresponding output flow is given by $k\sqrt{p}$, in which k is a positive constant depending on the geometry of the system. The pressure p is given by (neglecting the atmospheric pressure for simplicity) $p = \rho h$, in which h is the height of the water level in the tank and ρ is

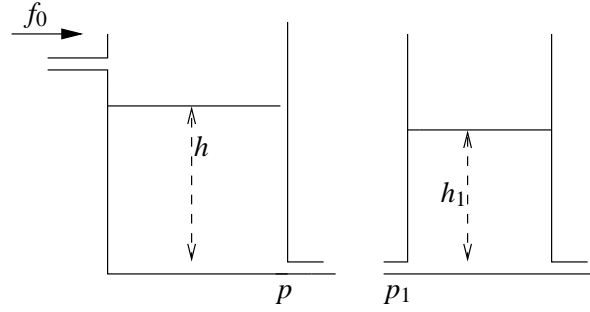


Figure 7.4: On the left, we represent a tank system that takes as input the constant flow f_0 and gives as output the pressure p at the output pipe. On the right, we show a downstream tank.

water density. Let A be the cross section of the tank, then the tank system can be represented by the equation

$$A \frac{dp}{dt} = \rho f_0 - \rho k \sqrt{p}. \quad (7.2)$$

Let us now connect the output pipe of the same tank to the input pipe of a downstream tank shown on the right of Figure 7.4. Let $p_1 = \rho h_1$ be the pressure generated by the downstream tank at its input and output pipes. Then, the flow at the output of the upstream tank will change and will now be given by $g(p, p_1) = k \sqrt{|p - p_1|}$ if $p > p_1$ and by $g(p, p_1) = -k \sqrt{|p - p_1|}$ if $p \leq p_1$. As a consequence, the time behavior of the pressure p generated at the output pipe of the upstream tank will change to

$$\begin{aligned} A \frac{dp}{dt} &= \rho f_0 - \rho g(p, p_1), \\ A_1 \frac{dp_1}{dt} &= \rho g(p, p_1) - \rho k_1 \sqrt{p_1}, \end{aligned} \quad (7.3)$$

in which A_1 is the cross section of the downstream tank and k_1 is a positive parameter depending on the geometry of the downstream tank. Thus, the input/output response of the tank measured in isolation (equation (7.2)) does not stay the same when the tank is connected through its output pipe to another tank (equation (7.3)).

◇

7.3 Retroactivity in Gene Circuits

In the previous section, we have defined retroactivity as a general concept modeling the fact that when an upstream system is input/output connected to a downstream one, its behavior can change. In this section, we focus on gene circuits and show what form retroactivity takes and what its net effects are.

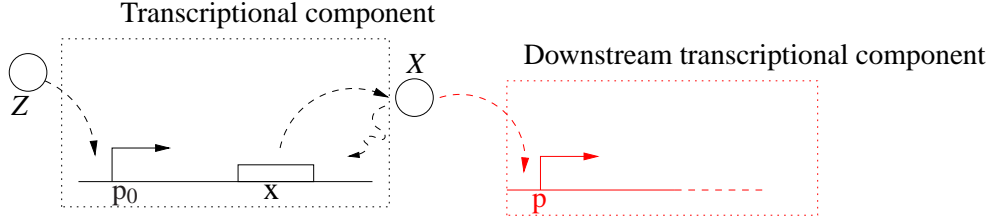


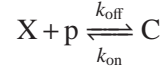
Figure 7.5: The transcriptional component takes as input u protein concentration Z and gives as output y protein concentration X . The transcription factor Z binds to operator sites on the promoter. The red part belongs to a downstream transcriptional component that takes protein concentration X as its input.

Consider the transcriptional system of Figure 7.5 in the dashed box. It is an input/output system that takes as input the transcription factor concentration Z and gives as output the transcription factor concentration $X(t)$. The activity of the promoter controlling gene x depends on the amount of Z bound to the promoter. If $Z = Z(t)$, such an activity changes with time. For simplifying notation, we denote it by $k(t)$. We assume here that the mRNA dynamics are at their quasi-steady state. The reader can verify that all the results hold unchanged when the mRNA dynamics are included (see exercises). We write the dynamics of X as

$$\frac{dX}{dt} = k(t) - \delta X, \quad (7.4)$$

in which δ is the decay rate of the protein. We refer to equation (7.4) as the *isolated system dynamics*.

Now, assume that X drives a downstream transcriptional module by binding to a promoter p with concentration p (Figure 7.5). The reversible binding reaction of X with p is given by



in which C is the complex protein-promoter and k_{on} and k_{off} are the binding and dissociation rates of the protein X to the promoter site p . Since the promoter is not subject to decay, its total concentration p_{tot} is conserved so that we can write $p + C = p_{\text{tot}}$. Therefore, the new dynamics of X are governed by the equations

$$\begin{aligned} \frac{dX}{dt} &= k(t) - \delta X + [k_{\text{off}}C - k_{\text{on}}(p_{\text{tot}} - C)X], \\ \frac{dC}{dt} &= -k_{\text{off}}C + k_{\text{on}}(p_{\text{tot}} - C)X, \end{aligned} \quad (7.5)$$

in which

$$s = k_{\text{off}}C - k_{\text{on}}(p_{\text{tot}} - C)X$$

. We refer to this system as *connected system*. The terms in the brackets represent the signal s , that is, the retroactivity to the output, while the second of equation

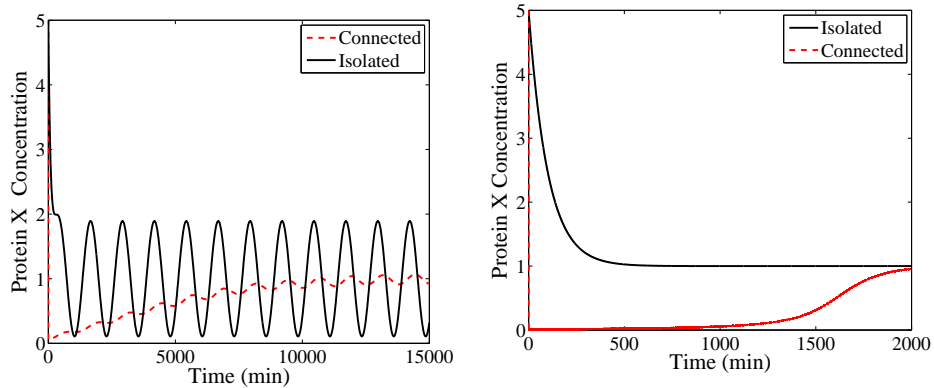


Figure 7.6: The effect of interconnection. Simulation results for the system in equations (7.5). The green plot (solid line) represents $X(t)$ originating by equations (7.4), while the blue plot (dashed line) represents $X(t)$ obtained by equation (7.5). Both transient and permanent behaviors are different. Here, $k(t) = 0.01(1 + \sin(\omega t))$ with $\omega = 0.005$ in the left side plots and $\omega = 0$ in the right side plots, $k_{\text{on}} = 10$, $k_{\text{off}} = 10$, $\delta = 0.01$, $p_{\text{tot}} = 100$, $X(0) = 5$. The choice of protein decay rate (in min^{-1}) corresponds to a half life of about one hour. The frequency of oscillations is chosen to have a period of about 12 times the protein half life in accordance to what is experimentally observed in the synthetic clock of [6].

(7.5) describes the dynamics of the downstream system driven by X . Then, we can interpret s as being a mass flow between the upstream and the downstream system. When $s = 0$, the first of equations (7.5) reduces to the dynamics of the isolated system given in equation (7.4).

How large is the effect of retroactivity s on the dynamics of X and what are the biological parameters that affect it? We focus on the retroactivity to the output s . We can analyze the effect of the retroactivity to the input r on the upstream system by simply analyzing the dynamics of Z , here modeled by $k(t)$, in the presence of its binding sites p_0 in Figure 7.5 in a way similar to how we analyze the dynamics of X in the presence of the downstream binding sites p .

The effect of retroactivity s on the behavior of X can be very large (Figure 7.6). By looking at Figure 7.6, we notice that the effect of retroactivity is to “slow down” the dynamics of $X(t)$ as the response time to a step input increases and the response to a periodic signal appears attenuated and phase-shifted. We will come back to this more precisely in the next section.

These effects are undesirable in a number of situations in which we would like an upstream system to “drive” a downstream one as is the case, for example, when a biological oscillator has to time a number of downstream processes. If, due to the retroactivity, the output signal of the upstream process becomes too low and/or out of phase with the output signal of the isolated system (as in Figure 7.6), the coordination between the oscillator and the downstream processes will be lost. We

next provide a procedure to obtain an operative quantification of the effect of the retroactivity on the dynamics of the upstream system.

Quantification of the retroactivity to the output

In this section, we provide a general approach to quantify the retroactivity to the output. To do so, we quantify the difference between the dynamics of X in the isolated system (7.4) and the dynamics of X in the connected system (7.5) by establishing conditions on the biological parameters that make the two dynamics close to each other. This is achieved by exploiting the difference of time scales between the protein production and decay processes and its binding and unbinding process to the promoter p . By virtue of this separation of time scales, we can approximate system (7.5) by a one dimensional system describing the evolution of X on the slow manifold (see Section 3.6).

Consider again the full system in equations (7.5), in which the binding and unbinding dynamics are much faster than protein production and decay, that is, $k_{\text{off}}, k_{\text{on}} \gg k(t), \delta$ and define $K_d = k_{\text{off}}/k_{\text{on}}$ as before. Even if the second equation goes to equilibrium very fast compared to the first one, the above system is not in standard singular perturbation form (see Section 3.6). To explicitly model the difference in time scales between the two equations of system (7.5), we introduce a parameter ϵ , which we define as $\epsilon = \delta/k_{\text{off}}$. Since $k_{\text{off}} \gg \delta$, we also have that $\epsilon \ll 1$. Substituting $k_{\text{off}} = \delta/\epsilon$, $k_{\text{on}} = \delta/(\epsilon K_d)$, and letting $y = X + C$ (the *total* protein concentration), we obtain the system in standard singular perturbation form

$$\frac{dy}{dt} = k(t) - \delta(y - C), \quad \epsilon \frac{dC}{dt} = -\delta C + \frac{\delta}{K_d}(p_{\text{tot}} - C)(y - C).$$

The reader can check as an exercise that the slow manifold of system (7.3) is locally exponentially stable (see exercises).

We can obtain an approximation of the dynamics of X in the limit in which ϵ is very small, by setting $\epsilon = 0$. This leads to

$$-\delta C + \frac{\delta}{K_d}(p_{\text{tot}} - C)X = 0 \rightarrow C = \gamma(X) \text{ with } \gamma(X) = \frac{p_{\text{tot}}X}{X + K_d}.$$

Since $\dot{y} = \dot{X} + \dot{C}$, we have that $\dot{y} = \dot{X} + (d\gamma/dX)\dot{X}$. This along with $\dot{y} = k(t) - \delta X$ lead to

$$\frac{d\bar{X}}{dt} = (k(t) - \delta\bar{X}) \left(\frac{1}{1 + d\gamma/d\bar{X}} \right). \quad (7.6)$$

The difference between the dynamics in equation (7.6) (the connected system after a fast transient) and the dynamics in equation (7.4) (the isolated system) is zero when the term $\frac{d\gamma(\bar{X})}{d\bar{X}}$ in equation (7.6) is zero. We thus consider the factor $\frac{d\gamma(\bar{X})}{d\bar{X}}$ as a quantification of the retroactivity s after a fast transient in the approximation in which $\epsilon \approx 0$. We can also interpret the factor $\frac{d\gamma(\bar{X})}{d\bar{X}}$ as a percentage variation of

the dynamics of the connected system with respect to the dynamics of the isolated system at the quasi steady state. We next determine the physical meaning of such a factor by calculating a more useful expression that is a function of key biochemical parameters.

By using the implicit function theorem, one can compute the following expression for $d\gamma(\bar{X})/d\bar{X}$:

$$\frac{d\gamma(\bar{X})}{d\bar{X}} = \frac{p_{\text{tot}}/K_d}{(\bar{X}/K_d + 1)^2} =: \mathcal{R}(\bar{X}). \quad (7.7)$$

The retroactivity measure \mathcal{R} is low basically whenever the ratio p_{tot}/K_d , which can be seen as an effective load, is low. This is the case if the affinity of the binding sites p is small (K_d large) or if p_{tot} is low. Also, the retroactivity measure is dependent on X in a nonlinear fashion and it is such that it is maximal when X is the smallest. The expression of $\mathcal{R}(\bar{X})$ provides an operative quantification of the retroactivity: such an expression can in fact be evaluated once the association and dissociation constants of X to p are known, the concentration of the binding sites p_{tot} is known, and \bar{X} is also known.

Summarizing, the modularity assumption introduced in Section 7.1 holds only when the value of $\mathcal{R}(\bar{X})$ is small enough. As a consequence, the design of a simple circuit can assume modularity if the interconnections among the composing modules can be designed so that the value of $\mathcal{R}(\bar{X})$ is low. From a design point of view, low retroactivity can be obtained by either choosing low-affinity binding sites p or making sure that the amounts of p is not too high. This can be guaranteed by placing the promoter sites p on low copy number plasmids or even on the chromosome (with copy number equal to 1). High copy number plasmids are expected to lead to non-negligible retroactivity effects on X .

However, in the presence of very low affinity and/or very low amount of promoter sites, the amount of complex C will be very low. As a consequence, the amplitude of the transmitted signal to downstream may be also very small. Hence, there will be a design compromise between guaranteeing a sufficiently high signal while minimizing retroactivity. A better approach is to design insulation devices (as opposed to designing the interconnection for low retroactivity) to buffer systems from retroactivity as explained later in the chapter.

Characterizing the effects of retroactivity

How do we explain the amplitude attenuation and phase shift due to retroactivity observed in Figure 7.6? In order to answer this question, we can linearize the system about its steady state and determine the effect of retroactivity on the frequency response. Let the input be $k(t) = \bar{k} + A_0 \sin(\omega t)$ and let $\bar{X} = \bar{k}/\delta$ and $\bar{C} = p_{\text{tot}}\bar{X}/(\bar{X} + K_d)$ be the equilibrium values corresponding to \bar{k} . The isolated system is already linear, so there is no need to perform linearization and the transfer

function from k to X is given by

$$T_I(s) = \frac{1}{s + \delta}.$$

For the connected system, denote the displacements with respect to the steady state $(\bar{k}, \bar{X}, \bar{C})$ by $\tilde{k} = k - \bar{k}$, $x = X - \bar{X}$, and $c = C - \bar{C}$. Then, the linearized dynamics are given by

$$\begin{aligned}\dot{x} &= \tilde{k}(t) - \delta x - \frac{\delta}{\epsilon K_d} x(p_{\text{tot}} - \bar{C}) + \frac{\delta}{\epsilon K_d} \bar{X}c + \frac{\delta}{\epsilon} c \\ \dot{c} &= \frac{\delta}{\epsilon K_d} x(p_{\text{tot}} - \bar{C}) - \frac{\delta}{\epsilon K_d} \bar{X}c - \frac{\delta}{\epsilon} c\end{aligned}$$

Letting $y := c + x$, these can be taken to standard singular perturbation form:

$$\begin{aligned}\dot{y} &= \tilde{k}(t) - \delta(y - c), \\ \epsilon \dot{c} &= \frac{\delta}{\epsilon K_d} x(p_{\text{tot}} - \bar{C}) - \frac{\delta}{\epsilon K_d} \bar{X}c - \frac{\delta}{\epsilon} c.\end{aligned}$$

Setting $\epsilon = 0$, gives the expression of the slow manifold as $c = x(p_{\text{tot}} - \bar{C})/(\bar{X}/K_d + 1) =: \bar{\gamma}(x)$, so that, using the facts that $\dot{x} + \dot{c} = \dot{y} = \tilde{k}(t) - \delta x$ and $\dot{c} = (d\bar{\gamma}/dx)\dot{x}$, we finally obtain the expression of the x dynamics on the slow manifold as

$$\dot{x} = (\tilde{k}(t) - \delta x) \frac{1}{1 + (p_{\text{tot}} - \bar{C})/(\bar{X}/K_d + 1)}.$$

Denoting $\bar{R} := (p_{\text{tot}} - \bar{C})/(\bar{X}/K_d + 1)$, we obtain the transfer function from \tilde{k} to x of the approximated connected system linearization as

$$T_C = \frac{1}{1 + \bar{R}} \frac{1}{s + \delta/(1 + \bar{R})}.$$

Hence, we have the following result for the frequency response amplitude and phase shift:

$$\begin{aligned}A_I(\omega) &= \frac{1}{\sqrt{\omega^2 + \delta^2}}, \quad \phi_I(\omega) = \tan^{-1}(-\omega/\delta), \\ A_C(\omega) &= \frac{1}{1 + \bar{R}} \frac{1}{\sqrt{\omega^2 + \delta^2/(1 + \bar{R})^2}}, \quad \phi_C(\omega) = \tan^{-1}(-\omega(1 + \bar{R})/\delta),\end{aligned}$$

from which one obtains that $A_I(0) = A_C(0)$ and, since $\bar{R} > 0$, the bandwidth of the connected system is lower than that of the isolated system. Also, the phase shift of the connected system will be larger than that of the isolated system.

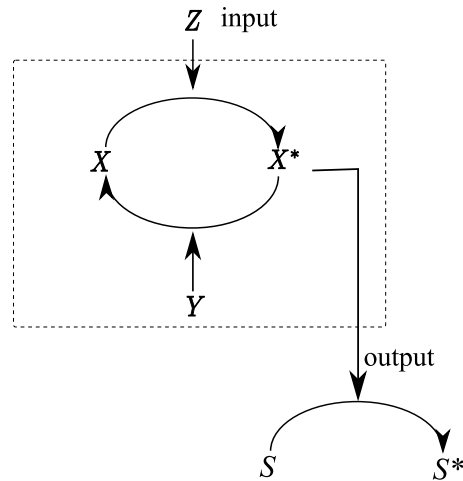


Figure 7.7: Covalent modification cycle (in the box) with its downstream system.

7.4 Retroactivity in Signaling Systems

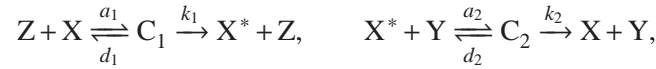
Signaling systems are circuits that take external stimuli and through a sequence of biomolecular reactions transform them to useful signals that establish how cells respond to their environment. These systems are usually composed of covalent modification cycles (phosphorylation, methylation, uridylation, etc.) connected in cascade fashion, in which each cycle has multiple downstream targets (or substrates). An example is that of the MAPK cascade, which we have analyzed in Section 2.5. Since covalent modification cycles always have downstream targets, such as DNA binding sites or other substrates, it is particularly important to understand whether and how retroactivity from these downstream systems affect the response of the upstream cycles to input stimulation. In this section, we study this question both for the steady state and dynamic response of a covalent modification cycle to its input (refer to Figure 7.7).

Steady state effects of retroactivity

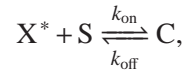
One important characteristic of signaling systems and, in particular, of covalent modification cycles, is the steady state characteristics (also called dose response). This describes the steady state output value in response to a constant input stimulation. For a single covalent modification cycle, this has been extensively studied as a function of important cycle parameters, such as the Michaelis-Menten constants and the total amount of protein. In particular, it was found that when the Michaelis-Menten constants are sufficiently small compared to the total protein amount, the cycle characteristic becomes ultrasensitive, a condition called zero-order ultrasen-

sitivity (Section 2.4).

However, when the cycle is interconnected to its downstream targets, this characteristic may change shape. In order to understand how this may change, we rewrite the reaction rates and corresponding differential equation model for the covalent modification cycle incorporating the binding of X^* to its downstream targets. Referring to Figure 7.7, we have the following reactions:



to which we add the binding reaction of X^* with its substrates S :



in which C is the complex of X^* with S . In addition to this, we have the conservation laws $X_{\text{tot}} = X^* + X + C_1 + C_2 + C$, $Z + C_1 = Z_{\text{tot}}$, and $Y + C_2 = Y_{\text{tot}}$. The rate equations governing the system are given by

$$\begin{aligned} \frac{dC_1}{dt} &= a_1 X Z - (d_1 + k_1) C_1 \\ \frac{dX^*}{dt} &= -a_2 X^* Y + d_2 C_2 + k_1 C_1 - k_{\text{on}} S X^* + k_{\text{off}} C \\ \frac{dC_2}{dt} &= a_2 X^* Y - (d_2 + k_2) C_2 \\ \frac{dC}{dt} &= k_{\text{on}} X^* S - k_{\text{off}} C. \end{aligned}$$

The input/output characteristics are found by solving this system for the equilibrium. In particular, by setting $dC_1/dt = 0$, $dC_2/dt = 0$, using that $Z = Z_{\text{tot}} - C_1$ and that $Y = Y_{\text{tot}} - C_2$, we obtain the familiar expressions for the complexes:

$$C_1 = \frac{Z_{\text{tot}} X}{K_1 + X}, \quad C_2 = \frac{Y_{\text{tot}} X^*}{K_2 + X^*}, \quad \text{with } K_1 = \frac{d_1 + k_1}{a_1} \text{ and } K_2 = \frac{d_2 + k_2}{a_2}.$$

By setting $dX^*/dt + dC_2/dt + dC/dt = 0$, we obtain $k_1 C_2 = k_2 C$, which leads to

$$V_1 \frac{X}{K_1 + X} = V_2 \frac{X^*}{K_2 + X^*}, \quad V_1 = k_1 Z_{\text{tot}} \text{ and } V_2 = k_2 Y_{\text{tot}}. \quad (7.8)$$

By assuming that the substrate X_{tot} is in excess compared to the enzymes, we have that $C_1, C_2 \ll X_{\text{tot}}$ so that $X \approx X_{\text{tot}} - X^* - C$, in which (from setting $dC/dt = 0$) $C = X^* S / K_d$ with $K_d = k_{\text{off}} / k_{\text{on}}$, leading to $X \approx X_{\text{tot}} - X^* (1 + S / K_d)$. Calling $\lambda = S / K_d$, equation (7.8) finally leads to

$$y := \frac{V_1}{V_2} = \frac{X^* \left(\frac{K_1}{1+\lambda} + \left(\frac{X_{\text{tot}}}{1+\lambda} - X^* \right) \right)}{(K_2 + X^*) \left(\frac{X_{\text{tot}}}{1+\lambda} - X^* \right)}. \quad (7.9)$$

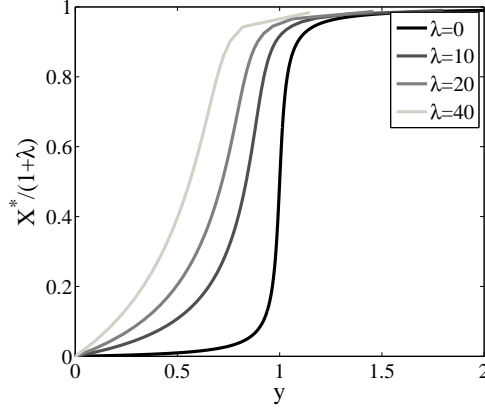


Figure 7.8: The addition of downstream target sites make the input/output characteristic more linear-like, that is, retroactivity makes a switch-like response into a more graded response.

Here, we can interpret λ as an effective load, which increases with the amount of targets of X^* but also with the affinity of these targets ($1/K_d$). The ratio $V_1/V_2 = y$ can be viewed as a normalized input stimulation as it linearly increases with the input Z_{tot} .

We are interested in the shape of the steady state curve of X^* as function of y . This shape is often characterized by two key parameters: the response coefficient, denoted R , and the point of half maximal induction, denoted y_{50} . Let y_α denote the value of y corresponding to having X^* equal $\alpha\%$ of the maximum value of X^* obtained for $y = \infty$. Then, the response coefficient (see Section 2.4)

$$R = \frac{y_{90}}{y_{10}},$$

measures how switch-like the response is.

In the case of the current system, we have that the maximal value of X^* obtained as $y \rightarrow \infty$ is given by $X_{\text{tot}}/(1 + \lambda)$. Hence, from equation (7.9), we have that

$$y_{90} = \frac{(\bar{K}_1 + 0.1)0.9}{(\bar{K}_2(1 + \lambda) + 0.9)0.1}, \quad y_{10} = \frac{(\bar{K}_1 + 0.9)0.1}{(\bar{K}_2(1 + \lambda) + 0.1)0.9}, \quad \bar{K}_1 := \frac{K_1}{X_{\text{tot}}}, \quad K_2 = \frac{K_2}{X_{\text{tot}}},$$

so that

$$R = 81 \frac{(\bar{K}_1 + 0.1)(\bar{K}_2(1 + \lambda) + 0.1)}{(\bar{K}_2(1 + \lambda) + 0.9)(\bar{K}_1 + 0.9)}.$$

One can check that this is a monotonically increasing function of λ . In particular, as λ increases, the value of R tends to $81(\bar{K}_1 + 0.1)/(\bar{K}_2 + 0.9)$, which, in turn, tends to 81 for $\bar{K}_1, \bar{K}_2 \rightarrow \infty$. When $\lambda = 0$, we recover the results of Section 2.4, according

to which R approaches 81 (Michelis-Menten type of response) for \bar{K}_1, \bar{K}_2 large, while R decreases for decreasing values of \bar{K}_1, \bar{K}_2 , corresponding to an ultrasensitive response. Independently of the values of \bar{K}_1 and \bar{K}_2 , the addition of the load makes any characteristic more linear-like (see Figure 7.8). This finding has been experimentally confirmed employing signal transduction circuits reconstituted *in vitro* [?].

We can also study the behavior of the point of half maximal induction

$$y_{50} = \frac{\bar{K}_1 + 0.5}{\bar{K}_2(1 + \lambda) + 0.5},$$

to find that as λ increases, it decreases. That is, as more downstream load is applied, a smaller stimulus is required to obtain a significant response of the output (see exercises).

Dynamic effects of retroactivity

In order to understand the dynamic effects of retroactivity on the signaling module, we seek a one dimensional approximation of the X^* dynamics, which can be easily analyzed. To do so, we exploit time scale separation and apply singular perturbation analysis.

Specifically, we have that $a_i, d_i, k_{\text{on}}, k_{\text{off}} \gg k_1, k_2$, so we can choose as a small parameter $\epsilon = k_1/k_{\text{off}}$ and slow variable $y = X^* + C_1 + C_2$. By setting $\epsilon = 0$, we obtain that $C_1 = Z_{\text{tot}}X/(K_1 + X)$, $C_2 = Y_{\text{tot}}X^*/(K_2 + X^*) =: \gamma(X^*)$, and $C = \lambda X^*$, in which Z_{tot} is now a time-varying signal. Hence, the dynamics of the slow variable y on the slow manifold is given by

$$\frac{dy}{dt} = k_1 \frac{Z_{\text{tot}}(t)X}{K_1 + X} - k_2 Y_{\text{tot}} \frac{X^*}{X^* + K_2}.$$

Using $\dot{y} = \dot{X}^* + \dot{C}_1 + \dot{C}_2$, $\dot{C}_1 = \lambda \dot{X}^*$, $\dot{C}_2 = \partial\gamma/\partial X^* \dot{X}^*$, and the conservation law $X = X_{\text{tot}} - X^*(1 + \lambda)$, we finally obtain the approximated X^* dynamics as

$$\frac{dX^*}{dt} = \frac{1}{1 + \lambda} \left(k_1 \frac{Z_{\text{tot}}(t)(X_{\text{tot}} - X^*(1 + \lambda))}{K_1 + (X_{\text{tot}} - X^*(1 + \lambda))} - k_2 Y_{\text{tot}} \frac{X^*}{X^* + K_2} \right), \quad (7.10)$$

where we have assumed that that $Y_{\text{tot}}/K_2 \ll S/K_d$, so that the effect of the binding dynamics of X^* with Y (modeled by $\partial\gamma/\partial X^*$) is negligible with respect to λ . The reader can verify this derivation as an exercise (see exercises).

From this expression, one can understand immediately the effect of the load λ on the rise time and decay time in response to extreme input stimuli. For the decay time, one has to assume an initial condition $X^*(0) \neq 0$ and $Z_{\text{tot}}(t) = 0$ for all t . In this case, we have that

$$\frac{dX^*}{dt} = -k_2 Y_{\text{tot}} \frac{X^*}{X^* + K_2} \frac{1}{1 + \lambda},$$

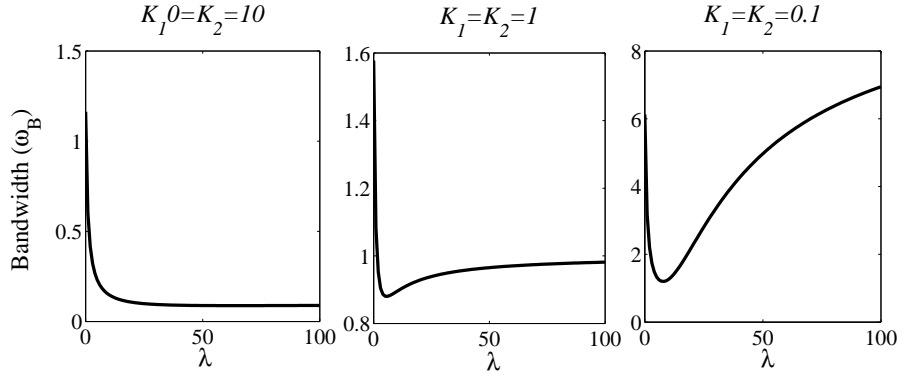


Figure 7.9: Behavior of the bandwidth as a function of the load for different values of the Michaelis-Menten constants K_1, K_2 .

from which, since $\lambda > 0$, it is apparent that the transient will be slower and hence that the system will have an increased decay time due to retroactivity. For the rise time, one can assume $Z_{\text{tot}} \approx \infty$ and $X^*(0) = 0$. Hence, we have that

$$(1 + \lambda) \frac{dX^*}{dt} = \left(k_1 \frac{Z_{\text{tot}}(t)(X_{\text{tot}} - X^*(1 + \lambda))}{K_1 + (X_{\text{tot}} - X^*(1 + \lambda))} \right),$$

which is the same expression for the isolated system in which X^* is scaled by $(1 + \lambda)$. So, the rise time is not affected.

In order to understand how the bandwidth of the system is affected by retroactivity, we consider $Z_{\text{tot}}(t) = \bar{Z} + A_0 \sin(\omega t)$. Let \bar{X} be the equilibrium of X^* corresponding to \bar{Z} and denote the displacements $z = Z_{\text{tot}} - \bar{Z}$ and $x = X^* - \bar{X}$. The linearized dynamics is given by

$$\dot{x} = -a(\lambda)x + b(\lambda)z(t),$$

in which

$$a(\lambda) = \frac{1}{1 + \lambda} \left(k_1 \bar{Z} \frac{K_1(1 + \lambda)}{(K_1 + (X_{\text{tot}} - \bar{X}(1 + \lambda)))^2} + k_2 Y_{\text{tot}} \frac{K_2}{(K_2 + \bar{X})^2} \right)$$

and

$$b(\lambda) = \frac{k_1}{1 + \lambda} \left(\frac{X_{\text{tot}} - \bar{X}(1 + \lambda)}{K_1 + (X_{\text{tot}} - \bar{X}(1 + \lambda))} \right),$$

so that the bandwidth of the system is given by $\omega_B = a(\lambda)$.

Figure 7.9 shows the behavior of the bandwidth as a function of the load. When the isolated system static characteristics are hyperbolic ($K_1, K_2 \gg X_{\text{tot}}$), the bandwidth monotonically decreases with the load. Hence applying any load decreases

system bandwidth. When the isolated system static characteristics are ultrasensitive ($K_1, K_2 \ll X_{\text{tot}}$), the bandwidth of the connected system can be larger than that of the isolated system for sufficiently large amounts of loads. In these conditions, one should expect that the response of the connected system becomes faster than that of the isolated system.

7.5 Insulation Devices: Retroactivity Attenuation

As explained earlier, it is not always possible or advantageous to design the downstream system so that it applies low retroactivity. This is because the downstream system may have already been designed and optimized for other purposes. A better approach, in analogy to what is performed in electrical circuits, is to design a device to be placed between the upstream system (the oscillator, for example) and the downstream load so that the device output is not changed by the load and the device does not affect the behavior of the upstream system. That is, the output of the device should follow the prescribed behavior independently of any loading applied by a downstream system.

Specifically, consider a system S such as the one shown in Figure 7.3 that takes u as input and gives y as output. We would like to design such a system so that

- (a) the retroactivity r to the input is very small;
- (b) the effect of the retroactivity s to the output on the internal dynamics of the system is very small independently of s itself;

Such a system is said to enjoy the *insulation* property and will be called an insulation device. Indeed, such a system will not affect an upstream system because $r \approx 0$ and it will keep the same output signal y *independently* of any connected downstream system.

Retroactivity to the input

In electronic amplifiers, r is very small because the input stage of an op amp absorbs almost zero current (Figure ??). This way, there is no voltage drop across the output impedance of an upstream voltage source. Equation (7.7) quantifies the effect of retroactivity on the dynamics of X as a function of biochemical parameters that characterize the interconnection mechanism with a downstream system. These parameters are the affinity of the binding site $1/K_d$, the total concentration of such binding site p_{tot} , and the level of the signal $X(t)$. Therefore, to reduce the retroactivity, we can choose parameters such that (7.7) is small. A sufficient condition is to choose K_d large (low affinity) and p_{tot} small, for example. Having small value of p_{tot} and/or low affinity implies that there is a small “flow” of protein X toward its target sites. Thus, we can say that a low retroactivity to the input is obtained when the “input flow” to the system is small.

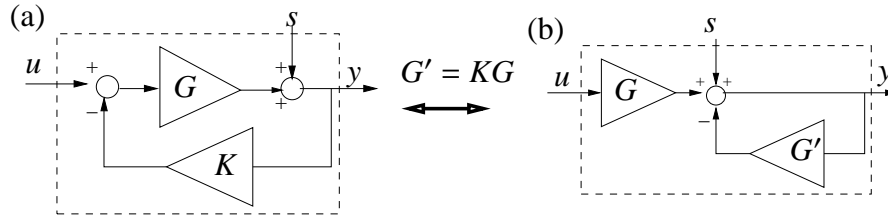


Figure 7.10: Diagram (a) shows the basic feedback/amplification mechanism by which amplifiers attenuate the effect of the retroactivity to the output s . Diagram (b) shows an alternative representation of the same mechanism of diagram (a), which will be employed to design biological insulation devices.

Attenuation of retroactivity to the output: Principle 1

The basic mechanism for retroactivity attenuation is based on the concept of disturbance attenuation presented in Section 3.2. In its simplest form, it can be illustrated by diagram (a) of Figure 7.10, in which the retroactivity to the output s plays the same role as an additive disturbance. For large gains G , the effect of the retroactivity s to the output is negligible as the following simple computation shows. The output y is given by

$$y = G(u - Ky) + s,$$

which leads to

$$y = u \frac{G}{1 + KG} + \frac{s}{1 + KG}.$$

As G grows, y tends to u/K , which is independent of the retroactivity s .

Therefore, a central enabler to attenuate the retroactivity effect at the output of a component is to (1) amplify the input of the component through a large gain and (2) apply a large negative output feedback. The inset illustrates this general idea in the context of a simple hydraulic system.

Inset. Consider the academic hydraulic example consisting of two connected tanks shown in Figure 7.11. The objective is to attenuate the effect of the pressure applied from the downstream tank to the upstream tank, so that the output pressure of the upstream system does not change when the downstream tank is connected. We let the input flow f_0 be amplified by a large factor G . Also, we consider a large pipe in the upstream tank with output flow $G' \sqrt{p}$, with $G' \gg k$ and $G' \gg k_1$. Let p be the pressure at the output pipe of the upstream tank and p_1 the pressure at the bottom of the downstream tank. One can verify that the only equilibrium value for the pressure p at the output pipe of the upstream tank is obtained for $p > p_1$ and it is given by

$$p_{eq} = \left(\frac{Gf_0}{G' + (kk_1)/\sqrt{k_1^2 + k^2}} \right)^2.$$

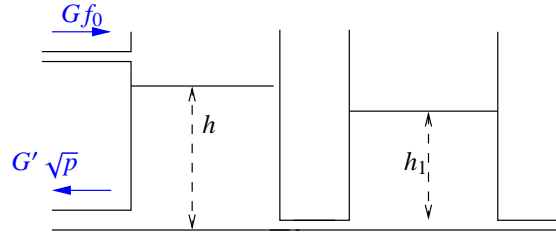


Figure 7.11: We amplify the input flow f_0 through a large gain G and we apply a large negative feedback by employing a large output pipe with output flow $G' \sqrt{p}$.

If we let G' be sufficiently larger than k_1 and k and we let $G' = KG$ for some positive $K = O(1)$, then for G sufficiently large $p_{eq} \approx (f_0/K)^2$, which does not depend on the presence of the downstream system. In fact, it is the same as the equilibrium value of the isolated upstream system $A \frac{dp}{dt} = \rho G f_0 - \rho G' \sqrt{p} - \rho k \sqrt{p}$ for G sufficiently large and for $G' = KG$ with $K = O(1)$.

◇

Going back to the transcriptional example, consider the approximated dynamics of equation (7.6) for X . Let us thus assume that we can apply a gain G to the input $k(t)$ and a negative feedback gain G' to X with $G' = KG$. This leads to the new differential equation for the connected system (7.6) given by

$$\frac{dX}{dt} = (Gk(t) - (G' + \delta)X)(1 - d(t)), \quad (7.11)$$

in which we have defined $d(t) = (d\gamma/dX)/(1 + d\gamma/dX)$. Since $d(t) < 1$, letting $G' = KG$, we can verify (see exercises) that as G grows $X(t)$ tends to $k(t)/K$ for both the connected system in the form of equation (7.11) and the isolated system

$$\frac{dX}{dt} = Gk(t) - (G' + \delta)X. \quad (7.12)$$

That is, the solutions $X(t)$ of the connected and isolated system tend to each other as G increases. As a consequence, the presence of the disturbance term $d(t)$ will not significantly affect the time behavior of $X(t)$. Since $d(t)$ is a measure of retroactivity, its effect on the behavior of $X(t)$ is attenuated by employing large gains G and G' .

The next questions we address is how we can implement such amplification and feedback gains in a biomolecular system.

Biomolecular realizations of Principle 1

In the previous section, we have proposed a general principle to attenuate the retroactivity to the output. Such a principle consists of a large amplification of the input and a large negative output feedback. In this section, we determine two

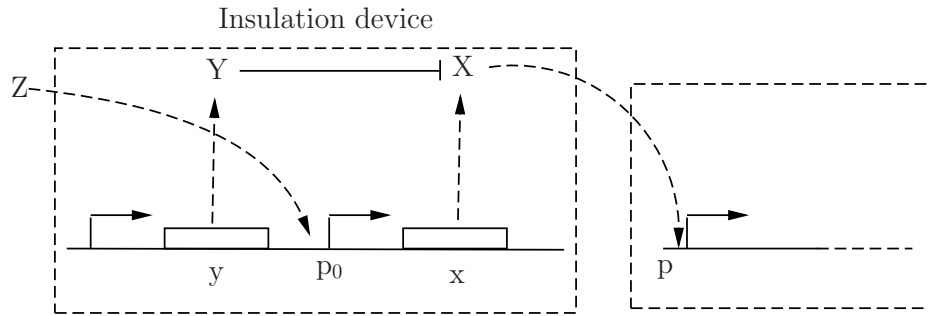


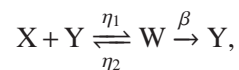
Figure 7.12: In this design, the input Z is amplified through a strong promoter p_0 . The negative feedback on the output X is obtained by enhancing its degradation through the protease Y .

possible biomolecular implementations to obtain a large amplification gain to the input Z of the insulation component and a large negative feedback on the output X . Both mechanisms realize the negative feedback through enhanced degradation. The first design realizes amplification through transcriptional activation, while the second design through phosphorylation.

Design 1: Amplification through transcriptional activation

In this design, we obtain a large amplification of the input signal $Z(t)$ by having promoter p_0 (to which Z binds) be a strong, non-leaky promoter. The negative feedback mechanism on X relies on enhanced degradation of X . Since this must be large, one possible way to obtain an enhanced degradation for X is to have a protease, called Y , be expressed by a strong constitutive promoter. The protease Y will cause a degradation rate for X , which is larger if Y is more abundant in the system. This design is schematically shown in Figure 7.12.

In order to investigate whether such a design realizes a large amplification and a large negative feedback on X as needed, we analyze the full input/output model for the block in the dashed box of Figure 7.12. In particular, the expression of gene x is assumed to be a two-step process, which incorporates also the mRNA dynamics. Incorporating these dynamics in the model is relevant for the current study because they may contribute to an undesired delay between the Z and X signals. The reaction of the protease Y with protein X is modeled as the two-step reaction



which can be found in Section 2.3.

The input/output system model of the insulation component that takes Z as an

input and gives X as an output is given by the following equations

$$\frac{dZ}{dt} = k(t) - \delta Z + [k_- Z_p - k_+ Z(p_{0,TOT} - Z_p)] \quad (7.13)$$

$$\frac{dZ_p}{dt} = k_+ Z(p_{0,TOT} - Z_p) - k_- Z_p \quad (7.14)$$

$$\frac{dm_X}{dt} = GZ_p - \delta_1 m_X \quad (7.15)$$

$$\frac{dW}{dt} = \eta_1 XY - \eta_2 W - \beta W \quad (7.16)$$

$$\frac{dY}{dt} = -\eta_1 YX + \beta W + \alpha G - \gamma Y + \eta_2 W \quad (7.17)$$

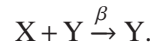
$$\frac{dX}{dt} = \nu m_X - \eta_1 YX + \eta_2 W - \delta_2 X + [k_{\text{off}} C - k_{\text{on}} X(p_{\text{tot}} - C)] \quad (7.18)$$

$$\frac{dC}{dt} = -k_{\text{off}} C + k_{\text{on}} X(p_{\text{tot}} - C), \quad (7.19)$$

in which we have assumed that the expression of gene z is controlled by a promoter with activity $k(t)$. In this system, we have denoted by k_+ and k_- the association and dissociation rates of Z with its promoter site p_0 in total concentration $p_{0,\text{tot}}$ is the total concentration of the promoter p_0 . Also, Z_p denotes the complex of Z with such a promoter site. m_X is the concentration of mRNA of X , C is the concentration of X bound to the downstream binding sites with total concentration p_{tot} , and γ is the decay rate of the protease Y . The promoter controlling gene y has strength αG , for some constant α , and it has the same order of magnitude strength as the promoter controlling x .

The terms in the square brackets in equation (7.13) represent the retroactivity r to the input of the insulation component in Figure 7.12. The terms in the box in equation (7.18) represent the retroactivity s to the output of the insulation component of Figure 7.12. The dynamics of equations (7.13)–(7.19) without s (the elements in the box in equation (7.18)) describe the dynamics of X with no downstream system.

Equations (7.13) and (7.14) simply determine the signal $Z_p(t)$ that is the input to equations (7.15)–(7.19). For the discussion regarding the attenuation of the effect of s , it is not relevant what the specific form of signal $Z_p(t)$ is. Let then $Z_p(t)$ be any bounded signal $\nu(t)$. Since equation (7.15) takes $\nu(t)$ as an input, we will have that $m_X = G\bar{\nu}(t)$, for a suitable signal $\bar{\nu}(t)$. Let us assume for the sake of simplifying the analysis that the protease reaction is a one step reaction, that is,



Therefore, equation (7.17) simplifies to

$$\frac{dY}{dt} = \alpha G - \gamma Y$$

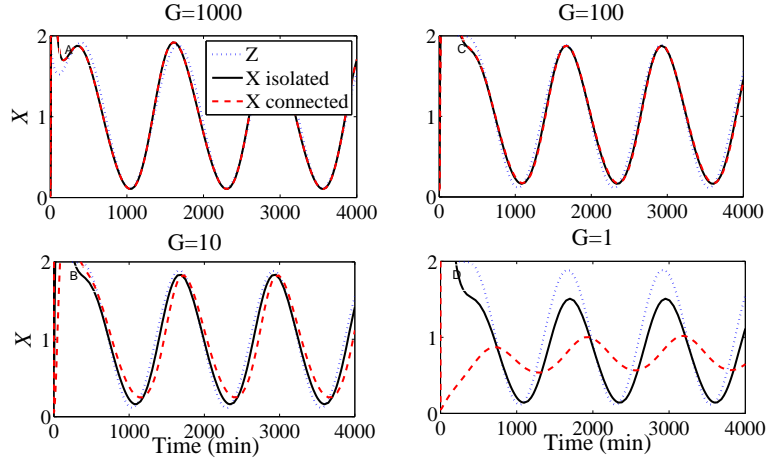


Figure 7.13: Design 1: results for different gains G . In all plots, $k(t) = 0.01(1 + \sin(\omega t))$, $p_{\text{tot}} = 100$, $k_{\text{off}} = k_{\text{on}} = 10$, $\delta = 0.01$, and $\omega = 0.005$. The parameter values are $\delta_1 = 0.01$, $p_{0,TOT} = 1$, $\eta_1 = \eta_2 = \beta = \gamma = 0.01$, $k_- = 200$, $k_+ = 10$, $\alpha = 0.1$, $\delta_2 = 0.1$, $\nu = 0.1$, and $G = 1000, 100, 10, 1$. The retroactivity to the output is not well attenuated for values of the gain $G = 1$ and the attenuation capability begins to worsen for $G = 10$.

and equation (7.18) simplifies to

$$\frac{dX}{dt} = \nu m_X - \beta Y X - \delta_2 X + k_{\text{off}} C - k_{\text{on}} X (p_{\text{tot}} - C).$$

If we consider the protease to be at its equilibrium, we have that $Y(t) = \alpha G / \gamma$.

As a consequence, the X dynamics become

$$\frac{dX}{dt} = \nu G \bar{\nu}(t) - (\beta \alpha G / \gamma + \delta_2) X + k_{\text{off}} C - k_{\text{on}} X (p_{\text{tot}} - C),$$

with C determined by equation (7.19). By using the same singular perturbation argument employed in the previous section, we obtain that the dynamics of X will be (after a fast transient) approximatively given by

$$\frac{dX}{dt} = (\nu G \bar{\nu}(t) - (\beta \alpha G / \gamma + \delta_2) X) (1 - d(t)), \quad (7.20)$$

in which $0 < d(t) < 1$ is the retroactivity measure. Then, as G increases, $X(t)$ becomes closer to the solution of the isolated system

$$\frac{dX}{dt} = \nu G \bar{\nu}(t) - (\beta \alpha G / \gamma + \delta_2) X,$$

as explained in the previous section.

We now turn to the question of minimizing the retroactivity to the input r because its effect can alter the input signal $Z(t)$. In order to decrease r , we guarantee that the retroactivity measure given in equation (7.7) in which we substitute Z in place of X and $p_{0,\text{tot}}$ in place of p_{tot} , is small. This is seen to be true if $(\bar{K}_d + Z)^2 / (p_{0,\text{tot}} \bar{K}_d)$ is very large, in which $1/\bar{K}_d = k_+/k_-$ is the affinity of the binding site p_0 to Z . Since after a short transient, $Z_p = (p_{0,\text{TOT}} Z) / (\bar{K}_d + Z)$, for Z_p not to be a distorted version of Z , it is enough to ask that $\bar{K}_d \gg Z$. This, combined with the requirement that $(\bar{K}_d + Z)^2 / (p_{0,\text{tot}} \bar{K}_d)$ is very large, leads to the requirement $p_{0,\text{tot}} / \bar{K}_d \ll 1$. Summarizing, for not having distortion effects between Z and Z_p and small retroactivity r , we need that

$$\bar{K}_d \gg Z \text{ and } p_{0,\text{tot}} / \bar{K}_d \ll 1. \quad (7.21)$$

Simulation results are presented for the insulation system of equations (7.13)–(7.19) as the mathematical analysis of such a system is only valid under the approximation that the protease reaction is a one step reaction. In all simulations, we consider protein decay rates to be 0.01 min^{-1} to obtain a protein half life of about one hour. We consider always a periodic forcing $k(t) = 0.01(1 + \sin(\omega t))$, in which we assume that such a periodic signal has been generated by a synthetic biological oscillator. Therefore, the oscillating signals are chosen to have a period that is about 12 times the protein half life in accordance to what is experimentally observed in the synthetic clock of [6]. All simulation results were obtained by using MATLAB (Simulink), with variable step ODE solver ODE23s.

For large gains ($G = 1000, G = 100$), the performance considerably improves compared to the case in which X was generated by a plain transcriptional component accepting Z as an input (Figure 7.6). For lower gains ($G = 10, G = 1$), the performance starts to degrade for $G = 10$ and becomes not acceptable for $G = 1$ (Figure 7.13). Since we can view G as the number of transcripts produced per unit time (one minute) per complex of protein Z bound to promoter p_0 , values $G = 100, 1000$ may be difficult to realize *in vivo*, while the values $G = 10, 1$ could be more easily realized. The values of the parameters chosen in Figure 7.13 are such that $\bar{K}_d \gg Z$ and $p_{0,\text{TOT}} \ll \bar{K}_d$. This is enough to guarantee that there is small retroactivity r to the input of the insulation device independently of the value of the gain G , according to relations (7.21). The poorer performance of the device for $G = 1$ is therefore entirely due to poor attenuation of the retroactivity s to the output.

To obtain a large gain, we need to guarantee high expression of the protease. This may be difficult to do because in general proteases are not specific and target for degradations all proteins. Hence, global undesired effects on the cll behavior may result. The next design avoids this problem by using dephosphorylation as the mechanism for enhanced degradation.

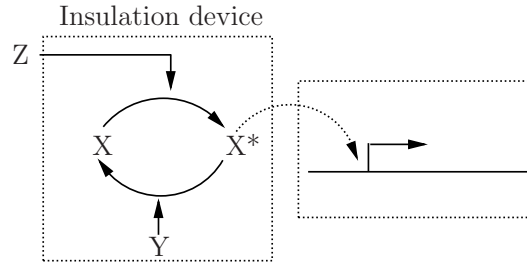
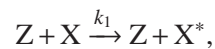


Figure 7.14: In this design, negative feedback occurs through a phosphatase Y that converts the active form X^* back to its inactive form X . Amplification occurs through Z activating the phosphorylation of X .

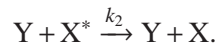
Design 2: Amplification through phosphorylation

In this design, the amplification gain G of Z is obtained by having Z activate the phosphorylation of a protein X , which is available in the system in abundance. That is, Z is a kinase for a protein X . The negative feedback gain G' on X^* is obtained by having a phosphatase Y activate the dephosphorylation of active protein X^* . Protein Y is also available in abundance in the system. This mechanism is depicted in Figure 7.14. A similar design has been proposed by [76, 77], in which a MAPK cascade plus a negative feedback loop that spans the length of the MAPK cascade is considered as a feedback amplifier. The design presented here is much simpler as it involves only one phosphorylation cycle and does not require any explicit feedback loop. In fact, a strong negative feedback can be realized by the action of the phosphatase that converts the active protein form X^* back to its inactive form X .

We consider a simplified model for the phosphorylation and dephosphorylation processes, which will help in obtaining a conceptual understanding of what reactions realize the desired gains G and G' . The one step model that we consider is the same as considered in Chapter 2 (Exercise 2.6):



and



We assume that there is an abundance of protein X and of phosphatase Y in the system and that these quantities are conserved. The conservation of X gives $X + X^* + C = X_{\text{tot}}$, in which X is the inactive protein, X^* is the phosphorylated protein that binds to the downstream sites p , and C is the complex of the phosphorylated

protein X^* bound to the promoter p . The X^* dynamics can be described by the first equation in the following model

$$\frac{dX^*}{dt} = k_1 X_{\text{tot}} Z(t) \left(1 - \frac{X^*}{X_{\text{tot}}} - \left[\frac{C}{X_{\text{tot}}} \right] \right) - k_2 Y X^* + [k_{\text{off}} C - k_{\text{on}} X^* (p_{\text{tot}} - C)] \quad (7.22)$$

$$\frac{dC}{dt} = -k_{\text{off}} C + k_{\text{on}} X^* (p_{\text{tot}} - C). \quad (7.23)$$

The terms in the square brackets represent the retroactivity s to the output of the insulation system of Figure 7.14. For a weakly activated pathway [38], $X^* \ll X_{\text{tot}}$. Also, if we assume that the concentration of total X is large compared to the concentration of the downstream binding sites, that is, $X_{\text{tot}} \gg p_{\text{tot}}$, equation (7.22) is approximately equal to

$$\frac{dX^*}{dt} = k_1 X_{\text{tot}} Z(t) - k_2 Y X^* + k_{\text{off}} C - k_{\text{on}} X^* (p_{\text{tot}} - C).$$

Let $G = k_1 X_{\text{tot}}$ and $G' = k_2 Y$. Exploiting again the difference of time scales between the X^* dynamics and the C dynamics, after a fast initial transient the dynamics of X^* can be well approximated by

$$\frac{dX^*}{dt} = (GZ(t) - G'X^*)(1 - d(t)), \quad (7.24)$$

in which $0 < d(t) < 1$ is the retroactivity contribution. Therefore, for G and G' large enough, $X^*(t)$ tends to the solution $X^*(t)$ of the isolated system $\frac{dX^*}{dt} = GZ(t) - G'X^*$, as explained in Section 7.5. As a consequence, the effect of the retroactivity to the output s is attenuated by increasing $k_1 X_{\text{tot}}$ and $k_2 Y$ enough. That is, to obtain large input and feedback gains, one should have large phosphorylation/dephosphorylation rates and/or a large amount of protein X and phosphatase Y in the system. This reveals that the values of the phosphorylation/dephosphorylation rates cover an important role toward the realization of the insulation property of the module of Figure 7.14.

From a practical point of view, the effective rates can be increased by increasing the total amounts of X and Y , which can be done by placing the corresponding genes under the control of inducible promoters. Experiments performed on a covalent modification cycle reconstituted *in vitro*, showed that increasing these protein amounts is an effective means to attain insulation [45].

Attenuation of retroactivity to the output: Principle 2

In this section, we present a more general mechanism for insulation, that is not inspired by the design of electrical circuits and is naturally implemented by the structure of biomolecular systems. For this purpose, consider Figure 7.15. We illustrate how the system can achieve insulation from s whenever its internal dynamics is

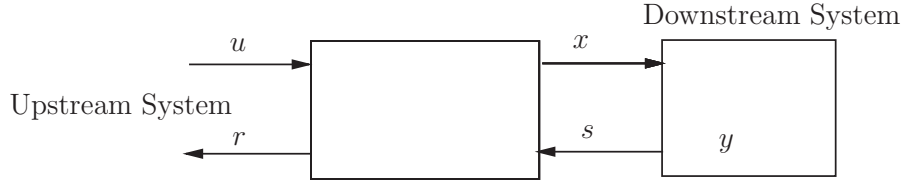


Figure 7.15: Interconnection of a device with input u and output x to a downstream system with internal state y applying retroactivity s .

much faster compared to the dynamics of the input u . To this end, we consider the following simple structure in which (for simplicity) we assume that all variables are scalar:

$$\begin{aligned}\frac{du}{dt} &= f_0(u, t) + r(u, x) \\ \frac{dx}{dt} &= Gf_1(x, u) + \bar{G}s(x, u) \\ \frac{dy}{dt} &= -\bar{G}s(x, y).\end{aligned}\tag{7.25}$$

Here, $G \gg 1$ models the fact that the internal dynamics of the device is much faster than that of the input; similarly, $\bar{G} \gg 1$ models the fact that the dynamics of the interconnection with downstream systems is also fast (as it is usually the case, being it due to binding mechanisms). The claim that we make about this system is the following.

If $G \gg 1$ and the Jacobian of f_1 has eigenvalues with negative real part, then $x(t)$ is not affected by retroactivity s after a short initial transient, independently of the value of \bar{G} .

This result states that independently of the characteristics of the downstream system, the device can be tuned (by making G large enough) so to function as an insulation device. To clarify why this would be the case, it is useful to rewrite the above system in standard singular perturbation form by employing $\epsilon := 1/G$ as a small parameter and $\tilde{x} := x + y$ as the slow variable. Hence, it can be re-written as

$$\begin{aligned}\frac{du}{dt} &= f_0(u, t) + r(u, x) \\ \epsilon \frac{d\tilde{x}}{dt} &= f_1(\tilde{x} - y, u) \\ \frac{dy}{dt} &= -\bar{G}s(\tilde{x} - y, y).\end{aligned}\tag{7.26}$$

Since $\partial f_1 / \partial \tilde{x}$ has eigenvalues with negative real part, one can apply standard singular perturbation (see Section 3.6) to show that after a very fast transient, the

trajectories are attracted to the slow manifold given by $f_1(\tilde{x} - y, u) = 0$. This is locally given by $x = \gamma(u)$ solving $f_1(x, u) = 0$. Hence, on the slow manifold we have that $x(t) = \gamma(u(t))$, which is independent of the downstream system, that is, it is not affected by retroactivity.

The same result holds for a more general class of systems in which the variables u, x, y are vectors:

$$\begin{aligned}\frac{du}{dt} &= f_0(u, t) + r(u, x) \\ \frac{dx}{dt} &= Gf_1(x, u) + \bar{G}As(x, u) \\ \frac{dy}{dt} &= -\bar{G}Bs(x, y)\end{aligned}\tag{7.27}$$

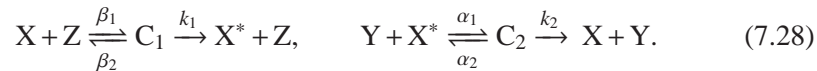
as long as there are matrices T and M such that $TA + MB = 0$ and T is invertible. In fact, one can take the system to new coordinates u, \tilde{x}, y with $\tilde{x} = Tx + My$, in which the system will have the form (7.26).

Biomolecular realizations of Principle 2

We next consider possible biomolecular structures that realize Principle 2. Since this principle is based on a fast time scale of the device dynamics when compared to that of the device input, we focus on signaling systems, which are known to evolve on faster time scales than those of protein production and decay.

Design 1: Implementation through phosphorylation

We consider a more complex model for the phosphorylation and dephosphorylation reactions in a phosphorylation cycle and perform a parametric analysis to highlight the roles of the various parameters for attaining the insulation properties. In particular, we consider a two-step reaction model as seen in Section 2.4. According to this model, we have the following two reactions for phosphorylation and dephosphorylation:



Additionally, we have the conservation equations $Y_{\text{tot}} = Y + C_2$, $X_{\text{tot}} = X + X^* + C_1 + C_2 + C$, because proteins X and Y are not degraded. Therefore, the differential

equations modeling the insulation system of Figure 7.14 become

$$\frac{dZ}{dt} = k(t) - \delta Z \left[-\beta_1 Z X_{\text{tot}} \left(1 - \frac{X^*}{X_{\text{tot}}} - \frac{C_1}{X_{\text{tot}}} - \frac{C_2}{X_{\text{tot}}} - \left[\frac{C}{X_{\text{tot}}} \right] \right) + (\beta_2 + k_1) C_1 \right] \quad (7.29)$$

$$\frac{dC_1}{dt} = -(\beta_2 + k_1) C_1 + \beta_1 Z X_{\text{tot}} \left(1 - \frac{X^*}{X_{\text{tot}}} - \frac{C_1}{X_{\text{tot}}} - \frac{C_2}{X_{\text{tot}}} - \left[\frac{C}{X_{\text{tot}}} \right] \right) \quad (7.30)$$

$$\frac{dC_2}{dt} = -(k_2 + \alpha_2) C_2 + \alpha_1 Y_{\text{tot}} X^* \left(1 - \frac{C_2}{Y_{\text{tot}}} \right) \quad (7.31)$$

$$\frac{dX^*}{dt} = k_1 C_1 + \alpha_2 C_2 - \alpha_1 Y_{\text{tot}} X^* \left(1 - \frac{C_2}{Y_{\text{tot}}} \right) + [k_{\text{off}} C - k_{\text{on}} X^* (p_{\text{tot}} - C)] \quad (7.32)$$

$$\frac{dC}{dt} = -k_{\text{off}} C + k_{\text{on}} X^* (p_{\text{tot}} - C), \quad (7.33)$$

in which the expression of gene z is controlled by a promoter with activity $k(t)$. The terms in the large square bracket in equation (8.1) represent the retroactivity r to the input, while the terms in the square brackets of equations (8.2) and (7.32) represent the retroactivity s to the output.

We assume that $X_{\text{tot}} \gg p_{\text{tot}}$ so that in equations (8.1) and (8.2) we can neglect the term C/X_{tot} because $C < p_{\text{tot}}$. Also, phosphorylation and dephosphorylation reactions in equations (7.28) can occur at a much faster rate than protein production and decay processes (see Chapter 2). Choosing X_{tot} and Y_{tot} sufficiently large, let $G = k_1 X_{\text{tot}}/\delta$ and $\bar{G} = k_{\text{off}}/\delta$, then we can re-write the system with $k_{\text{on}} = k_{\text{off}}/K_d$, $b_1 = \beta_1 X_{\text{tot}}/(\delta G)$, $a_1 = \alpha_1 Y_{\text{tot}}/(\delta G)$, $b_2 = \beta_2/(\delta G)$, $a_2 = \alpha_2/(\delta G)$, $c_i = k_i/(\delta G)$, and $k_{\text{on}} = \bar{G}\delta/K_d$. Letting $z = Z + C_1$ we obtain the system in the form

$$\begin{aligned} \frac{dz}{dt} &= k(t) - \delta(z - C_1) \\ \frac{dC_1}{dt} &= G \left(-\delta(b_2 + c_1)C_1 + \delta b_1(z - C_1) \left(1 - \frac{X^*}{X_{\text{tot}}} - \frac{C_1}{X_{\text{tot}}} - \frac{C_2}{X_{\text{tot}}} \right) \right) \\ \frac{dC_2}{dt} &= G \left(-\delta(c_2 + a_2)C_2 + \delta a_1 X^* \left(1 - \frac{C_2}{Y_{\text{tot}}} \right) \right) \\ \frac{dX^*}{dt} &= G \left(\delta c_1 C_1 + \delta a_2 C_2 - \delta a_1 X^* \left(1 - \frac{C_2}{Y_{\text{tot}}} \right) \right) + \bar{G} (\delta C - \delta/K_d (p_{\text{tot}} - C) X^*) \\ \frac{dC}{dt} &= -\bar{G} (\delta C - \delta/K_d (p_{\text{tot}} - C) X^*), \end{aligned} \quad (7.34)$$

which is in the form of system (7.27) with $u = z$, $x = (C_1, C_2, X^*)$, and $y = C$, in which one can choose T as the 3 by 3 identity matrix and $M = (0 \ 0 \ 1)'$. Hence, this system, for G sufficiently larger than 1 attenuates the effect of the retroactivity to the output s . For G to be large, one has to require that $k_1 X_{\text{tot}}$ is sufficiently large and that $\alpha_1 Y_{\text{tot}}$ is also comparatively large. These are the same design requirements obtained in the previous section based on the one-step reaction model of the enzymatic reactions.

In order to understand the effect of retroactivity to the input on the Z dynamics, one can perform the following calculations. Letting $K_m = (\beta_2 + k_1)/\beta_1$ and $\bar{K}_m = (\alpha_2 + k_2)/\alpha_1$ represent the Michaelis-Menten constants of the forward and backward enzymatic reactions and setting $\epsilon = 0$ in the third and fourth equations of (7.34) the following relationships can be obtained:

$$C_1 = F_1(X^*) = \frac{\frac{X^* Y_{\text{tot}} k_2}{\bar{K}_m k_1}}{1 + X^*/\bar{K}_m}, \quad C_2 = F_2(X^*) = \frac{\frac{X^* Y_{\text{tot}}}{\bar{K}_m}}{1 + X^*/\bar{K}_m}. \quad (7.35)$$

Using expressions (7.35) in the second of equations (7.34) with $\epsilon = 0$ leads to

$$F_1(X^*)(b_2 + c_1 + \frac{b_1 Z}{X_{\text{tot}}}) = b_1 Z \left(1 - \frac{X^*}{X_{\text{tot}}} - \frac{F_2(X^*)}{X_{\text{tot}}}\right). \quad (7.36)$$

Assuming for simplicity that $X^* \ll \bar{K}_m$, we obtain that $F_1(X^*) \approx X^* Y_{\text{tot}} k_2 / \bar{K}_m k_1$ and that $F_2(X^*) \approx X^* / \bar{K}_m Y_{\text{tot}}$. As a consequence of these simplifications, equation (7.36) leads to

$$X^* = \frac{b_1 Z}{\frac{b_1 Z}{X_{\text{tot}}} (1 + Y_{\text{tot}}/\bar{K}_m + (Y_{\text{tot}} k_2)/(\bar{K}_m k_1)) + \frac{Y_{\text{tot}} k_2}{\bar{K}_m k_1} (b_2 + c_1)} := m(Z).$$

In order not to have distortion from Z to X^* , we require that

$$Z \ll \frac{Y_{\text{tot}} \frac{k_2}{k_1} \frac{K_m}{\bar{K}_m}}{1 + \frac{Y_{\text{tot}}}{\bar{K}_m} + \frac{Y_{\text{tot}} k_2}{\bar{K}_m k_1}}, \quad (7.37)$$

so that $m(Z) \approx ZX_{\text{tot}} \bar{K}_m k_1 / Y_{\text{tot}} K_m k_2$ and therefore we have a linear relationship between X^* and Z with gain from Z to X^* given by $X_{\text{tot}} \bar{K}_m k_1 / Y_{\text{tot}} K_m k_2$. In order not to have attenuation from Z to X^* we require that the gain is greater than or equal to one, that is,

$$\text{input/output gain} \approx \frac{X_{\text{tot}} \bar{K}_m k_1}{Y_{\text{tot}} K_m k_2} \geq 1. \quad (7.38)$$

Requirements (7.37), (7.38) and $X^* \ll \bar{K}_m$ are enough to guarantee that we do not have nonlinear distortion between Z and X^* and that X^* is not attenuated with respect to Z . In order to guarantee that the retroactivity r to the input is sufficiently small, we need to quantify the retroactivity effect on the Z dynamics due to the binding of Z with X . To achieve this, we proceed as in Section 7.3 by computing the Z dynamics on the slow manifold, which gives a good approximation of the dynamics of Z if $\epsilon \approx 0$. Such a dynamics is given by

$$\frac{dZ}{dt} = (k(t) - \delta Z) \left(1 - \frac{dF_1}{dX^*} \frac{dX^*}{dz}\right),$$

in which $\frac{dF_1}{dX^*} \frac{dX^*}{dz}$ measures the effect of the retroactivity r to the input on the Z dynamics. Direct computation of $\frac{dF_1}{dX^*}$ and of $\frac{dX^*}{dz}$ along with $X^* \ll \bar{K}_m$ and with

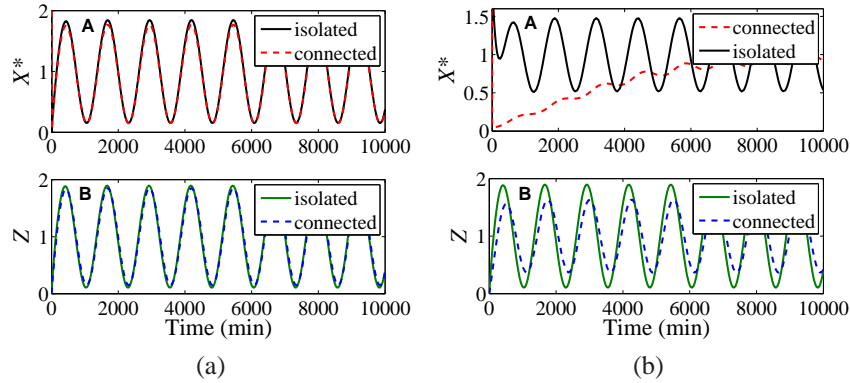


Figure 7.16: (a) Performance with fast time scales. Simulation results for system in equations (8.1–7.33). In all plots, $p_{\text{tot}} = 100$, $k_{\text{off}} = k_{\text{on}} = 10$, $\delta = 0.01$, $k(t) = 0.01(1 + \sin(\omega t))$, and $\omega = 0.005$. In subplots A and B, $k_1 = k_2 = 50$, $\alpha_1 = \beta_1 = 0.01$, $\beta_2 = \alpha_2 = 10$, and $Y_{\text{tot}} = X_{\text{tot}} = 1500$. In plot A, the isolated system is without downstream binding sites p and the connected system is with binding sites p . The small error shows that the effect of the retroactivity to the output s is attenuated very well. In subplot B, the isolated system stands for the case in which Z does not have X to bind to, while the connected system stands for the case in which Z binds to substrate X ($X_{\text{tot}} = 1500$). The small error confirms a small retroactivity to the input r . (b) Performance with slow time scale. Phosphorylation and dephosphorylation rates are slower than the ones in (a), that is, $k_1 = k_2 = 0.01$, while the other parameters are left the same, that is, $\alpha_2 = \beta_2 = 10$, $\alpha_1 = \beta_1 = 0.01$, and $Y_{\text{tot}} = X_{\text{tot}} = 1500$.

(7.37) leads to $\frac{dF_1}{dX^*} \frac{dX^*}{dz} \approx X_{\text{tot}}/K_m$, so that in order to have small retroactivity to the input, we require that

$$\frac{X_{\text{tot}}}{K_m} \ll 1. \quad (7.39)$$

Hence, a design trade-off appears: X_{tot} should be sufficiently large to provide a gain G large enough to attenuate the retroactivity to the output. Yet, X_{tot} should be small enough compared to K_m so to apply minimal retroactivity to the input.

Concluding, for having attenuation of the effect of the retroactivity to the output s , we require that the time scale of the phosphorylation/dephosphorylation reactions is much faster than the production and decay processes of Z (the input to the insulation device) and that $X_{\text{tot}} \gg p_{\text{tot}}$, that is, the total amount of protein X is in abundance compared to the downstream binding sites p . To obtain also a small effect of the retroactivity to the input, we require that $K_m \gg X_{\text{tot}}$. This is satisfied if, for example, kinase Z has low affinity to binding with X . To keep the input/output gain between Z and X^* close to one (from equation (7.38)), one can choose $X_{\text{tot}} = Y_{\text{tot}}$, and equal coefficients for the phosphorylation and dephosphorylation reactions, that is, $K_m = \bar{K}_m$ and $k_1 = k_2$.

System in equations (8.1–7.33) was simulated with and without the downstream binding sites p , that is, with and without, respectively, the terms in the small box

of equation (8.1) and in the boxes in equations (7.32) and (8.2). This is performed to highlight the effect of the retroactivity to the output s on the dynamics of X^* . The simulations validate our theoretical study that indicates that when $X_{\text{tot}} \gg p_{\text{tot}}$ and the time scales of phosphorylation/dephosphorylation are much faster than the time scale of decay and production of the protein Z , the retroactivity to the output s is very well attenuated (Figure 7.16(a), plot A). Similarly, the time behavior of Z was simulated with and without the terms in the large box in equation (8.1), that is, with and without X to which Z binds, to verify whether the insulation component exhibits retroactivity to the input r .

In particular, the accordance of the behaviors of $Z(t)$ with and without its downstream binding sites on X (Figure 7.16(a), plot B), indicates that there is no substantial retroactivity to the input r generated by the insulation device. This is obtained because $X_{\text{tot}} \ll K_m$ as indicated in equation (7.39), in which $1/K_m$ can be interpreted as the affinity of the binding of X to Z .

Our simulation study also indicates that a faster time scale of the phosphorylation/dephosphorylation reactions is necessary, even for high values of X_{tot} and Y_{tot} , to maintain perfect attenuation of the retroactivity to the output s and small retroactivity to the output r . In fact, slowing down the time scale of phosphorylation and dephosphorylation, the system loses its insulation property (Figure ??(b)). In particular, the attenuation of the effect of the retroactivity to the output s is lost because there is not enough separation of time scales between the Z dynamics and the internal device dynamics. The device also displays a non negligible amount of retroactivity to the input because the condition $K_m \ll X_{\text{tot}}$ is not satisfied anymore.

Design 2: Realization through phosphotransfer

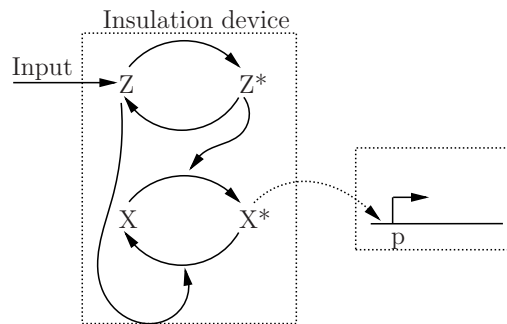
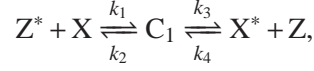


Figure 7.17: System Σ is a phosphotransfer system. The output X^* activates transcription through the reversible binding of X^* to downstream DNA promoter sites p .

Let X be a transcription factor in its inactive form and let X^* be the same transcription factor once it has been activated by the addition of a phosphate group. Let Z^* be a phosphate donor, that is, a protein that can transfer its phosphate group

to the acceptor X. The standard phosphotransfer reactions (see Chapter 2, Section 2.4) can be modeled according to the two-step reaction model



in which C_1 is the complex of Z bound to X bound to the phosphate group. Additionally, protein Z can be phosphorylated and protein X^* dephosphorylated by other phosphotransfer interactions. These reactions are modeled as one step reactions depending only on the concentrations of Z and X^* , that is, $Z \xrightarrow{\pi_1} Z^*$, $X^* \xrightarrow{\pi_2} X$. Protein X is assumed to be conserved in the system, that is, $X_{\text{tot}} = X + C_1 + X^* + C$. We assume that protein Z is produced with time-varying production rate $k(t)$ and decays with rate δ . The active transcription factor X^* binds to downstream DNA binding sites p with total concentration p_{tot} to activate transcription through the reversible reaction $p + X^* \xrightleftharpoons[k_{\text{off}}]{k_{\text{on}}} C$. Since the total amount of p is conserved, we also have that $C + p = p_{\text{tot}}$. The ODE model corresponding to this system is thus given by the equations

$$\begin{aligned} \dot{Z} &= k(t) - \delta Z + k_3 C_1 - k_4 X^* Z - \pi_1 Z \\ \dot{C}_1 &= k_1 X_{\text{tot}} \left(1 - \frac{X^*}{X_{\text{tot}}} - \frac{C_1}{X_{\text{tot}}} - \frac{C}{X_{\text{tot}}} \right) Z^* - k_3 C_1 - k_2 C_1 + k_4 X^* Z \\ \dot{Z}^* &= \pi_1 Z + k_2 C_1 - k_1 X_{\text{tot}} \left(1 - \frac{X^*}{X_{\text{tot}}} - \frac{C_1}{X_{\text{tot}}} - \frac{C}{X_{\text{tot}}} \right) Z^* \\ \dot{X}^* &= k_3 C_1 - k_4 X^* Z - k_{\text{on}} X^* (p_{\text{tot}} - C) + k_{\text{off}} C - \pi_2 X^* \\ \dot{C} &= k_{\text{on}} X^* (p_{\text{tot}} - C) - k_{\text{off}} C. \end{aligned} \tag{7.40}$$

Since phosphotransfer reaction are faster than protein production and decay, define $G_1 := X_{\text{tot}} k_1 / \delta$ so that $\bar{k}_1 := X_{\text{tot}} k_1 / G_1 = \delta$, $\bar{k}_2 := k_2 / G_1$, $\bar{k}_3 := k_3 / G_1$, $\bar{k}_4 := k_4 / G_1$, $\bar{\pi}_1 := \pi_1 / G_1$, $\bar{\pi}_2 := \pi_2 / G_1$ are of the same order of $k(t)$ and δ . Similarly, the process of protein binding and unbinding to promoter sites is much faster than protein production and decay. Therefore, for $\bar{G} \gg 1$ and we let $\bar{G} := k_{\text{on}} / \delta$, $K_d := k_{\text{off}} / k_{\text{on}}$ with $K_d = O(1)$. Assuming also that $p_{\text{tot}} \ll X_{\text{tot}}$, we have that $C \ll X_{\text{tot}}$ so that system (7.40) can be rewritten as

$$\begin{aligned} \dot{Z} &= k(t) - \delta Z + G (\bar{k}_3 C_1 - \bar{k}_4 Z X^* - \bar{\pi}_1 Z) \\ \dot{C}_1 &= G \left(\bar{k}_1 \left(1 - \frac{X^*}{X_{\text{tot}}} - \frac{C_1}{X_{\text{tot}}} \right) Z^* - \bar{k}_3 C_1 - \bar{k}_2 C_1 + \bar{k}_4 X^* Z \right) \\ \dot{Z}^* &= G \left(\bar{\pi}_1 Z + \bar{k}_2 C_1 - \bar{k}_1 \left(1 - \frac{X^*}{X_{\text{tot}}} - \frac{C_1}{X_{\text{tot}}} \right) Z^* \right) \\ \dot{X}^* &= G (\bar{k}_3 C_1 - \bar{k}_4 X^* Z - \bar{\pi}_2 X^*) - \bar{G} (\delta X^* (p_{\text{tot}} - C) + \delta K_d C) \\ \dot{C} &= \bar{G} (\delta X^* (p_{\text{tot}} - C) - \delta K_d C). \end{aligned} \tag{7.41}$$

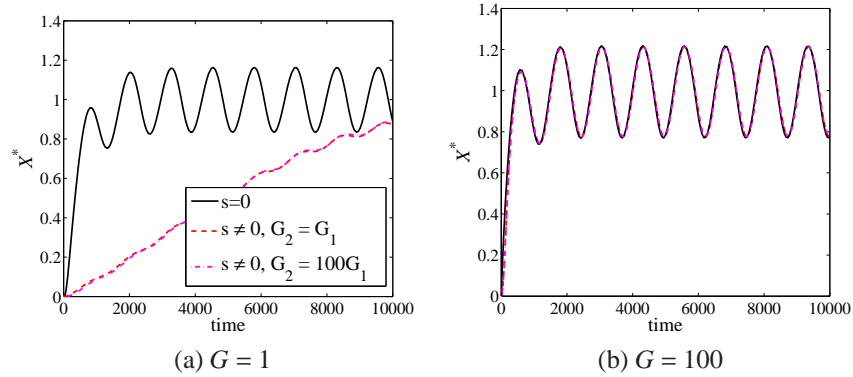


Figure 7.18: Output response of the phosphotransfer system with a periodic signal $k(t) = \delta(1 + 0.5\sin\omega t)$. The parameters are given by $\delta = 0.01$, $X_{\text{tot}} = 5000$, $k_1 = k_2 = k_3 = k_4 = \pi_1 = \pi_2 = 0.01G$ in which $G = 1$ (left-side panel), and $G = 100$ (right-side panel). The downstream system parameters are given by $K_d = 1$ and $k_{\text{off}} = 0.01G_2$, in which \bar{G} assumes the values indicated on the legend. The isolated system ($s = 0$) corresponds to $p_{\text{tot}} = 0$ while the connected system ($s \neq 0$) corresponds to $p_{\text{tot}} = 100$.

Taking $T = \mathbb{I}_{3 \times 3}$ and $M = \begin{bmatrix} 0 \\ 0 \\ 1 \end{bmatrix}$, the coordinate transformation $\tilde{x} = Tx + My$ brings the system to the form of system (7.27) with $u = Z$, $x = (C_1, Z^*, X^*)$, and $y = C$.

We illustrate the retroactivity to the output attenuation property of this system using simulations for the cases in which $G \gg \bar{G}$, $G = \bar{G}$, and $G \ll \bar{G}$. Figure 7.18 shows that, for a periodic input $k(t)$, the system with low value for G suffers the impact of retroactivity to the output. However, for a large value of G , the permanent behavior of the connected system becomes similar to that of the isolated system, whether $G \gg \bar{G}$, $G = \bar{G}$ or $G \ll \bar{G}$. Notice that, in the bottom panel of Figure 7.18, when $G \gg \bar{G}$, the impact of the retroactivity to the output is not as dramatic as it is when $G = \bar{G}$ or $G \ll \bar{G}$. This is due to the fact that s is scaled by \bar{G} and it is not related to the retroactivity to the output attenuation property. This confirms the theoretical result that, independently of the order of magnitude of \bar{G} , the system can arbitrarily attenuate retroactivity for large enough G .

Exercises

7.1 Include in the study of retroactivity in transcriptional systems the mRNA dynamics and demonstrate how/whether the results change. Specifically, consider the

following model of a connected transcriptional component

$$\begin{aligned}\frac{m_X}{dt} &= k(t) - \gamma m_X \\ \frac{dX}{dt} &= \beta m_X - \delta X + [k_{\text{off}}C - k_{\text{on}}(p_{TOT} - C)X], \\ \frac{dC}{dt} &= -k_{\text{off}}C + k_{\text{on}}(p_{TOT} - C)X,\end{aligned}$$

7.2 Consider the system in standard singular perturbation form, in which $\epsilon \ll 1$. Demonstrate that the slow manifold is locally exponentially stable.

$$\frac{dy}{dt} = k(t) - \delta(y - C), \quad \epsilon \frac{dC}{dt} = -\delta C + \frac{\delta}{k_d}(p_{TOT} - C)(y - C).$$

7.3 The characterization of retroactivity effects in a transcriptional module was based on the following model of the interconnection:

$$\begin{aligned}\frac{dX}{dt} &= k(t) - \delta X + [k_{\text{off}}C - k_{\text{on}}(p_{\text{tot}} - C)X], \\ \frac{dC}{dt} &= -k_{\text{off}}C + k_{\text{on}}(p_{\text{tot}} - C)X,\end{aligned}$$

in which it was implicitly assumed that the complex C does not dilute. This is often a fair assumption. However, depending on the experimental conditions, a more appropriate model may include dilution for the complex C. In this case, the model modified to

$$\begin{aligned}\frac{dX}{dt} &= k(t) - (\mu + \bar{\delta})X + [k_{\text{off}}C - k_{\text{on}}(p_{\text{tot}} - C)X], \\ \frac{dC}{dt} &= -k_{\text{off}}C + k_{\text{on}}(p_{\text{tot}} - C)X - \mu C,\end{aligned}$$

in which μ represents decay due to dilution and $\bar{\delta}$ represents protein degradation. Employ singular perturbation to determine the reduced X dynamics and the effects of retroactivity in this case. Is the steady state characteristic of the transcriptional module affected by retroactivity? How?

7.4 We have illustrated that the expression of the point of half-maximal induction in a covalent modification cycle is affected by the effective load λ as follows:

$$y_{50} = \frac{\bar{K}_1 + 0.5}{\bar{K}_2(1 + \lambda) + 0.5}.$$

Study the behavior of this quantity when the effective load λ is changed.

7.5 Show how equation (7.10) is derived in Section 7.4.

7.6 Demonstrate that in the following system

$$\frac{dX}{dt} = G(k(t) - KX)(1 - d(t)),$$

$X(t) - k(t)/K$ becomes smaller as G is increased.

7.7 Consider the activator-repressor clock from Atkinson *et al.* (Cell 2003), described in Section 6.5. Take the same simulation model derived for that exercise and pick parameter values to obtain a stable limit cycle. Then, assume that the activator A connects to another transcriptional circuit through the reversible binding of A with operator sites p to form activator-operator complex C : $A + p \xrightleftharpoons[k_{off}]{k_{on}} C$. This occurs, for example, if you want to use this clock as a source generator for some downstream system. Answer the following questions:

- Simulate the system with this new binding phenomenon and vary the total amount of p , that is, p_T . Explore how this affects the behavior of the clock.
- Give a mathematical explanation of the phenomenon you saw in (i). To do so, use singular perturbation to approximate the dynamics of the clock with downstream binding on the slow manifold (here, $k_{on}, k_{off} \gg \delta_A, \delta_B$). You can follow the process we used in class when we studied retroactivity for the transcriptional component with downstream binding.

Chapter 8

Design Tradeoffs

In this chapter, we describe a number of design tradeoffs due to the fact that the synthetic circuits interact with the host organism. We specifically focus on two issues: effects of retroactivity from synthetic circuits on the host organism and effects of biological noise on the design of insulation devices. In particular, circuits use a number of cellular resources that are shared among all circuits in the cell. Hence, they increase the loading on these resources, with possibly undesired repercussions on the functioning of the circuits themselves. Specifically, unconnected circuits are actually coupled through sharing common resources. We analyze the effects of this general phenomenon by illustrating it on the RNAP usage as an example. The same reasonings can be applied to any shared resource that is not in substantial excess with respect to the amounts of circuit copies placed in the cell. We will also illustrate possible mechanisms to avoid this problem by employing several of the robustness tools of Chapter 3. Further, we illustrate the possible tradeoffs between retroactivity attenuation and noise amplification, due to noisy cellular environments.

Prerequisites. Readers should have an understanding of the modeling of core processes of Chapter 2, the concepts of adaptation and robustness as outlined in Chapter 3, the tools to analyze noise as outlined in Chapter 4, and the principles for retroactivity attenuation discussed in Chapter 7.

8.1 Metabolic Burden

All biomolecular circuits use cellular resources, such as ribosomes, RNAP, and ATP, that are shared among all the circuitry of the cell, whether this circuitry is endogenous or exogenous. As a consequence, the introduction of synthetic circuits in the cell environment is potentially perturbing the availability of these resources, leading to undesired and often unpredictable side effects on cell metabolism. In this chapter, we study the effect of the retroactivity or “back-action” from the synthetic circuits to shared resources in the cellular environment by focusing on the demand for RNAP, for simplicity. The effects that we highlight are going to be significant for any resource whose availability is not in substantial excess compared to the added demand by synthetic circuits. We will then study possible mechanisms that can be engineered to attenuate the side effects of retroactivity on shared resources,

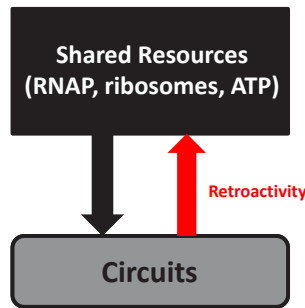


Figure 8.1: The cellular environment provides resources to synthetic circuits, such as RNAP, ribosomes, ATP, proteases, etc. Circuits use these resources and as a consequence, they affect (through retroactivity) the availability of resources for other circuits.

focusing on RNAP as an example, employing some of the adaptation techniques outlined in Chapter 3 and Chapter 6.

In order to illustrate the problem, we consider the example system shown in Figure 8.2, in which two modules, an inducible promoter (module A) and a constitutive promoter (module B), are both present in the cellular environment. In theory, module A should respond to changes in the inducer concentration while module B, featuring a constitutive promoter, should display a constant expression level that is independent of the inducer amount. Experimental results, however, indicate that this is not the case since module B also responds to changes in inducer concentration. We illustrate how this effect can be justified mathematically by accounting for competition of shared resources needed in gene expression. To simplify the analysis, we focus on one such shared resource, the RNAP.

Experimental observations indicate that increased amounts of inducer (independently of whether we have a positive inducer or a negative inducer) lead to decreased expression of the constitutive promoter in module B. In the case of a

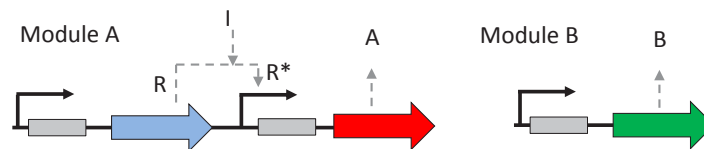


Figure 8.2: Module A has an inducible promoter that can be activated (or repressed) by transcription factor R. Such a transcription factor, when an activator, is activated by inducer I, while when a repressor, is repressed by the inducer. The output of Module A is protein A. Module B has a constitutive promoter producing protein B.

positive inducer, this can be qualitatively explained as follows. When the inducer amount is increased, an increased amount of active activator will be present leading to increased levels of transcription in module A. These increased levels of transcription will require increased demand for RNAP and, as a consequence, smaller amounts of RNAP will be free to promote transcription in module B. Hence, module B will experience a decreased transcription rate. At the same time, the presence of larger amounts of transcript in module A will require larger concentration of ribosomes for the translation process. As a result, smaller amounts of ribosomes will be free to promote translation in module B. The net result is that lower expression will be observed in module B when the inducer of module A is increased. A similar reasoning can be performed in the case of a negative inducer.

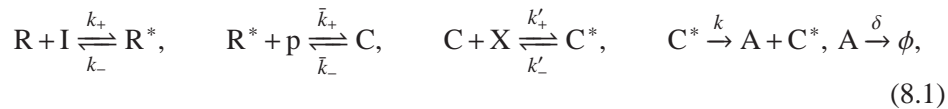
The extent of this effect will depend on the availability of resources and whether they are regulated. It is in fact known that RNAP and ribosomes are regulated by the cell through negative feedback [?, ?].

To mathematically demonstrate this phenomenon, we first perform a simple analytical study assuming that gene expression is a one-step process. We then perform a numerical study employing a mechanistic two-step model for gene expression.

Analytical study using a simple model with a positive inducer

To illustrate the essence of the problem under study, we assume that gene expression is a one-step process, in which the RNAP binds to the promoter region of a gene resulting in a transcriptionally active complex, which, in turn, produces the corresponding protein at some constant rate. We first analyze module A, assuming module B is not present, and module B, assuming module A is not present. Then, we consider the case in which both of them are present and compare the levels of output proteins to the cases in which only one module is present.

Only module A is present. Let X denote the RNAP, R the inactive activator, I the inducer, R^* the active activator, that is, R bound to the activator I , p the amount of promoter of module A, and A the output protein of module A. For any species Z , we denote in italics Z its concentration. The reactions describing the system are given by



in which C is the complex promoter-activator and C^* is the transcriptionally active complex promoter-activator-RNAP. In addition, we assume that the total amount of X is conserved and denote such a total amount by X_T . Further, we assume that the total amount of promoter p is conserved and denote such a total amount by p_T . Let $R_T := R + R^*$ denote the total amount of transcription factor. We are interested in determining the steady state levels of X and of A as a function of the inducer

amounts I . The steady state values satisfy

$$R^* = \frac{R_T I}{k_D + I} \quad \text{with} \quad k_D = k_- / k_+, \quad C = \frac{R^* p}{\bar{k}_D} \quad \text{with} \quad \bar{k}_D = \bar{k}_- / \bar{k}_+, \quad C^* = \frac{C X}{k'_D} \quad \text{with} \quad k'_D =$$

Combining these along with the conservation law $C + C^* + p = p_T$ leads to

$$p = \frac{p_T}{R^* / \bar{k}_D + R^* X / (k'_D \bar{k}_D) + 1},$$

in which, to simplify the derivations, we assume that

$$\frac{R^*}{\bar{k}_D} \left(1 + \frac{X}{k'_D} \right) \ll 1,$$

which, in turn, is satisfied if the amount of activator I is sufficiently small or if the total amount of protein R is small. As a consequence, we assume in the remainder of this section that $p \approx p_T$. Employing the conservation law for X , that is, $X_T = X + C^*$, we finally obtain that

$$X = \frac{X_T}{1 + \frac{p_T R^*}{k'_D \bar{k}_D}} = \frac{X_T}{1 + \frac{p_T R_T I}{k'_D \bar{k}_D (k_D + I)}},$$

as a consequence, as the positive inducer concentration I is increased, the amount of free RNAP (X) decreases (see Figure 8.3). Also, since $Y = (k/\delta)C^*$, we have that

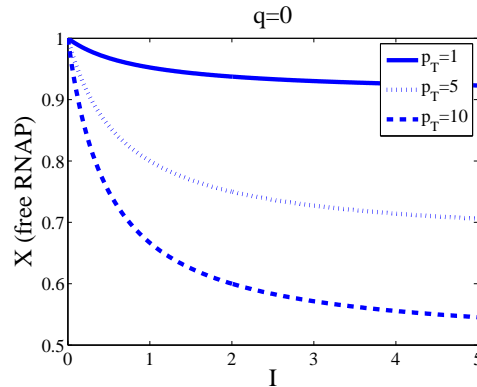


Figure 8.3: Plots showing that when the inducer level I is changed, the amount of X is also changed.

$$A = \frac{k}{\delta} \left(\frac{\frac{p_T X_T R_T I}{k_D + I}}{k'_D + \bar{k}_D + p_T \frac{R_T X_T I}{k_D + I}} \right),$$

which increases with I as expected.

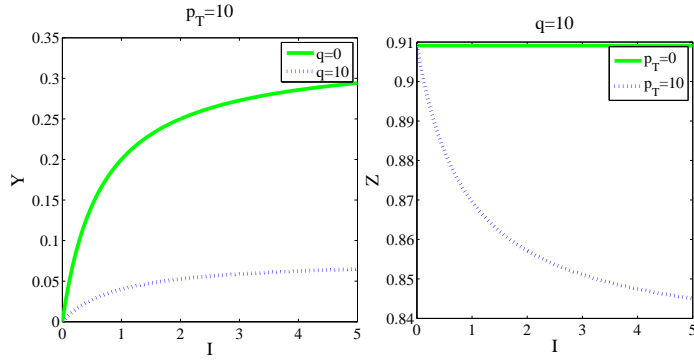
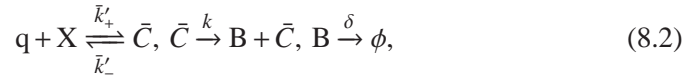


Figure 8.4: (Left) Effect on the expression of A when module B is added to the system: the expression level of A changes, but it maintains its response to the inducer. (Right) Effect on the expression of B when Module A is added to the system. When Module A is absent, the expression of B does not respond to inducer changes. By contrast, when Module A is present, the expression of B responds to inducer changes.

Only module B is present. When only module B is present, since its promoter is constitutive, it will display a constant expression level for any fixed X_T . Denoting q the amounts of promoter in Module B, we have the reactions



with conservation law for X given by $X_T = X + \bar{C}$. The steady state values satisfy

$$\bar{C} = \frac{Xq}{k'_D} \text{ with } \bar{k}'_D = \bar{k}'_-/\bar{k}'_+ \text{ and } B = \frac{k\bar{C}}{\delta}.$$

These relations along with the conservation law for X lead to

$$X = \frac{X_T}{1 + \frac{q}{\bar{k}'_D}} \text{ and } B = \frac{k}{\delta} \left(\frac{X_T q}{\bar{k}'_D + q} \right),$$

which increases with X_T and q as expected.

Both modules A and B are present. When both modules are present, the set of reactions describing the system is just the union of the set of reactions describing the two modules, that is, equations (8.1) and equations (8.2). The steady state values also still satisfy the same relations as before. The only difference is the conservation law for X , which is now given by

$$X + C^* + \bar{C} = X_T.$$

Employing this conservation law along with the steady state relations gives

$$X = \frac{X_T}{1 + \frac{R^* p_T}{k'_D \bar{k}_D} + \frac{q}{k'_D}},$$

$$A = \frac{k}{\delta} \left(\frac{\frac{p_T X_T R_T I}{k_D + I}}{k'_D + \bar{k}_D + p_T \frac{R_T X_T A}{k_D + I} + k'_D \bar{k}_D \frac{q}{k'_D}} \right) \text{ and } B = \frac{k}{\delta} \left(\frac{X_T q}{\bar{k}'_D \left(1 + \frac{p_T}{k'_D \bar{k}_D} \frac{R_T I}{k_D + I} \right) + q} \right).$$

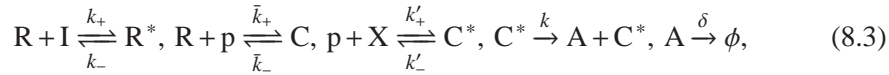
From this expression, it is clear that

- (1) Due to the presence of module B, the amounts of output protein Y of module A is lower for any given value of the inducer I ;
- (2) Module B also responds to the inducer of module A. Specifically, the amounts of output protein Z decreases when the amounts of inducer I is increased.

These conclusions are summarized in Figure 8.4 that shows the steady state values of B and A when the inducer amount I is changed as compared to the case in which the modules were not both present in the system.

Analytical study using a simple model with a negative inducer

A similar derivation can be carried if R were a repressor and R^* was the inactive form of the repressor when bound to the negative inducer, denoted I . The reactions in this case are given by



in which now C is the complex of the promoter bound to the repressor, to which the RNAP X cannot bind to start transcription, while C^* is the complex of X with the free promoter, which is transcriptionally active. Solving for the steady state yields

$$R = \frac{R_T k_D}{k_D + I}, \quad C = \frac{R p}{\bar{k}_D}, \quad C^* = \frac{X p}{k'_D}.$$

Using the conservation law $C + C^* + p = p_T$ leads to

$$p = \frac{p_T}{\frac{R}{\bar{k}_D} + \frac{X}{k'_D} + 1}.$$

Employing the conservation law $X_T = X + C^*$, using that $C^* = \frac{X}{k'_D} \frac{p_T}{\frac{R}{\bar{k}_D} + \frac{X}{k'_D} + 1}$, and assuming that $R/\bar{k}_D \gg X/k'_D$ (obtained with small amounts of inducer) so that $p \approx \frac{p_T}{R/\bar{k}_D + 1}$, leads to

$$X = \frac{X_T}{1 + \frac{p_T}{(k'_D/\bar{k}_D)R + k'_D}}$$

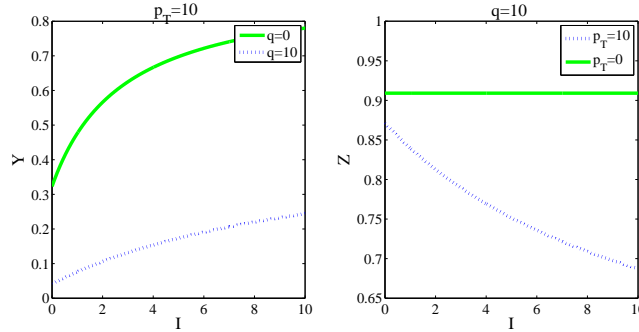
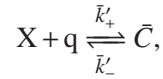


Figure 8.5: (Left) Effect on the expression of A when module B is added to the system: the expression level of A changes, but it maintains its response to the inducer. (Right) Effect on the expression of B when Module A is added to the system. When Module A is absent, the expression of B does not respond to inducer changes. By contrast, when Module A is present, the expression of B responds to inducer changes.

so that when I increases X decreases because there is going to be more promoter p free to bind X . Since $A = (k/\delta)C^*$, we have that

$$A = \frac{k}{\delta k'_D} \frac{X_T}{1 + \frac{p_T}{(k'_D/\bar{k}_D)R + k'_D}} \frac{p_T}{R/\bar{k}_D + 1}.$$

If we add a constitutive promoter q expressing B, we add the reaction



and modify the conservation law for X to $X_T = X + C^* + \bar{C}$, so that

$$X = \frac{X_T}{1 + \frac{p_T}{(k'_D/\bar{k}_D)R + k'_D} + q/\bar{k}'_D},$$

and

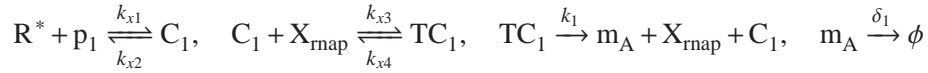
$$B = \frac{kq}{\delta \bar{k}'_D} \frac{X_T}{1 + \frac{p_T}{(k'_D/\bar{k}_D)R + k'_D} + q/\bar{k}'_D}.$$

As a consequence, B also responds to the addition of inducer I by decreasing when inducer I is increasing. This is qualitatively occurring because when inducer I is increased, more free promoter p will be able to bind to X , hence decreasing the free amount of X than can bind to promoter Q leading to B expression (see Figure 8.5).

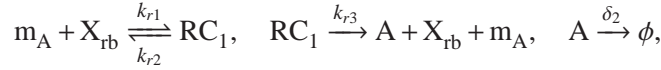
Numerical study using a mechanistic model with a positive inducer

In this section, we introduce a mechanistic model of the system in Figure 8.2, in which we consider both the RNAP and the ribosome usage, no approximating

assumption are made, and biochemical parameters are chosen from the literature. Specifically, we consider for inducer I is AHL, transcription factor R is LuxR, the output of module A is RFP, and the output of module B is GFP. We denote the concentration of RNAP by X_{rnap} and the concentration of ribosomes by X_{rb} . We denote by m_A and A the concentrations of the mRNA of RFP and of RFP protein, respectively, while we denote by m_B and B the concentrations of the mRNA of GFP and of GFP protein, respectively. Denoting by R^* the concentration of the complex of LuxR with AHL (equal to $LuxR_T I / (k_D + I)$ with $LuxR_T$ the total amount of LuxR), we have the following reactions for module A transcription



and for module A translation

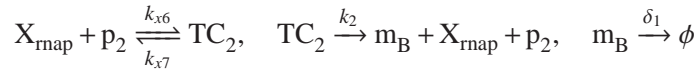


in which C_1 is the complex of active transcription factor with the promoter controlling A, TC_1 is the complex of C_1 with X_{rnap} , δ_1 is the decay rate of mRNA, δ_2 is the decay rate of protein, RC_1 is the complex of X_{rb} with the mRNA ribosome binding site, k_1 is the rate of transcription, and k_{r3} is the rate of translation. The resulting system of differential equations is given by

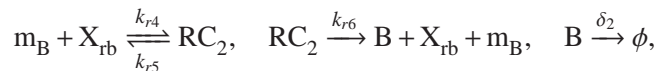
$$\begin{aligned} \frac{dC_1}{dt} &= k_{x1} R^* p_1 - k_{x2} C_1 - k_{x3} X_{rnap} C_1 + (k_{x4} + k_1) TC_1 \\ \frac{dTC_1}{dt} &= k_{x3} X_{rnap} C_1 - (k_{x4} + k_1) TC_1 \\ \frac{dm_A}{dt} &= k_1 TC_1 - k_{r1} X_{rb} m_A + k_{r2} RC_1 - \delta_1 m_A + k_{r3} RC_1 \\ \frac{dRC_1}{dt} &= k_{r1} X_{rb} m_A - (k_{r2} + k_{r3}) RC_1 \\ \frac{dA}{dt} &= k_{r3} RC_1 - \delta_2 A, \end{aligned} \quad (8.4)$$

In which, we have that $p_1 = p_{1,tot} - C_1 - TC_1$ by the conservation law of DNA in module A.

For module B, we have the following reactions for transcription



and the following reactions for translation



in which TC_2 is the transcriptionally active complex of promoter with RNAP, k_2 is the transcription rate, RC_2 is the complex of ribosome binding site with the ribosome, and k_{r6} is the translation rate. The resulting system of differential equations is given by

$$\begin{aligned}
 \frac{d TC_2}{dt} &= k_{x6} X_{rnap} p_2 - (k_{x7} + k_2) TC_2 \\
 \frac{d m_B}{dt} &= k_2 TC_2 - k_{r4} X_{rb} m_B + k_{r5} RC_2 - \delta_1 m_B + k_{r6} RC_2 \\
 \frac{d RC_2}{dt} &= k_{r4} X_{rb} m_B - (k_{r5} + k_{r6}) RC_2 \\
 \frac{d B}{dt} &= k_{r6} RC_2 - \delta_2 B,
 \end{aligned} \tag{8.5}$$

in which $p_2 = p_{2,tot} - TC_2$ from the conservation law of DNA in module B.

We consider two cases: (Independent case) either Module A or Module B is present in the cellular environment and (Competitive case) Module A and Module B are both present in the cellular environment. In either case, the differential equations for the two modules are the same. The difference between the two cases is in the conservation law for the shared resources X_{rnap} and X_{rb} . Specifically, in the independent case we have that

$$\text{Module A: } X_{rnap,tot} = X_{rnap} + TC_1, \quad X_{rb,tot} = X_{rb} + RC_1$$

and

$$\text{Module B: } X_{rnap,tot} = X_{rnap} + TC_2, \quad X_{rb,tot} = X_{rb} + RC_2,$$

while in the competitive case we have that

$$X_{rnap,tot} = X_{rnap} + TC_1 + TC_2, \quad X_{rb,tot} = X_{rb} + RC_1 + RC_2,$$

which leads to a coupling between the model of Module A and that of Module B.

The results are shown in Figure 8.6. The presence of module A, causes module B to also respond to the inducer of module A. The presence of module B also affects the response of module A to its inducer by decreasing the steady state values of the output and by increasing the effective K_m of the steady state characteristic.

Engineering adaptation to changing demands of cellular resources

When inserting a synthetic circuit in the cell, the amount of available resources such as RNAP and ribosomes decreases, leading to perturbations in the responses of other circuits present in the cell environment. In order to prevent this, there are two main techniques that can be employed. The first approach is to make the amount of free X robust to changes in the circuits that use it. That is, one would like to maintain a roughly constant X when circuits are added or removed from the

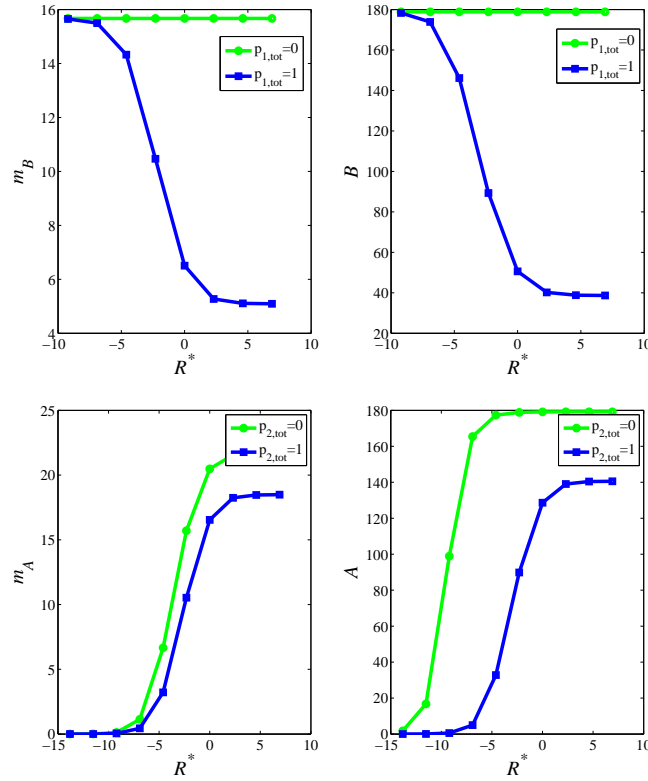


Figure 8.6: (Up: Module B) Effect on the mRNA and protein steady state response to the stimulus R^* in the presence of module A ($p_{1,tot} \neq 0$). In the presence of module A also module B responds to the stimulus of module A. (Down: Module A) Effect on the mRNA and protein steady state response to the stimulus R^* in the presence of module B ($p_{2,tot} \neq 0$). In the presence of module B, there is an increase of the apparent K_m of the steady state characteristic (right-side plot). The values of the parameters for the numerical simulation of the mechanistic model are given by $k_{x1} = 1$ ([10]), $k_{x2} = 1$ ([10]), $k_{x3} = 100$, $k_{x4} = 1$, $k_1 = 1$ ([10]), $k_{x6} = 2000$ (NYMU-Taipei iGEM 2009: pTet is 20x stronger than pLux), $k_{x7} = 1$ ([10]), $k_2 = 1$, $k_{r1} = 100$, $k_{r2} = 1$, $k_{r3} = 9$ ([10]), $k_{r4} = 100$, $k_{r5} = 1$, $k_{r6} = 9$ ([10]), $\delta_1 = 0.04$ ([10]), $\delta_2 = 0.05$ (extrapolated from [10]).

cell environment. The second approach is to allow potentially large excursions of X when circuits are added or removed from the cell environment, but engineer the circuit so that its function is unaltered by changes in X , that is, its function adapts to changes in X .

Engineering X robustness to changing demands by large fan-out. Assume that X has a large number of sites, denoted q , to which it can bind (and unbind) and assume that we add some more sites, denoted p , belonging, for example to synthetic circuits. The introduction of sites p will increase the demand of X and will tend to decrease the amount of free X . However, such a decrease can be compensated by

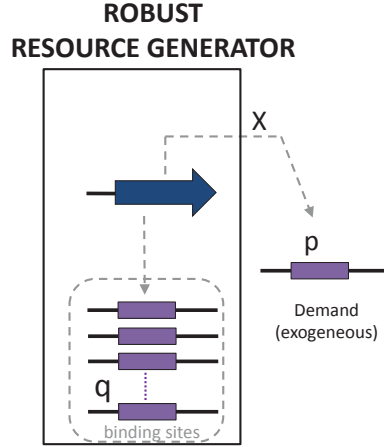


Figure 8.7: The role of q is to introduce a reservoir for X , so that more X is freed up from sites q when the demand increases.

having the X bound to sites q unbind them and increase the amount of free X . In this sense, sites q can be thought of a reservoir of X , from which X is released when needed. If this reservoir is much larger than the perturbation p , we should expect that X will stay about constant after the addition of sites p .

To mathematically justify this reasoning, assume that X is in total amount X_T and let $p \ll q$ (Figure ??). Denote C_0 the concentration of the complex of X with sites q and C_1 the concentration of the complex of X with sites p . The quasi-steady state approximation of these binding reactions gives $C_0 = (q/k_D)X$ and $C_1 = (p/k_D)X$, in which k_D is the dissociation constant of X with the sites. The conservation law for X gives the free amount of X as

$$X = \frac{X_T}{1 + (p/k_D) + (q/k_D)}.$$

Assume now that p is perturbed to $p + \Delta p$, then the resulting perturbation on X is given by

$$\Delta X = X_T \frac{\Delta p/k_D}{(1 + (p/k_D) + (q/k_D))(1 + (p/k_D) + (q/k_D) + (\Delta p/k_D))},$$

from which, it is clear that as q increases, the perturbation ΔX goes to zero. Since X also goes to zero as q increases, it is more meaningful to determine the percentage variation of X , which is given by

$$\frac{\Delta X}{X} = \frac{\Delta p/k_D}{(1 + (p/k_D) + (q/k_D) + (\Delta p/k_D))},$$

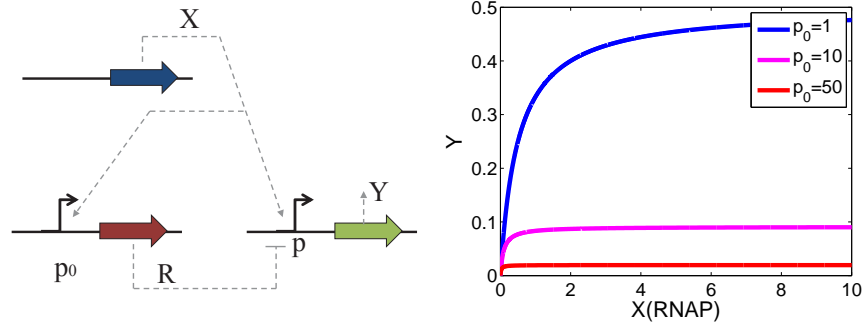


Figure 8.8: The output protein expression Y does not sensibly depend on the amounts of available RNAP (X) for sufficiently high values of p_0 .

which can be made arbitrarily small by increasing q . Hence, sufficiently large values of q lead to low sensitivity of the change in X when additional circuits are added or removed from the cell. As a consequence, the induced perturbation on the circuits in the cell can be reduced by increasing q .

Engineering adaptation in circuits to changes of X . We have seen in Chapter 3 that incoherent feedforward loops can engineer adaptation to changes in their input. Here, we show how this mechanism can be employed in order to make the expression level of a protein in a synthetic circuit independent of the availability of X (RNAP). For this sake, let Y be a protein that is constitutively expressed by a promoter p in total amounts p_T . Its expression level is going to be proportional to $X(p/k_D)$, so that if there is a perturbation in the free amount of X , there is going to be a proportional perturbation in the amount of Y . In order to make the expression level of Y independent of changes in X , we add to the circuit expressing Y an auxiliary circuit that constitutively expresses a repressor protein R , which competes with X for the promoter sites p , causing an effective repression of Y (Figure 8.8(Left)). The idea of this design is as follows. When the availability of X decreases, the steady state value of Y should also decrease. At the same time, the amounts of R also decreases, resulting in a consequent decrease of the repression of Y , so that the steady state value of Y should increase. If these two effects are well balanced, one should expect that no substantial change of Y is observed. This is mathematically studied by considering the reactions involved in the system and their associated ODE.

Specifically, let p_0 denote the amounts of promoter expressing protein R , let C' be the concentration of the complex of protein R with promoter p , and let C be the concentration of the complex of X with promoter p . Since X and R bind to p competitively, we have that $p_T = p + C + C'$. As a consequence, at the steady state, we have that

$$C = \frac{p_T(X/k_D)}{(X/k_D) + (R/k'_D) + 1},$$

in which $R = Kp_0(X/k_D)$ with K proportional to the strength of promoter p_0 and k'_D the dissociation constant of R with p . Since the steady state value of Y is proportional to the amount of complex C , we have that

$$Y \propto \frac{p_T(X/k_D)}{X(1/k_D + (Kp_0)/(k'_D k_D)) + 1}.$$

As p_0 becomes larger, we have that approximately $Y \propto (p_T k'_D)/(Kp_0)$, which is not dependent on X and, as a consequence, is not affected by changes in X . That is, the circuit's output Y adapts to changes in its input X . This is also shown in Figure 8.8 (Right), in which the steady state value of Y becomes more and more insensitive to changes in X as p_0 is increased. Of course, increasing p_0 decreases also the steady state value of Y , so the amounts of promoters p and p_0 should be chosen comparably large in such a way that a desired value of Y is not too low.

8.2 Stochastic Effects: Design Tradeoffs between Retroactivity and Noise

As we have seen in Chapter 7, a bio-molecular system can be rendered insensitive to retroactivity by implementing a large input amplification gain in a negative feedback loop. This type of design, however, relying on large amplifications, may have undesired effects on the internal noise of the system, as illustrated in Chapter 4. Also, it is not clear so far what the effect of retroactivity is on the noise content of the upstream system. Here, we employ the tools seen in Chapter 4 to answer these questions.

Consider a transcriptional system that takes a transcription factor U as an input and produces a transcription factor Z as output. The transcription rate of the gene z , which expresses the protein Z , is given by a time varying function $Gk(t)$ that depends on the transcription factor U . This dependency is not modeled, since it is not central to our discussion. The parameter G models the input amplification gain. The degradation rate of protein Z is also assumed to be tunable and thus identified by $G\delta$. The variable gain parameter G will be adjusted to improve the insulation properties.

The transcription factor Z is also an input to the downstream load through the reversible binding of Z to promoter sites p . Neglecting the Z messenger RNA dynamics, the system can be modeled by the chemical equations $0 \xrightleftharpoons[G k(t)]{G\delta} Z$ and $Z + p \xrightleftharpoons[k_{\text{on}}]{k_{\text{off}}} C$. We assume that $k(t)$ and δ are of the same order and denote $k_d = k_{\text{off}}/k_{\text{on}}$. We also assume that the production and decay processes are slower than binding and unbinding reactions, that is, $k_{\text{off}} \gg G\delta$, $k_{\text{on}} \gg G\delta$ as performed before. Let the total concentration of promoter be p_{tot} . The deterministic ordinary differ-

ential equation model is given by

$$\begin{aligned} [\dot{Z}] &= Gk(t) - G\delta[Z] + k_{\text{off}}[C] - k_{\text{on}}(p_{\text{tot}} - [C])[Z], \\ [\dot{C}] &= -k_{\text{off}}[C] + k_{\text{on}}(p_{\text{tot}} - [C])Z, \end{aligned} \quad (8.6)$$

in which $[Z]$ and $[C]$ denote the concentrations of Z and C respectively.

To identify by what amounts G should be increased to compensate the retroactivity effect, we perform a linearized analysis of (8.6) about $k(t) = \bar{k}$, and the corresponding equilibrium $[\bar{Z}] = \bar{k}/\delta$ and $[\bar{C}] = [\bar{Z}]p_{\text{tot}}/([\bar{Z}] + K_d)$. The dynamics of small perturbations about the equilibrium $(\bar{k}, [\bar{Z}], [\bar{C}])$ are, with abuse of notation, given by

$$\begin{aligned} [\dot{Z}] &= Gk(t) - (G\delta + k_{\text{on}}(p_{\text{tot}} - [\bar{C}]))[Z] \\ &\quad + (k_{\text{off}} + k_{\text{on}}[\bar{Z}])[C], \\ [\dot{C}] &= k_{\text{on}}(p_{\text{tot}} - [\bar{C}])[Z] - (k_{\text{off}} + k_{\text{on}}[\bar{Z}])[C]. \end{aligned} \quad (8.7)$$

Since $k_{\text{on}} \gg \delta$ and $k_{\text{off}} = k_{\text{on}}K_d$, write

$$k_{\text{on}} = \delta/\epsilon \text{ and } k_{\text{off}} = \delta K_d/\epsilon, \quad (8.8)$$

in which $\epsilon \ll 1$. Let $y = [Z] + [C]$. Substituting (8.8) into (8.7) and writing the system in terms of y and $[C]$, one obtains the system in the standard singular perturbation form

$$\begin{aligned} \dot{y} &= Gk(t) - (G\delta)(y - [C]) \\ \epsilon[\dot{C}] &= \delta(p_{\text{tot}} - [\bar{C}])y - \delta(p_{\text{tot}} - [\bar{C}] + K_d + [\bar{Z}])[C] \end{aligned}$$

Setting $\epsilon = 0$, one obtains the expression of the slow manifold as $[C] = K_d p_{\text{tot}} [Z] / ([\bar{Z}] + K_d)^2 := \gamma([Z])$. It can be shown that this manifold is exponentially stable. Defining the constant

$$R_l = \frac{K_d p_{\text{tot}}}{(\bar{k}/\delta + K_d)^2}, \quad (8.9)$$

the expression of the slow manifold can be rewritten as $\gamma([Z]) = R_l [Z]$. Letting $[Z] = y - \gamma([Z])$, we obtain that $[\dot{Z}] = \dot{y} - R_l [\dot{Z}]$, in which $\dot{y} = Gk(t) - G\delta[Z]$. The approximated dynamics of $[Z]$ on the slow manifold then become

$$[\dot{Z}] = \frac{G}{1 + R_l} (k(t) - \delta[Z]). \quad (8.10)$$

Thus, for small perturbations about the equilibrium, we should choose $G \approx 1 + R_l$ to compensate for retroactivity from the load. In real systems, however, there are practical limitations on how much the gain can be increased so that retroactivity may not be completely rejected.

Steady state effects of retroactivity

Let $P(Z, C, p; t | Z_0, C_0, p_0; t_0 = 0)$ denote the conditional probability that at time t , the number of molecules of the species Z , C and p are Z , C and p respectively, given that the number of molecules were Z_0 , C_0 and p_0 at the initial time $t_0 = 0$. Throughout this paper we omit the dependency on initial conditions and write $P(Z, C, p; t)$ for convenience. Let Ω denote the volume of the system. Then the relation between concentrations and number of molecules is given by $Z = \Omega[Z]$ and $C = \Omega[C]$. Define the step operator as $\mathbb{E}_X^a f(X) = f(X + a)$. The Master Equation

$$\begin{aligned} \dot{P}(Z, C, p; t) &= \left(Gk(t)\Omega(\mathbb{E}_Z^{-1} - 1) + G\delta(\mathbb{E}_Z^{+1} - 1) \right) Z \\ &+ k_{\text{on}}\Omega^{-1}(\mathbb{E}_Z^{+1}\mathbb{E}_p^{+1}\mathbb{E}_C^{-1} - 1)Zp \\ &+ k_{\text{off}}(\mathbb{E}_Z^{-1}\mathbb{E}_p^{-1}\mathbb{E}_C^{+1} - 1)C \Big) P(Z, C, p; t). \end{aligned}$$

Since $p + C = \Omega p_{\text{tot}}$ with probability one, the equation can be reduced to the two-state Master Equation

$$\begin{aligned} \dot{P}(Z, C; t) &= \left(Gk(t)\Omega(\mathbb{E}_Z^{-1} - 1) + G\delta(\mathbb{E}_Z^{+1} - 1) \right) Z \\ &+ k_{\text{on}}(\Omega^{-1}(\mathbb{E}_Z^{+1}\mathbb{E}_C^{-1} - 1)Z(\Omega p_{\text{tot}} - C) \\ &+ k_{\text{off}}(\mathbb{E}_Z^{-1}\mathbb{E}_C^{+1} - 1)C) P(Z, C; t). \end{aligned} \quad (8.11)$$

Since the coefficients of $P(Z, C; t)$ in equation (8.11) are not linear functions of the states, we cannot obtain a closed set of exact equations for the moments. To proceed with the analysis, we thus employ the Ω -expansion [?].

Define the change of variables

$$Z = \Omega\phi_Z + \Omega^{1/2}\zeta \text{ and } C = \Omega\phi_C + \Omega^{1/2}\xi, \quad (8.12)$$

in which ζ and ξ are random variables and ϕ_Z , ϕ_C are deterministic quantities. Let also $\Pi(\zeta, \xi; t) := P(\Omega\phi_Z + \Omega^{1/2}\zeta, \Omega\phi_C + \Omega^{1/2}\xi; t)$. Then, the left hand side of equation (8.11) becomes

$$\begin{aligned} \dot{P}(Z, C; t) &= \partial_t \Pi(\zeta, \xi; t) - \Omega^{1/2} \dot{\phi}_Z \partial_\zeta \Pi(\zeta, \xi; t) \\ &- \Omega^{1/2} \dot{\phi}_C \partial_\xi \Pi(\zeta, \xi; t), \end{aligned} \quad (8.13)$$

in which $\partial_x := \partial/\partial x$. By performing Taylor expansion of the step operator in the new variables ζ and ξ , we obtain the identities

$$\mathbb{E}_Z^a = \sum_{k=0}^{\infty} \frac{(a\Omega^{-1/2})^k}{k!} \partial_\zeta^k, \quad \mathbb{E}_C^a = \sum_{k=0}^{\infty} \frac{(a\Omega^{-1/2})^k}{k!} \partial_\xi^k. \quad (8.14)$$

Substituting (8.11) and (8.14) in equation (8.13), solving for $\partial_t \Pi(\zeta, \xi; t)$ and collecting the terms in powers of Ω up to order Ω^0 , we obtain

$$\begin{aligned}
\partial_t \Pi(\zeta, \xi; t) &= \Omega^{1/2} \left[(\dot{\phi}_Z - Gk(t) + G\delta\phi_Z + k_{\text{on}}\phi_Z(p_{\text{tot}} - \phi_C) \right. \\
&\quad - \phi_C) - k_{\text{off}}\phi_C \partial_\zeta + (\dot{\phi}_C - k_{\text{on}}\phi_Z(p_{\text{tot}} - \phi_C) \\
&\quad \left. + k_{\text{off}}\phi_C) \partial_\xi \right] \Pi(\zeta, \xi; t) \\
&+ \Omega^0 \left[\partial_\zeta ((G\delta + k_{\text{on}}(p_{\text{tot}} - \phi_C))\zeta + (-k_{\text{on}}\phi_Z - k_{\text{off}})\xi) \right. \\
&\quad + \partial_\xi (-k_{\text{on}}(p_{\text{tot}} - \phi_C)\zeta + (k_{\text{on}}\phi_Z + k_{\text{off}})\xi) \\
&\quad + \frac{1}{2} \partial_\zeta^2 (Gk(t) + G\delta\phi_Z + k_{\text{on}}\phi_Z(p_{\text{tot}} - \phi_C) + k_{\text{off}}\phi_C) \\
&\quad + \frac{1}{2} \partial_\xi^2 (k_{\text{on}}\phi_Z(p_{\text{tot}} - \phi_C) + k_{\text{off}}\phi_C) \\
&\quad \left. + \partial_\zeta \partial_\xi (-k_{\text{on}}\phi_Z(p_{\text{tot}} - \phi_C) - k_{\text{off}}\phi_C) \right] \Pi(\zeta, \xi; t) \\
&+ O(\Omega^{-1/2}). \tag{8.15}
\end{aligned}$$

Setting the coefficient of $\Omega^{1/2}$ in equation (8.15) to zero, one obtains the macroscopic laws for the deterministic variables ϕ_Z and ϕ_C :

$$\begin{aligned}
\dot{\phi}_Z &= Gk(t) - \delta\phi_Z - k_{\text{on}}\phi_Z(p_{\text{tot}} - \phi_C) + k_{\text{off}}\phi_C \\
\dot{\phi}_C &= k_{\text{on}}\phi_Z(p_{\text{tot}} - \phi_C) - k_{\text{off}}\phi_C. \tag{8.16}
\end{aligned}$$

By taking the volume to be large enough to make $O(\Omega^{-1/2})$ negligible in equation (8.15), we obtain the Fokker-Planck equation¹

$$\begin{aligned}
\partial_t \Pi(\zeta, \xi; t) &= \left[\partial_\zeta ((G\delta + k_{\text{on}}(p_{\text{tot}} - \phi_C))\zeta + (-k_{\text{on}}\phi_Z \right. \\
&\quad - k_{\text{off}})\xi) + \partial_\xi (-k_{\text{on}}(p_{\text{tot}} - \phi_C)\zeta + (k_{\text{on}}\phi_Z + k_{\text{off}})\xi) \\
&\quad + \frac{1}{2} \partial_\zeta^2 (Gk(t) + G\delta\phi_Z + k_{\text{on}}\phi_Z(p_{\text{tot}} - \phi_C) + k_{\text{off}}\phi_C) \\
&\quad + \frac{1}{2} \partial_\xi^2 (k_{\text{on}}\phi_Z(p_{\text{tot}} - \phi_C) + k_{\text{off}}\phi_C) \\
&\quad \left. + \partial_\zeta \partial_\xi (-k_{\text{on}}\phi_Z(p_{\text{tot}} - \phi_C) - k_{\text{off}}\phi_C) \right] \Pi(\zeta, \xi; t). \tag{8.17}
\end{aligned}$$

The above procedure, often referred to as Linear Noise Approximation (see Chapter 4), takes the jump Markov process defined by equation (8.11) and approximates it by the continuous Markov process that solves equation (8.17) [?]. This approximation is valid for large volumes and when the jumps on the original process are small compared to the total number of molecules [?]. Since all reactions

¹The function $\Pi(\zeta, \xi; t)$ was scaled so that it integrates to 1 [?].

have stoichiometry 1, this second condition is satisfied by guaranteeing $\Omega\phi_Z(t) \gg 1$ and $\Omega\phi_C(t) \gg 1$ for all time. Since we already take Ω large to satisfy the first condition, we just need to guarantee $\phi_C(t) > 0$ and $\phi_Z(t) > 0$.

Given a general Fokker-Planck equation of the form

$$\partial P_i(x; t) = - \sum_i \partial_i A_i(x, t) P(x, t) + \frac{1}{2} \sum_i \sum_j \partial_i \partial_j B_{ij}(x, t) P(x, t), \quad (8.18)$$

it is possible to derive differential equations for the expectancy of any polynomial function $f(x)$. Multiplying both sides of equation (8.18) by $f(x)$ and integrating both sides over the state space one obtains the differential equation [?]

$$\mathbb{E}(\dot{f}(x)) = \sum_i \mathbb{E}(A_i \partial_i f(x)) + \frac{1}{2} \sum_i \sum_j \mathbb{E}(B_{ij} \partial_i \partial_j f(x)). \quad (8.19)$$

Repeating this process with the Fokker-Planck equation (8.17), we obtain the differential equations for the first order moments as

$$\begin{aligned} \mathbb{E}(\dot{\zeta}) &= -\delta \mathbb{E}(\zeta) - k_{\text{on}}(p_{\text{tot}} - \phi_C) \mathbb{E}(\zeta) + k_{\text{on}} \phi_Z \mathbb{E}(\xi) \\ &\quad + k_{\text{off}} \mathbb{E}(\xi), \\ \mathbb{E}(\dot{\xi}) &= k_{\text{on}}(p_{\text{tot}} - \phi_C) \mathbb{E}(\zeta) - k_{\text{on}} \phi_Z \mathbb{E}(\xi) - k_{\text{off}} \mathbb{E}(\xi). \end{aligned} \quad (8.20)$$

Setting the initial conditions of the macroscopic equations (8.16) to correspond to the initial values of the number of species, that is, setting $\phi_Z(0) = \Omega^{-1} Z_0$ and $\phi_C(0) = \Omega^{-1} C_0$, then $\mathbb{E}(\zeta(0)) = 0$ and $\mathbb{E}(\xi(0)) = 0$. In doing so, $\mathbb{E}(\zeta(t)) = 0$ and $\mathbb{E}(\xi(t)) = 0$ for all time. Therefore, $\zeta(t)$ and $\xi(t)$ are zero-mean random processes.

Similarly, the dynamics of the second order moments are given by

$$\begin{aligned} \mathbb{E}(\dot{\zeta}^2) &= -2G\delta \mathbb{E}(\zeta^2) - 2k_{\text{on}}(p_{\text{tot}} - \phi_C) \mathbb{E}(\zeta^2) + 2k_{\text{on}} \phi_Z \mathbb{E}(\zeta \xi) \\ &\quad + 2k_{\text{off}} \mathbb{E}(\zeta \xi) + k_{\text{on}} \phi_Z (p_{\text{tot}} - \phi_C) + k_{\text{off}} \phi_C \\ &\quad + Gk(t) + G\delta \phi_Z \\ \mathbb{E}(\dot{\zeta} \xi) &= -G\delta \mathbb{E}(\zeta \xi) + k_{\text{on}} \phi_Z \mathbb{E}(\xi^2) + k_{\text{off}} \mathbb{E}(\xi^2) \\ &\quad + k_{\text{on}}(p_{\text{tot}} - \phi_C) \mathbb{E}(\zeta^2) - k_{\text{on}} \phi_Z \mathbb{E}(\zeta \xi) - k_{\text{off}} \zeta \xi \\ &\quad - k_{\text{on}} \phi_Z (p_{\text{tot}} - \phi_C) - k_{\text{off}} \phi_C \\ \mathbb{E}(\dot{\xi}^2) &= 2k_{\text{on}}(p_{\text{tot}} - \phi_C) \mathbb{E}(\zeta \xi) - 2k_{\text{on}} \phi_Z \mathbb{E}(\xi^2) - 2k_{\text{off}} \mathbb{E}(\xi^2) \\ &\quad + k_{\text{on}} \phi_Z (p_{\text{tot}} - \phi_C) + k_{\text{off}} \phi_C. \end{aligned} \quad (8.21)$$

To validate the Fokker-Planck approximation (8.17), we compare the time-dependent mean and standard deviation of the concentrations predicted by numerical integrations of equations (8.16) and (8.21) with the mean and standard-deviation from sample realizations given by a Stochastic Simulation Algorithm (SSA) implementation (see Chapter 4). Let the means be denoted by $\mu_{[Z]} = \mathbb{E}([Z])$

and $\mu_{[C]} = \mathbb{E}([C])$ and the standard deviations denoted by $\sigma_{[Z]} = \sqrt{\mathbb{E}((\Omega^{-1}Z)^2 - \mu_{[Z]}^2)}$ and $\sigma_{[C]} = \sqrt{\mathbb{E}((\Omega^{-1}C)^2 - \mu_{[C]}^2)}$. To obtain these quantities from the Fokker-Planck approximation, recall that ζ and ξ are zero-mean random variables and that ϕ_Z and ϕ_C are deterministic. Then, from the substitution of variables (8.12) the mean concentration of Z and C are given by $\mu_{[Z]} = \phi_Z$, $\mu_{[C]} = \phi_C$. The standard deviation of $[Z]$ is given by $\sigma_{[Z]} = \sqrt{\Omega^{-1}\mathbb{E}(\zeta^2)}$ and $\sigma_{[C]} = \sqrt{\Omega^{-1}\mathbb{E}(\xi^2)}$. To obtain these quantities from N realizations Z_i and C_i of the SSA we used the sample mean and the biased sample variance estimator, that is, $\mu_{[Z]} = \sum_i^N Z_i / (N\Omega)$, $\mu_{[C]} = \sum_i^N C_i / (N\Omega)$, $\sigma_{[Z]}^2 = \sum_{i=1}^N ((\Omega^{-1}Z_i)^2 - \mu_{[Z]}^2) / N$ and $\sigma_{[C]}^2 = \sum_{i=1}^N ((\Omega^{-1}C_i)^2 - \mu_{[C]}^2) / N$.

Figure 8.9 shows that the means and standard deviations of Z and C predicted by the Fokker-Planck equation are very close to the values obtained from the samples of the SSA. This comparison was made using different values of G , p_{tot} and K_d , all showing that the Fokker-Planck equation is a satisfactory approximation for the Master Equation.

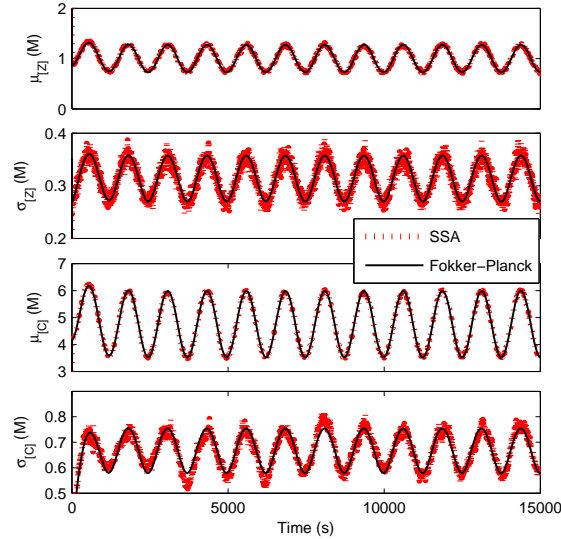


Figure 8.9: The sample means and variances from SSA and from Fokker-Planck equation are shown to be very close to each other. For these plots, $\delta = 0.01\text{M}^{-1}\text{s}^{-1}$, $K_d = 20\text{M}$, $k_{\text{off}} = 50\text{M}^{-1}\text{s}^{-1}$ with input signal $k(t) = \delta(1 + 0.8 \sin \omega t)\text{s}^{-1}$ and volume $\Omega = 10\text{M}^{-1}$. To simulate the time varying input in the SSA, we imposed a deterministic time-varying concentration of a Z protein messenger with concentration $k(t) = \delta(1 + 0.8 \sin(\omega t))$. Means from SSA were calculated using 500 realizations.

To calculate the values of $\bar{\sigma}^2$, set $k(t) = \bar{k}$ in equations (8.16) and (8.21). The corresponding equilibrium values of the deterministic variables ϕ_Z and ϕ_C are ob-

tained from equations (8.16) as

$$\bar{\phi}_Z = \frac{\bar{k}}{\delta} \text{ and } \bar{\phi}_C = \frac{p_{\text{tot}}\bar{\phi}_Z}{1 + \delta K_d/\bar{k}} = \frac{p_{\text{tot}}/K_d}{1 + \bar{\phi}_Z/K_d}. \quad (8.22)$$

Substituting (8.22) in equations (8.21) and setting the time derivatives to zero, the equilibrium values for the second-order moments become

$$\mathbb{E}(\bar{\zeta}^2) = \frac{\bar{k}}{\delta}, \quad \mathbb{E}(\bar{\zeta}\bar{\xi}) = 0 \text{ and } \mathbb{E}(\bar{\xi}^2) = \frac{\bar{\phi}_Z p_{\text{tot}} K_d}{(\bar{k}/\delta + K_d)^2} = \bar{\phi}_Z R_l,$$

in which R_l is the same constant defined in expression (8.9).

From the change of variables (8.12), and since ζ and ξ are zero-mean, we have that $\bar{\sigma}_{[Z]}^2 = \Omega^{-1}\mathbb{E}(\bar{\zeta}^2)$ and $\bar{\sigma}_{[C]}^2 = \Omega^{-1}\mathbb{E}(\bar{\xi}^2)$ leading to expressions

$$\bar{\sigma}_{[Z]}^2 = \frac{\bar{\phi}_Z}{\Omega} \text{ and } \bar{\sigma}_{[C]}^2 = \frac{\bar{\phi}_Z R_l}{\Omega}. \quad (8.23)$$

For small amplitudes of the signal $\tilde{k}(t)$, $\bar{\sigma}^2$ approximates the time-average value of the time-dependent variance $\sigma(t)$ when the system is subject to the input $k(t) = \bar{k} + \tilde{k}(t)$. This result implies that there is no effect of retroactivity on the steady state mean and variance of the upstream system.

Dynamic effects of retroactivity

We have shown that increasing the gain G is beneficial for rejecting retroactivity to the upstream component. However, as shown in Figure 8.10, increasing the gain G impacts the frequency content of the noise in a single realization. For low values of G , the error signal between a realization and the mean is of lower frequency when compared to a higher gain.

To study this problem, we employ the Langevin equation derived from the Master Equation (8.11). As shown in Chapter 4, a Master Equation of the form

$$\frac{dP(\mathbf{X}; t)}{dt} = \sum_{j=1}^M \left(\prod_{i=1}^N \mathbb{E}_{x_i}^{v_{ij}} - 1 \right) a_j(\mathbf{X}) P(\mathbf{X}; t),$$

can be approximated by a Langevin system of equations of the form

$$\frac{dX_i}{dt} = \sum_{j=1}^M v_{ij} a_j(\mathbf{X}(t)) + \sum_{j=1}^M v_{ij} a_j^{1/2}(\mathbf{X}(t)) \Gamma_j(t),$$

in which $\Gamma_j(t)$ are independent Gaussian white noise processes. Applying the above approximation to the Master Equation (8.11), one obtains the system of Langevin

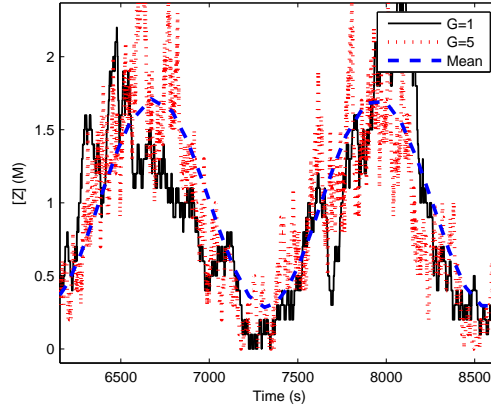


Figure 8.10: Increasing the value of G produces a disturbance signal of higher frequency. Two realizations are shown with different values for G without load. The parameters used in the simulations are $\delta = 0.01\text{M}^{-1}\text{s}^{-1}$, $K_d = 20\text{M}$, $k_{\text{off}} = 50\text{M}^{-1}\text{s}^{-1}$, $\omega = 0.005\text{rad/s}$ and $\Omega = 10\text{M}^{-1}$. The input signal used is $k(t) = \delta(1 + 0.8\sin\omega t)\text{s}^{-1}$. The mean of the signal is given as reference.

equations

$$\begin{aligned}
 \dot{Z} &= Gk(t) - G\delta Z - k_{\text{on}}(p_{\text{tot}} - C)Z + k_{\text{off}}C \\
 &\quad + \sqrt{Gk(t)}\Gamma_1(t) - \sqrt{G\delta Z}\Gamma_2(t) \\
 &\quad - \sqrt{k_{\text{on}}(p_{\text{tot}} - C)Z}\Gamma_3(t) + \sqrt{k_{\text{off}}C}\Gamma_4(t), \\
 \dot{C} &= k_{\text{on}}(p_{\text{tot}} - C)Z - k_{\text{off}}C + \sqrt{k_{\text{on}}(p_{\text{tot}} - C)Z}\Gamma_3(t) \\
 &\quad - \sqrt{k_{\text{off}}C}\Gamma_4(t).
 \end{aligned} \tag{8.24}$$

The above system can be viewed as a non-linear system with five inputs, $k(t)$ and $\Gamma_i(t)$ for $i = 1, 2, 3, 4$. Let $k(t) = \bar{k}$, $\Gamma_1(t) = \Gamma_2(t) = \Gamma_3(t) = \Gamma_4(t) = 0$ be constant inputs and let \bar{Z} and \bar{C} be the corresponding equilibrium points. Then for small amplitude signals $\tilde{k}(t)$ the linearization of the system (8.24) leads, with abuse of notation, to

$$\begin{aligned}
 \dot{Z} &= G\tilde{k}(t) - G\delta Z - k_{\text{on}}(p_{\text{tot}} - \bar{C})Z + k_{\text{on}}\bar{Z}\bar{C} + k_{\text{off}}C \\
 &\quad + \sqrt{G\tilde{k}}\Gamma_1(t) - \sqrt{\delta\bar{Z}}\Gamma_2(t) - \sqrt{k_{\text{off}}\bar{C}}\Gamma_3(t) \\
 &\quad + \sqrt{k_{\text{on}}(p_{\text{tot}} - \bar{C})\bar{Z}}\Gamma_4(t) \\
 \dot{C} &= k_{\text{on}}(p_{\text{tot}} - \bar{C})Z - k_{\text{on}}\bar{Z}\bar{C} - k_{\text{off}}C + \sqrt{k_{\text{off}}\bar{C}}\Gamma_3(t) \\
 &\quad - \sqrt{k_{\text{on}}(p_{\text{tot}} - \bar{C})\bar{Z}}\Gamma_4(t).
 \end{aligned}$$

We can further simplify the above expressions by noting that $\delta\bar{Z} = G\bar{k}$ and $k_{\text{on}}(p_{\text{tot}} -$

$\bar{C})\bar{Z} = k_{\text{off}}\bar{C}$. Also, since Γ_j are independent identical Gaussian white noises, we can write $\Gamma_1(t) - \Gamma_2(t) = \sqrt{2}N_1(t)$ and $\Gamma_3(t) - \Gamma_4(t) = \sqrt{2}N_2(t)$, in which $N_1(t)$ and $N_2(t)$ are independent Gaussian white noises identical to $\Gamma_j(t)$. This simplification leads to the system

$$\begin{aligned}\dot{Z} &= G\tilde{k}(t) - G\delta Z - k_{\text{on}}(p_{\text{tot}} - \bar{C})Z + k_{\text{on}}\bar{Z}C + k_{\text{off}}C \\ &\quad + \sqrt{2G\bar{k}}N_1(t) - \sqrt{2k_{\text{off}}\bar{C}}N_2(t), \\ \dot{C} &= k_{\text{on}}(p_{\text{tot}} - \bar{C})Z - k_{\text{on}}\bar{Z}C - k_{\text{off}}C \\ &\quad + \sqrt{2k_{\text{off}}\bar{C}}N_2(t).\end{aligned}\tag{8.25}$$

This is a system with three inputs: the deterministic input $\tilde{k}(t)$ and two independent white noise sources $N_1(t)$ and $N_2(t)$. One can interpret N_1 as the source of the fluctuations caused by the production and degradation reactions while N_2 is the source of fluctuations caused by binding and unbinding reactions. Since the system is linear, we can analyze the different contributions of each noise source separately and independent from the signal $\tilde{k}(t)$.

The transfer function from N_1 to Z is

$$T_1(s) = \frac{\sqrt{G\bar{k}}}{(s + G\delta)(s + k_{\text{on}}\bar{Z} + k_{\text{off}}) + sk_{\text{on}}(p_{\text{tot}} - \bar{C})}.$$

Employing substitutions (8.8) and setting $\epsilon = 0$, we simplify the transfer function to

$$T_1(s) = \frac{Z(s)}{N_1(s)} = \frac{\sqrt{2G\bar{k}}}{s(1 + R_l) + G\delta}.\tag{8.26}$$

The zero frequency gain of this transfer function is equal to $T_1(0) = \sqrt{2\bar{k}}/\sqrt{G}\delta$. Thus, as G increases, the zero frequency gain decreases. But for large enough frequencies ω , $j\omega(1 + R_l) + G\delta \approx j\omega(1 + R_l)$, and the amplitude $|T_1(j\omega)| \approx \sqrt{2\bar{k}}G/\omega(1 + R_l)$ becomes a monotone function of G . This effect is illustrated in the upper plot of Figure 8.11. The frequency at which the amplitude of $|T_1(j\omega)|$ computed with $G = 1$ intersects the amplitude $|T_2(j\omega)|$ computed with $G > 1$ is given by the expression

$$\omega_e = \frac{\delta\sqrt{G}}{(1 + R_l)}.$$

Thus, when increasing the gain from 1 to $G > 1$, we reduce the noise at frequencies lower than ω_e but we increase it at frequencies larger than ω_e .

The transfer function from the second white noise source N_2 to Z is given by

$$\begin{aligned}T_2(s) &= \left[\sqrt{2k_{\text{off}}\bar{C}}s \right] / \left[s^2 + (G\delta + k_{\text{on}}(p_{\text{tot}} - \bar{C}) + k_{\text{on}}\bar{Z} \right. \\ &\quad \left. + k_{\text{off}})s + G\delta(k_{\text{on}}\bar{Z} + k_{\text{off}}) \right].\end{aligned}$$

Using substitutions (8.8) and multiplying numerator and denominator by ϵ , we obtain the transfer function

$$T_2(s) = \frac{\left[\sqrt{\epsilon} \sqrt{2\delta\bar{C}}s \right]}{\left[\epsilon s^2 + (\epsilon G\delta + \delta(p_{\text{tot}} - \bar{C}) + \delta\bar{Z} + \delta K_d)s + G\delta(\delta\bar{Z} + \delta K_d) \right]}. \quad (8.27)$$

This transfer function has one zero at $s = 0$ and two poles at

$$s_{\pm} = \frac{\delta}{2\epsilon} \left[-\epsilon G - (p_{\text{tot}} - \bar{C}) - \bar{Z} + K_d \pm \sqrt{(\epsilon G + (p_{\text{tot}} - \bar{C}) + \bar{Z} + K_d)^2 - 4\epsilon G(\bar{Z} + K_d)} \right].$$

When $\epsilon \rightarrow 0$, $s_- \rightarrow -\infty$ and $s_+ \rightarrow -G\delta/(1 + R_l)$. Thus, the contribution of $N_2(t)$ to Z is relevant only on the high frequency range due to the high-pass nature of the transfer function. Furthermore, increasing the gain G increases the cutoff frequency given by the pole s_+ . It is also important to note that $N_2(s)$ is scaled by $\sqrt{\epsilon}$, making the noise on the low-frequency caused by $N_2(t)$ negligible when compared to that caused by $N_1(t)$. The Bode plot of the transfer function $T_2(s)$ is shown in the lower plot of Figure 8.11.

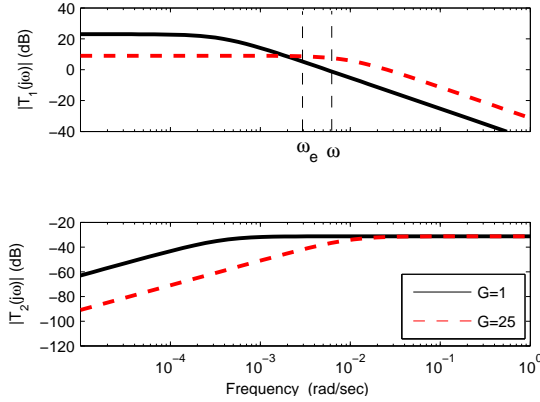


Figure 8.11: Magnitude of the transfer functions $T_1(s)$ and $T_2(s)$. The parameters used in this plot are $\delta = 0.01\text{M}^{-1}\text{s}^{-1}$, $K_d = 1\text{M}$, $k_{\text{off}} = 50\text{M}^{-1}\text{s}^{-1}$, $\omega = 0.005\text{rad/s}$, $p_{\text{tot}} = 100\text{M}$. When G increases from 1 to $1 + R_l = 25$, contribution from N_1 decreases but it now spreads to a higher range of the spectrum. Note that there was an increase on the noise at the frequency of interest ω . Increasing G reduces the contribution from N_2 in the low frequency range, leaving the high frequency range unaffected. Note also that the amplitude of T_2 is significantly smaller than that of T_1 .

Concluding, while retroactivity contributes to filtering noise in the upstream system as it decreases the bandwidth of the noise transfer function, high gains

contribute to increasing noise at frequencies higher than ω_e . In particular, when increasing the gain from 1 to G we reduce the noise in the frequency ranges below $\omega_e = \delta \sqrt{G}/(R_l + 1)$, but the noise at frequencies above ω_e increases. Starting from the original system suffering from retroactivity, it is possible to increase the gain up to $G = R_l + 1$ to recover the isolated system behavior. In this case we obtain $\omega_e = \delta / \sqrt{R_l + 1} < \delta$. This implies that if the input signal is on the same time-scale of the natural dilution rates, which is often the case, we increase the noise in the frequencies of interest. This effect is showed on the top plot of Figure 8.11. In theory, one should increase G beyond $(R_l + 1)^2$ so that $\omega_e > \delta$, but in practice this may be difficult to realize when R_l is very large.

Appendix A

Cell Biology Primer

This appendix provides a brief overview of some of the key elements of cell biology. It is not intended to be read sequentially, but rather to be used as a reference for terms and concepts that may not be familiar to some readers.

Note: The text and figures in this appendix are based on *A Science Primer* by the National Center for Biotechnology Information (NCBI) of the National Library of Medicine (NLM) at the National Institutes of Health (NIH) [65]. The text in this chapter is not subject to copyright and may be used freely for any purpose, as described by the NLM:

Information that is created by or for the US government on this site is within the public domain. Public domain information on the National Library of Medicine (NLM) Web pages may be freely distributed and copied. However, it is requested that in any subsequent use of this work, NLM be given appropriate acknowledgment.

Some minor modifications have been made, including insertion of additional figures (from the NHGRI Talking Glossary [66]), deletion of some of the text not needed here, and minor editorial changes to maintain consistency with the main text.

The original material included here can be retrieved from the following web sites:

- <http://www.ncbi.nlm.nih.gov/About/primer/genetics.html>
- <http://www.genome.gov/glossary>

We gratefully acknowledge the National Library of Medicine for this material.

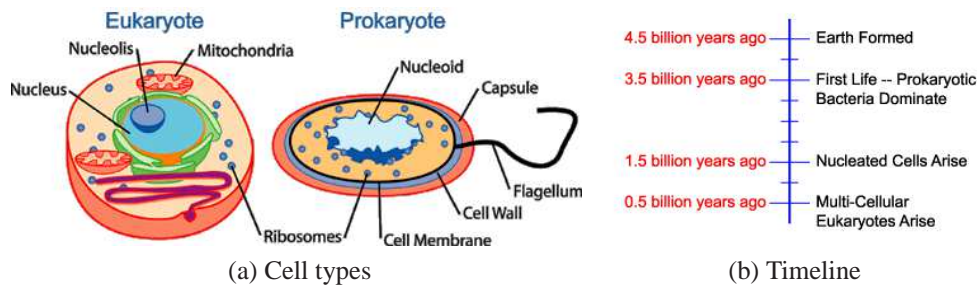


Figure A.1: Eukaryotes and prokaryotes. (a) This figure illustrates a typical human cell (*eukaryote*) and a typical bacterium (*prokaryote*). The drawing on the left highlights the internal structures of eukaryotic cells, including the nucleus (light blue), the nucleolus (intermediate blue), mitochondria (orange), and ribosomes (dark blue). The drawing on the right demonstrates how bacterial DNA is housed in a structure called the nucleoid (very light blue), as well as other structures normally found in a prokaryotic cell, including the cell membrane (black), the cell wall (intermediate blue), the capsule (orange), ribosomes (dark blue), and a flagellum (also black). (b) History of life on earth. Figures courtesy the National Library of Medicine.

A.1 What is a Cell

Cells are the structural and functional units of all living organisms. Some organisms, such as bacteria, are unicellular, consisting of a single cell. Other organisms, such as humans, are multicellular, or have many cells—an estimated 100,000,000,000,000 cells! Each cell is an amazing world unto itself: it can take in nutrients, convert these nutrients into energy, carry out specialized functions, and reproduce as necessary. Even more amazing is that each cell stores its own set of instructions for carrying out each of these activities.

Cell Organization

Before we can discuss the various components of a cell, it is important to know what organism the cell comes from. There are two general categories of cells: *prokaryotes* and *eukaryotes* (see Figure A.1a).

Prokaryotic Organisms

It appears that life arose on earth about 4 billion years ago (see Figure A.1b). The simplest of cells, and the first types of cells to evolve, were prokaryotic cells—organisms that lack a nuclear membrane, the membrane that surrounds the nucleus of a cell. Bacteria are the best known and most studied form of prokaryotic organisms, although the recent discovery of a second group of prokaryotes, called *archaea*, has provided evidence of a third cellular domain of life and new insights

into the origin of life itself.

Prokaryotes are unicellular organisms that do not develop or differentiate into multicellular forms. Some bacteria grow in filaments, or masses of cells, but each cell in the colony is identical and capable of independent existence. The cells may be adjacent to one another because they did not separate after cell division or because they remained enclosed in a common sheath or slime secreted by the cells. Typically though, there is no continuity or communication between the cells. Prokaryotes are capable of inhabiting almost every place on the earth, from the deep ocean, to the edges of hot springs, to just about every surface of our bodies.

Prokaryotes are distinguished from eukaryotes on the basis of nuclear organization, specifically their lack of a nuclear membrane. Prokaryotes also lack any of the intracellular organelles and structures that are characteristic of eukaryotic cells. Most of the functions of organelles, such as mitochondria, chloroplasts, and the Golgi apparatus, are taken over by the prokaryotic plasma membrane. Prokaryotic cells have three architectural regions: appendages called *flagella* and *pili*—proteins attached to the cell surface; a *cell envelope* consisting of a capsule, a *cell wall*, and a *plasma membrane*; and a *cytoplasmic region* that contains the *cell genome* (DNA) and ribosomes and various sorts of inclusions.

Eukaryotic Organisms

Eukaryotes include fungi, animals, and plants as well as some unicellular organisms. Eukaryotic cells are about 10 times the size of a prokaryote and can be as much as 1000 times greater in volume. The major and extremely significant difference between prokaryotes and eukaryotes is that eukaryotic cells contain membrane-bound compartments in which specific metabolic activities take place. Most important among these is the presence of a nucleus, a membrane-delineated compartment that houses the eukaryotic cell's DNA. It is this nucleus that gives the eukaryote—literally, true nucleus—its name.

Eukaryotic organisms also have other specialized structures, called *organelles*, which are small structures within cells that perform dedicated functions. As the name implies, you can think of organelles as small organs. There are a dozen different types of organelles commonly found in eukaryotic cells. In this primer, we will focus our attention on only a handful of organelles and will examine these organelles with an eye to their role at a molecular level in the cell.

The origin of the eukaryotic cell was a milestone in the evolution of life. Although eukaryotes use the same genetic code and metabolic processes as prokaryotes, their higher level of organizational complexity has permitted the development of truly multicellular organisms. Without eukaryotes, the world would lack mammals, birds, fish, invertebrates, mushrooms, plants, and complex single-celled organisms.

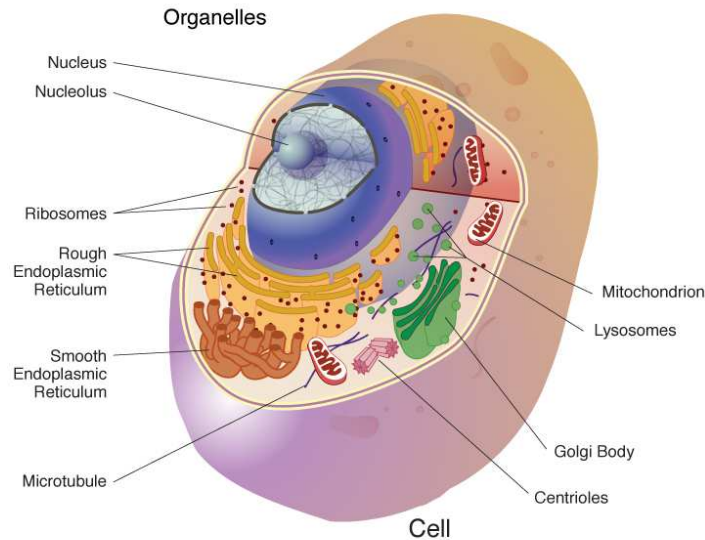


Figure A.2: An organelle is a subcellular structure that has one or more specific jobs to perform in the cell, much like an organ does in the body. Among the more important cell organelles are the nuclei, which store genetic information; mitochondria, which produce chemical energy; and ribosomes, which assemble proteins.

Cell Structures: The Basics

The Plasma Membrane—A Cell's Protective Coat

The outer lining of a eukaryotic cell is called the *plasma membrane*. This membrane serves to separate and protect a cell from its surrounding environment and is made mostly from a double layer of proteins and lipids, fat-like molecules. Embedded within this membrane are a variety of other molecules that act as channels and pumps, moving different molecules into and out of the cell. A form of plasma membrane is also found in prokaryotes, but in this organism it is usually referred to as the *cell membrane*.

The Cytoskeleton—A Cell's Scaffold

The *cytoskeleton* is an important, complex, and dynamic cell component. It acts to organize and maintain the cell's shape; anchors organelles in place; helps during *endocytosis*, the uptake of external materials by a cell; and moves parts of the cell in processes of growth and motility. There are a great number of proteins associated with the cytoskeleton, each controlling a cell's structure by directing, bundling, and aligning filaments.

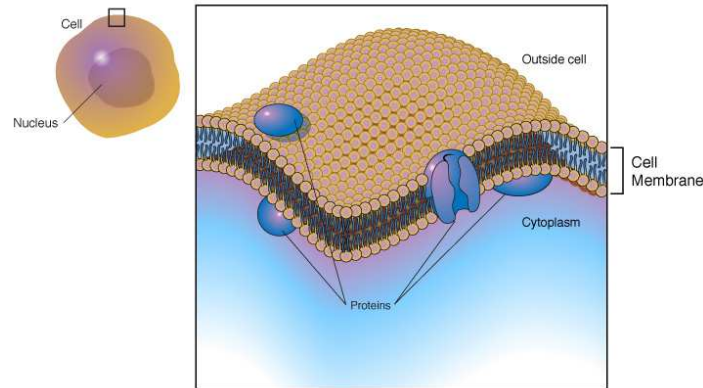


Figure A.3: The cell membrane, also called the plasma membrane, is found in all cells and separates the interior of the cell from the outside environment. The cell membrane consists of a lipid bilayer that is semipermeable. The cell membrane regulates the transport of materials entering and exiting the cell.

The Cytoplasm—A Cell's Inner Space

Inside the cell there is a large fluid-filled space called the *cytoplasm*, sometimes called the *cytosol*. In prokaryotes, this space is relatively free of compartments. In eukaryotes, the *cytosol* is the “soup” within which all of the cell’s organelles reside. It is also the home of the cytoskeleton. The cytosol contains dissolved nutrients, helps break down waste products, and moves material around the cell through a process called *cytoplasmic streaming*. The nucleus often flows with the cytoplasm changing its shape as it moves. The cytoplasm also contains many salts and is an excellent conductor of electricity, creating the perfect environment for the mechanics of the cell. The function of the cytoplasm, and the organelles which reside in it, are critical for a cell’s survival.

Genetic Material

Two different kinds of genetic material exist: *deoxyribonucleic acid (DNA)* and *ribonucleic acid (RNA)*. Most organisms are made of DNA, but a few viruses have RNA as their genetic material. The biological information contained in an organism is encoded in its DNA or RNA sequence. Prokaryotic genetic material is organized in a simple circular structure that rests in the cytoplasm. Eukaryotic genetic material is more complex and is divided into discrete units called *genes*. Human genetic material is made up of two distinct components: the *nuclear genome* and the *mitochondrial genome*. The nuclear genome is divided into 24 linear DNA molecules, each contained in a different *chromosome*. The *mitochondrial genome* is a circular DNA molecule separate from the nuclear DNA. Although the mitochondrial genome is very small, it codes for some very important proteins.

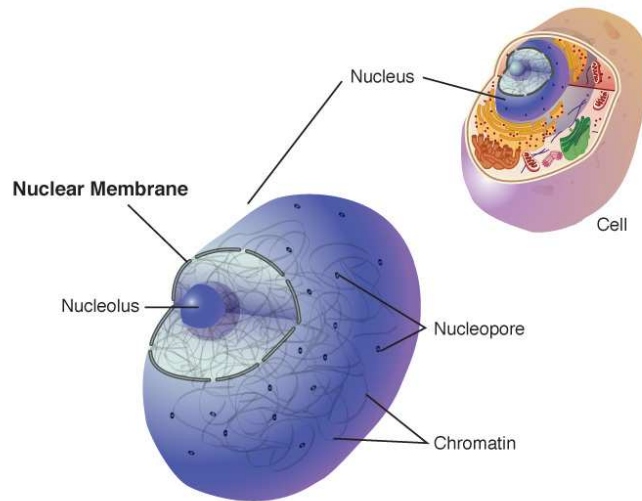


Figure A.4: A nuclear membrane is a double membrane that encloses the cell nucleus. It serves to separate the chromosomes from the rest of the cell. The nuclear membrane includes an array of small holes or pores that permit the passage of certain materials, such as nucleic acids and proteins, between the nucleus and cytoplasm.

Organelles

The human body contains many different organs, such as the heart, lung, and kidney, with each organ performing a different function. Cells also have a set of “little organs”, called *organelles*, that are adapted and/or specialized for carrying out one or more vital functions. Organelles are found only in eukaryotes and are always surrounded by a protective membrane. It is important to know some basic facts about the following organelles.

The Nucleus—A Cell’s Center. The *nucleus* is the most conspicuous organelle found in a eukaryotic cell. It houses the cell’s chromosomes and is the place where almost all DNA replication and RNA synthesis occur. The nucleus is spheroid in shape and separated from the cytoplasm by a membrane called the *nuclear envelope*. The nuclear envelope isolates and protects a cell’s DNA from various molecules that could accidentally damage its structure or interfere with its processing. During processing, DNA is *transcribed*, or synthesized, into a special RNA, called mRNA. This mRNA is then transported out of the nucleus, where it is translated into a specific protein molecule. In prokaryotes, DNA processing takes place in the cytoplasm.

The Ribosome—The Protein Production Machine. *Ribosomes* are found in both prokaryotes and eukaryotes. The ribosome is a large complex composed of many molecules, including RNAs and proteins, and is responsible for processing the ge-

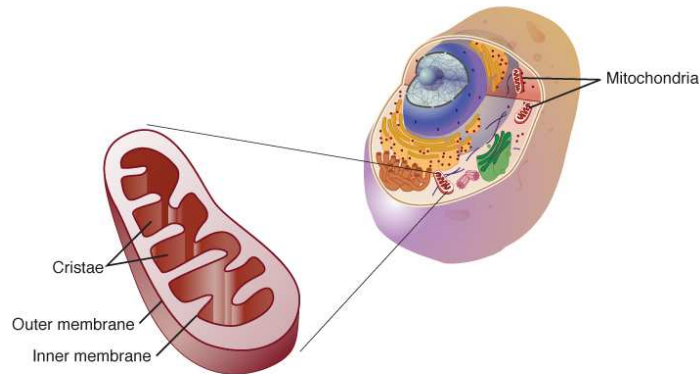


Figure A.5: Mitochondria are membrane-bound cell organelles (mitochondrion, singular) that generate most of the chemical energy needed to power the cell's biochemical reactions. Chemical energy produced by the mitochondria is stored in a small molecule called adenosine triphosphate (ATP). Mitochondria contain their own small chromosomes. Generally, mitochondria, and therefore mitochondrial DNA, are inherited only from the mother.

netic instructions carried by an mRNA. The process of converting an mRNA's genetic code into the exact sequence of amino acids that make up a protein is called *translation*. Protein synthesis is extremely important to all cells, and therefore a large number of ribosomes—sometimes hundreds or even thousands—can be found throughout a cell.

Ribosomes float freely in the cytoplasm or sometimes bind to another organelle called the endoplasmic reticulum. Ribosomes are composed of one large and one small subunit, each having a different function during protein synthesis.

Mitochondria and Chloroplasts—The Power Generators. Mitochondria are self-replicating organelles that occur in various numbers, shapes, and sizes in the cytoplasm of all eukaryotic cells. As mentioned earlier, mitochondria contain their own genome that is separate and distinct from the nuclear genome of a cell. Mitochondria have two functionally distinct membrane systems separated by a space: the *outer membrane*, which surrounds the whole organelle; and the *inner membrane*, which is thrown into folds or shelves that project inward. These inward folds are called *cristae*. The number and shape of cristae in mitochondria differ, depending on the tissue and organism in which they are found, and serve to increase the surface area of the membrane.

Mitochondria play a critical role in generating energy in the eukaryotic cell, and this process involves a number of complex pathways. Let's break down each of these steps so that you can better understand how food and nutrients are turned into energy packets and water. Some of the best energy-supplying foods that we eat contain complex sugars. These complex sugars can be broken down into a

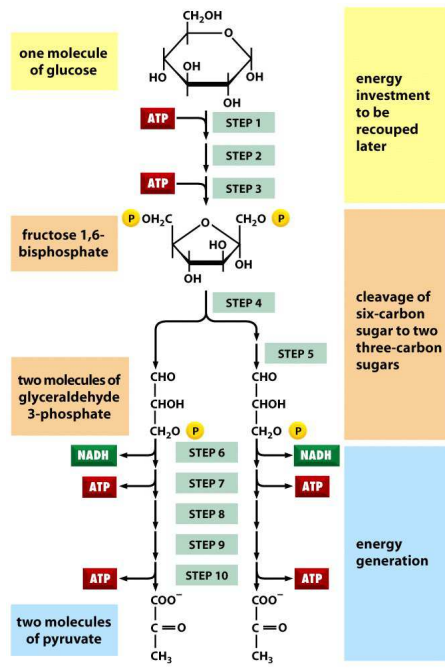


Figure 2-70 Molecular Biology of the Cell 5/e (© Garland Science 2008)

(a) Glycolysis

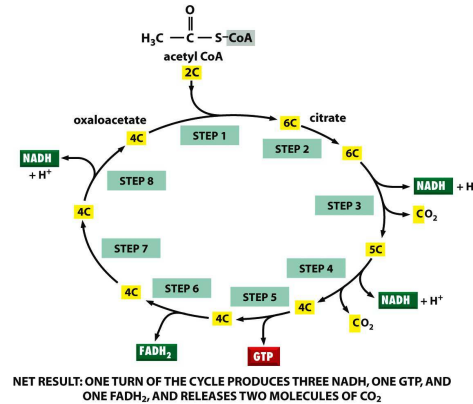
NET RESULT: ONE TURN OF THE CYCLE PRODUCES THREE NADH, ONE GTP, AND ONE FADH₂, AND RELEASES TWO MOLECULES OF CO₂

Figure 2-82 Molecular Biology of the Cell 5/e (© Garland Science 2008)

(b) Krebs's cycle

Figure A.6: Cell energy production. Reproduced from Alberts et al. [3]; permission pending.

less chemically complex sugar molecule called *glucose*. Glucose can then enter the cell through special molecules found in the membrane, called *glucose transporters*. Once inside the cell, glucose is broken down to make *adenosine triphosphate (ATP)*, a form of energy, via two different pathways.

The first pathway, *glycolysis*, requires no oxygen and is referred to as *anaerobic metabolism*. Glycolysis occurs in the cytoplasm outside the mitochondria. During glycolysis, glucose is broken down into a molecule called *pyruvate*. Each reaction is designed to produce some hydrogen ions that can then be used to make energy packets (*ATP*). However, only four *ATP* molecules can be made from one molecule of glucose in this pathway. In prokaryotes, glycolysis is the only method used for converting energy.

The second pathway, called the *Krebs's cycle*, or the *citric acid cycle*, occurs inside the mitochondria and is capable of generating enough *ATP* to run all the cell functions. Once again, the cycle begins with a glucose molecule, which during the process of glycolysis is stripped of some of its hydrogen atoms, transforming the glucose into two molecules of *pyruvic acid*. Next, pyruvic acid is altered by the removal of a carbon and two oxygens, which go on to form carbon dioxide. When the *carbon dioxide* is removed, energy is given off, and a molecule called *NAD+*

is converted into the higher energy form, NADH. Another molecule, *coenzyme A* (*CoA*), then attaches to the remaining acetyl unit, forming *acetyl CoA*.

Acetyl CoA enters the Krebs's cycle by joining to a four-carbon molecule called *oxaloacetate*. Once the two molecules are joined, they make a six-carbon molecule called citric acid. Citric acid is then broken down and modified in a stepwise fashion. As this happens, hydrogen ions and carbon molecules are released. The carbon molecules are used to make more carbon dioxide. The hydrogen ions are picked up by NAD and another molecule called *flavin-adenine dinucleotide* (*FAD*). Eventually, the process produces the four-carbon oxaloacetate again, ending up where it started off. All in all, the Krebs's cycle is capable of generating from 24 to 28 ATP molecules from one molecule of glucose converted to pyruvate. Therefore, it is easy to see how much more energy we can get from a molecule of glucose if our mitochondria are working properly and if we have oxygen.

Chloroplasts are similar to mitochondria but are found only in plants. Both organelles are surrounded by a double membrane with an intermembrane space; both have their own DNA and are involved in energy metabolism; and both have reticulations, or many foldings, filling their inner spaces. Chloroplasts convert light energy from the sun into ATP through a process called *photosynthesis*.

The Endoplasmic Reticulum and the Golgi Apparatus—Macromolecule Managers. The *endoplasmic reticulum* (*ER*) is the transport network for molecules targeted for certain modifications and specific destinations, as compared to molecules that will float freely in the cytoplasm. The ER has two forms: the *rough ER* and the *smooth ER*. The rough ER is labeled as such because it has ribosomes adhering to its outer surface, whereas the smooth ER does not. Translation of the mRNA for those proteins that will either stay in the ER or be *exported* (moved out of the cell) occurs at the ribosomes attached to the rough ER. The smooth ER serves as the recipient for those proteins synthesized in the rough ER. Proteins to be exported are passed to the *Golgi apparatus*, sometimes called a Golgi body or Golgi complex, for further processing, packaging, and transport to a variety of other cellular locations.

Lysosomes and Peroxisomes—The Cellular Digestive System. *Lysosomes* and *peroxisomes* are often referred to as the garbage disposal system of a cell. Both organelles are somewhat spherical, bound by a single membrane, and rich in digestive enzymes, naturally occurring proteins that speed up biochemical processes. For example, lysosomes can contain more than three dozen enzymes for degrading proteins, nucleic acids, and certain sugars called polysaccharides. All of these enzymes work best at a low pH, reducing the risk that these enzymes will digest their own cell should they somehow escape from the lysosome. Here we can see the importance behind compartmentalization of the eukaryotic cell. The cell could not house such destructive enzymes if they were not contained in a membrane-bound system.

One function of a lysosome is to digest foreign bacteria that invade a cell. Other

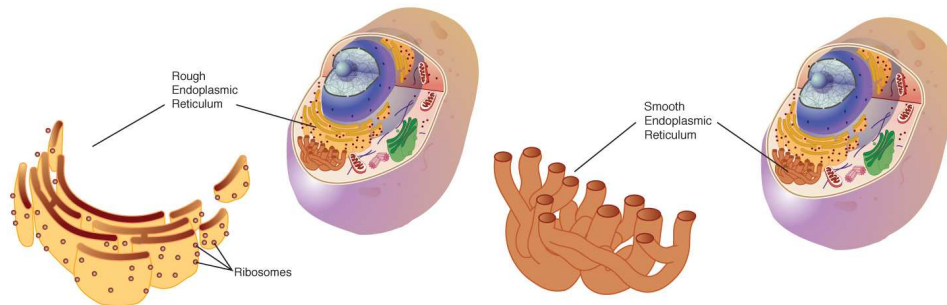


Figure A.7: Endoplasmic reticulum is a network of membranes inside a cell through which proteins and other molecules move. Proteins are assembled at organelles called ribosomes. (a) When proteins are destined to be part of the cell membrane or exported from the cell, the ribosomes assembling them attach to the endoplasmic reticulum, giving it a rough appearance. (b) Smooth endoplasmic reticulum lacks ribosomes and helps synthesize and concentrate various substances needed by the cell.

functions include helping to recycle receptor proteins and other membrane components and degrading worn out organelles such as mitochondria. Lysosomes can even help repair damage to the plasma membrane by serving as a membrane patch, sealing the wound.

Peroxisomes function to rid the body of toxic substances, such as hydrogen peroxide, or other metabolites and contain enzymes concerned with oxygen utilization. High numbers of peroxisomes can be found in the liver, where toxic byproducts are known to accumulate. All of the enzymes found in a peroxisome are imported from the cytosol. Each enzyme transferred to a peroxisome has a special sequence at one end of the protein, called a *PTS* or *peroxisomal targeting signal*, that allows the protein to be taken into that organelle, where they then function to rid the cell of toxic substances.

Peroxisomes often resemble a lysosome. However, peroxisomes are self replicating, whereas lysosomes are formed in the Golgi complex. Peroxisomes also have membrane proteins that are critical for various functions, such as for importing proteins into their interiors and to proliferate and segregate into daughter cells.

Where Do Viruses Fit?

Viruses are not classified as cells and therefore are neither unicellular nor multicellular organisms. Most people do not even classify viruses as “living” because they lack a metabolic system and are dependent on the host cells that they infect to

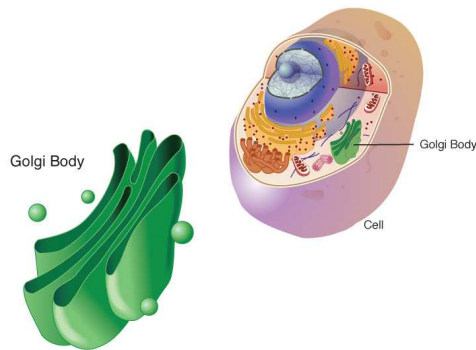


Figure A.8: A Golgi body, also known as a Golgi apparatus, is a cell organelle that helps process and package proteins and lipid molecules, especially proteins destined to be exported from the cell. Named after its discoverer, Camillo Golgi, the Golgi body appears as a series of stacked membranes.

reproduce. Viruses have genomes that consist of either DNA or RNA, and there are examples of viruses that are either double-stranded or single-stranded. Importantly, their genomes code not only for the proteins needed to package its genetic material but for those proteins needed by the virus to reproduce during its infective cycle.

Making New Cells and Cell Types

For most unicellular organisms, reproduction is a simple matter of *cell duplication*, also known as *replication*. But for multicellular organisms, cell replication and reproduction are two separate processes. Multicellular organisms replace damaged or worn out cells through a replication process called *mitosis*, the division of a eukaryotic cell nucleus to produce two identical *daughter nuclei*. To reproduce, eukaryotes must first create special cells called *gametes*—eggs and sperm—that then fuse to form the beginning of a new organism. Gametes are but one of the many unique cell types that multicellular organisms need to function as a complete organism.

Making New Cells

Most unicellular organisms create their next generation by replicating all of their parts and then splitting into two cells, a type of *asexual reproduction* called *binary fission*. This process spawns not just two new cells, but also two new organisms. Multicellular organisms replicate new cells in much the same way. For example, we produce new skin cells and liver cells by replicating the DNA found in that cell

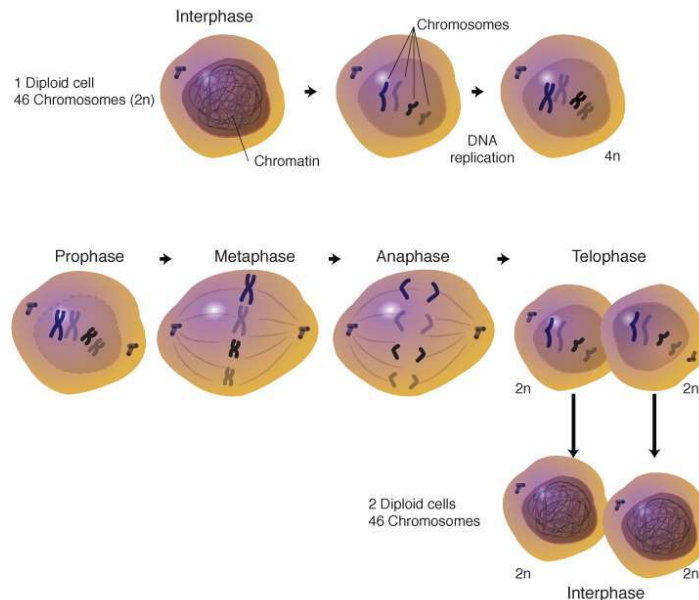


Figure A.9: Mitosis is a cellular process that replicates chromosomes and produces two identical nuclei in preparation for cell division. Generally, mitosis is immediately followed by the equal division of the cell nuclei and other cell contents into two daughter cells.

through mitosis. Yet, producing a whole new organism requires *sexual reproduction*, at least for most multicellular organisms. In the first step, specialized cells called *gametes*—eggs and sperm—are created through a process called *meiosis*. *Meiosis* serves to reduce the chromosome number for that particular organism by half. In the second step, the sperm and egg join to make a single cell, which restores the chromosome number. This joined cell then divides and differentiates into different cell types that eventually form an entire functioning organism.

Mitosis. Every time a cell divides, it must ensure that its DNA is shared between the two daughter cells. Mitosis is the process of “divvying up” the genome between the daughter cells. To easier describe this process, let’s imagine a cell with only one chromosome. Before a cell enters mitosis, we say the cell is in *interphase*, the state of a eukaryotic cell when not undergoing division. Every time a cell divides, it must first replicate all of its DNA. Because chromosomes are simply DNA wrapped around protein, the cell replicates its chromosomes also. These two chromosomes, positioned side by side, are called *sister chromatids* and are identical copies of one another. Before this cell can divide, it must separate these sister chromatids from one another. To do this, the chromosomes have to condense. This stage of mitosis is called *prophase*. Next, the nuclear envelope breaks down, and a large protein network, called the *spindle*, attaches to each sister chromatid. The chromosomes are now aligned perpendicular to the spindle in a process called *metaphase*. Next,

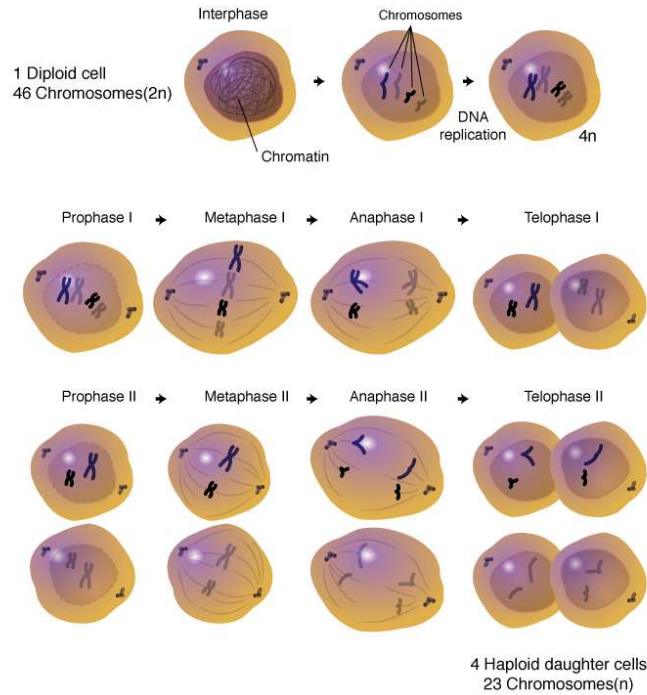


Figure A.10: Meiosis is the formation of egg and sperm cells. In sexually reproducing organisms, body cells are diploid, meaning they contain two sets of chromosomes (one set from each parent). To maintain this state, the egg and sperm that unite during fertilization must be haploid, meaning they each contain a single set of chromosomes. During meiosis, diploid cells undergo DNA replication, followed by two rounds of cell division, producing four haploid sex cells.

“molecular motors” pull the chromosomes away from the metaphase plate to the spindle poles of the cell. This is called *anaphase*. Once this process is completed, the cells divide, the nuclear envelope reforms, and the chromosomes relax and decondense during *telophase*. The cell can now replicate its DNA again during interphase and go through mitosis once more.

Meiosis. *Meiosis* is a specialized type of cell division that occurs during the formation of gametes. Although meiosis may seem much more complicated than mitosis, it is really just two cell divisions in sequence. Each of these sequences maintains strong similarities to mitosis.

Meiosis I refers to the first of the two divisions and is often called the *reduction division*. This is because it is here that the chromosome complement is reduced from *diploid* (two copies) to *haploid* (one copy). Interphase in meiosis is identical to interphase in mitosis. At this stage, there is no way to determine what type of division the cell will undergo when it divides. Meiotic division will only occur in cells associated with male or female sex organs. *Prophase I* is virtually identical

to prophase in mitosis, involving the appearance of the *chromosomes*, the development of the spindle apparatus, and the breakdown of the nuclear membrane. Metaphase I is where the critical difference occurs between meiosis and mitosis. In mitosis, all of the chromosomes line up on the metaphase plate in no particular order. In Metaphase I, the chromosome pairs are aligned on either side of the metaphase plate. It is during this alignment that the chromatid arms may overlap and temporarily fuse, resulting in what is called *crossovers*. During *Anaphase I*, the spindle fibers contract, pulling the homologous pairs away from each other and toward each pole of the cell. In *Telophase I*, a cleavage furrow typically forms, followed by *cytokinesis*, the changes that occur in the cytoplasm of a cell during nuclear division; but the nuclear membrane is usually not reformed, and the chromosomes do not disappear. At the end of Telophase I, each daughter cell has a single set of chromosomes, half the total number in the original cell, that is, while the original cell was diploid; the daughter cells are now haploid.

Meiosis II is quite simply a mitotic division of each of the haploid cells produced in Meiosis I. There is no Interphase between Meiosis I and Meiosis II, and the latter begins with *Prophase II*. At this stage, a new set of spindle fibers forms and the chromosomes begin to move toward the equator of the cell. During *Metaphase II*, all of the chromosomes in the two cells align with the metaphase plate. In *Anaphase II*, the centromeres split, and the spindle fibers shorten, drawing the chromosomes toward each pole of the cell. In *Telophase II*, a cleavage furrow develops, followed by cytokinesis and the formation of the nuclear membrane. The chromosomes begin to fade and are replaced by the *granular chromatin*, a characteristic of interphase. When Meiosis II is complete, there will be a total of four daughter cells, each with half the total number of chromosomes as the original cell. In the case of *male structures*, all four cells will eventually develop into *sperm cells*. In the case of the *female life cycles* in higher organisms, three of the cells will typically abort, leaving a single cell to develop into an egg cell, which is much larger than a sperm cell.

Recombination—The Physical Exchange of DNA. All organisms suffer a certain number of small *mutations*, or random changes in a DNA sequence, during the process of DNA replication. These are called *spontaneous mutations* and occur at a rate characteristic for that organism. *Genetic recombination* refers more to a large-scale rearrangement of a DNA molecule. This process involves pairing between complementary strands of two parental duplex, or double-stranded DNAs, and results from a physical exchange of chromosome material.

The position at which a gene is located on a chromosome is called a *locus*. In a given individual, one might find two different versions of this gene at a particular locus. These alternate gene forms are called *alleles*. During Meiosis I, when the chromosomes line up along the metaphase plate, the two strands of a chromosome pair may physically cross over one another. This may cause the strands to break apart at the crossover point and reconnect to the other chromosome, resulting in

the exchange of part of the chromosome.

Recombination results in a new arrangement of maternal and paternal alleles on the same chromosome. Although the same genes appear in the same order, the alleles are different. This process explains why offspring from the same parents can look so different. In this way, it is theoretically possible to have any combination of parental alleles in an offspring, and the fact that two alleles appear together in one offspring does not have any influence on the statistical probability that another offspring will have the same combination. This theory of “*independent assortment*” of alleles is fundamental to genetic inheritance. However, having said that, there is an exception that requires further discussion.

The frequency of recombination is actually not the same for all gene combinations. This is because recombination is greatly influenced by the proximity of one gene to another. If two genes are located close together on a chromosome, the likelihood that a recombination event will separate these two genes is less than if they were farther apart. *Linkage* describes the tendency of genes to be inherited together as a result of their location on the same chromosome. *Linkage disequilibrium* describes a situation in which some combinations of genes or genetic markers occur more or less frequently in a population than would be expected from their distances apart. Scientists apply this concept when searching for a gene that may cause a particular disease. They do this by comparing the occurrence of a specific DNA sequence with the appearance of a disease. When they find a high correlation between the two, they know they are getting closer to finding the appropriate gene sequence.

Binary Fission—How Bacteria Reproduce. Bacteria reproduce through a fairly simple process called *binary fission*, or the reproduction of a living cell by division into two equal, or near equal, parts. As just noted, this type of asexual reproduction theoretically results in two identical cells. However, bacterial DNA has a relatively high mutation rate. This rapid rate of genetic change is what makes bacteria capable of developing resistance to antibiotics and helps them exploit invasion into a wide range of environments.

Similar to more complex organisms, bacteria also have mechanisms for exchanging genetic material. Although not equivalent to sexual reproduction, the end result is that a bacterium contains a combination of traits from two different *parental* cells. Three different modes of exchange have thus far been identified in bacteria.

Conjunction involves the direct joining of two bacteria, which allows their circular DNAs to undergo recombination. Bacteria can also undergo *transformation* by absorbing remnants of DNA from dead bacteria and integrating these fragments into their own DNA. Lastly, bacteria can exchange genetic material through a process called *transduction*, in which genes are transported into and out of the cell by bacterial viruses, called *bacteriophages*, or by *plasmids*, an autonomous self-replicating extrachromosomal circular DNA.

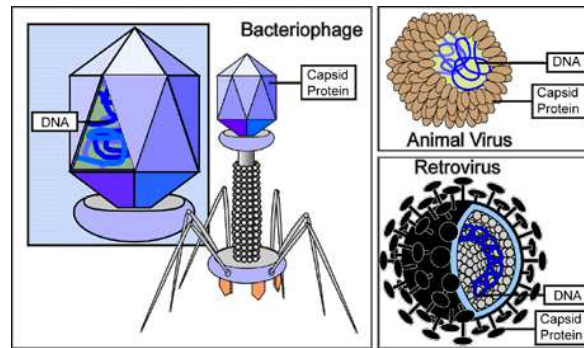


Figure A.11: Types of viruses. This illustration depicts three types of viruses: a bacterial virus, otherwise called a bacteriophage (left center); an animal virus (top right); and a retrovirus (bottom right). Viruses depend on the host cell that they infect to reproduce. When found outside of a host cell, viruses, in their simplest forms, consist only of genomic nucleic acid, either DNA or RNA (depicted as blue), surrounded by a protein coat, or capsid.

Viral Reproduction. Because viruses are acellular and do not use ATP, they must utilize the machinery and metabolism of a host cell to reproduce. For this reason, viruses are called *obligate intracellular parasites*. Before a virus has entered a host cell, it is called a virion—a package of viral genetic material. *Virions*—infectious viral particles—can be passed from host to host either through direct contact or through a vector, or carrier. Inside the organism, the virus can enter a cell in various ways. Bacteriophages—bacterial viruses—attach to the cell wall surface in specific places. Once attached, enzymes make a small hole in the cell wall, and the virus injects its DNA into the cell. Other viruses (such as HIV) enter the host via *endocytosis*, the process whereby cells take in material from the external environment. After entering the cell, the virus's genetic material begins the destructive process of taking over the cell and forcing it to produce new viruses.

There are three different ways genetic information contained in a viral genome can be reproduced. The form of genetic material contained in the *viral capsid*, the protein coat that surrounds the nucleic acid, determines the exact replication process. Some viruses have DNA, which once inside the host cell is replicated by the host along with its own DNA. Then, there are two different replication processes for viruses containing RNA. In the first process, the viral RNA is directly copied using an enzyme called *RNA replicase*. This enzyme then uses that RNA copy as a template to make hundreds of duplicates of the original RNA. A second group of RNA-containing viruses, called the *retroviruses*, uses the enzyme reverse transcriptase to synthesize a complementary strand of DNA so that the virus's genetic information is contained in a molecule of DNA rather than RNA. The viral DNA can then be further replicated using the host cell machinery.

Steps Associated with Viral Reproduction.

1. *Attachment*, sometimes called *absorption*: The virus attaches to receptors on the host cell wall.
2. *Penetration*: The nucleic acid of the virus moves through the plasma membrane and into the cytoplasm of the host cell. The capsid of a phage, a bacterial virus, remains on the outside. In contrast, many viruses that infect animal cells enter the host cell intact.
3. *Replication*: The viral genome contains all the information necessary to produce new viruses. Once inside the host cell, the virus induces the host cell to synthesize the necessary components for its replication.
4. *Assembly*: The newly synthesized viral components are assembled into new viruses.
5. *Release*: Assembled viruses are released from the cell and can now infect other cells, and the process begins again.

When the virus has taken over the cell, it immediately directs the host to begin manufacturing the proteins necessary for virus reproduction. The host produces three kinds of proteins: *early proteins*, enzymes used in nucleic acid replication; *late proteins*, proteins used to construct the virus coat; and *lytic proteins*, enzymes used to break open the cell for viral exit. The final viral product is assembled spontaneously, that is, the parts are made separately by the host and are joined together by chance. This self-assembly is often aided by molecular *chaperones*, or proteins made by the host that help the capsid parts come together.

The new viruses then leave the cell either by exocytosis or by lysis. Envelope-bound animal viruses instruct the host's endoplasmic reticulum to make certain proteins, called *glycoproteins*, which then collect in clumps along the cell membrane. The virus is then discharged from the cell at these exit sites, referred to as exocytosis. On the other hand, bacteriophages must break open, or *lyse*, the cell to exit. To do this, the phages have a gene that codes for an enzyme called *lysozyme*. This enzyme breaks down the cell wall, causing the cell to swell and burst. The new viruses are released into the environment, killing the host cell in the process.

One family of animal viruses, called the retroviruses, contains RNA genomes in their virus particles but synthesize a DNA copy of their genome in infected cells. Retroviruses provide an excellent example of how viruses can play an important role as models for biological research. Studies of these viruses are what first demonstrated the synthesis of DNA from RNA templates, a fundamental mode for transferring genetic material that occurs in both eukaryotes and prokaryotes.

Why Study Viruses? Viruses are important to the study of *molecular and cellular biology* because they provide simple systems that can be used to manipulate and investigate the functions of many cell types. We have just discussed how viral replication depends on the metabolism of the infected cell. Therefore, the study

of viruses can provide fundamental information about aspects of cell biology and metabolism. The rapid growth and small genome size of bacteria make them excellent tools for experiments in biology. Bacterial viruses have also further simplified the study of bacterial genetics and have deepened our understanding of the basic mechanisms of molecular genetics. Because of the complexity of an animal cell genome, viruses have been even more important in studies of animal cells than in studies of bacteria. Numerous studies have demonstrated the utility of animal viruses as probes for investigating different activities of eukaryotic cells. Other examples in which animal viruses have provided important models for biological research of their host cells include studies of *DNA replication*, *transcription*, *RNA processing*, and *protein transport*.

Deriving New Cell Types

Look closely at the human body, and it is clear that not all cells are alike. For example, cells that make up our skin are certainly different from cells that make up our inner organs. Yet, all of the different cell types in our body are all *derived*, or arise, from a single, fertilized egg cell through differentiation. *Differentiation* is the process by which an unspecialized cell becomes specialized into one of the many cells that make up the body, such as a heart, liver, or muscle cell. During differentiation, certain genes are turned on, or become *activated*, while other genes are switched off, or *inactivated*. This process is intricately regulated. As a result, a differentiated cell will develop specific structures and perform certain functions.

Mammalian Cell Types. Three basic categories of cells make up the mammalian body: *germ cells*, *somatic cells*, and *stem cells*. Each of the approximately 100 trillion cells in an adult human has its own copy, or copies, of the genome, with the only exception being certain cell types that lack nuclei in their fully differentiated state, such as red blood cells. The majority of these cells are *diploid*, or have two copies of each chromosome. These cells are called *somatic cells*. This category of cells includes most of the cells that make up our body, such as skin and muscle cells. *Germ line cells* are any line of cells that give rise to *gametes*—eggs and sperm—and are continuous through the generations. *Stem cells*, on the other hand, have the ability to divide for indefinite periods and to give rise to specialized cells. They are best described in the context of normal human development.

Human development begins when a sperm fertilizes an egg and creates a single cell that has the potential to form an entire organism. In the first hours after fertilization, this cell divides into identical cells. Approximately 4 days after fertilization and after several cycles of cell division, these cells begin to specialize, forming a hollow sphere of cells, called a *blastocyst*. The blastocyst has an outer layer of cells, and inside this hollow sphere, there is a cluster of cells called the inner *cell mass*. The cells of the inner cell mass will go on to form virtually all of the tissues of the human body. Although the cells of the inner cell mass can

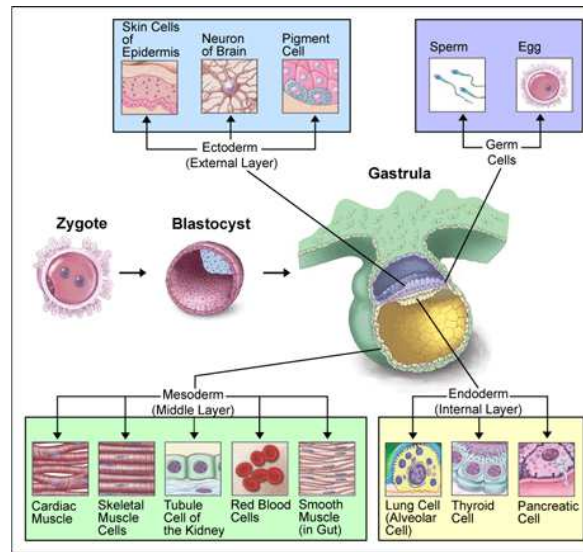


Figure A.12: Differentiation of human tissues. Human development begins when a sperm fertilizes an egg and creates a single cell that has the potential to form an entire organism, called the zygote (top panel, mauve). In the first hours after fertilization, this cell divides into identical cells. These cells then begin to specialize, forming a hollow sphere of cells, called a blastocyst (second panel, purple). The blastocyst has an outer layer of cells (yellow), and inside this hollow sphere, there is a cluster of cells called the inner cell mass (light blue). The inner cell mass can give rise to the germ cells—eggs and sperm—as well as cells derived from all three germ layers (ectoderm, light blue; mesoderm, light green; and endoderm, light yellow), depicted in the bottom panel, including nerve cells, muscle cells, skin cells, blood cells, bone cells, and cartilage. Reproduced with permission from the Office of Science Policy, the National Institutes of Health.

form virtually every type of cell found in the human body, they cannot form an organism. Therefore, these cells are referred to as *pluripotent*, that is, they can give rise to many types of cells but not a whole organism. Pluripotent stem cells undergo further specialization into stem cells that are committed to give rise to cells that have a particular function. Examples include blood stem cells that give rise to red blood cells, white blood cells, and platelets, and skin stem cells that give rise to the various types of skin cells. These more specialized stem cells are called *multipotent*—capable of giving rise to several kinds of cells, tissues, or structures.

The Working Cell: DNA, RNA, and Protein Synthesis

DNA Replication

DNA replication, or the process of duplicating a cell's genome, is required every time a cell divides. Replication, like all cellular activities, requires specialized proteins for carrying out the job. In the first step of replication, a special protein, called

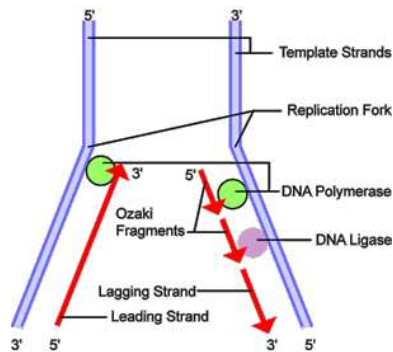


Figure A.13: An overview of DNA replication. Before a cell can divide, it must first duplicate its DNA. This figure provides an overview of the DNA replication process. In the first step, a portion of the double helix (blue) is unwound by a helicase. Next, a molecule of DNA polymerase (green) binds to one strand of the DNA. It moves along the strand, using it as a template for assembling a leading strand (red) of nucleotides and reforming a double helix. Because DNA synthesis can only occur 5' to 3', a second DNA polymerase molecule (also green) is used to bind to the other template strand as the double helix opens. This molecule must synthesize discontinuous segments of polynucleotides (called Okazaki Fragments). Another enzyme, DNA Ligase (yellow), then stitches these together into the lagging strand.

a *helicase*, unwinds a portion of the parental DNA double helix. Next, a molecule of *DNA polymerase*—a common name for two categories of enzymes that influence the synthesis of DNA— binds to one strand of the DNA. DNA polymerase begins to move along the DNA strand in the 3' to 5' direction, using the single-stranded DNA as a template. This newly synthesized strand is called the *leading strand* and is necessary for forming new nucleotides and reforming a double helix. Because DNA synthesis can only occur in the 5' to 3' direction, a second DNA polymerase molecule is used to bind to the other template strand as the double helix opens. This molecule synthesizes discontinuous segments of polynucleotides, called *Okazaki fragments*. Another enzyme, called *DNA ligase*, is responsible for stitching these fragments together into what is called the *lagging strand*.

The average human chromosome contains an enormous number of nucleotide pairs that are copied at about 50 base pairs per second. Yet, the entire replication process takes only about an hour. This is because there are many *replication origin sites* on a eukaryotic chromosome. Therefore, replication can begin at some origins earlier than at others. As replication nears completion, “bubbles” of newly replicated DNA meet and fuse, forming two new molecules.

With multiple replication origin sites, one might ask, how does the cell know which DNA has already been replicated and which still awaits replication? To date, two *replication control mechanisms* have been identified: one positive and one negative. For DNA to be replicated, each replication origin site must be bound by a

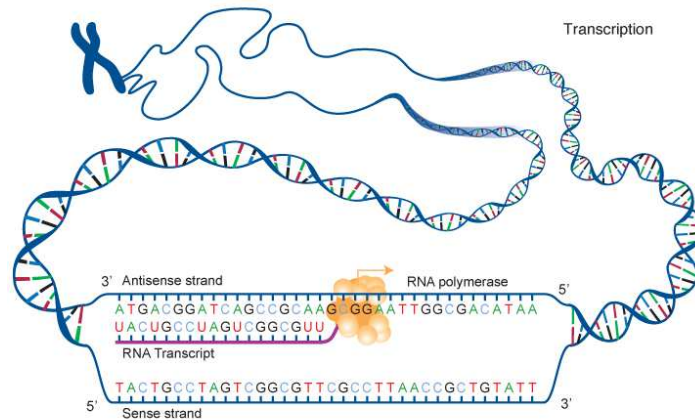


Figure A.14: Transcription is the process of making an RNA copy of a gene sequence. This copy, called a messenger RNA (mRNA) molecule, leaves the cell nucleus and enters the cytoplasm, where it directs the synthesis of the protein, which it encodes.

set of proteins called the *Origin Recognition Complex*. These remain attached to the DNA throughout the replication process. Specific accessory proteins, called *licensing factors*, must also be present for initiation of replication. Destruction of these proteins after initiation of replication prevents further replication cycles from occurring. This is because licensing factors are only produced when the nuclear membrane of a cell breaks down during mitosis.

DNA Transcription—Making mRNA

DNA transcription refers to the synthesis of RNA from a DNA template. This process is very similar to DNA replication. Of course, there are different proteins that direct transcription. The most important enzyme is *RNA polymerase*, an enzyme that influences the synthesis of RNA from a DNA template. For transcription to be initiated, RNA polymerase must be able to recognize the beginning sequence of a gene so that it knows where to start synthesizing an mRNA. It is directed to this initiation site by the ability of one of its subunits to recognize a specific DNA sequence found at the beginning of a gene, called the *promoter sequence*. The promoter sequence is a unidirectional sequence found on one strand of the DNA that instructs the RNA polymerase in both where to start synthesis and in which direction synthesis should continue. The RNA polymerase then unwinds the double helix at that point and begins synthesis of a RNA strand complementary to one of the strands of DNA. This strand is called the *antisense* or *template strand*, whereas the other strand is referred to as the *sense* or coding strand. Synthesis can then proceed in a unidirectional manner.

Although much is known about transcript processing, the signals and events that instruct RNA polymerase to stop transcribing and drop off the DNA template remain unclear. Experiments over the years have indicated that processed eukaryotic messages contain a *poly(A) addition signal* (AAUAAA) at their 3' end, followed by a string of adenines. This poly(A) addition, also called the *poly(A) site*, contributes not only to the addition of the poly(A) tail but also to transcription termination and the release of RNA polymerase from the DNA template. Yet, transcription does not stop here. Rather, it continues for another 200 to 2000 bases beyond this site before it is aborted. It is either before or during this termination process that the nascent transcript is *cleaved*, or cut, at the poly(A) site, leading to the creation of two RNA molecules. The upstream portion of the newly formed, or *nascent*, RNA then undergoes further modifications, called *post-transcriptional modification*, and becomes mRNA. The downstream RNA becomes unstable and is rapidly degraded.

Although the importance of the poly(A) addition signal has been established, the contribution of sequences further downstream remains uncertain. A recent study suggests that a defined region, called the *termination region*, is required for proper transcription termination. This study also illustrated that transcription termination takes place in two distinct steps. In the first step, the nascent RNA is cleaved at specific subsections of the termination region, possibly leading to its release from RNA polymerase. In a subsequent step, RNA polymerase disengages from the DNA. Hence, RNA polymerase continues to transcribe the DNA, at least for a short distance.

Protein Translation—How Do Messenger RNAs Direct Protein Synthesis?

The cellular machinery responsible for synthesizing proteins is the *ribosome*. The ribosome consists of structural RNA and about 80 different proteins. In its inactive state, it exists as two subunits: a *large subunit* and a *small subunit*. When the small subunit encounters an mRNA, the process of *translating* an mRNA to a protein begins. In the large subunit, there are two sites for amino acids to bind and thus be close enough to each other to form a bond. The “*A site*” accepts a new *transfer RNA*, or tRNA—the adaptor molecule that acts as a translator between mRNA and protein—bearing an amino acid. The “*P site*” *P site* binds the tRNA that becomes attached to the growing chain.

As we just discussed, the adaptor molecule that acts as a translator between mRNA and protein is a specific RNA molecule, the tRNA. Each tRNA has a specific *acceptor site* that binds a particular triplet of nucleotides, called a *codon*, and an *anti-codon site* that binds a sequence of three unpaired nucleotides, the anti-codon, which can then bind to the the codon. Each tRNA also has a specific *charger protein*, called an *aminoacyl tRNA synthetase*. This protein can only bind to that particular tRNA and attach the correct amino acid to the acceptor site.

The *start signal* for translation is the codon ATG, which codes for methionine.

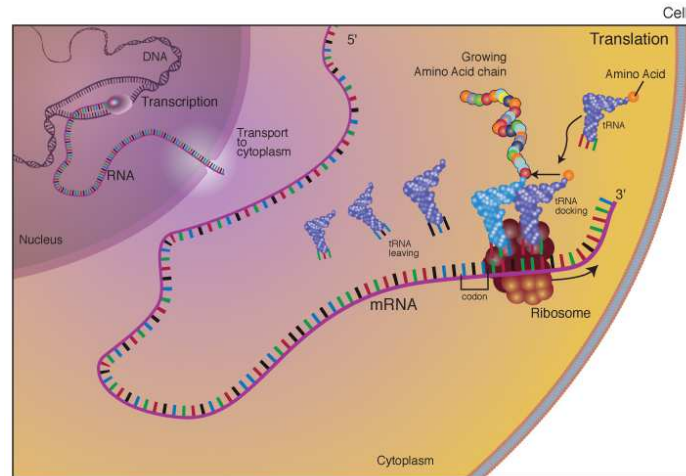


Figure A.15: Translation is the process of translating the sequence of a messenger RNA (mRNA) molecule to a sequence of amino acids during protein synthesis. The genetic code describes the relationship between the sequence of base pairs in a gene and the corresponding amino acid sequence that it encodes. In the cell cytoplasm, the ribosome reads the sequence of the mRNA in groups of three bases to assemble the protein.

Not every protein necessarily starts with methionine, however. Oftentimes this first amino acid will be removed in later processing of the protein. A tRNA charged with methionine binds to the translation start signal. The large subunit binds to the mRNA and the small subunit, and so begins *elongation*, the formation of the polypeptide chain. After the first charged tRNA appears in the A site, the ribosome shifts so that the tRNA is now in the P site. New charged tRNAs, corresponding the codons of the mRNA, enter the A site, and a bond is formed between the two amino acids. The first tRNA is now released, and the ribosome shifts again so that a tRNA carrying two amino acids is now in the P site. A new charged tRNA then binds to the A site. This process of elongation continues until the ribosome reaches what is called a *stop codon*, a triplet of nucleotides that signals the termination of translation. When the ribosome reaches a stop codon, no aminoacyl tRNA binds to the empty A site. This is the ribosome signal to break apart into its large and small subunits, releasing the new protein and the mRNA. Yet, this isn't always the end of the story. A protein will often undergo further modification, called *post-translational modification*. For example, it might be cleaved by a protein-cutting enzyme, called a protease, at a specific place or have a few of its amino acids altered.

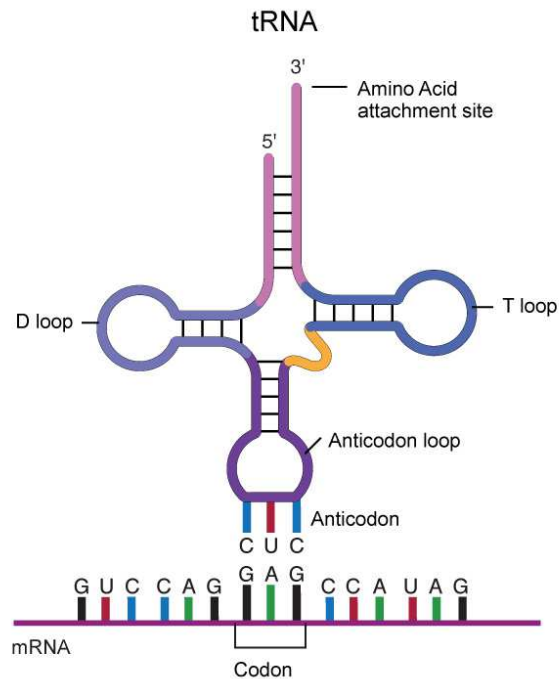


Figure A.16: Transfer RNA (tRNA) is a small RNA molecule that participates in protein synthesis. Each tRNA molecule has two important areas: a trinucleotide region called the anticodon and a region for attaching a specific amino acid. During translation, each time an amino acid is added to the growing chain, a tRNA molecule forms base pairs with its complementary sequence on the messenger RNA (mRNA) molecule, ensuring that the appropriate amino acid is inserted into the protein.

DNA Repair Mechanisms

Maintenance of the accuracy of the DNA genetic code is critical for both the long- and short-term survival of cells and species. Sometimes, normal cellular activities, such as duplicating DNA and making new gametes, introduce changes or *mutations* in our DNA. Other changes are caused by exposure of DNA to chemicals, radiation, or other adverse environmental conditions. No matter the source, genetic mutations have the potential for both positive and negative effects on an individual as well as its species. A positive change results in a slightly different version of a gene that might eventually prove beneficial in the face of a new disease or changing environmental conditions. Such beneficial changes are the cornerstone of evolution. Other mutations are considered *deleterious*, or result in damage to a cell or an individual. For example, errors within a particular DNA sequence may end up either preventing a vital protein from being made or encoding a defective protein. It is often these types of errors that lead to various disease states.

The potential for DNA damage is counteracted by a vigorous surveillance and

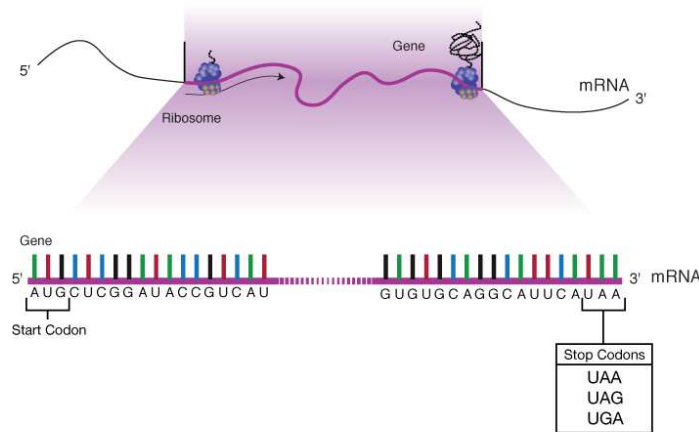


Figure A.17: A stop codon is a trinucleotide sequence within a messenger RNA (mRNA) molecule that signals a halt to protein synthesis. The genetic code describes the relationship between the sequence of DNA bases (A, C, G, and T) in a gene and the corresponding protein sequence that it encodes. The cell reads the sequence of the gene in groups of three bases. Of the 64 possible combinations of three bases, 61 specify an amino acid, while the remaining three combinations are stop codons.

repair system. Within this system, there are a number of enzymes capable of repairing damage to DNA. Some of these enzymes are specific for a particular type of damage, whereas others can handle a range of mutation types. These systems also differ in the degree to which they are able to restore the normal, or *wild-type*, sequence.

Categories of DNA Repair Systems.

- *Photoreactivation* is the process whereby genetic damage caused by ultraviolet radiation is reversed by subsequent illumination with visible or near-ultraviolet light.
- *Nucleotide excision repair* is used to fix DNA lesions, such as single-stranded breaks or damaged bases, and occurs in stages. The first stage involves recognition of the damaged region. In the second stage, two enzymatic reactions serve to remove, or excise, the damaged sequence. The third stage involves synthesis by DNA polymerase of the excised nucleotides using the second intact strand of DNA as a template. Lastly, DNA ligase joins the newly synthesized segment to the existing ends of the originally damaged DNA strand.
- *Recombination repair*, or *post-replication repair*, fixes DNA damage by a strand exchange from the other daughter chromosome. Because it involves

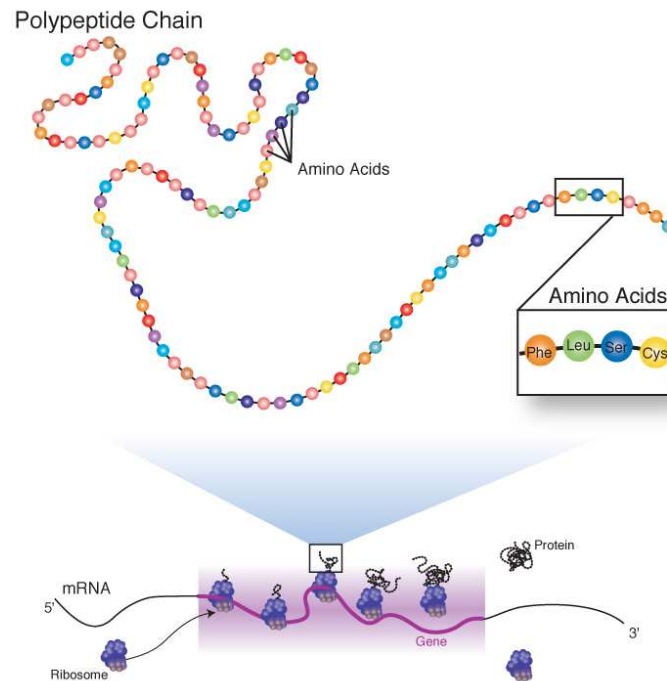


Figure A.18: A peptide is one or more amino acids linked by chemical bonds. The term also refers to the type of chemical bond that joins the amino acids together. A series of linked amino acids is a polypeptide. The cell's proteins are made from one or more polypeptides.

homologous recombination, it is largely error free.

- *Base excision repair* allows for the identification and removal of wrong bases, typically attributable to *deamination*—the removal of an amino group (NH₂)—of normal bases as well as from chemical modification.
- *Mismatch repair* is a multi-enzyme system that recognizes inappropriately matched bases in DNA and replaces one of the two bases with one that “matches” the other. The major problem here is recognizing which of the mismatched bases is incorrect and therefore should be removed and replaced.
- *Adaptive/inducible repair* describes several protein activities that recognize very specific modified bases. They then transfer this modifying group from the DNA to themselves, and, in doing so, destroy their own function. These proteins are referred to as inducible because they tend to regulate their own synthesis. For example, exposure to modifying agents induces, or turns on, more synthesis and therefore adaptation.
- *SOS repair* or *inducible error-prone repair* is a repair process that occurs in bacteria and is induced, or switched on, in the presence of potentially

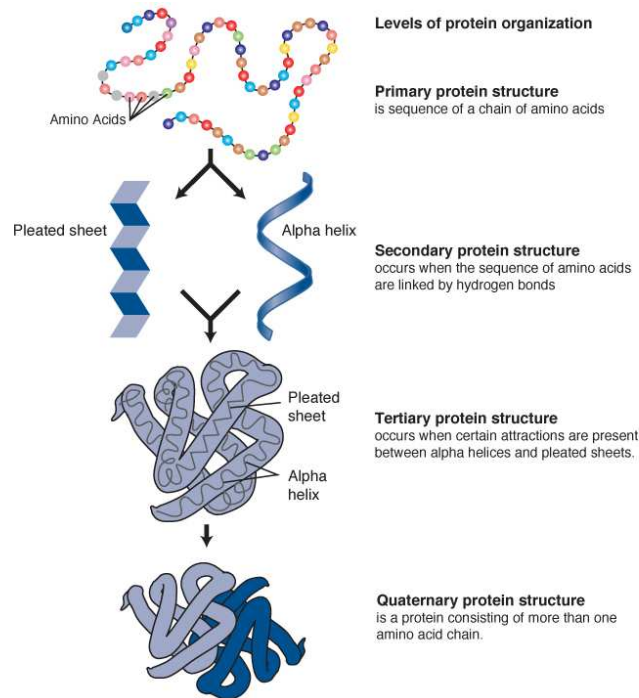


Figure A.19: Proteins are an important class of molecules found in all living cells. A protein is composed of one or more long chains of amino acids, the sequence of which corresponds to the DNA sequence of the gene that encodes it. Proteins play a variety of roles in the cell, including structural (cytoskeleton), mechanical (muscle), biochemical (enzymes), and cell signaling (hormones). Proteins are also an essential part of diet.

lethal stresses, such as UV irradiation or the inactivation of genes essential for replication. Some responses to this type of stress include *mutagenesis*—the production of mutations—or cell elongation without cell division. In this type of repair process, replication of the DNA template is extremely inaccurate. Obviously, such a repair system must be a desperate recourse for the cell, allowing replication past a region where the wild-type sequence has been lost.

From Cells to Genomes

Understanding what makes up a cell and how that cell works is fundamental to all of the biological sciences. Appreciating the similarities and differences between cell types is particularly important to the fields of cell and molecular biology. These fundamental similarities and differences provide a unifying theme, allowing the principles learned from studying one cell type to be extrapolated and generalized to other cell types.

Perhaps the most fundamental property of all living things is their ability to reproduce. All cells arise from pre-existing cells, that is, their genetic material must be replicated and passed from parent cell to progeny. Likewise, all multicellular organisms inherit their genetic information specifying structure and function from their parents. The next section of the genetics primer, What is a Genome, details how genetic information is replicated and transmitted from cell to cell and organism to organism.

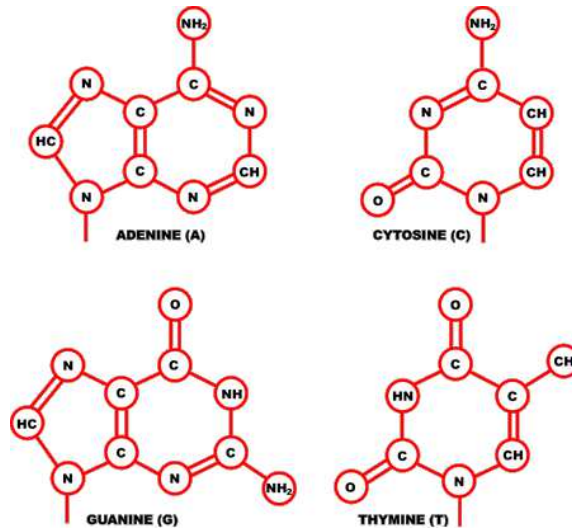


Figure A.20: The four DNA bases. Each DNA base is made up of the sugar 2'-deoxyribose linked to a phosphate group and one of the four bases depicted above: adenine (top left), cytosine (top right), guanine (bottom left), and thymine (bottom right).

A.2 What is a Genome

Life is specified by *genomes*. Every organism, including humans, has a genome that contains all of the biological information needed to build and maintain a living example of that organism. The biological information contained in a genome is encoded in its *deoxyribonucleic acid (DNA)* and is divided into discrete units called *genes*. Genes code for proteins that attach to the genome at the appropriate positions and switch on a series of reactions called gene expression.

The Physical Structure of the Human Genome

Nuclear DNA

Inside each of our cells lies a *nucleus*, a membrane-bounded region that provides a sanctuary for genetic information. The nucleus contains long strands of DNA that encode this genetic information. A *DNA* chain is made up of four chemical bases: *adenine (A)* and *guanine (G)*, which are called *purines*, and *cytosine (C)* and *thymine (T)*, referred to as *pyrimidines*. Each base has a slightly different composition, or combination of oxygen, carbon, nitrogen, and hydrogen. In a DNA chain, every base is attached to a sugar molecule (deoxyribose) and a phosphate molecule, resulting in a nucleic acid or *nucleotide*. Individual nucleotides are linked through the phosphate group, and it is the precise order, or sequence, of nucleotides that determines the product made from that gene.

A DNA chain, also called a strand, has a sense of direction, in which one end

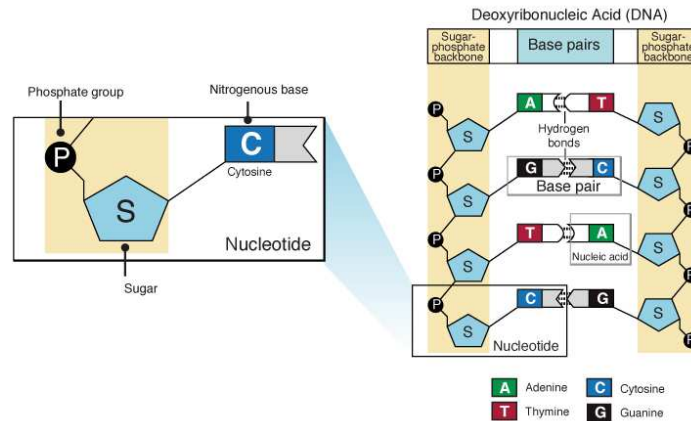


Figure A.21: A nucleotide is the basic building block of nucleic acids. RNA and DNA are polymers made of long chains of nucleotides. A nucleotide consists of a sugar molecule (either ribose in RNA or deoxyribose in DNA) attached to a phosphate group and a nitrogen-containing base. The bases used in DNA are adenine (A), cytosine (C), guanine (G), and thymine (T). In RNA, the base uracil (U) takes the place of thymine.

is chemically different than the other. The so-called 5' end terminates in a 5' phosphate group (-PO₄); the 3' end terminates in a 3' hydroxyl group (-OH). This is important because DNA strands are always synthesized in the 5' to 3' direction.

The DNA that constitutes a gene is a double-stranded molecule consisting of two chains running in opposite directions. The chemical nature of the bases in double-stranded DNA creates a slight twisting force that gives DNA its characteristic gently coiled structure, known as the double helix. The two strands are connected to each other by chemical pairing of each base on one strand to a specific partner on the other strand. Adenine (A) pairs with thymine (T), and guanine (G) pairs with cytosine (C). Thus, *A-T* and *G-C base pairs* are said to be *complementary*. This complementary base pairing is what makes DNA a suitable molecule for carrying our genetic information—one strand of DNA can act as a *template* to direct the synthesis of a complementary strand. In this way, the information in a DNA sequence is readily copied and passed on to the next generation of cells.

Organelle DNA

Not all genetic information is found in nuclear DNA. Both plants and animals have an organelle—a “little organ” within the cell—called the *mitochondrion*. Each mitochondrion has its own set of genes. Plants also have a second organelle, the *chloroplast*, which also has its own DNA. Cells often have multiple mitochondria, particularly cells requiring lots of energy, such as active muscle cells. This is because mitochondria are responsible for converting the energy stored in macro-

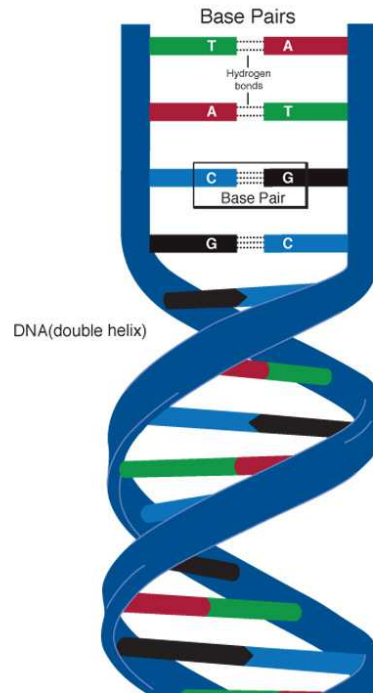


Figure A.22: A base pair is two chemical bases bonded to one another forming a "rung of the DNA ladder." The DNA molecule consists of two strands that wind around each other like a twisted ladder. Each strand has a backbone made of alternating sugar (deoxyribose) and phosphate groups. Attached to each sugar is one of four bases—adenine (A), cytosine (C), guanine (G), or thymine (T). The two strands are held together by hydrogen bonds between the bases, with adenine forming a base pair with thymine, and cytosine forming a base pair with guanine.

molecules into a form usable by the cell, namely, the *adenosine triphosphate (ATP)* molecule. Thus, they are often referred to as the power generators of the cell.

Unlike *nuclear DNA* (the DNA found within the nucleus of a cell), half of which comes from our mother and half from our father, mitochondrial DNA is only inherited from our mother. This is because mitochondria are only found in the female gametes or "eggs" of sexually reproducing animals, not in the male gamete, or sperm. Mitochondrial DNA also does not recombine; there is no shuffling of genes from one generation to the other, as there is with nuclear genes.

Large numbers of mitochondria are found in the tail of sperm, providing them with an engine that generates the energy needed for swimming toward the egg. However, when the sperm enters the egg during fertilization, the tail falls off, taking away the father's mitochondria.

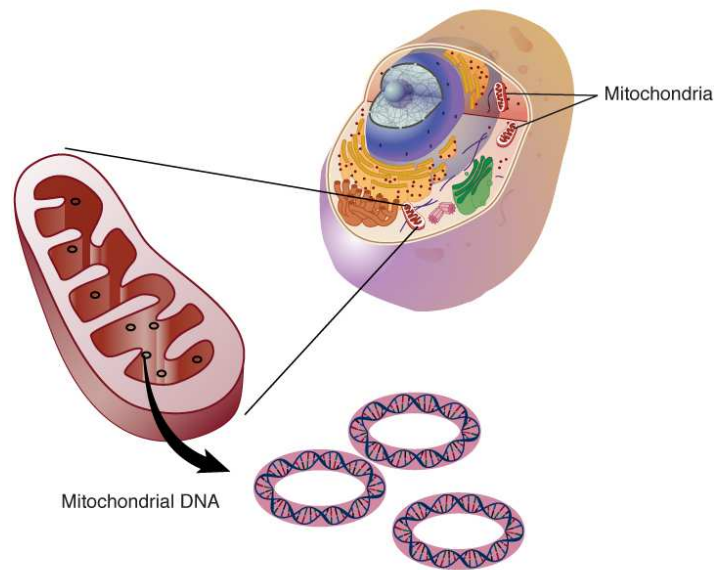


Figure A.23: Mitochondrial DNA is the small circular chromosome found inside mitochondria. The mitochondria are organelles found in cells that are the sites of energy production. The mitochondria, and thus mitochondrial DNA, are passed from mother to offspring.

Why Is There a Separate Mitochondrial Genome?

The energy-conversion process that takes place in the mitochondria takes place *aerobically*, in the presence of oxygen. Other energy conversion processes in the cell take place *anaerobically*, or without oxygen. The independent aerobic function of these organelles is thought to have evolved from bacteria that lived inside of other simple organisms in a mutually beneficial, or *symbiotic*, relationship, providing them with aerobic capacity. Through the process of evolution, these tiny organisms became incorporated into the cell, and their genetic systems and cellular functions became integrated to form a single functioning cellular unit. Because mitochondria have their own DNA, RNA, and ribosomes, this scenario is quite possible. This theory is also supported by the existence of a eukaryotic organism, called the amoeba, which lacks mitochondria. Therefore, amoeba must always have a symbiotic relationship with an aerobic bacterium.

Why Study Mitochondria?

There are many diseases caused by mutations in *mitochondrial DNA (mtDNA)*. Because the mitochondria produce energy in cells, symptoms of mitochondrial

diseases often involve degeneration or functional failure of tissue. For example, mtDNA mutations have been identified in some forms of diabetes, deafness, and certain inherited heart diseases. In addition, mutations in mtDNA are able to accumulate throughout an individual's lifetime. This is different from mutations in nuclear DNA, which has sophisticated repair mechanisms to limit the accumulation of mutations. Mitochondrial DNA mutations can also concentrate in the mitochondria of specific tissues. A variety of deadly diseases are attributable to a large number of accumulated mutations in mitochondria. There is even a theory, the *Mitochondrial Theory of Aging*, that suggests that accumulation of mutations in mitochondria contributes to, or drives, the aging process. These defects are associated with Parkinson's and Alzheimer's disease, although it is not known whether the defects actually cause or are a direct result of the diseases. However, evidence suggests that the mutations contribute to the progression of both diseases.

In addition to the critical cellular energy-related functions, mitochondrial genes are useful to evolutionary biologists because of their maternal inheritance and high rate of mutation. By studying patterns of mutations, scientists are able to reconstruct patterns of migration and evolution within and between species. For example, mtDNA analysis has been used to trace the migration of people from Asia across the Bering Strait to North and South America. It has also been used to identify an ancient maternal lineage from which modern man evolved.

Ribonucleic Acids

Just like DNA, *ribonucleic acid (RNA)* is a chain, or polymer, of nucleotides with the same 5' to 3' direction of its strands. However, the ribose sugar component of RNA is slightly different chemically than that of DNA. RNA has a 2' oxygen atom that is not present in DNA. Other fundamental structural differences exist. For example, uracil takes the place of the thymine nucleotide found in DNA, and RNA is, for the most part, a single-stranded molecule. DNA directs the synthesis of a variety of RNA molecules, each with a unique role in cellular function. For example, all genes that code for proteins are first made into an RNA strand in the nucleus called a *messenger RNA (mRNA)*. The mRNA carries the information encoded in DNA out of the nucleus to the protein assembly machinery, called the *ribosome*, in the cytoplasm. The ribosome complex uses mRNA as a template to synthesize the exact protein coded for by the gene.

In addition to mRNA, DNA codes for other forms of RNA, including ribosomal RNAs (rRNAs), transfer RNAs (tRNAs), and small nuclear RNAs (snRNAs). rRNAs and tRNAs participate in protein assembly whereas snRNAs aid in a process called splicing—the process of editing of mRNA before it can be used as a template for protein synthesis.

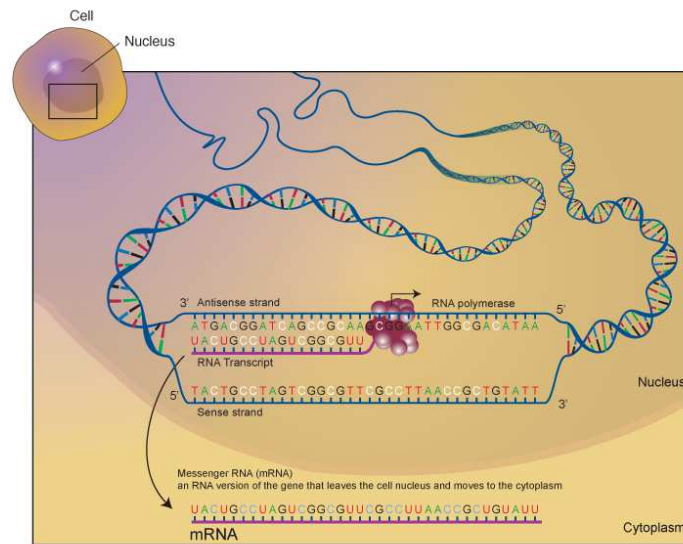


Figure A.24: Messenger RNA (mRNA) is a single-stranded RNA molecule that is complementary to one of the DNA strands of a gene. The mRNA is an RNA version of the gene that leaves the cell nucleus and moves to the cytoplasm where proteins are made. During protein synthesis, an organelle called a ribosome moves along the mRNA, reads its base sequence, and uses the genetic code to translate each three-base triplet, or codon, into its corresponding amino acid.

Proteins

Although DNA is the carrier of genetic information in a cell, proteins do the bulk of the work. Proteins are long chains containing as many as 20 different kinds of amino acids. Each cell contains thousands of different proteins: *enzymes* that make new molecules and catalyze nearly all chemical processes in cells; *structural components* that give cells their shape and help them move; hormones that transmit signals throughout the body; *antibodies* that recognize foreign molecules; and *transport molecules* that carry oxygen. The genetic code carried by DNA is what specifies the order and number of amino acids and, therefore, the shape and function of the protein.

The “*Central Dogma*”—a fundamental principle of molecular biology—states that genetic information flows from DNA to RNA to protein. Ultimately, however, the genetic code resides in DNA because only DNA is passed from generation to generation. Yet, in the process of making a protein, the encoded information must be faithfully transmitted first to RNA then to protein. Transferring the code from DNA to RNA is a fairly straightforward process called *transcription*. Deciphering the code in the resulting mRNA is a little more complex. It first requires that the mRNA leave the nucleus and associate with a large complex of specialized RNAs

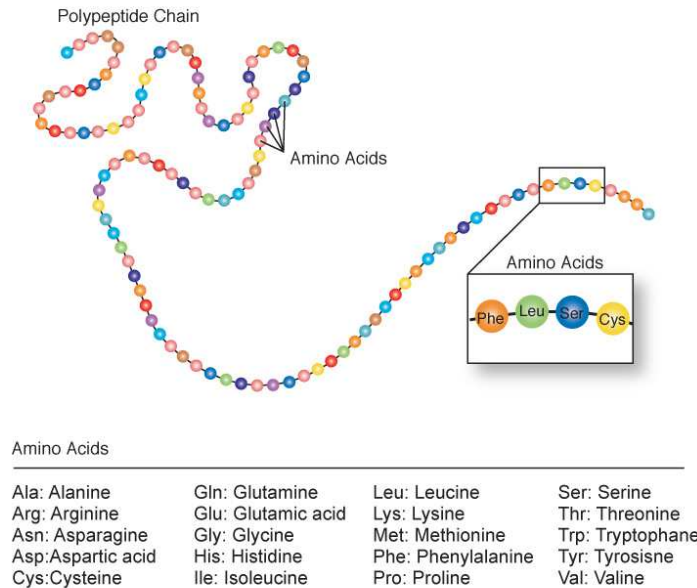


Figure A.25: Amino acids are a set of 20 different molecules used to build proteins. Proteins consist of one or more chains of amino acids called polypeptides. The sequence of the amino acid chain causes the polypeptide to fold into a shape that is biologically active. The amino acid sequences of proteins are encoded in the genes.

and proteins that, collectively, are called the *ribosome*. Here the mRNA is translated into protein by decoding the mRNA sequence in blocks of three RNA bases, called *codons*, where each codon specifies a particular amino acid. In this way, the *ribosomal complex* builds a protein one amino acid at a time, with the order of amino acids determined precisely by the order of the codons in the mRNA.

A given amino acid can have more than one codon. These redundant codons usually differ at the third position. For example, the amino acid serine is encoded by UCU, UCC, UCA, and/or UCG. This redundancy is key to accommodating mutations that occur naturally as DNA is replicated and new cells are produced. By allowing some of the random changes in DNA to have no effect on the ultimate protein sequence, a sort of genetic safety net is created. Some codons do not code for an amino acid at all but instruct the ribosome when to stop adding new amino acids.

The Core Gene Sequence: Introns and Exons

Genes make up about 1 percent of the total DNA in our genome. In the human genome, the coding portions of a gene, called *exons*, are interrupted by intervening sequences, called *introns*. In addition, a eukaryotic gene does not code for a protein

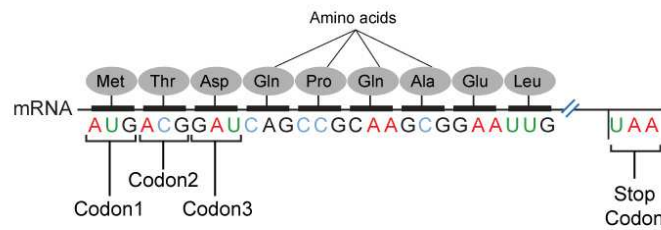


Figure A.26: A codon is a trinucleotide sequence of DNA or RNA that corresponds to a specific amino acid. The genetic code describes the relationship between the sequence of DNA bases (A, C, G, and T) in a gene and the corresponding protein sequence that it encodes. The cell reads the sequence of the gene in groups of three bases. There are 64 different codons: 61 specify amino acids while the remaining three are used as stop signals.

in one continuous stretch of DNA. Both exons and introns are “*transcribed*” into mRNA, but before it is transported to the ribosome, the primary mRNA transcript is edited. This editing process removes the introns, joins the exons together, and adds unique features to each end of the transcript to make a “*mature*” mRNA. One might then ask what the purpose of an intron is if it is spliced out after it is transcribed? It is still unclear what all the functions of introns are, but scientists believe that some serve as the site for *recombination*, the process by which progeny derive a combination of genes different from that of either parent, resulting in novel genes with new combinations of exons, the key to evolution.

Gene Prediction Using Computers

When the complete mRNA sequence for a gene is known, computer programs are used to align the mRNA sequence with the appropriate region of the genomic DNA sequence. This provides a reliable indication of the beginning and end of the coding region for that gene. In the absence of a complete mRNA sequence, the boundaries can be estimated by ever-improving, but still inexact, gene prediction software. The problem is the lack of a single sequence pattern that indicates the beginning or end of a eukaryotic gene. Fortunately, the middle of a gene, referred to as the *core gene sequence*—has enough consistent features to allow more reliable predictions.

From Genes to Proteins: Start to Finish

We just discussed that the journey from DNA to mRNA to protein requires that a cell identify where a gene begins and ends. This must be done both during the transcription and the translation process.

Table A.1: RNA triplet codons and their corresponding amino acids.

	U	C	A	G
U	UUU Phenylalanine UUC Phenylalanine UUA Leucine UUG Leucine	UCU Serine UCC Serine UCA Serine UCG Serine	UAU Tyrosine UAC Tyrosine UAA Stop UAG Stop	UGU Cysteine UGC Cysteine UGA Stop UGG Tryptophan
C	CUU Leucine CUC Leucine CUA Leucine CUG Leucine	CCU Proline CCC Proline CCA Proline CCG Proline	CAU Histidine CAC Histidine CAA Glutamine CAG Glutamine	CGU Arginine CGC Arginine CGA Arginine CGG Arginine
A	AUU Isoleucine AUC Isoleucine AUA Isoleucine AUG Methionine	ACU Threonine ACC Threonine ACA Threonine ACG Threonine	AAU Asparagine AAC Asparagine AAA Lysine AAG Lysine	AGU Serine AGC Serine AGA Arginine AGG Arginine
G	GUU Valine GUC Valine GUA Valine GUG Valine	GCU Alanine GCC Alanine GCA Alanine GCG Alanine	GAU Aspartate GAC Aspartate GAA Glutamate GAG Glutamate	GGU Glycine GGC Glycine GGA Glycine GGG Glycine

Transcription

Transcription, the synthesis of an RNA copy from a sequence of DNA, is carried out by an enzyme called *RNA polymerase*. This molecule has the job of recognizing the DNA sequence where transcription is initiated, called the *promoter site*. In general, there are two “promoter” sequences upstream from the beginning of every gene. The location and base sequence of each promoter site vary for *prokaryotes* (bacteria) and *eukaryotes* (higher organisms), but they are both recognized by RNA polymerase, which can then grab hold of the sequence and drive the production of an mRNA.

Eukaryotic cells have three different RNA polymerases, each recognizing three classes of genes. *RNA polymerase II* is responsible for synthesis of mRNAs from protein-coding genes. This polymerase requires a sequence resembling TATAA, commonly referred to as the *TATA box*, which is found 25-30 nucleotides upstream of the beginning of the gene, referred to as the *initiator sequence*.

Transcription terminates when the polymerase stumbles upon a termination, or stop signal. In eukaryotes, this process is not fully understood. Prokaryotes, however, tend to have a short region composed of G’s and C’s that is able to fold in on itself and form complementary base pairs, creating a stem in the new mRNA. This stem then causes the polymerase to trip and release the *nascent*, or newly formed, mRNA.

Translation

The beginning of *translation*, the process in which the genetic code carried by mRNA directs the synthesis of proteins from amino acids, differs slightly for prokary-

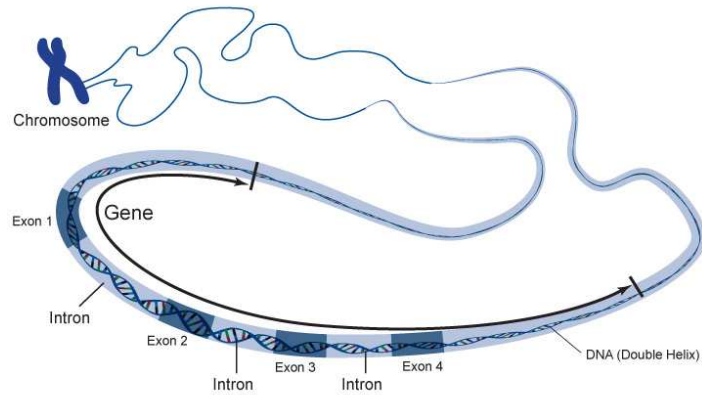


Figure A.27: An exon is the portion of a gene that codes for amino acids. In the cells of plants and animals, most gene sequences are broken up by one or more DNA sequences called introns. The parts of the gene sequence that are expressed in the protein are called exons, because they are expressed, while the parts of the gene sequence that are not expressed in the protein are called introns, because they come in between—or interfere with—the exons. In the cells of plants and animals, most gene sequences are broken up by one or more introns.

otes and eukaryotes, although both processes always initiate at a codon for methionine. For prokaryotes, the ribosome recognizes and attaches at the sequence AGGAGGU on the mRNA, called the *Shine-Delgarno sequence*, that appears just upstream from the methionine (AUG) codon. Curiously, eukaryotes lack this recognition sequence and simply initiate translation at the amino acid methionine, usually coded for by the bases AUG, but sometimes GUG. Translation is terminated for both prokaryotes and eukaryotes when the ribosome reaches one of the three stop codons.

Structural Genes, Junk DNA, and Regulatory Sequences

Over 98 percent of the genome is of unknown function. Although often referred to as “junk” DNA, scientists are beginning to uncover the function of many of these intergenic sequences—the DNA found between genes.

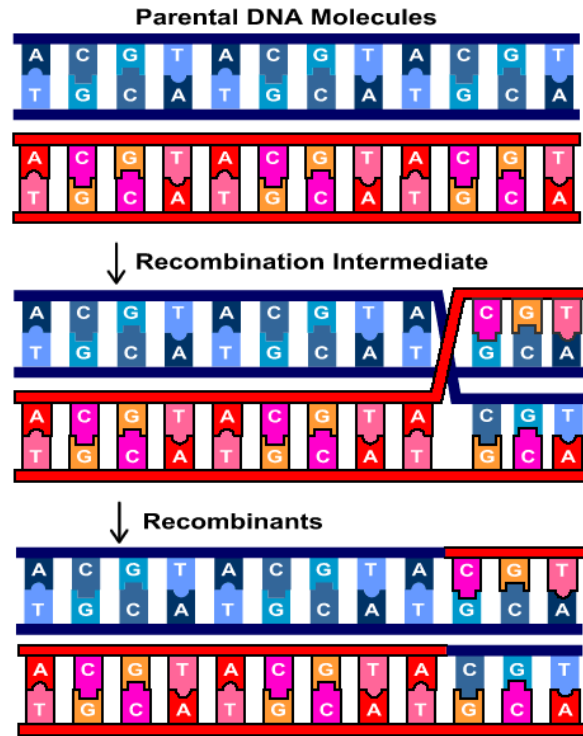


Figure A.28: Recombination. Recombination involves pairing between complementary strands of two parental duplex DNAs (top and middle panel). This process creates a stretch of hybrid DNA (bottom panel) in which the single strand of one duplex is paired with its complement from the other duplex.

Structural Genes. Sequences that code for proteins are called *structural genes*. Although it is true that proteins are the major components of structural elements in a cell, proteins are also the real workhorses of the cell. They perform such functions as transporting nutrients into the cell; synthesizing new DNA, RNA, and protein molecules; and transmitting chemical signals from outside to inside the cell, as well as throughout the cell—both critical to the process of making proteins.

Regulatory Sequences. A class of sequences called *regulatory sequences* makes up a numerically insignificant fraction of the genome but provides critical functions. For example, certain sequences indicate the beginning and end of genes, sites for initiating replication and recombination, or provide landing sites for proteins that turn genes on and off. Like structural genes, regulatory sequences are inherited; however, they are not commonly referred to as genes.

Other DNA Regions. Forty to forty-five percent of our genome is made up of short sequences that are repeated, sometimes hundreds of times. There are numerous forms of this “*repetitive DNA*”, and a few have known functions, such as stabilizing the chromosome structure or inactivating one of the two X chromosomes in

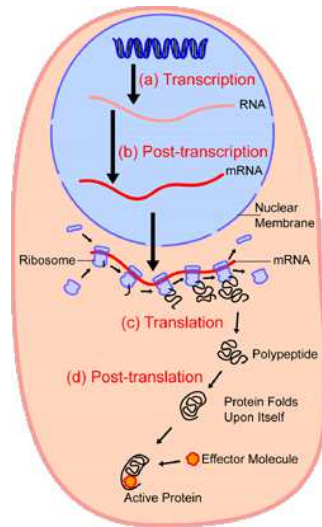


Figure A.29: An overview of transcription and translation. This drawing provides a graphic overview of the many steps involved in transcription and translation. Within the nucleus of the cell (light blue), genes (DNA, dark blue) are transcribed into RNA. This RNA molecule is then subject to post-transcriptional modification and control, resulting in a mature mRNA molecule (red) that is then transported out of the nucleus and into the cytoplasm (peach), where it undergoes translation into a protein. mRNA molecules are translated by ribosomes (purple) that match the three-base codons of the mRNA molecule to the three-base anticodons of the appropriate tRNA molecules. These newly synthesized proteins (black) are often further modified, such as by binding to an effector molecule (orange), to become fully active.

developing females, a process called *X-inactivation*. The most highly repeated sequences found so far in mammals are called “*satellite DNA*” because their unusual composition allows them to be easily separated from other DNA. These sequences are associated with chromosome structure and are found at the *centromeres* (or centers) and *telomeres* (ends) of chromosomes. Although they do not play a role in the coding of proteins, they do play a significant role in chromosome structure, duplication, and cell division. The highly variable nature of these sequences makes them an excellent “*marker*” by which individuals can be identified based on their unique pattern of their satellite DNA.

Another class of non-coding DNA is the “*pseudogene*”, so named because it is believed to be a remnant of a real gene that has suffered mutations and is no longer functional. Pseudogenes may have arisen through the duplication of a functional gene, followed by inactivation of one of the copies. Comparing the presence or absence of pseudogenes is one method used by evolutionary geneticists to group species and to determine relatedness. Thus, these sequences are thought to carry a record of our evolutionary history.

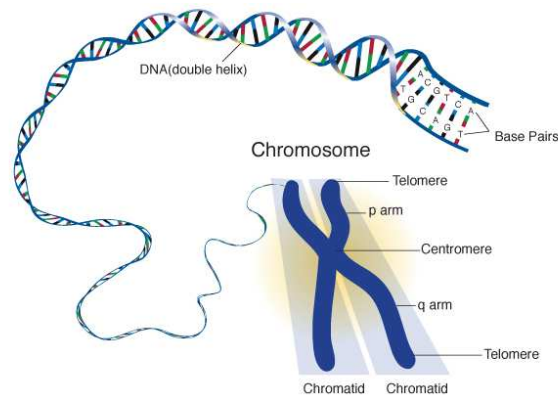


Figure A.30: A chromosome. A chromosome is composed of a very long molecule of DNA and associated proteins that carry hereditary information. The centromere, shown at the center of this chromosome, is a specialized structure that appears during cell division and ensures the correct distribution of duplicated chromosomes to daughter cells. Telomeres are the structures that seal the end of a chromosome. Telomeres play a critical role in chromosome replication and maintenance by counteracting the tendency of the chromosome to otherwise shorten with each round of replication.

How Many Genes Do Humans Have?

In February 2001, two largely independent draft versions of the human genome were published. Both studies estimated that there are 30,000 to 40,000 genes in the human genome, roughly one-third the number of previous estimates. More recently scientists estimated that there are less than 30,000 human genes. However, we still have to make guesses at the actual number of genes, because not all of the human genome sequence is annotated and not all of the known sequence has been assigned a particular position in the genome.

So, how do scientists estimate the number of genes in a genome? For the most part, they look for tell-tale signs of genes in a DNA sequence. These include: *open reading frames*, stretches of DNA, usually greater than 100 bases, that are not interrupted by a stop codon such as TAA, TAG or TGA; *start codons* such as ATG; specific sequences found at *splice junctions*, a location in the DNA sequence where RNA removes the non-coding areas to form a continuous gene transcript for translation into a protein; and *gene regulatory sequences*. This process is dependent on computer programs that search for these patterns in various sequence databases and then make predictions about the existence of a gene.

From One Gene—One Protein to a More Global Perspective

Only a small percentage of the 3 billion bases in the human genome becomes an expressed gene product. However, of the approximately 1 percent of our genome

that is expressed, 40 percent is alternatively spliced to produce multiple proteins from a single gene. *Alternative splicing* refers to the cutting and pasting of the primary mRNA transcript into various combinations of mature mRNA. Therefore the one gene—one protein theory, originally framed as “one gene—one enzyme”, does not precisely hold.

With so much DNA in the genome, why restrict transcription to a tiny portion, and why make that tiny portion work overtime to produce many alternate transcripts? This process may have evolved as a way to limit the deleterious effects of mutations. Genetic mutations occur randomly, and the effect of a small number of mutations on a single gene may be minimal. However, an individual having many genes each with small changes could weaken the individual, and thus the species. On the other hand, if a single mutation affects several alternate transcripts at once, it is more likely that the effect will be devastating—the individual may not survive to contribute to the next generation. Thus, alternate transcripts from a single gene could reduce the chances that a mutated gene is transmitted.

Gene Switching: Turning Genes On and Off

The estimated number of genes for humans, less than 30,000, is not so different from the 25,300 known genes of *Arabidopsis thaliana*, commonly called mustard grass. Yet, we appear, at least at first glance, to be a far more complex organism. A person may wonder how this increased complexity is achieved. One answer lies in the regulatory system that turns genes on and off. This system also precisely controls the amount of a gene product that is produced and can further modify the product after it is made. This exquisite control requires multiple regulatory input points. One very efficient point occurs at transcription, such that an mRNA is produced only when a gene product is needed. Cells also regulate gene expression by *post-transcriptional modification*; by allowing only a subset of the mRNAs to go on to translation; or by restricting translation of specific mRNAs to only when the product is needed. At other levels, cells regulate gene expression through DNA folding, chemical modification of the nucleotide bases, and intricate “*feedback mechanisms*” in which some of the gene’s own protein product directs the cell to cease further protein production.

Controlling Transcription

Promoters and Regulatory Sequences. Transcription is the process whereby RNA is made from DNA. It is initiated when an enzyme, *RNA polymerase*, binds to a site on the DNA called a *promoter sequence*. In most cases, the polymerase is aided by a group of proteins called “*transcription factors*” that perform specialized functions, such as DNA sequence recognition and regulation of the polymerase’s enzyme activity. Other regulatory sequences include *activators*, *repressors*, and

enhancers. These sequences can be *cis-acting* (affecting genes that are adjacent to the sequence) or *trans-acting* (affecting expression of the gene from a distant site), even on another chromosome.

The Globin Genes: An Example of Transcriptional Regulation. An example of transcriptional control occurs in the family of genes responsible for the production of globin. Globin is the protein that complexes with the iron-containing heme molecule to make hemoglobin. *Hemoglobin* transports oxygen to our tissues via red blood cells. In the adult, red blood cells do not contain DNA for making new globin; they are ready-made with all of the hemoglobin they will need.

During the first few weeks of life, embryonic globin is expressed in the yolk sac of the egg. By week five of gestation, globin is expressed in early liver cells. By birth, red blood cells are being produced, and globin is expressed in the bone marrow. Yet, the globin found in the yolk is not produced from the same gene as is the globin found in the liver or bone marrow stem cells. In fact, at each stage of development, different globin genes are turned on and off through a process of transcriptional regulation called “*switching*”.

To further complicate matters, globin is made from two different protein chains: an alpha-like chain coded for on chromosome 16; and a beta-like chain coded for on chromosome 11. Each chromosome has the embryonic, fetal, and adult form lined up on the chromosome in a sequential order for developmental expression. The developmentally regulated transcription of globin is controlled by a number of *cis-acting* DNA sequences, and although there remains a lot to be learned about the interaction of these sequences, one known control sequence is an enhancer called the *Locus Control Region (LCR)*. The LCR sits far upstream on the sequence and controls the alpha genes on chromosome 16. It may also interact with other factors to determine which alpha gene is turned on.

Thalassemias are a group of diseases characterized by the absence or decreased production of normal globin, and thus hemoglobin, leading to decreased oxygen in the system. There are alpha and beta thalassemias, defined by the defective gene, and there are variations of each of these, depending on whether the embryonic, fetal, or adult forms are affected and/or expressed. Although there is no known cure for the thalassemias, there are medical treatments that have been developed based on our current understanding of both gene regulation and cell differentiation. Treatments include blood transfusions, iron chelators, and bone marrow transplants. With continuing research in the areas of gene regulation and cell differentiation, new and more effective treatments may soon be on the horizon, such as the advent of gene transfer therapies.

The Influence of DNA Structure and Binding Domains. Sequences that are important in regulating transcription do not necessarily code for transcription factors or other proteins. Transcription can also be regulated by subtle variations in DNA structure and by chemical changes in the bases to which transcription factors

bind. As stated previously, the chemical properties of the four DNA bases differ slightly, providing each base with unique opportunities to chemically react with other molecules. One chemical modification of DNA, called *methylation*, involves the addition of a *methyl group* ($-CH_3$). Methylation frequently occurs at cytosine residues that are preceded by guanine bases, oftentimes in the vicinity of promoter sequences. The methylation status of DNA often correlates with its functional activity, where inactive genes tend to be more heavily methylated. This is because the methyl group serves to inhibit transcription by attracting a protein that binds specifically to methylated DNA, thereby interfering with polymerase binding. Methylation also plays an important role in *genomic imprinting*, which occurs when both maternal and paternal alleles are present but only one allele is expressed while the other remains inactive. Another way to think of genomic imprinting is as “*parent of origin differences*” in the expression of inherited traits. Considerable intrigue surrounds the effects of DNA methylation, and many researchers are working to unlock the mystery behind this concept.

Controlling Translation

Translation is the process whereby the genetic code carried by an mRNA directs the synthesis of proteins. *Translational regulation* occurs through the binding of specific molecules, called *repressor proteins*, to a sequence found on an RNA molecule. Repressor proteins prevent a gene from being expressed. As we have just discussed, the default state for a gene is that of being expressed via the recognition of its promoter by RNA polymerase. Close to the promoter region is another cis-acting site called the *operator*, the target for the repressor protein. When the repressor protein binds to the operator, RNA polymerase is prevented from initiating transcription, and gene expression is turned off.

Translational control plays a significant role in the process of embryonic development and cell differentiation. Upon fertilization, an egg cell begins to multiply to produce a ball of cells that are all the same. At some point, however, these cells begin to *differentiate*, or change into specific cell types. Some will become blood cells or kidney cells, whereas others may become nerve or brain cells. When all of the cells formed are alike, the same genes are turned on. However, once differentiation begins, various genes in different cells must become active to meet the needs of that cell type. In some organisms, the egg houses store immature mRNAs that become translationally active only after fertilization. Fertilization then serves to trigger mechanisms that initiate the efficient translation of mRNA into proteins. Similar mechanisms serve to activate mRNAs at other stages of development and differentiation, such as when specific protein products are needed.

Molecular Genetics: The Study of Heredity, Genes, and DNA

As we have just learned, DNA provides a blueprint that directs all cellular activities and specifies the developmental plan of multicellular organisms. Therefore, an understanding of DNA, gene structure, and function is fundamental for an appreciation of the molecular biology of the cell. Yet, it is important to recognize that progress in any scientific field depends on the availability of experimental tools that allow researchers to make new scientific observations and conduct novel experiments. The last section of the genetic primer concludes with a discussion of some of the laboratory tools and technologies that allow researchers to study cells and their DNA.

A.3 Molecular Genetics: Piecing It Together

Molecular genetics is the study of the agents that pass information from generation to generation. These molecules, our *genes*, are long polymers of *deoxyribonucleic acid*, or DNA. Just four chemical building blocks—guanine (G), adenine (A), thymine (T), and cytosine (C)—are placed in a unique order to code for all of the genes in all living organisms.

Genes determine *hereditary traits*, such as the color of our hair or our eyes. They do this by providing instructions for how every activity in every cell of our body should be carried out. For example, a gene may tell a liver cell to remove excess cholesterol from our bloodstream. How does a gene do this? It will instruct the cell to make a particular protein. It is this protein that then carries out the actual work. In the case of excess blood cholesterol, it is the receptor proteins on the outside of a liver cell that bind to and remove cholesterol from the blood. The cholesterol molecules can then be transported into the cell, where they are further processed by other proteins.

Many diseases are caused by *mutations*, or changes in the DNA sequence of a gene. When the information coded for by a gene changes, the resulting protein may not function properly or may not even be made at all. In either case, the cells containing that genetic change may no longer perform as expected. We now know that mutations in genes code for the *cholesterol receptor protein* associated with a disease called *familial hypercholesterolemia*. The cells of an individual with this disease end up having reduced receptor function and cannot remove a sufficient amount of low density lipoprotein (LDL), or bad cholesterol, from their bloodstream. A person may then develop dangerously high levels of cholesterol, putting them at increased risk for both heart attack and stroke.

How do scientists study and find these genetic mutations? They have available to them a variety of tools and technologies to compare a DNA sequence isolated from a healthy person to the same DNA sequence extracted from an afflicted person. Advanced computer technologies, combined with the explosion of genetic data generated from the various whole genome sequencing projects, enable scientists to use these molecular genetic tools to diagnose disease and to design new drugs and therapies. Below is a review of some common laboratory methods that geneticists—scientists who study the inheritance pattern of specific traits—can use to obtain and work with DNA, followed by a discussion of some applications.

Laboratory Tools and Techniques

The methods used by molecular geneticists to obtain and study DNA have been developed through keen observation and adaptation of the chemical reactions and biological processes that occur naturally in all cells. Many of the enzymes that copy DNA, make RNA from DNA, and synthesize proteins from an RNA template were first characterized in bacteria. These basic research results have become

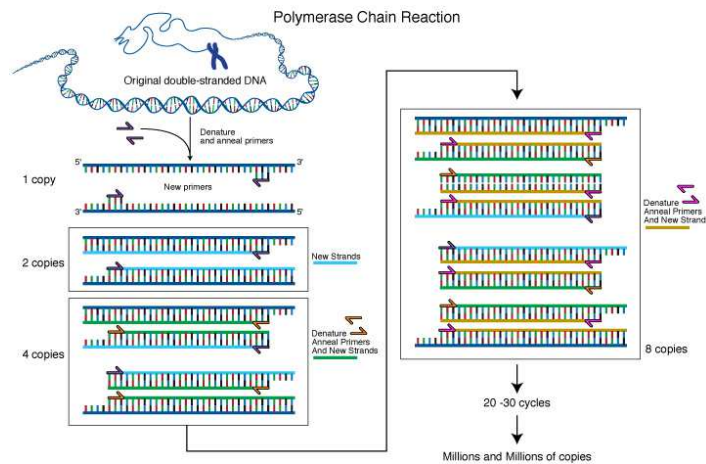


Figure A.31: Polymerase chain reaction (PCR) is a laboratory technique used to amplify DNA sequences. The method involves using short DNA sequences called primers to select the portion of the genome to be amplified. The temperature of the sample is repeatedly raised and lowered to help a DNA replication enzyme copy the target DNA sequence. The technique can produce a billion copies of the target sequence in just a few hours.

fundamental to our understanding of the function of human cells and have led to immense practical applications for studying a gene and its corresponding protein. For example, large-scale protein production now provides an inexpensive way to generate abundant quantities of certain therapeutic agents, such as insulin for the treatment of diabetes. As science advances, so do the number of tools available that are applicable to the study of molecular genetics.

Obtaining DNA for Laboratory Analysis

Isolating DNA from just a single cell provides a complete set of all a person's genes, that is, two copies of each gene. However, many laboratory techniques require that a researcher have access to hundreds of thousands of copies of a particular gene. One way to obtain this many copies is to isolate DNA from millions of cells grown artificially in the laboratory. Another method, called *cloning*, uses DNA manipulation procedures to produce multiple copies of a single gene or segment of DNA. The *polymerase chain reaction* (PCR) is a third method whereby a specific sequence within a double-stranded DNA is copied, or *amplified*. PCR amplification has become an indispensable tool in a great variety of applications.

Methods for Amplifying DNA

Cloning DNA in Bacteria. The word “cloning” can be used in many ways. In this document, it refers to making multiple, exact copies of a particular sequence of DNA. To make a clone, a target DNA sequence is inserted into what is called a *cloning vector*. A cloning vector is a DNA molecule originating from a virus, plasmid, or the cell of a higher organism into which another DNA fragment of appropriate size can be integrated without interfering with the vector’s capacity for self-replication. The target and vector DNA fragments are then *ligated*, or joined together, to create what is called a *recombinant DNA molecule*. Recombinant DNA molecules are usually introduced into *Escherichia coli*, or *E. coli*—a common laboratory strain of a bacterium— by *transformation*, the natural DNA uptake mechanism possessed by bacteria. Within the bacterium, the vector directs the multiplication of the recombinant DNA molecule, producing a number of identical copies. The vector replication process is such that only one recombinant DNA molecule can propagate within a single bacterium; therefore, each resulting clone contains multiple copies of just one DNA insert. The DNA can then be isolated using the techniques described earlier.

A *restriction enzyme* is a protein that binds to a DNA molecule at a specific sequence and makes a double-stranded cut at, or near, that sequence. Restriction enzymes have specialized applications in various scientific techniques, such as manipulating DNA molecules during cloning. These enzymes can cut DNA in two different ways. Many make a simple double-stranded cut, giving a sequence what are called *blunt* or *flush ends*. Others cut the two DNA strands at different positions, usually just a few nucleotides apart, such that the resulting DNA fragments have short single-stranded overhangs, called *sticky* or *cohesive ends*. By carefully choosing the appropriate restriction enzymes, a researcher can cut out a target DNA sequence, open up a cloning vector, and join the two DNA fragments to form a recombinant DNA molecule.

More on Cloning Vectors. In general, a bacterial genome consists of a single, circular chromosome. They can also contain much smaller extrachromosomal genetic elements, called *plasmids*, that are distinct from the normal bacterial genome and are nonessential for cell survival under normal conditions. Plasmids are capable of copying themselves independently of the chromosome and can easily move from one bacterium to another. In addition, some plasmids are capable of integrating into a host genome. This makes them an excellent vehicle, or *vector*, for shuttling target DNA into a bacterial host. By cutting both the target and plasmid DNA with the same restriction enzyme, complementary base pairs are formed on each DNA fragment. These fragments may then be joined together, creating a new circular plasmid that contains the target DNA. This *recombinant plasmid* is then coaxed into a bacterial host where it is copied, or *replicated*, as though it were a normal plasmid.

Bacterial plasmids were the first vectors used to transfer genetic information and are still used extensively. However, their use is sometimes limited by the amount of target DNA they can accept, approximately 15,000 bases, or 15 Kb. With DNA sequences beyond this size, the efficiency of the vector decreases because it now has trouble entering the cell and replicating itself. However, other vectors have been discovered or created that can accept larger target DNA including: *bacteriophages*, bacterial viruses that accept inserts up to 20 Kb; *cosmids*, recombinant plasmids with bacteriophage components that accept inserts up to 45 Kb; *bacterial artificial chromosomes* (BACs) that accept inserts up to 150 Kb; and *yeast artificial chromosomes* (YACs) that accept inserts up to 1000 kb. Many viruses have also been modified for use as cloning vectors.

Polymerase Chain Reaction (PCR). The *polymerase chain reaction (PCR)* is an amazingly simple technique that results in the exponential *amplification* of almost any region of a selected DNA molecule. It works in a way that is similar to DNA replication in nature. The primary materials, or reagents, used in PCR are:

- *DNA nucleotides*, the building blocks for the new DNA
- *Template DNA*, the DNA sequence that you want to amplify
- *Primers*, single-stranded DNAs between 20 and 50 nucleotides long that are complementary to a short region on either side of the template DNA
- *Taq polymerase*, a heat stable enzyme that drives, or catalyzes, the synthesis of new DNA

Taq polymerase was first isolated from a bacterium that lives in the hot springs in Yellowstone National Park. The Taq polymerase enzyme has evolved to withstand the extreme temperatures in which the bacteria live and can therefore remain intact during the high temperatures used in PCR.

The PCR reaction is carried out by mixing together in a small test tube the template DNA, DNA nucleotides, primers, and Taq polymerase. The primers must anneal, or pair to, the template DNA on either side of the region that is to be amplified, or copied. This means that the DNA sequences of these borders must be known so that the appropriate primers can be made. These oligonucleotides serve to initiate the synthesis of the new complementary strand of DNA. Because Taq polymerase, a form of DNA polymerase that catalyzes the synthesis of new DNA, is incredibly heat stable (thermostable), the reaction mixture can be heated to approximately 90 degrees centigrade without destroying the molecules' enzymatic activity. At this temperature, the newly created DNA strands detach from the template DNA.

The reaction mixture is then cooled again, allowing more primers to anneal to the template DNA and also to the newly created DNA. The Taq polymerase can now carry out a second cycle of DNA synthesis. This cycle of heating, cooling,

and heating is repeated over and over. Because each cycle doubles the amount of template DNA in the previous cycle, one template DNA molecule rapidly becomes hundreds of thousands of molecules in just a couple of hours.

PCR has many applications in biology. It is used in DNA mapping, DNA sequencing, and molecular phylogenetics. A modified version of PCR can also be used to amplify DNA copies of specific RNA molecules. Because PCR requires very little starting material, or template DNA, it is frequently used in forensic science and clinical diagnosis.

Preparing DNA for Experimental Analysis

Gel Electrophoresis: Separating DNA Molecules of Different Lengths. Gels are usually made from *agarose*—a chain of sugar molecules extracted from seaweed—or some other synthetic molecule. Purified agarose is generally purchased in a powdered form and is dissolved in boiling water. While the solution is still hot, it is poured into a special gel casting apparatus that contains three basic parts: a tray, a support, and a comb. The tray serves as the mold that will provide the shape and size for the gel. The support prevents the liquid agarose from leaking out of the mold during the solidification process. As the liquid agarose starts to cool, it undergoes what is known as *polymerization*. Rather than staying dissolved in the water, the sugar polymers crosslink with each other, causing the solution to *gel* into a semi-solid matrix much like Jello, only more firm. The support also allows the polymerized gel to be removed from the mold without breaking. The job of the comb is to generate small *wells* into which a DNA sample will be loaded.

Once a gel has polymerized, it is lifted from the casting tray, placed into a running tank, and submerged in a special aqueous buffer, called a *running buffer*. The gel apparatus is then connected to a power supply via two plugs, or *electrodes*. Each plug leads to a thin wire at opposite ends of the tank. Because one electrode is positive and the other is negative, a strong electric current will flow through the tank when the power supply is turned on.

Next, DNA samples of interest are dissolved in a tiny volume of liquid containing a small amount of glycerol. Because glycerol has a density greater than water, it serves to weight down the sample and stops it from floating away once the sample has been loaded into a well. Also, because it is helpful to be able to monitor a DNA sample as it migrates across a gel, charged molecules, called *dyes*, are also added to the sample buffer. These dyes are usually of two different colors and two different *molecular weights*, or sizes. One of the dyes is usually smaller than most, if not all, of the sample DNA fragments and will migrate faster than the smallest DNA sample. The other dye is usually large and will migrate with the larger DNA samples. It is assumed that most of the DNA fragments of interest will migrate somewhere in between these two dyes. Therefore, when the small dye reaches the end of the gel, electrophoresis is usually stopped.

Once the gel has been prepared and loaded, the power supply is turned on. The electric current flowing through the gel causes the DNA fragments to migrate toward the bottom, or *positively charged* end, of the gel. This is because DNA has an overall negative charge because of the combination of molecules in its structure. Smaller fragments of DNA are less impeded by the crosslinks formed within the polymerized gel than are larger molecules. This means that smaller DNA fragments tend to move faster and farther in a given amount of time. The result is a streak, or *gradient*, of larger to smaller DNA pieces. In those instances where multiple copies of DNA all have the same length, a concentration of DNA occurs at that position in the gel, called a band. Bands can result from a restriction enzyme digest of a sample containing thousands of copies of plasmid DNA, or PCR amplification of a DNA sequence. The banded DNA is then detected by soaking the gel briefly in a solution containing a dye called *ethidium bromide* (EtBr). EtBr is an *intercalating agent*, which means that it is capable of wedging itself into the grooves of DNA, where it remains. The more base pairs present within a DNA fragment, the greater the number of grooves available for EtBr to insert itself. EtBr also fluoresces under ultraviolet (UV) light. Therefore, if a gel soaked in a solution containing EtBr is placed under a UV source, a researcher can actually detect DNA by visualizing where the EtBr fluoresces. Because a scientist always loads and runs a “control” sample that contains multiple fragments of DNA with known sizes, the sizes of the sample DNA fragments can be estimated by comparing the control and sample bands.

DNA Blotting. The porous and thin nature of a gel is ideal for separating DNA fragments using electrophoresis, but as we mentioned earlier, these gels are delicate and rarely usable for other techniques. For this reason, DNA that has been separated by electrophoresis is transferred from a gel to an easy-to-handle inert membrane, a process called *blotting*. The term “blotting” describes the overlaying of the membrane on the gel and the application of a pad to ensure even contact, without disturbing the positions of the DNA fragments. In the first step, the DNA trapped in the gel is *denatured*—the double-stranded DNA is broken into single strands by soaking the gel in an alkaline solution. This readies the DNA for hybridization with a *probe*, a piece of DNA that is complementary to the sequence under investigation. A membrane, usually made of a compound called *nitrocellulose*, is then placed on top of the gel and compressed with a heavy weight. The DNA is transferred from the gel to the membrane by simple capillary action. This procedure reproduces the exact pattern of DNA captured in the gel on the membrane. The membrane can then be probed with a DNA marker to verify the presence of a target sequence.

Southern blotting is the name of the procedure for transferring denatured DNA from an agarose gel to a solid support membrane. This procedure takes advantage of a special property of nitrocellulose, its ability to bind very strongly to single-stranded DNA but not double-stranded DNA. On the other hand, *Northern blotting*

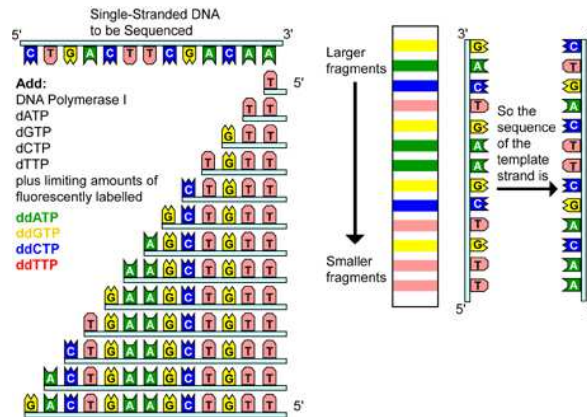


Figure A.32: Chain termination DNA sequencing. Chain termination sequencing involves the synthesis of new strands of DNA complementary to a single-stranded template (step I). The template DNA is supplied with a mixture of all four deoxynucleotides, four dideoxynucleotides (each labeled with a different colored fluorescent tag), and DNA polymerase (step II). Because all four deoxynucleotides are present, chain elongation proceeds until, by chance, DNA polymerase inserts a dideoxynucleotide. The result is a new set of DNA chains, all of different lengths (step III). The fragments are then separated by size using gel electrophoresis (step IV). As each labeled DNA fragment passes a detector at the bottom of the gel, the color is recorded. The DNA sequence is then reconstructed from the pattern of colors representing each nucleotide sequence (step V).

refers to any blotting procedure in which electrophoresis is performed using RNA.

Methods for Analyzing DNA

Once DNA has been isolated and purified, it can be further analyzed in a variety of ways, such as to identify the presence or absence of specific sequences or to locate nucleotide changes, called mutations, within a specific sequence.

DNA Sequencing. The process of determining the order of the nucleotide bases along a DNA strand is called *sequencing*. In 1977, 24 years after the discovery of the structure of DNA, two separate methods for sequencing DNA were developed: the *chain termination method* and the *chemical degradation method*. Both methods were equally popular to begin with, but, for many reasons, the chain termination method is the method more commonly used today. This method is based on the principle that single-stranded DNA molecules that differ in length by just a single nucleotide can be separated from one another using polyacrylamide gel electrophoresis, described earlier.

The DNA to be sequenced, called the *template DNA*, is first prepared as a single-stranded DNA. Next, a short oligonucleotide is *annealed*, or joined, to the same position on each template strand. The oligonucleotide acts as a primer for the synthesis of a new DNA strand that will be complementary to the template DNA. This

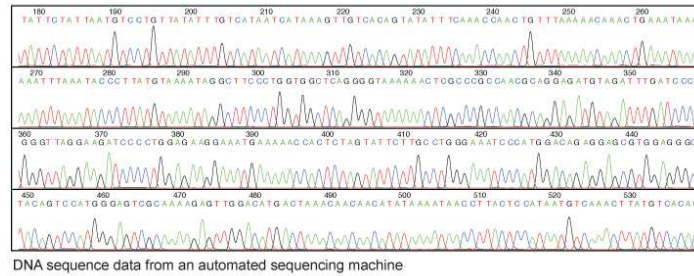


Figure A.33: DNA sequencing is a laboratory technique used to determine the exact sequence of bases (A, C, G, and T) in a DNA molecule. The DNA base sequence carries the information a cell needs to assemble protein and RNA molecules. DNA sequence information is important to scientists investigating the functions of genes. The technology of DNA sequencing was made faster and less expensive as a part of the Human Genome Project.

technique requires that four nucleotide-specific reactions—one each for G, A, C, and T—be performed on four identical samples of DNA. The four sequencing reactions require the addition of all the components necessary to synthesize and label new DNA, including:

- A *DNA template*
- A *primer* tagged with a mildly radioactive molecule or a light-emitting chemical
- *DNA polymerase*, an enzyme that drives the synthesis of DNA
- Four *deoxynucleotides* (G, A, C, and T)
- One *dideoxynucleotide*, either ddG, ddA, ddC, or ddT

After the first deoxynucleotide is added to the growing complementary sequence, DNA polymerase moves along the template and continues to add base after base. The strand synthesis reaction continues until a dideoxynucleotide is added, blocking further elongation. This is because dideoxynucleotides are missing a special group of molecules, called a 3'-hydroxyl group, needed to form a connection with the next nucleotide. Only a small amount of a dideoxynucleotide is added to each reaction, allowing different reactions to proceed for various lengths of time until by chance, DNA polymerase inserts a dideoxynucleotide, terminating the reaction. Therefore, the result is a set of new chains, all of different lengths.

To read the newly generated sequence, the four reactions are run side-by-side on a polyacrylamide sequencing gel. The family of molecules generated in the presence of ddATP is loaded into one lane of the gel, and the other three families, generated with ddCTP, ddGTP, and ddTTP, are loaded into three adjacent lanes. After electrophoresis, the DNA sequence can be read directly from the positions of the bands in the gel.

Variations of this method have been developed for automated sequencing machines. In one method, called *cycle sequencing*, the dideoxynucleotides, not the primers, are tagged with different colored fluorescent dyes; thus, all four reactions occur in the same tube and are separated in the same lane on the gel. As each labeled DNA fragment passes a detector at the bottom of the gel, the color is recorded, and the sequence is reconstructed from the pattern of colors representing each nucleotide in the sequence.

Impact of Molecular Genetics

Most sequencing and analysis technologies were developed from studies of non-human genomes, notably those of the bacterium *Escherichia coli*, the yeast *Saccharomyces cerevisiae*, the fruit fly *Drosophila melanogaster*, the roundworm *Caenorhabditis elegans*, and the laboratory mouse *Mus musculus*. These simpler systems provide excellent models for developing and testing the procedures needed for studying the much more complex human genome.

A large amount of genetic information has already been derived from these organisms, providing valuable data for the analysis of normal human gene regulation, genetic diseases, and evolutionary processes. For example, researchers have already identified single genes associated with a number of diseases, such as cystic fibrosis. As research progresses, investigators will also uncover the mechanisms for diseases caused by several genes or by single genes interacting with environmental factors. Genetic susceptibilities have been implicated in many major disabling and fatal diseases including heart disease, stroke, diabetes, and several kinds of cancer. The identification of these genes and their proteins will pave the way to more effective therapies and preventive measures. Investigators determining the underlying biology of genome organization and gene regulation will also begin to understand how humans develop, why this process sometimes goes awry, and what changes take place as people age.

Appendix B

Probability and Random Processes

This appendix provides a summary of random processes in continuous time with continuous and discrete states. Some of the material in this section is drawn from the AM08 supplement on Optimization-Based Control [62].

B.1 Random Variables

Random variables and processes are defined in terms of an underlying *probability space* that captures the nature of the stochastic system we wish to study. A probability space $(\Omega, \mathcal{F}, \mathbb{P})$ consists of:

- a *sample space* Ω that represents the set of all possible outcomes;
- a set of *events* \mathcal{F} that captures combinations of elementary outcomes that are of interest; and
- a *probability measure* \mathbb{P} that describes the likelihood of a given event occurring.

Ω can be any set, either with a finite, countable or infinite number of elements. The event space \mathcal{F} consists of subsets of Ω . There are some mathematical limits on the properties of the sets in \mathcal{F} , but these are not critical for our purposes here. The probability measure \mathbb{P} is a mapping from $\mathcal{F} \rightarrow [0, 1]$ that assigns a probability to each event. It must satisfy the property that given any two disjoint sets $A, B \in \mathcal{F}$, $\mathbb{P}(A \cup B) = \mathbb{P}(A) + \mathbb{P}(B)$.

With these definitions, we can model many different stochastic phenomena. Given a probability space, we can choose samples $\omega \in \Omega$ and identify each sample with a collection of events chosen from \mathcal{F} . These events should correspond to phenomena of interest and the probability measure \mathbb{P} should capture the likelihood of that event occurring in the system that we are modeling. This definition of a probability space is very general and allows us to consider a number of situations as special cases.

A *random variable* X is a function $X : \Omega \rightarrow S$ that gives a value in S , called the state space, for any sample $\omega \in \Omega$. Given a subset $A \subset S$, we can write the probability that $X \in A$ as

$$\mathbb{P}(X \in A) = \mathbb{P}(\{\omega \in \Omega : X(\omega) \in A\}).$$

We will often find it convenient to omit ω when working random variables and hence we write $X \in S$ rather than the more correct $X(\omega) \in S$. The term *probability distribution* is used to describe the set of possible values that X can take.

A *discrete random variable* X is a variable that can take on any value from a discrete set S with some probability for each element of the set. We model a discrete random variable by its *probability mass function* $p_X(s)$, which gives the probability that the random variable X takes on the specific value $s \in S$:

$$p_X(s) = \text{probability that } X \text{ takes on the value } s \in S.$$

The sum of the probabilities over the entire set of states must be unity, and so we have that

$$\sum_{s \in S} p_X(s) = 1.$$

If A is a subset of S , then we can write $\mathbb{P}(X \in A)$ for the probability that X will take on some value in the set A . It follows from our definition that

$$\mathbb{P}(X \in A) = \sum_{s \in A} p_X(s).$$

Definition B.1 (Bernoulli distribution). The Bernoulli distribution is used to model a random variable that takes the value 1 with probability p and 0 with probability $1 - p$:

$$\mathbb{P}(X = 1) = p, \quad \mathbb{P}(X = 0) = 1 - p.$$

Alternatively, it can be written in terms of its probability mass function

$$p(s) = \begin{cases} p & s = 1 \\ 1 - p & s = 0 \\ 0 & \text{otherwise.} \end{cases}$$

Bernoulli distributions are used to model independent experiments with binary outcomes, such as flipping a coin.

Definition B.2 (Binomial distribution). The *binomial distribution* models the probability of successful trials in n experiments, given that a single experiment has probability of success p . If we let X_n be a random variable that indicates the number of success in n trials, then the binomial distribution is given by

$$p_{X_n}(k) = \mathbb{P}(X_n = k) = \binom{n}{k} p^k (1 - p)^{n-k}$$

for $k = 1, \dots, n$. The probability mass function is shown in Figure B.1a.

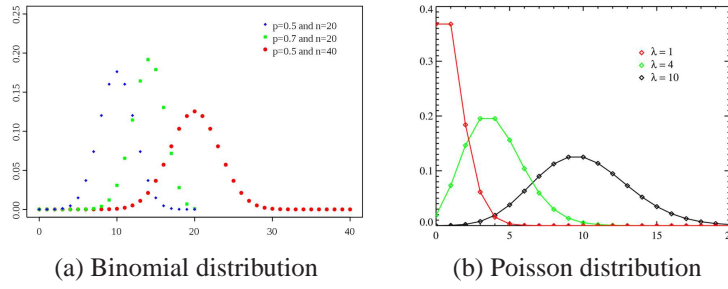


Figure B.1: Probability mass functions for common discrete distributions.

Definition B.3 (Poisson distribution). The *Poisson distribution* is used to describe the probability that a given number of events will occur in a fixed interval of time t . The Poisson distribution is defined as

$$p_{N_t}(k) = \mathbb{P}(N_t = k) = \frac{(\lambda t)^k}{k!} e^{-\lambda t}, \quad (\text{B.1})$$

where N_t is the number of events that occur in a period t and λ is a real number parameterizing the distribution. This distribution can be considered as a model for a counting process, where we assume that the average rate of occurrences in a period t is given by λt and λ represents the rate of the counting process. Figure B.1b shows the form of the distribution for different values of k and λt .

A *continuous (real-valued) random variable* X is a variable that can take on any value in the set of real numbers \mathbb{R} . We can model the random variable X according to its *probability distribution function* $F : \mathbb{R} \rightarrow [0, 1]$:

$$F(x) = \mathbb{P}(X \leq x) = \text{probability that } X \text{ takes on a value in the range } (-\infty, x].$$

It follows from the definition that if X is a random variable in the range $[L, U]$ then $\mathbb{P}(L \leq X \leq U) = 1$. Similarly, if $y \in [L, U]$ then $\mathbb{P}(L \leq X < y) = 1 - \mathbb{P}(y \leq X \leq U)$.

We characterize a random variable in terms of the *probability density function* (pdf) $p(x)$. The density function is defined so that its integral over an interval gives the probability that the random variable takes its value in that interval:

$$\mathbb{P}(x_l \leq X \leq x_u) = \int_{x_l}^{x_u} p(x) dx. \quad (\text{B.2})$$

It is also possible to compute $p(x)$ given the distribution \mathbb{P} as long as the distribution function is suitably smooth:

$$p(x) = \frac{\partial F}{\partial x}(x).$$

We will sometimes write $p_X(x)$ when we wish to make explicit that the pdf is associated with the random variable X . Note that we use capital letters to refer to a random variable and lower case letters to refer to a specific value.

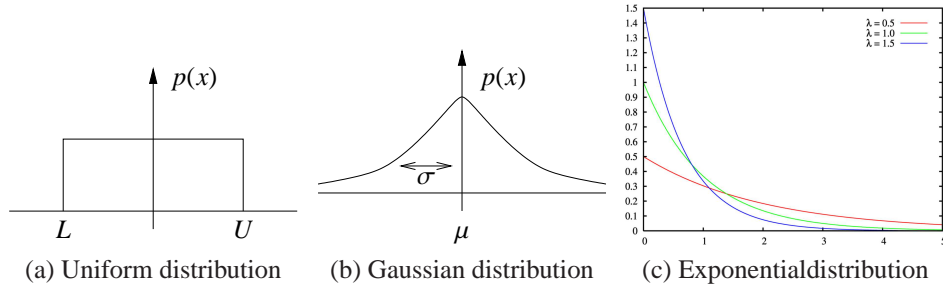


Figure B.2: Probability density function (pdf) for uniform, Gaussian and exponential distributions.

Definition B.4 (Uniform distribution). The *uniform distribution* on an interval $[L, U]$ assigns equal probability to any number in the interval. Its pdf is given by

$$p(x) = \frac{1}{U - L}. \quad (\text{B.3})$$

The uniform distribution is illustrated in Figure B.2a.

Definition B.5 (Gaussian distribution). The *Gaussian distribution* (also called a *normal distribution*) has a pdf of the form

$$p(x) = \frac{1}{\sqrt{2\pi\sigma^2}} e^{-\frac{1}{2}\left(\frac{x-\mu}{\sigma}\right)^2}. \quad (\text{B.4})$$

The parameter μ is called the *mean* of the distribution and σ is called the *standard deviation* of the distribution. Figure B.2b shows a graphical representation a Gaussian pdf.

Definition B.6 (Exponential distribution). The exponential distribution is defined for positive numbers and has a pdf of the form

$$p(x) = \lambda e^{-\lambda x}, \quad x > 0$$

where λ is a parameter defining the distribution. A plot of the pdf for an exponential distribution is shown in Figure B.2c.

We now define a number of properties of collections of random variables. We focus on the continuous random variable case, but unless noted otherwise these concepts can all be defined similarly for discrete random variables (using the probability mass function in place of the probability density function).

If two random variables are related, we can talk about their *joint probability distribution*: $\mathbb{P}_{X,Y}(A, B)$ is the probability that both event A occurs for X and B occurs for Y . This is sometimes written as $P(A \cap B)$, where we abuse notation by implicitly assuming that A is associated with X and B with Y . For continuous random

variables, the joint probability distribution can be characterized in terms of a *joint probability density function*

$$F_{X,Y}(x,y) = \mathbb{P}(X \leq x, Y \leq y) = \int_{-\infty}^y \int_{-\infty}^x p(u,v) du dv. \quad (\text{B.5})$$

The joint pdf thus describes the relationship between X and Y , and for sufficiently smooth distributions we have

$$p(x,y) = \frac{\partial^2 F}{\partial x \partial y}.$$

We say that X and Y are *independent* if $p(x,y) = p(x)p(y)$, which implies that $F_{X,Y}(x,y) = F_X(x)F_Y(y)$ for all x,y . Equivalently, $\mathbb{P}(A \cap B) = \mathbb{P}(A)\mathbb{P}(B)$ if A and B are independent events.

The *conditional probability* for an event A given that an event B has occurred, written as $\mathbb{P}(A | B)$, is given by

$$\mathbb{P}(A | B) = \frac{\mathbb{P}(A \cap B)}{\mathbb{P}(B)}. \quad (\text{B.6})$$

If the events A and B are independent, then $\mathbb{P}(A | B) = \mathbb{P}(A)$. Note that the individual, joint and conditional probability distributions are all different, so if we are talking about random variables we can write $P_{X,Y}(A, B)$, $P_{X|Y}(A | B)$ and $P_Y(B)$, where A and B are appropriate subsets of \mathbb{R} .

If X is dependent on Y then Y is also dependent on X . *Bayes' theorem* relates the conditional and individual probabilities:

$$\mathbb{P}(A | B) = \frac{\mathbb{P}(B | A)\mathbb{P}(A)}{\mathbb{P}(B)}, \quad \mathbb{P}(B) \neq 0. \quad (\text{B.7})$$

Bayes' theorem gives the conditional probability of event A on event B given the inverse relationship (B given A). It can be used in situations in which we wish to evaluate a hypothesis H given data D when we have some model for how likely the data is given the hypothesis, along with the unconditioned probabilities for both the hypothesis and the data.

The analog of the probability density function for conditional probability is the *conditional probability density function* $p(x | y)$

$$p(x | y) = \begin{cases} \frac{p(x,y)}{p(y)} & 0 < p(y) < \infty \\ 0 & \text{otherwise.} \end{cases} \quad (\text{B.8})$$

It follows that

$$p(x,y) = p(x | y)p(y) \quad (\text{B.9})$$

and

$$\begin{aligned}\mathbb{P}(X \leq x | y) &:= P(X \leq x | Y = y) \\ &= \int_{-\infty}^x p(u | y) du = \frac{\int_{-\infty}^x p(u, y) du}{p(y)}.\end{aligned}\quad (\text{B.10})$$

If X and Y are independent then $p(x | y) = p(x)$ and $p(y | x) = p(y)$. Note that $p(x, y)$ and $p(x | y)$ are different density functions, though they are related through equation (B.9). If X and Y are related with joint probability density function $p(x, y)$ and conditional probability density function $p(x | y)$ then

$$p(x) = \int_{-\infty}^{\infty} p(x, y) dy = \int_{-\infty}^{\infty} p(x | y) p(y) dy.$$

Example B.1 (Conditional probability for sum). Consider three random variables X , Y and Z related by the expression

$$Z = X + Y.$$

In other words, the value of the random variable Z is given by choosing values from two random variables X and Y and adding them. We assume that X and Y are independent Gaussian random variables with mean μ_1 and μ_2 and standard deviation $\sigma = 1$ (the same for both variables).

Clearly the random variable Z is not independent of X (or Y) since if we know the values of X then it provides information about the likely value of Z . To see this, we compute the joint probability between Z and X . Let

$$A = \{x_l \leq x \leq x_u\}, \quad B = \{z_l \leq z \leq z_u\}.$$

The joint probability of both events A and B occurring is given by

$$\begin{aligned}\mathbb{P}_{X,Z}(A \cap B) &= \mathbb{P}(x_l \leq x \leq x_u, z_l \leq x + y \leq z_u) \\ &= \mathbb{P}(x_l \leq x \leq x_u, z_l - x \leq y \leq z_u - x).\end{aligned}$$

We can compute this probability by using the probability density functions for X and Y :

$$\begin{aligned}\mathbb{P}(A \cap B) &= \int_{x_l}^{x_u} \left(\int_{z_l - x}^{z_u - x} p_Y(y) dy \right) p_X(x) dx \\ &= \int_{x_l}^{x_u} \int_{z_l}^{z_u} p_Y(z - x) p_X(x) dz dx =: \int_{z_l}^{z_u} \int_{x_l}^{x_u} p_{Z,X}(z, x) dx dz.\end{aligned}$$

Using Gaussians for X and Y we have

$$\begin{aligned}p_{Z,X}(z, x) &= \frac{1}{\sqrt{2\pi}} e^{-\frac{1}{2}(z - x - \mu_Y)^2} \cdot \frac{1}{\sqrt{2\pi}} e^{-\frac{1}{2}(x - \mu_X)^2} \\ &= \frac{1}{2\pi} e^{-\frac{1}{2}((z - x - \mu_Y)^2 + (x - \mu_X)^2)}.\end{aligned}$$

A similar expression holds for $p_{Z,Y}$.

∇

Given a random variable X , we can define various standard measures of the distribution. The *expectation* or *mean* of a random variable is defined as

$$\mathbb{E}(X) = \langle X \rangle = \int_{-\infty}^{\infty} x p(x) dx,$$

and the *mean square* of a random variable is

$$\mathbb{E}(X^2) = \langle X^2 \rangle = \int_{-\infty}^{\infty} x^2 p(x) dx.$$

If we let μ represent the expectation (or mean) of X then we define the *variance* of X as

$$\mathbb{E}((X - \mu)^2) = \langle (X - \langle X \rangle)^2 \rangle = \int_{-\infty}^{\infty} (x - \mu)^2 p(x) dx.$$

We will often write the variance as σ^2 . As the notation indicates, if we have a Gaussian random variable with mean μ and (stationary) standard deviation σ , then the expectation and variance as computed above return μ and σ^2 .

Example B.2 (Exponential distribution). The exponential distribution has mean and variance given by

$$\mu = \frac{1}{\lambda}, \quad \sigma^2 = \frac{1}{\lambda^2}.$$

▽

Several useful properties follow from the definitions.

Proposition B.1 (Properties of random variables).

1. If X is a random variable with mean μ and variance σ^2 , then αX is random variable with mean $\alpha\mu$ and variance $\alpha^2\sigma^2$.
2. If X and Y are two random variables, then $\mathbb{E}(\alpha X + \beta Y) = \alpha\mathbb{E}(X) + \beta\mathbb{E}(Y)$.
3. If X and Y are Gaussian random variables with means μ_X, μ_Y and variances σ_X^2, σ_Y^2 ,

$$p(x) = \frac{1}{\sqrt{2\pi\sigma_X^2}} e^{-\frac{1}{2}\left(\frac{x-\mu_X}{\sigma_X}\right)^2}, \quad p(y) = \frac{1}{\sqrt{2\pi\sigma_Y^2}} e^{-\frac{1}{2}\left(\frac{y-\mu_Y}{\sigma_Y}\right)^2},$$

then $X + Y$ is a Gaussian random variable with mean $\mu_Z = \mu_X + \mu_Y$ and variance $\sigma_Z^2 = \sigma_X^2 + \sigma_Y^2$,

$$p(x+y) = \frac{1}{\sqrt{2\pi\sigma_Z^2}} e^{-\frac{1}{2}\left(\frac{x+y-\mu_Z}{\sigma_Z}\right)^2}.$$

Proof. The first property follows from the definition of mean and variance:

$$\begin{aligned}\mathbb{E}(\alpha X) &= \int_{-\infty}^{\infty} \alpha x p(x) dx = \alpha \int_{-\infty}^{\infty} x p(x) dx = \alpha \mathbb{E}(X) \\ \mathbb{E}((\alpha X)^2) &= \int_{-\infty}^{\infty} (\alpha x)^2 p(x) dx = \alpha^2 \int_{-\infty}^{\infty} x^2 p(x) dx = \alpha^2 \mathbb{E}(X^2).\end{aligned}$$

The second property follows similarly, remembering that we must take the expectation using the joint distribution (since we are evaluating a function of two random variables):

$$\begin{aligned}\mathbb{E}(\alpha X + \beta Y) &= \int_{-\infty}^{\infty} \int_{-\infty}^{\infty} (\alpha x + \beta y) p_{X,Y}(x,y) dx dy \\ &= \alpha \int_{-\infty}^{\infty} \int_{-\infty}^{\infty} x p_{X,Y}(x,y) dx dy + \beta \int_{-\infty}^{\infty} \int_{-\infty}^{\infty} y p_{X,Y}(x,y) dx dy \\ &= \alpha \int_{-\infty}^{\infty} x p_X(x) dx + \beta \int_{-\infty}^{\infty} y p_Y(y) dy = \alpha \mathbb{E}(X) + \beta \mathbb{E}(Y).\end{aligned}$$

The third item is left as an exercise. □

B.2 Continuous-State Random Processes

A *random process* is a collection of time-indexed random variables. Formally, we consider a random process X to be a joint mapping of sample and a time to a state: $X : \Omega \times \mathcal{T} \rightarrow S$, where \mathcal{T} is an appropriate time set. We view this mapping as a generalized random variable: a sample corresponds to choosing an entire function of time. Of course, we can always fix the time and interpret $X(\omega, t)$ as a regular random variable, with $X(\omega, t')$ representing a different random variable if $t \neq t'$. Our description of random processes will consist of describing how the random variable at a time t relates to the value of the random variable at an earlier time s . To build up some intuition about random processes, we will begin with the discrete time case, where the calculations are a bit more straightforward, and then proceed to the continuous time case.

A *discrete-time random process* is a stochastic system characterized by the *evolution* of a sequence of random variables $X[k]$, where k is an integer. As an example, consider a discrete-time linear system with dynamics

$$X[k+1] = AX[k] + BU[k] + FW[k], \quad Y[k] = CX[k] + V[k]. \quad (\text{B.11})$$

As in AM08, $X \in \mathbb{R}^n$ represents the state of the system, $U \in \mathbb{R}^p$ is the vector of inputs and $Y \in \mathbb{R}^q$ is the vector of outputs. The (possibly vector-valued) signal W represents disturbances to the process dynamics and V represents noise in the measurements. To try to fix the basic ideas, we will take $u = 0$, $n = 1$ (single state) and $F = 1$ for now.

We wish to describe the evolution of the dynamics when the disturbances and noise are not given as deterministic signals, but rather are chosen from some probability distribution. Thus we will let $W[k]$ be a collection of random variables where the values at each instant k are chosen from a probability distribution with pdf $p_{W,k}(x)$. As the notation indicates, the distributions might depend on the time instant k , although the most common case is to have a *stationary* distribution in which the distributions are independent of k (defined more formally below).

In addition to stationarity, we will often also assume that distribution of values of W at time k is independent of the values of W at time l if $k \neq l$. In other words, $W[k]$ and $W[l]$ are two separate random variables that are independent of each other. We say that the corresponding random process is *uncorrelated* (also defined more formally below). As a consequence of our independence assumption, we have that

$$\mathbb{E}(W[k]W[l]) = \mathbb{E}(W^2[k])\delta(k-l) = \begin{cases} \mathbb{E}(W^2[k]) & k = l \\ 0 & k \neq l. \end{cases}$$

In the case that $W[k]$ is a Gaussian with mean zero and (stationary) standard deviation σ , then $\mathbb{E}(W[k]W[l]) = \sigma^2 \delta(k-l)$.

We next wish to describe the evolution of the state x in equation (B.11) in the case when W is a random variable. In order to do this, we describe the state x as a sequence of random variables $X[k]$, $k = 1, \dots, N$. Looking back at equation (B.11), we see that even if $W[k]$ is an uncorrelated sequence of random variables, then the states $X[k]$ are not uncorrelated since

$$X[k+1] = AX[k] + FW[k],$$

and hence the probability distribution for X at time $k+1$ depends on the value of X at time k (as well as the value of W at time k), similar to the situation in Example B.1.

Since each $X[k]$ is a random variable, we can define the mean and variance as $\mu[k]$ and $\sigma^2[k]$ using the previous definitions at each time k :

$$\begin{aligned} \mu[k] &:= \mathbb{E}(X[k]) = \int_{-\infty}^{\infty} x p(x, k) dx, \\ \sigma^2[k] &:= \mathbb{E}((X[k] - \mu[k])^2) = \int_{-\infty}^{\infty} (x - \mu[k])^2 p(x, k) dx. \end{aligned}$$

To capture the relationship between the current state and the future state, we define the *correlation function* for a random process as

$$\rho(k_1, k_2) := \mathbb{E}(X[k_1]X[k_2]) = \int_{-\infty}^{\infty} x_1 x_2 p(x_1, x_2; k_1, k_2) dx_1 dx_2$$

The function $p(x_i, x_j; k_1, k_2)$ is the *joint probability density function*, which depends on the times k_1 and k_2 . A process is *stationary* if $p(x, k+d) = p(x, d)$ for all k ,

$p(x_i, x_j; k_1 + d, k_2 + d) = p(x_i, x_j; k_1, k_2)$, etc. In this case we can write $p(x_i, x_j; d)$ for the joint probability distribution. We will almost always restrict to this case. Similarly, we will write $p(k_1, k_2)$ as $p(d) = p(k, k + d)$.

We can compute the correlation function by explicitly computing the joint pdf (see Example B.1) or by directly computing the expectation. Suppose that we take a random process of the form (B.11) with $X[0] = 0$ and W having zero mean and standard deviation σ . The correlation function is given by

$$\begin{aligned}\mathbb{E}(X[k_1]X[k_2]) &= E\left\{\left(\sum_{i=0}^{k_1-1} A^{k_1-i} BW[i]\right)\left(\sum_{j=0}^{k_2-1} A^{k_2-j} BW[j]\right)\right\} \\ &= E\left\{\sum_{i=0}^{k_1-1} \sum_{j=0}^{k_2-1} A^{k_1-i} BW[i]W[j]BA^{k_2-j}\right\}.\end{aligned}$$

We can now use the linearity of the expectation operator to pull this inside the summations:

$$\begin{aligned}\mathbb{E}(X[k_1]X[k_2]) &= \sum_{i=0}^{k_1-1} \sum_{j=0}^{k_2-1} A^{k_1-i} B \mathbb{E}(W[i]W[j]) BA^{k_2-j} \\ &= \sum_{i=0}^{k_1-1} \sum_{j=0}^{k_2-1} A^{k_1-i} B \sigma^2 \delta(i-j) BA^{k_2-j} \\ &= \sum_{i=0}^{k_1-1} A^{k_1-i} B \sigma^2 BA^{k_2-i}.\end{aligned}$$

Note that the correlation function depends on k_1 and k_2 .

We can see the dependence of the correlation function on the time more clearly by letting $d = k_2 - k_1$ and writing

$$\begin{aligned}\rho(k, k + d) &= \mathbb{E}(X[k]X[k + d]) = \sum_{i=0}^{k_1-1} A^{k-i} B \sigma^2 BA^{d+k-i} \\ &= \sum_{j=1}^k A^j B \sigma^2 BA^{j+d} = \left(\sum_{j=1}^k A^j B \sigma^2 BA^j\right) A^d.\end{aligned}$$

In particular, if the discrete time system is stable then $|A| < 1$ and the correlation function decays as we take points that are further departed in time (d large). Furthermore, if we let $k \rightarrow \infty$ (i.e., look at the steady state solution) then the correlation function only depends on d (assuming the sum converges) and hence the steady state random process is stationary.

In our derivation so far, we have assumed that $X[k + 1]$ only depends on the value of the state at time k (this was implicit in our use of equation (B.11) and the

assumption that $W[k]$ is independent of X). This particular assumption is known as the *Markov property* for a random process: a Markovian process is one in which the distribution of possible values of the state at time k depends only on the values of the state at the prior time and not earlier. Written more formally, we say that a discrete random process is Markovian if

$$p_{X,k}(x | X[k-1], X[k-2], \dots, X[0]) = p_{X,k}(x | X[k-1]).$$

Markov processes are roughly equivalent to state space dynamical systems, where the future evolution of the system can be completely characterized in terms of the current value of the state (and not its history of values prior to that).

We now consider the case where our time index is no longer discrete, but instead varies continuously. A fully rigorous derivation requires careful use of measure theory and is beyond the scope of this text, so we focus here on the concepts that will be useful for modeling and analysis of important physical properties.

A *continuous-time random process* is a stochastic system characterized by the evolution of a random variable $X(t)$, $t \in [0, T]$. We are interested in understanding how the (random) state of the system is related at separate times. The process is defined in terms of the “correlation” of $X(t_1)$ with $X(t_2)$. We assume, as above, that the process is described by continuous random variables, but the discrete state case (with time still modeled as a real variable) can be handled in a similar fashion.

We call $X(t) \in \mathbb{R}^n$ the *state* of the random process at time t . For the case $n > 1$, we have a vector of random processes:

$$X(t) = \begin{pmatrix} X_1(t) \\ \vdots \\ X_n(t) \end{pmatrix}$$

We can characterize the state in terms of a (joint) time-varying pdf,

$$\mathbb{P}(\{x_{i,l} \leq X_i(t) \leq x_{i,u}\}) = \int_{x_{1,l}}^{x_{1,u}} \dots \int_{x_{n,l}}^{x_{n,u}} p_{X_1, \dots, X_n}(x; t) dx_n \dots dx_1.$$

Note that the state of a random process is not enough to determine the exact next state, but only the distribution of next states (otherwise it would be a deterministic process). We typically omit indexing of the individual states unless the meaning is not clear from context.

We can characterize the dynamics of a random process by its statistical characteristics, written in terms of joint probability density functions:

$$\begin{aligned} \mathbb{P}(x_{1l} \leq X_i(t_1) \leq x_{1u}, x_{2l} \leq X_j(t_2) \leq x_{2u}) \\ = \int_{x_{2l}}^{x_{2u}} \int_{x_{1l}}^{x_{1u}} p_{X_i, X_j}(x_1, x_2; t_1, t_2) dx_1 dx_2 \end{aligned}$$

The function $p(x_i, x_j; t_1, t_2)$ is called a *joint probability density function* and depends both on the individual states that are being compared and the time instants over which they are compared. Note that if $i = j$, then p_{X_i, X_i} describes how X_i at time t_1 is related to X_i at time t_2 .

In general, the distributions used to describe a random process depend on the specific time or times that we evaluate the random variables. However, in some cases the relationship only depends on the difference in time and not the absolute times (similar to the notion of time invariance in deterministic systems, as described in AM08). A process is *stationary* if $p(x, t + \tau) = p(x, t)$ for all τ , $p(x_i, x_j; t_1 + \tau, t_2 + \tau) = p(x_i, x_j; t_1, t_2)$, etc. In this case we can write $p(x_i, x_j; \tau)$ for the joint probability distribution. Stationary distributions roughly correspond to the steady state properties of a random process and we will often restrict our attention to this case.

We are often interested in random processes in which changes in the state occur when a random event occurs (such as a molecular reaction or binding event). In this case, it is natural to describe the state of the system in terms of a set of times $t_0 < t_1 < t_2 < \dots < t_n$ and $X(t_i)$ is the random variable that corresponds to the possible states of the system at time t_i . Note that time instants do not have to be uniformly spaced and most often (for physical systems) they will not be. All of the definitions above carry through, and the process can now be described by a probability distribution of the form

$$\mathbb{P}\left(X(t_i) \in [x_i, x_i + dx_i], i = 1, \dots, n\right) = p(x_n, x_{n-1}, \dots, x_0; t_n, t_{n-1}, \dots, t_0) dx_n dx_{n-1} dx_1,$$

where dx_i are taken as infinitesimal quantities.

Just as in the case of discrete time processes, we define a continuous time random process to be a Markov process if the probability of being in a given state at time t_n depends *only* on the state that we were in at the previous time instant t_{n-1} and not the entire history of states prior to t_{n-1} :

$$\begin{aligned} \mathbb{P}\left(X(t_n) \in [x_n, x_n + dx_n] \mid X(t_i) \in [x_i, x_i + dx_i], i = 1, \dots, n-1\right) \\ = \mathbb{P}\left(X(t_n) \in [x_n, x_n + dx_n] \mid X(t_{n-1}) \in [x_{n-1}, x_{n-1} + dx_{n-1}]\right). \end{aligned} \quad (\text{B.12})$$

In practice we do not usually specify random processes via the joint probability distribution $p(x_i, x_j; t_1, t_2)$ but instead describe them in terms of a *propogater function*. Let $X(t)$ be a Markov process and define the Markov propogater as

$$\Xi(dt; x, t) = X(t + dt) - X(t), \text{ given } X(t) = x.$$

The propogater function describes how the random variable at time t is related to the random variable at time $t + dt$. Since both $X(t + dt)$ and $X(t)$ are random

variables, $\Xi(dt; x, t)$ is also a random variable and hence it can be described by its density function, which we denote as $\Pi(\xi, x; dt, t)$:

$$\mathbb{P}(x \leq X(t+dt) \leq x+\xi) = \int_x^{x+\xi} \Pi(dx, x; dt, t) dx.$$

The previous definitions for mean, variance and correlation can be extended to the continuous time, vector-valued case by indexing the individual states:

$$\begin{aligned} E\{X(t)\} &= \begin{pmatrix} E\{X_1(t)\} \\ \vdots \\ E\{X_n(t)\} \end{pmatrix} =: \mu(t) \\ E\{(X(t) - \mu(t))(X(t) - \mu(t))^T\} &= \begin{pmatrix} E\{X_1(t)X_1(t)\} & \dots & E\{X_1(t)X_n(t)\} \\ & \ddots & \vdots \\ & & E\{X_n(t)X_n(t)\} \end{pmatrix} =: \Sigma(t) \\ E\{X(t)X^T(s)\} &= \begin{pmatrix} E\{X_1(t)X_1(s)\} & \dots & E\{X_1(t)X_n(s)\} \\ & \ddots & \vdots \\ & & E\{X_n(t)X_n(s)\} \end{pmatrix} =: R(t, s) \end{aligned}$$

Note that the random variables and their statistical properties are all indexed by the time t (and s). The matrix $R(t, s)$ is called the *correlation matrix* for $X(t) \in \mathbb{R}^n$. If $t = s$ then $R(t, t)$ describes how the elements of x are correlated at time t (with each other) and in the case that the processes have zero mean, $R(t, t) = \Sigma(t)$. The elements on the diagonal of $\Sigma(t)$ are the variances of the corresponding scalar variables. A random process is uncorrelated if $R(t, s) = 0$ for all $t \neq s$. This implies that $X(t)$ and $X(s)$ are independent random events and is equivalent to $p_{X,Y}(x, y) = p_X(x)p_Y(y)$.

If a random process is stationary, then it can be shown that $R(t+\tau, s+\tau) = R(t, s)$ and it follows that the correlation matrix depends only on $t - s$. In this case we will often write $R(t, s) = R(s - t)$ or simply $R(\tau)$ where τ is the correlation time. The covariance matrix in this case is simply $R(0)$.

In the case where X is also scalar random process, the correlation matrix is also a scalar and we will write $r(\tau)$, which we refer to as the (scalar) correlation function. Furthermore, for stationary scalar random processes, the correlation function depends only on the absolute value of the correlation function, so $r(\tau) = r(-\tau) = r(|\tau|)$. This property also holds for the diagonal entries of the correlation matrix since $R_{ii}(s, t) = R_{ii}(t, s)$ from the definition.

Definition B.7 (Ornstein-Uhlenbeck process). Consider a scalar random process defined by a Gaussian pdf with $\mu = 0$,

$$p(x, t) = \frac{1}{\sqrt{2\pi\sigma^2}} e^{-\frac{1}{2} \frac{x^2}{\sigma^2}},$$

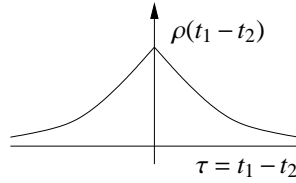


Figure B.3: Correlation function for a first-order Markov process.

and a correlation function given by

$$r(t_1, t_2) = \frac{Q}{2\omega_0} e^{-\omega_0 |t_2 - t_1|}.$$

The correlation function is illustrated in Figure B.3. This process is known as an *Ornstein-Uhlenbeck process* and it is a stationary process.

Note on terminology. The terminology and notation for covariance and correlation varies between disciplines. The term covariance is often used to refer to both the relationship between different variables X and Y and the relationship between a single variable at different times, $X(t)$ and $X(s)$. The term “cross-covariance” is used to refer to the covariance between two random vectors X and Y , to distinguish this from the covariance of the elements of X with each other. The term “cross-correlation” is sometimes also used. Finally, the term “correlation coefficient” refers to the normalized correlation $\bar{r}(t, s) = \mathbb{E}(X(t)X(s))/\mathbb{E}(X(t)X(t))$.

MATLAB has a number of functions to implement covariance and correlation, which mostly match the terminology here:

- `cov(X)` - this returns the variance of the vector X that represents samples of a given random variable or the covariance of the columns of a matrix X where the rows represent observations.
- `cov(X, Y)` - equivalent to `cov([X(:), Y(:)])`. Computes the covariance between the columns of X and Y , where the rows are observations.
- `xcorr(X, Y)` - the “cross-correlation” between two random sequences. If these sequences came from a random process, this is correlation function $r(t)$.
- `xcov(X, Y)` - this returns the “cross-covariance”, which MATLAB defines as the “mean-removed cross-correlation”.

The MATLAB help pages give the exact formulas used for each, so the main point here is to be careful to make sure you know what you really want.

We will also make use of a special type of random process referred to as “white noise”. A *white noise process* $X(t)$ satisfies $E\{X(t)\} = 0$ and $R(t, s) = W\delta(s - t)$,

where $\delta(\tau)$ is the impulse function and W is called the *noise intensity*. White noise is an idealized process, similar to the impulse function or Heaviside (step) function in deterministic systems. In particular, we note that $r(0) = E\{X^2(t)\} = \infty$, so the covariance is infinite and we never see this signal in practice. However, like the step and impulse functions, it is very useful for characterizing the response of a linear system, as described in the following proposition. It can be shown that the integral of a white noise process is a Wiener process, and so often white noise is described as the derivative of a Wiener process.

B.3 Discrete-State Random Processes

There are a number of specialized discrete random processes that are relevant for biochemical systems. In this section we give a brief introduction to these processes.

A *birth-death* process is one in which the states of the process represent integer-value counts of different species populations and the transitions between states are restricted to either incrementing (birth) or decrementing (death) a given species. This type of model is often used to represent chemical reactions such as the production and degradation of proteins.

Example B.3 (Protein production). ∇

A more general type of discrete random process is a *Markov chain*. In a Markov chain, evolution of the discrete states occurs by execution of allowable transitions between two states. Each transition has a specified probability, which is used to determine whether a system will transition from its current state into a different state (corresponding to an allowable transition). An important property, called the *Markov property*, is that the transition probability only depends on the value of the current state, not the previous values of the state.

We define a Markov chain by giving the set of transition probabilities

$$q_{ij}(t, \tau) = \mathbb{P}(X(t + \tau) = s_j | X(t) = s_i),$$

where $s_i, s_j \in S$, t is the current time and τ is the time interval over which we are interested. If $q_{ij}(t, \tau) \neq 0$ for some $\tau \neq 0$ then we say that the transition is allowable at time t . If q_{ij} is independent of t then we say that the process is *stationary* and we omit the argument t . In the special case that we are only interested in a fixed τ (i.e., we are using a discrete-time model) then we omit this argument as well.

It is generally difficult to describe the probability of being in a particular state in a Markov process at a given time. Instead, we often resort to describing the steady state distributions, assuming that they exist. For a stationary Markov chain, we can look at the equilibrium distributions, which are those distributions π that satisfy

$$\pi_i = q_{ij}(\tau)\pi_j, \quad \text{for all } i, j.$$

Example B.4 (Protein expression). ∇

Bibliography

- [1] BioNumbers: The database of useful biological numbers. <http://bionumbers.org>, 2012.
- [2] K. J. Åström and R. M. Murray. *Feedback Systems: An Introduction for Scientists and Engineers*. Princeton University Press, 2008. Available at <http://www.cds.caltech.edu/~murray/amwiki>.
- [3] B. Alberts, D. Bray, J. Lewis, M. Raff, K. Roberts, and J. D. Watson. *The Molecular Biology of the Cell*. Garland Science, fifth edition edition, 2008.
- [4] U. Alon. *An introduction to systems biology. Design principles of biological circuits*. Chapman-Hall, 2007.
- [5] W. Arber and S. Linn. DNA modification and restriction. *Annual Review of Biochemistry*, 38:467–500, 1969.
- [6] M. R. Atkinson, M. A. Savageau, J. T. Meyers, and A. J. Ninfa. Development of genetic circuitry exhibiting toggle switch or oscillatory behavior in *Escherichia coli*. *Cell*, pages 597–607, 2003.
- [7] D. W. Austin, M. S. Allen, J. M. McCollum, R. D. Dar, J. R. Wilgus, G. S. Saylor, N. F. Samatova, C. D. Cox, and M. L. Simpson. Gene network shaping of inherent noise spectra. *Nature*, 2076:608–611, 2006.
- [8] D. Baker, G. Church, J. Collins, D. Endy, J. Jacobson, J. Keasling, P. Modrich, C. Smolke, and R. Weiss. ENGINEERING LIFE: Building a FAB for biology. *Scientific American*, June 2006.
- [9] N Barkai and S Leibler. Robustness in simple biochemical networks. *Nature*, 387(6636):913–7, 1997.
- [10] S Basu, R Mehreja, S. Thiberge, M-T Chen, and R. Weiss. Spatiotemporal control of gene expression with pulse-generating networks. *PNAS*, 101(17):6355–6360, 2004.
- [11] A. Becskei and L. Serrano. Engineering stability in gene networks by autoregulation. *Nature*, 405:590–593, 2000.
- [12] D. Bell-Pedersen, V. M. Cassone, D. J. Earnest, S. S. Golden, P. E. Hardin, T. L. Thomas, and M. J. Zoran. Circadian rhythms from multiple oscillators: lessons from diverse organisms. *Nature Reviews Genetics*, 6(7):544, 2005.
- [13] L Bleris, Z. Xie, D. Glass, A. Adadey, E. Sontag, and Y. Benenson. Synthetic incoherent feedforward circuits show adaptation to the amount of their genetic template. *Molecular Systems Biology*, 7:519, 2011.

- [14] B. Canton, A. Labno, and D. Endy. Refinement and standardization of synthetic biological parts and devices. *Nature Biotechnology*, 26(7):787–93, 2008.
- [15] M. Chalfie, Y. Tu, G. Euskirchen, W. Ward, and D. Prasher. Green fluorescent protein as a marker for gene expression. *Science*, 263(5148):802–805, 1994.
- [16] A. J. Courey. *Mechanisms in Transcriptional Regulation*. Wiley-Blackwell, 2008.
- [17] R. S. III Cox, M. G. Surette, and M. B. Elowitz. Programming gene expression with combinatorial promoters. *Mol Syst Biol*, page 3:145, 2007.
- [18] H. de Jong. Modeling and simulation of genetic regulatory systems: A literature review. *Journal of Computational Biology*, 9:67–103, 2002.
- [19] D. Del Vecchio. Design and analysis of an activator-repressor clock in *e. coli*. In *Proc. American Control Conference*, 2007.
- [20] D. Del Vecchio and H. El-Samad. Repressilators and promotilators: Loop dynamics in gene regulatory networks. In *Proc. American Control Conference*, 2005.
- [21] D. Del Vecchio, A. J. Ninfa, and E. D. Sontag. Modular cell biology: Retroactivity and insulation. *Nature/EMBO Molecular Systems Biology*, 4:161, 2008.
- [22] L. Desborough and R. Miller. Increasing customer value of industrial control performance monitoring—Honeywell’s experience. In *Sixth International Conference on Chemical Process Control*. AICHe Symposium Series Number 326 (Vol. 98), 2002.
- [23] L. N. M. Duysens and J. Ames. Fluorescence spectrophotometry of reduced phosphopyridine nucleotide in intact cells in the near-ultraviolet and visible region. *Biochim. Biophys. Acta*, 24:19–26, 1957.
- [24] H. El-Samad, J. P. Goff, and M. Khammash. Calcium homeostasis and parturient hypocalcemia: An integral feedback perspective. *J. Theoret. Biol.*, 214:17–29, 2002.
- [25] S. P. Ellner and J. Guckenheimer. *Dynamic Models in Biology*. Princeton University Press, Princeton, NJ, 2005.
- [26] M. B. Elowitz and S. Leibler. A synthetic oscillatory network of transcriptional regulators. *Nature*, 403(6767):335–338, 2000.
- [27] Michael B Elowitz, Arnold J Levine, Eric D Siggia, and Peter S Swain. Stochastic gene expression in a single cell. *Science (New York, NY)*, 297(5584):1183–1186, 2002.
- [28] D. Endy. Foundations for engineering biology. *Nature*, 438:449–452, 2005.
- [29] T.S. Gardner, C.R. Cantor, and J.J. Collins. Construction of the genetic toggle switch in *Escherichia Coli*. *Nature*, page 339342, 2000.
- [30] Daniel G. Gibson, John I. Glass, Carole Lartigue, Vladimir N. Noskov, Ray-Yuan Chuang, Mikkel A. Algire, Gwynedd A. Benders, Michael G. Montague, Li Ma, Monzia M. Moodie, Chuck Merryman, Sanjay Vashee, Radha Krishnakumar, Nacyra Assad-Garcia, Cynthia Andrews-Pfannkoch, Evgeniya A. Denisova, Lei Young, Zhi-Qing Qi, Thomas H. Segall-Shapiro, Christopher H. Calvey, Prashanth P. Parmar, Clyde A. Hutchison, Hamilton O. Smith, and J. Craig Venter. Creation of a Bacterial Cell Controlled by a Chemically Synthesized Genome. *Science*, 329(5987):52–56, 2010.

- [31] D. T. Gillespie. *Markov Processes: An Introduction For Physical Scientists*. Academic Press, 1976.
- [32] D. T. Gillespie. A rigorous derivation of the chemical master equation. *Physica A*, 188:404–425, 1992.
- [33] L. Goentoro, O. Shoval, M. W. Kirschner, and U. Alon. The incoherent feedforward loop can provide fold-change detection in gene regulation. *Molecular Cell*, 36:894–899, 2009.
- [34] A. Goldbeter and D. E. Koshland. An amplified sensitivity arising from covalent modification in biological systems. *PNAS*, pages 6840–6844, 1981.
- [35] J. Greenblatt, J. R. Nodwell, and S. W. Mason. Transcriptional antitermination. *Nature*, 364(6436):401–406, 1993.
- [36] J. Greenblatt, J. R. Nodwell, and S. W. Mason. Transcriptional antitermination. *Nature*, 364(6436):401–406, 1993.
- [37] J. Guckenheimer and P. Holmes. *Nonlinear Oscillations, Dynamical Systems, and Bifurcations of Vector Fields*. Springer, 1983.
- [38] R. Heinrich, B. G. Neel, and T. A. Rapoport. Mathematical models of protein kinase signal transduction. *Molecular Cell*, 9:957–970, 2002.
- [39] B. Hess, A. Boiteux, and J. Kruger. Cooperation of glycolytic enzymes. *Adv. Enzyme Regul*, 7:149–167, 1969.
- [40] Andreas Hilfinger and Johan Paulsson. Separating intrinsic from extrinsic fluctuations in dynamic biological systems. *Proceedings of the National Academy of Sciences*, 108(29):12167–12172, 2011.
- [41] C. F. Huang and J. E. Ferrell. Ultrasensitivity in the mitogen-activated protein kinase cascade. *Proc. Natl. Acad. Sci.*, 93(19):10078–10083, 1996.
- [42] T. P. Hughes. *Elmer Sperry: Inventor and Engineer*. John Hopkins University Press, Baltimore, MD, 1993.
- [43] B. Ingalls. A frequency domain approach to sensitivity analysis of biochemical networks. *Journal of Physical Chemistry B-Condensed Phase*, 108(3):143–152, 2004.
- [44] F. Jacob and J. Monod. Genetic regulatory mechanisms in the synthesis of proteins. *J. Mol. Biol.*, 3:318–56, 1961.
- [45] P. Jiang, A. C. Ventura, S. D. Merajver, E. D. Sontag, A. J. Ninfa, and D. Del Vecchio. Load-induced modulation of signal transduction networks. *Science Signaling*, 4(194):ra67, 2011.
- [46] N. G. Van Kampen. *Stochastic Processes in Physics and Chemistry*. Elsevier, 1992.
- [47] A. S. Khalil and J. J. Collins. Synthetic biology: applications come of age. *Nature Reviews Genetics*, 11(5):367, 2010.
- [48] E. Klipp, W. Liebermeister, C. Wierling, A. Kowald, H. Lehrach, and R. Herwig. *Systems Biology: A Textbook*. Wiley-VCH, 2009.
- [49] P. Kundur. *Power System Stability and Control*. McGraw-Hill, New York, 1993.

- [50] M. T. Laub, L. Shapiro, and H. H. McAdams. Systems biology of *caulobacter*. *Annual Review of Genetics*, 51:429–441, 2007.
- [51] J.-C. Leloup and A. Goldbeter. A molecular explanation for the long-term suppression of circadian rhythms by a single light pulse. *American Journal of Physiology*, 280:1206–1212, 2001.
- [52] W. Lohmiller and J. J. E. Slotine. On contraction analysis for non-linear systems. *Automatica*, 34:683–696, 1998.
- [53] H. Madhani. *From a to alpha: Yeast as a Model for Cellular Differentiation*. CSHL Press, 2007.
- [54] J. Mallet-Paret and H.L. Smith. The Poincaré-Bendixson theorem for monotone cyclic feedback systems. *J. of Dynamics and Differential Equations.*, 2:367–421, 1990.
- [55] J. E. Marsden and M. J. Hoffman. *Elementary Classical Analysis*. Freeman, 2000.
- [56] S. Marsigliante, M. G. Elia, B. Di Jeso, S. Greco, A. Muscella, and C. Storelli. Increase of $[Ca^{2+}]_i$ via activation of ATP receptors in pc-cl3 rat thyroid cell line. *Cell. Signal*, 14:61–67, 2002.
- [57] C. R. McClung. Plant circadian rhythms. *Plant Cell*, 18:792–803, 2006.
- [58] M. W. McFarland, editor. *The Papers of Wilbur and Orville Wright*. McGraw-Hill, New York, 1953.
- [59] P. Miller and X. J. Wang. Inhibitory control by an integral feedback signal in prefrontal cortex: A model of discrimination between sequential stimuli. *PNAS*, 103:201–206, 2006.
- [60] C. J. Morton-Firth, T. S. Shimizu, and D. Bray. A free-energy-based stochastic simulation of the tar receptor complex. *Journal of Molecular Biology*, 286(4):1059–74, 1999.
- [61] J. D. Murray. *Mathematical Biology*, Vols. I and II. Springer-Verlag, New York, 3rd edition, 2004.
- [62] R. M. Murray. *Optimization-Based Control*. <http://www.cds.caltech.edu/~murray/amwiki/OBC>, Retrieved 20 December 2009.
- [63] C. J. Myers. *Engineering Genetic Circuits*. Chapman and Hall/CRC Press, 2009.
- [64] T. Nagashima, H. Shimodaira, K. Ide, T. Nakakuki, Y. Tani, K. Takahashi, N. Yumoto, and M. Hatakeyama. Quantitative transcriptional control of erbB receptor signaling undergoes graded to biphasic response for cell differentiation. *J. Biol. Chem.*, 282:40454056, 2007.
- [65] National Center for Biotechnology Information. A science primer. Retrieved 20 December 2009, 2004. <http://www.ncbi.nlm.nih.gov/About/primer/genetics.html>.
- [66] National Human Genome Research Institute. Talking glossary of genetic terms. Retrieved 20 December 2009. <http://www.genome.gov/glossary>.
- [67] R. Neshher and E. Cerasi. Modeling phasic insulin release: Immediate and time-dependent effects of glucose. *Diabetes*, 51:53–59, 2002.

- [68] R. Phillips, J. Kondev, and J. Theriot. *Physical Biology of the Cell*. Garland Science, 2008.
- [69] M. Ptashne. *A genetic switch*. Blackwell Science, Inc., 1992.
- [70] P. E. M. Purnick and R. Weiss. The second wave of synthetic biology: from modules to systems. *Nature Reviews Molecular Cell Biology*, 10(6):410–422, 2009.
- [71] E. K. Pye. Periodicities in intermediary metabolism. *Biochronometry, National Acad. Sci.*, 1971.
- [72] L. Qiao, R. B. Nachbar, I. G. Kevrekidis, and S. Y. Shvartsman. Bistability and oscillations in the Huang-Ferrell model of MAPK signaling. *PLoS Computational Biology*, 3:e184, 2007.
- [73] C. V. Rao, J. R. Kirby, and A. P. Arkin. Design and diversity in bacterial chemotaxis: A comparative study in *Escherichia coli* and *Bacillus subtilis*. *PLoS Biology*, 2(2):239–252, 2004.
- [74] J. M. Rohwer, N. D. Meadow, S. Roseman, H. V. Westerhoff, and P. W. Postma. Understanding glucose transport by the bacterial phosphoenolpyruvate: glucose phosphotransferase system on the basis of kinetic measurements in vitro. *The Journal of biological chemistry*, 275(45):34909–34921, November 2000.
- [75] N. Rosenfeld, M. B. Elowitz, and U. Alon. Negative autoregulation speeds the response times of transcription networks. *J. Molecular Biology*, 323(5):785–793, 2002.
- [76] H. M. Sauro and B. Ingalls. MAPK cascades as feedback amplifiers. Technical report, <http://arxiv.org/abs/0710.5195>, Oct 2007.
- [77] H. M. Sauro and B. N. Kholodenko. Quantitative analysis of signaling networks. *Progress in Biophysics & Molecular Biology*, 86:5–43, 2004.
- [78] D. E. Seborg, T. F. Edgar, and D. A. Mellichamp. *Process Dynamics and Control*. Wiley, Hoboken, NJ, 2nd edition, 2004.
- [79] Thomas S Shimizu, Yuhai Tu, and Howard C Berg. A modular gradient-sensing network for chemotaxis in *Escherichia coli* revealed by responses to time-varying stimuli. *Molecular Systems Biology*, 6:382, 2010.
- [80] O. Shimomura, F. Johnson, and Y. Saiga. Extraction, purification and properties of aequorin, a bioluminescent protein from the luminous hydromedusa, *Aequorea*. *J Cell Comp Physiol*, 59(3):223–239, 1962.
- [81] O. Shoval, U. Alon, and E. Sontag. Symmetry invariance for adapting biological systems. *SIAM J. APPLIED DYNAMICAL SYSTEMS*, 10:857886, 2011.
- [82] Peter S Swain, Michael B Elowitz, and Eric D Siggia. Intrinsic and extrinsic contributions to stochasticity in gene expression. *Proceedings of the National Academy of Sciences of the United States of America*, 99(20):12795–12800, 2002.
- [83] J. Tsang, J. Zhu, and A. van Oudenaarden. MicroRNA-mediated feedback and feed-forward loops are recurrent network motifs in mammals. *Mol. Cell*, 26:753–767, 2007.

- [84] K. V. Venkatesh, S. Bhartiya, and A. Ruhela. Multiple feedback loops are key to a robust dynamic performance of tryptophan regulation in *Escherichia coli*. *FEBS Letters*, 563:234–240, 2004.
- [85] O. Venturelli, H. El-Samad, and R. M. Murray. Dual positive feedback loops compensate for generating robust bistability in the gal regulatory network. In preparation, 2012.
- [86] O. Venturelli, H. El-Samad, and R. M. Murray. Synergistic dual positive feedback loops generate robust bimodal response. Submitted, 2012.
- [87] L. Villa-Komaroff, A. Efstratiadis, S. Broome, P. Lomedico, R. Tizard, S. P. Naber, W. L. Chick, and W. Gilbert. A bacterial clone synthesizing proinsulin. *Proc. Natl. Acad. Sci. U.S.A.*, 75(8):372731, 1978.
- [88] C. A. Voigt. Genetic parts to program bacteria. *Current Opinions in Biotechnology*, 17(5):548–557, 2006.
- [89] S. Wiggins. *Introduction to Applied Nonlinear Dynamical Systems and Chaos*. Springer, 2003.
- [90] L. Yang and P. A. Iglesias. Positive feedback may cause the biphasic response observed in the chemoattractant-induced response of dictyostelium cells. *Systems Control Lett.*, 55:329–337, 2006.
- [91] T.-M. Yi, Y. Huang, M. I. Simon, and J. C. Doyle. Robust perfect adaptation in bacterial chemotaxis through integral feedback control. *Proc. of the National Academy of Sciences*, 97(9):4649–4653, 2000.
- [92] N. Yildirim and M. C. Mackey. Feedback regulation in the lactose operon: A mathematical modeling study and comparison with experimental data. *Biophysical Journal*, 84(5):2841–2851, 2003.

Index

- Ω expansion, 4-17
- A site, A-22
- absorption, A-17
- acceptor site, A-22
- acetyl CoA, A-9
- acetylation, 1-21
- activated genes, A-18
- activation, 1-14
- activator, 1-14
- activators, A-42
- actuators, 1-32
- adaptive/inducible repair, A-26
- adenine, A-29
- adenosine triphosphate (ATP), A-8, A-31
- aerobically, A-32
- aerospace systems, 1-25
- agarose, A-50
- alleles, A-14
- alternative splicing, A-42
- aminoacyl tRNA synthetase, A-22
- amplification, *see also* polymerase chain reaction
- amplification, of DNA, A-48, A-49
- amplified, A-47
- anaerobic metabolism, A-8
- anaerobically, A-32
- anaphase, A-13
- Anaphase I, A-14
- Anaphase II, A-14
- annealed, A-52
- anti-codon, A-22
- anti-codon site, A-22
- antibodies, A-34
- anticipation, in controllers, 1-29
- antisense strand, A-21
- antitermination, 1-18
- archaea, A-2
- asexual reproduction, A-11
- assembly, of a virus, A-17
- asymptotic stability, 3-3, 3-4, 3-8, 3-9
- ATP, A-8
- attachment, A-17
- attractor (equilibrium point), 3-4
- automotive control systems, 1-26
- autopilot, 1-25, 1-26
- bacteria, A-15
- bacterial artificial chromosomes (BACs), A-49
- bacterial plasmids, A-49
- bacteriophages, A-16
- bacteriophages, A-15, A-49
- base excision repair, A-26
- base pairs, A-30
- Bell Labs, 1-24
- bifurcation, 3-44
- bifurcation diagram, 3-44
- bifurcations, 3-43–3-45
- bimodality, 1-7
- binary fission, A-11, A-15
- binomial distribution, B-2
- biological circuits, 1-4
 - repressilator, 1-37–1-38, 2-22–2-23
- birth-death, B-15
- bistability, 1-6, 1-38, 1-39
- bistable, 3-44
- Black, H. S., 1-24, 1-26
- blastocyst, A-18
- block diagonal systems, 3-8
- blotting, A-51
- blunt ends, A-48
- Bode plot, 3-12
- capsid, *see* viral capsid A-16, A-17
- carbon dioxide, A-8
- CDKs, *see* cyclin dependent kinases 3-33
- cell
 - organization, A-2–A-3
- cell duplication, A-11
- cell envelope, A-3
- cell genome, A-3
- cell mass, A-18
- cell membrane, A-4

- cell types, A-11, A-18
- cell wall, A-3
- center (equilibrium point), 3-4
- Central Dogma, A-34
- centromeres, A-14, A-40
- chain termination method, A-52
- chaperones, A-17
- characteristic polynomial, 3-7
- charger protein, A-22
- chemical degradation method, A-52
- chemical kinetics, 2-4-2-5
- chemical Langevin equation, 4-14, 4-15
- chloroplast, A-30
- chloroplasts, A-9
- cholesterol receptor protein, A-46
- chromatid arms, A-14
- chromosome, A-5, A-12, A-13
- chromosomes, A-13, A-14
- cis-acting, A-43, A-44
- citric acid cycle, A-8
- cleaved, A-22
- cloning, A-47, A-48
- cloning vector, A-48
- closed complex, 1-9
- closed loop, 1-22
 - versus open loop, 1-22
- secoenzyme A, A-9
- coding strand, A-21
- codon, A-22
- codons, A-35
- coenzyme A, A-9
- cohesive ends, A-48
- combinatorial promoters, 1-17
- complementary, A-30
- complexity, of control systems, 1-26
- conjunction, A-15
- contracting, 3-26
- control
 - early examples, 1-23, 1-26
- control matrix, 1-34
- control signal, 1-32
- cooperative, 2-11
- coordinate transformations, 3-8
- core gene sequence, A-36
- cosmids, A-49
- cristae, A-7
- crossovers, A-14
- cruise control, 1-23
 - robustness, 1-23
- Curtiss seaplane, 1-26
- cycle sequencing, A-54
- cyclin dependent kinases, 3-33
- cyclins, 3-32
- cytokinesis, A-14
- cytoplasm, A-5
- cytoplasmic region, A-3
- cytoplasmic streaming, A-5
- cytosine, A-29
- cytoskeleton, A-4, A-5
- cytosol, A-5

- daughter nuclei, A-11
- dead zone, 1-28
- deamination, A-26
- degree of cooperativity, 4-5
- deleterious mutation, A-24
- denatured, A-51
- deoxynucleotides, A-53
- deoxyribonucleic acid, A-46
- deoxyribonucleic acid (DNA), A-5, A-29
- derivative action, 1-29, 1-30
- derived cells, A-18
- design of dynamics, 1-24-1-26, 3-9
- diagonal systems, 3-7
 - transforming to, 3-8
- dideoxynucleotide, A-53
- differentiation, A-18, A-44
- diffusion term, 4-16
- diploid, A-13, A-14, A-18
- direct term, 1-34
- dissociation constant, 2-10
- disturbance attenuation
 - in biological systems, 3-14
- disturbances, 1-33
- DNA, A-29
- DNA ligase, A-20, A-25
- DNA looping, 1-15
- DNA nucleotides, A-49
- DNA polymerase, A-20, A-25, A-53
- DNA repair systems, A-25
- DNA replication, A-18, A-19
- DNA template, A-53
- drift term, 4-16
- dyes, A-50
- dynamical systems, 1-21
 - linear, 3-7

- dynamics matrix, 1-34
- early proteins, A-17
- economic systems, 1-27
- egg, A-18
- egg cell, A-14
- eigenvalues, 3-7, 3-45
 - invariance under coordinate transformation, 3-8
- eigenvectors, 3-8
- electrical circuits, 1-4
- electrodes, A-50
- elongation, A-23
- Elowitz, M. B., 2-22
- endocytosis, A-4, A-16
- endoplasmic reticulum, A-7
- endoplasmic reticulum (ER), A-9
- energy production, in a cell, A-7–A-9
- enhancers, A-43
- enthalpy, 4-7
- enzymes, A-34
- equilibrium points, 3-2, 3-7
 - bifurcations of, 3-43
 - for planar systems, 3-4
 - region of attraction, 3-4
- ethidium bromide, A-51
- eukaryotes, A-2–A-3, A-37
- events, B-1
- exocytosis, A-17
- exons, A-35
- expectation, B-7
- exported proteins, A-9
- familial hypercholesterolemia, A-46
- feedback
 - as technology enabler, 1-25
 - drawbacks of, 1-22, 1-26
 - properties, 1-27
 - robustness through, 1-23
 - versus feedforward, 1-27
- feedback mechanisms, A-42
- feedforward, 1-27
- female life cycles, A-14
- filters
 - for measurement signals, 1-26
- flagella, A-3
- flavin-adenine dinucleotide (FAD), A-9
- flight control, 1-25
- fluorescent reporters, 1-37
- flush ends, A-48
- Fokker-Planck equations, 4-16
- forward Kolmogorov equation, 4-11
- fragmentation, 1-37
- free energy, 4-7
- frequency response, 1-31, 3-12
- gametes, A-11, A-12, A-18
- Gaussian distribution, B-4
- gel, A-50
- gels, A-50
- gene, 1-9
- gene prediction, A-36
- gene regulation, A-42–A-44
- gene regulatory sequences, A-41
- genes, A-5, A-29, A-46
- genetic marker, A-40
- genetic material, A-5
- genetic recombination, A-14
- genetic switch, 1-39
- genomes, A-29
- genomic imprinting, A-44
- germ cells, A-18
- germ line cells, A-18
- Gibbs free energy, 4-7
- global behavior, 3-4
- glucose, A-8, A-9
- glucose transporters, A-8
- glycolysis, A-8
- glycoproteins, A-17
- Golgi apparatus, A-9
- gradient, A-51
- granular chromatin, A-14
- guanine, A-29
- haploid, A-13, A-14
- heat shock, 1-16
- helicase, A-20
- hemoglobin, A-43
- hereditary traits, A-46
- Hill coefficient, 4-5
- Hill functions, 2-11
- homologous recombination, A-26
- Hopf bifurcation theorem, 3-46
- human development, A-18
- human genome, A-41
- hysteresis, 1-28

- implicit function theorem, 3-48
- inactivated genes, A-18
- independent assortment, A-15
- inducer, 1-16
- inducible error-prone repair, A-26
- initiator sequence, A-37
- inner membrane, of mitochondria, A-7
- input/output models, 1-30, 1-32
- input/output models relationship to state space models, 1-32
- inputs, 1-32
- integral action, 1-29, 1-30
- intercalating agent, A-51
- interphase, A-12, A-13
- introns, A-35
- isomerization, 1-9

- Jacobian matrix, 3-9
- junk DNA, A-38

- kinase, 1-20, 2-33
- Kozak sequence, 1-12
- Kreb's cycle, A-8, A-9

- lagging strand, A-20
- large subunit, A-22
- late proteins, A-17
- leading strand, A-20
- licensing factors, A-21
- ligation, 1-37, A-48
- limit cycle, 3-37
- linear noise approximation, 4-17
- linear systems, 1-31, 1-34, 3-6
- linear time-invariant systems, 1-31, 1-34
- linearization, 3-9
- linkage, A-15
- linkage disequilibrium, A-15
- local behavior, 3-3, 3-9
- locally asymptotically stable, 3-3
- locus, A-14
- Locus Control Region (LCR), A-43
- lysis, A-17
- lysosomes, A-9
- lysozyme, A-17
- lytic proteins, A-17

- male structures, A-14
- Markov chain, B-15
- Markov property, B-15
- maturation time, 1-12
- mature mRNA, 1-12, A-36
- mean, B-4, B-7
- measured signals, 1-32, 1-33
- mechanics, 1-32
- meiosis, A-12–A-14
- Meiosis I, A-13, A-14
- Meiosis II, A-14
- memory, 1-6
- messenger RNA (mRNA), A-33
- Metaphase, A-14
- metaphase, A-12
- Metaphase II, A-14
- metaphase plate, A-14
- methionine, A-22
- methyl group (-CH₃), A-44
- methylation, 1-21, A-44
- Michaelis-Menten constant, 2-14
- Michaelis-Menten kinetics, 2-14
- mismatch repair, A-26
- mitochondria, A-7–A-9
- mitochondrial DNA (mtDNA), A-32
- mitochondrial genome, A-5
- Mitochondrial Theory of Aging, A-33
- mitochondrion, A-30
- mitosis, A-11–A-13
- modeling simplified models, use of, 1-33
- modularity, 7-2
- molecular and cellular biology, A-17
- molecular dynamics, 2-2
- molecular genetics, A-46
- molecular weights, A-50
- multipotent, A-19
- multistable, 3-44
- mutagenesis, A-27
- mutations, A-14, A-24, A-46

- NAD⁺, A-8
- NADH, A-9
- nascent RNA, A-22, A-37
- negative inducer, 1-16
- networking, 1-4
- neutral stability, 3-3, 3-4
- nitrocellulose, A-51
- noise intensity, B-15
- nonlinear systems, 1-32, 3-9
 - linear approximation, 3-9

- normal distribution, B-4
 northern blotting, A-51
 nuclear DNA, A-31
 nuclear envelope, A-6, A-12, A-13
 nuclear genome, A-5
 nuclear membrane, A-14
 nucleic acid, A-29
 nucleotide, A-29
 Nucleotide excision repair, A-25
 nucleus, A-6, A-29
 Nyquist plot, 3-13
- obligate intracellular parasites, A-16
 observability, 1-32
 Okazaki fragments, A-20
 omega limit set, 3-39
 omega-limit point, 3-39
 on-off control, 1-28
 open complex, 1-9
 open loop, 1-22
 open reading frames, A-41
 operator, A-44
 operator region, 1-15
 operon, 1-15
 order, of a system, 1-33
 organelles, A-3, A-6
 Origin Recognition Complex, A-21
 Ornstein-Uhlenbeck process, B-14
 outer membrane, of mitochondria, A-7
 oxaloacetate, A-9
- P site, A-22
 parametric stability diagram, 3-44, 3-45
 parent of origin differences, A-44
 parental, A-15
 partition function, 2-3, 4-7
 penetration, of a virus, A-17
 peroxisomal targeting signal (PTS), A-10
 peroxisomes, A-9, A-10
 phosphatase, 2-33
 phosphotransferase, 1-20
 photoreactivation, A-25
 photosynthesis, A-9
 PI control, 1-23, 1-29
 PID control, 1-28–1-29
 pili, A-3
 planar dynamical systems, 3-4
 plasma membrane, A-3, A-4
- plasmids, A-15, A-48
 platelets, A-19
 pluripotent, A-19
 Poisson distribution, B-3
 poles, 3-12
 poly(A) tail, A-22
 polymerase chain reaction, A-47
 polymerase chain reaction (PCR), A-49
 polymerization, A-50
 polypeptide chain, A-23
 positive feedback, 1-27
 positive inducer, 1-16
 positively charged, A-51
 post-replication repair, A-25
 post-transcriptional modification, A-22, A-42
 post-translational modification, A-23
 pre-mRNA, 1-12
 prediction, in controllers, 1-29
 primer, A-53
 primers, A-49
 probability mass function, B-2
 probability measure, B-1
 probability space, B-1
 probe, A-51
 process control, 1-4
 prokaryotes, A-2–A-3, A-37
 promoter sequence, A-21, A-42
 promoter site, A-37
 propensity function, 4-10
 prophase, A-12
 Prophase I, A-13
 Prophase II, A-14
 protease, A-23
 protein transport, A-18
 proteins, A-34–A-35
 pseudogene, A-40
 purines, A-29
 pyrimidines, A-29
 pyruvate, A-8, A-9
 pyruvic acid, A-8
- quasi-steady state approximation, 2-14
- random process, B-8
 random variable, B-1
 reachability, 1-32
 recombinant DNA molecule, A-48
 recombinant plasmid, A-48

- recombination, A-14–A-15, A-36
- recombination repair, A-25
- red blood cells, A-18, A-19
- reduced stoichiometry matrix, 3-27
- reduction division, A-13
- reference signal, 1-28
- regulatory sequences, A-39
- release, of a virus, A-17
- repetitive DNA, A-39
- replication, A-11, A-19, A-48
- replication control mechanisms, A-20
- replication origin sites, A-20
- replication, of a virus, A-17
- reporter genes, 6-3
- repressilator, 1-37–1-38, 2-22–2-23
- repression, 1-14
- repressor, 1-38, 3-17
- repressor proteins, A-44
- repressors, A-42
- restriction enzyme, A-48
- restriction enzymes, 1-36
- retroviruses, A-16
- reverse transcriptase, A-16
- ribonucleic acid (RNA), A-5, A-33
- ribosomal complex, A-35
- ribosome, A-22, A-33, A-35
 - large and small subunits, A-7
- ribosome binding site (RBS), 1-12
- ribosomes, A-6
- RNA polymerase, A-21, A-22, A-37, A-42
- RNA polymerase II, A-37
- RNA processing, A-18
- RNA replicase, A-16
- robustness, 1-23–1-24
- root locus diagram, 3-45, 3-46
- rough ER, A-9
- running buffer, A-50

- saddle (equilibrium point), 3-4
- sample space, B-1
- satellite DNA, A-40
- scale invariance, 3-24
- screening, 1-37
- self-repression, 3-16
- sense strand, A-21
- sensor matrix, 1-34
- sequencing, A-52
- sexual reproduction, A-12

- Shine-Delgarno, 1-12
- Shine-Delgarno sequence, A-38
- sigma factors, 1-16
- sink (equilibrium point), 3-4
- sister chromatids, A-12
- slow manifold, 3-48
- small subunit, A-22
- smooth ER, A-9
- somatic cells, A-18
- SOS repair, A-26
- source (equilibrium point), 3-4
- Southern blotting, A-51
- sperm, A-18
- sperm cells, A-14
- spindle, A-12, A-14
- splice junctions, A-41
- spontaneous mutations, A-14
- stability, 1-24, 3-2
 - asymptotic stability, 3-3, 3-9
 - in the sense of Lyapunov, 3-3
 - local versus global, 3-3
 - neutrally stable, 3-3, 3-4
 - of a system, 3-7
 - of equilibrium points, 3-4
 - of linear systems, 3-6–3-9
 - of solutions, 3-3
 - unstable solutions, 3-3
 - using linear approximation, 3-9
- standard deviation, B-4
- start codon, 1-12, A-22, A-41
- state, of a dynamical system, 1-32, 1-33
- state space, 1-33
- state vector, 1-33
- stationary, B-15
- statistical mechanics, 2-2–2-4
- steam engines, 1-23
- stem cells, A-18
- step input, 1-31
- step response, 1-31, 1-32
- sticky ends, A-48
- stop codon, 1-12, A-23
- structural components, A-34
- structural genes, A-39
- superposition, 1-31
- switching (transcriptional regulation, A-43
- switching behavior, 1-27
- symbiotic, A-32

- Taq polymerase, A-49
- TATA box, A-37
- telomeres, A-40
- telophase, A-13
- Telophase I, A-14
- Telophase II, A-14
- template DNA, A-49, A-52
- template strand, A-21, A-30
- termination region, 1-11, A-22
- terminator, 1-11
- thalassemias, A-43
- thymine, A-29
- time-invariant systems, 1-33
- trans-acting, A-43
- transcription, 1-9, A-6, A-18, A-21, A-34, A-36, A-37, A-42–A-44
- transcription factors, A-42
- transcriptional regulation, 1-14
- transduction, A-15
- transfection, 1-37
- transfer function, 3-12
- transfer RNA (tRNA), A-22
- transformation, A-15, A-48
- translation, 1-12, A-7, A-22, A-37, A-44
- translational regulation, A-44
- transport molecules, A-34

- ubiquitination, 1-21
- uncertainty, 1-23–1-24, 1-33
 - disturbances and noise, 1-33
- uniform distribution, B-4
- unstable solution, for a dynamical system, 3-3, 3-4, 3-9

- vector, A-48
- viral capsid, A-16
- virion, A-16
- virions, A-16
- viruses, A-10, A-15, A-17
 - reproduction, A-16–A-17

- Watt steam engine, 1-23
- wells, A-50
- white blood cells, A-19
- wild-type, A-25
- Wright, W., 1-25

- X-inactivation, A-40

- yeast artificial chromosomes (YACs), A-49

- zero frequency gain, 3-12
- zero-order kinetics, 2-15
- zeros, 3-12

